

BULGARIAN CHEMICAL COMMUNICATIONS

2017 Volume 49 / Special Issue E

Selected papers delivered at the 7th Bulgarian Peptide Symposium,
Blagoevgrad, June 10-12, 2016

*Journal of the Chemical Institutes
of the Bulgarian Academy of Sciences
and of the Union of Chemists in Bulgaria*

BULGARIAN CHEMICAL COMMUNICATIONS

A quarterly published by

THE BULGARIAN ACADEMY OF SCIENCES

and

THE UNION OF CHEMISTS IN BULGARIA

Volume 49, Special Issue E

ИЗВЕСТИЯ ПО ХИМИЯ

Тримесечно издание на

БЪЛГАРСКА АКАДЕМИЯ НА НАУКИТЕ

и

СЪЮЗ НА ХИМИЦИТЕ В БЪЛГАРИЯ

Том 49, Специален брой Е

2017

Editor-in-Chief:

V. Beschkov

Guest editors:

I. Stoineva, R. Kalfin

EDITORIAL BOARD

Ch. Bonev, P.R. Bontchev, L. Boyadzhiev, I. Gutzow, I. Havezov, E. Ivanova, K. Petkov, K. Petrov, L. Petrov, I. Pojarlieff, S. Rakovsky, D. Stoychev, L. Terlemezyan, D. Tsalev, D. Vladikova, D. Yankov

Members from abroad:

J. M. Albella (Spain), S. Berger (Germany), J. C. Breakman (Belgium), J. Etourneau (France), M. Farina (Italy), K. Friedrich (Germany), J. Gyenis (Hungary), A. J. Kirby (United Kingdom), T. Kowalska (Poland), K. Kutchitsu (Japan), A. Lasia (Canada), O. V. Mazurin (Russia), B. Mutafschiev (France), E. Peter Kündig (Switzerland), S. De Rosa (Italy), T. F. Tadros (United Kingdom), K. Valko (Hungary)

The annual subscription (for 4 issues) for vol. 49 (2017) is € 160. – including postage, handling and packaging charge.

Payments should be delivered to:

*Editorial Board of Bulgarian Chemical Communications, Institute of Chemical Engineering,
Unicredit Bulbank, IBAN: BG65UNCR76303400001748; BIC - UNCRBGSF (for Euro €).*

Unicredit Bulbank, IBAN: BG18UNCR96603119903312; SWIFT BIC - UNCRBGSF (for local currency BGN).



Preface

The present special issue of the journal *Bulgarian Chemical Communications* contains selected papers from the presentations delivered at the 7th Bulgarian Peptide Symposium.

The 1st meeting of “Structure and function of peptides, proteins and enzymes“ was held in 1986 in Sofia and ten years later the Bulgarian Peptide Society was established during the 1st Bulgarian Peptide Symposium in Rila mountain with founders Prof. Ch. Ivanov, Prof. B. Aleksiev, Prof. D. Petkov, Prof. L. Vezenkov and Prof. L. Kasakov. Till now Bulgarian Peptide Symposium is a regular scientific conference, taking place every two years.

The 7th Bulgarian Peptide Symposium was held from 10th to 12th June 2016 in the Educational centre of South-West University – “Bachinovo”, near Blagoevgrad. The Symposium was proceeded under the auspices of the European Peptide Society (EPS). More than 70 active scientists from peptides/proteins chemistry, biologists, biochemists, biophysicists, as well as medical doctors and pharmacists participated by 13 oral and 60 poster presentations. The scientific program was divided into sections on different topics: amino acids and peptides synthesis, peptide mimetics, biologically active peptides, analytical methods in peptide chemistry, structure and conformation analysis. The main objection of such a selection was the consolidation of fundamental research with attempts to its application at the understanding of the molecular mechanism of pathogenic processes, diagnosis of diseases characteristic for modern civilization and introduction into practice of a new generation of drugs that are based on the most biocompatible active substances, undoubtedly peptides and proteins.

During the symposium there were invited lectures: Prof. Andreas Tzakos - University of Ioannina, Greece, Prof. Dirk Tourwe - Free University Brussels, Belgium, Prof. Krzysztof Rolka - University of Gdansk, Poland. It worths to underline the active participation of young scientists at 7th Bulgarian Peptide Symposium, both with oral presentations, as well as with posters. The Scientific Committee evaluated 40 posters presented by young participants. The winners of the competition for the best posters were: Petya. Hadzhibozheva - Trakia University, Department of Physiology, Stara Zagora and Dessislava Marinkova, University of Chemical Technology and Metallurgy, Sofia.



The financial support from the European Peptide Society, Bulgarian Peptide Society, and several private companies as FOT OOD, Sigma-Aldrich, Corning, Chromservis OOD, Bio Compounds, Waters, Globaltest, made it possible to invite several distinguished scientists and to cover the participation of more than 10 young scientists and students.

April, 2017

Guest editors

Ivanka Stoineva
Reni Kalfin

Synthesis, analysis and biological evaluation of new RGD mimetics

A.A. Balacheva^{1*}, M.K. Lambev², I. Pashov³, R.L. Detcheva¹, P. Sázelova³, G.Ts. Momekov³, V. Kašička⁴, T.I. Pajpanova¹, E.V. Golovinsky¹

¹*Institute of Molecular Biology “Acad. Roumen Tsanev”, Bulgarian Academy of Sciences, Acad. G. Bonchev Str., bl.21, 1113 Sofia, Bulgaria*

²*Medical University of Varna “Prof.Dr.Paraskev Stoyanov”, Faculty of Pharmacy, 55 Marin Drinov str., Varna 9002, Bulgaria*

³*Medical University Sofia, Faculty of Pharmacology, Pharmacotherapy and Toxicology, 2 Dunav str., Sofia 1000, Bulgaria*

⁴*Institute of Organic Chemistry and Biochemistry, Academy of Sciences of the Czech Republic, Flemingovo 2, 166 10 Prague 6, Czech Republic*

Received October 10, 2016; Revised February 15, 2017

The amino acid sequence L-arginyl-glycyl-L-aspartic acid (RGD) is a part of many extracellular proteins. It is a specific recognition site by integrins. Some synthetic RGD analogues bind specifically with integrin receptors on the cell membrane, which are over-expressed on the surface of various malignant human tumour and angiogenic endothelial cells. These peptides exert dual role by: inhibiting proliferation and migration of tumour cells and on the other hand by inhibiting angiogenesis. In recent years, many RGD cytotoxic agents have been developed, that showed promising results *in vitro* and *in vivo*. Herein we present the synthesis, analysis and biological evaluation of two new RGD analogues, modified in position 1 with Arg mimetics (Agb or Agp). Our pilot studies on their cytotoxicity were presented in comparison to parent RGD as standard.

Key words: RGD; biologically active peptides; cytotoxicity

INTRODUCTION

One of the major problems in cancer chemotherapy is poor selectivity of anticancer agents to cancer versus normal cells. Although cancer cells share many common characteristics with normal cells, certain receptors are over-expressed on their surface. Among receptors over-expressed on tumour cells, integrins are particularly attractive pharmacological targets. These heterodimeric transmembrane cell adhesion glycoproteins have a fundamental role in increasing migration, invasion, proliferation and survival of tumour cells. In addition, integrins have been linked to tumour angiogenesis, which is an essential process for tumour growth and metastasis [1].

The discovery of the minimal peptide sequence RGD, which plays a prominent role in cell adhesion via integrin interaction, has led to a large increase in biomedical and biomaterials research on this motif. Various RGD-containing peptides have been increasingly developed for adapting to versatile applications including tumour imaging and therapy, drug delivery vector, targeted gene transfer, and biomaterial or tissue engineering [2, 3].

Although RGD analogues have been approved for clinical use, their application is still ineffective because of their low bioavailability. This is largely

due to the metabolic instability of this class of compounds in the presence of proteases and peptidases.

We gave our contribution in the field by developing several RGD peptide analogues with enhanced cytotoxic activity [4].

In the present report we describe the synthesis, analysis and biological evaluation of novel RGD mimetics, in which the arginine residue was replaced with Agb and Agp (Fig. 1), two of its structural analogues.

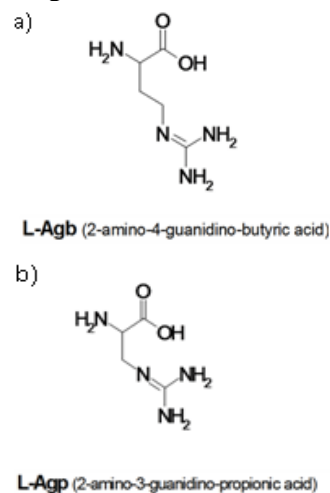


Fig 1. Arginine mimetics: a) L-Agb (2-amino-4-guanidino butyric acid); b) L-Agp (2-amino-3-guanidino-prionic acid)

* To whom all correspondence should be sent:
E-mail: neli_bal@abv.bg

EXPERIMENTAL

Peptide synthesis and analysis

Resins and Fmoc-amino acids used in peptide synthesis were purchased from Merck (Darmstadt, Germany) and Iris Biotech GMBH (Germany). Solvents of dimethylformamide (DMF) and dichloromethane (DCM) were purchased from Merck (Darmstadt, Germany). Electrophoretic experiments were performed using a BeckmanP/ACE (Beckman Coulter Inc., Pasadena, CA, USA).

Synthesis of all peptides was performed by the conventional and manual stepwise Fmoc solid-phase synthesis on 2-chlorotriyl chloride resin with substitution, 1.4 mmol/g. The coupling of each amino acid was performed in the presence of 3 mol excess of Fmoc-amino acid, 3 mol excess of N-hydroxybenzotriazole (HOBt), 3 mol excess of diisopropylcarbodiimide (DIC), and 5 mol excess of diisopropylamine (DIPEA) in dimethylformamide (DMF). Completion of coupling reactions were monitored by the Kaiser test and the Fmoc groups were removed by adding 20% piperidine in DMF.

The peptides were cleaved from the resin and the final deprotection was done in a cocktail containing trifluoroacetic acid (TFA), triisopropylsilane (TIPS), thioanisole, and water (92.5: 2.5: 2.5: 2.5). The crude peptides were precipitated into cold petroleum ether/diisopropyl ether (50:50). Then, the precipitate was dissolved in 10% CH₃COOH and desalted by gel filtration on a Sephadex G25. The chemical purity of peptides was characterized by RP-HPLC and capillary electrophoresis.

Cell cultures

The HepG2 cells (human liver hepatocellular carcinoma cell line) were cultured in Dulbecco Modified Eagle's medium (DMEM) (Gibco, Austria) supplemented with 10% fetal bovine serum (Gibco, Austria), 100 U/ml penicillin (Lonza, Belgium) and 0.1 mg/ml streptomycin (Lonza, Belgium) under a humidified 5% CO₂ atmosphere at 37°C. Plastic flasks supplied by Greiner, Germany, were used to grow the cells. Cells were trypsinized using Trypsin-EDTA (FlowLab, Australia) when they reached approximately 80% confluence. For experiments the cells in exponential phase of growth after treatment with Trypsin-EDTA were seeded into 96-well plates (Greiner, Germany) in a concentration 1.5x10⁵ cells/ml. 24 hours incubation post seeding

(under a humidified 5% CO₂ atmosphere at 37°C) allowed the cells to attach to the wells.

Cytotoxicity assay – MTT test

The cultivated cells were treated with RGD and RGD-analogues (AgbGD and AgpGD) for cytotoxic effect in a wide concentration range (2 - 0.0039 mM). Untreated cells were used as controls. Empty wells were blank controls. Cytotoxicity was measured by colorimetric assay based on tetrasolium salt MTT (3-(4,5-dimethylthiazol-2-yl)-2,5-diphenyltetrazolium bromide) (Sigma Chemical Co.).

The MTT assay is based on the protocol first described by Mossman [5]. In this assay, living cells reduce the yellow MTT to insoluble purple formazan crystals. The peptides were dissolved in dimethyl sulfoxide (DMSO). The final concentration of DMSO in samples did not affect the viability of the cells. The assay was performed on HepG2 cell line.

The assay was performed 72 hours after treatment with the amino acid analogues. For this purpose, MTT solution was prepared at 5 mg/ml in PBS and was filtered through a 0.2 µm filter. Then 1 ml of MTT solution was added to 15 ml DMEM and 100 µl of this solution were added into each well, including the cell free blank wells. Then the plates were further incubated for 3 hours to allow MTT to be metabolized. After lysis buffer (DMSO: ethanol (1:1)) was added, optical density (OD) was determined at a wavelength of 540 nm and a reference wavelength of 620 nm by ELIZA plate reader (TECAN, Sunrise TM, Grodig/Sazburg, Austria).

Cell cytotoxicity determined by MTT assay was expressed as per cent of dead cells:

% cytotoxicity = $(1 - (\text{OD sample} - \text{OD blank control}) / (\text{OD control} - \text{OD blank control})) \times 100$.

RESULTS AND DISCUSSION

In our lab a series of arginine analogues have been designed and synthesized and their cytotoxic potential has been studied. Guanidinium group of Arg is crucial for various bioactivities as the regulation of structure and function of proteins. There is evidence that if arginine is replaced with a homologue comprising one or two methylene groups less (Agb or Agp) (Fig. 1), there is an improvement in stability of proteins to enzymatic degradation [6].

As mentioned above we obtained two new RGD mimetics that contain the sequence Xaa-GD (Fig. 2), where Xaa is structural analogue of Arg with

shortened side chain: L-Agb (2-amino-4-guanidino butyric acid) and L-Agp (2-amino-3-guanidine-pronic acid).

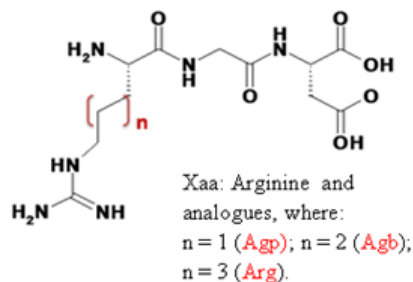


Fig. 2 Arginine and analogues.

A target peptide is assembled on a 2-chlorotrityl chloride resin by standard Fmoc-SPPS. The N-terminal amino group of the peptides was protected with a Fmoc group, and the side guanidine groups of arginine mimetics with Boc group. After final deprotection from the resin the peptides were purified with simple gel filtration on a Sephadex G25. The obtained purity characterized by RP-HPLC and capillary electrophoresis, was 87-94% (Fig. 3).

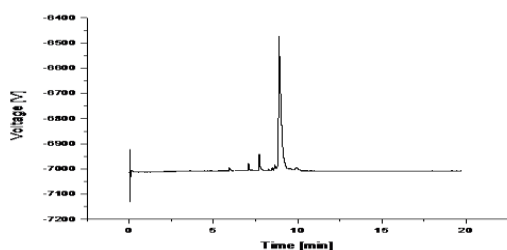


Fig 3. Electropherogramme of AgbGD, running buffer: 20 mMTris, 5mM H₃PO₄, 50 mM SDS, pH 7; Effective capillary length: 290/400 mm

Next we investigated the cytotoxic activities of RGD and its newly synthesized analogues on HepG2 tumour cell line using MTT analysis. All peptides were tested for cytotoxic effect in a wide concentration range (2 mM - 0.0039 mM) (Fig 4).

The modification of Arg by shortening of its side chain (in the case of Agb or Agp) didn't show significant increase of the cytotoxic effect of the compounds in comparison to parent RGD molecule.

We also compared the cytotoxic activity of these analogues with RGD-mimetics modified at the C-terminus, previously synthesized and reported by us [7]. It was shown that our new peptides have weaker cytotoxic effect in comparison to the methyl ester (RGD-OMe). The cytotoxic activity of some of the synthesized peptides are demonstrated by

half maximal inhibitory concentrations (IC₅₀ values), shown in Table 1.

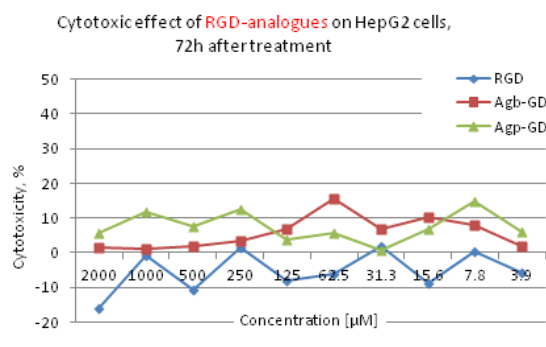


Fig. 4. Cytotoxic effect of novel RGD-analogues on HepG2 cells after 72 h treatment in concentrations from 2 mM to 0.0039 mM.

Table 1. Comparative table of cytotoxic effect of the RGD and its analogues (RGD-OMe, Agb-GD and Agp-GD), in 3T3 and HepG2 cells after 72 h of treatment [7].

Compounds	Mean IC ₅₀ values (mM), after 72h	
	3T3	HepG2
RGD*	>2mM	>2mM
RGD-OMe*	0.758±0.0504 mM	0.524±0.0766 mM
Agb-GD	-	>2mM
Agp-GD	-	>2mM

In conclusion, the modification in the carboxylic group of RGD peptide even with simple esterification (RGD-OMe) leads to the highest cytotoxic effect on HepG2 cells [7] in comparison with parent RGD molecule and newly synthesized Agb-GD and Agp-GD analogues.

Acknowledgements: The work was supported by project No. 34 of the cooperation between ASCR and BAS in the period 2014-2016.

REFERENCES

1. F. Danhier, A. Le Breton, V. Pr at, *Mol. Pharmaceutics*, **9**, 2961 (2012).
2. J. Thundimadathil, *Journal of Amino Acids*, ID 967347, **13** (2012).
3. I. Saiki, J. Murata, J. Iida, T. Sakurai, N. Nishi, K. Matsun, I. Azuma, *Br. J. Cancer*, **60**, 722 (1989).
4. T. Dzimbova, I. Iliev, K. Georgiev, R. Detcheva, A. Balacheva, T. Pajpanova, *Biotechnol & Biotechnol Eq.*, **26**, 180 (2012).
5. T. Mossman, *Journal of Immunological methods*, **65**, 55 (1983).

6. P. Henklein, Th.Bruckdorfer, *Peptides. The Proceedings of 21st American Peptide Symposium*, **44** (2009).
7. A. Balacheva, I. Iliev, R. Detcheva, T. Dzimbova, T. Pajpanova, E. Golovinsky, *BioDiscovery* **4**, 1 (2012).

СИНТЕЗ, АНАЛИЗ И БИОЛОГИЧНА ОЦЕНКА НА НОВИ RGD МИМЕТИЦИ
А.А. Балачева¹ *, М.К. Ламбев², И. Пашов³, Р.Л. Дечева¹, П. Сазелова³, Г.Ц. Момеков³, В. Кашичка⁴, Т.И. Пайпанова¹, Е.В. Головински¹

¹Институт по молекулярна биология "Акад. Румен Цанев", Българска Академия на Науките, ул. „Акад. Г. Бончев”, Бл.21, 1113 София, България

²Медицински университет Варна "Проф. Д-р Параскев Стоянов", Фармацевтичен факултет, ул. "Марин Дринов" 55, Варна 9002, България

³Медицински университет София, Факултет по фармакология, фармакотерапия и токсикологи, ул. "Дунав" 2, София 1000, България

⁴Институт по органична химия и биохимия, Академия на науките на Чешката република, Фламингово 2, 166 10 Прага 6, Чехия

Постъпила на 10 октомври, 2016 г.; Коригирана на 15 февруари, 2017 г.

(Резюме)

Аминокиселинната последователност L-аргинил-глицил-L-аспаргинова киселина (RGD) е част от много протеини от екстрацелуларния матрикс и е специфично място за разпознаване от интегрини. Някои синтетични RGD аналози се свързват специфично с интегринови рецептори върху клетъчната мембрана, които са свръхекспресирани при различни злокачествени човешки туморни и ангиогенни ендотелни клетки. Тези пептиди упражняват двойна роля чрез инхибиране на пролиферацията и миграцията на туморни клетки, и от друга страна инхибиране на ангиогенезата. През последните години са разработени много RGD цитотоксични агенти, които показват обещаващи резултати *in vitro* и *in vivo*. В настоящия доклад ние представяме синтез, анализ и първоначална биологична оценка на два нови RGD аналога, модифицирани в 1-ва позиция с Arg миметици (Agb или Agr). Тяхната цитотоксичност е сравнена с тази на изходния RGD пептид, използван като стандарт.

Molecular design and chemical synthesis of peptide inhibitors of Angiotensin I converting enzyme (ACE) for prevention and therapy of hypertension

B. K. Yakimova*, D. Petkova and I. B. Stoineva

Institute of Organic Chemistry with Centre of Phytochemistry, Bulgarian Academy of Sciences, Acad.G. Bonchev str. bl.9, 1113 Sofia, Bulgaria

Received September 30, 2016; Revised January 17, 2017

Angiotensin I-converting enzyme plays a central role to the regulation of renin-angiotensin system (RAS). The inhibitors of ACE are an attractive target for drug design due to its critical role in hypertension and cardiovascular diseases. The creation of new more effective inhibitors of ACE with less undesirable side effects, requires the search for new molecular and synthetic design of desired compounds. Another focus is development of functional foods as a possible prophylaxis for hypertension.

The targeted short peptides -H-Ile-Ala-Pro-OH, H-Leu-Ala-Pro-OH, H-Val-Ala-Pro-OH and H-Val-Ala-Trp-OH were synthesized by Fmoc-SPPS strategy. The newly synthesized peptides were purified by HPLC and characterized by UPLC and NMR analysis. For determination of ACE inhibitory activity was used modified method of *Jimsheena and Gowda*, based on interaction between ACE and the specific synthetic substrate hippuryl-histidyl-leucine (HHL). Chemically synthesized tripeptides exhibit inhibitory activity comparable to that of a commercially used in medicine lisinopril

Keywords: cardiovascular diseases (CVD), renin-angiotensin system (RAS), angiotensin-I converting enzyme (ACE), inhibitors of ACE

INTRODUCTION

Angiotensin I converting enzyme (ACE) is a zinc and chloride dependent dipeptidyl carboxypeptidase. Its main function is the activation of the renin- angiotensin system (RAS) [1,2] by catalyzing the cleavage of two amino acids from carboxyl terminus of angiotensin I to form the active octapeptide angiotensin II, which is an extremely powerful vasoconstrictor. Many synthetic drugs as Captopril, Benazepril, Lisinopril, Enalapril, ect. are widely used in the clinical practice. All of them have the same mechanism of action. In recent years studies have been mainly focused on the identification of effective peptides, able to inhibit ACE activity with the aim to control hypertension and prevent cardiovascular diseases. Most of peptides inhibitors of ACE are relatively short sequences containing from 2 to 12 amino acids. Among them di- and tripeptides are more favorable as potential functional food additives candidates due to their high antihypertensive activity and low bitterness. Fernandez et al. [3] emphasize the role of ACE inhibitor peptides as a target for drug design resulting from the function of ACE in cardiovascular and renal diseases.

The aim of this study is to synthesize a short peptides, as a novel inhibitors of angiotensin-I

converting enzyme (ACE), which were predicted to possess better ACE inhibitory activity and lesser side effects and as well as potential candidate as additives in functional foods of hypertension.

EXPERIMENTAL

Synthesis of the peptides

The chemical synthesis of target short peptides H-Ile-Ala-Pro-OH, H-Leu-Ala-Pro-OH, H-Val-Ala-Pro-OH and H-Val-Ala-Trp-OH was realized by Fmoc- strategy of solid phase peptide synthesis (SPPS) or by microwave assisted SPPS, performed on Syro Wave Peptide Synthesizer from Biotage. The TBTU/DIPEA method was used for coupling of each amino acid. For the synthesis of the peptides with free C-terminal group 2-chlorotriyl chloride resin (CLTR) and Wang resin were used by us successfully. On each step of the synthesis was checked for free amino group with acetaldehyde/chloranil test. The target peptides were synthesized in similar procedure.

The synthesis begins with the coupling of the first amino acid Fmoc-Ala-OH to the resin. To the pre-activated resin are added 4 equiv. Fmoc-Ala - OH (0,093 g, 0,30 mmol), 4 eq. coupling agent TBTU (0,9563 g, 0,30 mmol), 8 eq. base DIPEA (0,7621 g, 0,60 mmol), dissolved in 2 ml DMF. The reaction mixture was allowed to mix for 1 hour and 30 minutes at a Vortex mixer.

* To whom all correspondence should be sent:
E-mail: bkq_1982@abv.bg

Completion of coupling reactions were monitored by the Kaiser test and the Fmoc groups were removed by adding 20% piperidine in DMF. After completion of the reaction is carried acetaldehyde / chloranil test and in the case of is absence of a free -NH₂ group the reaction continue with the next step. Deblocking was performed with 20% piperidine solution. The second amino acid - Fmoc-Val-OH was added in the following way: to 2 ml DMF was added 4 equiv. Fmoc-Val -OH (0,105 g, 0,30 mmol), 4 eq. coupling agent TBTU (0,9563 g, 0,30 mmol) and 8 eq. base DIPEA (0,102 ml, 0,60 mmol). The mixture thus obtained was added to the resin in the reaction vessel. The reaction system was of a Vortex mixer for 1.5 h. After this Fmoc protection is accomplished by blocking with 20% solution of piperidine. The final step of the synthesis of the tripeptide is its removal from the resin. The most commonly used reagent for removal of the synthesized peptide from the resin is trifluoro acetic acid (TFA). During the reaction are formed highly reactive carbocations. This requires the use of quenchers that prevent adverse reactions. In our case we used water and triisopropyl silane (TIS). A solution consists of 95% TFA: 2,5% H₂O: 2,5% TIS, was added to the resin and reaction mixture was mixed for 3 h under magnetic stirring at room temperature. After completion of the reaction the flask contents were filtered and washed with TFA, evaporated under nitrogen and precipitate by diethyl ether under ice. The organic solvents were removed and the peptides were freeze drying.

Purification and characterization of target peptides

The obtained tripeptides were purified by HPLC and characterized by UPLC-MS and NMR analysis. ¹H NMR (600 MHz, DMSO-*d*₆, δ ppm): data for **H-Leu-Ala-Pro-OH**: 4.63 (1H, α -H-Ala), 4.23 (1H, α -H-Pro), 3.60, 3.41 (2H, δ -CH₂-Pro), 3.21 (1H, α-Leu), 2.33, 1.94 (4H, CH₂-Pro), 1,79 (1H γ- CH-Leu), 1,45, 1.38 (2H, β- CH₂-Leu), 1.41 (3H, CH₃-Ala), 0,92 (6H, CH₃-Leu); **Ile-Ala-Pro-OH**: 4.76 (1H, α-H-Ala), 4.43 (1H, α-H-Pro), 4.03 (1H, α-H-Ile), 3.61, 3.74 (2H, δ-CH₂-Pro), 2.2 -1.84 (4H, CH₂-Pro), 1.96 (H, β-CH-Ile), 1.56 (3H, CH₃-Ala), 0,96 (3H, CH₃-Ile), 0.82 (3H, CH₃-Ile); **H-Val-Ala-Pro-OH**: 4.56 (1H, α-H-Ala), 4.13 (1H, α-H-Pro), 4.06 (1H, α-H-Val), 3.61, 3.54 (2H, δ-CH₂-Pro), 2.2 -1.84 (4H, CH₂-Pro), 1.94 (H, β-CH-Val), 1.56 (3H, CH₃-Ala), 1.01 (3H, CH₃-Val), 0.92 (3H, CH₃-Val); **H-Val-Ala-Trp-OH**: 7,49-6.93 (4H Ar Trp), 7.10 (1H Trp) (1H 4.90 (1H, α-H-Trp), 4.34 (1H, α-H-Ala), 3.76 (1H, α-H-Val), 3.31-3,01 (2H, β-CH₂-

Trp), 1.82 (H, β-CH-Val), 1.50 (3H, CH₃-Ala), 0.92 (6H, CH₃-Val).

The analyses of the peptides were performed by UPLC connected with MS detector. The samples were applied to a column: ACQNTITY HPLC BEH C18, 1,7 mm, isocratic gradient elution with mobile phase: CH₃CN/0.1 % TFA:H₂O/0.1 % TFA (30:70 v/v) and after that purified with High liquid performance chromatography - HPLC Agilent 1200, column : RP Synergi 4 Fusion, mobile phase AcCN:H₂O (30:70 v/v).

Determination of ACE inhibitory activity of the peptides

To determine ACE inhibitory activity was used modified method of *Jimsheena and Gowda* [4]. The analysis is based on interaction between ACE and the specific synthetic peptide hippuryl-histidyl-leucine (HHL) in borate buffer pH 8,3 at 37°C. The released hippuric acid (HA) when complexed with pyridine and benzene sulfonyl chloride (BSC) forms a yellow color, which is measured at 410 nm.

For each assay, a sample solution of ACE inhibitor (25μl) with 50 ml of 5 mM Hip-His-Leu in 125 μl 0,05 M sodium borate buffer with pH 8,3 containing 300 mM NaCl was preincubated at 37°C for 30 min. with 25μl ACE from rabbit lung, as obtained mixture was stirred at Vortex mixer for 5 min. The reaction was stopped by adding 100 μl 1N HCl, followed by added of freshly distilled 400 μl pyridine and 200 μl BSC at Vortex mixer for 1 min and cooled with ice bath. The absorbance was measured at 410 nm on Thermo Scientific Evolution 300 UV-VIS.

The extent of inhibition was calculated as follows:

$$\text{ACE inhibitory activity (\%)} = [1 - (A/B)] \times 100,$$

Where: A is the absorbance of the sample, containing enzyme, substrate and inhibitor, B is the absorbance of the sample, containing enzyme and substrate.

All measurements were performed in triplicate. A calibration curve was obtained by plotting the absorbance at 410 nm versus different hippuric acid (HA) concentrations. As reference was used Lizinopril, which inhibit 100 % ACE.

RESULTS AND DISCUSSION

The inhibitors of ACE are among the most prospective resources at therapy of hypertension, heart attack, diabetic hypertension as different cardiovascular diseases. Major efforts worldwide are directed towards synthesis of effective peptides

and peptidomimetics, as inhibitors of Angiotensin I-converting enzyme for the pharmacy and like supplements for functional foods. It is known that all experiments on peptide inhibitors of ACE are conducted with samples isolated from different natural sources. Biologically active peptides, which have been identified are contained in a number of natural and processed food products -milk, eggs, fish, soya, rice, spinach, different hydrolysates and etc. [5,6,7,8,9,10,11], whose activity results in the formation of versatile effects - immunomodulating, antibacterial, opioid, antithrombotic, antihypertensive (ACE inhibitors). The design of peptides for therapeutic purposes requires detailed information on conformational requirements and maximum biological activity.

Based on the relationship between structure-function of ACE inhibitors can be found some general similarities between them [12]. They are rich in hydrophobic amino acids on S₂' subsite and many of them contain proline, lysine or arginine as C-terminal residues. The majority among ACE-peptide inhibitors are di- or tri- peptides that are resistant to endopeptidase of the digestive tract and can be readily absorbed into the blood [13]. The amounts of these peptides is insignificantly and vary in milligram amounts. Of interest is to investigate the inhibitory activity of the chemically synthesized peptide inhibitors of ACE.

The chosen approach with Fmoc-strategy in solid phase synthesis, proved particularly effective and yields of target peptides in this study were within 65-77% of the pure substance. Strategy using 2-Cl-trityl-chloride resin has proved particularly effective in the synthesis of the proline tripeptides. The reaction scheme of synthesis of the H-Val-Ala-Pro-OH is shown on Fig.1.

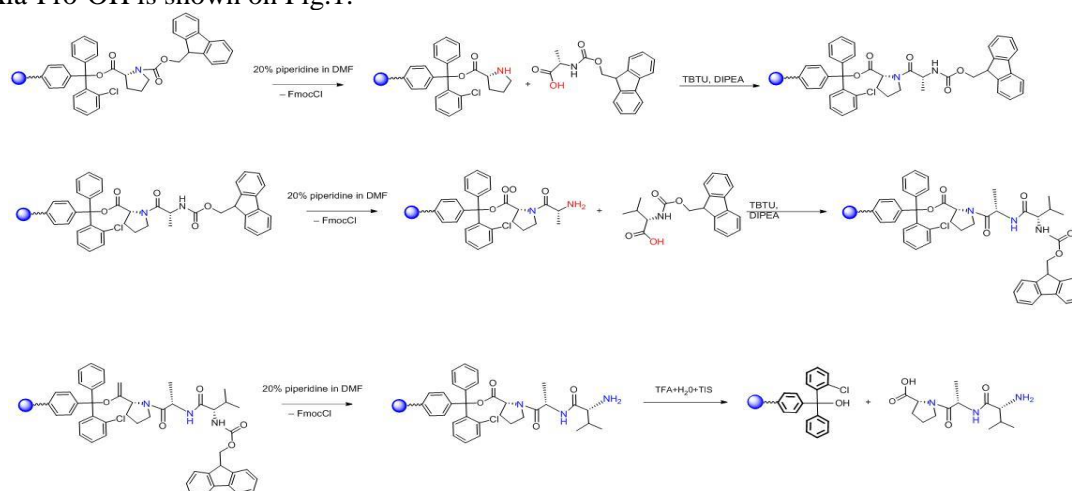


Fig.1. Reaction scheme of the synthesis of H-Val-Ala-Pro-OH

To determine the ACE inhibitory activity we used a modified colorimetric method of Jimsheena

All synthesized peptides H-Ile-Ala-Pro-OH, H-Leu-Ala-Pro-OH, H-Val-Ala-Pro-OH and H-Val-Ala-Trp-OH were identified and characterized by ¹H NMR and UPLC. The UPLC chromatogram of the purified H-Val-Ala-Pro-OH are shown on Fig.2.

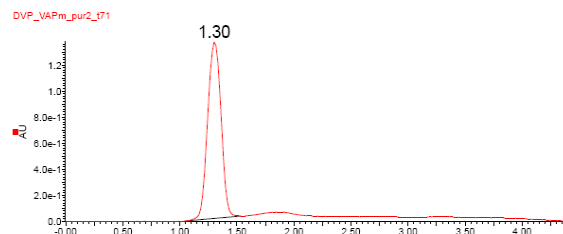


Fig.2. UPLC chromatogram of the purified peptide H-Val-Ala-Pro-OH

The activity of ACE inhibitors can be determined by various analytical methods. The most popular tests for determination of ACE inhibitory activity of peptides in vitro are based on spectrophotometric, fluorimetric, colorimetric and radiochemical methods and chromatographic techniques. The measurement of IC₅₀ is a marker for biological activity, but not for antihypertensive action.

It is not established a clear relationship between ACE inhibitors and antihypertensive activity. It is possible the antihypertensive activity to exceed expectations or in some cases there is no antihypertensive activity. The most significant reasons for this are the oral bioavailability of studied peptides and mechanisms other than the inhibition of ACE.

and Gowda. The analysis of the ACE inhibitory activity is based on the interaction of ACE with the

specific synthetic substrate HHL (hippuryl-L-histidyl-L-leucine) in phosphate buffer with pH 8.3 at 37 ° C, which leads to the release of hippuric acid and dipeptide histidyl- L-leucine (HL).

The released hippuric acid forms a complex with pyridine and benzenesulfonyl chloride. On fig.3 is shown a possible mechanism of the reaction of hippuric acid with pyridine and benzenesulfonyl chloride.

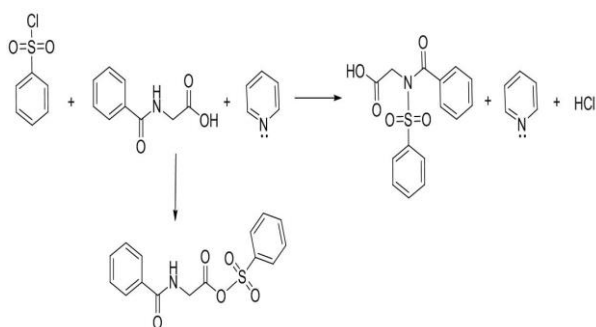


Fig. 3. A possible mechanism of interaction between hippuric acid and benzene sulfonyl chloride in the presence of pyridine

The complex of pyridine and BSC with hippuric acid gives yellow color and measured at 410nm. The color intensity is correlated with the concentration of hippuric acid. In the presence of ACE inhibitor in the reaction mixture the release of the product hippuric acid is inhibited, which can affect the absorbance values.

The determined relative inhibitory activity of synthesized peptides is shown on Fig.4.

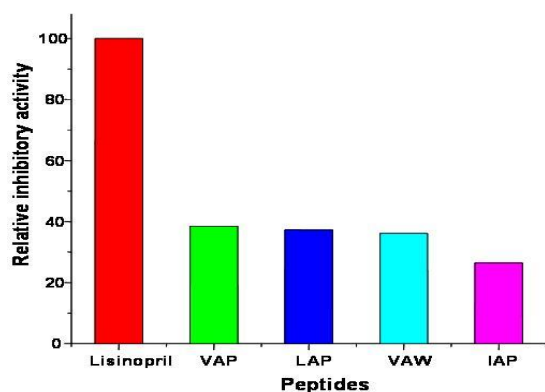


Fig. 4. Relative inhibitory potential of synthesized peptides

The figure shows that the VAP is with the highest inhibitory activity, and the lowest activity shows IAK.

The synthesized peptides, H-Ile-Ala-Pro-OH, H-Leu-Ala-Pro-OH, H-Val-Ala-Pro-OH and H-Val-Ala-Trp-OH be juxtapose with the commercially used Lisinopril. We hope they will be good additives in functional foods of hypertension.

CONCLUSION

Important role of RAS in cardiovascular system causes recently more and more attention. ACE inhibitors have always been used as the first line treatment of hypertension and heart failure. The design and synthesis of new synthetic structures as H-Ile-Ala-Pro-OH, H-Leu-Ala-Pro-OH, H-Val-Ala-Pro-OH and H-Val-Ala-Trp-OH that are good inhibitors of ACE is very promising for receiving a new drugs for heart diseases and functional foods for prevention of hypertension.

REFERENCES

1. M.A., Ondetti, D.W. Cushman, *Annu. Rev.Biochem.* **51**, 283 (1982).
2. H. Roks, Buikema, Y.M. Pinto, W.H. van Gilst, *Heart Vessels*, **12**, 119 (1997).
3. J.H. Fernandez, G. Neshich, A. Camargo, *Genet. Mol. Res*, **3**, 554 (2004).
4. V.K. Jimsheena, L.R. Gowda, *Anal. Chem.* **81**, 9388 (2009).
5. G.-H. Li, H. Liu, Y.-H. Shi, G.W. Le, *J. Pharmaceut. Biomed. Anal.*, **37**, 219 (2005).
6. J.Tsai, J.-L., Chen, B.S. Pan, *Proc.Biochem.*, **43**, 743 (2008).
7. Y. Nakamura, N. Yamamoto, K. Sakai, T. Takano, *J. Dairy Sci.*, **78**, 6 (1995).
8. H., Wu, H.-L. He, X.-L., Chen, C.-Y., Sun, Y.-Z., Zhang, B.-C. Zhou *Proc.Biochem.*, **43**, 457 (2008).
9. A. Jang, M. Lee, *Meat Science*, **69**, 653 (2005).
10. D, Kitts, K. Weiler, *Current Pharmaceuti. Design*, **9**, 1309 (2003).
11. Y. Yang, E.D. Marczak, H. Usui, Y. Kawamura, M. Yoshikawa, *Journal of Agricultural and Food Chemistry*, **52**(8), 2223 (2004).
12. N. Yamamoto, *Biopolymers*, **43**, 129 (1997).
13. P. Sandeya, A text book of medicinal chemistry, Third edition, Elsevier, India, 2004, Chap. 27, 33.

МОЛЕКУЛЕН ДИЗАЙН И СИНТЕЗ НА ПЕПТИДНИ ИНХИБИТОРИ НА АНГИОТЕНЗИН I ПРЕВРЪЩАЩИЯ ЕНЗИМ ЗА ЛЕЧЕНИЕ И ПРЕВЕНЦИЯ НА ХИПЕРТОНИЯ

Б. Якимова, Д. Петкова И. Стойнева

Институт по Органична Химия с Център по Фитохимия, Българска Академия на Науките, ул. Акад.Г. Бончев, бл.9, 1113, София, България

Постъпила на 30 септември, 2016 г.; Коригирана на 17 януари , 2017 г.

(Резюме)

Хипертонията и сърдечно-съдовите заболявания са едни от най-рисквите заболявания и представяват около 60% от общата статистика на заболяемост у нас. С въвеждането на синтетичните инхибитори на ангиотензин превръщащия ензим (АСЕ) в клиничната практика настъпва нова ера в лечението на тези заболявания. Получените чрез твърдо фазен пептиден синтез нови късоверижни пептидни инхибитори на АСЕ - Н-Ile-Ala-Pro-OH, Н-Leu-Ala-Pro-OH, Н-Val-Ala-Pro-OH и Н-Val-Ala-Trp-OH бяха пречистени чрез HPLC и анализирани чрез UPLC-MS и ЯМР анализи. Те проявяват инхибиторна активност сравнима с тази на търговския препарат Lisinopril, което води до получаването на важна информация за различни синтетични структури като потенциални инхибитори на АСЕ, което дава възможност за молекулен дизайн и синтез на лекарствени форми с ясно изразен антихипертензивен ефект при пациенти страдащи от сърдечно-съдови заболявания.

Amino acids amides of anti-influenza drugs: synthesis and biological activities

B. Stoykova¹, M. Chochkova^{1*}, L. Georgiev¹, G. Ivanova², L. Mukova³, N. Nikolova³, L. Nikolaeva-Glomb³, Ts. Milkova¹, M. Štícha⁴

¹ Department of Chemistry, South-West University "Neofit Rilski", 2700 Blagoevgrad, Bulgaria

² Departamento de Química e Bioquímica, Faculdade de Ciências, Universidade do Porto, 4169-007 Porto, Portugal

³ The Stephan Angeloff Institute of Microbiology Bulgarian Academy of Sciences, 1113 Sofia, Bulgaria

⁴ Department of Organic Chemistry, Faculty of Science, Charles University, 12843 Prague 2, Czech Republic

Received October 25, 2016; Revised January 30, 2017

Influenza A viruses are amongst the most severe human pathogens leading to high morbidity and mortality worldwide. Due to the high mutation rate and the unpredictable potential for influenza pandemic outbreaks, the development of novel anti-influenza drugs is an undeniably attractive area of research.

In the present study amino acid amides of rimantadine and oseltamivir were synthesized and their *in vitro* antiviral activity against influenza A viruses (A/H3N2) was studied. Results revealed that amide modification of *N*_α- and side chain protected tyrosine, histidine, aspartic- and glutamic acids did not exhibit significant enhancement of the *in vitro* effect against influenza A virus strain.

Keywords: amino acids amides, aminoadamantanes, influenza virus neuraminidase inhibitors

INTRODUCTION

Influenza viruses are RNA viruses responsible for an acute infectious disease, commonly known as a flu. Those pathogens belong to *Orthomyxoviridae* family and they are classified into three types (A, B and C) on the basis of differences in their nucleoprotein antigens [1, 2]. Unlike the antigenic stability of influenza type C, the genetic variation of hemagglutinin (HA) and neuraminidase (NA) antigens in types A and B leads to a frequent occurrence of viral mutations through the mechanisms of antigenic drift and shift. Thus, a rise to a rapid development of new virus strains is given which could be a serious threat to the human population [3, 4].

In recorded world history influenza infection has generated some of the worst pandemics. The 1918-1919, influenza pandemic (Spanish flu) swept across the world in three waves and was responsible directly or indirectly for over 20 million deaths-more than doubling the total casualty of the previous leader, the Black Death [5]. Since then, at least 3 pandemics and numerous milder localized influenza epidemics have been recorded.

At the present time, influenza continues to be a serious threat to human health. Affecting the population irrespective of age, it causes tremendous economic losses and also poses a global concern due to its unpredictable, pandemic potential and

pathogenesis.

Although vaccination is the mainstay of influenza prophylactic treatment, this primary prevention strategy is associated with significant drawbacks. For instance, annual update is required due to the widely varying virus prevalence between years. Moreover, vaccines and circulating virus strains must be closely matched, and there have been well recognized vaccine failures [6].

Therefore, effective antiviral agents are of utmost importance for influenza treatment [7]. Although two clinically relevant classes of anti-influenza compounds are available, the effectiveness of the neuraminidase inhibitors (oseltamivir, zanamivir) is preferable because of the high level of resistance to the amantadine (amantadine, rimantadine) observed worldwide [7, 8].

A promising approach for "resuscitation" the antiviral properties of M2 ion channel blockers would be the modification of the structure of the antiviral compound by incorporating additional active functional groups. The main goal is disruption of the proton transport through the virus membrane via interacting with the transmembrane domain. A source of such active functional groups could be amino acids and peptides, which can finally play key role as inhibitors of enzymes included in different diseases [9]. The use of amino acid scaffolds as building blocks during drug discovery [10] and the unusual role of amino acids

* To whom all correspondence should be sent:
E-mail: mayabg2002@yahoo.com

as reactants for important drug-like compounds [11] (e.g., benzodiazepines) are potentially relevant for a wide number of applications in the medicinal chemistry. The conserved backbones and variable side chains of amino acids along with their high bioavailability, make them readily enter in biochemical reactions.

Recently *Shibnev V. A. et. al.* reported for several adamantane derivatives with amino acid residues which inhibit resistant to rimantadine influenza A virus strains [12]. Subsequently, in order to investigate the antiviral activity of similar compounds, we modified anti-influenza agents (amantadine, rimantadine and oseltamivir) with amino acid residues.

EXPERIMENTAL

General information

All chemicals were of analytical grade and were purchased from Sigma-Aldrich. Ethyl (3R,4R,5S)-4-acetamido-5-amino-3-(1-ethylpropoxy)-1-cyclohexene-1-carboxylate (oseltamivir) was obtained from Aopharm (China).

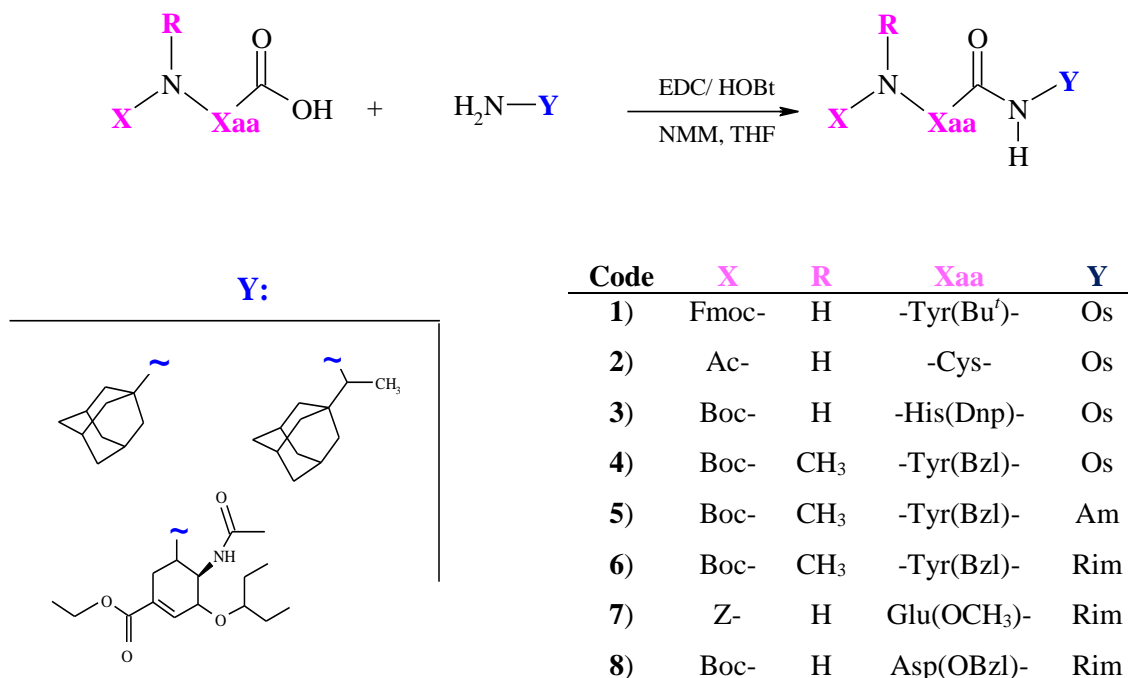
Melting points were determined using an apparatus „Stuart SMP10“. UV spectra of the

amides were measured with an Agilent 8453 UV–Vis spectrophotometer. Attenuated total reflectance infrared spectroscopy (ATR-IR) measurements were performed using Thermo Scientific Nicolet iS10 FT-IR device with ID5 ATR accessory (diamond crystal). ^1H NMR and ^{13}C NMR were obtained with Bruker Avance II+ 600 and Bruker Avance III 400. The ESI mass spectra were recorded on an Esquire3000 plus instrument. Thin-layer chromatography (TLC) was conducted on precoated Kieselgel 60F254 plates (Merck, Germany). Separation of the compounds by preparative thin layer chromatography with silica gel 60 GF254 (Merck, Bulgaria).

Synthesis of anti-influenza drug derivatives incorporating amino acid residues

The synthesis of the desired molecules is outlined in Scheme 1. The couplings between protected amino acid analogues and anti-influenza drugs were performed with EDC/HOBt in tetrahydrofuran [13,14].

The physico-chemical parameters and the IR, NMR MS spectral data of the compounds **1-8** are as follows:



Scheme 1. General scheme for obtaining amino acid derivatives of anti-influenza drugs

N-(9-Fluorenylmethoxycarbonyl)-*O*-*tert*-butyl-*L*-tyrosyl-oseltamivir

(Table 1, Entry 1 (Fmoc-Tyr(Bu^t)-Os)); Yield: 21 %; mp: 226-228°C; UV (C₂H₅OH) λ_{\max} = 205, 318 nm; IR (ATR) ν_{\max} : 3283.1, 2969.2, 2929.6, 1717.4, 1645.8, 1537.4, 1506.5, 1237.9, 737.4; ¹H NMR (600 MHz, CDCl₃): 0.86 (t, *J* = 7.5 Hz, 3H, -CH₂CH₃), 0.88 (t, *J* = 7.2 Hz, 3H, -CH₂CH₃), 1.23 (s, 9H, -C(CH₃)₃), 1.32 (t, 3H, -OCH₂CH₃), 1.46 (m, 4H, 2 x -CH₂CH₃), 2.02 (s, 3H, -C(O)CH₃), 2.31 (m, 1H, =CH-CH_{2a}-), 2.61 (dd, *J* = 17.7, 5.0 Hz, 1H, =CH-CH_{2b}-), 2.74 (dd, *J* = 14.4, 11.4 Hz, 1H, Ar-CH_{2a}-), 3.10 (br. d, *J* = 14.4 Hz, 1H, Ar-CH_{2b}-), 3.40 (m, 1H, >CHCH₂CH₃), 3.81 (ddd, *J* = 10.6, 9.6, 8.7 Hz, 1H, CH₃C(O)NHCH<), 3.92 (m, 1H, -CH₂CHNH-), 4.08 (t, *J* = 8.7 Hz, 1H, -OCH<), 4.19 (q, *J* = 7.2 Hz, 2H, -CH₂CH₃), 4.46 (t, 1H, -CH-CH₂-O), 4.92 (ddd, *J* = 7.4, 5.8, 5.4 Hz, 1H, >N-CHCH₂-), 5.04 (d, 2H, -O-CH₂), 6.65 (s, 1H, =CH-), 6.72 (d, *J* = 8.5 Hz, 2H, Ar-H), 7.06 (d, 2H, *J* = 8.5 Hz, Ar-H), 7.66 (1H, -C(O)NH-), 7.54-7.82 (m, 8H, Ar-H), 8.0 (1H, CH₃C(O)NH-); ESI-MS: 754.3[M+H]⁺, 776.4[M+Na]⁺.

N-Acetyl-*L*-cysteinyl-oseltamivir

(Table 1, Entry 2 (Ac-Cys-Os)): Yield: 10 %; mp: 200-202°C; UV (C₂H₅OH) λ_{\max} = 206 nm; IR (ATR) ν_{\max} : 3265.4, 2933.0, 2935.3, 2859.7, 1716.8, 1652.0, 1537.9, 1369.6, 1242.5, 1054.1 cm⁻¹; ¹H NMR (600 MHz, CDCl₃): δ 0.97 (t, *J* = 7.34 Hz, 3H, -CH₂CH₃), 0.99 (t, *J* = 7.34 Hz, 3H, -CH₂CH₃), 1.39 (m, 3H, -OCH₂CH₃), 1.45 (s, 1H, -SH), 1.47 (m, 4H, 2 x -CH₂CH₃), 1.89 (s, 3H, -C(O)CH₃), 2.03 (s, 3H, -C(O)CH₃), 2.28-2.56 (m, 2H, =CH-CH_{2a}-), 2.93-3.19 (m, 2H, -CH₂SH), 3.54 (m, 1H, =CH-CHOCH(CH₂CH₃)₂), 3.85 (t, 1H, -OCH(CH₂CH₃)₂), 3.92 (m, 1H, -CHNHCO-), 4.06 (m, 1H, -NH-CHCH₂-), 4.21 (q, *J* = 7.2 Hz, 2H, -OCH₂CH₃), 4.82-4.86 (m, 1H, H α), 6.66 (d, *J* = 6.2 Hz, 1H, -C(O)NH), 6.77 (d, 1H, =CH-), 7.88 (d, *J* = 8.5 Hz, 1H, -C(O)NH-), 7.95 (d, *J* = 9.2 Hz, 1H, -C(O)NH-). ESI-MS: 458.2 [M+H]⁺, 480.1 [M+Na]⁺.

N α -*tert*-Butoxycarbonyl-*N*_(im)-(2,4-dinitrophenyl)-*L*-histidyl-oseltamivir

(Table 1, Entry 3 (Boc-His(Dnp)-Os)): Yield: 14 %; mp: 150-153°C; UV (C₂H₅OH) λ_{\max} = 207, 265, 300 nm; IR (ATR) ν_{\max} : 3366.7, 3189.3, 2935.3, 2859.7, 1704.7, 1678.3, 1623.8, 1515.5, 1338.4, 1156.6 cm⁻¹; ¹H NMR (600 MHz, CDCl₃): δ 0.87 (t, *J* = 7.5 Hz, 3H, -CH₂CH₃), 0.89 (t, *J* = 7.2 Hz, 3H, -CH₂CH₃), 1.31 (t, 3H, -OCH₂CH₃), 1.42 (s, 9H, -C(CH₃)₃), 1.46 (m, 4H, 2 x -CH₂CH₃), 2.05 (s, 3H, -C(O)CH₃), 2.33 (m, 1H, =CH-CH_{2a}-), 2.59 (dd, *J* = 17.8, 5.2 Hz, 1H, =CH-CH_{2b}-), 3.05-3.14 (m, 2H,

-CH₂-im), 3.36 (m, 1H, -CH(CH₂CH₃)₂), 3.84 (ddd, *J* = 10.5, 9.6, 8.6 Hz, 1H, CH₃C(O)NHCH<), 3.93 (m, 1H, -CH₂CHNH-), 4.10 (t, *J* = 8.6 Hz, 1H, -OCH<), 4.22 (q, *J* = 7.2 Hz, 2H, -OCH₂CH₃), 4.62-4.78 (m, 1H, α -CH), 5.73 (d, 1H, *J* = 8.0 Hz, NH-Boc), 6.69 (s, 1H, =CH-), 6.86 (s, 1H, Ar^{im}-H), 7.63 (s, 1H, Ar^{im}-H), 7.68 (d, 1H, *J* = 8.8 Hz, Ar^{Dnp}-H), 7.89 (1H, -C(O)NH-), 8.05 (1H, CH₃C(O)NH-), 8.57 (ddd, *J* = 8.8, 2.6, 1.6 Hz, 1H, Ar^{Dnp}-H), 8.89 (1H, Ar^{Dnp}-H); ESI-MS: 716.3 [M+H]⁺, 738.2 [M+Na]⁺.

O-Benzyl-*N* α -*tert*-butoxycarbonyl-*N* α -methyl-*L*-tyrosyl-oseltamivir

(Table 1, Entry 4 (Boc-N(CH₃)-Tyr(Bzl)-Os)): Yield: 46 %; mp ~ 90-94°C; UV (C₂H₅OH) λ_{\max} = 206, 225, 277 nm; IR (ATR) ν_{\max} : 3295, 2971, 2933, 2876, 1695, 1651, 1613, 1511 cm⁻¹; ¹H NMR (600 MHz, CDCl₃): 0.77 (t, *J* = 7.5 Hz, 3H, -CH₂CH₃), 0.82 (t, *J* = 7.2 Hz, 3H, -CH₂CH₃), 1.20 (s, 9H, -C(CH₃)₃), 1.22 (m, 3H, -OCH₂CH₃), 1.41 (m, 4H, 2 x -CH₂CH₃), 1.77 (s, 3H, -C(O)CH₃), 2.28 (m, 1H, =CCH_{2a}-), 2.56 (dd, *J* = 17.7, 5.0 Hz, 1H, =CCH_{2b}-), 2.63 (s, 3H, >NCH₃), 2.74 (dd, *J* = 14.4, 11.4 Hz, 1H, Ar-CH_{2a}-), 3.05 (br. d, *J* = 14.4 Hz, 1H, Ar-CH_{2b}-), 3.40 (m, 1H, >CHCH₂CH₃), 3.81 (ddd, *J* = 10.6, 9.6, 8.7 Hz, 1H, CH₃C(O)NHCH<), 3.92 (m, 1H, -CH₂CHNH-), 4.08 (t, *J* = 8.7 Hz, 1H, -OCH<), 4.14 (q, *J* = 7.2 Hz, 2H, -CH₂CH₃), 4.7 (1H, >N-CHCH₂-), 5.04 (s, 2H, -O-CH₂Ar), 6.65 (s, 1H, =CH-), 6.90 (d, *J* = 8.1 Hz, 2H, *m*-Ar), 7.11 (d, 2H, *o*-Ar), 7.30 (2H, *m*-Ar), 7.30 (t, *J* = 7.2 Hz, 1H, *p*-Ph), 7.37 (t, *J* = 7.2 Hz, 2H, *m*-Ph), 7.41 (d, *J* = 7.2 Hz, 2H, *o*-Ar), 7.66 (1H, -C(O)NH-), 7.92 (1H, CH₃C(O)NH-); ¹³C NMR (150 MHz, DMSO-*d*₆): 9.1 (-CH₂CH₃), 9.4 (-CH₂CH₃), 14.1 (-O-CH₂CH₃), 22.7 (-CH₃), 25.3 (>CHCH₂CH₃), 25.8 (>CHCH₂CH₃, isomer), 27.7 (3 x -CH₃), 27.9 (3 x -CH₃, isomer), 29.9 (>CH₂), 30.9 (>NCH₃), 33.4 (>CH₂), 47.5 (-HN-CH<), 47.9 (-HN-CH<, isomer), 53.0 (-C(O)HN-CH<), 59.0 (>NCHCH₂-), 60.5 (-OCH₂CH₃), 69.1 (-OCH₂Ph), 74.7 (-OCH<), 78.9 (-OCH<), 81.3 (-OCH<, isomer), 114.6 (=CH-, Ar), 127.5 (=CH-, *o*-Ar), 127.7 (=CH-, *p*-Ar), 128.4 (=CH-, *m*-Ar), 129.8 (=CH-, Ar), 137.2 (=CH-), 137.9 (=CH-, isomer), 129.3 (=Cq), 137.7 (=CHC(O)-), 154.6 (-O(O)C-NCH₃), 156.9 (OCq, Ar), 165.5 (155.4 (-O(O)CC=), 169.8 (HNC=O), 170.0 (-NH-C(O)CH₃); ESI-MS: 580.3 [M+H-Boc+H]⁺, 624.2 [M+H-56]⁺, 680.4 [M+H]⁺, 702.4 [M+Na]⁺.

O-Benzyl- *N*_α-tert-butoxycarbonyl- *N*_α-methyl-*L*-tyrosyl-amantadine

(Table 1, Entry 5 (Boc-N(CH₃)-Tyr(Bzl)-Am)): Yield: 52 %; mp ~ 110-114°C; UV (C₂H₅OH) λ_{max} = 206, 226, 277 nm; IR (ATR)_umax: 3368, 2971, 2909, 2847, 1677, 1662, 1512, 1453, 1388, 1363 cm⁻¹; ¹H NMR (600 MHz, DMSO-*d*₆): 1.28 (s, 9H, -C(CH₃)₃), 1.60 (6H, 3 x >CH₂), 1.90 (6H, 3 x >CH₂), 1.99 (3H, 3 x >CH-), 2.68 (3H, >NCH₃), 2.75 (m, 1H, >CHCH_{2a}-), 2.97 (dd, *J*=14.2, 5.2 Hz, 1H, >CCH_{2b}-), 4.62 (1H, >NCHCH₂-), 5.04 (s, 2H, -O-CH₂Ar), 6.90 (2H, *m*-Ar), 7.13 (2H, *o*-Ar), 7.31 (t, *J*=7.2 Hz, 1H, *p*-Ph), 7.37 (t, *J*= 7.2 Hz, 2H, *m*-Ph), 7.41 (d, *J*=7.2 Hz, 2H, *o*-Ar); ¹³C NMR (150 MHz, DMSO-*d*₆): 27.9 (3 x -CH₃), 28.8 (3 x >CH-), 30.3 (>NCH₃), 36.0 (3 x >CH₂), 40.9 (-CH₂CH<), 50.8 (-HN-Cq), 58.4 (>N-CHCH₂-), 60.1 (>N-CHCH₂- isomer), 69.1 (-OCH₂Ph), 78.7 (-O)(CH₃)₃, 114.6 (>CH-, Ar), 127.6 (>CH-, *o*-Ar), 127.7 (>CH-, *p*-Ar), 128.3 (>CH-, *m*-Ar), 129.8 (>CH-, Ar), 137.2 (=CH-), 137.9 (=CH-, isomer), 129.3 (=Cq), 137.7 (=CHC(O)-), 154.9 (-OOCN), 156.8 (OCq, Ar), 169.7 (-HNC=O); ESI-MS: 419.2 [M+H-Boc+H]⁺, 463.1 [M+H-56]⁺, 519.2 [M+H]⁺, 541.2 [M+Na]⁺.

O-Benzyl- *N*_α-tert-butoxycarbonyl- *N*_α-methyl-*L*-tyrosyl-rimantadine

(Table 1, Entry 6 (Boc-N(CH₃)-Tyr(Bzl)-Rim)): Yield: 57 %; mp ~ 89-93°C; UV (C₂H₅OH) λ_{max} = 205, 226, 277 nm; IR (ATR)_umax: 3399, 3257, 2974, 2902, 2883, 1678, 1660, 1641, 1509, 1446, 1391, 1364 cm⁻¹; ¹H NMR (600 MHz, DMSO-*d*₆): 0.86 (d, 3H, -NHCHCH₃), 1.30 (s, 9H, -C(CH₃)₃), 1.42 (6H, 3 x >CH₂), 1.60 (6H, 3 x >CH₂), 1.89 (3H, 3 x >CH-), 2.72 (3H, >NCH₃), 2.82 (m, 1H, >CHCH_{2a}-), 3.00 (m, 1H, =CCH_{2b}-), 3.51 (br. s, 1H, -NHCHCH₃), 4.80 (1H, >NCHCH₂-), 5.04 (s, 2H, -O-CH₂Ar), 6.90 (2H, *m*-Ar), 7.16 (2H, *o*-Ar), 7.30 (t, *J*=7.0 Hz, 1H, *p*-Ph), 7.37 (t, *J*= 7.0 Hz, 2H, *m*-Ph), 7.41 (d, *J*=7.0 Hz, 2H, *o*-Ar); 150 MHz ¹³C NMR (150 MHz, DMSO-*d*₆): 14.0 (-CH₃), 27.7 (3 x -CH₃), 28.0 (3 x >CH-), 30.2 (>NCH₃), 34.2 (>CH₂), 36.6 (3 x >CH₂), 37.9 (3 x >CH₂), 51.9 (-HN-CH<), 58.4 (>N-CHCH₂-), 59.0 (>N-CHCH₂- isomer), 69.1 (-OCH₂Ph), 78.7 (-OC(CH₃)₃), 114.6 (>CH-, Ar), 127.6 (>CH-, *o*-Ar), 127.7 (>CH-, *p*-Ar), 128.4 (>CH-, *m*-Ar), 129.6 (>CH-, Ar), 137.2 (=CH-), 137.9 (=CH-, isomer), 129.3 (=Cq), 137.7 (=CHC(O)-), 154.9 (-OOCN), 156.8 (OCq, Ar), 169.5 (HNC=O); ESI-MS: 447.1 [M+H-Boc+H]⁺, 491.3 [M+H-56]⁺, 547.3 [M+H]⁺, 569.2 [M+Na]⁺.

γ-Methyl ester of *N*_α-(Carbobenzyloxy)-*L*-glutamyl-rimantadine

(Table 1, Entry 7 (Z-Glu(OCH₃)-Rim)): Yield: 42 %; mp ~ 132-134°C; UV (C₂H₅OH) λ_{max} = 208 nm; IR (ATR)_umax: 3292, 2902, 1730, 1690, 1647, 1514, 1454 cm⁻¹; ¹H NMR (600 MHz, DMSO-*d*₆): 0.89 (3H, >CHCH₃), 1.3-1.7 (12H, 6 x -CH₂-; rimantadyl-), 1.78 (1H, >CHCH_{2a}-), 1.89 (4H, 3 x >CH-, rimantadyl-, + 1H >CHCH_{2b}-), 2.34 (m, 2H, -C(O)CH₂-), 3.48 (m, 1H, -HNCHCH₂-), 3.58 (s, 3H, -OCH₃), 4.04 (m, 1H, -NHCHCH₃), 5.02 (2H, -O-CH₂-), 7.2-7.5 (5H (Ar) + 2H >NH); ¹³C NMR (150 MHz, DMSO-*d*₆): 14.1 (1C, >CHCH₃), 27.7 (-CH₂CH₂C(O)-), 27.7 (3C, >CH-; rimantadyl-), 30.0 (-CH₂CH₂C(O)-), 35.4 (Cq), 36-39 (6C, -CH₂-; rimantadyl-), 51.3 (1C, -OCH₃), 52.0 (-HN-CHCH₃), 54.0 (-C(O)HN-CH<), 65.4 (-OCH₂-), 127.0-128.5 (5 x =CH-), 155.8 (-CH₂OC(O)-), 170.4 (-HNCHC(O)NH-), 172.7 (-C(O)OCH₃). ESI-MS: 457.1 [M+H]⁺, 479.1 [M+Na]⁺.

β-Benzyl ester of *N*-tert-butoxycarbonyl-*L*-aspartyl-rimantadine

(Table 1, Entry 8 (Boc-Asp(OBzl)-Rim)): Yield: 54 %; mp ~ 71-74°C; UV (C₂H₅OH) λ_{max} = 207, nm; IR (ATR)_umax: 3331, 2979, 2919, 1729, 1695, 1655, 1514, 1393, 1367 cm⁻¹; ¹H NMR (600 MHz, DMSO-*d*₆): 0.89 (d, 3H, >CHCH₃), 1.39 (s, 9H, -C(CH₃)₃), 1.42-1.63 (12H, 6 x -CH₂-; rimantadyl-), 1.89 (3H, 3 x >CH-; rimantadyl-), 2.89 (m, 2H, >CHCH₂C(O)O-), 3.46 (m, 1H, -HNCHCH₂-), 4.32 (m, 1H, -NHCHCH₃), 5.12 (s, 2H, -O-CH₂-), 7.06-7.37 (5H (Ar) + 2H >NH); ¹³C NMR (150 MHz, DMSO-*d*₆): δ 14.0 (1C, >CHCH₃), 27.7 (3 x -CH₃), (-CH₂C(O)-), 28.1 (3C, >CH-; rimantadyl-), 36.4-36.6 (6C, -CH₂-; rimantadyl-), 37.7 (-CH₂-), 51.1 (-HN-CH(CH₃)-), 52.2 (-HN-CH<), 65.5 (-OCH₂-), 78.4 (-OC(CH₃)₃), 127.7-127.9 (5 x =CH-), 128.3 (=Cq), 136.1 (=CHC(O)-), 155.3 (-COC(O)-NH-), 169.8 (-HNCHC(O)NH-), 170.1 (-C(O)OCH₂-); ESI-MS: 385.1 [M+H-Boc+H]⁺, 429.0 [M+H-C(CH₃)₃+H]⁺, 485.1 [M+H]⁺, 507.3 [M+Na]⁺.

Antiviral activity assay

Cells and viruses. MDCK cells for the propagation of influenza virus A originated from the collection of the Stephan Angeloff Institute of Microbiology, Bulgarian Academy of Sciences, Sofia, Bulgaria, and were grown in a growth medium containing Dulbecco modified

Table 1. Effect of the amino acids linked to rimantadine, amantadine and oseltamivir against the influenza virus A/Aichi/2/68 (H3N2)

Entry	Compound	MTC	CC ₅₀ ^a	IC ₅₀	SI
		(μ M)	(μ M)		(CC ₅₀ /IC ₅₀)
1	Fmoc-Tyr(But)-Os	100	306.47±20.92	-	
2	Ac-Cys-Os	100	307.14±11.94	-	
3	Boc-His(Dnp)-Os	56	140.99±20.24	-	
4	Boc-N(CH ₃)-Tyr(Bzl)-Os	>1000		-	
5	Boc-N(CH ₃)-Tyr(Bzl)-Am	0.3	1.00±0.57	-	
6	Boc-N(CH ₃)-Tyr(Bzl)-Rim	100		-	
7	Z-Glu(OCH ₃)-Rim	3200		-	
8	Boc-Asp(OBzl)-Rim	32	10.12±1.60	-	
	Rimantadine	100	175	0.2	875
	Amantadine	100	330	1.6	206

CC₅₀: 50% cytotoxic concentration; MTC: maximal tolerance concentration; SI: selective index;

^aData are shown as mean \pm SD of four independent determinations

Eagles' medium (DMEM) (Gibco BRL, USA), supplemented with 10 % fetal bovine serum, 10 mM HEPES buffer (Merck, Germany) and antibiotics (penicillin 100 IU mL⁻¹ and streptomycin 100 μ g mL⁻¹). The cells were cultured as confluent monolayers in a humidified atmosphere containing 5 % CO₂ at 37 °C.

Influenza virus A/Aichi/2/68 (H3N2) from the collection of the Stephan Angeloff Institute of Microbiology, Bulgarian Academy of Sciences, was grown in MDCK cells in a maintenance medium of Dulbecco modified Eagles' medium (DMEM) (Gibco BRL, USA), containing 0.5 % fetal bovine serum, 10 mM HEPES buffer and antibiotics, as well as 3 mg mL⁻¹ trypsin (Gibco BRL).

Cytopathic effect (CPE) inhibition test. Monolayer MDCK cells in 96-well microplates (Costar, USA) were inoculated, following the removal of the growth medium, with 0.1 mL virus suspension containing 100 CCID₅₀ (cell culture infectious dose 50 %). After 1 h at 37 °C for virus adsorption, the inoculum was washed out and replaced by 0.1 mL of non-cytotoxic 0.5 log₁₀ dilutions in the maintenance medium of the newly synthesized compounds. Each dilution was applied in quadruplicate. Cells that were not inoculated with virus were left for cell controls (with only maintenance medium) and toxicity controls (with respective dilution of the compound in the maintenance medium). Cells inoculated with virus but not treated with a compound were left for virus

controls. Then cells were incubated for 48 h in a humidified atmosphere with 5 % CO₂ at 37 °C or until the virus specific cytopathic effect had destroyed 100 % of the cells in the virus control wells. Then cells were stained according to the neutral red uptake procedure and the percentage of CPE inhibition, if present, was calculated using the following formula [15]:

$$\% \text{ CPE} = \frac{(OD_{\text{test sample}} - OD_{\text{virus control}})}{(OD_{\text{toxicity control}} - OD_{\text{virus control}})} - 100.$$

RESULTS AND DISCUSSION

Chemistry

Despite the extensive efforts have been invested in designing of potential influenza antivirals, the continuing risk of a future pandemic flu remains very real.

Emerging from the restoration of the antiviral activity of amino acid analogues with anti-influenza drugs [12], herein we modify the anti-viral drugs amantadine, rimantadine and oseltamivir with amino acid moiety. The synthetic route for amino acid analogues is outlined in Schemes 1. As shown, the synthesized amides were obtained in low to good yields by the classical EDC/HOBt method of peptide chemistry [13, 14]. The desired compounds (**1-8**) were purified by preparative thin layer chromatography and their structures were assessed by means of melting points, UV, IR, ¹H-NMR, ¹³C-NMR and ESI-MS.

ESI-MS spectra in positive mode of ionization clearly reveal that the monitored base peaks are consistent to anticipated adducts $[M+H]^+$, $[M+Na]^+$ for all target compounds. The formation of amide bond is confirmed in 1H -NMR spectra by presence of a signal for amide proton at $\delta \sim 6.5$ - 7.5 ppm. Whereas ^{13}C -NMR spectra show a signal at about $\delta \sim 175$ ppm for carbonyl carbon of amide bond. Additional information is collected from IR spectra bands. The observed absorbance at ~ 1640 - 1680 cm^{-1} corresponds to N-C=O group.

Biological activity

According literature data the protection of α -amino- and side chain polar functional groups of amino acids produced the very active anti-influenza compounds [12]. These promising results enforced us to study antiviral activity of protected amino acid analogues with amantadine, rimantadine and oseltamivir.

Preliminary antiviral activities of the synthesized compounds (**1-8**) against influenza A (H3N2) were evaluated *in vitro* through their ability to prevent cytopathic effects (CPE) in influenza A virus (H3N2) infected Madin-Darby canine kidney (MDCK) cells. The data of the tested amides (Table 1) were compared to the positive controls-amantadine (Am) and rimantadine (Rim).

The newly synthesized compounds did not reveal an enhanced antiviral activity as compared to the generic antivirals.

Acknowledgements: For the financial support of this work we are grateful to project RP-A09/16 from the South-West University „Neofit Rilski”, Blagoevgrad. The Bruker Avance III 600 HD spectrometer was purchased under the framework of QREN, through Project NORTE-07-0162-

FEDER-000048, and is part of the Portuguese NMR Network created with support of FCT through Contract REDE/1517/RMN/2005, with funds from POCI 2010 (FEDER).

REFERENCES

1. R. G. Webster., W. J. Bean, O. T. Gorman, T. M. Chambers, Y. Kawaoka, *Microbiol. Mol. Biol. Rev.*, **56**, 152 (1992).
2. R. Wagner, M. Matrosovich, H.-D. Klenk, *Rev Med Virol*, **12**, 159 (2002).
3. J. K. Taubenberger, A. H. Reid, A. E. Kraft, K. E. Bijwaard, T. G. Fanning, *Science*, **275**, 1793 (1997).
4. J. K. Taubenberger, A. H. Reid, T. G. Fanning, *Virology*, **274**, 241 (2000).
5. A. W. Crosby, *America's Forgotten Pandemic: The Influenza of 1918*, Cambridge Univ. Press, UK, 1989.
6. X. Wang, W. Jia, A. Zhao, X. Wang, *Phytother. Res.*, **20**, 335 (2006).
7. A. Moscona, *N. Engl. J. Med.*, **353**, 1363 (2005).
8. E. De Clercq, *J. Clin. Virol.*, **22**, 73 (2001).
9. D. Danalev, *Mini-review in Med. Chem.*, **12**, 721 (2012).
10. V. Kapras, R. Pohl, I. Císařová, U. Jahn, *Org. Lett.*, **16**, 1088 (2014).
11. A. Jakubowska, K. Kulig, *Curr. Org. Synth.*, **10**, 547 (2013).
12. V. A. Shibnev, T. M. Garaev, M. P. Finogenova, E. S. Shevchenko, E. I. Burtseva, *Pharm. Chem. J.*, **46**, 1 (2012).
13. J. C. Sheehan, J. J. Hlavka, *J. Org. Chem.*, **21**, 439 (1956).
14. M. Chochkova, G. Ivanova, A. Galabov, Ts. Milkova, in: *Peptides (Proc. 32nd Eur. Pept. Symp., Athens, 2012)*, G. Kokotos, V. Constantinou-Kokotou, J. Matsoukas (eds.), European Peptide Society, 2012. p. 580.
15. C. Pannecouque, D. Daelemans, E. De Clercq, *Nat. Protoc.*, **3**, 427 (2008).

АМИНОКИСЕЛИННИ АМИДИ НА ПРОТИВОГРИПНИ ЛЕКАРСТВЕНИ СРЕДСТВА: СИНТЕЗ И БИОЛОГИЧНО ДЕЙСТВИЕ

Б. Стойкова¹, М. Чочкова^{1*}, Л. Георгиев¹, Г. Иванова², Л. Мукова³, Н. Николова³,
Л. Николаева-Гломб³, Ц. Милкова¹, М. Щиха⁴

¹Катедра по химия, Югозападен университет „Неофит Рилски“, 2700 Благоевград, България

²Департамент по химия и биохимия, Университет в Порто, 4169-007 Порто, Португалия

³Институт по микробиология „Стефан Ангелов“, Българска академия на науките, София, България

⁴Департамент по органична химия, Карлов университет, 12843 Прага 2, Чехия

Постъпила на 25 октомври 2016 г.; Коригирана на 30 януари, 2017 г.

(Резюме)

Грипните вируси тип А са сред най-вирулентните респираторни патогени, водещи до значителна заболяемост и смъртност. Високата честота на антигенни вариации на грипния вирус е причина за възникване на пандемични взривове. Ето защо създаването на нови противогрипни средства е изключително атрактивна изследователска област.

В настоящето изследване е разгледан синтеза и е изследвана противогрипната активност на аминокиселинни амиди на римантадин и оселтамивир. Изпитването за антивирусен ефект е проведено *in vitro* спрямо грипен вирус тип А (А/Н3N2). Резултатите от скрининга показват, че амидното свързване на аминокиселинните аналози (тирозин, хистидин, аспарагинова и глутаминова киселини) с оселтамивир и римантадин не водят до повишаване противовирусната активност спрямо изпитвания щам.

QSAR modelling and molecular docking studies of three models of delta opioid receptor

F. I. Sapundzhi^{1*}, T. A. Dzimbova², N. S. Pencheva¹, P. B. Milanov^{1,3}

¹South-West University "Neofit Rilski", Bulgaria, 2700 Blagoevgrad

²Institute of Molecular Biology, Bulgarian Academy of Sciences, Bulgaria, 1113 Sofia

³Institute of Mathematics and Informatics, Bulgarian Academy of Sciences, Bulgaria, 1113 Sofia

Received September 30, 2016 ; Revised March 07, 2017

Delta-opioid receptor (DOR) takes part in the control of chronic pain and emotional responses. Therefore it is an interesting object for QSAR modelling and molecular docking studies with delta-opioid selective enkephalin analogues.

The purpose of this study is to find the structure-activity relationship of a series of delta-opioid selective enkephalin analogues, basing on the quantitative parameters of *in vitro* bioassay (efficacy, affinity and potency) and the results of the molecular docking with three models of DOR: (1) a theoretical model of DOR (PDBe:1ozc); (2) a model of DOR with crystal structure (PDBid:4ej4); (3) a model of DOR obtained by homology modelling (named *Model B*). The relationship of the quantitative parameters of *in vitro* bioassay with the results from the molecular docking was modelled with first to third degree polynomials and surface fitted method.

We suggest that the polynomial surface fitting of the third order has the best fit, assessed by least squares method for model of DOR obtained by homology modelling. Hence, the third order of polynomial could be used for determining the relationship structure-biological activity between the three models of DOR and a series of delta-opioid selective enkephalin analogues.

Key words: QSAR, Docking, Ligand-receptor interaction, GOLD, Delta opioid receptor.

INTRODUCTION

Computer modelling and quantitative structure-activity relationship (QSAR) approaches have played a major role in the search and prediction of new biologically active substances based on the properties of compounds with known biological activities.

This research paper discusses QSAR modelling and approaches of computer and mathematical modelling to establish relationships between molecular structure of investigated compounds and their biological effects.

By computer modelling of the ligand-receptor interactions it was analyzed relationships between virtual data analogues of endogenous opioid peptides and experimental data for the same activity in experiments on isolated tissues.

The discovery of novel potent and selective ligands to the delta-opioid receptor (DOR) is related with a large amount of investigations with enkephalin analogues. The enkephalins are endogenous opioid peptides (enkephalins, endorphins or dynorphins) [1-4] and they are typically assigned to mu-, kappa-, and delta- opioid receptors.

In the last years computer-aided drug design has extensive impact in the field of the drug design and

the natural sciences [5]. The design of selective and effective ligands for DOR is related with most researchers with different enkephalin analogues. These analogues were synthesized and biologically tested in previous studies [6,7]. According to the *in vitro* results and the mathematical model of a partial agonism [8], it could be calculated with the explicit formulas the *potency* (concentration, which produce 50% of the maximal response of the tissue – IC_{50}), the *affinity* (reciprocal of the dissociation constant, K_A) of the respective analogues and relative *efficacy* (e_{rel}).

There are two broad categories of computational techniques in virtual screening: 1) a ligand-based screening uses pharmacophore maps and QSAR, which requires knowledge of some ligands that exhibit the desired bioactivity; 2) a structure-based virtual screening uses molecular docking of ligands into a protein structure by applying the scoring function to estimate the probability that the compound will bind to the biological target (in our case models of DOR) [9,10].

We would like to find a relationship between the values of quantitative parameters of *in vitro* tests (e_{rel} , K_A , IC_{50}) and the results of the molecular docking (the minimum energy conformation for each ligand-receptor complex, the scoring functions to calculate binding affinities of protein-ligand complexes based on experimental structure and data

* To whom all correspondence should be sent:
E-mail: sapundzhi@swu.bg

from *in vitro* bioassay, etc.) in order to predict biological activity of chemical compounds.

To achieve the goal the following tasks should be solved: 1) performance of molecular docking calculations of the models of DOR and δ -selective enkephalin analogues, and calculation of the total energies of formed ligand-receptor complex after molecular docking experiments and (2) finding a function $z = f(x,y)$ from some class polynomials, that fits given n distinct data points $\{(x_i, y_i, z_i)_{i=1}^n$ in R^3 by the least square method.

MATERIALS AND METHODS

Objects

Receptor-DOR

Three models of DOR were used:

(1) a theoretical model of DOR (PDBe:1ozc), published in Protein Data Base (www.rcsb.org) [11];

(2) a model of DOR with crystal structure (PDBid:4ej4) [12];

(3) a model of DOR obtained by homology modelling (named *Model B*) [13];

Ligands

Eleven ligands, investigated for their potency, selectivity and efficacy to DOR with *in vitro* bioassay in previous study [6,7,8] were selected for docking studies with the models of DOR.

The primary structures of the used ligands are presented in Table 1 (including selective ligand DPDPE ([D-Pen2,5]-enkephalin, selective δ -opioid receptor agonist [14] and endogenous enkephalins ([Leu5]- and [Met5]-enkephalin) and their analogues.

Table 1. Ligands used in this study.

Primary structure	Ligand	Mouse vas deferens		
		IC ₅₀ (nM)	K _A (nM)	e _{rel}
Tyr-D-Pen-Gly-Phe-D-Pen	DPDPE	6.18±1.17	180±35	30.2±10.0
Tyr-Gly-Gly-Phe-Leu	[Leu ⁵]-enk	11.45±2.06	54.9±13.1	5.8±1.0
Tyr-Gly-Gly-Phe-Met	[Met ⁵]-enk	18.91±2.15	48.4±7.5	3.6±0.3
Tyr-Cys(Bzl)-Gly-Phe-Leu	[Cys(Bzl) ² , Leu ⁵]-enk	8.30±1.40	68.5±29.7	9.3±3.2
Tyr-Cys(Bzl)-Gly-Phe-Met	[Cys(Bzl) ² , Met ⁵]-enk	9.53±1.20	23.8±3.0	3.5±0.3
Tyr-Cys(O ₂ NH ₂)-Gly-Phe-Leu	[Cys(O ₂ NH ₂) ² , Leu ⁵]-enk	1.29±0.31	36.4±16.4	29.2±9.5
Tyr-Cys(O ₂ NH ₂)-Gly-Phe-Met	[Cys(O ₂ NH ₂) ² , Met ⁵]-enk	2.22±0.45	14.1±5.4	7.3±2.0
Tyr-D-Cys(O ₂ NH ₂)-Gly-Phe-Leu	[DCys(O ₂ NH ₂) ² , Leu ⁵]-enk	11.40±2.01	73.4±12.7	7.4±1.9
Tyr-D-Cys(O ₂ NH ₂)-Gly-Phe-Met	[DCys(O ₂ NH ₂) ² , Met ⁵]-enk	75.96±11.67	463±161	7.1±1.8
Tyr-HCys(O ₂ NH ₂)-Gly-Phe-Leu	[HCys(O ₂ NH ₂) ² , Leu ⁵]-enk	31.92±5.10	76.4±7.1	3.4±0.2
Tyr-HCys(O ₂ NH ₂)-Gly-Phe-Met	[HCys(O ₂ NH ₂) ² , Met ⁵]-enk	16.09±1.90	55.7±6.1	4.5±0.3

Software

Docking procedure

The structures of 11 ligands were prepared for docking in the software Avogadro (open source, <http://avogadro.openmolecules.net/>).

All docking calculations were performed with the software GOLD (Genetic Optimisation for Ligand Docking) 5.2 using all four scoring functions available in the program: ChemPLP, GoldScore, ChemScore and ASP (Astex Statistical Potential) scoring functions, [15,16,17,18]. The DOR belong to the GPCRs, characterized by seven putative transmembrane domains. It is known from the literature that the residues within 10 Å around an aspartic acid residue at position 128 (Asp128) in transmembrane domain 3 of the DOR contributes to

the conformation of the receptor binding pocket [19].

The total energies for obtained ligand-receptor complex after docking procedure in GOLD 5.2 were calculated by software Molegro Molecular Viewer (MMV Version 2.5) using MolDock scoring function [20].

Correlation and fitting methods

Finding the correlation between the quantitative parameters of the *in vitro* tests (e_{rel} , K_A , IC_{50}) and the docking results (scoring functions) for the three models of DOR was carried out in software GraphPad Prism 3.0 (<http://www.graphpad.com/scientific-software/prism>). In this investigation the Pearson's correlation coefficient was used, which is a measure of the

correlation (linear dependence) between normally distributed variables.

$$\min_{(a_{00}, \dots, a_{0n})} F(a_{00}, \dots, a_{0n}) = \sum_{s=1}^m \left(z_s - \sum_{0 \leq i+j \leq n} a_{ij} x_s^i y_s^j \right)^2 \quad (1)$$

$$z = \sum_{0 \leq i+j \leq n} a_{ij} x^i y^j \quad (2)$$

Where s is the number of points; m is the number of ligand-receptor complexes; z is a dependent variable, x and y are independent variables. The values of z_1, z_2, \dots, z_n represent the values of *in vitro* parameters; the values of x_1, x_2, \dots, x_n represent the result from the docking procedure (scoring functions); the values of y_1, y_2, \dots, y_n represent the total energies for ligand-receptor complex; a_{ij} are the parameters of the model; n - the degree of the polynomial ($0 \leq i + j \leq n$), which gives the number of coefficients to be fit and the highest power of the predictor variable.

To investigate the fitting behaviour of degree of some polynomial functions, it was carried out a set of fittings, starting from the first-degree to the third-degree polynomial. The Surface Fitting Toolbox of MATLAB was applied for analysing the behaviour of one variable which depended on more independent variables and the individual model could be interpreted as a surface fitting function of the experimental data by least squares method (<http://www.mathworks.com/products/matlab>) [21]. The following parameters are used to evaluate the goodness of fit:

SSE (Sum of squares due to error) – this parameter represents the total deviation of the response values from the curve fit to the response values, where the value of *SSE* near to 0 shows that the model has a smaller random error component and then the fit will be more useful for prediction [22, 23].

R-Square (R^2) – this parameter measures how successful the fit is in explaining the variation of the data and it is defined as the ratio of the sum of squares of the regression and the total sum of squares about the mean. The values of R^2 closer to 1 indicate that a greater proportion of variance is accounted by the model [22, 23].

Adjusted R-square – this parameter is the best indicator of the fit quality when two models are comparing. The *adj/R²* statistic can take on any value less than or equal to 1, with a value closer to 1 indicating a better fit [22,23].

RMSE (Root Mean Squared Error) – this parameter presents the standard error of the

The fitting of experimental data can be presented as follows (Eqns.1,2):

regression and an estimate of the standard deviation of the random component in the data. The values of *RMSE* closer to 0 indicates a fit that is more useful for prediction [22,23].

RESULTS AND DISCUSSION

Docking results

The molecular docking experiments with the three models of DOR ((1) a theoretical model of DOR (PDBe:1ozc), (2) a model of DOR with crystal structure (PDBid:4ej4) and (3) a model of DOR obtained by homology modelling (named Model B)) and all 11 ligands were carried out with software GOLD 5.2 and all four scoring functions embedded in the program: GoldScore, ChemScore, ASP and ChemPLP.

The active site of the DOR is the residues within 10 Å around an Asp128 residue [19]. Molecular docking with GOLD 5.2 generates several probable ligand binding conformations at the active site around the protein target - DOR. The scoring functions in GOLD 5.2 are used to rank these ligand conformations by evaluating the binding density of each of the probable complexes. Docking results show the relative pose prediction performance of GOLD 5.2 by all scoring functions the values of which are calculated by using only the best scored pose for each binding site or the solution with the highest score.

When the results were analysed we found correlation between the docking results (the values of all four scoring functions available in GOLD 5.2) and the values of *in vitro* bioassay (IC_{50} , K_A or e_{rel}). The correlation between these data was assessed by the Pearson's correlation test in GraphPad Prism 3.0 [22]. The highest values of the Pearson's correlation coefficient for the theoretical model of DOR (PDBe:1ozc) were obtained between the values of GoldScore scoring function from docking experiments and the values of e_{rel} from *in vitro* parameters ($R = -0.7209$) [24]. Significant correlations were obtained for the model with crystal structure of DOR (PDBid:4ej4) between the values of ASP scoring function and e_{rel} from *in vitro* parameters ($R = -0.6366$); and the values of ChemPLP scoring function and e_{rel} from *in vitro* parameters ($R = -0.6742$) [12]. The highest value of the Pearson's correlation coefficient for Model B of DOR was obtained between the values of ASP scoring function and the values of IC_{50} from *in vitro* parameters ($R = -0.86$) [5,25]. These data indicate that GOLD5.2 software gives reliable results in the

docking of the 11 delta-opioid ligands with three models of DOR [26,27,28,29].

In order to investigate the appropriate relationship between biological activity of the delta-opioid ligands and docking results (the values of all four scoring functions in GOLD 5.2 it was applied the Surface Curve Fitting Toolbox in software MATLAB.

The total energies of the ligand-receptor complexes, which are formed after molecular docking with the three models of DOR and the best pose of the corresponding ligands, were calculated by MolDock scoring function in software MMV 2.5 [20].

By using a polynomial least squares surface fitting technique, a first to a third order polynomial was fitted to the experimental data in both the X-axis and Y-axis. The experimental data can be represented as follows: 1) the values of z represent the values of *in vitro* parameters (e_{rel} , K_A or IC_{50}) which were obtained by Mathematical model of partial agonism [2]; 2) the values of x represent the result from the docking procedure- the values of GoldScore, ChemScore, ChemPLP and ASP scoring functions; 3) the values of y represent the total energies for ligand-receptor complex – the values of MolDock scoring function [20] for the ligand-receptor complexes forming after the docking with corresponding scoring functions.

The best results of the parameters used for surface fitting in MATLAB of the three models of DOR can be represented as follows: 1) for DOR (PDBe:1ozc): the values of z represent the values of e_{rel} from *in vitro* parameters, the values of x represent

the values of GoldScore function, the values of y represent the values of the total energy for ligand-receptor complexes; 2) for DOR (PDBid:4ej4): the values of z represent the values of e_{rel} from *in vitro* parameters, the values of x represents the values of ChemScore function and the values of y represents the values of the total energy for the ligand-receptor complexes; 3) for *Model B* of DOR: the values of z represent the values of IC_{50} from *in vitro* parameters, the values of x represents the values of ASP function and the values of y represents the values of the total energy for the ligand-receptor complexes. The values of the main parameters used for surface fitting in MATLAB for the three models of DOR are presented in Table 2. The surface fitting by third degree of the polynomial of the experimental data from Table 2 for the three models of DOR is presented in Fig.1 (A,B,C).

All polynomial models from first to third degree were evaluated on how well they fitted the data and how precisely they could predict. The models were estimated with the statistical criteria of goodness of fit – SSE , R^2 , *adjusted* R^2 , $RMSE$. The results obtained for the statistic parameters are presented in Table 3.

As it can be seen from the results in Table 3 the goodness of fit statistics shows that the obtained model for fitting of the data for three models of DOR with the third degree for x and the third degree for y is a good one. The polynomial model of third degree is with the highest values of R^2 for the three models of DOR and the value closer to 1 indicating that a greater proportion of variance is explained by the model.

Table 2. The values of the main parameters used for surface fitting in MATLAB for the three models of DOR (1) a theoretical model of DOR (PDBe:1ozc), (2) a model of DOR with crystal structure (PDBid:4ej4), (3) a model of DOR obtained by homology modeling (named *Model B*)).

Ligands	DOR (PDBe:1ozc)				DOR (PDBid:4ej4)			DOR (Model B)	
	Values of Gold Score	Values of Mol Dock	Values of e_{rel}	Values of Chem Score	Values of MolDock	Values of e_{rel}	Values of ASP score	Values of MolDock	Values of IC_{50}
[Cys(Bzl) ² , Leu ⁵]-enk	64,68	-107.022	9.3	38.91	-170.657	9.3	20.26	-77.135	8.3
[Cys(Bzl) ² , Met ⁵]-enk	81,49	-89.091	3.5	35.19	-125.108	3.5	25.16	-98.91	9.53
[Cys(O ₂ NH ₂) ² , Leu ⁵]-enk	67,72	-97.619	29.2	28.48	-118.805	29.2	22.66	-99.678	1.29
[Cys(O ₂ NH ₂) ² , Met ⁵]-enk	73,91	-91.246	7.3	25.82	-87.343	7.3	26.18	-88.498	2.22
[DCys(O ₂ NH ₂) ² , Leu ⁵]-enk	74,73	-84.852	7.4	31.84	-136.187	7.4	24.31	-66.115	11.4
[DCys(O ₂ NH ₂) ² , Met ⁵]-enk	75,13	-86.221	7.1	31.55	-139.449	7.1	-12.82	897.265	75.96
[HCys(O ₂ NH ₂) ² , Leu ⁵]-enk	57,67	-109.709	30.2	32.75	-100.702	30.2	19.58	-75.943	6.18
[HCys(O ₂ NH ₂) ² , Met ⁵]-enk	68,43	-62.774	3.4	26.55	-112.164	3.4	18.87	-90.567	31.92
DPDPE	78,65	-93.301	4.5	29.23	896.877	4.5	23.84	-80.137	16.09
[Leu ⁵]-enk	73,42	-81.869	5.8	31.62	-119.009	5.8	22.45	-104.149	11.45
[Met ⁵]-enk	73,26	-118.971	3.6	32.22	-106.792	3.6	33.9	-112.752	18.91

Table 3. The goodness of fit for the polynomial models obtained by least squares method for the three models of DOR in MATLAB.

Degree	DOR (PDBid:1ozc)			
	SSE	R ²	Adj R ²	RMSE
First	443.5817	0.5446	0.4308	7.4463
Second	167.1000	0.8285	0.6569	5.7810
Third	0.0092	1.0000	0.9999	0.0960
Degree	DOR (PDBid:4ej4)			
	SSE	R ²	Adj R ²	RMSE
First	940.0461	0.0350	-0.2063	10.8400
Second	895.3748	0.0809	-0.8383	13.3819
Third	0.9631	0.9990	0.9901	0.9814
Degree	DOR (Model B)			
	SSE	R ²	Adj R ²	RMSE
First	752.844	0.8318	0.7897	9.7011
Second	287.3484	0.9358	0.8716	7.5809
Third	0.0246	1.0000	0.9999	0.1568

Table 4. The mean values (confidence bounds) of the coefficients of the third order polynomial model chosen as optimal model for the three models of DOR.

Coefficients	Mean (with 95% confidence bounds)					
	DOR (PDBe:1ozc)		DOR (PDBid:4ej4)		DOR (Model B)	
a ₀₀	11.51	(9.823, 13.19)	-188.4	(-705.4; 373.7)	416.5	(319.1; 514)
a ₁₀	-11.07	(-16.13, -6.008)	1855	(-17.99; 3279)	-2420	(-3089; -1751)
a ₀₁	-22.37	(-33.1, -11.64)	-828.1	(-4019; 2363)	111.7	(-248.9; 472.4)
a ₂₀	16.71	(14.65, 18.78)	740.8	(48.93; 1433)	-3299	(-3796; -2801)
a ₁₁	3.451	(-6.742, 13.64)	1.3	(-397.5; 2.639)	-2.164	(-2.687; -1.639)
a ₀₂	-0.6185	(-3.866, 2.629)	839.8	(-1929; 3609)	-1.439	(-1.829; -1.049)
a ₃₀	-12.15	(-14.89, -9.411)	83.1	(29.72; -136.5)	-864.7	(-989.5; -739.8)
a ₂₁	19.03	(11.96, 26.11)	2506	(119.9, 4892)	-1.301	(-1.493; -1.109)
a ₁₂	44.7	(29.97, 59.43)	2.3	(-1630; 4.563)	-4.613	(-5.623; -3.602)
a ₀₃	14	(7.377, 20.62)	4556	(-1526; 1.065)	-3.382	(-4.211; -2.552)

The values of *SSE* for the cubic polynomial for the three models of DOR are close to 0. Therefore this value of *SSE* shows that the model of third-degree has a smaller random error component and then the fit will be more useful for prediction. The values of *Adj R²* for the cubic polynomial for the DOR are closer to 0 and indicate a fit that is more useful for prediction. This shows that the obtained polynomial model for the surface fitting data is a good model and it explains a high proportion of the variability in experimental data, and it is able to predict new observations with high certainty [11,12,13].

The best results for fitting of experimental data for the three models of DOR according to the results in

$$f(x,y) = a_{00} + a_{10} * x + a_{01} * y + a_{20} * x^2 + a_{11} * x * y + a_{02} * y^2 + a_{30} * x^3 + a_{21} * x^2 * y + a_{12} * x * y^2 + a_{03} * y^3 \quad (3)$$

three models of DOR are less than 1. This statistic parameter is a good indicator of the fit quality when two models are compared and with a value closer to 1 indicating a better fit. The values of the *RMSE* for the third degree of polynomial for three models of

Table 2 were obtained for surface fitting by a cubic polynomial in three-dimensional for determining the relationship between biological activities and docking results of investigated compounds. By using a polynomial least squares surface fitting technique, a third order polynomial was fitted to the data and it is represented as the following Eqns.(3):

The coefficients of the surface fitting for the three models of DOR by a cubic polynomial in three-dimensions are presented in Table 4.

The efficacy as a function of the values of GoldScore function and the values of the total energy for the formed complexes for DOR (PDBe:1ozc) was presented in Fig.1A). The efficacy as a function of the values of GhemScore function and the values of the total energy for DOR (PDBid:4ej4) was presented in Fig.1B). The potency as a function of the values of ASP function and the values of the total energy for *Model B* was presented in Fig.1C).

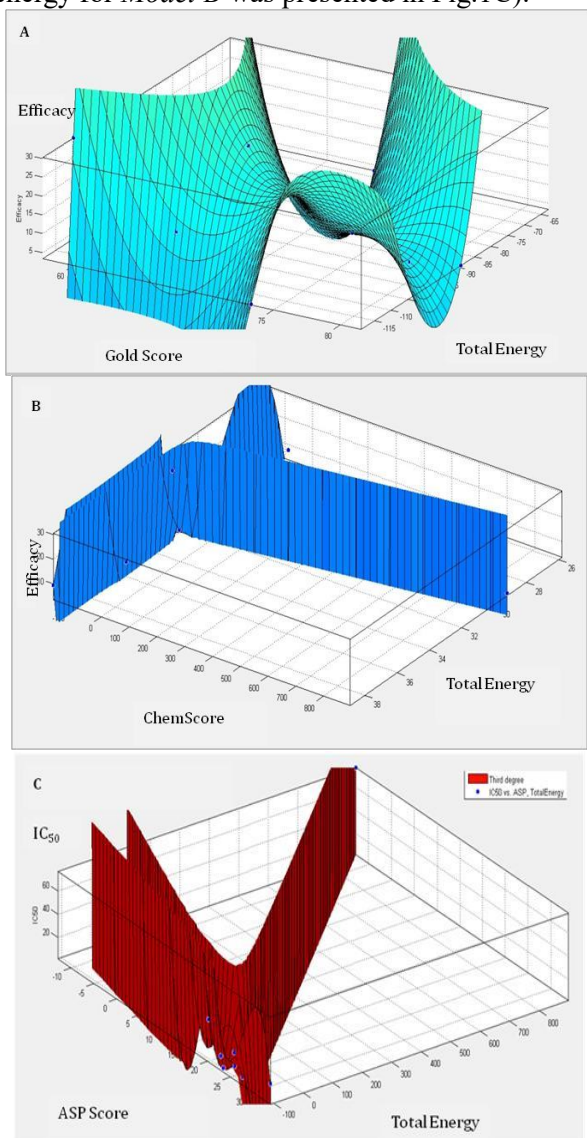


Fig. 1. A 3D surface fitting of experimental data with third degree of polynomial, which represent the biological activity of the ligands as a function of the values of scoring function from docking procedure and the values of the total energy for ligand-receptor complex: (A) Model of DOR (PDBe:1ozc); (B) Model of DOR (PDBid:4ej4); (C) Model B. The polynomial surface fitting model was obtained by Surface Fitting Toolbox in MATLAB.

Significant correlations is established between the values of ASP function and the values of IC_{50} from *in vitro* tests complexes, ($R=0.9120$) for *Model B* of DOR. The established correlations between these parameters are important because they give the best description of the fitting of experimental data with polynomials of two variables. The relationship between the values of docking experiments and the values of ASP function for *Model B* of DOR is also confirmed by the fitting of experimental data with a third order polynomial with two. Therefore the model of DOR developed by homology modelling allows to optimally determining the binding affinity by ASP scoring function.

A graphic chart representation of the relationship between the three numeric variables in 2D is presented in Fig.2: 1) the values of the GoldScore function and the values of the total energy are for X and Y axes for DOR (PDBe:1ozc), where the values of e_{rel} are for contour levels; 2) the values of the ChemScore function and the values of total energy are for X and Y axes for DOR (PDBid:4ej4), where the values of e_{rel} are for contour levels; 3) the values of the ASP function and the values of total energy are for X and Y axes for *Model B*, where the values of the IC_{50} are for contour levels. For the fitting by a cubic polynomial in 3D the contour plot (Fig.2) makes it easier to see points that have the same height. The main advantage of this chart is that it allows for precise examination and analysis of the shape of the surface.

Polynomial models are commonly used as empirical models for curve fitting of data, because they have a simple form and two essential respects: a quantitative - the degrees of the polynomials (the number of parameters of model) and a qualitative - the regression function is linear in terms of the unknown parameters. Thus, we can use the polynomial models to find the optimal regression coefficients using the method of least squares.

CONCLUSION

The obtained model for the experimental data showed good fitting properties and significant predictive ability. Therefore this model of third-degree polynomial is suitable for determine the relationship structure-biological activity. The ASP scoring function and total energy obtained from docking could be used for describing the biological activity of newly designed compounds. This would be helpful in shortening the drug design process. Analysis and comparison of the data from *in vitro* tests and docking studies could help to better

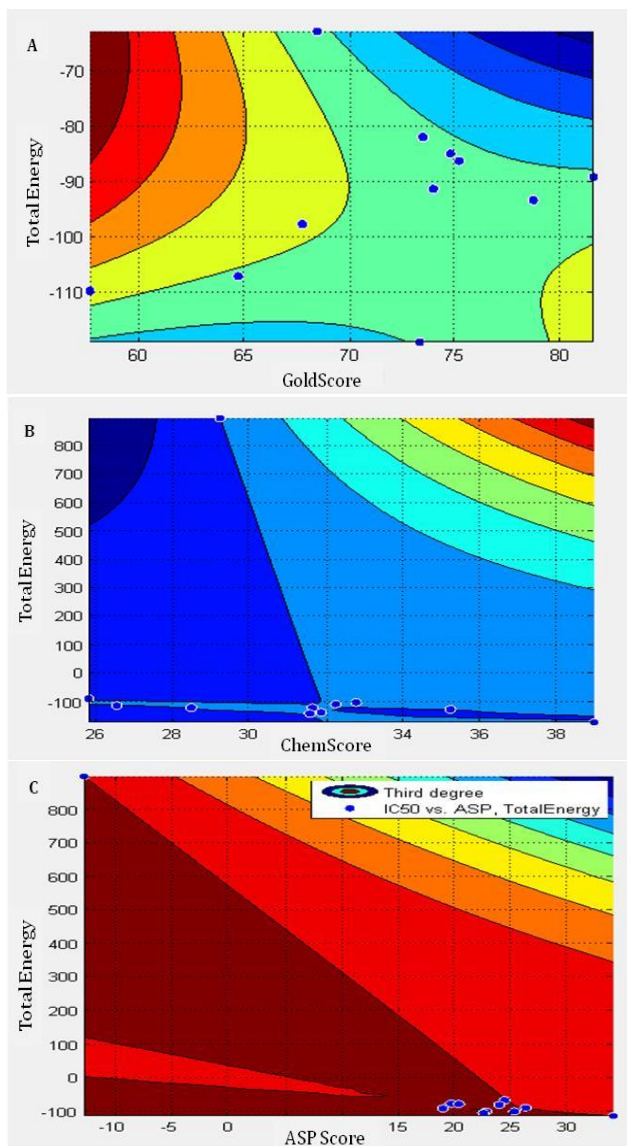


Fig. 2. A 2D contour plot of the 3D surface in the Fig.1: X represents the values of scoring functions from GOLD 5.2 and Y represents the values of total energy from MMV. (A) Model of DOR (PDB:1o2c); (B) Model of DOR (PDB:4ej4); (C) Model B. These diagrams were generated with the MATLAB.

understand the relationship between the biological effects of ligands and docking studies and to answer whether the models of the biological macromolecules (DOR) correspond to the real 3D structure.

Acknowledgements. This work is partially supported by the project of the Bulgarian National Science Fund, entitled: Bioinformatics research: protein folding, docking and prediction of biological activity, NSF I02/16, 12.12.14.

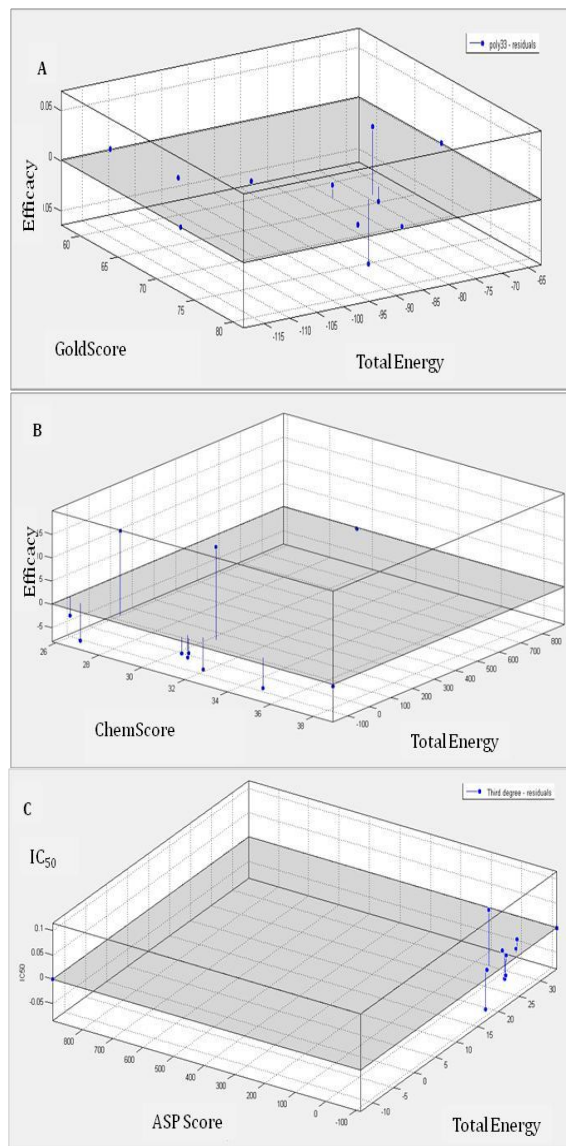


Fig. 3. The Residuals Plot for the obtained polynomial models of the third degree: A) Model of DOR (PDB:1o2c); B) Model of DOR (PDB:4ej4); C) Model B of DOR.

REFERENCES

1. P. Law, Y. Wong, H. Loh, *Ann. Rev.Pharmacol.Toxicol.*, **40**, 389 (2000).
2. J. Lord, A. Waterfield, J. Hughes, H. Kosterlitz. *Nature*, **267**, 495 (1977).
3. R. Maldonado, R. Severini, W. Hans, B. Kiefer, P. Melchiorri, L. Negri. *British Journal of Pharmacology*, **132**: 1485 (2001).
4. R. Bodnar *J. Peptides*, **60**, 65 (2013).
5. U. Rester. *Curr Opin Drug Discov Devel*, **11**, 559 (2008).
6. N. Pencheva, P. Milanov, L. Vezekov, T. Pajpanova, E. Naydenova, *Eur. J. Pharmacol.*, **498**, 249 (2004).
7. N. Pencheva, A. Bocheva, E. Dimitrov, C. Ivancheva, *Eur. J. Pharmacol*, **304**, 99 (1996).
8. P. Milanov, N. Pencheva, *Serdica J. Computing*, **5**, 333 (2011).

9. U. Rester. *Curr Opin Drug Discov Devel*, **11**,559 (2008).
10. H. Kubinyi. *Springer Science & Business Media*, Netherlands (1994).
11. F. Sapundzhi, T. Dzimbova, P. Milanov, N. Pencheva, *J. Comput. Methods Molec. Design*, **5**, 98 (2015).
12. F. Sapundzhi, T. Dzimbova, P. Milanov, N. Pencheva, *Biomath Communications*, **2**, P81, (2015).
13. F. Sapundzhi, T. Dzimbova, P. Milanov, N. Pencheva, *Proceedings of the 6th International Scientific Conference - FMNS2015*, **1**, 104-112, (2015).
14. J. Clark, Y. Itzhak, V. Hruby, H. Yamamura, G. Pasternak, *Eur. J. Pharmacol.*, **128**, 303-304, (1986).
15. GOLD, version 5.2 UserGuide, *CCDC Software Ltd.: Cambridge, UK*, (2010).
16. G. Jones, P. Willett, R. Glen, A. Leach, R. Taylor, *J. Mol. Biol.*, **267**, 727 (1997).
17. M. Verdonk, J. Cole, M. Hartshorn, C. Murray, R. Taylor. *Proteins*, **52**: 609 (2003).
18. R. Reinscheid, H. Nothacker, A. Bourson, A. Ardati, R. Henningsen, J. Bunzow, D. Grandy, H. Langen, F. Monsma, O. Civelli, *Science*, **270**, 792 (1995).
19. K. Befort, L. Tabbara, S. Bausch, C. Chavkin, C. Evans, B. Kieffer, *Mol. Pharmacol.*, **49**, 216 (1996).
20. R. Thomsen, M. Christensen. *J. Med. Chem.*, **49**, 3315 (2006).
21. P. Lancaster, *Ser. C: Math. Phys. Sci.*, **49**, 91 (1979).
22. D. Sun, A. Whitty, J. Papadatos, M. Newman, J. Donnelly, S. Bowes, S. Josiah. *J. Biomol. Screen.* **10**, 508 (2005).
23. (<http://www.mathworks.com/products/matlab>)
24. F. Sapundzhi, T. Dzimbova, N. Pencheva, P. Milanov, *Biomath Communications*, **1**, P84 (2014).
25. T. Dzimbova, F. Sapundzhi, N. Pencheva, P. Milanov, *Int. J. Bioautomation*, **17**, 5 (2013).
26. F. Sapundzhi, T. Dzimbova, N. Pencheva, P. Milanov, *Der Pharma Chemica*, **8**, 118 (2016).
27. T. Dzimbova, F. Sapundzhi, N. Pencheva, P. Milanov, *Journal of Peptide Science*, **18** (S1), S84, (2012).
28. F. Sapundzhi, T. Dzimbova, N. Pencheva, P. Milanov, *Journal of Peptide Science*, **20** (S1), S294, (2014).
29. F. Sapundzhi, T. Dzimbova, N. Pencheva, P. Milanov, *Bul. Chem. Commun.*, **47**, 613 (2015).

QSAR МОДЕЛИРАНЕ И ДОКИНГ ЕКСПЕРИМЕНТИ С ТРИ МОДЕЛА НА δ -ОПИОИДЕН РЕЦЕПТОР

Ф. И. Сапунджи^{1*}, Т. А. Дзимбова², Н. С. Пенчева¹, П. Б. Миланов^{1,3}

¹Югозападен университет „Неофит Рилски“, България, 2700 Благоевград

²Институт по молекулярна биология, Българска академия на науките, Bulgaria, 1113 Sofia

³Институт по математика и информатика, Българска Академия на Науките, Bulgaria, 1113 Sofia

Постъпила на 30 септември 2016 г.; Коригирана на 07 март, 2017 г.

(Резюме)

Делта-опиоидния рецептор (ДОР) участва в контрола на хроничната болка и емоционалните реакции. Ето защо ДОР е интересен обект за QSAR моделиране и докинг експерименти с делта-опиоидни селективни енкефалинови аналози.

Целта на това изследване е да се намери връзката структура-активност на серия от делта-опиоидни селективни енкефалинови аналози, базирайки се на количествените параметри от *in vitro* изследвания (ефикасност, афинитет и потентност) и резултати от молекулен докинг с три модела на ДОР: (1) теоретичен модел на ДОР (PDBe: 1ozc); (2) модел на ДОР с кристална структура (PDBid: 4ej4); (3) модел на ДОР получен чрез хомоложно моделиране (наречен *Model B*). Биологичната активност на делта-селективните енкефалинови аналози е описана чрез тримерно моделиране с полином на две променливи от трета степен, при което *in vitro* параметрите афинитет, ефикасност и потентност са представени като функции от стойностите на скоринг функцията от докинга и тоталната енергия на формираните лиганд-рецепторни комплекси. Това е един начин за определяне на QSAR.

Synthesis and characterization of new endomorphin analogs with N-terminal phosphonate

P.T. Todorov*, P.N. Peneva, Z.N. Genova, E.D. Naydenova

University of Chemical Technology and Metallurgy, Department of Organic Chemistry, Sofia 1756 (Bulgaria),

Received October 10, 2016; Revised January 18, 2017

Endomorphins are small endogenous neuropeptides that are produced by the body and act to reduce pain. They are tetrapeptides with the highest known affinity and selectivity for the μ -opioid receptor. This report refers to the synthesis and characterization of novel endomorphin analogues containing phosphonate moiety. The new endomorphins with N-terminal phosphonate were prepared using solid phase peptide synthesis by Fmoc chemistry. The phosphonate moiety was incorporated by modification of Kabachnik-Fields reaction. The crude neuropeptides were purified on a reversed-phase high-performance liquid chromatography and the molecular weights were determined, using electrospray ionization mass-spectrometry, and also determining of the specific angles of optical rotation.

Keywords: Opioid peptides; Endomorphin analogues; Peptide synthesis

INTRODUCTION

The numerous endogenous opioid peptides (endomorphins, enkephalins, nociceptin, etc.) and the exogenous opioids (such as morphine) exert their effects through the activation of receptors belonging to four main types: μ , δ , κ and ϵ . The endomorphins are a group of endogenous opioid peptides consisting of endomorphin-1 (H-Tyr-Pro-Trp-Phe-NH₂) and endomorphin-2 (H-Tyr-Pro-Phe-Phe-NH₂). They are tetrapeptides with the highest known affinity and selectivity for the μ -opioid receptor. Since chronic pain is notoriously difficult to treat using currently available therapeutics, the development of analgesics represents a major pharmaceutical objective. Endogenous opioids are intensively and extensively studied in search for a new powerful analgesic, lacking the adverse effects of most alkaloid opioids. Some of the greatest achievements in medicine in theoretical and in clinical aspect are connected with the research on pain and especially on the development of analgesic drugs [1-6].

Phosphonopeptides are phosphorus analogues of naturally occurring peptides containing a tetrahedral phosphorus atom. Their importance is obvious from the fact that they have been widely used as enzyme inhibitors and, as happens in catalytic antibody research, because they can be considered as stable mimetics of tetrahedral transition states in ester and amide hydrolysis and formation [7-10]. To date, several efficient synthetic routes have been developed for synthesis of phosphonopeptides and phosphinopeptides,

containing C-terminal α -aminoalkylphosphinic acids [11-10]. As part of our research, the synthesis, the characterization and the biological activity of new series of small peptides with aminophosphonates moiety as NOP receptor ligands, have previously been described [13-14].

Herein, we report the synthesis and characterization of novel endomorphin analogues containing phosphonate moiety. The new endomorphins with N-terminal phosphonate were prepared using SPPS by Fmoc (9-fluorenylmethoxy-carbonyl) chemistry. The phosphonate moiety was incorporated by modification of Kabachnik-Fields reaction. All of the newly synthesized peptide was C-terminal amides. It has been determined that the peptides with C-terminal amide group are more resistant to enzyme degradation and that their conformation suits better the interaction with μ -opioid receptors [15,16].

RESULTS AND DISCUSSION

The new endomorphin analogues with N-terminal phosphonate shown in Table 1 were prepared with good yield by solid phase synthesis using TBTU, an efficient peptide-coupling reagent. Rink-amide resin was used as a solid-phase carrier. All coupling reactions were performed, using for amino acid/TBTU/HOBt/DIEA/resin a molar ratio of 3/2.9/3/6/1. A 20%-piperidine solution in N,N-dimethylformamide (DMF) was used to remove the Fmoc group at every step. The phosphonate moiety was incorporated by modification of Kabachnik-Fields reaction. The peptidyl-resin with deprotected amino group, as amino-component, was treated with paraformaldehyde or benzaldehyde, as

* To whom all correspondence should be sent:
E-mail: pepi_37@abv.bg

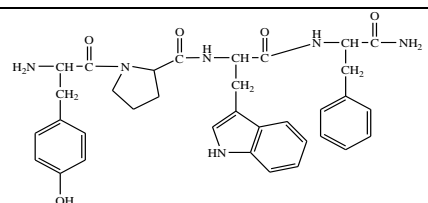
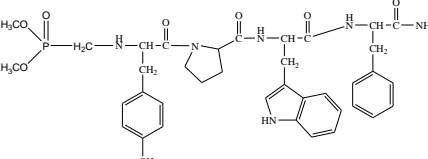
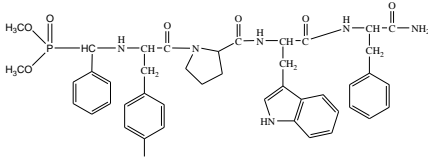
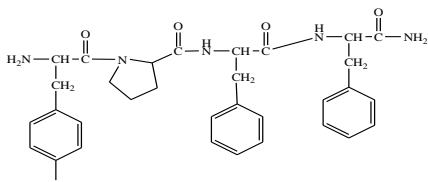
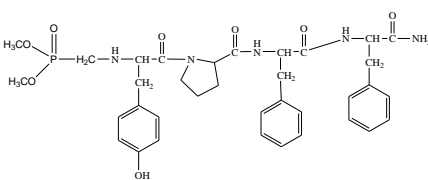
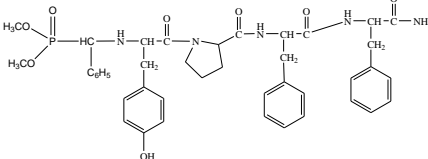
carbonyl component, in the presence of triethylamine in methanol and dimethyl hydrogen-H-phosphonate. With both the aliphatic and aromatic aldehyde the reaction conditions were the same. The reaction mixtures, monitored by Kaiser test, were stirred at 65-70°C for 7 h and gave the expected endomorphin analogues containing phosphonate moiety **1-6**.

The coupling and deprotection reactions were checked by the Kaiser test. The cleavage of the synthesized peptide from the resin was done, using a mixture of 95 % trifluoroacetic acid (TFA), 2.5 % triisopropylsilan (TIS) and 2.5 % water.

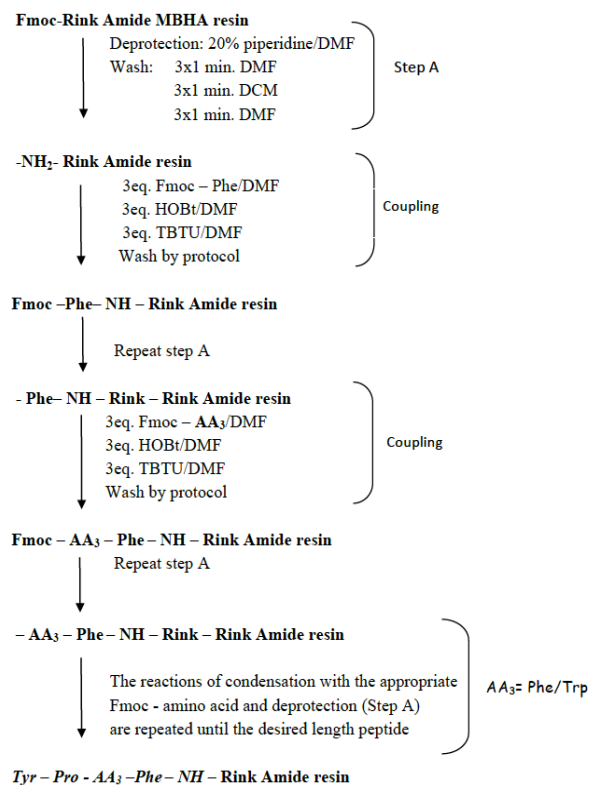
After filtration of the exhausted resin, the solvent was concentrated in vacuum and the residue

trituated with cool ether. The purity of the peptides was checked by RP-HPLC, column: SymmetryShield™ RP-18, 3.5μ, (50 x 4.6mm), flow: 1 ml/min, H₂O (0.1 % TFA)/CH₃CN (0.1 % TFA), gradient 0→100 % (15 min) and 100 % (4 min). The crude peptides were purified using semi-preparative HPLC, column XBridge™ Prep C18 10μm (10 x 250mm), flow: 5ml/min, H₂O (0.1 % TFA)/CH₃CN (0.1 % TFA), gradient 20→70 % (20 min). The ESI mass spectra were recorded with a platform II quadrupole mass spectrometer fitted with an electrospray source. Optical rotations were measured with a Perkin Elmer 341 polarimeter.

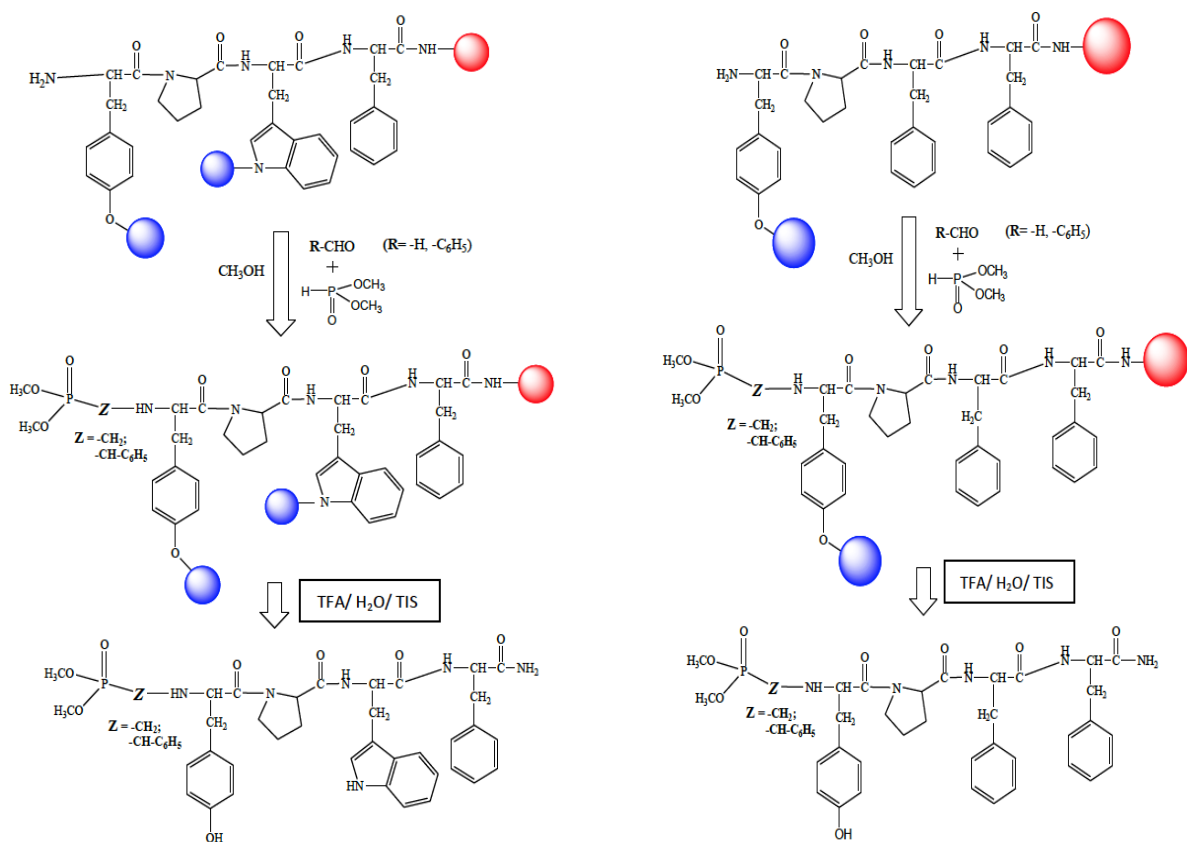
Table 1. Analytical data of synthetic peptides.

№	Peptides	[α] _D ^a (°)	^b t _R , min	^c ESI MS: (MH) ⁺	
				calculated	found
1		-29	6.17	610.3	611.2
2		-26	7.12	732.3	733.7
3		-28	7.53	808.8	809.6
4		-31	4.58	571.6	572.2
5		-27	6.20	693.7	694.7
6		-32	7.05	769.8	770.3

^a Optical rotation in methanol (*c* = 1) at 20 °C; ^b t_R is the retention time determined by HPLC; ^c The mass ion (MH⁺) was obtained by electrospray mass spectrometry.



Scheme 1. Solid Phase Peptide Synthesis of endomorphin analogues.



Scheme 2. SPSS of endomorphin-1 and endomorphin-2 analogues.

The synthetic routes for preparation of new endomorphin analogues are shown in Scheme 1 and Scheme 2.

CONCLUSION

We describe the synthesis and characterization of novel N-modified analogues of endomorphin-1 and endomorphin-2 with phosphonate moiety. The newly synthesized compounds were obtained by solid-phase peptide synthesis - Fmoc-strategy. The phosphonate moiety was incorporated by modification of Kabachnik-Fields reaction. The neuropeptides were purified on an RP-HPLC and the molecular weights were determined, using ES-MS, and also determining of the specific angles of optical rotation. The biological trials are in the progress.

Acknowledgements: We gratefully acknowledge the financial support by University of Chemical Technology and Metallurgy (UCTM), Sofia, Bulgaria, and the Scientific Research Center at UCTM - contract 11607/2016.

REFERENCES

1. M.A. Greco, P.M. Fuller, T.C. Jhou, S. Martin-Schild, J.E. Zadina, Z. Hu, P. Shiromani, *J. Brain Research*, **1245**, 96 (2008).
2. S. Offermanns, *Walter Rosenthal*, 904 (2008).
3. S. Brain, P.K. Moore, *Springer Science & Business Media*, 28 (1999).
4. W.D. Willis, E. Richard, *Coggeshall Springer Science & Business Media*, 343 (2004).
5. Austin, *MIT Press*, 125 (2015).
6. C.T. Dooley, C.G. Spaeth, I.P. Berzetei-Gurske, K. Craymer, I.D. Adapa, S.R. Brandt, R.A. Houghten, L. Toll, *J. Pharmacol. Exp. Ther.*, **283**, 735 (1997).
7. F. Palacios, A.M. Ochoa de Retana, E. Martínez de Marigorta, M. Rodriguez, J. Pagalday, *Tetrahedron* **59**, 2617 (2003).
8. R. Hirschmann, C.M. Taylor, P.A. Benkovic, S.D. Taylor, K.M. Yager, P.A. Sprengeler, S.J. Benkovic, *Science*, **265**, 234 (1994).
9. P. Kafarski, B. Lejczak, Synthesis of phosphono- and phosphinopeptides. In: V.P. Kukhar, H.R. Hudson (eds) *Aminophosphonic and aminophosphinic acids chemistry and biological activity*, Chap 6. Wiley, Chichester, 2000, 173.
10. P. Kafarski, B. Lejczak, The biological activity of phosphono- and phosphinopeptides. In: V.P. Kukhar, H.R. Hudson (eds) *Aminophosphonic and aminophosphinic acids: chemistry and biological activity*, Wiley, Chichester, 2000, Chap 12., 407.
11. V.P. Kukhar, V.A. Soloshonok, V.A. Solodenko, *Phosphorus Sulfur Silicon Relat. Elem.*, **92**, 239 (1994).
12. V.A. Soloshonok, Y.N. Belokon, N.A. Kuzmina, V.I. Maleev, N.Y. Svistunova, V.A. Solodenko, V.P. Kukhar, *J. Chem. Soc. Perkin. Trans.*, **1**, 1525 (1992).
13. P. Todorov, P. Mateeva, R. Zamfirova, N. Pavlov, E. Naydenova, *Amino Acids*, **43**, 1217 (2012).
14. E. Naydenova, P. Todorov, P. Mateeva, R. Zamfirova, N. Pavlov, S. Todorov, *Amino Acids*, **39**, 1537 (2010).
15. U.H. Mortensen, M. Raaschou-Nielsen, K. Breddam, *J. Biol. Chem.*, **269**, 15528 (1994).
16. I.D. Pogozeva, M.J. Przydzial, H.I. Mosberg, *The AAPS Journal*, **7**, 2 (2005).

СИНТЕЗ И ОХАРАКТЕРИЗИРАНЕ НА НОВИ N-МОДИФИЦИРАНИ АНАЛОЗИ НА ЕНДОМОРФИНТЕ С ФОСФОНАТЕН ОСТАТЪК

Петър Т. Тодоров*, Петя Н. Пенева, Златина Н. Генова, Емилия Д. Найденова

*Химикотехнологичен и Металургичен Университет, Катедра "Органична химия",
1756 София, България,*

Постъпила на 07 октомври, 2016 г.; Коригирана на 18 януари, 2017 г.

(Резюме)

Ендоморфините са малки ендогенни опиоидни пептиди, които се произвеждат от организма и действат за намаляване на болката. Те са тетрапептиди с най-висок афинитет и селективност към μ -опиоидния рецептор. В статията ние описваме синтеза и охарактеризирането на нови ендоморфинови аналози, съдържащи фосфонатна група. Новите N-модифицирани аналози на ендоморфините, с фосфонатен остатък бяха получени с помощта на твърдофазен пептиден синтез. Фосфонатният остатък беше въведен чрез модификация на реакцията на Кабачник-Филдс. Невропептидите бяха пречистени с помощта на обратно-фазова високоефективна течна хроматография, бяха определени и молекулните им маси, използвайки електроспрей йонизационна масспектрометрия, а също така и специфичните ъгли на оптично въртене.

Rapid screening of anti-inflammatory properties of newly synthesized derivatives of indomethacin

P.I. Mateeva¹, R.Y. Prodanova², M.N. Marinov², E.D. Naydenova^{3*}, P.T. Todorova¹, R.N. Zamfirova¹

¹*Institute of Neurobiology, Bulgarian Academy of Sciences, 1113 Sofia, Bulgaria*

²*Agricultural University – Plovdiv, Faculty of Plant Protection and Agroecology, Department of General Chemistry, 4000 Plovdiv, 12 “Mendeleev” Blvd, Bulgaria*

³*University of Chemical Technology and Metallurgy, Department of Organic Chemistry, 1756 Sofia, 8 “Kliment Ohridski” Blvd, Bulgaria*

Received October 07, 2016; Revised January 25, 2017

Anti-inflammatory effects of newly synthesized derivatives of indomethacin with 3-aminospirohydantoin and 3-amino-5-methyl-5-phenylimidazolidine-2,4-dione, have been studied. It was found that the compounds tested possess an inhibitory activity on acute inflammation, but not stronger than that of indomethacin. The structure of spirohydantoin residue influences the effects of the new molecules.

Keywords: Inflammation, Indomethacin, 3-aminospirohydantoin, 3-amino-5-methyl-5-phenylimidazolidine-2,4-dione

INTRODUCTION

Non-steroid anti-inflammatory drugs (NSAD) are widely used in therapy of inflammation, fever and pain. The main mode of their action is the inhibition of cyclooxygenase (COX) isoenzymes COX1 and COX2. Thus they suppress the synthesis and reduce the amount of prostaglandins, which increases during inflammation. Irrespective of their numerous side effects the drugs of this group (aspirin, paracetamol, indomethacin, ibuprofen, diclofenac, etc.) are still commonly prescribed in the cases of acute and chronic inflammatory diseases because of their remarkable effectiveness.

Different substituted hydantoin and their derivatives have also revealed various activities, including inhibition of allergy reactions, mediated by serotonergic, cholinergic, adrenergic, dopaminergic mediatory systems [1 - 6]. Spirohydantoin derivatives are intensively synthesized and studied like drugs for mental diseases such as schizophrenia, anxiety and/or depression [7], antitumor agent [8] and in inflammatory processes of allergic diseases such as asthma, allergic rhinitis, and atopic dermatitis. It was found also that indomethacin shares partly the same mechanism on allergic inflammatory processes as spirohydantoin derivatives [9]. That is why in the present study we tested the possible anti-inflammatory effect of the newly synthesized by Marinov et al. [10] compounds, derivatives of indomethacin with 3-aminospirohydantoin and 3-amino-5-methyl-5-phenylimidazolidine-2,4-dione.

EXPERIMENTAL

Materials

The new amides shown in Table 1 were prepared with good yield by interaction of a series of 3-aminospirohydantoin and 3-amino-5-methyl-5-phenylimidazolidine-2,4-dione with indomethacin.

Methods

The anti-inflammatory activity of the new compounds was tested on male Wistar rats (160-200g), using a carrageenan-induced paw edema model. Acute inflammation was induced by intraplantar (i.pl.) injection of 0.1 ml λ -carrageenan (CG, 1%, w/v) into the right hind paw. The compounds in a volume of 0.1 ml/100g was administered intraperitoneally (i.p.) 30 min before the induction of the CG-inflammation. The paw volume was measured plethysmographically (Ugo Basile, Italy) before the injection of CG, to obtain a control value, and then every 60 min for a period of 4 hours. Data are expressed as edema rate (%). Values for each group represent the mean +SEM of 5-7 animals. The effects of derivatives, as well as of indomethacin have been compared to that of the control group.

To make the results comparable, we tested the effects of derivatives in equimolar doses, relative to indomethacin 3mg/kg. All compounds investigated, as well as the referent drug indomethacin were suspended with Twin 80 in saline. The rats in the control group were injected only with saline. All

* To whom all correspondence should be sent:
E-mail: e_naydenova@abv.bg

institutional and national guidelines for care and use of laboratory animals were followed.

Statistics

The data were statistically analyzed by one-way ANOVA (Dunnett post hoc test), $P < 0.05$ being accepted as the minimum level of statistical significance of the established differences.

RESULTS AND DISCUSSION

The compounds shown in Table 1 have been tested.

Our study has shown, that most of newly synthesized compounds exert an anti-inflammatory

effect, but none of them possesses efficacy, stronger than that of indomethacin. The effects of compounds 1-4 (in which a spirohydantoin residue is incorporated) on acute inflammation are presented on fig 1, 2 and 3. Comp 1 with C5- ring in spirohydantoin moiety did not improve the anti-inflammatory properties of indomethacin. Applied in a concentration, equimolar to 3mg/kg indomethacin, it decreased the paw volume significantly, compared to the control, in the first 120 min of observation, but the effect was not significant to the end of the experiment.

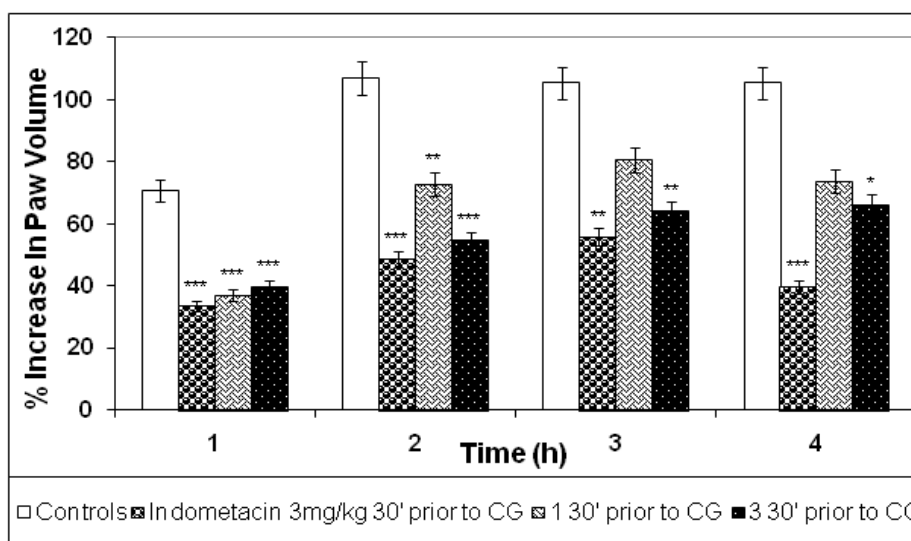


Fig. 1. Anti-inflammatory effect of indomethacin (3 mg/kg) and its derivatives 1 and 3 in doses equimolar to indomethacin, applied 30 min prior to carrageenan (CG). Values represent the mean \pm SEM of 6-8 animals. Statistically significant differences versus control with CG * $p < 0.05$; ** $p < 0.01$.

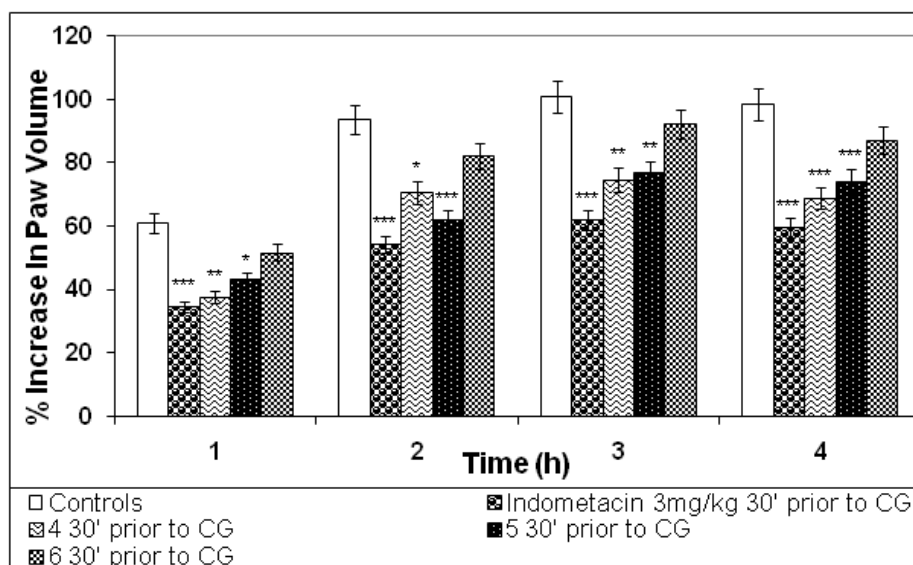


Fig. 2. Anti-inflammatory effect of indomethacin (3 mg/kg) and its derivatives 4, 5 and 6 in doses equimolar to indomethacin, applied 30 min prior to carrageenan (CG). Values represent the mean \pm SEM of 6-8 animals. Statistically significant differences versus control with CG * $p < 0.05$; ** $p < 0.01$.

Table 1. Structures of new compounds

№ / FW	Structure
1 C ₂₆ H ₂₅ ClN ₄ O ₅ 508.95	
2 C ₂₇ H ₂₇ ClN ₄ O ₅ 522.98	
3 C ₂₈ H ₂₉ ClN ₄ O ₅ 537.01	
4 C ₂₈ H ₂₉ ClN ₄ O ₅ 537.01	
5 C ₂₉ H ₂₅ ClN ₄ O ₅ 544.99	
6 C ₃₀ H ₂₅ ClN ₄ O ₅ 556.99	
7 C ₃₁ H ₂₇ ClN ₄ O ₅ 571.02	
8 C ₃₄ H ₂₅ ClN ₄ O ₅ 605.04	

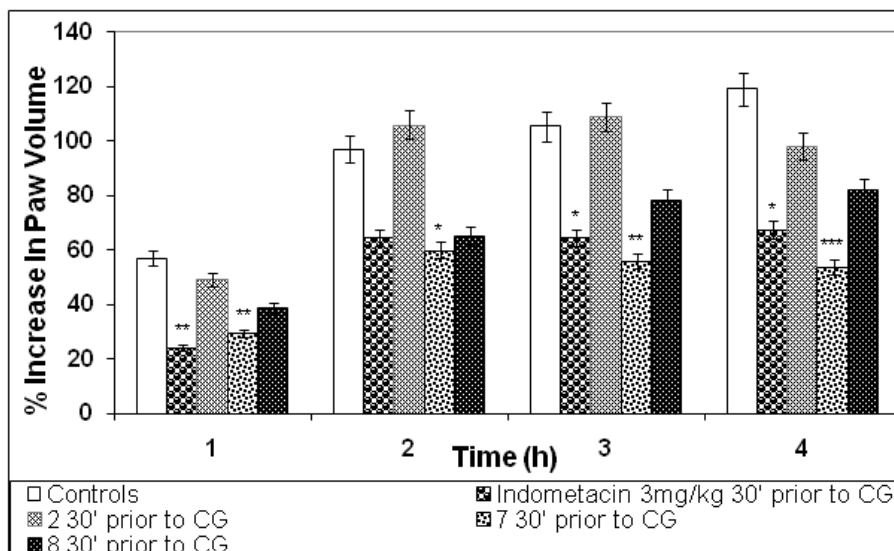


Fig. 3. Anti-inflammatory effect of indomethacin (3 mg/kg) and its derivatives 2, 7 and 8 in doses equimolar to indomethacin, applied 30 min prior to carrageenan (CG). Values represent the mean \pm SEM of 6-8 animals. Statistically significant differences versus control with CG * p <0.05; ** p <0.01.

The expanding of the ring (C6 instead of C5) in a spirohydantoin residue eliminated completely the anti-inflammatory capacity of the new substance (comp. 2, fig 3). This compound did not affect the increase of rats paw, induced by carrageenan, the rise being comparable to that of the controls (fig 3). However, the experiments have shown that the attachment of a methyl group in the C6 cycle (comp. 3 and 4) recovered the inhibitory potency of derivatives on inflammation and leads to effects, comparable with that of equimolar concentration indomethacin. It was found also that the rate of suppression is irrespective of the position of the methyl group- the percentage of inhibition evoked by the two isomers were very similar during the entire period of observation. It could be suggested that methyl group leads to conformational changes, affecting the activity.

In the second group (5-8) compounds 6 and 8 in dose equivalent to 3mg/kg indomethacin trend to reduce, but not significantly, the increase of inflamed paw volume, while comp.5 and comp.7 inhibited the inflammation as strong as indomethacin.

CONCLUSIONS

The results obtained showed, that most of the tested derivatives of indomethacin with 3-aminospirohydantoin and 3-amino-5-methyl-5-phenylimidazolidine-2,4-dione, poses an anti-inflammatory activity but not stronger than that of indomethacin. The structure of spirohydantoin

residue influences the anti-inflammatory activity of the newly synthesized compounds.

REFERENCES

1. E. Naydenova, N. Pencheva, J. Popova, M. Lazarova, B. Aleksiev. *Il Farmaco*, **57**, 189 (2002).
2. H. Byrtus, M Pawłowski, S. Chara kchieva-Minol, B. Duszyńska, M.J. Mokrosz, J.L Mokrosz, A. Zijc, *Arch. Pharmacol. (Weinheim)*, **6**, 283, (1996).
3. M.L. López-Rodríguez, M.J. Morcillo, E. Fernández, E. Porras, L. Orensanz, M.E. Beneytez, JManzanares, J.A. Fuentes. *J. Med. Chem.* **44**, 86 (2001).
4. M.L. López-Rodríguez, M.J. Morcillo, E. Fernández, M.L. Rosado, L. Pardo, K. Schaper. *J. Med. Chem.* **4**, 198 (2001).
5. M.L. López-Rodríguez, M.L. Rosado, B. Benhamú, M.J. Morcillo, A.M. Sanz, L. Orensanz, M.E. Beneitez, J.A. Fuentes, J. Manzanares. *J. Med. Chem.* **39**, 4439 (1996).
6. I. Wolska, H. Byrtus, A. Zejc. *Pol. J. Chem.* **71**, 1005 (1997).
7. A. Czopek, M. Kołaczkowski, A. Bucki, H. Byrtus, M. Pawłowski, G.Kazek, A. J.Bojarski, A. Piaskowska, J. Kalinowska-Thuścik, A. Partyka, A. Wesółowska. *Bioorg. Med. Chem.* **23**, 3436 (2015).
8. C.V. Kavitha, M. Nambiar, C.S. Ananda Kumar, B. Choudhary, K. Muniyappa, K.S. Rangappa, S.C. Raghavan, *Biochem. Pharmacol.* **77**, 348 (2009).
9. S. Crosignani, C. Jorand-Lebrun, P. Page, G.Campbell, V. Colovray, M. Missotten, Y. Humbert, C. Cleva, J.-F. Arrighi, M. Gaudet, Z. Johnson, P. Ferro, A. Chollet. *ACS Med. Chem. Lett.* **2**, 644 (2011).
10. M.N. Marinov, E.D. Naydenova, R.Y. Prodanova, S. H. Tsoneva, N. M. Stoyanov. *Bulg. Chem. Commun.*, (2017) in press.

БЪРЗ СКРИНИНГ НА ПРОТИВОВЪЗПАЛИТЕЛНИТЕ СВОЙСТВА НА НОВОСИНТЕЗИРАНИ ПРОИЗВОДНИ НА ИНДОМЕТАЦИН

П.И. Матеева¹, Р. Й. Проданова², М. Н. Маринов², Е. Д. Найденова^{3*}, П.Т. Годорова¹,
Р.Н. Замфирова¹

¹*Институт по невробиология, Българска академия на науките, 1113 София, България*

²*Аграрен университет – Пловдив, Факултет по растителна защита и агроекология, Катедра „Обща химия”,
4000 Пловдив, бул. „Менделеев” 12, България*

³*Химикотехнологичен и металургичен университет, Катедра „Органична химия”, 1756 София, бул. „Климент
Охридски” 8, България*

Постъпила на 07 октомври 2016 г.; Коригирана на 25 януари, 2017 г.

(Резюме)

Изследвани са противовъзпалителните ефекти на новосинтезирани производни на индометацин със серия от 3-аминоспирохидантоини и 3-амино-5-метил-5-фенилимидазолидин-2,4-дион. Установено е, че изследваните съединения потискат възпалителния процес, но не по-силно от индометацина. Установена е зависимост между структурата на спирохидантоиновия остатък и проявения ефект.

Synthesis of new indomethacin derivatives with 3-aminospirohydantoin and 3-amino-5-methyl-5-phenylimidazolidine-2,4-dione

M.N. Marinov¹, E.D. Naydenova^{2*}, R.Y. Prodanova¹, S.H. Tsoneva³, N.M. Stoyanov⁴

¹Agricultural University – Plovdiv, Faculty of Plant Protection and Agroecology, Department of General Chemistry, 4000 Plovdiv, 12 “Mendeleev” Blvd, Bulgaria

²University of Chemical Technology and Metallurgy, Department of Organic Chemistry, 1756 Sofia, 8 “Kliment Ohridski” Blvd, Bulgaria

³Plovdiv University “Paisii Hilendarski”, Faculty of Chemistry, Department of Analytical Chemistry and Computer Chemistry, 4000 Plovdiv, 24 “Tzar Asen” St, Bulgaria

⁴“Angel Kanchev” University of Ruse, Razgrad Branch, Department of Chemistry and Chemical Technologies, 7200 Razgrad, 47 “Aprilsko Vastanie” Blvd, Bulgaria

Received October 07, 2016; Revised January 25, 2017

This article presents the synthesis of new amides, based on the interaction of a series of 3-aminospirohydantoin and 3-amino-5-methyl-5-phenylimidazolidine-2,4-dione with Indomethacin. The target compounds were prepared with the aim of developing new products with anti-inflammatory properties. The structures of all obtained amides were verified via physicochemical parameters, FTIR-ATR, Raman, ¹H and ¹³C NMR spectroscopy.

Keywords: Synthesis, Indomethacin, 3-aminospirohydantoin, 3-amino-5-methyl-5-phenylimidazolidine-2,4-dione

INTRODUCTION

The synthesis and research of different types of biological activity of 3-aminospirohydantoin were reported in previous works of ours. The anticonvulsive effect of a series of 3-aminocycloalkanespiro-5-hydantoin with 5-, 6-, 7-, 8- and 12-membered rings (Figure 1) was investigated. The results obtained from the conducted experiments showed the absence of anticonvulsive activity. The tested cyclohexane-, cycloheptane- and cyclododecane- derivatives even induced seizures [1].

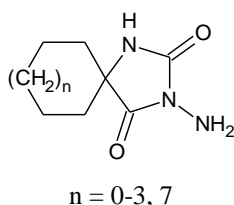


Fig. 1. 3-Aminocycloalkanespiro-5-hydantoin

The cytotoxic effect of 3-amino-9'-fluorenespiro-5-hydantoin (Figure 2) on the retinoblastoma cell line WERI-Rb-1 and its antimicrobial activity against both Gram-positive *Staphylococcus aureus* and Gram-negative *Escherichia coli* bacteria and the yeasts *Candida albicans* were examined. It was found that this

compound could not serve as potential anticancer agent, but it showed pronounced antibacterial activity against the bacteria *Escherichia coli* and no activity towards *Staphylococcus aureus* and *Candida albicans* [2].

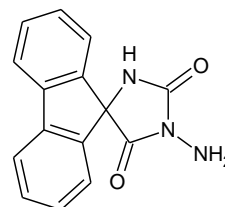
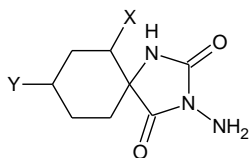


Fig. 2. 3-Amino-9'-fluorenespiro-5-hydantoin

An evaluation of the antimicrobial action of 3-amino-6-methyl-1,3-diazaspiro[4.5]decane-2,4-dione (Figure 3a), 3-amino-8-methyl-1,3-diazaspiro[4.5]decane-2,4-dione (Figure 3b), 3-amino-8-ethyl-1,3-diazaspiro[4.5]decane-2,4-dione (Figure 3c) and 3-amino-8-propyl-1,3-diazaspiro[4.5]decane-2,4-dione (Figure 3d) was also performed. The studied compounds showed no activity against Gram-positive bacteria *Staphylococcus aureus* and *Bacillus subtilis*, Gram-negative bacteria *Escherichia coli*, *Pseudomonas aeruginosa* and *Salmonella abony*, the yeasts *Candida albicans* and *Saccharomyces cerevisiae*, the molds *Penicillium chrysogenum* and *Aspergillus niger*, the plant pathogenic fungi *Fusarium oxysporum* and *Pythium ultimum* and a plant pathogenic bacterium *Pseudomonas syringae* [3].

* To whom all correspondence should be sent:
E-mail: e_naydenova@abv.bg



a) X = Me-, Y = H-; b) X = H-, Y = Me-; c) X = H-, Y = Et-; d) X = H-, Y = Pr-

Fig. 3. Substituted 3-aminocyclohexanespiro-5-hydantoin

The aim of the current research is to present the synthesis of new organic compounds with potential anti-inflammatory properties. The interaction of 3-aminospirohydantoin and 3-amino-5-methyl-5-phenylimidazolidine-2,4-dione with Indomethacin was studied for this purpose.

EXPERIMENTAL

General

All used chemicals were purchased from Merck and Sigma-Aldrich. The melting points were determined by a SMP-10 digital melting point apparatus. The purity of the compounds was checked by thin layer chromatography on Kieselgel 60 F₂₅₄, 0.2 mm Merck plates, eluent system (vol. ratio): ethyl acetate : petroleum ether = 1 : 2. The elemental analysis data were obtained with an automatic analyzer Carlo Erba 1106, giving results within ± 0.2 % of the calculated values. The Attenuated Total Reflection FTIR (ATR) spectra were registered on a Bruker FT-IR VERTEX 70 Spectrometer by ATR accessory MIRacle™ with a one-reflection ZnSe element (Pike). The stirred crystals were pressed by an anvil to the reflection element and the spectra were measured from 4500 cm^{-1} to 600 cm^{-1} at resolution 2 cm^{-1} with 16 scans. The Raman spectra (the stirred crystals placed in aluminium disc) were measured on a RAM II (Bruker Optics) with a focused laser beam of 200-500 mW power of Nd:YAG laser (1064 nm) from 4000 cm^{-1} to 51 cm^{-1} at resolution 2 cm^{-1} with 25 scans. The NMR spectra were taken on a Bruker Avance II + 600 MHz spectrometer, operating at 600.130 and 150.903 MHz for ^1H and ^{13}C , respectively, using the standard Bruker software. The chemical shifts were referenced to tetramethylsilane (TMS). The measurements in DMSO-*d*₆ solutions were carried out at ambient temperature.

Synthesis of amides **4a-4h** (Scheme 1) [4]

A mixture of Indomethacin (3.58 g, 0.01 mol, Figure 4) and 0.01 mol of the corresponding 3-aminospirohydantoin (**3a-3d** and **3f-3h**) and 3-

amino-5-methyl-5-phenylimidazolidine-2,4-dione (**3e**, 2.05 g, 0.01 mol) was dissolved in 50 ml of tetrahydrofuran with stirring at room temperature. *N,N'*-dicyclohexylcarbodiimide (DCC, 2.06 g, 0.01 mol) was added to the reaction mixture and the latter was left overnight. After this interaction, the *N,N'*-dicyclohexylcarbamide formed was filtered off and 1 ml of glacial acetic acid was added to the filtrate for removing of the unreacted reagent. After filtration, the solvent was evaporated to dryness and the amides obtained (**4a-4h**) were recrystallized from ethanol.

RESULTS AND DISCUSSION

The synthesis of the target compounds (**4a-4h**) was performed in accordance with Scheme 1. The cycloalkanespiro-5-hydantoin (**2a-2d**) and 5-methyl-5-phenylimidazolidine-2,4-dione (**2e**) were synthesized by the Bucherer-Lieb method [5], based on the interaction between the corresponding ketones (**1a-1e**), sodium cyanide, ammonium carbonate and ethanol. The 2',3'-dihydro-2*H*,5*H*-spiro[imidazolidine-4,1'-indene]-2,5-dione (**2f**) and spiro[fluorene-9,4'-imidazolidine]-2',5'-dione (**2h**) were obtained in accordance with Nagasawa et al. [6]. The 3',4'-dihydro-2*H*,2'*H*,5*H*-spiro[imidazolidine-4,1'-naphthalene]-2,5-dione (**2g**) was prepared in accordance with Marinov et al. [7] through a modification of the method reported by Sarges et al. [8]. The 3-aminoderivatives (**3a-3h**) were synthesized by a treatment of compounds **2a-2h** with concentrated hydrazine hydrate, following a modified technique [4] of the previously published procedures [1, 2, 7, 9]. Compounds **3a-3h** were subjected to an interaction with Indomethacin (Figure 4) in accordance with the DCC-method [10], resulted in the formation of the corresponding amides (**4a-4h**).

The physicochemical parameters, FTIR-ATR, Raman and NMR spectral data of the synthesized compounds (**4a-4h**) are listed in Tables 1-4 respectively.

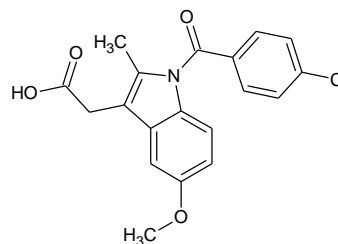
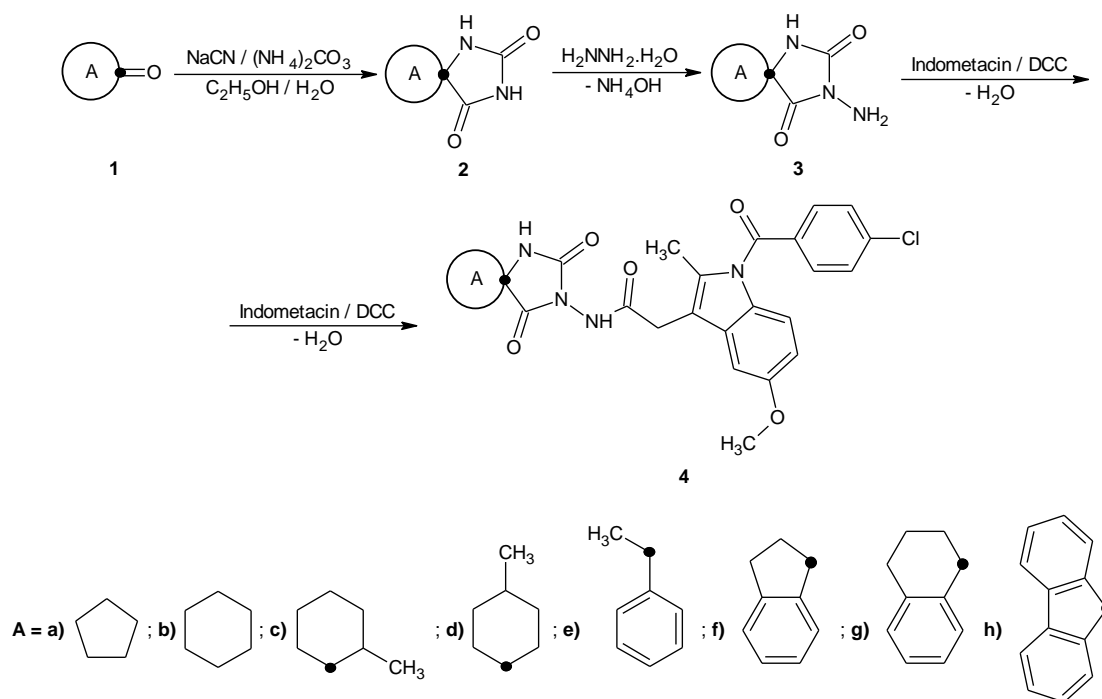


Fig. 4. Indomethacin (INN, BAN), Indomethacin (AAN, USAN, BAN), /Systematic name: 2-[1-(4-chlorobenzoyl)-5-methoxy-2-methyl-indol-3-yl]acetic acid/

Scheme 1. Synthesis of amides **4a-4h**Table 1. Physicochemical parameters of compounds **4a-4h**

N_{e}^*	Systematic name	Yield, %	M. p., °C	R_{f}^{**}
4a	2-[1-(4-Chlorobenzoyl)-5-methoxy-2-methyl-1H-indol-3-yl]-N-(2,4-dioxo-1,3-diazaspiro[4.4]nonan-3-yl)acetamide	85	224-225	0.65
4b ***	2-[1-(4-Chlorobenzoyl)-5-methoxy-2-methyl-1H-indol-3-yl]-N-(2,4-dioxo-1,3-diazaspiro[4.5]decan-3-yl)acetamide	89	234-235	0.57
4c	2-[1-(4-Chlorobenzoyl)-5-methoxy-2-methyl-1H-indol-3-yl]-N-(6-methyl-2,4-dioxo-1,3-diazaspiro[4.5]decan-3-yl)acetamide	83	188-189	0.45
4d	2-[1-(4-Chlorobenzoyl)-5-methoxy-2-methyl-1H-indol-3-yl]-N-(8-methyl-2,4-dioxo-1,3-diazaspiro[4.5]decan-3-yl)acetamide	92	236-237	0.52
4e	2-[1-(4-Chlorobenzoyl)-5-methoxy-2-methyl-1H-indol-3-yl]-N-(4-methyl-2,5-dioxo-4-phenylimidazolidin-1-yl)acetamide	94	148-149	0.63
4f	2-[1-(4-Chlorobenzoyl)-5-methoxy-2-methyl-1H-indol-3-yl]-N-(2,5-dioxo-2',3'-dihydrospiro[imidazolidine-4,1'-indene]-1-yl)acetamide	87	186-187	0.54
4g	2-[1-(4-Chlorobenzoyl)-5-methoxy-2-methyl-1H-indol-3-yl]-N-(2,5-dioxo-3',4'-dihydro-2'H-spiro[imidazolidine-4,1'-naphthalene]-1-yl)acetamide	91	207-208	0.51
4h	2-[1-(4-Chlorobenzoyl)-5-methoxy-2-methyl-1H-indol-3-yl]-N-(2',5'-dioxospiro[fluorene-9,4'-imidazolidine]-1'-yl)acetamide	84	181-182	0.46

* The compounds numbering is in accordance with Scheme 1.

** Eluent system (vol. ratio): ethyl acetate : petroleum ether = 1 : 2.

*** Ref. 4.

Table 2. FTIR-ATR spectral data (cm⁻¹) of compounds **4a-4h**

№	ν _{NH}	ν _{CH} (arom.)	ν _{aliph.}		ν _{C=O}	ν _{C=O} (amide)	ν _{CC} (arom.)	ν _{CN}
			ν _{as}	ν _s				
4a	3279	3022	2933	2854	1798, 1736, 1706	1681	1596	1371
4b*	3253	3001	2926	2856	1800, 1735, 1705	1681	1599	1372
4c	3165	3057	2932	2859	1766, 1731, 1708	1647	1590	1343
4d	3266	3019	2929	2856	1786, 1727, 1683	1656	1591	1356
4e	3280	3015	2930	2857	1795, 1741, 1692	1678	1595	1369
4f	3221	3008	2931	2852	1794, 1737, 1715	1690	1592	1378
4g	3223	3014	2931	2855	1792, 1737, 1715	1687	1593	1379
4h	3282	3018	2930	2853	1798, 1740, 1687	1660	1573	1358

* Ref. 4.

Table 3. Raman spectral data (cm⁻¹) of compounds **4a-4h**

№	mW	ν _{max} , cm ⁻¹
4a	250	3069, 2930, 1679, 1591, 1446, 1372, 1259, 1224, 1150, 1089, 831, 756, 412
4b*	200	3068, 3002, 2928, 2852, 1782, 1738, 1680, 1590, 1577, 1447, 1393, 1350, 1222, 1182, 1124, 1066, 830, 736, 663
4c	250	3072, 2930, 1728, 1689, 1680, 1649, 1616, 1580, 1457, 1395, 1226, 1093, 742, 413
4d	200	3070, 2932, 1682, 1651, 1610, 1458, 1396, 1369, 1356, 1223, 1090, 739, 411
4e	500	3069, 2929, 1693, 1679, 1613, 1579, 1456, 1396, 1369, 1089, 904, 754, 401
4f	250	3068, 2932, 1667, 1652, 1620, 1591, 1447, 1394, 1366, 1226, 1090, 758, 409
4g	200	3068, 2929, 1787, 1651, 1626, 1593, 1580, 1459, 1434, 1387, 1266, 1177, 1090, 973, 760, 741, 402
4h	200	3070, 2945, 1672, 1648, 16109, 1583, 1458, 1395, 1372, 1229, 1089, 739, 416

* Ref. 4.

Table 4. NMR spectral data of compounds **4a-4h**

№	¹ H NMR (DMSO- <i>d</i> ₆), δ / ppm
4a	1.22-1.73 (m, 4H, CH ₂), 2.15 (s, 3H, CH ₃), 3.74 (s, 3H, CH ₃), 6.68-7.58 (m, 7H, CH), 7.70 (s, 1H, NH, urea), 8.79 (s, 1H, NH, sec. amide)
4b	1.39-1.86 (m, 10H, CH ₂), 2.22 (s, 3H, CH ₃), 3.38 (s, 3H, CH ₃), 6.16-6.77 (m, 3H, CH, indole), 7.43-7.64 (m, 4H, CH, benzene), 7.83 (s, 1H, NH, urea), 8.95 (s, 1H, NH, sec. amide)
4c	1.08 (s, 3H, CH ₃), 1.42-1.95 (m, 8H, CH ₂ , cyclohexane), 2.29 (s, 3H, CH ₃), 2.47 (s, 2H, CH, cyclohexane), 3.30 (s, 2H, CH ₂), 3.76 (s, 3H, CH ₃), 6.18-6.73 (m, 3H, CH, indole), 7.42-7.68 (m, 4H, CH, benzene), 7.87 (s, 1H, NH, urea), 9.10 (s, 1H, NH, sec. amide)
4d	1.11 (s, 3H, CH ₃), 1.54 (s, 1H, CH, cyclohexane), 1.38-1.89 (m, 8H, CH ₂ , cyclohexane), 2.33 (s, 3H, CH ₃), 3.35 (s, 2H, CH ₂), 3.82 (s, 3H, CH ₃), 6.29-6.81 (m, 3H, CH, indole), 7.48-7.76 (m, 4H, CH, benzene), 7.94 (s, 1H, NH, urea), 10.2 (s, 1H, NH, sec. amide)
4e	1.85 (s, 3H, CH ₃), 2.23 (s, 3H, CH ₃), 3.55 (s, 2H, CH ₂), 3.74 (s, 3H, CH ₃), 6.56-7.02 (m, 7H, CH), 7.49 (m, 5H, CH), 7.71 (s, 1H, NH, urea), 8.84 (s, 1H, NH, sec. amide)
4f	2.25 (s, 3H, CH ₃), 2.49 (s, 2H, CH ₂ , indane), 3.02 (s, 2H, CH ₂ , indane), 3.43 (s, 2H, CH ₂), 6.68-6.91 (m, 3H, CH, indole), 7.24-7.36 (m, 4H, CH, indane), 7.41-7.63 (m, 4H, CH, benzene), 7.87 (s, 1H, NH, urea), 8.58 (sec. amide)
4g	1.51 (s, 2H, CH ₂ , 1,2,3,4-tetrahydronaphthalene), 1.72 (s, 3H, CH ₃), 2.07 (s, 2H, CH ₂ , 1,2,3,4-tetrahydronaphthalene), 2.73 (s, 2H, CH ₂ , 1,2,3,4-tetrahydronaphthalene), 3.01 (s, 2H, CH ₂), 3.75 (s, 3H, CH ₃), 6.13-6.92 (m, 3H, CH, indole), 6.95-7.15 (m, 4H, CH, 1,2,3,4-tetrahydronaphthalene), 7.20-7.61 (m, 4H, CH, benzene), 7.94 (s, 1H, NH, urea), 8.99 (s, 1H, NH, sec. amide)

Table 4 - continuation.

N₂	¹H NMR (DMSO-<i>d</i>₆), δ / ppm
4h	2.15 (s, 3H, CH ₃), 3.27 (s, 2H, CH ₂), 3.76 (s, 3H, CH ₃), 6.22-6.71 (m, 3H, CH, indole), 7.39-7.47 (m, 4H, CH, benzene), 7.31-7.88 (m, 8H, CH, fluorene), 8.11 (s, 1H, NH, urea), 9.8 (s, 1H, NH, sec. amide)
	¹³C NMR (DMSO-<i>d</i>₆), δ / ppm
4a	191.1 (C=O), 175.7 (C=O, amide), 168.4 (C=O, spirohyd. ring), 156.1 (C=O, spirohyd. ring), 138.1 (CH, indole), 136.1 (CH, indole), 134.5 (CH, benzene), 129.3 (CH, benzene), 113.3 (CH, indole), 66.5 (spiro C-atom), 55.8 (CH ₃), 29.2 (CH ₂), 25.8 (CH ₂), 25.1 (CH ₂), 13.7 (CH ₃)
4b	189.9 (C=O), 176.6 (C=O, amide), 165.7 (C=O, spirohyd. ring), 156.4 (C=O, spirohyd. ring), 132.2 (CH, benzene), 139.6 (CH, benzene), 114.4 (CH, indole), 108.3 (CH, indole), 104.9 (CH, indole), 62.4 (spiro C-atom), 56.3 (CH ₃), 33.1 (CH ₂ , cyclohexane), 29.2 (CH ₂ , cyclohexane), 26.9 (CH ₂ , cyclohexane), 19.8 (CH ₂ , cyclohexane), 13.4 (CH ₃)
4c	192.3 (C=O), 178.6 (C=O, amide), 167.6 (C=O, spirohyd. ring), 158.2 (C=O, spirohyd. ring), 132.6 (CH, benzene), 129.6 (CH, benzene), 114.3 (CH, indole), 108.3 (CH, indole), 104.5 (CH, indole), 69.1 (spiro C-atom), 58.8 (CH ₃), 35.4 (CH, cyclohexane), 30.8 (CH ₂ , cyclohexane), 27.2 (CH ₂ , cyclohexane), 25.3 (CH ₂ , cyclohexane), 20.5 (CH ₂ , cyclohexane), 17.4 (CH ₂), 13.2 (CH ₃)
4d	195.2 (C=O), 178.6 (C=O, spirohyd. ring), 171.3 (C=O, amide), 158.2 (C=O, spirohyd. ring), 133.4 (CH, benzene), 130.6 (CH, benzene), 115.4 (CH, indole), 110.1 (CH, indole), 105.7 (CH, indole), 64.1 (spiro C-atom), 58.3 (CH ₃), 31.6 (CH ₂ , cyclohexane), 29.4 (CH ₂), 28.6 (CH, cyclohexane), 26.4 (CH ₂ , cyclohexane), 19.3 (CH ₃), 14.1 (CH ₃)
4e	188.1 (C=O), 172.6 (C=O, amide), 168.4 (C=O, hyd. ring), 156.1 (C=O, hyd. ring), 138.1 (CH, indole), 135.6 (CH, indole), 134.6 (CH, benzene), 131.6 (CH, benzene), 131.2 (CH, benzene), 130.6 (CH, benzene), 115.0 (CH, benzene), 111.7 (CH, indole), 68.3 (C), 55.8 (CH ₃), 29.9 (CH ₂), 25.3 (CH ₃), 13.6 (CH ₃)
4f	190.5 (C=O), 172.3 (C=O, amide), 167.9 (C=O, spirohyd. ring), 158.2 (C=O, spirohyd. ring), 132.3 (CH, benzene), 130.6 (CH, benzene), 129.5 (CH, indane), 126.3 (CH, indane), 115.5 (CH, indole), 108.3 (CH, indole), 106.1 (CH, indole), 68.5 (spiro C-atom), 55.8 (CH ₃), 32.1 (CH ₂ , indane), 25.8 (CH ₂ , indane), 24.8 (CH ₂ , aliph.), 13.7 (CH ₃)
4g	189.6 (C=O), 174.1 (C=O, amide), 168.4 (C=O, spirohyd. ring), 157.8 (C=O, spirohyd. ring), 138.2 (CH, benzene), 136.1 (CH, benzene), 134.5 (CH, 1,2,3,4-tetrahydronaphthalene), 131.7 (CH, 1,2,3,4-tetrahydronaphthalene), 130.7 (CH, indole), 129.5 (CH, indole), 112.3 (CH, indole), 65.2 (spiro C-atom), 55.8 (CH ₃), 39.6 (CH ₂ , 1,2,3,4-tetrahydronaphthalene), 39.4 (CH ₂ , 1,2,3,4-tetrahydronaphthalene), 29.5 (CH ₂ , 1,2,3,4-tetrahydronaphthalene), 27.6 (CH ₂), 13.7 (CH ₃)
4h	192.6 (C=O), 171.3 (C=O, amide), 168.2 (C=O, spirohyd. ring), 158.4 (C=O, spirohyd. ring), 132.3 (CH, benzene), 130.1 (CH, benzene), 129.2 (CH, fluorene), 128.4 (CH, fluorene), 127.1 (CH, fluorene), 125.9 (CH, fluorene), 113.3 (CH, indole), 108.4 (CH, indole), 104.3 (CH, indole), 67.2 (spiro C-atom), 56.6 (CH ₃), 29.4 (CH ₂), 12.8 (CH ₃)
	¹³C DEPT 135 (DMSO-<i>d</i>₆), δ / ppm
4a	138.1 (CH, indole), 136.1 (CH, indole), 134.5 (CH, benzene), 129.3 (CH, benzene), 113.3 (CH, indole), 55.8 (CH ₃), 29.2 (CH ₂), 25.8 (CH ₂), 25.1 (CH ₂), 13.7 (CH ₃)
4b	132.2 (CH, benzene), 139.6 (CH, benzene), 114.4 (CH, indole), 108.3 (CH, indole), 104.9 (CH, indole), 56.3 (CH ₃), 33.1 (CH ₂ , cyclohexane), 29.2 (CH ₂ , cyclohexane), 26.9 (CH ₂ , cyclohexane), 19.8 (CH ₂ , cyclohexane), 13.4 (CH ₃)
4c	132.6 (CH, benzene), 129.6 (CH, benzene), 114.3 (CH, indole), 108.3 (CH, indole), 104.5 (CH, indole), 58.8 (CH ₃), 35.4 (CH, cyclohexane), 30.8 (CH ₂ , cyclohexane), 27.2 (CH ₂ , cyclohexane), 25.3 (CH ₂ , cyclohexane), 20.5 (cyclohexane), 17.4 (CH ₂), 13.2 (CH ₃)
4d	133.4 (CH, benzene), 130.6 (CH, benzene), 115.4 (CH, indole), 110.1 (CH, indole), 105.7 (CH, indole), 58.3 (CH ₃), 31.6 (CH ₂ , cyclohexane), 29.4 (CH ₂), 28.6 (CH, cyclohexane), 26.4 (CH ₂ , cyclohexane), 19.3 (CH ₃), 14.1 (CH ₃)
4e	138.1 (CH, indole), 135.6 (CH, indole), 134.6 (CH, benzene), 131.6 (CH, benzene), 131.2 (CH, benzene), 130.6 (CH, benzene), 115.0 (CH, benzene), 111.7 (CH, indole), 55.8 (CH ₃), 29.9 (CH ₂), 25.3 (CH ₃), 13.6 (CH ₃)
4f	132.3 (CH, benzene), 130.6 (CH, benzene), 129.5 (CH, indane), 126.3 (CH, indane), 115.5 (CH, indole), 108.3 (CH, indole), 106.1 (CH, indole), 55.8 (CH ₃), 32.1 (CH ₂ , indane), 25.8 (CH ₂ , indane), 24.8 (CH ₂ , aliph.), 13.7 (CH ₃)

Table 4 - continuation.

№	¹ H NMR (DMSO-d ₆), δ / ppm
4g	138.2 (CH, benzene), 136.1 (CH, benzene), 134.5 (CH, 1,2,3,4-tetrahydronaphthalene), 131.7 (CH, 1,2,3,4-tetrahydronaphthalene), 130.7 (CH, indole), 129.5 (CH, indole), 112.3 (CH, indole), 55.8 (CH ₃), 39.6 (CH ₂ , 1,2,3,4-tetrahydronaphthalene), 39.4 (CH ₂ , 1,2,3,4-tetrahydronaphthalene), 29.5 (CH ₂ , 1,2,3,4-tetrahydronaphthalene), 27.6 (CH ₂), 13.7 (CH ₃)
4h	132.3 (CH, benzene), 130.1 (CH, benzene), 129.2 (CH, fluorene), 128.4 (CH, fluorene), 127.1 (CH, fluorene), 125.9 (CH, fluorene), 113.3 (CH, indole), 108.4 (CH, indole), 104.3 (CH, indole), 56.6 (CH ₃), 29.4 (CH ₂), 12.8 (CH ₃)

CONCLUSIONS

Indomethacin derivatives with 3-amino-1,3-diazaspiro[4.4]nonane-2,4-dione, 3-amino-1,3-diazaspiro[4.5]decane-2,4-dione, 3-amino-6-methyl-1,3-diazaspiro[4.5]decane-2,4-dione, 3-amino-8-methyl-1,3-diazaspiro[4.5]decane-2,4-dione, 3-amino-5-methyl-5-phenylimidazolidine-2,4-dione, 1-amino-2',3'-dihydro-2*H*,5*H*-spiro[imidazolidine-4,1'-indene]-2,5-dione, 1-amino-3',4'-dihydro-2*H*,2'*H*,5*H*-spiro [imidazolidine-4,1'-naphthalene]-2,5-dione and 1'-aminospiro[fluorene-9,4'-imidazolidine]-2',5'-dione were successfully synthesized. The structures of the amides obtained were proven by physicochemical parameters, FTIR-ATR, Raman, ¹H and ¹³C NMR spectroscopy.

REFERENCES

1. E. Naydenova, N. Pencheva, J. Popova, N. Stoyanov, M. Lazarova, B. Aleksiev, *Il Farmaco.*, 189 (2002).
2. P. Marinova, M. Marinov, Y. Feodorova, M. Kazakova, D. Georgiev, V. Lekova, P. Penchev, N. Stoyanov, *C. R. Acad. Bulg. Sci.*, **67**, 513 (2014).
3. M. Marinov, E. Naydenova, R. Prodanova, N. Markova, P. Marinova, I. Kostova, I. Valcheva, D. Draganova, M. Naydenov, P. Penchev, N. Stoyanov, *Agric. Sci.*, **19**, 117 (2016).
4. M. Marinov, I. Kostova, E. Naydenova, R. Prodanova, P. Marinova, P. Penchev, N. Stoyanov, *Univ. of Ruse "Angel Kanchev" Proc.*, **54** (10.2), 62 (2015).
5. H. T. Bucherer, V. A. Lieb, *J. Prakt. Chem.*, **141**, 5 (1934).
6. H. T. Nagasawa, J. A. Elberling, F. N. Shirota, *J. Med. Chem.*, **16**, 823 (1973).
7. M. Marinov, P. Marinova, N. Stoyanov, N. Markova, V. Enchev, *Acta Chim. Slov.*, **61**, 420 (2014).
8. R. Sarges, R. C. Schnur, J. L. Belletire, M. J. Peterson, *J. Med. Chem.*, **31**, 230 (1988).
9. R. A. Wildonger, M. B. Winstead, *J. Med. Chem.*, **10**, 981 (1967).
10. J. C. Sheehan, G. P. Hess, *J. Am. Chem. Soc.*, **77**, 1067 (1955).

СИНТЕЗ НА НОВИ ИНДОМЕТАЦИНОВИ ПРОИЗВОДНИ С 3-АМИНОСПИРОХИДАНТОИНИ И 3-АМИНО-5-МЕТИЛ-5-ФЕНИЛИМИДАЗОЛИДИН-2,4-ДИОН

М. Н. Маринов¹, Е. Д. Найденова^{2*}, Р. Й. Проданова¹, С. Х. Цонева³, Н. М. Стоянов⁴

¹Аграрен университет – Пловдив, Факултет по растителна защита и агроекология, Катедра „Обща химия“, 4000 Пловдив, бул. „Менделеев“ 12, България

²Химикотехнологичен и металургичен университет, Катедра „Органична химия“, 1756 София, бул. „Климент Охридски“ 8, България

³Пловдивски университет, Химически факултет, Катедра „Аналитична химия и компютърна химия“, 4000 Пловдив, ул. „Цар Асен“ 24, България

⁴Русенски университет „Ангел Кънчев“, Филиал – Разград, Катедра „Химия и химични технологии“, 7200 Разград, бул. „Априлско въстание“ 47, България

Постъпила на 07 октомври, 2016 г.; Коригирана на 25 януари, 2017 г.

(Резюме)

Статията представя синтез на нови амиди, основан на взаимодействието на серия от 3-аминоспирохидантоини и 3-амино-5-метил-5-фенилимидазолидин-2,4-дион с Индометацин. Целевите съединения бяха получени с цел разработване на нови продукти с противовъзпалителни свойства. Структурите на всички получени амиди бяха потвърдени чрез физикохимични параметри, FTIR-ATR, Раманова, ¹H и ¹³C ЯМР спектроскопия.

Pharmacological and toxicological investigations of newly synthesized benzazepine derivatives comprising peptide fragment

I.I. Kostadinova^{1*}, N.D. Danchev¹, I.N. Nikolova¹, L.T. Vezekov², Tch.B. Ivanov², M.G. Georgieva²

¹Department of Pharmacology, Pharmacotherapy and Toxicology, Faculty of Pharmacy, Medical University - Sofia, 2 Dunav Str, 1000 Sofia (Bulgaria)

²University of Chemical Technology and Metallurgy - Sofia, 8 Kl. Ohridski Blvd, 1756 Sofia (Bulgaria)

Received October 25, 2016 ; Revised February 20, 2017

In the present study, we investigated the toxicological and pharmacological effects of four benzazepine derivatives comprising modified dipeptides holding the residue of the N-(3, 4-dichlorophenyl)-D,L-Ala-OH. The newly synthesized compounds were tested for acute intraperitoneal toxicity (LD₅₀), potential antidepressant activity and for improvement of cognitive function in mice. The results indicated that one of the newly synthesized compounds showed lower toxicity (3 times) and antidepressant activity in forced swim test in comparison with the reference substance Mirtazapine. The compounds didn't reverse scopolamine-induced memory deficit in mice and this result indicated lack of cholinergic activity.

Key words: benzazepine derivatives, Alzheimer's disease, depression, mirtazapine, mice.

INTRODUCTION

Psychiatric disturbances affect as many as 90% of patients with Alzheimer's disease (AD) and are a major focus of treatment. Depression is one of the most frequent psychiatric complications of AD, affecting as many as 50% of patients. In this context, depression is a significant public health problem that has a serious consequences for patients and their caregivers [1].

Identifying depression in someone with Alzheimer's can be difficult, since dementia can cause some of the same symptoms. Examples of symptoms common to both depression and dementia include: apathy, loss of interest in activities and hobbies, social withdrawal, isolation, trouble concentrating, impaired thinking [2].

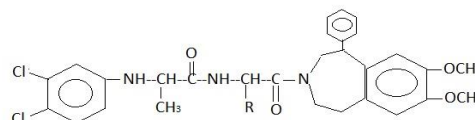
The present study is devoted to the pharmacological and toxicological investigations of newly synthesized benzazepine derivatives including dipeptide residue. In order to evaluate the most active compounds we use standard tests for antidepressant activity and memory-induced deficit in animals.

MATERIALS AND METHODS

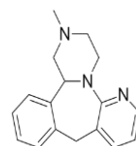
Compounds

The investigated compounds (synthesized in University of Chemical Technology and

Metallurgy-Sofia) comprise benzazepine heterocycle, connected with N-(3,4-dichlorophenyl)-D,L-Ala-OH [3] Scheme 1.



R= 1) -CH₂CH(CH₃)₂, 2) -H, 3) -CH(CH₃)₂, 4) -CH₂C₆H₅



Mirtazapine

Scheme 1. Chemical structure of new compounds and reference compound mirtazapine.

Treatment solutions

Test compounds were homogenized with 1-2 drops of Tween 80, dissolved in distilled water and administered intraperitoneally (i.p.) in dose 1/20 part of LD₅₀ in forced swim and passive avoidance tests – compound 1 in dose 54 mg/kg, compound 2 in dose 48 mg/kg, compound 3 in dose 71 mg/kg, compound 4 in dose 82,5 mg/kg. The reference compound mirtazapine was also dissolved in distilled water and administered intraperitoneally in dose of 5 mg/kg. Compounds were administered in a volume of 10 ml/kg body weight. The newly synthesized compounds are with similar molecular weights (between 556 and 645 g/mol).

* To whom all correspondence should be sent:

E-mail: vanq_don25@abv.bg

Animals

Male albino mice line H, 25-32 g body weight. The animals were housed according GLP instruction of animal care, water and food being supplied ad libitum; animal room temperature 22 ± 3 °C; humidity 30 %; lighting schedule 12 h light/dark cycle. Animals were trained and tested during light part of the cycle. The studies were approved by the Institutional Animal Care Committee at the Medical University of Sofia, Bulgaria.

Toxicity test

The newly synthesized compounds were tested for acute intraperitoneal toxicity (LD_{50}). The acute toxicity (LD_{50}) was estimated by OECD-425 FDA method on male mice (12-15 mice per studied compound), line H, weight 25-30 g and the data are presented as mg/kg body weight [4].

Forced swim test

In a single session, mice (8 per group) are forced to swim in a narrow cylinder from which they cannot escape - 13 cm in diameter and 24 cm high, containing water (22°C) to 10 cm. Thirty minutes after intraperitoneal administration of the tested compound, the animals are placed in water containing cylinders and their behavior was observed for 6 minutes [5].

From the second minute onward, immobility of each mouse is recorded.

Scopolamine-induced amnesia in mice

The scopolamine test is performed in groups of 6 male mice weighing 25-32 g in a one-trial, passive avoidance paradigm. Thirty minutes after i.p. administration of 3 mg/kg scopolamine hydrobromide, each mouse is individually placed in the bright part of a two-chambered apparatus for training (Gemini Avoidance System, San Diego, California). After a brief orientation period, the mouse enters the second darker chamber. Once inside the second chamber, the door is closed which prevents the mouse from escaping, and a 1 mA, 3-s foot shock is applied through the grid floor. The mouse is then returned to the home cage. Twenty-four hours later, testing is performed by placing the animal in the bright chamber. The latency time in seconds for entering the second darker chamber within a 5 min test session is measured electronically. The test compounds were administered 90 min before training. A prolonged latency indicates that the animal remembers that it

has been punished and, therefore, does avoid the darker chamber [6].

STATISTICAL ANALYSES

The data were processed on personal computer using standard Student t-test.

RESULTS AND DISCUSSION

The newly synthesized compounds are less toxic after i.p. administration than reference substance mirtazapine with LD_{50} values between 958 and 1650 mg/kg body weight (Figure 1).

The results showed that compounds 1, 2 and 3 decrease the duration of immobility in forced swim test in mice. There is significant difference between mirtazapine group treated with 5mg/kg and group of compound 2 with dose 48 mg/kg (Figure 2, $p < 0.05$).

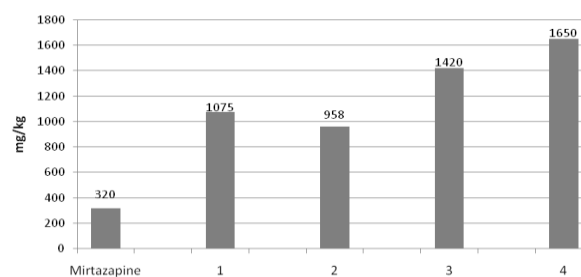


Fig. 1. Comparison between LD_{50} values of mirtazapine and newly synthesized compounds

The results showed that single administration of scopolamine (3 mg/kg, i.p.) impaired memory processes which is demonstrated with decrease in latency time. Compounds 1-4 didn't reverse scopolamine-induced memory impairment and didn't cause statistically significant increase in step-trough latency in comparison with the control group.

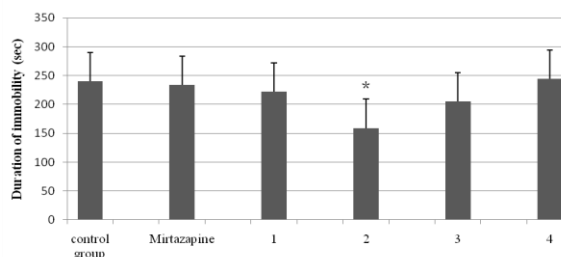


Fig. 2. The effects of compounds on the duration of immobility in the forced swim test in mice (n=8). * $p \leq 0,05$ (two tailed Student t-test)

Compounds 2, 3 and 4 prolonged latency times in comparison with mirtazapine (Figure 3). Acquisition trial is the first trial before administration of scopolamine and compounds. On

the second day the trial is conducted 30 minutes after scopolamine administration in dose 3 mg/kg i.p. and the retention trial is on the third day 24 h after scopolamine and 90 min after i.p. administration of compounds. For control group were performed only acquisition trial on the first day and retention trial on the second day.

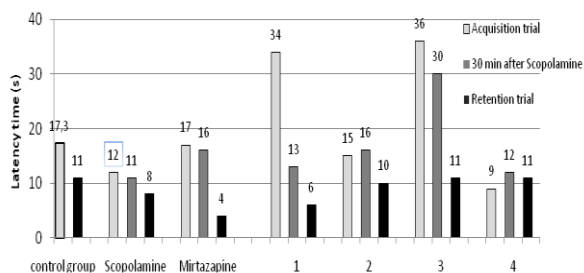


Fig. 3. Effects of investigated compounds and mirtazapine on scopolamine-induced memory deficit on passive avoidance task (n=6)

Mirtazapine is an atypical antidepressant, centrally active presynaptic alpha 2-antagonist, which increases central noradrenergic and serotonergic neurotransmission. The enhancement of serotonergic neurotransmission is specifically mediated via 5-HT₁ receptors, because 5-HT₂ and 5-HT₃ receptors are blocked by mirtazapine. Both enantiomers of mirtazapine are presumed to contribute to the antidepressant activity, the S(+) enantiomer by blocking α 2 and 5-HT₂ receptors and the R(-) enantiomer by blocking 5-HT₃ receptors.

The histamine H₁-antagonistic activity of mirtazapine is responsible for its sedative properties. Mirtazapine is generally well tolerated. It has practically no anticholinergic activity and, at therapeutic doses, has practically no effect on the cardiovascular system [7].

Mirtazapine was used as a reference substance in acute toxicity, forced swim and passive avoidance experiments because of benzazepine ring, which is reason for chemical similarity to newly synthesized compounds.

Many of the primary symptoms of depression (depressed mood, low self-esteem, guilt, difficulty in concentration, suicidal ideation, thoughts of death) are by their nature difficult to model in animals. This problem is further confounded by their unknown etiology. Most theories of depression concur in suggesting that stressful life events play an important role [8].

The first tests for screening antidepressants were based on pharmacological interactions. The most common of these was reserpine antagonism. Not only had reserpine sometimes been associated with the induction of depression in humans, it also was

known to cause depletion of neuronal stores of monoamines. It was effective in detecting antidepressants with mechanisms of action similar to those already in clinical use (inhibitors of monoamine uptake and metabolism), thereby demonstrating the predictive validity of reserpine antagonism.

The advent of atypical antidepressants, such as iprindole and mianserin, that showed little or no activity in these tests, necessitated the search for new screens that were not based on pharmacological interactions. One of the earliest was the forced swim or “behavioral despair” test, in which rodents become immobile when forced to swim in a restricted space from which there is no exit [5]. During the past 20 years, the behavioral despair test, in both rats and mice, has become one of the most widely used antidepressant screens in experimental pharmacology [9].

The forced swim and tail suspension procedures are best viewed as simple tests for antidepressants rather than as models of depression, because the dependent variable (immobility) is a direct reaction to the test itself and does not persist outside the test situation. There is no obvious induction of a “depressive state,” although there are elements of construct validity (stressful inducing conditions, decreased behavioral output). Rodents forced to swim in a narrow space from which there is no escape adopt, after an initial period of vigorous activity become a characteristic immobile posture, moving only when necessary to keep their heads above the water. The animals’ immobility was hypothesized to show they had learned that escape was impossible and had given up hope. Immobility was therefore given the name “behavioral despair.” It was subsequently found that immobility could be reduced by a wide range of clinically active antidepressant drugs. This simple behavioral procedure has since become a useful test for screening novel antidepressants [5].

There is a data that in Porsolt test mirtazapine showed decreased immobility time, but only after a 14 days treatment [10].

The administration of antimuscarinic agent to young human volunteers produces transient memory deficits [11]. Analogously, scopolamine has been shown to impair memory retention when given to mice shortly before training in a dark avoidance task [12]. The ability of a range of different cholinergic agonists to reverse the amnesic effects of scopolamine are well documented [13].

Disruption of cognitive performance by antidepressants has been documented for the

tricyclics, and occasionally observed with other compounds such as fluoxetine. The antidepressant mirtazapine has been reported to induce less disruption in tests of psychomotor performance than classical antidepressants in both man and rats. The potential advantage of mirtazapine over other antidepressants in sparing cognitive function was investigated using an autoshaping task. The effects of mirtazapine were compared with a number of clinically available antidepressant drugs: imipramine, amitriptyline, desipramine and fluoxetine. The results showed that, in rats, mirtazapine is less likely to interfere with some aspects of cognition, in this case the ability to acquire and use new information [14].

Acute LD₅₀ of mirtazapine is 600-720 mg/kg in mice after oral administration [15] and 320 mg/kg after i.p. administration which indicate that this compound is slight toxic. New compounds are 3 to 5 times less toxic than standard after intraperitoneal administration.

CONCLUSION

Our results indicates that the most perspective is compound 2, which possess low toxicity (958 mg/kg) after i.p. administration in mice, reduce immobility in forced swim test in comparison with control group, mirtazapine and other compounds. Compound 2 and other newly synthesized compounds didn't reverse scopolamine induced memory impairment and this result indicates that compounds didn't possess cholinergic activity.

ФАРМАКОЛОГИЧНИ И ТОКСИКОЛОГИЧНИ ИЗСЛЕДВАНИЯ НА НОВОСИНТЕЗИРАНИ БЕНЗАЗЕПИНОВИ ПРОИЗВОДНИ С ПЕПТИДЕН ФРАГМЕНТ

И.И. Костадинова^{1*}, Н.Д. Данчев¹, И.Н. Николова¹, Л.Т. Везенков², Ч. Иванов, М.Г. Георгиева²

¹ Катедра по фармакология, фармакотерапия и токсикология, Фармацевтичен факултет, ул. „Дунав“ 2, 1000 София (България)

² Химикотехнологичен и металургичен университет, бул. „Климент Охридски“ 8, 1756 София (България)

Постъпила на 25 октомври, 2016 г.; Коригирана на 20 февруари, 2017 г.

(Резюме)

В настоящото експериментално проучване, представяме токсикологичните и фармакологични ефекти на четири бензазепинови производни, съдържащи модифицирани дипептиди с N-(3,4-дихлорофенил)-D,L-Ala-OH в N-края. На съединенията беше определена остра интраперитонеална токсичност (LD₅₀), потенциалната антидепресивна активност и влиянието върху когнитивните функции на мишки. Резултатите показват, че едно от новосинтезираните съединения показва по-ниска токсичност (3 пъти) и антидепресивна активност в доза 48 мг/кг телесно тегло при теста за принудително плуване (forced swim test) спрямо референтното вещество Миртазапин. Съединенията не премахват скополамин-индуцирания паметов дефицит при мишки, което говори за липса на холинергична активност.

REFERENCES

1. C.G. Lyketsos, J. Olin, *Biol. Psych.*, **52**, 243 (2002).
2. <https://www.alz.org/care/alzheimers-dementia-depression.asp>
3. M. Georgieva, L. Vezenkov, Tch. Ivanov, G. Ivanova, *Proc. Bulg. Acad. Sci.*, **57**, № 9, 13-18, (2004).
4. <https://www.epa.gov/pesticide-science-and-assessing-pesticide-risks/acute-oral-toxicity-and-down-procedure>
5. V. Castagne, P. Moser, S. Roux, R. Porsolt, *Curr. Protoc. Pharmacol.*, **49**, 5.8.1 (2010).
6. H. G. Vogel (Ed.), *Drug Discovery and Evaluation*, Second edition, Springer-Verlag, Berlin Heidelberg, 623, (2002).
7. *Mirtazapine 30 mg Tablets, SPC, Public Assessment Report, Medicines and Healthcare products Regulatory Agency, UK (2006)*
8. O.Berton, E.J. Nestler, *Nat. Rev. Neurosci.*, **7**, 137-151, (2006).
9. F. Borsini, A. Meli, *Psychopharmacology*, **94**, 147 (1988).
10. E. Nowakowska, A. Chodera, K. Kus, A. Massakowska, *Pol J Pharmacol.*, **51**(6), 463, (1999).
11. D.A. Drachman, J. Leavitt, *Arch. Neurol.*, **30**, 113, (1974).
12. S.L. Dilts, C.A. Berry, *J Pharmcol. Exp. Ther.*, **158**, 279, (1976).
13. S. D. Iversen, *Behavioural Naunyn-Schmiedeberg's Arch. Pharmacol.*, **358**(12), R 371 (1998).
14. J.S. Andrews, S. Bloks, J.H.M. Jansen, *Biol. Psych.*, **42**, 238 (1997).
15. <http://www.drugbank.ca/drugs/DB00370>

In silico investigation of single-chain variable fragment (scFv) antibody, structurally similar to native C1q globular heads

M.A. Rangelov^{1*}, N.H. Todorova², I.G. Tsacheva^{3*}

¹ Institute of Organic Chemistry with Centre of Phytochemistry (IOCCP), Bulgarian Academy of Sciences, Acad. G. Bontchev str. bl. 9, 1113 Sofia, Bulgaria

² Institute of Biodiversity and Ecosystem Research (IBER), Bulgarian Academy of Sciences, Yurii Gagarin Str.2, 1113 Sofia, Bulgaria

³ Biology Faculty, Sofia University "St. Kliment Ohridski", 8 Dragan Tsankov Blv., 1164 Sofia, Bulgaria

Received September 29, 2016; Revised February 04, 2017

Homology model of a selected single-chain variable fragment (scFv) inhibitory antibody A1 is generated using Generalized Born/Volume Integral (GB/VI) methodology and MMFF94 force field. Comparative analysis of scFvA1 homology model and ghC1q chains is further used to find conformational and electrostatic similar regions, crucial for the biological binding regions in C1q globular heads.

Key words: homology modeling, anti-C1q scFv

INTRODUCTION

Phage-displayed single-chain variable fragment (scFv) antibodies obtain serious advantages that make them preferable tool for application in research, laboratory diagnostics and medicine. Recent progress in antibody engineering together with the microbial expression systems are milestones for design and production of antibodies for numerous applications [1]. Variety of selection and screening strategies could be used to simultaneously derive many high-affinity scFv with different relevance [2]. Importance of their diverse collection relies on high specificity and selectivity of antibodies, while offering distinct biological profiles in tissue distributions of unique molecules [3].

C1q is the recognizing first subcomponent of the classical complement pathway, which undergo a conformation transition by its activation, exposing neo-epitopes. Naive phage library is used to create a single-chain variable fragment (scFv) antibody, that mimics the globular head regions of native C1q (ghC1q). It is further used in *in-silico* modelling to characterise crucial for biological binding regions in C1q globular heads.

EXPERIMENTAL

scFv A1 construction and sequencing

'Griffin' library, provided by Greg Winter, MRC, Cambridge, UK, is used to create large, nonimmunized fully human scFv repertoires [4],

* To whom all correspondence should be sent:
E-mail: marangelov@gmail.com

with high specificity of binding to human self-antigens [5]. This kind of library construction of naturally rearranged V genes in a phagemid vector ensures natural diversity in length of the VH CDR3 and a higher number of functional scFv [2]. ScFv A1, showing functional mimicry with only to the globular head region of C1q, is obtained after several panning rounds. pHEN2 region, containing genes for scFv A1 is amplified by using *in-situ* polymerase chain reaction (PCR) of the *Escherichia coli* clone and primers LMB3 (5'-CAGGAAACAGCTATGAC-3') and fd-SEQ1 (5'-GAATTTTCTGTATGAGG-3'), using amplification program of Liners *et al.* 2005 [6]. The product is purified and further send for *iboth* sides sequencing (Macrogen Europe). Derived sequence is deposited in GenBank under accession number KX981596.

Homology Search

Searches for protein structures that are homologous to a query sequence are performed on a database of protein structures and sequences that have been clustered into families. A scan is performed to create an initial list of candidates using a generalized version of the FASTA methodology [7]. Expectation value (E-Value) is determined for each sequence and low E-Values, that correspond to good scores were used as evaluation criteria.

Homology Model of scFv A1

We performed alignment of the target sequence to the selected parts of best scored selected proteins according to the modified version of Needleman

and Wunsch algorithm [8] with sequence alignment imposed on amino acid BLOSUM 62 substitution matrix. Homology Model is carried out by Boltzmann-weighted randomized modeling procedure using coulomb and generalized Born implicit solvent [9] interaction energies. Best models were further refined by Merck Molecular Forcefield MMFF94 [10] for all energy minimization.

Comparative analysis of scFvA1 homology model and ghC1q chains

Sequence comparison of crystallized globular heads domains of human C1q, according to the 1PK6 PDB and H-chain of generated homology model of scFv A1 is performed, using secondary structure information of those sequences having associated atomic coordinates. The target sequence is sequence-to-group aligned to each one of ghC1q chains. Manual alignment is used for refining CDR frames of scFv A1 H-chain and loops in A-, B- and C- ghC1q.

RESULTS AND DISCUSSION

Sequence and structure similarity analysis

Analysis of the CDR3 regions of scFv clones from the library, both VH and VL, shows considerable variability in their length, which is similar to the distribution of the length of CDR3 in unselected library.

ScFv A1 nucleotide sequence is translated to amino acids (Fig. 1), compared to deposited germline V genes and most likely CDR regions in both VL and VH were predicted in VBASE2 [11]. Heavy chain V segment is of the IGHV4 family, while the one of the light chain used IGKV1 subgroup. No J-segment is discovered in the VL, but the junction in VH participated as expected in the CDR3 formation

The scFv A1 model

Sequence alignment is performed using MOE [12] software with database deposited scFv antibodies by BLOSUM 62 algorithm as substitution scoring matrix, with algorithm penalty for gap opening -12 and gap extension -2 and evaluated with E-value accepted $1.e^{-12}$. The first five hits (PDB ID: 1YNL, 1A5F, 1ETZ, 1DEE, 1AD9) showing statistically significant similarity, the most similar one having $E \sim 2.e^{-42}$, were chosen for further analysis (Fig. 2).

Further multiple sequence alignment determines the correspondences between residues of selected related protein chains employing *sequence-derived* and *structure-based* information. BLOSUM 62 substitution matrix is chosen as based on observed alignments and immunoglobulin superfamily having many specific members.

```

>Amino acid sequence of H-chain scFv A1
RCSSRSRGAGLLKPSETLSLTCVYGGSFSGYYWSWIRQPPGKGLEWIGEINHSGSTNYPNPSLKSRVT
ISVDTSKNQFSLKLSVTAADTAVYYCARSHSAAWQGTLVTVS

>Amino acid sequence of L-chain scFv A1
DIQLTQSPSFLSASVGDRTITCRASQGISSYLAWYQQKPGKAPKLLIYAASSTLQSGVPSRFSGSGSGT
EFTLTISLQPEDFATYHCQQLNSY

CDR analysis of H-chain scFv A1
GGSFSGYY...__INHSGST...__ARSHSAA
---CDR1---> <--CDR2--> <---CDR3----

CDR analysis of L-chain scFv A1
QGISSY.....__AAS.....__QQLNSY
---CDR1---> <--CDR2--> <---CDR3----
    
```

Fig. 1. ScFv A1 H- and L-chain amino acid sequence, derived from nucleotide sequence, using standard genetic code in VBASE2, with predicted CDR 1, 2 and 3 in H- and L-chains.

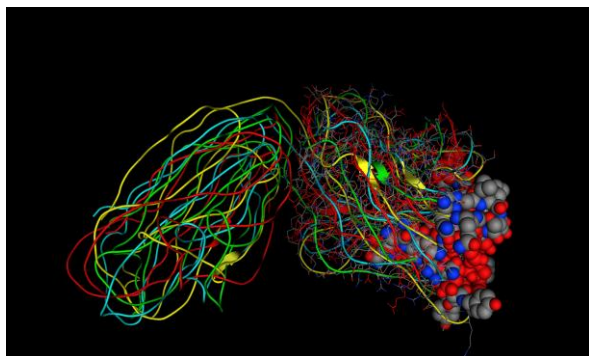


Fig. 2. Comparison of scFv VL and VH structure to high scored similar PDBs of crystallized antibodies, shown in different colors. CDR1, 2 and 3 of VH is visualized as CPK.

Homology model of scFv A1 is generated using Generalized Born/Volume Integral (GB/VI) methodology and MMFF94 force field (Fig. 3).



Fig. 3. Representation of the known 3D structure of crystallized antibodies in red and the generated model backbone of scFv A1 in color coding (yellow beta-structure, blue for loops).

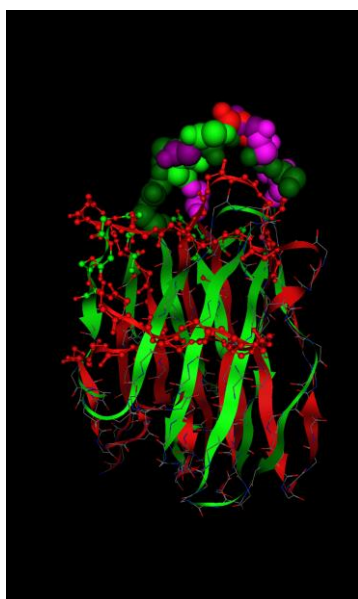


Fig. 4. CDR1 H-chain scFv A1 according to the model: GGSFSGYY dark color and A-chain of C1q: TTNKGLF; light color.

ScFv A1 H-chain and ghC1q comparison and loop similarity analysis

ScFv A1 CDR1, 2 and 3 were compared loop by loop with C1q separate chains loop. Similarity in using AA coding is: polar + and – separately; polar uncharged and nonpolar. Backbone is analyzed only as amino acid side chain (R) polarity due to the mobility of R in solution, and not as a chain position in the loop. The following color coding is formed according to amino acid R-chain properties analysis (Table 1):

Table 1. Good correlation of R polarity between C1q globular head chains and CDR loops of H-chain scFv A1 is achieved for B-chain and CDR2, A-chain and CDR1 and C-chain and CDR3.

CDR1	H		G	G	S	F	S	G	Y	Y	
Aclq	55-60	L	S	Q	W	E	I	C	L		
Bclq	82-91	D	Y	A	Y	N	T	F	Q	V	
Cclq	79	H	T	S	K	T	N	Q	V		
CDR2	H		I	N	H	S	G	S	T		
Aclq	121-128	D	A	E	S	G	Q	Y	I		
Bclq	116-123	G	N	E	G	A	N	S	I		
Cclq	56-63	A	S	H	T	A	N	L	C		
CDR3	H		A	R	S	H	S	A	A		
Aclq	81-88	T	T	N	K	G	L	F	Q		
Bclq	36-43	A	S	S	R	G	N	L	C		
Cclq	112-119	V	G	I	Q	G	S	D	S		

R,H,K -> positively charged in darker gray; D,E -> negatively charged in dark gray; S,T,N,Q,P,C -> polar uncharged (H-bonds) in gray; G,A,V,I,L,M,F,Y,W -> hydrophobic in light gray.

CONCLUSIONS

Based on the nucleotide sequence of an inhibitory scFv A1, a structural 3D model of resulting polypeptide chain is generated, as homology model according to alignment on the deposited crystallized scFv PDBs. The resulting structure is used to find conformational (Fig. 4) and electrostatic similar regions between homology structure and native human C1q globular heads. This similarity helps to clarify crucial recognising regions from C1q molecule. The presented model will be further helpful giving insights into new scFv binding properties that represent a step toward understanding the recognition mechanisms of C1q and their biological targets.

REFERENCES

1. Z.A. Ahmad, S.K. Yeap, A.M. Ali, W.Y. Ho, N.B.M. Alitheen, M. Hamid, *Clin Dev Immunol.*, **2012**, 1 (2012).
2. S. Lennard, Standard Protocols for the Construction of scFv Libraries, Vol. 178 Methods in Molecular Biology Series, Humana Press, Inc., Tutowa NJ, 2002.
3. A.L. Nelson, *Mabs*, **2**, 77 (2010).
4. A.S. Zlatarova, I. Tsacheva, M.S. Kojouharova, *Biotechnol. & Biotechnol. Eq.*, **19**, 2 (2005).

5. A.D. Griffiths, M. Malmqvist, J.D. Marks, J.M. Bye, M.J. Embleton, J. McCafferty, M. Baier, K.P. Holliger, B.D. Gorick, N.C. Hughes-Jones, H.R. Hoogenboom, G. Winter, *The EMBO Journal*, **12**, 725 (1993).
6. F. Liners, W. Helbert, P. Van Cutsem, *Glycobiology*, **15**, 849 (2005).
7. W. R. Pearson, *Meth. Enz.*, R. F. Doolittle, ed. (San Diego: Academic Press) **266**, 227 (1996).
8. S.B. Needleman, C.D. Wunsch, *Journal of Molecular Biology*, **48**, 443 (1970).
9. P. Labute, *J. Comp. Chem.*, **29**, 1693 (2008).
10. T.A. Halgren, *J. Comput. Chem.*, **17**, 490 (1996).
11. I. Retter, H.H. Althaus, R. Münch, W. Müller, *Nucleic Acids Res.*, **33** (Database issue), D671 (2005).
12. Molecular Operating Environment (MOE), 2011.10; Chemical Computing Group Inc., 1010 Sherbooke St. West, Suite #910, Montreal, QC, Canada, H3A 2R7, 2011.

In silico ИЗСЛЕДВАНЕ НА ЕДНОВЕРИЖНИ АНТИТЕЛА (scFv), СТРУКТУРНО ПОДОБНИ НА НАТИВНИТЕ ГЛОБУЛАРНИ ФРАГМЕНТИ НА C1q

М.А. Рангелов^{1*}, Н.Х. Тодорова², И.Г. Цачева^{3*}

¹ *Институт по органична химия с Център по фитохимия (ИОХЦФ), Българска академия на науките, ул. "Акад. Г. Бончев" бл. 9, 1113 София, България*

² *Институт по биоразнообразие и екосистемни изследвания (ИБЕИ), Българска Академия на Науките, ул. "Юрий Гагарин" 2, 1113 София, България*

³ *Биологически факултет, Софийски университет "Св. Климент Охридски", бул. "Драган Цанков" 8, 1164 София, България*

Постъпила на 29 септември 2016 г.; Коригирана на 4 февруари, 2017 г.

(Резюме)

Генериран е хомоложен модел на избрано едноверижно инхибиращо анти тяло (single-chain variable fragment (scFv) A1 посредством алгоритъма Generalized Born/Volume Integral (GB/VI) и MMFF94 силово поле. Анализирани са хомоложния модел на scFvA1 спрямо глобуларните фрагменти на C1q (ghC1q) резултатите от анализа са използвани за откриване на конформационни и електростатични региони на подобие, критични за биологичните функции на свързване в глобуларните региони на C1q.

Synthesis and FT-IR spectral elucidation of dipeptide with aromatic amino acid

T.E. Dzimbova¹, R.K. Georgiev², A.G. Chapkanov^{2*}

¹Institute of Molecular Biology, Bulgarian Academy of Sciences, 21 Acad. G.Bonchev str., 1113 Sofia (Bulgaria)

²South-West University "N. Rilski", 66 "I. Mihailov" Str., 2700 Blagoevgrad (Bulgaria)

Received October 04, 2016; Revised January 20, 2017

Small peptides can provide useful models for studying the interaction forces responsible for the structure and activity of larger proteins. One approach is to study small peptide by "protecting" the ends with groups that eliminate the functionality of the N and C terminus. The synthesis of dipeptide containing aromatic amino acid was carried out by well known procedures - method of mixed anhydrides was applied, where N-protected Phe and C-protected Ala react in the presence of Piv-Cl. The FT-IR- spectral analysis in solid state was used for characterization and elucidation of typical bands of the investigated compound. The obtained results for the IR-bands of amide C=O-NH fragments and other vibrations of the aromatic residues can be provides a structural information about the configuration of amide O=C-NH group in the peptide molecules and corresponding amide planes in the peptide molecules.

Key words: amino acids, dipeptide H-Phe-Ala-OH, IR - spectral analysis

INTRODUCTION

Phenylalanine is one of the twenty biologically naturally occurring amino acids that can be found in protein. It contains an amino group, a phenyl ring and a carboxylic group. It is an essential amino acid.

Small, biologically active peptides were first described about 40 years ago. Bioactive peptides are specific protein fragments, that have a positive impact on body functions or conditions and may ultimately influence on the health [1]. Upon oral administration, they may affect the major body systems - namely, the cardiovascular, digestive, immune and nervous systems, depending on their amino acid sequence. Essentially, these molecules play a hormonal role: they act at specific receptor sites at different locations in the organism. Mostly the peptides are transported from the site of release to the site of biological activity through the blood or lymphatic fluid.

Many studies of receptor binding have been carried out to determine the affinity and specificity of the peptides for the target cells. Different kinds of analysis have been undertaken to understand better the mechanisms of recognition, binding and signal triggering when the peptide interacts with the cellular surface. It became clear, that peptides might have tremendous potential for medical and pharmaceutical applications.

The short peptides are potential drug candidates for pharmaceutical and biotech industries. Synthetic short peptides are also extensively developed as

agonistic or antagonistic ligands, that function in a similar manner to antibodies, soluble receptors and protein ligands. Characterization of the peptides in solution is often performed in the presence of organic solvents, which can presumably generate the structure bound to the target surface and also enhance the solubility of the peptides [2].

There have been several spectroscopic studies on the behavior of many amino acids and peptides including phenylalanine and on complexes involving amino acids, organic molecules and metal ions [3–8]. Infrared spectroscopy is often used for obtaining both structural and conformational information from biological samples, especially proteins [9–14] and amino acids [15–18].

On the other hand, the possibilities of the IR- and especially IR-LD spectroscopy have been demonstrated in series of papers, dealing with the IR-characteristic band assignment and structural elucidation of small peptides [19–22]. As a part of these systematic study our aim is to be presented the synthesis of the dipeptide *L*-phenylalanyl-*L*-alanine (*H*-Phe-Ala-OH) and examination of the correlation IR-spectroscopic characteristics-structure of the dipeptide depicted in Fig. 1.

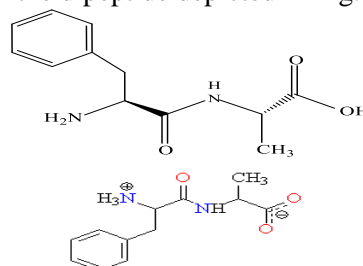


Fig. 1. Chemical diagram of the Phe-Ala-OH and zwitterionic structure.

* To whom all correspondence should be sent:

E-mail: chapkanov@swu.bg

EXPERIMENTAL

Synthesis

Boc-Phe-OH (1): Phenylalanine (1.7 g, 10 mM) was added to the solution of NaHCO_3 (0.9 g, 10.5 mM) in 25 ml water and was cooled to 0°C . A solution of Boc_2O (2.3 g, 10.5 mM) in 25 ml *i*-PrOH was added to this mixture. The reaction mixture was stirred for 24 hours at room temperature. The process was monitored by TLC CT_1 (CHCl_3 : MeOH : H_2O , 80 : 30 : 5). At the end of the process *i*-PrOH was evaporated, aqueous solution was acidified with dry NaHSO_4 to pH 3 and three extractions with EtOAc were made (3 x 30 ml). Combined organic layers were washed with saturated solution of NaCl, dried over Na_2SO_4 , filtered and EtOAc was evaporated. Pure Boc-Phe-OH crystallized on air and 2.5 g (98 %) was obtained.

HCl.Ala-OMe (2): 10 ml Methanol were cool to -10°C and SO_2Cl (2.9 ml, 40 mM) was added dropwise. After 5 min alanine (1.8 g, 20 mM) was added. The reaction was completed after 2 hours, methanol was evaporated and white crystal product (2.3 g (76 %) was obtained.

Boc-Phe-Ala-OMe (3): Boc-Phe-OH (1.5 g, 6 mM) and NMM (0.66 ml, 6 mM) were dissolved in THF (10 ml) and were cooled to -10°C . Piv-Cl (0.74 ml, 6 mM) was added carefully at this temperature. After 10 min a solution of HCl.Ala-OMe (0.9 g, 6 mM) in THF (10 ml) with Et_3N (0.9 ml, 6 mM) was added. The reaction completed after 24 hours. THF was evaporated under reduced pressure, residue was dissolved in EtOAc (30 ml) and was washed consequently with NaHCO_3 (3 x 30 ml), NaHSO_4 (3 x 30 ml), and water to pH 7. Organic layer was dried over Na_2SO_4 and EtOAc was evaporated. 1.1 g (53 %) was obtained.

Boc-Phe-Ala-OH (4): Fully protected dipeptide 3 (1.1 g, 3.1 mM) was dissolved in mixture of dioxane : water 1:1 (20 ml). A drop of methanol solution of thymolphthaleine was added and after that 1N NaOH was added dropwise until color of the solution (blue) remained constant. Dioxane was evaporated and aqueous solution was acidified with dry NaHSO_4 to pH 3. The dipeptide was obtained from aqueous solution with EtOAc extractions (3 x 20 ml). Combined organic layers were washed with water to pH 7, dried over Na_2SO_4 and EtOAc was evaporated. 0.8 g (73%) product was obtained.

Phe-Ala (5): Boc-Phe-Ala-OH (0.8 g, 2.5 mM) was dissolved in CH_2Cl_2 (2 ml) and TFA (1 ml) was added. The reaction completed in 1 hour at room

temperature. The solvent was evaporated and the crude product was purified by column purification.

Methods

The IR-spectra of the compound were recorded using a Thermo Scientific Nicolet iS10 FT-IR spectrometer ($4000 - 400 \text{ cm}^{-1}$) with ATR accessory. A spectral resolution of $\pm 4 \text{ cm}^{-1}$ was used and 64 scans were accumulated. The solid state IR spectra were recorded using ATR accessory and technique.

RESULTS AND DISCUSSION

Peptides and proteins play an important role in modern biology. A key step in peptide production is the formation of the peptide bond, which involves amide bond formation [23]. The process usually requires activation of a carboxylic acid moiety in the presence of coupling reagents. Activation consists of the replacement of the hydroxyl group of the carboxylic acid with a leaving group as the acid would otherwise simply form salts with the amine. The reaction of the activated intermediate and the amine is known as the coupling reaction and the activators are coupling reagents [24].

The dipeptide, Phe-Ala was synthesized using synthetic scheme shown in Fig. 2. Method of mixed anhydrides was applied, where N-protected Pro and C-protected Ala reacted in the presence of Piv-Cl. In order to obtain free dipeptide, protecting groups (Me ester and Boc-group) were removed subsequently. Alkaline hydrolysis was used for ester removal and acid hydrolysis – for Boc-group deprotection. Crude product was purified by gel filtration.

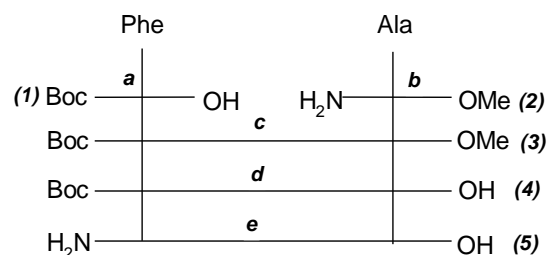


Fig. 2. Synthesis of *L*-phenylalanyl-*L*-alanine: a) Boc_2O , NaHCO_3 , *i*-PrOH, H_2O ; b) SO_2Cl , MeOH; c) Piv-Cl, NMM, Et_3N , THF; d) 1N NaOH, dioxin: H_2O (1:1); TFA, CH_2Cl_2 .

IR-spectral analysis

Like in our previous investigations on peptide systems [25, 26], the vibrational analysis support well the experimental IR-characteristic bands only assigned to molecular motions of

functional groups which does not participate in intermolecular interactions in solid-state.

The obtained results about the investigated compound are assigned on the basis of known IR-data about similar systems. The characteristic IR-bands of the dipeptide *H-Phe-Ala-OH* are listed and assigned in Table (1). The comparison and assignment of the solid-state IR-spectra of the studied compound is done, using the statement that pure dipeptide stabilize H_3N^+ , R-COO^- (*Phe-Ala-OH*) as a zwitterion with characteristic IR-spectral bands of $-\text{NH}_3^+$ and $-\text{COO}^-$ groups.

The IR-characteristic bands assignment shown in Table 1 is done by preliminary deconvolution and curve-fitting on the IR-spectroscopic patterns. The spectral analysis shows the presence of bands assigned of the protonated amino group $-\text{NH}_3^+$ in the $3300 - 2400 \text{ cm}^{-1}$ region. The broad maximum for studied compound in this region corresponds to symmetric and asymmetric stretching vibrations of protonated NH_3^+ -group.

The IR-spectrum of *H-Phe-Ala-OH* is characterized with an intensive band of ν_{NH} at 3250 cm^{-1} . The obtained low frequency shifting is a result of the participation of NH amide group in intermolecular interactions. The discussed band is low-frequency shifted too in corresponding hydrochloride of *H-Phe-Ala-OH* with $\sim 70 \text{ cm}^{-1}$ supposing the participation of the NH group in strong hydrogen bonding (Tabl.1).

The $\delta^{\text{as}}_{\text{NH}_3^+}$, $\delta^{\text{as}}_{\text{NH}_3^+}$, and $\delta^{\text{s}}_{\text{NH}_3}$, bending maxima are at about $1690 - 1620 \text{ cm}^{-1}$ region. The observed two bands at $1692, 1684 \text{ cm}^{-1}$ characterized asymmetric banding vibrations ($\delta^{\text{as}}_{\text{NH}_3^+}$). The band at 1546 cm^{-1} is assigned to the symmetric banding vibrations ($\delta^{\text{s}}_{\text{NH}_3^+}$). The *amide I* bands of the peptide is observed about 1679 cm^{-1} , while the *amide II* (1525 cm^{-1}) is strongly depends of the type of intermolecular interactions. The typical COO^- maxima are in the $1600 - 1400 \text{ cm}^{-1}$ spectral range. The character of the band at 1610 cm^{-1} and 1403 cm^{-1} are assigned and belonging to the asymmetric and symmetric stretching modes of COO^- -fragment ($\nu^{\text{as}}_{\text{COO}^-}$ and $\nu^{\text{s}}_{\text{COO}^-}$) in the molecule.

The protonation of the zwitterionic dipeptide leads to disappearance of the characteristic IR-bands of COO^- , i.e. $\nu^{\text{as}}_{\text{COO}^-}$, $\nu^{\text{s}}_{\text{COO}^-}$ and an observation of the bands of COOH group. The protonation leads to disappearance of the typical $-\text{COO}^-$ maxima in $1600-1400 \text{ cm}^{-1}$ spectral range. The character of the 1610 cm^{-1} and 1403 cm^{-1} bands as $\nu^{\text{as}}_{\text{COO}^-}$ and $\nu^{\text{s}}_{\text{COO}^-}$ in *H-Phe-Ala-OH* is confirmed in addition by the obtained IR-spectrum of protonated form as hydrochloride salt. It is characterized with the disappearance of the maxima

above and a new peak at 1735 cm^{-1} is appeared, which correspond to $\nu_{\text{C=O}}$ stretching vibration of the restored COOH group in the salt.

Table 1. IR-characteristic bands of *Phe-Ala-OH* and *Phe-Ala-OH.HCl*

Assignment ν (cm^{-1})	H-Phe-Ala- OH.	H-Phe-Ala- OH.HCl
$\nu^{\text{as}}_{\text{NH}_3^+}, \nu^{\text{s}}_{\text{NH}_3^+}, \nu^{\text{as}}_{\text{NH}_3^+}$	3200 – 2700	3200 – 2700
ν_{OH}	3365	3400
ν_{NH}	3275	3200
$\delta^{\text{as}}_{\text{NH}_3^+}, \delta^{\text{s}}_{\text{NH}_3^+}$	1692, 1684	1654, 1650
$\delta^{\text{s}}_{\text{NH}_3^+}$	1546	1511
$\nu_{\text{C=O}}$ (COOH group)	-	1735
$\nu_{\text{C=O}}$ (<i>Amide I</i>)	1679	1670
δ_{NH} (<i>Amide II</i>)	1525	1571
$\nu^{\text{as}}_{\text{COO}^-}$	1610	-
$\nu^{\text{s}}_{\text{COO}^-}$	1403	-

CONCLUSSION

The dipeptide *H-Phe-Ala-OH* was synthesized by well know method of mixed anhydrides in the presence of Piv-Cl. The spectral investigation, inclucuds IR-characteristic bands determination of the studied dipeptide *H-Phe-Ala-OH* were carried out.

Acknowledgements: This work was supported by Scientific Research Fund of SWU "N. Rilski", № RP-B3/16/2016.

REFERENCES

1. D.D. Kitts, K.Weiler, *Curr. Pharm. Des.* **9**, 1309 (2003).
2. T. Arakawa, T. Niikura, Y. Kita, F. Arisaka, *Drug Discov. Ther.* **3**(5), 208 (2009).
3. X. Cao, G. Fischer, *J. Mol. Struct.*, **519**, 153 (2000).
4. S. Stewart, P.M. Fredericks, *Spectrochim. Acta*, **55**, 1641 (1999).
5. S.P.A. Fodor, R.A. Copeland, C.A. Gryon, T.G. Spiro, *J. Am. Chem. Soc.*, **111**, 5509. (1989).
6. V. Naik, *Int. J. Pept. Protein Res.*, **42**, 2125.York, 1973. (1993).
7. J. Pessoa, I. Cavaco, I. Correia, M.T. Duarte, R.D. Gillard, R.T. Henriques, F.J. Higes, C. Madeira, T. Tomaz, *Inorg. Chim. Acta.*, **293**, 1. (1999).
8. F. Ota, S. Higuchi, Y. Gohshi, K. Furuya, M. Ban, M. Kyoto, *J. Raman Spectrosc.*, **28**, 849. (1997).
9. L. Tamm, S.A. Tatulian, *Q. Rev. Biophys.*, **30**, 365 (1997).
- 10 D. Moore, R. H. Sills, R. Mendelsohn, *Biospectrosc.*, **1**, 133 (1995).

11. F. Parker, Application of Infrared, Raman and Resonance Raman Spectroscopy in Biochemistry, Plenum Press, New York, 1983.
12. Y. Ozaki, K. Murayama, Y. Wang, *Vib. Spectrosc.*, **20**, 127 (1999).
13. Y. Wang, K. Murayama, Y. Myojo, R. Tsenkova, N. Hayashi, Y. Ozaki, *J. Phys. Chem.B.*, **102**, 6655 (1998).
14. L. Smeller, K. Heremans, *Vib. Spectrosc.*, **19**, 375 (1999).
15. J.-J. Max, M. Trudel, and C. Chapados, *Appl. Spectrosc.*, **52**, 226 (1998)
16. J. Casado, J. T. Lo'pez Navarrete, F. J. Ram' rez, *J. Raman Spectrosc.*, **26**, 1003 (1995).
17. X. Cao, G. Fischer, *J. Phys. Chem.*, A **103**, 9995 (1999).
18. X. Cao, G. Fischer, *Spectrochim. Acta, Part A*, **55**, 2329 (1999).
19. B. Ivanova, *J. Coord. Chem.*, **58**, 587 (2005).
20. B. Ivanova, *Spectrochim Acta* **65A**, 5 (2005).
21. B. Koleva., Ts. Kolev., S. Zareva, M. Spitteller *J. Mol. Struct.*, **831**, 165 (2007).
22. T. Kolev, S. Zareva, B. Koleva, M. Spitteller, *Inorg. Chim. Acta*, **359**, 436 (2006).
23. E. Valeur, M. Bradley, *Chem. Soc. Rev.*, **38**, 606 (2009).
24. S. Han, Y. Kim, *Tetrahedron*, **60**, 2447 (2004).
25. A. Chapkanov, S. Zareva, *Protein & Peptide Letters*, **16**(11), 1277 (2009).
26. A. Chapkanov, S. Zareva, *Spect. Lett.*, **43**(2), 79 (2010).

СИНТЕЗ И ИЧ-ФТ СПЕКТРАЛНО ИЗЯСНЯВАНЕ НА ДИПЕПТИДИ С АРОМАТНА АМИНОКИСЕЛИНА

Т. Е. Дзимбова¹, Р. К. Георгиев², А. Г. Чапкънов^{2*}

¹Институт по молекулярна биология, Българска академия на науките, ул. Акад. Г. Бончев 21, 1113 София (България)

²Югозападен университет „Н. Рилски“, ул. „И. Михайлов“ 66, 2700 Благоевград (България)

Постъпила на 04 октомври 2016 г.; Коригирана на 06 март, 2017 г.

(Резюме)

Малките пептиди могат да представляват полезни модели за изучаване силите на взаимодействие, отговорни за структурата и активността на по-големи протеини. Синтезът на дипептид, съдържащ ароматна аминокиселина е извършен по добре известна методика - приложен е метода на смесените анхидриди, където аминокиселините фенилаланин е N-защитена, а аланин C-защитена реагират в присъствие на пивалоил хлорид. Спектралният ИЧ-ФТ анализ в твърдо състояние може да се използва за допълнително охарактеризиране и изясняване на типични ивици от изследваното съединение. Получените резултати за ивиците на amid фрагментите (C=O, NH), както и на други ивици от ароматния остатък могат да дадат полезна структурна информация относно конфигурацията на amidната група и съответните amidни равнини в пептидните молекули.

Chemical stability of thiazole analogues of rimantadine and amantadine

K. Chuchkov, D. Mitreva, V. Markova, I. Stankova*

Department of Chemistry, South-West University "Neofit Rilsky", Blagoevgrad, Bulgaria,

Received October 25, 2016; Revised March 07, 2017

At present, two classes antivirals of influenza virus are available: the neuraminidase inhibitors (oseltamivir, peramivir, zanamivir) and the M2 proton channel blockers (amantadine and rimantadine). Since vaccination and existing antiviral therapy and rapid emergence of M2 proton channel blockers resistance cannot guarantee protection against influenza, battling this virus remains important health care task that requires design and development of new drugs. In the search of new prodrugs effective against influenza virus were synthesized thiazole analogues with amantadine and rimantadine (RS) -1 - (1-adamantyl) ethanamine) and their antiviral activity was studied [1]. The chemical stability of them was studied at pH 1 and 7.4 temperature of 37°C. An HPLC method was developed for quantification of the unchanged ester concentration.

Keywords: adamantanes, thiazole, chemical stability

INTRODUCTION

Modification of antiviral agents by peptidomimetics, with chemical structures different from the natural peptides but maintaining the same ability to interact with specific receptors, is of great interest [2]. Based on the known structure/activity relationship we designed a new series of analogues of amantadine and rimantadine with peptidomimetics [3].

Novel rimantadine and amantadine analogues have been synthesized with amino acids containing thiazole and thiazole rings and their activity on the Influenza virus A/Hongkong/68 have been explored. The rimantadine analogues with thiazole ring showed moderate activity against influenza virus A/Hongkong. The remaining compounds were considerably less effective.

The object of this study was to assess the chemical stability of some of the synthesised adamantane esters with peptidomimetics at pH 1.0 and pH 7.4 at 37°C [4].

EXPERIMENTAL

General information

Chemicals

Acetonitrile for HPLC the buffer components HCl, Na₂H₂PO₄ of the purest grade, were purchased from Merck (Germany). The Grace Vidac chromatographic column was used (USA).

Chromatography

Chromatography was carried out isocratically, on a modular KNAUER HPLC system (Germany), consisting of a Smartline Pump 1000, a Smartline Manager 5000 solvent degasser, an injector with a 20 µl loop and a Smartline UV Detector 2600 diode array. The analyses were controlled and the data were acquired with EuroChrom software. The mobile phase consisted of acetonitrile/water in a ratio of 30:70 or 50:50 v/v depending on the polarity of the compound and a flow rate 1 ml/min was used. The detection was performed at relevant λ_{\max} for the respective compound (range 252–262 nm).

Kinetic study

A single chromatographic method was used to detect the studied adamantane esters with thiazole rings containing amino acid glycine in aqueous buffer solutions at pH 1.0 (0.1 M HCl) and pH 7.4 (phosphate buffer). Twenty microlitres of each sample were injected into a reverse phase HPLC C18 column. The mobile phase consisted of acetonitrile/water at a ratio of 30:70 or 50:50 v/v depending on the polarity of the compound. The analyses of the esters of amantadine and rimantadine with amino acid containing thiazole rings were validated. The specificity of the method was investigated by observing potential interference between the esters of amantadine and rimantadine and its parent drug. No interfering peaks were presented in the chromatograms. The linearity of the relationship between the peak area and concentration was determined by analysing six standard solutions in a concentration range of 0.1–1.0 mmol/l. For all analytes, the relationship

* To whom all correspondence should be sent:
E-mail: ivastankova@abv.bg

between the peak area ratio of the drug to the internal standard and concentration was linear over the entire examined concentration range. The correlation coefficients of the calibration curves were greater than 0.997. For all of the examined compounds the coefficient of variation calculated for the six analysed samples did not exceed 5%.

Hydrolysis of adamantane esters with thiazole rings containing amino acid Glycine was studied at pH 1.0 (HCl) and pH 7.4 (phosphate buffered saline). Stock solutions of the prodrugs were prepared and used immediately for stability studies. Aliquots (9.8 ml) of the buffer were placed in a screw-capped vial and allowed equilibrate at 37°C. A prodrug stock solution (0.2 ml) was added to the buffer. The vial was placed in a constant shaker bath set at 37°C and 60 rpm. Each sample was directly analysed by HPLC.

RESULTS AND DISCUSSION

The chemical stability of adamantane esters: HCl-2-aminomethyl-thiazole-amantadine (**1**), HCl-2-aminomethyl-thiazole-rimantadine (**2**) was studied under experimental conditions of biological relevance, i.e. at pH 1 and pH 7.4, at a temperature of 37°C. The compounds were synthesised as previously described. The structures of the compounds under investigation are presented on Fig. 1.

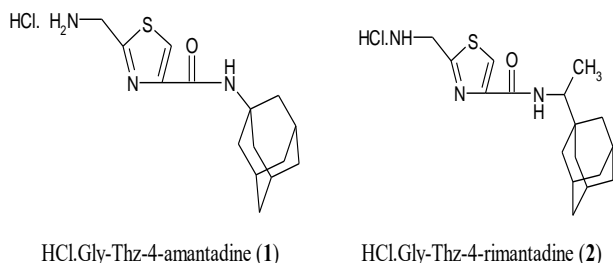


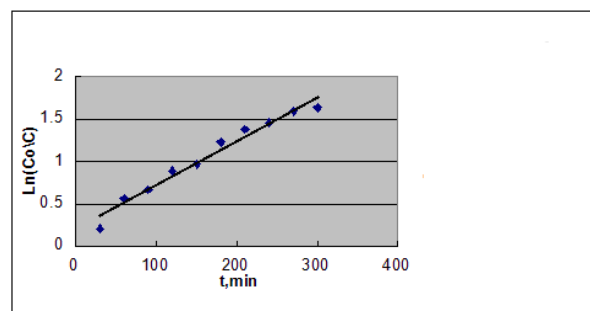
Fig.1. Adamantane esters with peptidomimetics

It was established that, under the described experimental conditions, some esters underwent decomposition by hydrolysis [5]. The hydrolysis followed apparent first order kinetics, and the rate constants (K) were obtained as slopes from the semi-logarithmic plots of the unchanged ester concentration versus time. The chemical stability was assessed by means of the decomposition half-lives:

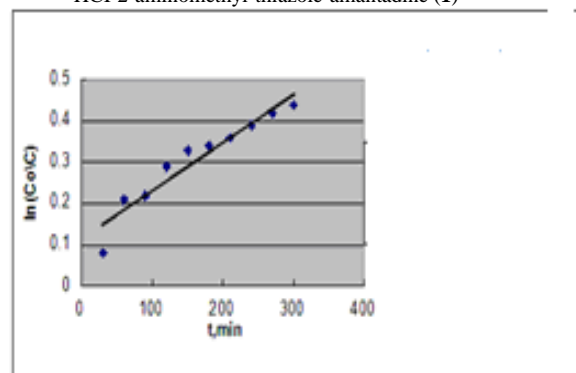
$$t_{1/2} = \ln \frac{2}{K}$$

Chemical stability measurements revealed that the thiazolyl esters of amantadine and rimantadine

were relatively unstable at acidic pH (Tabl.1., Fig. 2.).

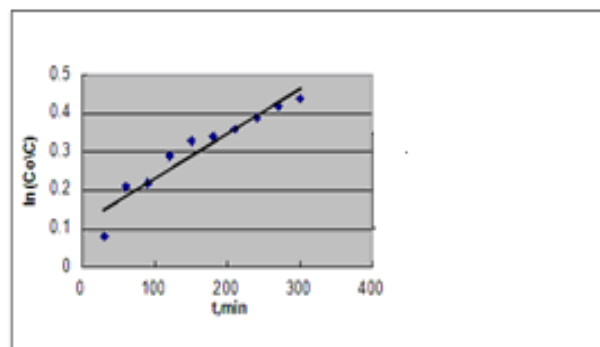


HCl-2-aminomethyl-thiazole-amantadine (**1**)

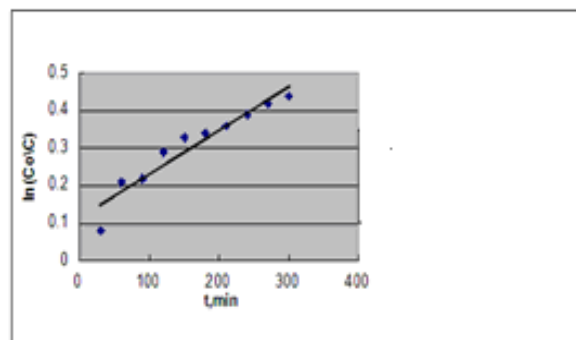


HCl-2-aminomethyl-thiazole-rimantadine (**2**)

Fig. 2. Decrease of the concentration of the esters at pH 1.0 (HCl)



HCl-2-aminomethyl-thiazole-amantadine (**1**)



HCl-2-aminomethyl-thiazole-rimantadine (**2**)

Fig. 3. Decrease of the concentration of the examined prodrugs in buffer solution at pH 7.4 (phosphate buffer)

Table 1. Half-lives (h) of thiazole analogues of amantadine and rimantadine at 37°C.

Compounds	pH=1	pH=7
1	0.53 h	1.03 h
2	1.48 h	6.05 h

The HCl-2-aminomethyl-thiazole-amantadine (1) and HCl-2-aminomethyl-thiazole-rimantadine (2) were less stable than the Boc-thiazole-OH at pH 1.0. Esters (1) and (2) manifest lower stability at pH 7.4. It was proved that the compound (2) is stable at the pH 7.4 (Fig. 3, Table 1.).

CONCLUSION

The chemical stability of thiazolyl esters of amantadine (1) and rimantadine (2) was studied in experimental conditions simulating some relevant biological medias (pH 1.0 and 7.4, 37°C). Test compounds are stable at pH 7.4 and 37°C where the

highest stability manifests Boc-thiazole with rimantadine ($t_{1/2}=6.05$ h) at pH 1.0 and 37°C the most stable is analogues of Boc-thiazole with rimantadine ($t_{1/2}=1.48$ h).

Acknowledgements: The authors gratefully acknowledge financial support from South-West University "Neofit Rilski" – grant RP-A9/16.

REFERENCES

1. I. Stankova, K. Chuchkov, R. Georgiev, G. Ivanova, A. S. Galabov, *FMNS Blagoevgrad*, **14**, 3 (2013).
2. J.C. Watts, P. Marvin, U.S. Patent, **3**, 310, (1967).
3. M. D. Duque, E. Torres, E. Valverde, M. Guardiola, M. Rey, S. Vázquez, *Rec. Adv.Pharm. Sci.*, 35 (2011).
4. G. Hristov, I. Stankova, *Sci. Pharm.*, **79**, 259 (2011)
5. 5.Weinstock, M.,D. Zuccotti, G., *J. Am. Med. Assoc.*, **8**, 934 (2006)

ХИМИЧНА СТАБИЛНОСТ НА ТИАЗОЛОВИ ПРОИЗВОДНИ НА РИМАНТАДИН И АМАНТАДИН

К. Чучков, Д. Митрева, В. Маркова И. Станкова

¹Катедра по химия, Югозападен университет „Неофит Рилски“, ул. „Иван Михайлов“ № 66, 2700
Благоевград, България

Постъпила на 25 октомври 2016 г.; Коригирана на 7 март, 2017 г.

(Резюме)

Нови аналози на амантадин и римантадин съдържащи тиазолов пръстен бяха синтезирани и бе изследвана противовирусната им активност спрямо грипен вирус [1].

Химичната стабилност на тиазоловите производни на амантадина и римантадина бе изследвана при pH=1, pH=7.4 и T=37°C с използване на високоефективна течна хроматография.

Amantadine analogues – synthesis and biological activity

R. Chayrov^{1*}, L. Mukova², A. Galabov², Y. Mitrev³, I. Stankova¹

¹Department of Chemistry, South-West University “Neofit Rilsky”, Blagoevgrad, Bulgaria, ²Stefan Angeloff Institute of Microbiology, Bulgarian Academy of Sciences, 1113 Sofia, Bulgaria

³Laboratory “Bulgarian NMR Centre”, Institute of Organic Chemistry with Centre of Phytochemistry, 1113 Sofia, Bulgaria

Received October 30, 2016 ; Revised February 25, 2017

The biological activity of adamantane derivatives is due to the symmetry and steric bulkiness of the structure and the significant lipophilicity of the rigid hydrocarbon framework. This enables them to penetrate easily through biological membranes. Therefore, modification of organic compounds by an adamantyl radical changes significantly their biological activity, often enhancing it. A large number of strains that are completely resistant to amantadine are currently known. The number of resistant influenza strains increases every year because of spontaneous mutations in the virus genome. This necessitates expanded research on the reasons for the development of resistance and ways of overcoming it by creating new antiviral drugs [1].

Keywords: adamantanes, amino acids, amino acid amides, antiviral activity

INTRODUCTION

Amantadine was a drug that was once used to treat the influenza virus A. The influenza virus A became resistant to amantadine due to the misuse of the drug. In 2005 the drug was used in China as a way to treat the avian influenza. The Chinese gave approximately 2.6 billion doses of amantadine to the chickens, which is what caused it to become resistant [2]. The avian flu threat served as a catalyst for scientists to prepare a new antibiotic that could be used to treat the drug-resistant bacterial and viral strains [3]. According to Plumb’s Veterinary Drug Handbook, amantadine is safe to use in small animals and equine. It also states that amantadine is still able to treat some influenza viruses, but they have found that the greatest interest in its use is treating chronic pain. The influenza virus it is able to treat is found in equine and is known as equine-2 influenza virus. The handbook states that amantadine is safe for humans and that it is no longer used for fighting the influenza virus but used in Parkinsonian Syndrome [4]. Amantadine is an amino-analogue of adamantane.

Our goal was to modify amantadine with L-Valine, L-Alanine and L-Lys and to investigate their antiviral activity against influenza virus A (H3N2) (Scheme 1). The structures of new analogues were confirmed by NMR and MS analyses.

EXPERIMENTAL

General information

All amino acids (N-(tert-Butoxycarbonyl)-L-alanine, N-(tert-Butoxycarbonyl)-L-valine and N^{α,ε}-

bis-Boc-L-lysine dicyclohexylammonium salt), amantadine hydrochloride, as well as isobutyl chloroformate (IBCF), triethylamine (TEA), were purchased from Sigma Aldrich (FOT, Bulgaria). Dichloromethane was obtained from Fisher Chemical (Bulgaria) and further was distilled. Chloroform was of reagent grade and used without further purification. Thin-layer chromatography (TLC) was conducted on pre-coated Kieselgel 60F254 plates (Merck, Germany).

The NMR experiments were recorded on Bruker Avance III 600 or Bruker Avance III 400 spectrometer, operating at 600.13 and 400.15 MHz for protons respectively. The measurements in CDCl₃ solutions were carried out at ambient temperature (300 K) and tetramethylsilane (TMS) was used as an internal standard. The UV spectra of the compounds were measured with an “Agilent 8453” UV-vis spectrophotometer. Electrospray Ionisation (ESI) and EI mass spectra were recorded corresponding on an Esquire 3000 and MAT 8230.

General procedures. Synthesis of 3a - c

The tert-butyloxycarbonyl (Boc) amino acids (Boc-Val-OH, Boc-Ala-OH, Boc-Lys(Boc)-OH) (69 mmol) were dissolved in 2 ml CH₂Cl₂. The solution was cooled to -15°C, added TEA (69 mmol) and dropwise isobutyl chloroformate (69 mmol). The amantadine (46 mmol) were dissolved in 2 ml mix CH₂Cl₂/CHCl₃ in ratio 1:1, added TEA (46 mmol). After 15 min the solutions were mixed and stirred for 1,5h at -15°C. The mixture was poured into 5% NaHCO₃, extracted with CHCl₃, washed with brine, dried over Na₂SO₄ and concentrated in vacuo. The residues were purified by

* To whom all correspondence should be sent:
E-mail: rchayrov@swu.bg

TLC on Kieselgel 60F254 using the solvent system chloroform/ methanol (95:5).

The resulting white solid, Boc-Valyl-Amantadine, Boc-Alanyl-Amantadine and oil Boc-Lysinyl(Boc)-Amantadine were dissolved in 2 ml of 50% TFA/ CH₂Cl₂ and stirred at 0°C for 1h to remove the Boc group.

Boc-Valyl-Amantadine (Boc-Val-Am) - M.W. = 350,5;

ESI-MS: 723.4 [2M+Na]⁺, 389.1 [M+K]⁺, 373.2 [M+Na]⁺, 351.2 [M+H]⁺; **¹H NMR** (CDCl₃) /600 MHz/ δ (ppm): 0.901 (d, J=6.8 Hz, 3H), 0.937 (d, J=6.5 Hz, 3H), 1.435 (s, 9H), 1.664 (br t, 6H), 1.985 (s, 6H), 2.03 (overlapping, 1H), 2.06 (s, 3H), 3.705 (br t, J= 7.9 Hz, 1H), 5.09 (d, J= 8.2 Hz, 1H), 5.478 (s, 1H).

After removing the Boc group - white powder, 36% yield;

ESI-MS: 523.2 [2M+Na]⁺, 273.1 [M+Na]⁺

Boc-Alanyl-Amantadine (Boc-Ala-Am) - M.W. = 322,5;

ESI-MS: 667.2 [2M+Na]⁺, 361.1 [M+K]⁺, 345.1 [M+Na]⁺, 323.1 [M+H]⁺; **¹H NMR** (CDCl₃) /600 MHz/ δ (ppm): 1.30, (d, J=7Hz, 3H), 1.44 (s, 9H), 1.66 (s, 6H), 1.973 (s, 6H), 2.065 (s, 3H), 4.024 (br s, 1H, CH), 5.024 (br s, 1H, NH), 5.796 (br s, 1H, NH).

After removing the Boc group – white powder, 58% yield;

ESI-MS: 467.1 [2M+Na]⁺, 245.0 [M+Na]⁺

Boc-Lysinyl(Boc)-Amantadine (Boc-Lys(Boc)-Am) - M.W.= 479,7;

ESI-MS: 981.4 [2M+Na]⁺, 502.2 [M+Na]⁺, 480.3 [M+H]⁺; **¹H NMR** (CDCl₃) /600 MHz/ δ (ppm): 1.44 (s, 18H, Me), 1.40-1.90 (m, 6H, CH₂), 3.11 (br s, 2H, CH₂), 4.13 (br s, 1H, CH), 4.80 (br s, 1H, NH), 5.44 (br s, 1H, NH).

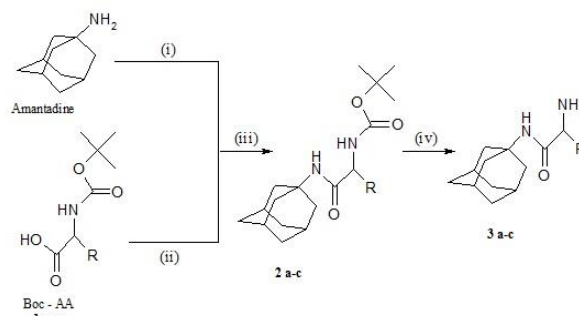
After removing the Boc groups – white to yellow powder, 28% yield;

ESI-MS: 581.8 [2M+Na]⁺, 302.1 [M+Na]⁺.

Viral suspension is from the collection of the section "Virology" of the "Stefan Angelov" Institute of Microbiology, Bulgarian Academy of Sciences.

The virus is cultured in a maintenance environment DMEM (Dulbecco's Modified Eagles's Medium) (Gibco BRL, USA) with 0.5% fetal veal serum, 10 mM HEPES (Merk, Germany) and antibiotics (penicillin 100 UI / mL and streptomycin 100 µg / mL) at 37 ° C in the presence of 5% CO₂. After seeding in microtitre plates, MDCK cells were incubated at 5 % CO₂, 37 ° C and 95 % humidity for 48 h. Thereafter, the cell culture medium was aspirated and serially diluted compound concentrations in fresh cell culture

medium were added (100 µl/well; 2 parallels/concentration, dilution factor 2). Six untreated wells were used as cell control (negative control). 72 h after compound addition and incubation cell were stained with a crystal violet/methanol solution. After dissolving away the stain, the optical density (OD) of individual wells was determined in a Dynatech microplate Photometer (550 /630 nm) and compared with the mean optical density of the 6 cell controls.



R = CH(CH₃)₂ - Valine (a) R = CH₃ - Alanine (b) R = (CH₂)₄NH₂ - Lysine (c)

Scheme 1. (i) Et₃N, CH₂Cl₂/CHCl₃ 1:1, -15°C; (ii) Et₃N, IBCF, CH₂Cl₂, -15°C, 15min; (iii) 1,5h, -15°C; (iv) TFA/ CHCl₃

RESULTS AND DISCUSSION

We presents test results for the ability of the prepared compounds to inhibit virus A/H3N2 strain Aichi and the cytotoxic activity of the compounds on MDCK cell culture.

Antiviral activity of the compounds was studied at a concentration of 5µg/mL. The percent inhibition of the compounds given in Table 1 is the arithmetic mean.

It can be concluded by analyzing the results that the antiviral activity is depends by the length the carbohydrate chain. There is an optimal size and structure.

As we can see in the table branched chain amino acids valine did not show activity, even it's hydrophobic portion together with the lipophilic carbocyclic adamantane created the optimum structure for penetrating the membrane bilayer of the virus capsule and disrupting replication processes valine derivative (3 a) behaved no antiviral activity on A(H3N2) virus. Compound 3 b represented amantadine linked to the amino acid alanine. It slightly inhibited A(H3N2). The moderate inhibition activity of this compound possibly is due to its compact structure, which fit into M2 protein envelope and partially obstructs proton conduction.

Table 1. Antiviral activity against influenza virus A (H3N2) and cytotoxicity of the amantadine derivatives.

Compounds	Cytotoxicity (CC ₅₀)	Inhibition (IC ₅₀)
Val-Am (3 a)	189.02	0
Ala-Am (3 b)	211.16	33.28
Lys-Am (3 c)	206.13	15.32
Amantadine	> 200	n/a

Based on the activity of the ornithine derivative, which Shibnev and etc. report, we synthesized close structural analog – lysinyl-amantadine (3 c). The activity of the compound was slightly less than that of 3 b. Carbohydrate chain is much longer compare to 3 b, but in this derivative are two amino groups, which increase the basic properties and inclination to formation hydrogen bonds with M2 protein [5].

CONCLUSION

We synthesized and tested three compounds of amantadine analogues with the amino acids valine, alanine and lysine. The new analogues 3 a-c were

evaluated for their antiviral activity towards influenza virus A(H3N2). This study shows that the antiviral properties of amantadine amino acid derivatives could resuscitation the antiviral properties and the resistance was overcome.

Acknowledgements: The authors gratefully acknowledge financial support from South-West University “Neofit Rilski” – grant RP-A9/16.

REFERENCES

1. V. A. Shibnev et al., *Pharm. Chem. J.*, **46**, 1, (2012).
2. R. A. Bright et al., *The Lancet*, **366**, 1175 (2005).
3. X. Chen et al., *Europ. J. of Med. Chem.*, **93**, 182 (2015).
4. D. C. Plumb, *PharmaVet.*, **6**, 508 (2005).
5. V. Gaiday et al., *Intern. Conf. on Computational Sci.*, 360 (2008).
6. S. S. Anchuri et al., *Biointerf. Research in Applied Chem.*, **6**, 1491 (2016).

АМАНТАДИНОВИ АНАЛОЗИ – СИНТЕЗ И БИОЛОГИЧНА АКТИВНОСТ

Р. Чайров^{1*}, Л. Мукова², А. Гълъбов², Я. Митрев³, И. Станкова¹

¹Катедра по химия, Югозападен университет „Неофит Рилски“, ул. „Иван Михайлов“ № 66, 2700 Благоевград, България

²Институт по микробиология „Стефан Ангелов“, ул. „Акад. Георги Бончев“ бл. 26, 1113 София, България

³Институт по органична химия с Център по фитохимия, ул. „Акад. Георги Бончев“ бл. 9, 1113 София, България

Постъпила на октомври 30, 2016 г.; Коригирана на 25 феврури, 2017 г.

(Резюме)

Пространственото разположение, значителната липофилност, лесно преминаване през биологичните мембрани на аминокиселините са причините, които оказват влияние върху повишена биологичната активност на техни производни с амантадина.

Известни са голям брой грипни щамове резистентни към амантадина. Техният брой се увеличава всяка година заради спонтанни мутации във вирусния геном. Създаване на нови аминокиселинни аналози на амантадина са възможност за преодоляване на резистентността [1].

Kinetic investigation and tyrosinase inhibition activity of peptide analogues of galanthamine

S.A. Yaneva^{1*}, D.A. Marinkova², L. Ilieva³, L.T. Vezekov³, L.K. Yotova², D.L. Danalev¹

University of Chemical Technology and Metallurgy, Sofia 1756, Bulgaria, 8 blvd. Kliment Ohridski,

¹*Department of Fundamentals of Chemical Technology*

²*Biotechnology Department, phone (+359 2) 8163310, e-mail: dancho.danalev@gmail.com*

³*Department of Organic Chemistry*

Received October 4., 2016; Revised February 20, 2017

The hyper production of melanin is a reason for malignant melanoma, the most life-threatening skin cancer. Recently, tyrosinase inhibitors attract a lot of attention because of their ability to influence the activity of this key enzyme. Such kind of compounds is increasingly used as ingredients in cosmetic creams and products. Peptides containing aspartic or glutamic acid residues usually do not bind very well to tyrosinase. Strong tyrosinase-binding peptides always contain one or more arginine residues, often in combination with phenylalanine, while lysine residues can be found equally among nonbinding peptides as well as moderate tyrosinase-binding peptides. The presence of the hydrophobic, aliphatic residues valine, alanine or leucine appears to be important for tyrosinase inhibition. Therefore, good tyrosinase inhibitory peptides preferably contain arginine and/or phenylalanine in combination with valine, alanine and/or leucine. A special place is given to peptides, because of their good bioavailability and low or lack of toxicity.

Herein, we report the kinetic investigation, inhibitory activity and IC₅₀ of two peptide amide of galanthamine Boc-Asp(norGal)-Asp-Leu-Ala-Val-NH-Bzl and Boc-Asp(norGal)-Asp-Leu-β-Ala-Val-NH-Bzl.

Key words: peptides, enzymes, inhibitors; pharmaceutical application

INTRODUCTION

Tyrosinase (EC 1.14.18.1.) is a metalloenzyme containing Cu⁺² as a cofactor in the active site that catalysis two districts reaction of melanin synthesis, the hydroxylation of a monophenol and the bioconversion of o-diphenol to the corresponding o-quinone [1]. The latter undergoes several reactions to form melanin (figure 1).

Currently a great interest is the involvement of melanin (one of the most common pigments including in human skin) in several dermatological disorders. The hyper production of melanin is a reason for malignant melanoma, the most life-threatening skin cancer. Recently, tyrosinase inhibitors attract a lot of attention because of their ability to influence the activity of this key enzyme. Such kind of compounds is increasingly used as ingredients in cosmetic creams and products [2]. A special place is given to peptides, because of their good bioavailability and low or lack of toxicity [3]. Herein, we report the kinetic investigation and inhibitory activity of two peptide amide of galanthamine Boc-Asp(norGal)-Asp-Leu-Ala-Val-NH-Bzl and Boc-Asp(norGal)-Asp-Leu-β-Ala-Val-NH-Bzl.

MATERIALS AND METHODS

Tyrosinase inhibition activity

All kinetic investigations and IC₅₀ determinations were done using an **optical biosensor** with tyrosinase from mushrooms (EC 1.14.18.1), immobilized **onto** hybrid membranes synthesized by sol-gel technology. Synthesis of used membranes containing cellulose acetate propionate with high molecule weight (~25 000) (CAP), methyl triethoxysilane (MTES) and copolymer of acrylamide/acrylonitrile is described in [4]. The quantity of protein immobilized onto the membranes, was determine using Lowry's methodology [5]. Initially, the activity of the immobilized tyrosinase was measured without presence of inhibitor. Diphenolase activity was determined spectrophotometrically with 10 mM substrate L-DOPA (L-3,4-dihydroxyphenylalanine) as a substrate, at 25 °C, using spectrophotometer with optical fibers (AvaSpec, Avantes, USA).

The diphenolase activity does not show any lag period. The dopachrome assay was performed. The increase in absorption at 475 nm, due to the formation of dopachrome ($\epsilon_{475} = 3\ 600\ \text{M}^{-1}\text{cm}^{-1}$), was monitored as a function of time. The activity is expressed as mole of L-DOPA oxidized per minute.

* To whom all correspondence should be sent:

E-mail: sp_yaneva@uctm.edu

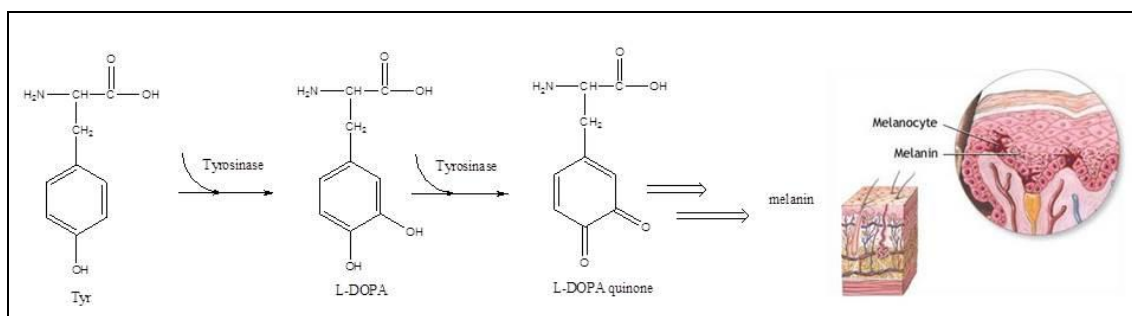


Fig. 1. Two stages of tyrosinase participation in melanin synthesis

1 ml of 0.001M potassium phosphate buffer (pH=7) and 1 ml 13.3×10^{-5} M L-DOPA were stirring. Further, synthesized peptides at different concentrations from 5 μ M to 100 μ M were diluted in 1.0 ml of 0.001M potassium phosphate buffer (pH=7). 50mg of membranes with the immobilized enzyme were added directly to the solution and were incubated together for 30 min at 25° C. The membranes with immobilized tyrosinase, were moved out from the solution and the residual activity was measured following the procedure according to Worthington [6].

Peptide inhibitors were synthesized according to methodology described in [7]. They all are amides or esters of natural galanthamine with following structures:

Boc-Asp-(norGal)-Asp-Leu-Ala-Val-NH-Bzl – inhibitor 1- (**I₁**);

Boc-Asp-(norGal)-Asp-Leu- β -Ala-Val-NH-Bzl – inhibitor 2- (**I₂**).

The inhibitory effects of all the analyzed Tyrosinase inhibitors was calculated by measuring the difference in the enzyme activity before and after incubation with inhibitor. The measurement was done at 460 nm for 5 min.

The inhibition percentage was calculated according to equation.

$$\text{Inhibition (\%)} = [(E_0 - E_i)/E_0] * 100,$$

Where E_0 is the initial inhibited sensor activity and E_i is the inhibited sensor activity. The sensitivity of the biosensor toward tyrosinase was measured.

RESULTS AND DISCUSSION

A lot of scientific groups are investigated peptides with different structures as potential inhibitors of tyrosinase in order to estimate role of different amino acids for inhibitory activity. Schurink et al. reveal that strong peptide based tyrosinase inhibitors always contain one or more arginine residues, often in combination with phenylalanine. In addition they prove that the presence of hydrophobic, aliphatic residue like

valine, alanine or leucine is key factor for tyrosinase inhibitory potential [3]. In contrary, Noh et al. describe series of 22 tripeptides combined with kojic acid where all compounds with strong inhibitory activity against tyrosinase contain minimum one hydrophilic amino acid [8]. Many researchers studied inhibitors from natural sources such as silk, yogurt and more [9-12]. A lot of other examples appear in the scientific literature but finally one is clear that still there is no exactly defined structure-activity relationship for peptide containing molecules and their anti-tyrosinase activity. That's why we studied inhibition activity of two peptide containing analogues of norgalanthamine including combination of hydrophobic (Leu, Ala/ β -Ala, Val) and one hydrophilic (Asp) residue. C-terminus of aim peptides is modified as benzamide in order to have hydrophobic properties. In addition, both aim peptide analogues differ by the presence of Ala or β -Ala in their structure in order to evaluate their influence on inhibitory activity.

All investigations for inhibitory activity of both compounds are made using optical biosensor containing tyrosinase immobilized on hybrid matrix. Initially, we made the calibration curves with inhibitors.

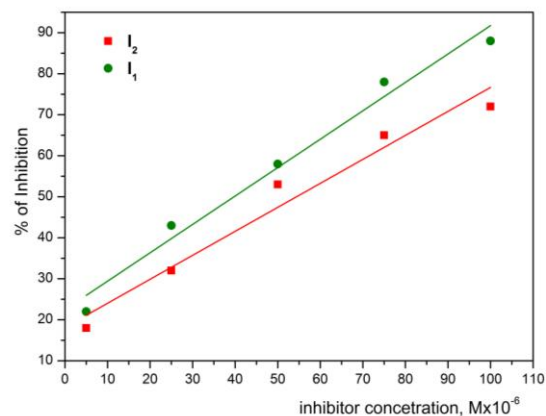
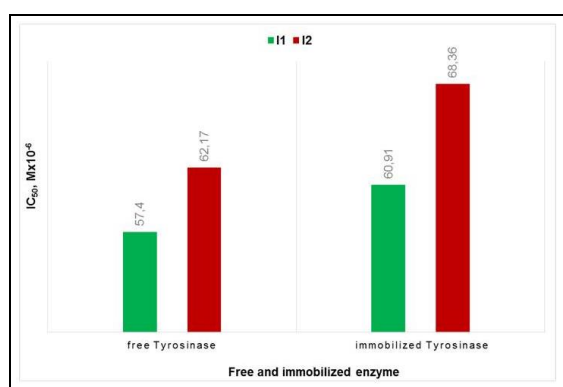


Fig. 2. Calibration curves for free and immobilized tyrosinase with the peptide inhibitors **I₁**, **I₂**

Table 1. Ki value for I₁ and I₂ for free and immobilized tyrosinase

Inhibitor concentration, Mx10 ⁻⁶	Ki free tyrosinase, Mx10 ⁻⁶		Ki immobilized tyrosinase, Mx10 ⁻⁶	
	I ₁	I ₂	I ₁	I ₂
5	0.65	0.29	1.84	1.25
25	2.75	1.61	3.11	3.47
50	4.82	3.99	5.68	6.36
75	5.92	5.95	7.56	7.09

They are illustrated on Figure 2 in the presence of tyrosinase at 13.3×10^{-5} M concentration. The calibration curves exhibited linear response in the concentration range $5 \cdot 10^{-6} \div 100 \cdot 10^{-6}$ M.

**Fig. 3.** IC₅₀ determined for I₁ and I₂ for free and immobilized tyrosinase

After drawing the calibration curves, the IC₅₀ values for the used inhibitors are determined and they are shown in figure 3.

The results shown IC₅₀ for free enzyme is $57.4 \cdot 10^{-6}$ and $62.17 \cdot 10^{-6}$ M for I₁ and I₂, respectively. IC for immobilized tyrosinase was calculated $60.91 \cdot 10^{-6}$ and $68.36 \cdot 10^{-6}$ M for I₁ and I₂.

The values of Ki for both inhibitors concentrations for free and immobilized tyrosinase are presented at Table 1. The results showed that inhibitors act as uncompetitive for tyrosinase.

After the spectrophotometric determination of inhibitory activity of peptide derivatives of galanthamine, samples containing substrate L-DOPA, enzyme and inhibitor were stored in the dark at $t = 4$ °C for 30 days. Periodically on the first, 15th and 30th day the samples are measured to determine the effect of the inhibitors in time and final product formation - melanin. The results of the tests show that both inhibitors have excellent inhibitory properties against tyrosinase,

by suppressing formation of melanin for a period of - longer than 15 days.

CONCLUSIONS

The results from our study shows that inhibitors of two peptide amide of galanthamine Boc-Asp(norGal)-Asp-Leu-Ala-Val-NH-Bzl and Boc-Asp(norGal)-Asp-Leu-β-Ala-Val-NH-Bzl acting uncompetitive against tyrosinase. The obtained peptides could find potential applications into the medical cosmetology and prevention of diseases related to pigmentation disorders.

Acknowledgments: This work was supported by Scientific Research Fund of UCTM, project 11527.

REFERENCES

1. Y.J. Kim, H. Uyama, *CMLS, Cell. Mol. Life Sci.*, **62**, 15 (2005).
2. L. Zhang, T. J. Falla, *Clinics in Dermatology*, **27**, 485 (2009).
3. M. Schurink M.S. Willem, J.H. van Berkel, H.J. Wichers, C.G. Boeriu, *Peptides*, **28**, 2 (2007).
4. L. Yotova, S. Yaneva, *Bul. Chem. Comm.*, **45**, 4 (2013).
5. O.H. Lowry, N.J. Rosbrough, A.L. Farr, R.J. Randall, *J. Biol. Chem.*, **193**, 265 (1951).
6. A. Decker, L. Worthington, *Enzyme Manual, Polyphenol oxidase*, Worthington Biochemical Corporation, 1977, 39.
7. L.T. Vezenkov, M. Georgieva, D.L. Danalev, Tch. Ivanov, G. Ivanova, *Protein and Peptide Lett.*, **16**, 1024 (2009).
8. J.M. Noh, S.Y. Kwak, D.H. Kim, Y.S. Lee, *Biopolymers*, **88**(2), 300 (2007).
9. S. Ates, *Journal of Food Biochemistry*, **25**, 127 (2001).
10. J. M. Chen, R. J. Liu, F. J. Sheu, W. C. Lin and L. C. Chuang, *Asian-Aust. J. Anim. Sci.* **19**, 6, (2006).
11. G. Gillis, K. Bojanowski, G. Majewski, R. Bohm, *Cosmetic Science Technology*, **30**, (2009).
12. M.R. Loizzo, R. Tundis, F. Menichini, *Food Sci. Food Safety*, **11**, 378 (2012).

ИЗСЛЕДВАНЕ ИНХИБИТОРНАТА АКТИВНОСТ ВЪРХУ ТИРОЗИНАЗА НА ПЕПТИДНИ АНАЛОЗИ НА ГАЛАНТАМИН

С.А. Янева^{1*}, Д.А. Маринкова², Л.И. Илиева³, Л.Т. Везенков³, Л.К. Йотова², Д.Л. Даналев²

Химикотехнологичен и металургичен университет, София 1756, България, 8 бул. Св. Климент Охридски,

¹*Катедра Основи на химичната технология*

²*Катедра Биотехнология*

³*Катедра Органична химия*

Постъпила на 4 октомври, 2016 г.; Коригирана на 20 февруари, 2017 г.

(Резюме)

Хипер производството на меланин е причина за възникването на малигнен меланом – вид агресивен рак на кожата. Хипофункцията на меланин в организма се отключва все по-често срещаното заболяване, свързано със загуба на пигментация – витилиго. В последните години инхибиторите на тирозиназата както и нейните активатори привличат вниманието на изследователите, заради способността да се повлиява действието на ензима. Този вид съединения все по-често се включват като съставка в козметични кремове и продукти

Пептиди, съдържащи остатъци на аспаргинова и глутаминова киселини, обикновено не се свързват добре с тирозиназата. Ефективно свързване се постига с пептиди, съдържащи един или повече аргининови остатъци, често заедно с фенилаланин. От друга страна лизиновите остатъци имат двойствен характер и се срещат както при несвързващите, така и при умерено свързващите тирозиназата пептиди. Присъствието на хидрофобните алифатни остатъци валин, аланин или левцин са важни за инхибирането на тирозиназата. Следователно, добри тирозиназни инхибитори са пептидите съдържащи в състава си аргинин и/или фенилаланин заедно с валин, аланин и/или левцин. Инхибиторите с пептидна структура са особено подходящи за приложение поради тяхната натурална природа и ниска или отсъстваща токсичност.

В настоящата работа докладваме изследването на инхибиторната активност и IC_{50} на два пептида amidни аналози на галантамин Boc-Asp (norGal) -Asp-Leu-Ala-Val-NH-Bzl и Boc-Asp (norGal) -Asp-Leu-β-Ala-Val-NH-Bzl.

Synthesis and radical scavenging activity of cinnamic acid esters

M. Chochkova^{1*}, B. Stoykova¹, P. Petrova¹, N. Gyoshkova¹, G. Ivanova², M. Štícha³, Ts. Milkova¹

¹ Department of Chemistry, South-West University "Neofit Rilski", 66 Ivan Mihailov Str.,
2700 Blagoevgrad (Bulgaria)

² REQUIMTE-UCIBIO, Departamento de Química e Bioquímica, Faculdade de Ciências, Universidade do Porto, Rua
do Campo Alegre s/n, 4169-007 Porto (Portugal)

³ Department of Organic Chemistry, Faculty of Science, Charles University, Hlavova 2030/8, 12843 Prague 2
(Czech Republic)

Received October 10, 2016; Revised January 20, 2017

Cinnamic and hydroxycinnamic acid esters (α , β -unsaturated esters), functional derivatives of cinnamic acids (cinnamic, ferulic, sinapic, caffeic) are secondary plant metabolites derived from phenylpropanoid pathway. Cinnamates, of both natural and synthetic origin, continue to elicit great interest due to diversity of biological activities they possess, such as: antioxidant, antimicrobial, anticancer, anti-inflammatory, anti-tyrosinase and etc.

Herein, the reduction of N_α - and side chain protected amino acids to N -protected amino alcohols and the coupling of the latest with hydroxycinnamic (sinapic and ferulic) acids is described. 1,1-Diphenyl-2-picrylhydrazyl (DPPH[•]) scavenging activities of hydroxycinnamates were compared with their corresponding N -hydroxycinnamoyl amino acid amides. Free hydroxycinnamic acids were used as positive controls. The results indicated that N -hydroxycinnamoyl amino acid amides exhibited lower scavenging ability than the corresponding free hydroxycinnamic acids, but higher one than hydroxycinnamates.

Keywords: N -protected amino alcohols, hydroxycinnamates, N -hydroxycinnamoyl amino acid amides, DPPH[•] scavenging activity

INTRODUCTION

Cinnamic (3-phenyl propenoic) acid and its patterns with different hydroxylated and methoxylated phenyl moiety: *p*-coumaric (4-hydroxycinnamic acid), ferulic (4-hydroxy-3-methoxycinnamic acid), caffeic (3,4-dihydroxycinnamic acid), sinapic (3,5-dimethoxy-4-hydroxy-cinnamic acid) acids, belong to a diverse group of phenolic compounds. These secondary plant metabolites are biosynthesized via shikimate pathway that is involved in plant adaptation to environmental stress (e. g. microbial pathogens, mechanical wounding, UV irradiation, salinity) [1]. They are found in higher plants predominantly as free cinnamic acids and may occur either in their conjugated forms: *amides* (conjugated with mono- or polyamines, amino acids, or peptides); *simple esters or cinnamates* (derived from corresponding cinnamic acids and alcohol component of quinic acid, shikimic acid, and tartaric acid, and their sugar derivatives) [2]. In particular, chlorogenic acids are the most commonly occurred natural esters of caffeic, ferulic, *p*-coumaric acids with quinic acid [3,4]. Being important biosynthetic polyphenolic intermediates in green coffee, chlorogenic acids are

known with numerous bioactive properties, mostly related to their antioxidant activity [5-7].

Besides antioxidant activity, cinnamates have been regarded as photoprotectors, antimicrobials, and effective as anticancer, anti-inflammatory, analgesic, antimicrobial and antithrombotic agents [8-11].

Whereas hydroxycinnamates with alcohols, phenols, saccharides and flavonoids are common phytochemical constituents, those with the participation of the OH group of the side chain of amino acids are very scanty. There are only few reports of such metabolites - caffeic acid esters, derived from insects: *O*-caffeoyltyrosine from *Aonidiella aurantii* (California red scale), *O*-caffeoylserine from *Phenacoccus herreni* (Cassava mealybug) [12, 13] and from plant origin: *L*-*O*-caffeoylhomoserine [14]. In addition, *O*-caffeoylserine has been also synthetically obtained [15].

The revealed pharmacological activities of hydroxycinnamic acid esters and their small quantities in plants, evoked the interest of organic researchers to design their synthetically analogues.

Ester functionalization of cinnamic acids comprises classical procedures-accomplished via cinnamoylchloride [16], *N,N'*-dicyclohexylcarbodiimide (DCC) [17] or BOP [18] as coupling agents. Moreover, those compounds can also be obtained using Wittig reaction under different

* To whom all correspondence should be sent:
E-mail: mayabg2002@yahoo.com

conditions [19-22] and as well as green esterification procedures [23-27].

Considering the importance of phenolic compounds, e.g. hydroxycinnamic acid esters for removal of oxidative stress, and thus to prevent lifestyle-related diseases such as cancer, diabetes or heart diseases, herein we prepared hydroxycinnamic acid esters and tested them as scavengers against DPPH radical.

EXPERIMENTAL

General information

All amino acid derivatives, ferulic (3-methoxy-4-hydroxy-cinnamic, **FA**), sinapic (3,5-dimethoxy-4-hydroxy-cinnamic, **SA**) acids, as well as isobutyl chloroformate (IBCF), 4-methylmorpholine (NMM), 4-(dimethylamino)pyridine (DMAP), dicyclohexylcarbodiimide (DCC), NaBH₄, 1,1-diphenyl-2-picrylhydrazyl radical (DPPH[•]) were purchased from Sigma Aldrich (FOT, Bulgaria). Tetrahydrofuran was obtained from Fisher Chemical (Bulgaria) and further was distilled over LiAlH₄ and stored under argon. All other solvents were of reagent grade and used without further purification.

Thin-layer chromatography (TLC) was conducted on precoated Kieselgel 60F254 plates (Merck, Germany). Separation of the compounds by preparative thin layer chromatography with silica gel 60 GF254 (Merck, Bulgaria).

The NMR experiments were recorded on Bruker Avance III 600 or Bruker Avance III 400 spectrometer, operating at 600.13 and 400.15 MHz for protons respectively. The measurements in CDCl₃ solutions were carried out at ambient temperature (300 K) and tetramethylsilane (TMS) was used as an internal standard. The UV spectra of the compounds were measured with an "Agilent 8453" UV-vis spectrophotometer. Electrospray Ionisation (ESI) and EI mass spectra were recorded corresponding on an Esquire 3000 and MAT 8230. Attenuated total reflectance infrared spectroscopy (ATR-IR) measurements were performed using Thermo Scientific Nicolet iS10 FT-IR device with ID5 ATR accessory (diamond crystal).

N-protected amino acids (Boc-Cys(Bzl)-OH (**1a**) and Boc-Val-OH (**1b**) were converted into corresponding alcohols Boc-Cys(Bzl)-ol (**2a**) and Boc-Val-ol (**2b**), following a modified procedure developed by Kokotos [28] (Scheme 1).

General procedures

Synthesis of 2a, b (a modified method reported by Kokotos [28]). A solution of 1.6 mmol *N*-protected amino acid (**1a, b**) in 10 ml dry THF is cooled to -15°C and added 0.18 ml (1.6 mmol) *N*-

methylmorpholine. Isobutyl chloroformate (0.24 ml, 1.7 mmol) is added dropwise to make sure that the internal temperature does not rise above -10 °C. About 5-8 minutes later, to the white suspension of formed isobutylcarbonic acid mixed anhydrides[29] is added 0.104 g (2.74 mmol) NaBH₄ in 10 ml THF, and for a period of 10 min abs.CH₃OH (5 ml) is added dropwise. Stirring is continued and the progress of the reaction is monitored by thin layer chromatograms (hexane:ethylacetate=1:1).

At the completion of the reduction (2h) the solvent is evaporated under reduced pressure. The residue is dissolved in ethylacetate and is washed twice consequently with 5% NaHSO₄, 5% NaHCO₃ and finally with saturated sodium chloride solution. The organic phase is dried over Na₂SO₄, filtered and the solvent removed *in vacuo*. The obtained crude product is purified by preparative thin layer chromatography (hexane:ethylacetate= 3:1).

S-Benzyl-*N*-(*tert*-butoxycarbonyl)-*L*-cysteinol (**Boc-Cys(Bzl)-ol**) (**2a**) white crystal, 61% yield; **ESI-MS**: 617.1 [2M+Na]⁺, 595.1 [2M+H]⁺, 336.3 [M+K]⁺, 320.1 [M+Na]⁺, 298.2 [M+H]⁺; **IR (ATR)**u_{max}: 3342.65, 1679.47, 1527.03, 1340.92, 1311.44, 1284.20, 1164.34, 1004.33, 698.47 cm⁻¹;

N-(*tert*-butoxycarbonyl)-*L*-valinol (**Boc-Val-ol**) (**2b**) yellow oil, 53% yield;

¹H NMR (CDCl₃, δ ppm): 0.9 (dd, 6H, -CH(CH₃)₂), 1.2 (s, 9H, -C(CH₃)₃), 1.8-1.84 (m, 1H, -CH(CH₃)₂), 3.4-3.6 (m, 3H, -CH₂OH, -NH-CH<), 4.8 (br. s, 1H, NH); **EI-MS**: 57.1, 73, 116.1, 130, 172.1, 203 [M⁺]; **IR (ATR)**u_{max}:3318.1, 3189.5, 2978.6, 1679.7, 1366.5, 1289.4, 1150.7, 1011.8, 908.9, 772.0, 699.4

Esterification of cinnamic acids with *N*-protected amino alcohol [30]. Cinnamic acids (1.5 mmol), DCC (1.5 mmol) and DMAP (0.0224 mmol) are dissolved in 10 mL of dry THF. The reaction mixture is stirred under argon at 0°C and then, after 10 min *N*-protected amino alcohol (0.6 mmol) is added. The mixture is kept under vigorous stirring and cooling (0°C) for 60 min and then is allowed to stand at room temperature overnight. The residue of dicyclohexylcarbamide is filtered and washed with cold ethylacetate. The combined solutions are evaporated under vacuum and the residue is purified by column chromatography on silica.

Ferulate of Boc-Val-ol, 35% yield. **UV** (C₂H₅OH) λ max = 203, 218, 236, 328 nm; **IR (ATR)**u_{max}: 3335.5, 2959.6, 2932.1, 1707.2, 1627.4, 1592.3, 1510.9, 1365.5, 1269.7, 1246.7, 1157.4, 1119.8, 1029.32, 978.9 cm⁻¹; **¹H NMR** (CDCl₃)/600 MHz/ δ = 0.9 (dd, 6H, -CH(CH₃)₂), 1.2 (s, 9H, -C(CH₃)₃), 1.8 (m, 1H, -CH(CH₃)₂), 3.7 (s, 2H, -OCH₂-), 3.8 (s, 3H, -OCH₃), 4.1 (m, 1H, -NH-CH<), 5.0 (br. s, 1H, NH), 6.2 (d, 1H, J=15.5 Hz, -CH=CH-

), 7.00-7.03 (m, 3H, Ar-H), 7.5 (d, 1H, J=15.5 Hz, -CH=CH-); **ESI-MS**: 380.2 [M+H]⁺, 409.12 [M+Na]⁺

Sinapate of Boc-Val-ol, 49 % yield. UV (C₂H₅OH) λ max = 203,229, 329 nm; **IR (ATR)**u_{max}: 3376.3, 2936.4, 2844.2, 1704.6, 1632.7, 1594.5, 1456.2, 1419.11, 1338.1, 1275.2, 1204.2, 1111.6, 980.1, 822.8 cm⁻¹; **¹H-NMR** (CDCl₃) /600 MHz/ δ = 0.9 (dd, 6H, -CH(CH₃)₂), 1.2 (s, 9H, -C(CH₃)₃), 1.8 (m, 1H, -CH(CH₃)₂), 3.7 (s, 2H, -OCH₂-), 3.8 (s, 6H, 2 x-OCH₃), 4.2 (m, 1H, NH-CH), 5.6 (br. s, 1H, NH), 6.5 (d, 1H, J = 15.5 Hz, -CH=CH-), 6.7 (s, 2H, Ar-H), 7.5 (d, 1H, J = 15.5 Hz, -CH=CH-); **EI-MS**: 57.1, 207.1, 308, 238.1, 336.2, 353.2, 409.2 [M⁺].

Ferulate of Boc-Cys(Bzl)-ol, 20 % yield. UV (C₂H₅OH) λ max = 203,217, 236, 327 nm; **IR (ATR)**u_{max}: 3343.4, 1679.7, 1526.6, 1364.7, 1340.9, 1311.3, 1284.1, 1163.2, 1076.9, 1003.9, 698.6 cm⁻¹; **¹H NMR** (DMSO-*d*₆, ppm): δ 1.42 (s, 9H, -C(CH₃)₃), 3.21 (dd, J=14.2, 5.2 Hz, 1H, CHCH_{2a}), 3.4 (dd, J=14.2, 4.6 Hz, 1H, CHCH_{2b}), 3.66 (d, J=5.6 Hz, 2H, -S-CH₂-Ph), 3.73 (s, 3H, OCH₃), 4.42 (d, 2H, -CH₂-O -), 4.87 (ddd, J= 7.0, 5.2, 4.6 Hz, 1H, CHCH₂), 5.82 (br. s, 1H, OH), 6.28 (d, J=7.0 Hz, 1H, NH), 6.32 (d, J=15.6 Hz, 1H, -CH=CH-), 6.93 (d, J=8.0 Hz, 1H, m-ArH), 7.01 (d, J=1.6 Hz, 1H, o-ArH), 7.06 (dd, J=8.0, 1.6 Hz, 1H, o-ArH), 7.24 (m, 5H, Ar-H), 7.57 (d, J=15.6 Hz, 1H, -CH=CH-); **EI-MS**: 57.1, 91.0, 177.1, 473.3 [M⁺]

Sinapate of Boc-Cys(Bzl)-ol, yield 25 %

UV (C₂H₅OH) λ max = 203,228, 330 nm; **IR (ATR)**u_{max}: 3392.8, 1705.1, 1597.5, 1507.1, 1456.8, 1418.8, 1108.3, 870.4, 659.0 cm⁻¹; **¹H NMR** (DMSO-*d*₆, ppm): δ 1.42 (s, 9H, -C(CH₃)₃), 3.71

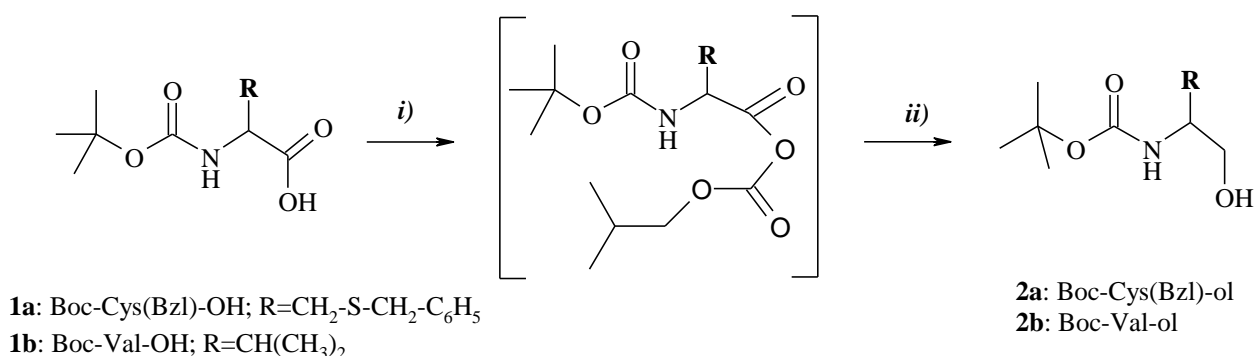
(dd, J=14.2, 5.2 Hz, 1H, CHCH_{2a}), 3.4 (dd, J=14.2, 4.6 Hz, 1H, CHCH_{2b}), 3.68 (d, J=5.6 Hz, 2H, -S-CH₂-Ph), 3.73 (s, 6H, 2x OCH₃), 4.51 (d, 2H, -CH₂-O-), 4.63 (ddd, J= 7.0, 5.2, 4.6 Hz, 1H, CHCH₂), 5.72 (s, 1H, OH), 6.28 (d, J=7.0 Hz, 1H, NH), 6.32 (d, J=15.6 Hz, 1H, =CH), 6.7 (s, 2H, Ar-H), 7.28-7.51 (m, 5H, Ar-H), 7.59 (d, J=15.6 Hz, 1H, =CH); **EI-MS**: 57.1, 91.0, 207.1, 238.1, 266.1, 386.3, 447.1, 503.3 [M⁺].

RESULTS AND DISCUSSION

Herein, in order to elucidate the antiradical activity of cinnamic acid esters, we firstly obtained synthetically the amino alcohols (used as intermediates).

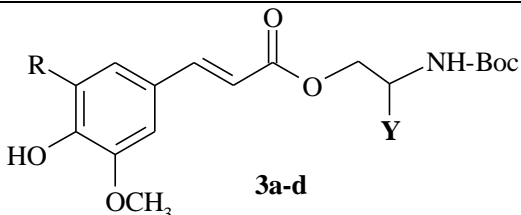
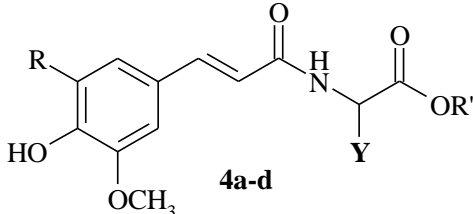
By applying a modified method [28], the NaBH₄ reduction of protected amino acids (Scheme 1; **1a,b**) into corresponding amino alcohols (**2a, b**) was occurred by means of *in situ* formed isobutylcarbonic acid mixed anhydrides in THF. However, the establishment that the reducing power of NaBH₄ in THF increases when methanol is added drop-wise [28] enforces us to accomplish the reaction in the same manner. The expected amino alcohols were isolated on silica gel by preparative thin layer chromatography (hexane:ethylacetate) in moderate yields.

The hydroxycinnamic acid esters (**Table 1, 3a-d**) were prepared by esterification of sinapic- (SA) and ferulic (FA) acids with compounds **2a, b** using DCC/DMAP method [30]. The structures of desired hydroxycinnamates were elucidated by UV, IR, ESI(EI)-MS and ¹H-NMR spectroscopic analyses.



Scheme 1. i) IBCF/NMM, THF, -15 °C ii) NaBH₄, CH₃OH

Table 1. Structures of hydroxycinnamic derivatives studied and their DPPH•-scavenging activity.

Compounds	RSA %			
	R	R'	Y	3.6 mM 20'
 3a-d				
FA ester of BocCys(Bzl)ol (3a)	H	-	-CH ₂ -S-Bzl	27.0±0.1
SA ester of BocCys(Bzl)ol (3b)	OCH ₃	-	-CH ₂ -S-Bzl	29.9±0.2
FA ester of BocVal-ol (3c)	H	-	-CH(CH ₃) ₂	17.6±0.2
SA ester of BocVal-ol (3d)	OCH ₃	-	-CH(CH ₃) ₂	19.7±0.1
 4a-d				
FA-Cys(Bzl)-OEt* (4a)	H	C ₂ H ₅	-CH ₂ -S-Bzl	38.4±1.2
SA-Cys(Bzl)-OEt* (4b)	OCH ₃	C ₂ H ₅	-CH ₂ -S-Bzl	47.4±2.4
FA-Val-OCH ₃ (4c)	H	CH ₃	-CH(CH ₃) ₂	30.8±0.2
SA-Val-OCH ₃ (4d)	OCH ₃	CH ₃	-CH(CH ₃) ₂	35.1±0.1
Sinapic acid (SA)		-	-	68.0±0.3
Ferulic acid (FA)		-	-	45.2±0.1

% RSA—percent radical scavenging activity; % RSA = $[Abs_{516nm}(t=0) - Abs_{516nm}(t=t')] \times 100 / Abs_{516nm}(t=0)$; sinapic- and ferulic acids were used as standards.

*The RSA of hydroxycinnamoylamides were previously reported [32] and were used for comparison.

The values of the proton-proton vicinal coupling constants ($^3J_{H/H}$ about 15.5 Hz) measured for the olefinic protons of feruloyl- and sinapoyl moieties define *E* configuration of the double bond of the studied compounds (**3a-d**).

Highlighting the valuable role of hydroxycinnamic acid derivatives as antioxidants, the search for new, more effective and better radical scavengers is a major challenge.

1,1-Diphenyl-2-picrylhydrazyl radical (DPPH•) scavenging activity

Being stable and commercially available organic nitrogen radical, DPPH• is often used for primary assessment of antioxidant activity. DPPH method gives rapid and highly reproducible results, therefore we applied this method to estimate and compared the radical scavenging abilities of the synthesized hydroxycinnamic acid derivatives (esters and amides).

As shown in Table 1, % RSA values of hydroxycinnamic acid (sinapic and ferulic) and their derivatives are presented for 20-min reaction period (3.6 mM), as proposed by Nenadis et al. [31].

The DPPH scavenging activity of hydroxycinnamates (**3a-d**) was compared with those of corresponding previously synthesized amides (**4a-d**). Results obtained indicated that amide derivatives (**4a-d**) were found to be more potent than corresponding hydroxycinnamic esters (**3a-d**). The established increase of antiradical activity in hydroxycinnamoyl amino acid amides may be due to the presence of other hydrogen-donating amide group. By comparison of DPPH activity of studied esters and amides with their corresponding free cinnamic acids the higher radical scavenging ability of the parent acids was established. Actually, *N*-sinapoyl amide of cysteine (SA-Cys(Bzl)-OEt (**4b**)) showed similar DPPH scavenging activity as ferulic acid was [32]. Moreover, our results are in a good correlation with those presented elsewhere, that

introduction of additional methoxyl group in an *ortho*-position to a hydroxyl group (such as in sinapic acid series, Table_1) is an important for the radical scavenging activities of phenolic acids.

CONCLUSION

In our study *N*-protected amino alcohols were chemically obtained and further used as intermediate analogues for synthesis of hydroxycinnamates.

The sinnapic and ferulic acid derivatives (esters and amides) were tested and compared for their *in vitro* antiradical activity towards DPPH radical. It was found that *N*-hydroxycinnamoyl amino acid amides showed better radical scavenging activity than the corresponding hydroxycinnamates, whereas the free hydroxycinnamic acids (used as standards) remained the most active ones in this test.

Acknowledgements: The authors gratefully acknowledge financial support from South-West University "Neofit Rilski" – grant RP-A9/16.

REFERENCES

1. K. M. Hermann, *Plant Physiol.*, **107**, 7 (1995).
2. K. Herrmann, *CRC Crit. Rev. Food Sci. Nutr.*, **28**, 315 (1989).
3. M. N. Clifford, *J. Sci. Food Agric.*, **79**, 362 (1999).
4. M. N. Clifford, *J. Sci. Food Agric.*, **80**, 1033 (2000).
5. C. A. Rice-Evans, N. J. Miller, G. Paganga, *Trends Plant Sci.*, **2**, 152 (1997).
6. H. Kasai, S. Fukada, Z. Yamaizumi, S. Sugie, H. Mori, *Food Chem. Toxicol.*, **38**, 467 (2000).
7. T. Tanaka, T. Kojima, T. Kawamori, A. Wang, M. Suzui, K. Okamoto, H. Mori, *Carcinogenesis*, **14**, 1321 (1993).
8. M. Sova, *Mini-Rev. Med. Chem.* **12**, 749 (2012).
9. S. Son, B.A. Lewis, *J. Agric. Food. Chem.*, **50**, 468 (2002).
10. A. Ivanova, Ts. Milkova, A. S. Galabov, L. Nikolaeva, E. Voynova, *Z. Naturforsch.*, **52c**, 516 (1997).
11. M. D. Santos, M. C. Almeida, N. P. Lopes, G.E.P. Souza, *Biol Pharm Bull.*, **29**, 2236 (2006).
12. J.G. Miller, J.D. Hare, *J. Chem. Ecol.*, **19**, 1721 (1993).
13. P.A. Calatayud, J. Auger, E. Thibout, S. Rousset, A.M., Caicedo, S. Calatayud, H Buschmann, J. Guillaud, M. Mandon, A.C. Bellotti, *J. Chem. Ecol.*, **27**, 2203 (2001).
14. T. Kimura, M. Suzuki, M. Takenaka, K. Yamagishi, H. Shinmoto, *Phytochemistry*, **65**, 423 (2004).
15. Z. Lin, M. Neamati, H. Zhao, Y. Kiryu, J.A. Tuppin, C. Aberham, K. Strebels, K. Kohn, M Witvrouw., C. Pannecouque, Z. Debyser, E. De Clercq, W.G. Rice, Y. Pommier, T. R. Burke, *J. Med. Chem.*, **42**, 1401 (1999).
16. E. Womack, J. McWhirter, *Org. Synth. Coll.*, **3**, 714 (1955).
17. N. Isaacs, T. Najem, *J. Chem. Soc. Perkin Trans.*, **2**, 557 (1988).
18. S. Gobec, M. Sova, K. Kristan, T. L. Rizner, *Bioorg. Med. Chem. Lett.*, **14**, 3933 (2004).
19. R. Mali, A. Papalkar, *J. Chem. Res. (S)* **10**, 603 (2003).
20. I. Elenkov, D. Todorova, V. Bankova, Ts. Milkova, *J. Nat. Prod.*, **58**, 280 (1995).
21. M. Spasova, V. Bankova, G. Ivanova, T. Pajpanova, Ts. Milkova, *Oxid. Commun.*, **29**, 172 (2006).
22. J. Westman, *Org. Lett.*, **3**, 3745 (2001).
23. D. M. Ruiz, G. P. Romanelli, D. O. Bennardi, G. T. Baronetti, H. J. Thomas, J. C. Autinoa, *Arkivoc*, **12**, 269 (2008).
24. V. Palermo, D. Ruiz, J. Autino, P. Vázquez, G. Romanelli, *Pure Appl. Chem.*, **84**, 529 (2012).
25. M. Nakayama, A Sato, K. Ishihara, H. Yamamoto, *Adv. Synth. Catal.*, **346**, 1275 (2004).
26. A. Sinha, A. Sharma, A. Swaroop, V. Kumar, *Tetrahedron*, **63**, 1000 (2007).
27. G. Romanelli, D. Ruiz, P. Vázquez, H. Thomas, J. Autino, *Chem. Eng. J.*, **161**, 355 (2010).
28. G. Kokotos, *Synthesis*, **1990**, 299 (1990).
29. J. R. Vaughan, R. L. Jr., Osato, *J. Amer. Chem. Soc.*, **73**, 3547 (1951).
30. B. Neises, W. Steglich, *Angew. Chem., Int. Ed. Engl.*, **17**, 522 (1978).
31. N. Nenadis, M. Tsimidou, *JAOCs*, **79**, 1191 (2002).
32. M. G. Chochkova, E. Y. Chorbadzhiyska, G. I. Ivanova, H. Najdenski, M. Ninova, Ts. S. Milkova, *Nat. Prod. J.*, **2**, 50 (2012).

СИНТЕЗ И ИЗСЛЕДВАНЕ НА РАДИКАЛ-УЛАВЯЩА АКТИВНОСТ НА ЕСТЕРИ НА КАНЕЛЕНИТЕ КИСЕЛИНИ

М. Чочкова^{1*}, Б. Стойкова¹, П. Петрова¹, Н. Гьошкова¹, Г. Иванова²,
М. Щиха³, Ц. Милкова¹

¹*Катедра по химия, Югозападен университет „Неофит Рилски“, ул. „Иван Михайлов“ № 66, 2700
Благоевград (България)*

²*Департамент по химия и биохимия, Университет в Порто, ул. Кампо Алегре с/н, 4169-007 Порто
(Португалия)*

³*Департамент по органична химия, Карлов университет, Хлавова 2030/8,
12843 Прага 2 (Чехия)*

Постъпила на 10 октомври, 2016 г.; Коригирана на 20 януари, 2017 г.

(Резюме)

Канелената, хидроксиканелените киселини (ферулова, синапова, кафеена) и техните естери представляват вторични растителни метаболити, биосинтезирани от фенилпропаноидния метаболитен път. Природните хидроксицинаматите и техните синтетични аналози привличат вниманието на изследователите поради широкия спектър от биологични активности като: антиоксидантна, антимикробиална, противотуморна, противовъзпалителна, тирозиназно-инхибиторна и др.

В настоящето изследване е разгледана редукция на карбоксилната група на защитени аминокарбоксилни киселини на N_{α} -място и в страничната верига. След естерифициране на получените аминокалкохоли с хидроксиканелени (синапова и ферулова) киселини, новосинтезираните производни са подложени на изследване за радикалулавяща активност спрямо 1,1-Дифенил-2-пикрилхидразилов радикал (DPPH[•]). Резултатите от антирадикаловата активност на хидроксицинаматите са сравнени с тези на съответните хидроксицинамоиламиди с аминокарбоксилни киселини. Като стандартни антиоксиданти са използвани свободните хидроксиканелени киселини. Установено е, че хидроксицинамоиламидите показват по-ниска антирадикалова активност от съответните свободни хидроксиканелени киселини, но по-висока от тази на хидроксицинаматите.

Synthesis and study of cytotoxic effect of novel AVPI-RGD hybrid peptides

M.G. Georgieva*, R.L. Detcheva, T.I. Pajpanova

Institute of Molecular Biology “Acad. Roumen Tsanev”, Bulgarian Academy of Sciences, Acad. G. Bonchev Str., bl.21, 1113 Sofia, Bulgaria

Received September 30, 2016 ; Revised February 18, 2017

Targeting critical apoptosis regulators is a promising strategy for development of new classes of anticancer drugs. Herein, we focused on synthesis and study of novel bi-functional AVPI-RGD hybrid peptides. Despite of, being functionally different motifs of separate proteins, AVPI and RGD peptides are still both known for their pro-apoptotic potential and therefore interesting objects of pharmacology design. Herein, we report for hybrid molecules and their monomeric subunits. Fmoc solid phase peptide strategy (SPPS) was preferred as synthesis method, whereas proline and arginine residues were subjected to modifications. Cytotoxic potential of molecules was examined by initial screening over two cell lines – HepG2 and MDA-MB-231 cells – by MTT colorimetric assay. It was found that almost all tested compounds had weak or none cytotoxic effect when they were used as single agents. However, we showed that AVPI-RGD hybrids exert comparatively higher cytotoxic effect than individual AVPI and AVHyPI peptides .

Ke ywords: AVPI, RGD, apoptosis, SPPS

INTRODUCTION

Resistance to apoptosis is an important hallmark of cancer cells and partly reason for their resistance to conventional anti-cancer treatment. Vast number of IAP-inhibitors, Smac-mimetics, AVPI-, and RGD- mimetics, have been synthesized over the past decade, as new promising agents for overwhelming higher apoptotic thresholds of cancer cells, as some of them have entered clinical trials [1].

Inhibitors of apoptosis proteins (IAP) are important regulators of processes - cell death and survival. At this time, 8 different IAP proteins are known in mammals. Three of them (cIAP-1, cIAP-2, XIAP) are well recognized as regulators of apoptosis. These functions they perform either by directly inhibiting caspases (XIAP) or by interfering formation of death-receptor complexes (cIAP1, cIAP2).

Distinctive for these IAPs is the presence of N-terminal BIR (baculoviral IAP repeat) domains and C-terminal RING domain - essential for their anti-apoptotic effects. While BIR domains mediate the interaction with caspases, RING domain exhibits ubiquitin-E3 ligase activity so IAPs can promote their own as well as proteasome degradation of binded-partner molecules.

Function of cIAP-1/2 is mainly dependent on their RING domains. On the other hand, XIAP is known to bind directly and inhibiting initiator

(caspase-9) and effector (caspases-3 and -7) caspases via its BIR3 and BIR2-linker regions, respectively [2].

AVPI (Ala-Val-Pro-Ile) is a tetrapeptide sequence of the N-terminus of the mature pro-apoptotic Smac protein. AVPI itself is the major IAP-binding motif (IBM) in mammals, and fruit flies. Via its AVPI motif Smac directly interacts with BIR2 and BIR3 domains of IAPs, releasing inhibitory effect of XIAP and stimulating c-IAPs autoubiquitination and proteasomal degradation [3, 4], that ultimately re-activates apoptosis.

Smac is localized in mitochondrial intermembrane space, but it is released into the cytoplasm upon apoptotic stimuli. Several studies established inverse correlation between Smac expression levels and cancer progression so prompted the development of Smac- and/ or AVPI-mimetics as therapeutic agents [5, 6]. Some of them are reported to be efficient in the induction of apoptosis in tumorigenic cells as single agents, others - in combination with different therapeutic agents (cisplatin, doxorubicin, etoposide, TRAIL, etc) [1, 7 – 9].

The RGD (L-arginyl-glycyl-L-aspartic acid) peptide sequence is found in many proteins of extracellular matrix, as well as in intracellular proteins such as caspases. RGD is also known to interact with specific over-expressed proteins on the membrane of cancer cells (example - $\alpha\beta3$, $\alpha\beta5$ integrins). That sets RGD-peptide motif as an advantageous tumor-targeting ‘device’ for selective inhibition and elimination of cancer cells that is still

* To whom all correspondence should be sent:

E-mail: m.geo@abv.bg

an overwhelming problem for most of the drugs [10].

Regarding that synthesis of hybrid-peptides, combining two or more pharmacological effects is an advantageous pharmacological approach, we focused on synthesis of new AVPI-RGD hybrid molecules and examination of their cytotoxic potential.

EXPERIMENTAL

Peptide design, synthesis and analysis

Synthesis of all peptides was performed by the conventional and manual stepwise Fmoc solid-phase synthesis on 2-chlorotrityl chloride resin with substitution, 1.4 mmol/g. The coupling of each amino acid was performed in the presence of 3 mol excess of Fmoc-amino acid, 3 mol excess of N-hydroxybenzotriazole (HOBt), 3 mol excess of Diisopropylcarbodiimide (DIC), and 5 mol excess of diisopropylamine (DIPEA) in Dimethylformamide (DMF). Completion of coupling reactions were monitored by the Kaiser test and the Fmoc groups were removed by adding 20% piperidine in DMF.

The peptides were cleaved from the resin and the final deprotection was done in a cocktail containing trifluoroacetic acid (TFA), triisopropylsilane (TIPS), thioanisole, and water (92.5 : 2.5 : 2.5 : 2.5).

The crude peptides were precipitated into cold petroleum ether/diisopropyl ether (50:50). Then, the precipitate was dissolved in 10% CH₃COOH and desalted by gel filtration on a Sephadex G25.

Peptides' purity was characterized by RP-HPLC and capillary electrophoresis.

Cell cultures

Both cell lines (HepG2 and MDA-MB-231) were cultured in Dulbecco Modified Eagle's medium (DMEM) (Gibco, Austria) supplemented with 10% fetal bovine serum (Gibco, Austria), 100 U/ml penicillin (Lonza, Belgium) and 0.1 mg/ml streptomycin (Lonza, Belgium) under a humidified 5% CO₂ atmosphere at 37°C. Cells were trypsinized using Trypsin-EDTA (FlowLab, Australia) when they reached approximately 80% confluence. The cells in the exponential phase of growth after treatment with Trypsin-EDTA were seeded into 96-well plates (Greiner, Germany) in a concentration of 1x10⁴ cells/well for further MTT assay.

Cytotoxicity assay - MTT test

Cell cytotoxicity was determined by colorimetric assay based on tetrasolium salt MTT (3-(4,5-Dimethylthiazol-2-yl)-2,5-

diphenyltetrazolium bromide) (Sigma Chemical Co.). The MTT assay is based on the protocol first described by Mossman [11]. In this assay, living cells reduce the yellow MTT to insoluble purple formazan crystals, dissolved later in lysis buffer (1:1, ethanol : DMSO).

Cell suspension (100 µl) was added to each well of 96-well plates except for blank control wells. Cells were treated 24 h later with newly synthesized peptides in a wide concentration range (2 mM - 0.004 mM), and incubated for further 72 h. Then MTT was added followed by 3-hour incubation. MTT absorbance was read by ELIZA plate reader (TECAN, Sunrise TM, Grodig/Sazburg, Austria) at a wavelength of 540 nm and a reference wavelength of 620 nm. Cell cytotoxicity determined by MTT assay was expressed as the percentage of dead cells:

$$\% \text{ cytotoxicity} = (1 - (\text{OD sample} - \text{OD blank control}) / (\text{OD control} - \text{OD blank control})) \times 100.$$

RESULTS AND DISCUSSION

We focused our work on synthesis and study of the cytotoxic effect of bifunctional AVPI-RGD hybrid peptides over two cell lines.

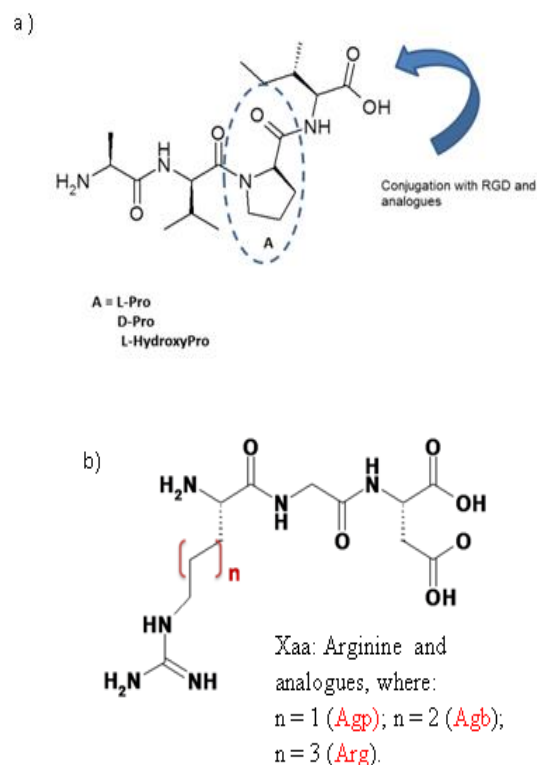


Fig. 1. Functional subunits: a) AVPI analogues; b) Tripeptide XaaGD and analogues

Regarding the data about Smac- and AVPI-mimetics and pharmacophore regions of AVPI, we decided to modify the proline at position 3 in AVPI

(Fig. 1a). We synthesized original AVPI peptide with L-Pro, and next Hydroxy-Pro (HyP) instead of proline itself. Next we prepared two new RGD analogues, containing an Arg-mimetic (Agb or Agp) with shortened side chain (with one or two –CH₂– groups respectively), in order to improve the stability and cytotoxicity of RGD molecule (Fig. 1b). Next corresponding AVPI-RGD hybrids were made. All peptides were synthesized by stepwise Fmoc solid-phase peptide strategy.

Analysis

The purity of the crude peptides characterized by RP-HPLC and capillary electrophoresis, was 87 – 97% (Fig. 2). All synthesized peptides were found to be stable in aqueous solution even after 72 hrs period and different values of pH, available physiologically.

Cytotoxicity

Next we performed initial screening for cytotoxic potential of peptides by colorimetric MTT analysis. Peptides were tested in a wide concentration range (2mM - 0.004 mM). The assay was performed on two cell lines - HepG2 cells (hepatocellular carcinoma cells) and MDA-MB-231 cells (breast cancer cells) recommended by literature data.

It was found that almost all tested compounds had weak or none cytotoxic effect when they were used as single agents (Fig. 3). Still that is in concordance with the literature data describing most of the AVPI- and Smac-mimetics as agents sensitizing cells to chemotherapeutics. Regarding that we are going to test our peptides with agents initiating apoptotic pathways, particularly TRAIL (cytotoxic death ligand) and cisplatin (triggering intrinsic pathway).

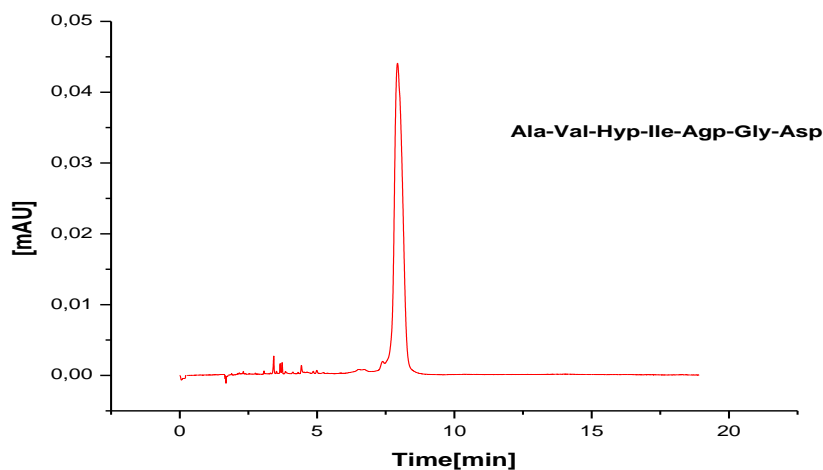


Fig. 2. Electrophoregramme of Ala-Val-HyP-Ile-Agp-Gly-Asp.

Conditions: Capillary: fused silica, 50/375 μ m, 30,4/40,6; BGE: 20 mM Tris, 5 mM H₃PO₄, 50 mM SDS; pH 8,6; U = 15 kV, I = 38 μ A; T = 23° C; 6,9 mbar, 10 s; UV 200 nm.

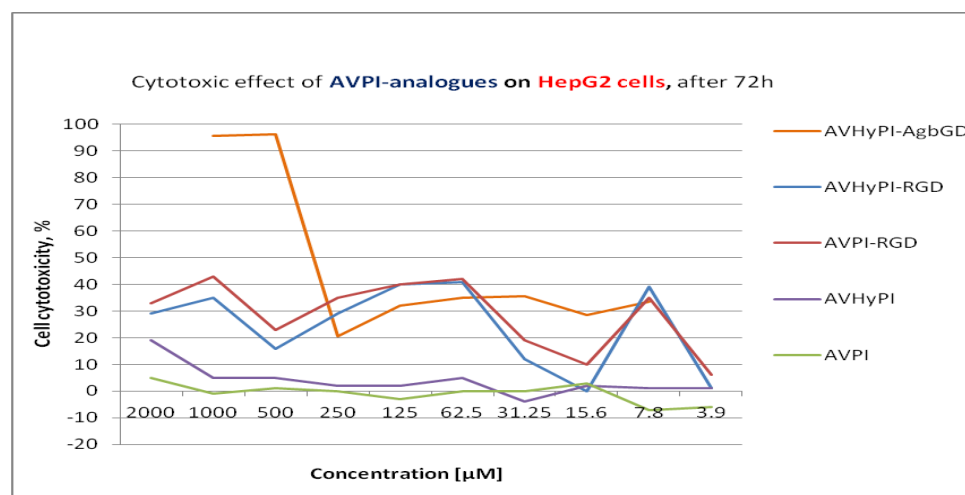


Fig. 3. Comparison of cytotoxic effect of AVPI-RGD-hybrids and AVPI / AVHyPI structural subunits on HepG2 cells after 72 h treatment (MTT-dye reduction assay).

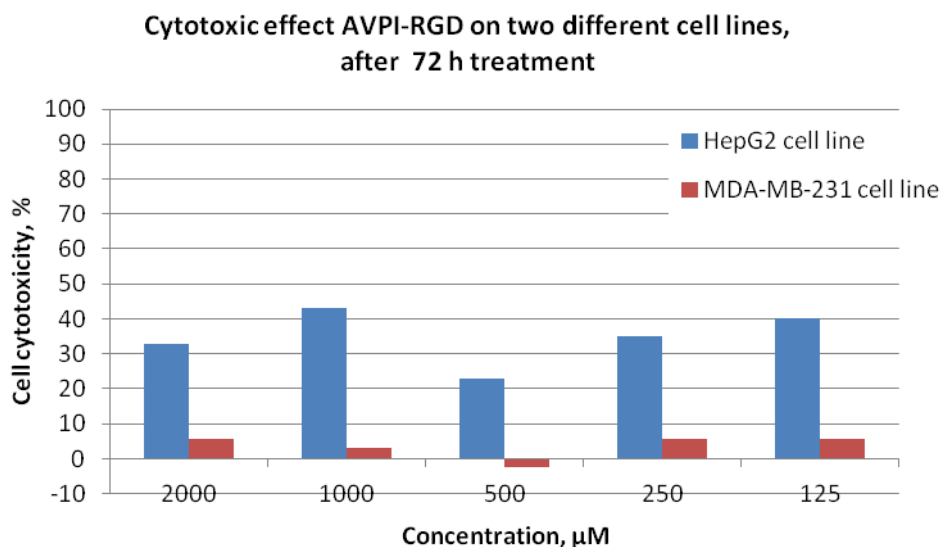


Fig. 4. Comparative graph of cytotoxic effect AVPI-RGD-hybrid over two different cell lines (HepG2 and MDA-MB-231) after 72 h treatment.

Nevertheless, we showed that AVPI-RGD hybrids exert comparatively higher cytotoxic effect than individual subunits - AVPI, AVHyPI (Fig. 3). One of the hybrids - Ala-Val-HyP-Ile-Agb-Gly-Asp (AVHyPI-AgbGD), double modified, showed higher activity, so we may speculate it is caused by the substitution of Arg amino acid in RGD with its analogue Agb.

Besides that, cytotoxic activity of peptides over both cell lines was compared, as it was shown slightly higher effect of AVPI-RGD on HepG2 cells in comparison to MDA-MB-231 cells (Fig. 4).

That pilot experiments directed us to further examination of peptides over the same and additional cell lines, in search for repeatability and selective effect over different cells. We need further combination of these peptides with other cytotoxic agents in search of sensitizing effect.

Acknowledgements: The work was supported by project no. 34 of the cooperation between ASCR and BAS in the period 2014-2016.

REFERENCES

1. D. J. Chen and S. Huerta, *Anti-cancer Drugs*, **20**, 646 (2009).
2. E. N. Shiozaki and Y. Shi, *Trends Biochem.Sci.*, **39**, 9 (2004).

3. J. E. Vince, W. Wong, N. Khan, R. Feltham, D. Chau, A. Ahmed, C. A. Benetatos, S. K. Chunduru, S. M. Condon, M. McKinlay, R. Brink, M. Leverkus, V. Tergaonkar, P. Schneider, B. A. Callus, F. Koentgen, D. I. Vaux, J. Silke, *Cell*, **131**, 682 (2007).
4. A. Schimmer, K. Welsh, C. Pinilla, Zh. Wang, M. Krajewska, M-J. Bonneau, I. Pedesen, Sh. Kitada, F. Scoff, B. Bailly-Maitre, G. Glinsky, D. Scudiero, E. Sausville, G. Salvesen, A. Nefzi, J. Ostresh, R. Houghten, J. Reed, *Trends in Genetics*, **18**, 7 (2002).
5. G. Martinez-Ruiz, V. Maldonado, G. Ceballos-Cancino, J.P. Reyes, G.J. Melendez-Zajgla, *J. Experimental & Clinical Cancer Res.* **27**, 48 (2008).
6. N. Elsayed, D. El Ella, R. A.T. Serya, K. A.M. Abouzid, *Future J.Pharmaceut. Sci.*, **1**, 16 (2015).
7. L. Bai, D. C. Smith, S. Wang, *Pharmacol. Therap.* **144**, 82 (2014).
8. D. Lecis, C. Drago, L. Manzoni, P. Seneci, C. Scolastico, E. Mastrangelo, M. Bolognesi, A. Anichini, H. Kashkar, H. Walczak, D. Delia, *British J. Cancer* **102**, 1707 (2010).
9. E. C. LaCasse, D. J. Mahoney, H. H. Cheung, S. Plenchette, S. Baird and R. G. Korneluk, *Oncogene* **27**, 6252 (2008).
10. M. Mingozzi, L. Manzoni, D. Arosio, A. Dal Corso, M. Manzotti, F. Innamorati, L. Pignataro, D. Lecis, D. Delia, P. Seneci, C. Gennari, *Org. Biomol. Chem.*, **12**, 3288 (2014).
11. T. Mossman, *J. Immunol. Methods*, **65**, 55 (1983).

СИНТЕЗ И АНАЛИЗ НА ЦИТОТОКСИЧНИЯ ПОТЕНЦИАЛ НА НОВИ AVPI-RGD ХИБРИДНИ ПЕПТИДИ

М.Г. Георгиева, Р.Л. Дечева, Т.И. Пайпанова

Институт по Молекулярна биология „Акад. Румен Цанев”, Българска Академия на Науките, ул. Акад. Г. Бончев, бл. 21, 1113 София, България

Постъпила на 30 септември, 2016 г.; Коригирана на 18 февруари, 2017 г.

(Резюме)

Разработването на агенти, повлияващи селективно критични апоптотични регулатори в раковите клетки, е обещаваща стратегия за развитие на нови по-селективни и ефективни класове противоракови лекарства. В настоящия доклад ние се фокусирахме върху синтез и изследване на цитотоксичния потенциал на нови AVPI-RGD хибридни пептиди. AVPI- и RGD- пептидните последователности са познати със своя про-апоптотичен потенциал. Това ги превърна в интересен обект на фармакологичен дизайн през последното десетилетие. Чрез Fmoc твърдофазен пептиден подход (SPPS) ние синтезирахме AVPI-, RGD-аналози, както и съответните им конюгати. Химични модификации бяха направени в аминокиселинните остатъци на пролин и аргинин. Цитотоксичният потенциал на пептидите беше изследван върху две различни ракови клетъчни линии (HerG2, MDA-MB-231) чрез МТТ тест. При първоначалните изследвания, беше установено, че пептидите, прилагани самостоятелно, имат слаб или нямат цитотоксичен ефект. Въпреки това, показахме, че конюгатите имат висока активност в сравнение с пептидите AVPI и AVHyPI.

Aminophenoxy-substituted zinc(II) phthalocyanines as basic photosensitizers for conjugation with biologically active moieties *via* amide bond

M.B. Aliosman^{1*}, I.Z. Eneva¹, I.B. Stoineva¹, M. Durmus², V.N. Mantareva¹

¹ Institute of Organic Chemistry with Centre of Phytochemistry,
Bulgarian Academy of Sciences, Acad. G. Bonchev, Bld. 9, 1113 Sofia, Bulgaria

² Gebze Technical University, Department of Chemistry, Gebze, Kocaeli, 41400 Turkey

Received September 29, 2016; Revised January 25, 2017

Photodynamic therapy with a photosensitizer functionalized with biologically active compounds such as amino acids or short peptides appears to be a promising strategy for targeted-oriented therapy. The photodynamic process is based on effective action between a photosensitizer, atmospheric molecular oxygen and specific light from visible to near infrared spectra (630 – 850 nm). Thus results in generation of singlet oxygen and other reactive oxygen species which can oxidize the varieties of biomolecules with consequential photocytotoxicity. Particular functionalization of phthalocyanine macrocycle with biologically-active units as amino acids and peptides aims to improve the solubility of the molecule of phthalocyanine as well as to enhance the cellular uptake of the photosensitizer and to improve the selectivity to the pathogenic cells.

The study presents optimization of several synthetical pathways for synthesis of tetra- and octa- aminophenoxy substituted Zn (II) phthalocyanines which functional groups namely aminophenoxy- moiety is a suitable unit for coupling through amide bond.

Keywords: phthalodinitriles, photosensitizer, Zn (II) phthalocyanine, amide bond, photodynamic therapy

INTRODUCTION

The photosensitizer conjugation to different type biomolecules such as cell penetrating, cell specific or biologically active amino acids or short peptides has been well documented as successful method to enhance the selectivity, intracellular delivery and efficacy of photodynamic method [1-7]. Peptides are attractive molecules for drug functionalization due to their relatively small size (<50 amino acid residues) which make them non-immunogenic, with a good tissue penetration, including crossing malfunctioning blood-brain barrier, and many of them interact with a given biological target without eliciting significant toxic responses. Peptides can be easily modified, allowing alterations in the sequence and straightforward conjugation to other chemical substances including phthalocyanine photosensitizers [8-10].

Phthalocyanines (Pcs) have been developed as a prospective second generation photosensitizers for biomedical applications, especially the metal complexes (MPcs) coordinated with diamagnetic ions [11-13]. The known MPcs show strong absorption (extinction coefficient $\epsilon > 10^5 \text{ M}^{-1} \text{ cm}^{-1}$) at far red wavelengths ($> 670 \text{ nm}$) and strong singlet oxygen generation abilities. The macrocyclic molecule is flexible to structural modifications which allow the binding on

peripheral or non-peripheral position of different functional groups and also at the central metal ion for the metals with higher than 2 coordination number. It is also possible to bind bulky axial substitution groups. The photophysicochemical properties of MPcs are strongly dependent on the substituents around the Pc aromatic core or the central ions. The proper functionalization of MPc macrocycle aims to intensify the absorption in the red region of visible light, to have non-toxic effect in the absence of light, to be selective for the targeted cells and to the normal tissue with an efficient generation of singlet oxygen. A large number of new photosensitizers have been proposed for clinical PDT; however their properties have still several limitations [14, 15].

Amino groups have ability of strong interaction and moreover the covalent bonding with biologically active molecules through carboxylic group. Hence, they are preferred functionalizations for preparation of pathogenic cell targeting photosensitizer [16].

One possible synthetical pathway for preparation of amino- substituted phthalocyanines started from synthesis of amino- substituted phthalodinitriles as precursors followed by cyclotetramerization reaction. Nyokong et. al. successfully synthesized tetraaminophenoxy substituted In(III) phthalocyanine in quinoline in the presence of urea [17].

* To whom all correspondence should be sent:

E-mail: meliha_aliosman@yahoo.com

Most of the reported amino- substituted phthalocyanines involved phthalocyanine formation from nitro- substituted phthalodinitriles followed by cyclotetramerization reaction to obtain nitro-substituted phthalocyanine and by reduction to the amino- substituted phthalocyanines. There are reports about the possible reaction routes for synthesis of aminophenoxy- functionalized zinc(II) phthalocyanines [18-22]. Wohrle and co-authors obtained tetra aminophenoxy substituted Zn(II) phthalocyanine by reduction of the nitro analogs with SnCl₂ [18]. The group of Prof. Ahmet Gul obtained the aminophenoxy phthalocyanine by reduction of the nitro groups using hydrazine hydrate and 10% Pd/C [21]. Nyokong et. al. synthesized the octa- aminophenoxy substituted phthalocyanine by the reduction of nitro analogs with sodium sulfide nonahydrate [20]. The applications of phthalocyanine complexes as photosensitizers require the use of biocompatible and diamagnetic metal ions to obtain the phthalocyanine complexes for PDT.

The study presents the optimization of the synthetical pathways for synthesis of tetra- and octa- aminophenoxy- substituted Zn (II) phthalocyanines. The altering of the reaction conditions of the chemical procedures was applied in order to obtain high yield and purity of the target compounds.

EXPERIMENTAL

General

All reagents and solvents were of reagent-grade quality obtained from commercial suppliers. All solvents used for synthesis such as dimethylformamide (DMF), tetrahydrofuran (THF), 1-pentanol were dried or distilled and stored over molecular sieves (3 Å) before experiments. The salt zinc acetate (hydrate)₂ was dried in Glass oven over P₂O₅. The catalyst 1,8-Diazabicyclo[5.4.0]undec-7-ene (DBU) was used as received. The purity of the products was tested in each step using thin layer chromatography (TLC). Silica gel 60 Å was purchased from Merck. All reactions were carried out under nitrogen atmosphere. FT-IR spectra were recorded on a Perkin Elmer Spectrum 100 spectrometer. ¹H NMR spectra were recorded on a Varian 500 MHz spectrometer (Gebze Technical University, Turkey) in DMSO-d₆, CDCl₃-d₁ for compounds **1**, **2**, **2a** and on Bruker 600 MHz spectrometer (Institute of Organic Chemistry with Centre of Phytochemistry) in DMSO-d₆ solutions for compounds **1a,3,4,5,6**.

Synthesis

Synthesis of 4-(4-nitrophenoxy) phthalonitrile (**1**)

4-Nitro phthalonitrile (1 g, 5.78 mmol) was dissolved in dry DMF and 4-nitrophenol (0,960 g 6.93 mmol) was added and stirred at room temperature under nitrogen atmosphere. Dry, powdered K₂CO₃ (800 mg, 5.79 mmol) was added as a base. After 24 h second portion K₂CO₃ (800 mg, 5.79 mmol) was added. The mixture was stirred until the ending of the starting 4-nitro phthalonitrile. Reaction was monitored by TLC. Then the reaction mixture was poured into ice water and stirred for 15 minutes. The obtained white precipitate was filtered off, washed several times with cold water dried under vacuum at 80 °C. Yield: 1.4 g (91 %). Molecular formula: C₁₄H₇N₃O₃. Molecular weight: 265,22 g/mol. FT-IR [$\nu_{\max}/\text{cm}^{-1}$]: 3108, 3078, 3037 (CH arom), 2232 (-C≡N), 1580, 1343 (-NO₂), 1512, 1481 (ARC=C), 1246 (Ar-O-Ar), 1309, 1213, 948, 849, 758; ¹HMR (d₁-CDCl₃), δ , ppm: 8.39-8.35 (d, 2H, CH), 7.87-7.85 (d, 1H, CH), 7.45 (d, 1H, CH), 7.40-7.38 (d, 1H, CH), 7.24-7.22 (d, 2H, CH).

Synthesis of 4-(4-aminophenoxy) phthalonitrile (**1a**)

4-Nitro phthalonitrile (1 g, 5.78 mmol) and 4-aminophenol (0.693 g, 6.35 mmol) were put in a round bottom flask and dry DMF was added while stirring. Dry potassium carbonate (1.6 g 11.56 mmol) was added when the mixture above became clear and after 24 h second portion potassium carbonate (0.800 g 5.78 mmol) was added. The reaction was carried out under argon atmosphere for 48 h. Then the solution was poured into ice water. The precipitated solid product was filtered off, washed with excess of water and then dried in a vacuum at 50 °C. Yield: 1.3g (91 %). Molecular formula: C₁₄H₉N₃O, Molecular weight: 235.25 g/mol. FT-IR [$\nu_{\max}/\text{cm}^{-1}$]: 3456, 3375 (NH₂), 3108, 3073, 3047 (CH arom), 2236 (-C≡N), 1598, 1608 (NH), 1508, 1485 (ARC=C), 1204, 1253 (C-O-C). ¹H-NMR (d₆-DMSO), δ , ppm: 8.03-8.01 (d, 1H, CH arom), 7.60-7.59 (d, 1H, CH arom), 7.25-7.23 (dd, 1H, CH arom), 6.86-6.83 (dt, 2H, CH arom), 6.64-6.62 (dt, 2H, CH arom), 5.17 (s, 2H, NH₂).

Synthesis of 4,5 bis (nitrophenoxy) phthalonitrile (**2**)

The reaction was carried out at different reaction conditions such as time, temperature and ratio in order to improve the purity and yield. A solution of 4,5-dichlorophthalonitrile (1 g, 5.08 mmol), and p-nitrophenol (2.11 g, 15.24 mmol) in dry DMF was heated while stirring at 90 °C under argon

atmosphere with the presence of dry K₂CO₃ (5,52 g 40 mmol) which was added in portions. Reaction was monitored by TLC. After finishing the starting phthalonitrile the reaction mixture was added to ice water to get precipitation and was filtered off, washed with excess of water. Obtained product was purified with column chromatography with eluent dichloromethane. Yield: 0.200 g (10%). Molecular Formula: C₂₀H₁₀N₄O₆, Molecular weight: 403 g/mol. FT-IR [$\nu_{\max}/\text{cm}^{-1}$]: 3105, 3077, 3037 (CH arom), 2238 (-C≡N), 1581, 1345 (NO₂), 1519, 1482 (ArC=C), 1271 (Ar-O-Ar). ¹H-NMR (d₆-DMSO), δ , ppm: 8.30-8.29 (d, 4H, CH arom), 7.52 (s, 2H, CH arom), 7.06-7.04 (d, 4H, CH arom).

Synthesis of 4,5 bis (aminophenoxy) phthalonitrile (2a)

A solution of (1, 5.08 mmol) 4,5-dichlorophthalodinitrile and (1.66 g, 15.2 mmol) aminophenol in dry DMF was heated while stirring at 90 °C under argon atmosphere with the presence (5.52 g, 40 mmol) dry K₂CO₃ which was added in portions. The mixture was stirred until finishing the starting nitrile, and then the reaction mixture was added to ice water to precipitate and filtered off, washed with excess of water. The obtained crude product was purified by column chromatography with eluent dichloromethane /acetone (9:1) Yield: 0.880 g (51%). FT-IR [$\nu_{\max}/\text{cm}^{-1}$]: 3443, 3355 (-NH₂), 3110, 3047, 3000 (CH arom), 2226 (-C≡N), 1581, 1495 (ArC=C), 1204 (C-O-C). ¹HMR (d₆-DMSO), δ , ppm: 7.29 (s, 2H, CH), 6.85 (d, 4H, CH arom), 6.62 (d, 4H, CH arom), 5.15 (4H, NH₂).

Synthesis of 2(3), 9(10), 16 (17), 23(24) tetra (4-nitrophenoxy) substituted Zn (II) phthalocyanine (3)

The mixture of 920 mg (3.47 mmol) of compound 1 was dissolved in 4 mL 1-pentanol and 158 mg (0.86 mmol) anhydrous zinc(II) acetate and 12 drops of DBU were added and stirred at reflux under nitrogen atmosphere. The reaction was monitored by TLC. When the reaction finished, then reaction mixture was cooled to room temperature from 137 °C and precipitated in hexane, filtrated and washed with excess of hexane, methanol and ethanol. The obtained crude product was purified by column chromatography with eluent CHCl₃/THF (10:1.5) Yield: 680 mg (69%). Molecular Formula: C₅₆H₂₈N₁₂O₁₂Zn, Molecular weight: 1126.29 g/mol. FT-IR [$\nu_{\max}/\text{cm}^{-1}$]: 2928 (CH arom), 1644, 1586, 1339 (NO₂), 1514, 1487 (ArC=C), 1393, 1236, 1110, 1084, 942, 847, 726.

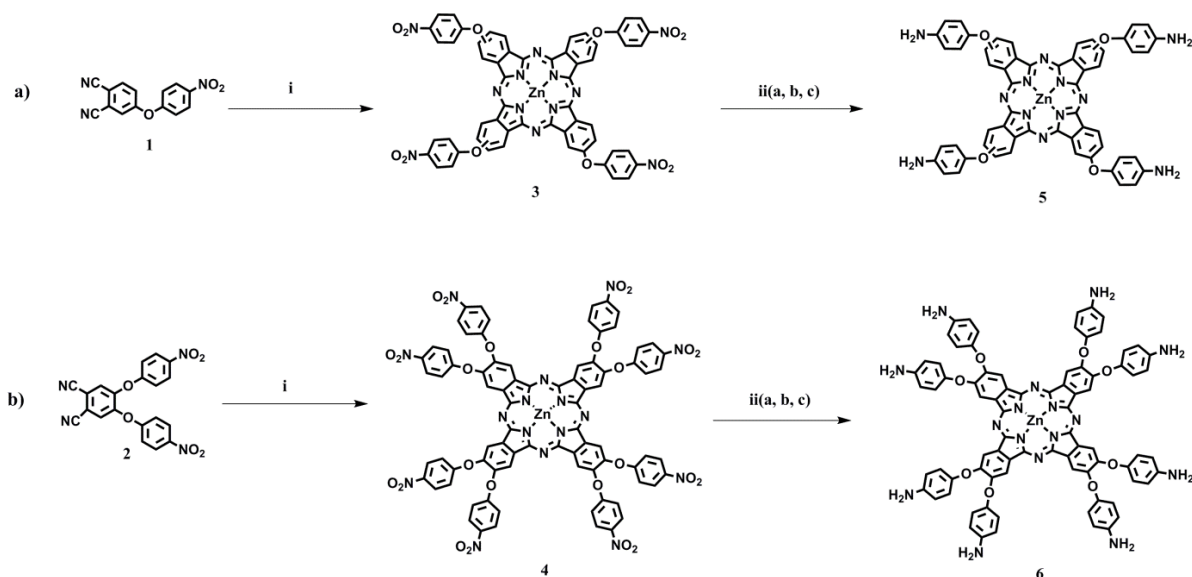
UV-Vis (DMF) λ_{\max} (log ϵ): 675 (4.07), 610 (3.31), 350 (3.71). ¹HMR (d₆-DMSO), δ , ppm: 8.47-8.40 (m, 6H, CH Ar), 8.35-8.29 (m, 6H, CH Ar), 7.96-7.90 (m, 4H, CH Ar), 7.73-7.53 (m, 10H, CH arom), 7.33-7.30 (d, 2H, CH arom).

Synthesis of 2,3,9,10,16,17,23,24 octa nitrophenoxy substituted Zn(II) phthalocyanine (4)

830 mg (1.97 mmol) 4,5 bis (nitrophenoxy) phthalonitrile 2 was dissolved in 4 mL 1-pentanol and then 90 mg (0.49 mmol) anhydrous zinc(II) acetate and 14 drops DBU were added and stirred under reflux at nitrogen atmosphere. The reaction was monitored with TLC. Then reaction mixture was cooled to room temperature and precipitated in hexane, filtrated and washed with excess of hexane, methanol and ethanol. The obtained crude product was purified by column chromatography with eluent CHCl₃/EtOH (10:1) Yield: 680 mg (82 %). Molecular Formula: C₈₀H₄₀N₁₆O₄Zn. Molecular weight: 1674,67 g/mol. FT-IR [$\nu_{\max}/\text{cm}^{-1}$]: 3099, 3075(CH arom), 1520, 1342(NO₂), 1515, 1488 (ArC=C), 1217. UV-Vis (DMF) λ_{\max} (log ϵ): 675 (3.34), 645 (2.42), 610 (2.42), 350 (3.11). ¹HMR (d₆-DMSO), δ , ppm: 8.74 (s, 4H, CH arom), 8.22-8.20 (m, 17H, CH arom), 7.95 (s, 1H, CH arom), 7.81 (s, 2H, CH arom), 7.40 (s, 12H, CH arom), 7.20-7.19 (d, 4H, CH arom).

Synthesis of 2(3), 9(10), 16 (17), 23(24) tetra (4-aminophenoxy) substituted Zn (II) phthalocyanine (5)

520 mg (0.46 mmol) of compound 3 was dissolved in dry THF, then (40 mg) Pd/C was added and stirred under hydrogen atmosphere at ice bath. The reaction was monitored by TLC. Reaction mixture was filtrated to remove the Pd/C and washed with excess of DMF and the solvent was vacuum evaporated with pump. Yield: 280 mg (70 %). Molecular Formula: C₅₆H₃₆N₁₂O₄Zn; Molecular weight: 1006,36 g/mol. FT-IR [$\nu_{\max}/\text{cm}^{-1}$]: 3351, 1603 (NH), 2925,2855 (CH arom), 1505, 1483 (ArC=C), 1392, 1335, 1260, 1234. UV-Vis (DMF) λ_{\max} (log ϵ): 685 (3.01), 615 (2.26), 350 (2.89). ¹HMR (d₆-DMSO), δ , ppm: 7.95 (s, 6H, CH arom), 7.77-7.75 (d, 2H, CH arom), 7.25-7.24 (d, 4H, CH arom), 7.05-7.04 (d, 3H, CH arom), 6.87-6.85 (d, 6H, CH arom), 6.65-6.64 (d, 7H, CH arom) 5.16 (s, 8H, NH₂).



Scheme 1a, b. Reaction routes for synthesis of tetra- and octa- aminophenoxy substituted Zn(II) phthalocyanines. Reagents and conditions for procedures: **a)** and **b)** (i) Zn acetate, DBU, 1-pentanol; (ii) dry DMF, H₂, Pd/C, ice bath; (iib) Ethanol, SnCl₂/ HCl; (iic) DMF, Na₂S.H₂O.

Synthesis of 2,3,9,10,16,17,23,24 octa aminophenoxy substituted Zn(II) phthalocyanine (6)

500 mg (0.31 mmol) of compound **4** was dissolved in dry DMF, then (80 mg) Pd/C was added and stirred at ice bath under hydrogen atmosphere. The reaction was monitored by TLC. Reaction mixture was filtrated to remove the Pd/C and washed with excess of DMF and the solvent was vacuum evaporated. Yield: 400 mg (90 %). Molecular Formula: C₈₀H₅₆N₁₆O₈Zn, Molecular weight: 1434 g/mol. FT-IR [$\nu_{\max}/\text{cm}^{-1}$]: 1613 (NH), 1504, 1399 (ArC=C), 1200, 1079. UV-Vis (DMF) λ_{\max} (log ϵ): 679 (3.52), 647 (2.96), 615 (289), 301 (3.73). ¹HMR (d₆-DMSO), δ , ppm: 8.22-8.20 (m, 20H, CH arom), 7.20-7.19 (d, 20H, CH arom), 4.37 (s, 16H, NH).

RESULTS AND DISCUSSION

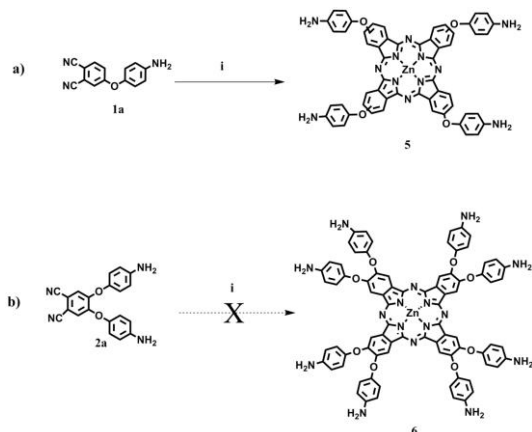
Synthesis and characterizations

Two different reaction pathways were applied to obtain the desired tetra- and octa- aminophenoxy Zn(II) phthalocyanines (**Scheme 1** and **2**). First reaction route shown in Scheme 1 started with synthesis of the corresponding nitrophenoxy-substituted phthalodinitriles, followed by the formation of the phthalocyanine molecules and by reduction of the nitro units to obtain the desired zinc(II) aminophenoxy substituted phthalocyanines. Synthetic procedure of nitrophenoxy substituted phthalonitriles is presented in **Scheme 1a and 1b**. The starting compounds 4-(4-nitrophenoxy)

phthalonitrile (**1**) and 4,5-bis-(nitrophenoxy)-phthalonitrile (**2**) were prepared by modification of the known reaction procedure described elsewhere [20, 23]. Compounds (**1**) and (**2**) were synthesized with the starting 4-nitrophenol and 4, 5-dinitrophenol and p-nitrophenol in presence of K₂CO₃ in dry DMF under nitrogen atmosphere. The base catalyzed nucleophilic aromatic displacement reaction takes place. To obtain compound (**2**) different reaction conditions such as time, temperature and ratio in order to have high purity and yield were tried. The most proper reaction pathway is shown in **Scheme 1b**. The IR spectra of (**1**) and (**2**) confirmed the characteristic vibrations of the -C≡N stretching with sharp and narrow peak at position at 2232 cm⁻¹ and also the characteristic vibrations of NO₂ group at positions 1345, 1580 cm⁻¹ and 1345, 1581 cm⁻¹, respectively. The ¹H-NMR spectra of the phthalonitriles (**1**) and (**2**) were consistent with the predicted structures.

Tetra and octa nitrophenoxy- substituted Zn(II) phthalocyanines were synthesized according to the literatures [20-22]. The cyclotetramerization of the compounds (**1**) and (**2**) was carried out in the presence of anhydrous ZnCl₂ and DBU as catalyst in 1-pentanol at 140 °C under nitrogen atmosphere (**Scheme 1a and 1b**). The IR spectra of Zn(II) phthalocyanines (**3**) and (**4**) clearly indicates the cyclotetramerization of the phthalonitrile derivatives (**1**) and (**2**) with the disappearance of the -C≡N peak at 2232 cm⁻¹. The ¹H-NMR spectra of the starting phthalonitriles (**1**) and (**2**) were consistent with the predicted structures.

Tetra- and octa- aminophenoxy substituted Zn(II) phthalocyanines (**5**) and (**6**) were synthesized by reduction of the nitro groups of compounds (**3**) and (**4**) with reaction procedures which is given in **Scheme 1a** and **b**. Several reduction procedures with different reducing agents were tested namely $\text{Na}_2\text{SxH}_2\text{O}$ (a) and tin dichloride/HCl (b) which resulted to compounds (**5**) and (**6**) [18-22]. The most efficient reduction method was the reaction procedure of bubbling hydrogen gas in nitro-phthalocyanine solution in the presence of 10% Pd/C at ice bath. This synthetic approach was described for the first time in this study (**Scheme 1a** and **b, iia**). In the IR spectra of compound (**5**) and (**6**) the $-\text{NH}_2$ group was observed as strong peaks at 1603 and 1618 cm^{-1} , respectively and the characteristics NO_2 groups were disappeared which clearly established the formation of the target compounds. The $^1\text{H-NMR}$ spectra of (**5**) and (**6**) in deuterated DMSO solutions showed broad singlet band attributed to the $-\text{NH}_2$ protons at 5.16 and 4.37, respectively.



Scheme 2a, b. Synthetic routes of tetra- and octa-aminophenoxy substituted Zn(II) phthalocyanines. Reagents and conditions for procedures: **a**) and **b**) (i) Zn acetate, DBU, 1-pentanol.

Zn(II) phthalocyanines (**5**) and (**6**) were obtained by the second pathway which is shown in **Scheme 2a** and **b**. In this case the starting phthalonitriles were directly used for cyclotetramerization reaction. This allows reducing the step of the reduction reaction. For this reason the phthalonitriles (**1a**) and (**2a**) were prepared. Compound (**5**) was successfully obtained from the phthalonitrile (**1a**) in presence of anhydrous ZnCl_2 and DBU as catalyst in 1-pentanol at refluxing temperature under nitrogen atmosphere. However the obtained crude product was with limited solubility. Zn(II) phthalocyanine (**6**) was not obtained from the phthalonitrile (**2a**). Different reaction conditions were selected to obtain the

compound (**6**) such as solvent, temperature, presence of catalyst and without catalyst and metal salt (ZnCl_2) to speed the complex formation. Another pathway by passing through metal free phthalocyanine was also carried out, but the reaction was not completed. The possible reasons could be the high reactivity of the amino groups which tend to form hydrogen bond between them and also of the steric hindrance effect. Therefore this synthetic pathway was not sufficient.

Ground state electronic absorption and fluorescence spectra

The electronic absorption spectra of Zn(II) phthalocyanines (**5**) and (**6**) were recorded in DMF on a Perkin Elmer Lambda 25 UV/Vis Spectrometer. (Fig.1). They showed characteristic absorption bands in the visible region with absorption maximum at 683 nm for compound (**5**) and 679 nm for compound (**6**), respectively. In the UV region the second B band was recorded. ZnPc (**5**) was observed with band at around 350 nm with half of the intensity of absorption of the Q band. A sharp and intense B band at around 375-378 nm was observed for ZnPc (**6**). The obtained spectra showed monomeric behavior which is evidenced by a single, narrow Q band typical for metallated phthalocyanine complexes.

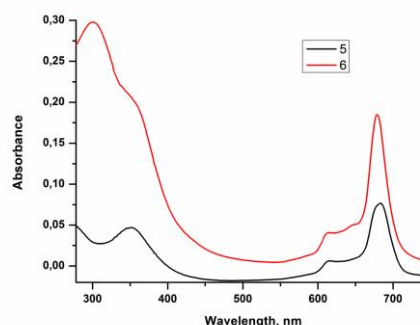


Fig.1. Absorption spectra of Zn(II) phthalocyanines (**5**) and (**6**) in DMF at concentration 12 μM .

In phthalocyanine chemistry the aggregation is usually depicted as a coplanar association of rings or physical conjugation throughout the substituents which are progressing from monomer molecule to dimer and higher associate of molecules. This phenomenon depends on the concentration, nature of the solvent, substituents, central metal ions and temperature [24]. The formation of oligomers of phthalocyanines for PDT usage should be avoided because of the lack of the proper photochemistry such as life-time and quantum yield of the triplet state of the photosensitizer. In order to evaluate the aggregation behavior of the studied ZnPc (**5**) and (**6**) the Beer's law was proven. The absorption

spectra were recorded in DMF for the concentration range between 3-16 μM for compound (5) and 12-2 μM for compound (6) in room temperature. The recorded spectra showed that, the intensity of the Q band increased with increment of the concentration. The new bands did not occur which suggested the lack of the formation of aggregates.

Fluorescence emission spectra of compounds (5) and (6) were recorded on a Perkin Elmer LS 55 Spectrometer at excitation 610 nm for the diluted solutions in DMF (Fig.2). The fluorescence emission maxima are red shifted as compared to the absorption maxima, which are as followed: 690 nm with a shift of 7 nm for compound (5) and 685 nm (6 nm shift) for compound (6).

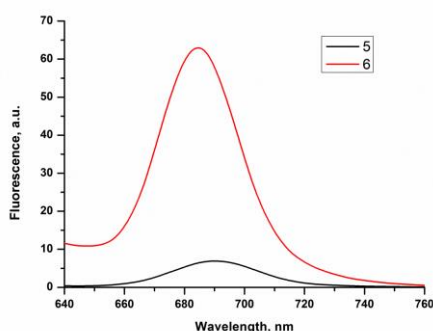


Fig.2. Fluorescence spectra of Zn(II) phthalocyanines (5) and (6) recorded in DMF. Excitation wavelength at 610 nm was used.

CONCLUSION

Tetra- and octa- aminophenoxy Zn(II) phthalocyanines were synthesized by following different reaction schemes. The efficient, simple and modified reaction conditions were chosen in order to obtain the products in a high yields and purity. A newly proposed synthetical pathway *via* reduction of the nitro- groups of tetra- and octa-nitrophenoxy- Zn(II) phthalocyanines using as reducing agent hydrogen gas, cooling and 10%Pd/C was applied for the both Zn(II) phthalocyanines with amonophenoxy- substitutions.

Acknowledgements: MA thanks for the fellowship 2216 of TUBITAK and the Program for career development of young scientists (project No 150) of Bulgarian Academy of Sciences.

REFERENCES

1. B. G. Ongarora, K.R. Fontenot, X. Hu, J. Sengal, S.D. Satyanarayana-Jois, M. G. H. Vicente, *J. Med. Chem.*, **55**, 3725 (2012).

2. Y. Choi, J.R. McCarthy, W.P. Weissleder, C. H. Tung, *ChemMedChem.*, **1**, 458 (2006).
3. M. R. Ke, S.L. Yeung, W.P. Fong, D. K. P, Ng, P.C. Lo, *Chem. Eur. J.*, **18**, 4225 (2012).
4. L. Bourre, F. Giuntini, Ian M. Eggleston, C. A. Mosse, A.J MacRobert, M. Wilson, *Photochem Photobiol. Sci.*, **9**, 1613 (2010).
5. W. Shi. G. Zhang, G. Cai, Y. Zhang, J. Zhao, J. Tao, *Bioorganic Med. Chem.*, **16**, 5665 (2008).
6. F. Li, Q.Liu, Z. Liang, J. Wang, M. Pang, W. Huang, W. Wu, Z. Hong, *Organic Biomolecular Chem.*, **14**, 3409 (2016).
7. L. Mamone, D. D. Ferreyra, L. Gandara, G. Di Venosa, P.Vallecora, D. Saenz, G. Calvo, A. Batlle, F. Buzzola, E. N. Durantini, A. Casas, *Photochem. Photobiol.*, **161**, 222 (2016).
8. N. Sewald, H.-D. Jakubke, Application of Peptides and Proteins, Wiley-VCH Verlag GmbH & Co. KGaA, Darmstadt, 2009.
9. M. Shadidi, M. Sioud, *Drug Resist. Updates*, **6**, 363 (2003).
10. Liu W, Hao GY, Long MA, Anthony T, Hsieh JT Sun XK. *Angew. Chem. Int. Ed.* **48**, 7346 (2009).
11. N. Sekkat, H van den Bergh, T. Nyokong, N.Lange, *Molecules*, **17**, 98 (2012).
12. G.Jori, C. Fabris, S. Soncin, S. Ferro, O. Coppellotti, D. Dei, L. Fantetti, G. Chiti, G. Roncucci, *Lasers Surg. Med.*, **38** 468, (2006).
13. T.G.S. Denis, T. Dai, A. Izikson, C. Astrakas, R. R. Anderson, M. R. Hamblin, G.P. Tegos, *Virulence*, **2**, 1 (2011).
14. M. Wainwright, *Anticancer Agents Med. Chem.* **8**,280, (2008)
15. R.R. Allison, G.H. Downie, E.R. Cuenca, X. H. Hu, C.J.H. Childs, C.H. Sibata, *Photosensitizers in clinical PDT. Photodiagn. Photodyn. Ther.*, **1**, 27 (2004).
16. <http://dx.doi.org/10.1016/j.bmc.2016.07.003>
17. K. Sanusi, E. K. Amuhaya, T. Nyokong, *J. Phys. Chem.*, **118**, 7057 (2014).
18. D. Wöhrle, G.Krawczyk, M. Paliuras, *Macromolecular Chemistry and Physics*, **189**, 1001 (1988).
19. R. Shankar, P. Sharma, A. Cabrera, G. Espinosa, N. Rosas, *Indian Journal of Chemistry Section B- Organic Chemistry Including Medicinal Chemistry*, **35**, 894 (1996).
20. S.E. Maree, T. Nyokong, *J Porphy. And Phthal.* **5**, 578 (2001).
21. F. Cong, B. Ning, X. Du, C. Ma, H. Yu, B. Chen, *Dyes Pigm.* **66**, 149 (2005)
22. G.K. Karaođlan, G. Gümrukçü, A. Koca, A. Gül, *Dyes Pigm.* **88**, 247 (2011).
23. D. Wöhrle, N. Iskander, G. Grashew, H. Sinn, E. A. Friedrich, W. Maier-Brost, J. Stern, P. Schlag, *Photochem. Photobiol.* **51**, 351 (1990)
24. A. Ogunsiye, D. Maree and T. Nyokong, *J. Mol. Struct.*, **650**, 131 (2004)

АМИНОФЕНОКСИ ЗАМЕСТЕНИ ФТАЛОЦИАНИНОВИ КОМПЛЕКСИ НА ЦИНК КАТО БАЗОВИ СТРУКТУРИ ЗА КОНЮГИРАНЕ С БИОЛОГИЧНИ АКТИВНИ ГРУПИ ЧРЕЗ АМИДНА ВРЪЗКА

М. Б. Алиосман¹, И. З. Енева¹, И. Б. Стойнева¹, М. Дурмуш², В. Н. Мантарева¹

¹Институт по органична химия с Център по фитохимия, Българска академия на науките, ул. Акад.
Г. Бончев, бл. 9, 1113 София, България

²Технически Университет Гебзе, Департамент по химия, Гебзе, 41400 Турция

Постъпила на 29 септември 2016 г.; Коригирана на 25 януари, 2017 г.

(Резюме)

Фотодинамичната терапия с фотосенсибилизатори, функционализирани с биологично активни съединения като аминокиселини или къси пептиди се явява обещаваща стратегия за насочената към таргета терапия. Фотодинамичният процес е резултат от ефективното взаимодействие на фотосенсибилизатор, атмосферен молекулен кислород и специфична светлина от видимата и близката инфрачервена област (630-850 nm). В резултат на това се генерират синглетен кислород и други реактивоспособни кислородни форми, които могат да окисляват биомолекули с последваща цитотоксичност. Функционализирането на фталоциановия макроцикъл с биологично-активни пептиди цели да подобри разтворимостта на фталоцианиновата молекула, както и да повиши клетъчното усвояване на фотосенсибилизатора и да подобри таргетната му селективност спрямо органели. Пептиди като клетъчно проникващи, клетъчно специфични, биологично-активни пептиди, рецептор свързващи секвенции, вътреклетъчно локализиращи секвенции могат да повишат действието на фотосенсибилизатора чрез двойна ефективност спрямо целевите клетки и тъкани, известно като синергична фотодинамична терапия и пептидна цитотоксичност.

Настоящото научно изследване представя оптимизирането на няколко синтетични пътища за синтез на тетра- и окта аминофенокси заместени цинкови (II) фталоцианини, чиято функционална група, наречена аминофенокси- група е подходяща единица за свързване с биологично-активни пептиди.

Synthesis and antibacterial activity of amino acids modified with specifically substituted pyrrole heterocycle

S.P. Vladimirova², D.L. Danalev^{1*}, D.A. Marinkova¹, R.N. Raykova¹, D.S. Manova¹,
S.R. Marinova¹, D.I. Marinova¹, S.A. Yaneva³

¹University of Chemical Technology and Metallurgy, Sofia 1756, Bulgaria, 8 blvd. Kliment Ohridski, Biotechnology Department

²University of Chemical Technology and Metallurgy, Sofia 1756, Bulgaria, 8 blvd. Kliment Ohridski, Department of Organic Synthesis and Fuels

³University of Chemical Technology and Metallurgy, Sofia 1756, Bulgaria, 8 blvd. Kliment Ohridski, Department of Fundamentals of Chemical Technology

Received October 01, 2016; Revised January 15, 2017

Since last century studying the properties of various heterocyclic compounds including pyrrole, as anti-inflammatory and anti-pain agents is explored strongly. It is interesting to note that a number of molecules containing in its structure pyrrole heterocycle are approved as drugs with diverse activities in medical practice.

Design of a series of substituted with specifically modified pyrrole heterocycle at N-terminus amino acids was done. The aim compounds were synthesized in acid conditions using Paal-Knorr reaction between substituted pyrrole and natural amino acids. Further, after purification and characterization antibacterial activity against model Gram positive (*Bacillus cereus* 1085), Gram negative (*Pseudomonas fluorescens*) microorganisms and fungi (*Candida lipolytica*) were studied by means of standard disk diffusion method. The highest activity against model strain Gram positive bacteria (*Bacillus cereus* 1085) show compounds Pyr-Ile (1d) and Pyr-β-Phe (1f). The best activity against model Gram negative microorganism (*Pseudomonas fluorescens* 1442) was revealed for compounds Pyr-Met (1e) and Pyr-β-Phe (1f). All tested compounds have not any activity against model strain fungi *Yarrowia lipolytica* 3344. Compound Pyr-β-Phe (1f) shows strong bacteriostatic effect against strain *Bacillus cereus* 1085.

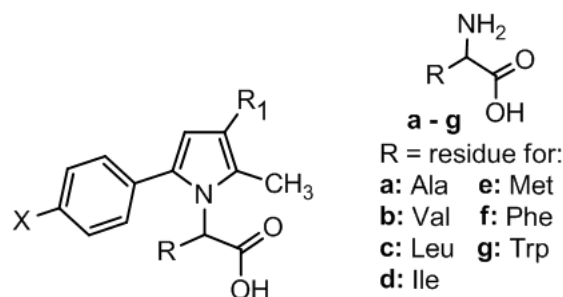
Key words: pyrrole, Paal-Knorr reaction, *Bacillus cereus* 1085, *Pseudomonas fluorescens*, *Candida lipolytica*

INTRODUCTION

Since last century studying the properties of various heterocyclic compounds including pyrrole, as anti-inflammatory and anti-pain agents is explored strongly [1]. It is interesting to note that a number of molecules containing in its structure pyrrole heterocycle [2, 3] as well as unnatural amino acids are approved as drugs with diverse activities in medical practice [4-6]. Pyrrole derivatives are essential in finding new drugs with pharmacological activity as anti-inflammatory, cytotoxicity, in vitro cytotoxic activity against tumors [7], in the treatment of hyperlipidemia [8], etc. Pyrrole-containing heterocyclic derivatives show biological activity as COX-1/COX-2 inhibitors and cytotoxic activity against different human tumor models [9]. They also show antioxidant [10], anticonvulsant [11], HIV-inhibiting action [12]. Pyrrole heterocycle participate in the classic Non-steroidal anti-inflammatory drugs (NSAIDs): Tolmeline, Zomepirac and Klopiprac, and in recent years their important biological activity is confirmed in many

investigations in different directions [13-15].

Design of a series of substituted with specifically modified pyrrole heterocycle at N-terminus amino acids was done. The targeted products (fig. 1) were synthesized via Paal-Knorr cyclization by condensation of seven amino-acids (a-g), acting as primary amines and 1,4-dicarbonyl compounds. The later was prepared by C-alkylation of commercially available β-dicarbonyl compound with ω-bromoacetophenone and then used *in situ* [16].



where **1a-1g**: X = Cl, R₁ = COOC₂H₅.

Fig.1. Structure of pyrrolylamino acids tested for antibacterial activity

Herein we report the antibacterial activity against model Gram positive (*Bacillus cereus* 1085), Gram negative (*Pseudomonas fluorescens*)

* To whom all correspondence should be sent:
E-mail: dancho.danalev@gamil.com

microorganisms and fungi (*Candida lipolytica*) by means of standard disk diffusion method.

EXPERIMENTAL

Material and Methods

Pseudomonas fluorescens 1442, *Bacillus cereus* 1085 and *Yarrowia lipolytica* 3344-microbial strains were supplied by the National Bank for Industrial Microorganisms and Cell Cultures (NBIMCC). Salts for nutrient medium were obtained from Merck (Germany). Glucose and bovine serum albumin (BSA) were obtained from Fluka (Switzerland). Agar and LB for nutrient microbial growth mediums were obtained from Sigma-Aldrich. Sterile disks impregnated with Gentamicin (10 μ g) and Fluconazole (25 μ g) were supplied by FOT (Bulgaria).

Cell cultures

Bacillus cereus 1085, *Pseudomonas fluorescens* 1442 and *Yarrowia lipolytica* 3344 were cultivated on solid agar nutrient medium containing meat extract, peptone, glucose, NaCl at 30°C for 24 h. After incubation process the bacterial colonies were picked up and suspended in liquid nutrient medium containing LB and 10% glucose for 24h in water bath shaker at 30 °C, pH 7.2-7.4. Further the cells were suspended in fresh liquid medium, containing LB and 10% glucose and the biomass was used for investigation of antimicrobial activity.

The yeast colonies were suspended in liquid nutrient medium containing yeast extract, malt extract, peptone and 10 % glucose. The biomass was cultivated for 24h in water bath shaker at 30°C, pH 6.

Standard disk diffusion test was used for studding of antimicrobial activity of target compounds. Discs impregnated with Gentamicin (10 μ g) and fluconazole (25 μ g) were used as refers.

Standard DNS method was used for determination of glucose consumption by *Bacillus cereus* 1085.

RESULTS AND DISCUSSION

The activity of newly synthesized compounds are tested against model Gram negative microorganisms - *Pseudomonas fluorescens* 1442, Gram positive microorganisms - *Bacillus cereus* 1085, and fungi - *Yarrowia lipolytica* 3344.

All impregnated sterile disks with different concentration of N-pyrrolyl amino acids (**1a-1g**), are incubated in petri dishes with biomass of strain *Bacillus cereus* 1085. 24 hours later obtained inhibition zones are measured and all data are

summarized in table 1. Sterile disks impregnated with 10 μ g Gentamicin (commercially available) were used as check samples.

Table 1. Inhibition zones in mm for tested compounds 1a-1g at concentrations 50mM and 25mM against *B.cereus*

Test compound	Zone of inhibition of <i>B. Cereus</i> at 50 mM concentration [mm]	Zone of inhibition of <i>B. Cereus</i> at 25mM concentration [mm]
1a	10	no effect
1b	13	10
1c	11	9
1d	16	15
1f	15	14
1g	8	8
Gentamicin	23	23

As it can be seen from the data in table 1, the highest activity reveals compounds Pyr-Ile (1d) and Pyr- β -Phe (1f) at both 50mM and 25mM concentrations. *Bacillus cereus*1085 is resistant against compounds 1a, 1c and 1g at 50 mM and 25 mM concentrations. According to compound 1b *Bacillus cereus* 1085 is moderately sensitive at 50 mM and microorganism is resistant at 25mM. Because of the good activity of compounds 1d and 1f they were also tested at 10 mM concentration. The obtained inhibition zones are 10mm which show that at this concentration strain *Bacillus cereus* 1085 is resistant.

Table 2. Inhibition zones in mm for tested compounds 1a-1g at concentrations 50mM and 25mM against *Pseudomonas fluorescens* 1442

Test compound	Zone of inhibition of <i>Ps. fluorescens</i> at 50 mM [mm]	Zone of inhibition of <i>Ps. fluorescens</i> at 25 mM [mm]
1a	13	no effect
1b	10	8
1c	10	9
1d	15	11
1e	20	no effect
1f	23	12
1g	no effect	no effect
Gentamicin	23	23

The same methods were used for determination of antibacterial activity of newly synthesized compounds against Gram negative microorganism

Ps. fluorescens 144. All studies were done again at 25mM and 50mM concentrations.

Sterile disks impregnated with 10µg gentamicin (commercially available) were again used as check sample. Results are summarized at table 2.

Data in table 2 show that compounds 1b, 1c and 1g have no activity against strain *Pseudomonas fluorescens* 1442. Strain is moderately sensible to compounds 1a and 1d at 50mM concentration, but it is resistant at concentration 25mM. Compounds 1e and 1f have strong antibacterial activity at 50 mM concentration but strain is resistant at 25 mM

All compounds did not exhibit any antifungal activity against model strain *Yarrowia lipolytica* 3344.

Investigation of antimicrobial activity of *Bacillus cereus* 1085 in presence of compound Pyr-β-Phe

Monitoring of bacterial growth is an additional method for investigation of antibacterial activity. Monitoring of bacterial growth is an additional method for investigation of antibacterial properties of compounds. Herein, we studied biomass growth of *Bacillus cereus* 1085 in presence and absence of compound 1f. For this purpose we used blank sample without compound and biomass in presence of 10 mM concentration of 1f. The absorbance of the biomass were measured at 590 nm spectrophotometrically during 98h of incubation time (Fig.2)

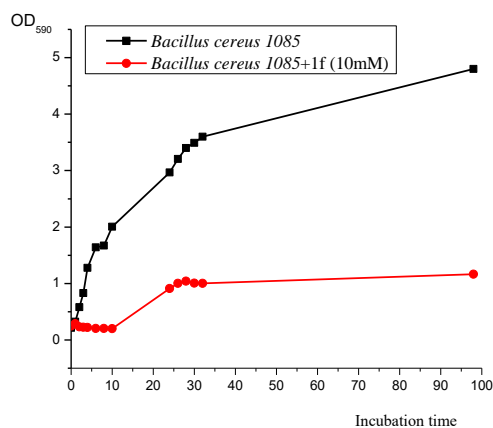


Fig. 2. Growth curves of *Bacillus cereus* 1085 in presence and absence of 1f

From the figure is noticed that lag-phase of the cells without compound 1f is shorter in comparison of those in presence of investigated compound. The cells are rapidly entered into exponential phase lasting up to 32 hours. After that the growth of cells is in steady state but don't enter in the stationary phase until the end of the incubation time. In terms

of cultivation of test compound (1f) is observed a longer initial phase, approximately 10 hours of incubation time. The exponential phase is prolonged to 28h. After that is observed the stationary stage of the cells culture. It can be concluded from the obtained data that compound 1f shows bacteriostatic effect to test microorganism *Bacillus cereus*.

In addition, the dynamic of glucose accumulation by *Bacillus cereus* cells in presence and absence of Pyr-β-Phe (1f) compound by using DNS method (Fig.3) were studied.

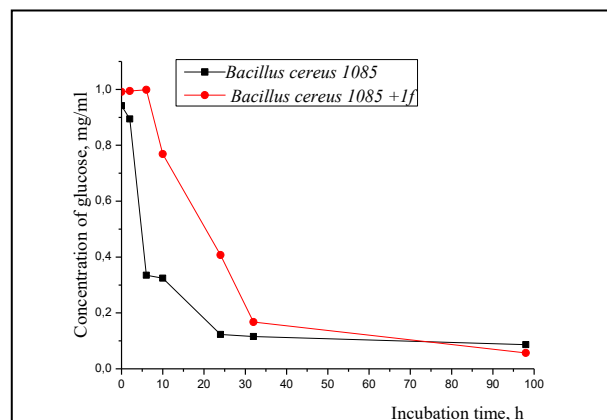


Fig.3. Glucose accumulation of *Bacillus cereus* in presence and absence of Pyr-β-Phe (1f)

The figure shows that the nutrient source accumulation by *Bacillus cereus* cells in the terms of cultivation without 1f is proportional of the incubation time. In the presence of Pyr-β-Phe (1f) the assimilation of glucose begins after 10h of incubation time. The glucose is accumulated completely up to 35h of incubation time.

CONCLUSION

Antibacterial activity against model Gram positive (*Bacillus cereus* 1085), Gram negative (*Pseudomonas fluorescens*) microorganisms and fungi (*Candida lipolytica*) of six newly synthesized pyrrolylamino acids were studied. The obtained results show that the highest activity against model strain Gram-positive bacteria (*Bacillus cereus* 1085) show compounds Pyr-1le (1d) and Pyr-β-Phe (1f). The best activity against model gram negative microorganism (*Pseudomonas fluorescens* 1442) was revealed for compounds Pyr-Met (1e) and Pyr-β-Phe (1f). All tested compounds have no any activity against model strain fungi *Yarrowia lipolytica* 3344.

Bacteriostatic effect is observed onto growth of *Bacillus cereus* cells in the presence of Pyr-β-Phe (1f).

Acknowledgments: This study was particularly supported by the project 11570 with Scientific Fund of UCTM.

REFERENCES

1. J.A.H. Lainton, J.W. Huffman, B.R. Martin, D.R. Compton, *Tetrahedron Lett.*, **36**, 1401(1995).
2. M. Artico, R. Silvestri, E. Pagnozzi, B. Bruno, E. Novellino, S.M. Greco, A. Ettore, A.G. Loi, G.F. Scintu, P. La Colla, *J. Med. Chem.*, **43**, 1886 (2000).
3. W. Malinka, M. Sieklucka-Dziuba, G. Rajtar, R. Rejdak, K. Rejdak, Z. Kleinrok, *Pharmazie*, **55**, 9 (2000).
4. K. Georgiev, T. Dzimbova, I. Iiev, A. Balacheva, R. Detcheva, T. Pajpanova, *Der Pharma Chemica*, **6**, 360 (2014).
5. T. Dzimbova, I. Iiev, K. Georgiev, R. Detcheva, A. Balacheva, T. Pajpanova *Collec. Czech Chem. Suppl.*, **13**, 34 (2011).
6. S.G. Bayryamov, N.G. Vassilev, M.A. Rangelov, A.P. Mladjova, D.D. Petkov. *Protein and Peptide Letters*, **16**, 392 (2009).
7. N. Amishiro, A. Okamoto, C. Murakata, T. Tamaoki, M. Okabe, H. Saito, *J. Med. Chem.*, **42**, 2946 (1999).
8. P.R. Bovy, J.T. Collins, R.E. Manning, US Pat. 6,008,368 (1999).
9. A.M. Almerico, P. Diana, P. Barraja, G. Dattolo, F. Mingoia, A.G. Loi, F. Scintu, C. Milia, I. Puddu, P. La Colla, *Farmaco*, **53**, 33 (1998).
10. Y. Fumoto, T. Eguchi, H. Uno, N. Ono, *J. Org. Chem.*, **64**, 6518 (1999).
11. J.R. Carson, R.J. Carmosin, P.M. Pitis, J.L. Vaught, H.R. Almond, J.P. Stables, H.H. Wolf, E.A. Swinyard, H.S. White, *J. Med. Chem.* **40**, 1578 (1997).
12. M. Artico, R. Silvestri, E. Pagnozzi, B. Bruno, E. Novellino, G. Greco, S. Massa, A. Ettore, A. Giulia, L. Franca, S. P. La Colla, *J Med. Chem.* **43**, 1886 (2000)
13. C. Peifer, A. Krasowski, N. Hämmerle, O. Kohlbacher, G. Dannhardt, F. Totzke, C. Schächtele, S. Laufer, *J. Med. Chem.*, **49**, 7549 (2006).
14. J.M. Richter, B.W. Whitefield, T.J. Maimone, D.W. Lin, M.P. Castroviejo, *J. Am. Chem. Soc.*, **129**, 12857 (2007).
15. H. Wang, M. Chen, L. Wang, *Chemical & pharmaceutical bulletin*, **55**, 1439 (2007).
16. S. Vladimirova, A. Bijev, *Heterocycl. Commun.*, **20**, 111 (2014).

СИНТЕЗ И АНТИБАКТЕРИАЛНА АКТИВНОСТ НА АМИНОКИСЕЛИНИ МОДИФИЦИРАНИ СЪС СПЕЦИФИЧНО ЗАМЕСТЕН ПИРОЛОВ ХЕТЕРОЦИКЪЛ

С.П. Владимирова², Д. Л. Даналев^{1*}, Д. А. Маринкова¹, Р. Н. Райкова¹, Д. С. Манова¹, С. Р. Маринова¹, Д. И. Маринова¹, С.А. Янева³

¹Химикотехнологичен и Металургичен Университет, София, 1756, България, бул. Климент Охридски 8, катедра Биотехнология

²Химикотехнологичен и Металургичен Университет, София, 1756, България, бул. Климент Охридски 8, катедра Органичен Синтез и Горива

³Химикотехнологичен и Металургичен Университет, София, 1756, България, бул. Климент Охридски 8, катедра Основи на химичните технологии

Постъпила на октомври, 2016 г.; Коригирана на 15 януари, 2017 г.

(Резюме)

Свойствата на различни съединения, съдържащи пиролов хетероцикъл се изследват широко от началото на века като противовъзпалителни и противоболкови агенти. Интересно е, също така, че редица молекули, съдържащи пиролов хетероцикъл са доказани лекарства с разнообразна активност в медицинската практика.

Беше направен дизайн на серия от аминокиселини, чиито N-край е включен в специфично заместени пиролови производни. Целевите съединения бяха синтезирани в кисела среда по реакцията на Паал-Кнор между заместен пирол и природни аминокиселини. След пречистване и охарактеризиране, съединенията бяха подложени на изследвания за антибактериална активност спрямо моделни Грам положителни (*Bacillus cereus* 1085), Грам отрицателни (*Pseudomonas fluorescens*) микроорганизми и гъби (*Candida lipolytica*) чрез използване на стандартен дисково-дифузионен метод. Най-висока активност срещу моделния Грам положителен щам микроорганизми (*Bacillus cereus* 1085) показаха съединенията Prg-Ile (1d) и Prg-β-Phe (1f). Най-добра активност по отношение на моделните Грам отрицателни микроорганизми (*Pseudomonas fluorescens* 1442) беше установена за съединенията Prg-Met (1e) и Prg-β-Phe (1f). Всички тествани съединения не показаха активност спрямо моделният щам гъби *Yarrowia lipolytica* 3344. Съединението Prg-β-Phe (1f) показва силен бактериостатичен ефект спрямо моделния щам *Bacillus cereus* 1085.

Acetylcholinesterase inhibition activity of peptide analogues of galanthamine with potential application for treatment of Alzheimer`s disease

S.A.Yaneva^{1*}, I.I. Stoykova², L.I. Ilieva³, L.T. Vezekov³, D.A. Marinkova², L.K. Yotova², R.N. Raykova², D. L. Danalev²

University of Chemical Technology and Metallurgy, Sofia 1756, Bulgaria, 8 blvd. Kliment Ohridski,

¹ Department of Fundamentals of Chemical Technology, *sp_yaneva@uctm.edu*

² Biotechnology Department

³ Department of Organic Chemistry

Received October 4, 2016; Revised January 15, 2017

An acetylcholinesterase inhibitor (AChEI) or anti-cholinesterase is a compound that inhibits the cholinesterase enzyme from breaking down acetylcholine, increasing both level and duration of action of the neurotransmitter ACh. AChEIs occur naturally as venoms and poisons; they are used as weapons in the form of nerve agents, and as constituents of medicines for Myasthenia Gravis treatment. They are used to increase neuromuscular transmission to treat Glaucoma and Alzheimer disease (AD) as well as an antidote to anticholinergic poisoning.

Herein, we report the kinetic investigation of five peptide amide and esters of galanthamine Boc-Val-Asn-Leu-Ala-Gly-Ogal, Boc-Val-Asn-Leu-Ala-Val-Gly-Ogal, Boc-Asp-(norGal)-Asp-Leu-Ala-Val-NH-Bzl, Boc-Asp-(norGal)-Asp-Leu-β-Ala-Val-NH-Bzl, Boc-Asp-(norGal)-Val-Asn-Leu-β-Ala-Val-NH-Bzl, inhibitors of AChE. In addition, IC₅₀ values (50 % inhibition effect on the enzyme) according to AChE were determined. Finally, we compare the obtained IC₅₀ values for synthetic peptides with those of two pesticides Parathion and Carbofuran, well know AChEI`s.

Key words: peptides, enzymes, inhibitors; pharmaceutical application

INTRODUCTION

Acetylcholinesterase (AChE) (E.C.3.1.1.7) is a serine hydrolase that catalyzes the hydrolytic degradation of acetylcholine to choline and acetic acid. According to cholinergic hypothesis AChE is one of both choline esterases (together with butyrylcholine esterase BuChE) which plays key role for progression of Alzheimer`s disease [1]. One of possible approaches for treatment of patients with Alzheimer`s disease is using of acetylcholinesterase inhibitors (AChEIs) [2]. AChEIs could have different origin, extracted from natural sources (galanthamine, huperzine A, uleine etc.) [3-6] or synthetic (including organophosphates, carbamates, peptides, etc.) one [7-10]. Parathion and carbofuran are compounds that belongs to two main groups of pesticides-organophosphorus (OPs) and carbamates. They are still widely used in veterinary practice and in agriculture as fungicides, insecticides and herbicides. Since carbamates, as well as OPs, are AChE inhibitors, both compounds cause similar toxic acute effects and symptoms derived from poisoning. The principal difference between OPs and carbamate induced inhibitory action is that the AChE-OP complex is much more stable than

AChE-carbamate, making carbamates the potential candidates for the treatment of Alzheimer`s disease [8].

Herein we report the acetylcholine esterase inhibition activity of several synthetic peptide amide and esters, derivatives of natural AChEI galanthamine. We also obtained IC₅₀ values for synthesized hybrid structures and additionally, we compared these data with those for two synthetic pesticides: one from the OP group and one carbamate.

EXPERIMENTALS

AChE inhibition activity

All kinetic investigations and IC₅₀ determinations were done using an optical biosensor with Acetylcholinesterase (AChE) (EC.3.1.1.7) from *Electrophorus electricus* (electric eel), Type VI-S, AChE from electric eel, immobilized onto hybrid membranes synthesized by sol-gel technology. Synthesis of used membranes containing cellulose acetate propionate with high molecule weight (~25 000) (CAP), methyl triethoxysilane (MTES) and Polyamidoamine (PAMAM) dendrimers is described in [11]. The quantity of protein immobilized onto the membranes, was determine using Lowry`s methodology [12]. Initially, the activity of the immobilized AChE was measured

* To whom all correspondence should be sent:
E-mail: *sp_yaneva@uctm.edu*

without presence of inhibitor. The experimental procedure was run at 25° C in 1 ml of 0.1M sodium phosphate buffer (pH 8) containing 90 µl of ACh iodide (7.5 AM) and 45 µl of 5,5'- dithiobis-2-nitrobenzoic acid (DTNB, 10 µM) and stirring. Further, newly synthesized compounds at different concentrations from 5 µM to 100µM were diluted in 1,5 ml of 0,1M sodium phosphate buffer (pH 8). 50mg of membranes with the immobilized enzyme were added directly to the solution and were incubated together for 30 min at 25° C. The membranes with immobilized AChE, were moved out from the solution and the residual activity was measured following the procedure according to Elman's method with DTNB reagent [13].

Peptide inhibitors were synthesized according to methodology described in [14]. They all are amides or esters of natural galanthamine with following structures:

Boc-Asp-(norGal)-Asp-Leu-β-Ala-Val-NH-Bzl (I₁), Boc-Asp-(norGal)-Asp-Leu-Ala-Val-NH-Bzl (I₂), Boc-Asp-(norGal)-Val-Asn-Leu-s-Ala-Val-

NH-Bzl (I₃), Boc-Val-Asn-Leu-Ala-Val-Gly-OGal (I₄), Boc-Val-Asn-Leu-Ala-Gly-OGal (I₅)

The inhibitory effects of all the analyzed AChEIs (the newly synthesized peptides, as well as the pesticides) was calculated by measuring the difference in the enzyme activity before and after incubation with inhibitor. The measurement was done at 412 nm for 8 min.

The inhibition percentage was calculated according to equation.

$$\text{Inhibition (\%)} = [(E_0 - E_i)/E_0] * 100,$$

Where E₀ is the initial inhibited sensor activity and E is the inhibited sensor activity. The sensitivity of the biosensor toward ACh was measured.

RESULTS AND DISCUSSION

Galantamine is one of the most selectively inhibitors of AChE which is one of the commonly used inhibitors to treat patients with mild to moderate AD. Therefore, syntheses of novel peptides compounds containing galantamine analogues are very important.

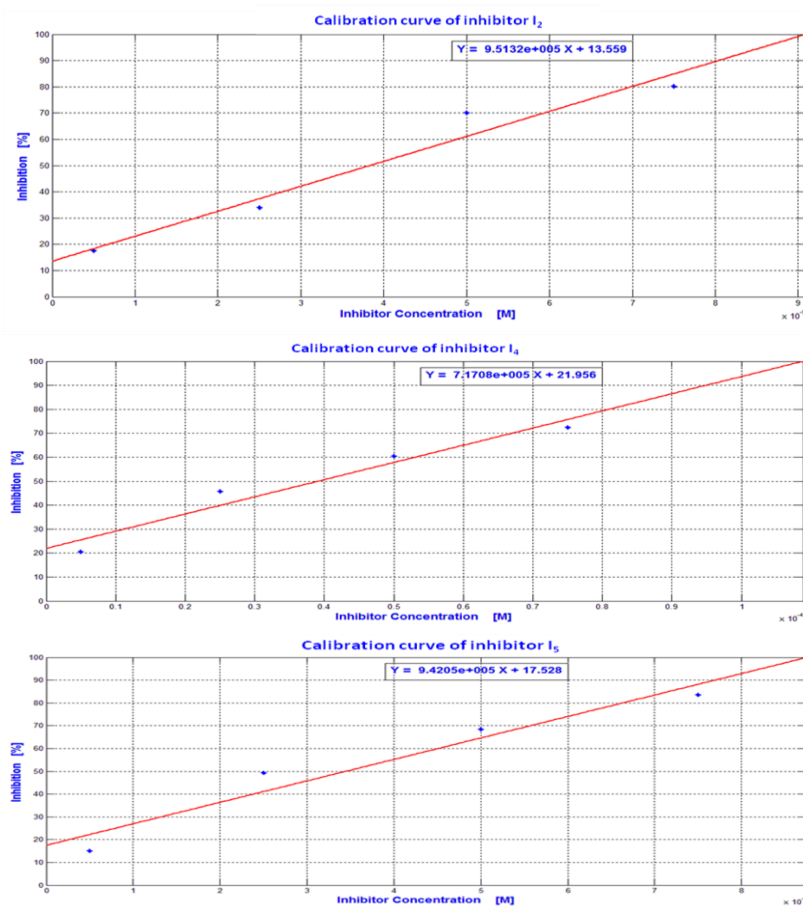


Fig. 1. Calibration curves for free AChE and the peptide inhibitors I₂, I₄ and I₅

Table 2. IC₅₀ values for the synthesized and the some pesticides

Symbols	Amino acid sequence	IC ₅₀ [M x10 ⁻⁶]
I ₁	Boc-Asp(norGal)-Val-Asn-Leu-β-Ala-Val-NH-Bzl	-
I ₂	Boc-Asp(norGal)-Asp-Leu-β-Ala-Val-NH-Bzl	40.70±0,10
I ₃	Boc-Asp(norGal)-Asp-Leu-Ala-Val-NH-Bzl	38.30±0,18
I ₄	Boc-Val-Asn-Leu-Ala-Val-Gly-OGal	39.11±0,12
I ₅	Boc-Val-Asn-Leu-Ala-Gly-OGal	34.46±0,07
Gal*	galanthamine	5.00
	Parathion	1.75**
	Carbofuran	0.65**

* data from literature [15], **both values are x10⁻¹⁰

Table 3. The values of Ki for different newly inhibitors concentrations for immobilized AChE

Inhibitor concentration, (Mx10 ⁻⁶)	Ki (Mx10 ⁻⁶) MTES (AChE)			
	I ₁	I ₂	I ₄	I ₅
5	0.45624	0.26209	41.482	0.21175
25	3.85745	1.51692	2.28114	1.43737
50	5.62258	4.79799	5.46817	3.36793
75	9.28964	6.96592	8.72065	9.52302

In this part examination of the effect of some types of those newly synthesized inhibitors that were designed in [14] was achieved. In addition, their IC₅₀ values (50% inhibition effect on the enzyme) against AChE were determined. Five different peptide inhibitors, galantamine derivatives were investigated. The results showed that four of them (I₅, I₄, I₂ and I₁) have inhibitory effect towards the enzyme AChE. Surprisingly compound I₃ has no inhibitory effect towards enzyme, but it reacts as an activator. Therefore, the study was continued only with the other four inhibitors (I₅, I₄, I₂ and I₁). Initially, we made the calibration curves with inhibitors I₁, I₂, I₄ and I₅. They are illustrated on Fig. 1 in the presence of ACh at 7,5μM concentration. The plots appear linear response for concentration of the inhibitor from 5 μM to 100μM.

After drawing the calibration curves, the IC₅₀ values for the newly synthesized inhibitors are determined and they are summarized in Table 2. The IC₅₀ values for the inhibitors I₁, I₂, I₄, and I₅, for immobilized AChE on MTES hybrid membranes is presented in Table 2. These values are obtained from the experimental work and compared to the obtained ones from the mathematical model.

The values of Ki for different newly inhibitors concentrations for immobilized AChE are presented at Table 3. The results showed that all newly

inhibitors compound I₁, I₂, I₄ and I₅ act as competitive inhibitor for immobilized AChE.

IC₅₀ values for the novel peptides compounds inhibitors for immobilized AChE on MTES hybrid membranes, obtained from experimental work and theoretical mathematical model were compared using simple regression analysis. The results are shown on a regression line in Figure 2 The obtained regression equations for different inhibitors are as follows:

I₁: Y = 3.4243 X – 251.95, correlation (r) = 0.782.

I₂: Y = 5.1909 X – 405.52, correlation (r) = 0.696;

I₄: Y = 0.47351 X + 7.0091, correlation (r) = 0.239;

I₅: Y = 3.854 X – 261.21, correlation (r) = 0.7501;

A good correlation existed between the results of experimental method and theoretical mathematical model for inhibitors I₅ and I₁. Data from these statistical calculations confirmed the precision of the proposed model.

As it can be seen from the table 1 four of five galanthamine derivatives have inhibition activity and the IC₅₀ values are in micromolar range, but they are 7-8 times lower than those of natural galanthamine. The comparison of obtained data shows that carbamate and phosphororganic pesticides are one million times more potent inhibitors of AChE. Eventhough, looking to the IC₅₀ values for both pesticides, carbofuran seems

stronger inhibitor than parathion, it is actually less toxic because of the inhibition mechanism. Carbamates are considered to be safer than OP insecticides that irreversibly inhibit AChE causing more severe cholinergic poisoning.

It is proved that OP as well as the organochlorine pesticides that are also irreversible

inhibitors, are toxic to the nervous system, reproductive organs, and endocrine system. Moreover, they can cause cancer and increase the risk of developing Alzheimer's disease. As a result of their wide use in agriculture, traces of them can further be found into animal tissues, milk, honey, eggs, etc.

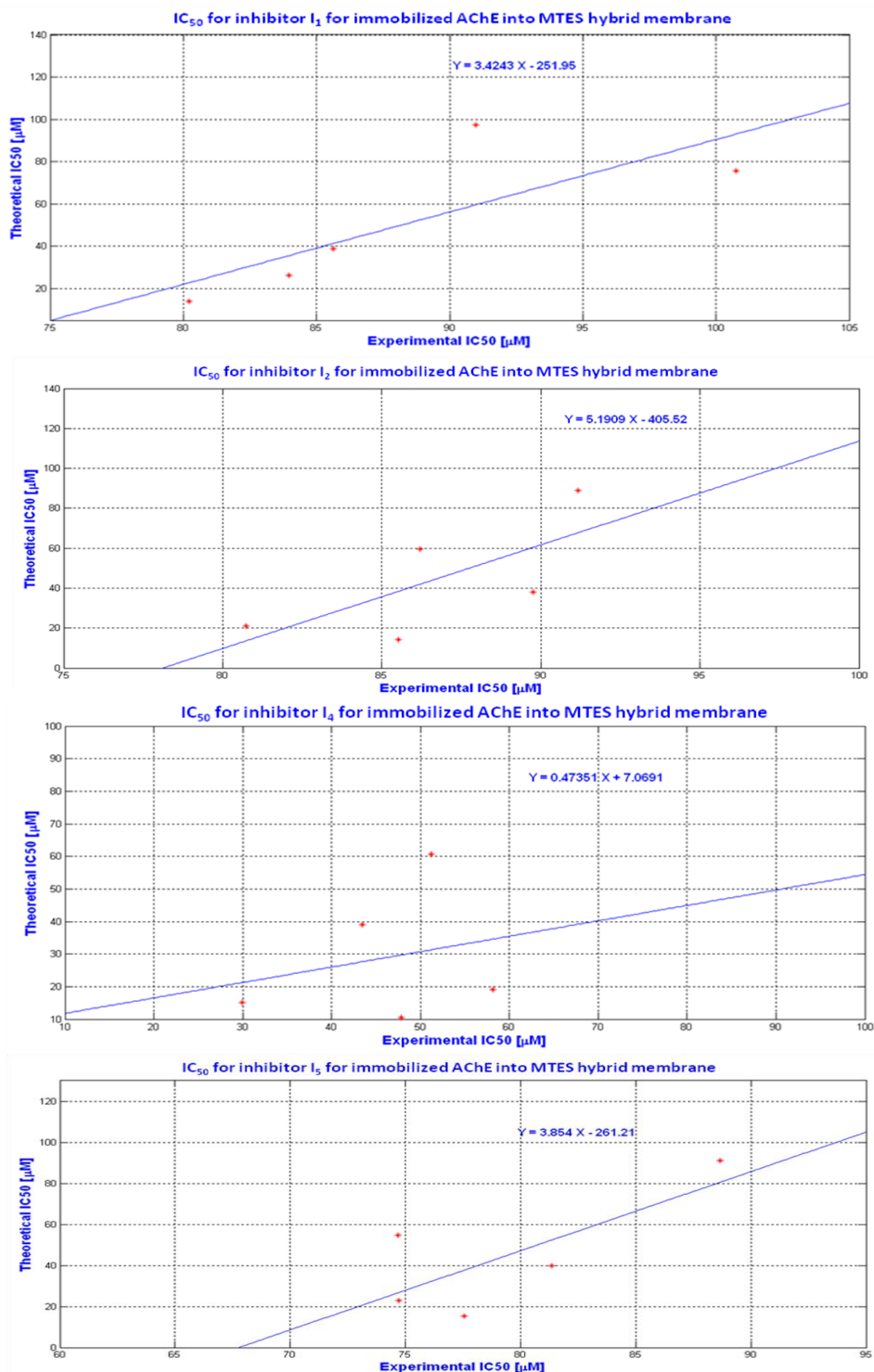


Fig. 2. IC₅₀ correlation curve for the newly compounds inhibitor I₁, I₂, I₄ and I₅ and immobilized AChE onto MTES hybrid membrane

CONCLUSION

Therefore, food safety is an integral part of the EU policy for protection of consumer's health and maximum residue levels for pesticides are defined in specific Regulations. However, some carbamates, due to their reversible AChE inhibitory action, found an important application in human medicine as pharmacologically active compounds. For example, rivastigmine is a carbamate with probably the most meaningful pharmacological application, being validated in the symptomatic treatment of Alzheimer's disease.

Acknowledgments: The present work was supported by "National Fund Scientific Research", project DUNK 01/03, 2009.

REFERENCES

1. A. Mary, D.Z. Renko, C. Guillou, C. Thal, *Bioorg. Med. Chem.*, **6**, 1835 (1998).
2. K. P. Kepp, *Chem. Rev.*, **112**, 5193 (2012).
3. L.J. Scott, K.L. Goa, *Drugs*, **60**, 1095 (2000).
4. X. Gao, C.Y. Zheng, L. Yang, X.C. Tang, H.Y. Zhang, *Free Radical Biol. Med.*, **46**, 1454, (2009).
5. N. Kitisripanya, P. Saparpakorn, P. Wolschann, S. Hannongbua, *Nanomed. Nanotechnol.*, **7**, 60 (2011).
6. Seidl, B.L. Correia, A.E. Stingham, C.A. Santos, *Z. Naturforsch C*, **65**, 440 (2010).
7. R. L. Metcalf, "Insect Control", Ullmann's Encyclopedia of Industrial Chemistry, Weinheim: Wiley-VCH, doi:10.1002/14356007, 2005.
8. M. B. Čolović, D. Z. Krstić, T. D. Lazarević-Pašti, A. M. Bondžić, V. M Vasić, *Curr. Neuropharmacol.*, **11**, 315 (2013).
9. L.Vezenkov, J. Sevalle, D. Danalev, T. Ivanov, A. Bakalova, M. Georgieva and F. Checler, *Curr. Alz. Res.*, **9**, 600 (2012).
10. T. A. Dzimbova, P.B. Milanov, T.I. Pajpanova, *J. Amino Acids*, **2013**, 7 (2013).
11. Yotova, Sp.Yaneva, D. Marinkova, S. Serfaty, , *Biotechnol. & Biotechnol. Eq.*, **27**, 3 (2013).
12. Lowry, N.J. Rosbrough, A.L. Farr, R.J. Randall, *J. Biol. Chem.*, **193**, 265 (1951).
13. G.L. Ellman, D.K. Courtney, V. Andreas, R.M. Featherstone, *Biochem. Pharmacol.*, **7**, 88 (1961).
14. L.T. Vezenkov, M. Georgieva, D.L. Danalev, Tch. Ivanov, G. Ivanova, *Protein and Peptide Lett.*, **16**, 1024 (2009).
15. Z. Rakonczay, *Acta Biol. Hungarica*, **54**, 183 (2003).

ИЗСЛЕДВАНЕ ИНХИБИТОРНАТА АКТИВНОСТ ВЪРХУ АЦЕТИЛХОЛИНЕСТЕРАЗА НА ПЕПТИДНИ АНАЛОЗИ НА ГАЛАНТАМИН, С ПОТЕНЦИАЛНО ПРИЛОЖЕНИЕ ПРИ ПАЦИЕНТИ С БОЛЕСТТА НА АЛЦХАЙМЕР

С.А. Янева^{1*}, И.И. Стойкова², Л.И. Илиева³, Л.Т. Везенков³, Д.А. Маринкова², Л.К. Йотова², Р.Н. Райкова², Д. Л. Даналев²

Химикотехнологичен и металургичен университет, София 1756, България, 8 бул. Св. Климент Охридски,

¹ Катедра Основи на химичната технология, sp_yaneva@uctm.edu

² Катедра Биотехнология

³ Катедра Органична химия

Постъпила на 04 октомври, 2016 г.; Коригирана на 15 януари, 2017 г

(Резюме)

Ацетилхолинестеразен инхибитор или анти-холинестеразно вещество е съединение, което инхибира ензима холинестераза като блокира ацетилхолина, което води до увеличаване както на нивото, така и продължителността на действие на невротрансмитера ацетилхолин.

Ацетилхолинестеразното инхибиране може да възникне при въздействие на различни отрови и токсини върху организма. Свойствата на този тип инхибитори са изследвани и прилагани като оръжие за масово поразяване, а от друга страна се включват в състава на лекарства за различни заболявания като миастения гравис. Също така се прилагат за увеличаване на нервномускулния пренос на импулси, при лечение на глаукома, болестта на Алцхаймер, както и като противоотрова при антихолинергично отравяне.

В настоящата работа, ние докладваме резултатите от кинетичните изследвания на пет пептида, amidни и естерни аналози на галантамин: Boc-Val-Asn-Leu-Ala-Gly-Ogal, Boc-Val-Asn-Leu-Ala-Val-Gly-Ogal, Boc-Asp-(norGal)-Asp-Leu-Ala-Val-NH-Bzl, Boc-Asp-(norGal)-Asp-Leu-β-Ala-Val-NH-Bzl, Boc-Asp-(norGal)-Val-Asn-Leu-β-Ala-Val-NH-Bzl, като потенциални инхибитори на ацетилхолинестераза. Определени са стойностите на IC₅₀ (50% инхибиране активността на ензима) спрямо ацетилхолинестераза. В допълнение ние сравняваме получените стойности за IC₅₀ с тези на два моделни пестицида, които са добре известни мощни инхибитори на ацетилхолинестеразата.

New amino acid modified silica gel sorbents for solid phase extraction of Au (III)

P. Petrova^{1*}, I. Karadjova², M. Chochkova¹, I. Dakova², M. Karadjov³

¹ South-West University "Neofit Rilski", Faculty of Mathematics and Natural Sciences, Department of Chemistry, 66, Ivan Mihailov Str, 2700, Blagoevgrad, Bulgaria

² Sofia University, "St. Kliment Ohridski", Faculty of chemistry and pharmacy, 1, blv. J. Boucher, 1164 Sofia, Bulgaria

³ Geological Institute, Bulgarian Academy of Science, Acad. G. Bonchev Str. bl.24, 1113 Sofia, Bulgaria

Received December 10, 2016; Revised March 5, 2017

Two new sorbents, silica gel modified with Cystine (Sig-Cys-S-S-Cys) and silica gel modified with *N*-Benzyloxycarbonyl-*L*-Methionine (Sig-Z-Met-OH) were prepared and examined for quantitative extraction of Au (III) from hydrochloric acid solutions. Several parameters affecting the sorption efficiency such as pH of the sample solution, sorption time, eluent type and volume were optimised in order to achieve quantitative extraction of Au (III). Experiments performed showed that under optimized conditions the degree of Au (III) sorption does not exceed 43 % by using Sig-Cys-S-S-Cys whereas Sig-Z-Met-OH enables fast and quantitative retention of Au (III) from 0.1-0.01 mol L⁻¹ HCl and could be used for the separation and preconcentration of Au (III). The analytical procedure was developed for the determination of Au in gold containing cosmetics based on two steps: solid phase extraction of Au (III) and measurement of extracted Au by ICP-OES. The limit of detection achieved is 0.1 µg g⁻¹ Au in the face cream and the relative standard deviation varied in the range 6-11% for the concentration range 0.1-1 µg g⁻¹ Au in the face cream. The accuracy of the developed analytical procedure was verified by direct analysis using ICP-MS.

Keywords: solid phase extraction, noble metals, atomic spectrometry

INTRODUCTION

Platinum group elements (PGEs) and gold are distributed at very low concentration in the earth crust. The typical concentration of gold in ore is in the range of 5-30 g/t [1]. However, their application in electrical and electronic industries, in medicine and in jewelry leads to their spread in the environment where significant quantities of noble metals are converted into bioavailable forms, mainly as chloro or organic complexes [2-5]. Despite the elevated anthropogenic PGEs levels, their concentration remains quite low for direct instrumental determination and usually analytical procedure which includes preliminary separation and concentration of analytes has to be used [6]. As a rule reliable results could be obtained after careful optimization of the parameters of analytical method which combines the application of sensitive analytical techniques such as ICP-MS, ICP-OES or ETAAS with suitable enrichment procedure. Solid phase extraction technique using different kind of solid sorbents ensures high enrichment factor, rapid phase separation and the ability of combination with different detection techniques [7]. Silica gel has been widely used as a sorbent or as a support due to its good mechanical and chemical properties, high porosity, large surface, resistance to

swelling, as well as high thermal stability. The extraction efficiency and selectivity of silica gel has been improved by its physical and chemical modification with various chemical reagents, in this way suitable functional groups have been chemically or physically bonded to the reactive sites on the silica surface. Chelating agents with *N*- and *S*- containing groups are highly efficient for the selective sorption of noble metals and could be used for physical modification of silica gel [8, 9]. In the presence of HCl noble metals' chlorocomplexes could form stable ion associates with protonated nitrogen-containing reagent and quantitatively retained on the surface of silica gel [9, 10].

The immobilization of chitosan and amino acids such as glycine, valine, leucine, serine and lysine has been already used as an approach for preconcentration of Au (III), Pt (IV) and Pd (II) [12-14]. Recently *Hastuti et al.* [15] used *L*-arginine functionalized silica gel as an effective adsorbent for gold (III), *Mladenova et al.* prepared and studied sorbent based on cysteine modified silica gel for preconcentration and separation of noble metals Au (III), Pd (II), Pt (II), Pt (IV) [16].

The aim of the present work is to prepare silica gel sorbents physically modified with sulfur containing amino acids *Z*-Methionine (*N*-Benzyloxycarbonyl-Methionine) and Cystine (unmodified), and to investigate their sorption efficiency towards Au (III). Additionally our interest is to examine the reliability of physical

* To whom all correspondence should be sent:
E-mail: petya_dukova@yahoo.com

functionalization of silica particles and to check out if the simplified preparation technique provides satisfactory results. Analytical application of sorbents prepared for Au determination in cosmetics is presented.

EXPERIMENTAL

Reagents

All chemicals were of analytical reagent grade and were used without further purification. The stock standard solution for Au (III) (1000 mg L⁻¹) was Sigma–Aldrich (Germany) in 5% HCl. Working standard solutions for Au were prepared daily by appropriate dilution of the stock standard solution. Silica gel for column chromatography ≤0.063 mm, ≥230 mesh ASTM, the amino acids cystine and *L*-methionine and *N*-(Benzyloxycarbonyloxy) succinimide were purchased from Sigma-Aldrich Ltd. Analytical grade sodium bicarbonate (NaHCO₃, Sigma-Aldrich, Germany), acetone (CH₃COCH₃, Sigma-Aldrich, Germany), ethyl acetate (CH₃COOC₂H₅, 99.8%, Sigma-Aldrich, Germany) and sodium sulfate (Na₂SO₄, Merck, Germany) were used for synthesis of *N*-Benzyloxycarbonyl-*L*-methionine. HCl (37%), HNO₃ (68%) and NH₃ (25%) were purchased from Merck, Germany.

Apparatus

FAAS measurements were carried out on a Perkin- Elmer AAnalyst 400 spectrometer, with air/acetylene flame under optimal instrumental parameters, ensuring maximal signal to noise ratio. The light source was hollow cathode lamps for Au. The spectral bandpass and wavelengths used were as recommended by the manufacturer. The wavelength used for Au AAS measurement is 242.8 nm. ICP-OES measurements were performed on an ICP-OES spectrometer Ultima 2, Jobin Yvon under optimized instrumental parameters using wavelength 242.795 nm.

A Milestone Ethos 900-Mega II microwave oven with a PTFE-vessel rotor was employed for samples digestion.

The centrifuge K-1000 (KUBOTA Corporation, Osaka, Japan) was used for the centrifugation of modified silica sorbent in batch experiments.

Synthesis of N-Benzyloxycarbonyl-L-methionine (Z-Met-OH) [17]

The suspension of *L*-methionine (1.5 g, 10 mmol) in deionized water (20 mL) was prepared and mixed with NaHCO₃ (0.84 g, 10 mmol) and 25 mL acetone. Then *N*-(Benzyloxycarbonyloxy) succinimide (2.5 g, 10

mmol) was added and the reaction mixture was stirred at room temperature overnight. After evaporation of the acetone *in vacuo*, the aqueous layer was acidified with 1 mol L⁻¹ HCl to pH 2.5 and extracted with ethylacetate (3 x 20 mL). The combined organic phases were washed with brine, dried over anhydrous Na₂SO₄ and evaporated *in vacuo*. Yield (65%); mp 67-69°C.

Preparation of modified silica gels: silica gel modified with Z-methionine and silica gel modified with cystine

The silica gel modified with Z-Methionine (Sig-Z-Met-OH) and silica gel modified with Cystine (Sig-Cys-S-S-Cys) were prepared following the procedure described by *Bartyzel et al.* [18] and further optimized by Petrova et al. [19].

The commercially available silica gel was activated by refluxing with concentrated HCl for 4 h, because the commercial silica gel possesses a low concentration of suitable surface silanol groups, required for further modification. Thereafter it was filtered, washed with deionized water until the filtrate was neutral and dried in an oven at 150 °C for 12 h to remove surface adsorbed water. The activated silica gel was refluxed separately with the modifiers Z-methionine or cystine in ratio 9:1 w/w in an acetone media for 8 h. Finally the mixture was vigorously stirred at room temperature to complete the solvent evaporation and then dried at 40°C for 1 h.

Sorption/desorption studies

Aqueous standard solution (10 mL) containing Au (10 mg L⁻¹) was mixed with 50 mg of the sorbent in the presence of various concentrations of HCl. The mixture was shaken for 10-40 min with an electric shaker and then centrifuged. In order to investigate the degree of sorption supernatant solution was removed and analyzed by FAAS as effluante. The sorbent was washed with deionized water and Au was eluted from the sorbent particles with different eluate solutions. In order to investigate the degree of elution, metal ion content in eluate was determined by FAAS after sorbent centrifugation. The degree of sorption, D%, and elution, R% is calculated using the following equations:

$$D\% = [(C_{\text{initial}} - C_{\text{effluante}})/C_{\text{initial}}] \times 100,$$

$$R\% = [(C_{\text{initial}} - C_{\text{effluante}})/C_{\text{eluate}}] \times 100,$$

where C_{initial} is the initial amount of Au, $C_{\text{effluante}}$ is the amount of Au measured in the supernatant (effluante solution) and C_{eluate} is the amount of Au measured in the eluate solution.

Determination of Au in cream samples

Digestion of cream samples: All plastic and glassware were soaked in 5% HNO₃ solution for 24 h and rinsed with deionized water before use.

The cream sample was dried in an oven at 105 °C to constant weight and then stored in desiccator. About 0.3 g of the dried sample was directly weighed into PTFE digestion vessel. Then 10.0 mL HCl (37%) and 3.5 mL HNO₃ (68%) were added and the mixture was left at room temperature for 24 h. The MW digestion programme was as follows: 10 min at 250 W; 5 min at 400 W; 5 min at 500 W; 5 min at 600 W. After cooling, the solution was quantitatively transferred in a volumetric flask and diluted up to 25 mL with 0.02 mol L⁻¹ HCl [20].

Determination of Au: 20 mL of above prepared solution of digested cream sample were transferred in a centrifuge tube, 50 mg sorbent was added and mixture was shaken for 30 min. After centrifugation the sorbent was washed with deionized water and eluted with 1 mL 0.7 mol L⁻¹ thiourea in 2 mol L⁻¹ HCl. The concentration of Au in an eluate obtained was measured by ICP-OES.

RESULTS AND DISCUSSION

Optimization of the experimental conditions for SPE of Au (III)

Influence of pH on Au (III) sorption

The pH of the solution is an important factor influencing the degree of sorption because it affects the protonation of the functional groups on the sorbent surface and also defines the chemistry of Au ions.

The effect of the HCl molarity on Au (III) adsorption was investigated in batch mode for the two studied sorbents by varying the HCl concentration in the range 0.01 - 2.7 mol L⁻¹, applying the procedure described in section 2.5. The results obtained are presented in Table 1.

The quantitative sorption of Au (III) on Sig-Z-Met-OH was achieved at HCl concentration in the

range 0.1-0.01 mol L⁻¹ reaching 96-98%. The high degree of Au (III) sorption on Sig-Z-Met-OH in the presence of HCl might be explained with the fact that Au (III) forms anionic chlorocomplexes [AuCl₄]⁻ whereas amino- and S-methyl thioether groups on the sorbent surface are protonated and thus charged positively [13,14,21,22,23]. Therefore, the Au (III) adsorption is due to the strong electrostatic attraction between the positively charged adsorbent surface and negatively charged chloride complex of Au [15,24].

The two sorbents differ remarkably in their extraction efficiency toward Au (III). Theoretically more considerable sorption capacity is expected for Sig-Cys-S-S-Cys due to the presence of two amino groups and two S atoms in the cystine molecule ([HOOC(NH₂)CHCH₂S-]₂) in comparison with Sig-Z-Met-OH (Z-NH-CH(CH₂CH₂SCH₃)-COOH), with one amino group and one S atom per mol amino acid. However it is obvious that Sig-Cys-S-S-Cys does not ensure satisfactory extraction (less than 44 % for all HCl molarities studied) of Au (III), whereas the sorption on Sig-Z-Met-OH is higher in the whole acidity range. One probable explanation for this observation could be very slow kinetics of sorption on the surface of Sig-Cys-S-S-Cys, as it was mentioned in the literature [23].

Another reason could be the formation of large ion associates which cannot be quantitatively sorbed on the surface of this material as discussed by A. Dubenskiy et al. [25]. Due to the low sorption activity or slow kinetics of sorption process on the surface of Sig-Cys-S-S-Cys, further studies were performed only with Sig-Z-Met-OH sorbent.

Influence of contact time

The kinetics of the Au (III) sorption was investigated in a batch system following the procedure described in section 2.5. It was found that the quantitative sorption was reached within 30 min, which is sufficiently fast for practical applications. The effect of contact time on the Au (III) ions adsorption is presented in Fig. 1.

Table 1. Degree of sorption of Au (III) on Sig-Z-Met-OH and Sig-Cys-S-S-Cys. Data represent an average of three independent experiments

Sorbent	Degree of sorption, %				
	0.01 mol L ⁻¹ HCl	0.1 mol L ⁻¹ HCl	1 mol L ⁻¹ HCl	2 mol L ⁻¹ HCl	2.7 mol L ⁻¹ HCl
Sig-Z-Met-OH	96±3	98±5	92±3	85±4	80±5
Sig-H-Cys-Cys-OH	18±4	18±3	42±4	10±3	4±5

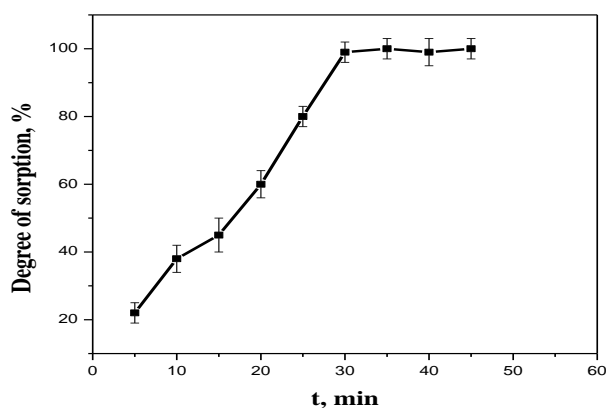


Fig. 1. Adsorption kinetic curves for the Sig-Z-Met-OH ($m_{\text{sorbent}} = 50$ mg, $V = 10$ mL, $C_{\text{Au (III)}} = 10$ mg L⁻¹). Data represent an average of three independent experiments.

Selection of appropriate eluent for Au (III) desorption

Very important factors affecting the extraction efficiency of particular sorbent are the type, volume and concentration of the eluent used for quantitative removal of sorbed metal ions. A series of eluents, presented in Table 2 were tested in order to find the most suitable eluent for desorption of Au(III).

The summarized results (Table 2) showed that the highest recovery was achieved by using 0.7 mol L⁻¹ thiourea in 2 mol L⁻¹ HCl as an eluent.

By varying the eluent volume (from 1 to 10 mL) it was found that the optimal volume for full desorption of Au (III) was 1 mL.

ANALYTICAL APPLICATION

The prepared Sig-Z-Met-OH sorbent was examined under optimized chemical parameters for SPE of Au (III) from cosmetics samples, digested using the analytical procedure described in section 2.6. The recovery experiments were performed by spiking cream sample with known amount of Au (III) before MW digestion. Recoveries achieved for spiked cosmetic samples varied between 90 and 103%, confirming the applicability of Sig-Z-Met-OH for Au determination in cosmetic creams (Table 3). Analytical procedure developed permits quantification (LOQ) of 0.1 µg g⁻¹ Au in cosmetic cream sample. Relative standard deviations for the concentration range 0.1–1 µg g⁻¹ Au in cream sample varied between 6–11 % (Table 3).

The procedure was applied for the determination of Au (III) in gold-containing face cream, purchased from the market. The sample was digested according to the procedure described in section 2.6 and the developed SPE-ICP-OES method was used for Au quantification. Further, the results obtained by the proposed method were compared with direct Au determination in the same face cream. Results (0.62±0.07) µg g⁻¹ obtained by SPE-ICP-OES and (0.68±0.06) µg g⁻¹ obtained by direct ICP-MS (performed in external lab) determination agreed very well (Student t-test, 95% confidence limit) thus demonstrating that there are no statistically significant differences between the results obtained by the two methods and confirming the accuracy of developed SPE-ICP-OES method for Au determination in cosmetic creams.

Table 2. Effect of eluent type and concentration on the desorption of gold ions

Eluent	R,%
0.5 mol L ⁻¹ NaClO ₄ and 0.5 mol L ⁻¹ thiourea in 1 mol L ⁻¹ HCl	67±5
0.7 mol L ⁻¹ thiourea in 2 mol L ⁻¹ HCl	98±2
0.1 mol L ⁻¹ thiourea in 1 mol L ⁻¹ HCl	70±5
0.5 mol L ⁻¹ NaClO ₄ in 0.1 mol L ⁻¹ HCl	32±6
96 % ethanol	25±7
0.01 mol L ⁻¹ EDTA in methanol	30±6

Table 3. Analytical figures of merit for the developed SPE-ICP-OES method for Au determination in cosmetic creams (three parallel determinations).

Added, $\mu\text{g g}^{-1}$	Found, (mean \pm sd) $\mu\text{g g}^{-1}$	RSD, %	Recovery, %
0.20	0.18 \pm 0.03	11	90
0.50	0.51 \pm 0.04	8	102
1.0	1.03 \pm 0.06	6	103

CONCLUSION

Two new sorbents Sig-Cys-S-S-Cys and Sig-Z-Met-OH were prepared by simple non-covalently amino acid bonding on the silica surface and were examined for SPE of Au (III). The influence of various important factors such as pH, contact time, eluent type, concentration and volume were studied and Au (III) sorption mechanism was proposed. The experiments demonstrated that the quantitative Au (III) sorption is achieved with Sig-Z-Met-OH in 0.1 mol L⁻¹ HCl reaching degree of sorption 98 \pm 2 %. The developed, optimized solid phase extraction procedure combined with ICP-OES measurements is applied for the determination of Au in gold-containing cosmetics. The accuracy of proposed analytical method was verified by parallel direct analysis with ICP-MS and recovery tests.

Acknowledgements: The authors gratefully acknowledge financial support from South-West University "Neofit Rilski" – grant RP-A9/16.

REFERENCES

1. T. Ogata, Y. Nakano, *Water Res.*, **39**, 4281 (2005).
2. C. Tasdelen, S. Aktas, E. Acma, Y. Guvenilir, *Hydrometallurgy*, **96**, 253 (2009).
3. C. Hagelüken, C.W. Corti, *Gold Bull.*, **43**, 209 (2010).
4. Iavicoli, B. Bocca, L. Fontana, S. Caimi, A. Bergamaschi, A. Alimonti. *Toxicol Ind Health*; **26** 183 (2010).
5. B. Godlewska-Żyłkiewicz, J. Malejko, B. Leśniewska, A. Kojło. *Microchim Acta*, **163**, 327 (2008).
6. F. Zereini, C. Wiseman (Eds), *Platinum Metals in the Environment*, Springer, 2006.
7. V. Camel, *Spectrochimica Acta B*, **58**, 1177 (2003).
8. K. Pyrzynska, *Analytica Chimica Acta*, **741**, 9 (2012).
9. P. Tzvetkova, R. Nickolov, *Journal of the University of Chemical Technology and Metallurgy*, **47**, 498 (2012).
10. Y.A. Zolotov, G.I. Tsysin, S.G. Dmitrienko, E.I. Morosanova, *Sorption Pre-concentration of Microcomponents From Solutions, Application in Inorganic Analysis*, Nauka, Moscow, 2007.
11. V.S. Schmid, *Extraction Using Amines*, Atomizdat, Moscow, 1980.
12. K. Oshita, T. Takayanagi, M. Oshima, S. Motomizu, *Anal. Sci.*, **23**, 1431 (2007).
13. Ramesh, H. Hasegawa, W. Sugimoto, T. Maki, K. Ueda, *Bioresour. Technol.*, **99**, 3801 (2008).
14. K. Fujiwara, A. Ramesh, T. Maki, H. Hasegawa, K. Ueda, *J. Hazard. Mater.*, **146**, 39 (2007).
15. Sri Hastuti, Nuryono, Agus Kuncaka, *Indones. J. Chem.*, **15**, 108 (2015).
16. E. Mladenova, I. Dakova, I. Karadjova, M. Karadjov, *Microchemical Journal*, **101**, 59 (2012).
17. A. Paquet, *Canadian Journal of Chemistry*, **60**, 976, (1982).
18. A. Bartyzel, E. Cukrowska, *Analytica Chimica Acta*, **707**, 204 (2011).
19. P. Petrova, I. Karadjova, M. Chochkova, I. Dakova, *Chemistry*, **24**, 441 (2015).
20. A. Bocca, G. Forte, F. Petrucci, A. Cristaudo, *Journal of Pharmaceutical and Biomedical Analysis*, **44**, 1197 (2007).
21. H. Wang, C. Bao, F. Li, X. Kong, J. Xu, *Microchim. Acta*, **168**, 99 (2010).
22. A. Afzali, A. Mostafavi, M. Mirzaei, *Journal of Hazardous Materials*, 181, 957 (2010).
23. B. Tong, Y. Akama, S. Tanaka, *Anal. Chim. Acta*, 230, 179 (1990).
24. M. Barczak, J. Dobrzynska, M. Oszust, E. Skwarek, J. Ostrowski, E. Zieba, P. Borowski, R. Dobrowolski, *Materials Chemistry and Physics*, **181**, 126 (2016).
25. A. S. Dubenskiy, I. F. Seregina, Z. K. Blinnikova, M. P. Tsyurupa, L. A. Pavlova, V. A. Davankov, M. A. Bolshov, *Talanta*, **153**, 240 (2016).

СИЛИКАГЕЛ, МОДИФИЦИРАН С АМИНОКИСЕЛИНИ КАТО СОРБЕНТ ЗА ТВЪРДОФАЗНА ЕКСТРАКЦИЯ НА Au (III)

П. Петрова^{1*}, И. Караджова², М. Чочкова¹, И. Дакова², М. Караджов³

¹ Югозападен университет „Неофит Рилски“, Природо-математически факултет, Катедра по „Химия“, 66, Иван Михайлов, 2700, Благоевград, България

² Софийски университет „Св. Климент Охридски“, Факултет по „Химия и фармация“, 1, бул. Джеймс Баучер, 1164 София, България

³ Българска Академия на Науките, Геоложки Институт, , София 1113, България

Постъпила на 10 декември, 2016 г.; Коригирана на 05 март, 2017 г.

(Резюме)

Синтезирани са два нови сорбента- силикагел, модифициран с цистин (Sig-Cys-S-S-Cys) и силикагел, модифициран с *N*-бензилоксикарбонил-*L*-метионин (Sig-Z-Met-OH). Изследвани са техните сорбционни свойства за количествена екстракция на Au (III) из разтвори на солна киселина. Оптимизирани са няколко параметъра, засягащи сорбционната ефективност, като рН на разтвора, времето за сорбция, вида и обема на елуента, с цел постигане количествена екстракция на Au (III). Показано е, че при оптимални условия степента на сорбция не надхвърля 43%, използвайки сорбента Sig-Cys-S-S-Cys, докато Sig-Z-Met-OH осигурява бърза и количествена сорбция на Au (III) в 0.1-0.01 mol L⁻¹ HCl и може да бъде използван за разделяне и концентриране на Au (III). Предложена е аналитична процедура за определяне на Au (III) в злато-съдържаща козметика, включваща две стъпки: твърдофазна екстракция на Au (III) и определяне на извлечените Au йони с ICP-OES. Постигнатите граници на откриване са 0.1 µg g⁻¹ Au в крем за лице, като относителното стандартно отклонение варира в границите 6-11% за концентрационен интервал 0.1-1 µg g⁻¹ Au в крема за лице. Точността на разработената аналитична процедура е доказана чрез директен анализ с ICP-MS.

Alpha-galactosidase and invertase from *Penicillium chrysogenum* sp.23: purification, characteristics and hydrolysis of raffinose

B.K. Yakimova, B.P. Tchorbanov, I.B. Stoineva*

Institute of Organic Chemistry with Centre of Phytochemistry, Bulgarian Academy of Sciences, Acad.G. Bonchev str. bl.9, 1113 Sofia, Bulgaria

Received September 30, 2016; Revised February 3, 2017

The shaking fermentation of fungal strain *Penicillium chrysogenum* sp.23 on soy meal resulting in a high α -galactosidase yield of 4200 U/l and was accompanied by the excretion of invertase activity. An ultrafiltration method was applied to obtain enzyme product and further purification procedure was developed to obtain pure α -galactosidase. The optimal parameters pH 4.5-5.0 and temperature 50°C of α -galactosidase fraction were determined by using p-nitrophenyl- α -D-galactopyranoside as substrate. The hydrolysis of raffinose catalyzed by α -galactosidase in the presence of side excreted invertase was followed by HPLC analysis. The results were compared with data from raffinose hydrolysis of α -galactosidase without any traces of invertase using fungal strain *Humicola lutea* 120-5. It is shown clearly that the presence of invertase in this case provoked a significant transformation of the raffinose to melibiose and fructose mainly.

Key words: α -galactosidase, *Penicillium chrysogenum* sp.23, invertase, hydrolysis of raffinose

INTRODUCTION

Human consumption of soy products is increasing due to their high nutritional value, acceptable price as well as their health effects, such as reduction the cardiovascular diseases, osteoporosis and cancer risks [1]. In spite of these advantages, they also contain a certain amount of oligosaccharides of raffinose type, which are not assimilated by humans and non-ruminants animals causing flatulence and discomfort. They pass on intact into the large intestine, where anaerobic microorganisms ferment them and cause gastrointestinal disturbances [2]. Degradation of these oligosaccharides from soybeans and legumes foods to low molecular weight compounds such as glucose and fructose is necessary to reduce substantially or completely prevent of the flatus formation (flatulence). Many researchers have noted the degradation of these oligosaccharides using a mixed crude enzyme system consisting of alpha-galactosidase and invertase [3]. The main problem is that the hydrolysis of these oligosaccharides as raffinose does not run completely to the formation of galactose, glucose and fructose, and in the hydrolyzate were found significant amounts of melibiose.

α -Galactosidase (EC 3.2.1.22) and invertase (EC 3.2.1.26) with official name β -fructosidase are enzymes belonging to the class of hydrolases,

subclass glycosidases (3.2.1) i.e enzymes hydrolyzing glycosyl oxygen compounds. α -Galactosidase is an enzyme which is a glycoprotein with a carbohydrate and a protein part in a ratio of 1:6. It catalyzes the hydrolysis of non-reducing α -1, 6 linked galactose residues of different substrates, including linear and branched oligosaccharides, polysaccharides, and synthetic substrates such as p-nitrophenyl- α -D-galactopyranoside [4]. This enzyme is widely distributed in microorganisms, plants and animals [4]. Among all the sources of α -galactosidases, the fungal α -galactosidases were most suitably exploited for their biotechnological applications mainly due to their extracellular localization, acidic pH optima, and broad stability profiles.

At present, the industrial applications of α -galactosidase are related to the beet sugar industry, pulp and paper industry, soy food processing, and animal feed processing [5, 6]. Another important application of α -galactosidase is its use in blood group transformation, the treatment of Fabry's disease and xenotransplantation [7,8].

The invertase is an enzyme that has the ability to hydrolyze α -1,2 glycosidic bonds, and thus degrades sucrose to glucose and fructose in a ratio of 1:1 [9]. There are several isoforms of invertase, differing in pH optimum of activity, which may be neutral, acid or alkaline [10]. The enzymatic activity of invertase has been characterized mainly in plants [11] and microorganisms [12,13].

In the present study we describe the production, purification, pH and thermal stability of an α -

* To whom all correspondence should be sent:
E-mail: istoineva@yahoo.com

galactosidase from *Penicillium chrysogenum* sp. 23. The special attention was focused on to the raffinose hydrolysis in the presence of the secondary enzyme invertase.

EXPERIMENTAL

Medium and culture conditions

In this research we used mesophilic filamentous strain *Penicillium chrysogenum* sp.23, cultivated as a source of extracellular α -galactosidase. The fungal culture was maintained on beer agar slants. Five ml of spore suspension (approximately $2 \times 10^9 - 10^{10}$ spores/ml) were added to flasks (500 ml capacity) containing 50 ml of soy meal extract (SME) which is an extract of waste processing of soy protein isolates with 5% dry content. The cultivation was carried out stationary on rotary shaker at 30°C. In a laboratory bioreactor (working volume 3 l) the cultivation conditions were 30°C, agitation 600 rpm and aeration 1.0 l/min⁻¹. Samples were taken in different hours of cultivation and at the end of the fermentation process fungal biomass was separated from the culture fluid by filtration through paper filter. The filtrate was used for assaying α -galactosidase and invertase activity. After the fermentation, the culture supernatant was subjected to ultrafiltration for concentration and desalination and after that it was lyophilized, as in that form the enzyme retains activity for a long time.

Enzyme assay

α -Galactosidase activity was assayed by the modified method of Dey et al. [14], which is very accurate and sensitive, using 0,003 M p-nitrophenyl- α -D-galactopyranoside (pNPG) as substrate at pH 5.5 supporting by 0.1 M citrate-phosphate buffer. The reaction mixture was incubated at 50°C for 15 min. The reaction was stopped by the addition of 0.1 M sodium carbonate. The amount of p-nitrophenol released was measured from absorbance at 405 nm. One unit (U) of α -galactosidase activity is defined as the amount of enzyme liberating 1 μ mol of p-nitrophenol per min under the described conditions and corresponds to 16.7 nkat.

Invertase activity was determined using sucrose as a substrate [15] and the reducing sugars produced was then determined by the dinitrosalicylic acid method [16] using glucose as standard. One unit of the enzyme was defined as the amount of protein necessary to produce 1 μ mol glucose equivalent in 1 ml of solution per minute at pH 5 and 37°C. The absorbance was measured at 530 nm.

The data presented are mean values of triplicate assays. Standard deviations values were always smaller than 5 % of the mean value.

Determination of protein content by Lowry method

To determine the protein content was used the method of Lowry [17]. The method is based on the colorimetric measurement of the blue coloration which is obtained as a result of the reaction of the peptide bonds in proteins with copper ions under alkaline conditions and reduction of phosphotungstic acid and phosphomolybdic acid from Folin-Ciocalteu reagent. The amount of protein is determined from a standard curve using bovine serum albumin with different concentrations (0-100 μ g/ml). The absorbance was measured at $\lambda = 750$ nm. All measurements were performed in triplicate.

α -Galactosidase purification

For separation and purification of enzyme sample were used gel-filtration and ion-exchange chromatography. The lyophilized enzyme sample (700 mg) was dissolved in 5 ml 0.02 M sodium-acetate buffer pH 5.5 and applied on Sephadex G₁₀₀ column (80 x 2.5 cm) equilibrated with 0.02 M sodium acetate buffer with pH 5.5. The absorbance was monitored at $\lambda = 280$ nm. The proteins were eluted at a flow rate of 18 ml/h and 3.8 ml fractions were collected. Fractions of the active peak after gel-filtration chromatography containing α -galactosidase and invertase activity were pooled and were applied on DEAE-cellulose column (16 cm x 1.7 cm), equilibrated with 0.02 M sodium acetate buffer with pH 5.5. Proteins were eluted at a flow rate of 30 ml/h, with a linear gradient of NaCl (0.1-0.5 M). Fractions containing α -galactosidase and invertase activity were pooled, lyophilized and used in further studies.

HPLC analysis of saccharides hydrolysis

HPLC analysis was performed with a Agilent 1100 chromatograph equipped with Evaporative Light-scattering detector. An analytical column LiChrosorb NH₂ (250-4 mm, 5 μ m) was applied for carbohydrates separation. Sample injection was via a Rheodyne injector equipped with a 10 μ l sample loop. The mobile phase consisted of acetonitrile/water (70:30 v/v) for separation and flow rate was fixed at 1 ml/min. Peak identification of the chromatographs was done by comparing the retention time with the standards - galactose, glucose, sucrose, raffinose and melibiose were purchased from Sigma. Stock solutions of mono-,

di- and trisaccharides were prepared with equal concentrations - 10 mg/ml, 0.1 M citrate-phosphate buffer with pH 5.5, which was used for the enzyme hydrolysis.

After determination the retention times of the standart sugars it was conducted the hydrolysis of raffinose catalyzed by the enzyme sample from *Penicillium chrysogenum* sp.23 with the activity - 2U. The reaction mixtures contained 100 µl 0.05 mmol raffinose in 800 µl 0.1 M citrate-phosphate buffer with pH 5.5, 2 units of the enzyme and 100 µl buffer. The reaction mixtures were incubated at 40 C for 5 min, cooled and applied to HPLC.

To prove the effect of invertase accompanying α -galactosidase produced by strain *Penicillium chrysogenum* sp.23, were conducted comparative kinetic studies using pure α -galactosidase produced by strain *Humicola lutea* 120-5 with the activity - 2U and without invertase activity.

Determination of pH optimum and pH stability

The effect of pH on the enzyme activity was established by 0.1 M citrate - phosphate buffer with different pH from 2.6 to 7.0. The enzyme activity was measured by the method described above using the synthetic substrate p-nitrophenyl- α -D-galactopyranoside. The amount of p-nitrophenol, which releases the enzyme was determined spectrophotometrically at SPECORD UV VIS at $\lambda=405$ nm.

The pH stability was determined by incubating the suitably diluted enzyme in the above buffers incubated at room temperature for 2 h and for 24 h at 4°C and measuring residual enzyme activity at pH 4.5 , 50°C and reaction time 15 min by the modified method of *Dey et al.*

Thermal stability experiments of the enzyme

The thermal stability of α -galactosidase was investigated by measuring the residual activity of the enzyme after incubation at different temperatures in the range from 25 ° to 70° C. The diluted with distilled water enzyme solutions were incubated for 2 h at a thermostat and the activity of the samples was measured under standard conditions described above.

RESULTS AND DISCUSSION

The fungal strain *Penicillium chrysogenum* sp.23 produces high levels extracellular α -galactosidase in combination with invertase, like other eukaryotic microorganisms. After the fermentation, the cultural supernatant was subjected to ultrafiltration for concentration and desalination.

The cultural supernatant was lyophilized because in that form the enzyme retains activity for a long period of time. After purification of the α -galactosidase by gel filtration on Sephadex G-100 column, we registered two closed protein fractions, which have a common enzymatic activity of 65.6 U (fig.1)

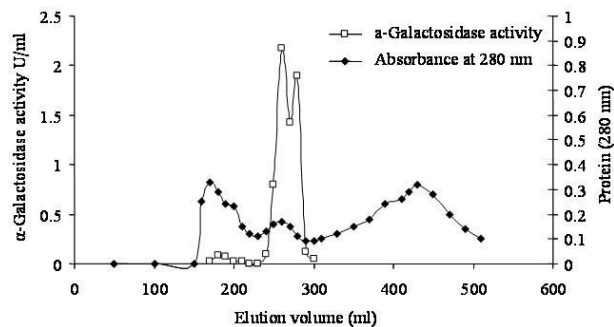


Fig 1. Elution profile of α -galactosidase from *Penicillium chrysogenum* sp.23 on Sephadex G-100 column

The fractions of the active peaks after gel filtration on Sephadex G-100 column were subjected to ion exchange chromatography on DEAE-cellulose column (16 cm \times 1.7 cm), equilibrated with 0.02 M sodium acetate buffer with pH 5.5. Proteins were eluted at a flow rate of 30 ml / h, with a linear gradient of NaCl (0.1-0.5M). There is one major peak, having the α -galactosidase activity of 27 U, which was eluted with a linear gradient at a concentration of 0.3 M NaCl (fig.2).

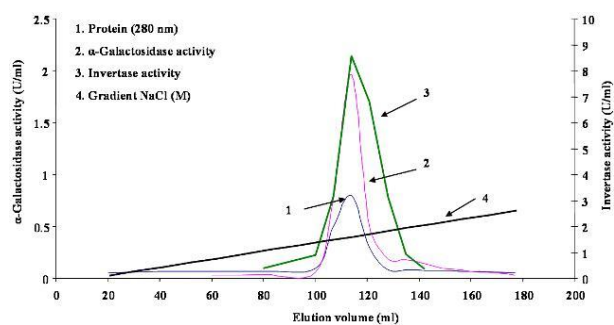


Fig.2. Elution profile of the α -galactosidase from *Penicillium chrysogenum* sp.23 on DEAE-cellulose column

It was established that the active fraction exhibiting α -galactosidase activity coincides with that of invertase activity. After DEAE ion-exchange chromatography the two enzymes are still not separated. This procedure resulted in a partially purified α -galactosidase fraction, which has and invertase activity with specific enzyme activity of 30 U/mg, purification factor 65.2 and recovery level about 28 %.

The results of the purification of the enzyme are summarized in the Table 1.

Table 1. Summary of protein content, enzymatic activity and yield at different purification steps of extracellular α -galactosidase produced by *Penicillium chrysogenum* sp.23

Purification	Total protein [mg]	Total activity [U]	Specific activity [U/mg]	Purification factor	Yield [%]
Lyophilized extract	210	96.6	0.46	1	100
Gel-filtration	9	65.6	7.28	15.8	67.9
Ion-exchange chromatography	0.9	27	30	65.2	28

Kinetic studies were performed by using HPLC analysis for tracking the hydrolysis of raffinose using two different enzymes from fungal strains-*Penicillium chrysogenum* sp.23 and *Humicola lutea* 120-5.

The HPLC analysis of the kinetic study with enzyme from fungal strain *Humicola lutea* 120-5 clearly shows that the enzyme does not possess invertase activity (fig.3, fig.4)

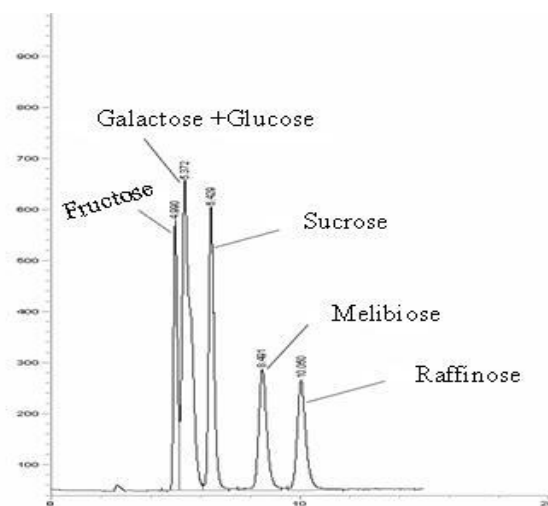


Fig 3. HPLC chromatogram of a standard mixture of sugars (mobile phase -acetonitrile: water (70:30 v/v, flow rate -1 ml/min)

Kinetic studies using HPLC analysis of the hydrolysis of raffinose catalyzed by *Penicillium chrysogenum* sp.23 showed the presence of fructose and depletion of raffinose. The appearance of a new peak for a disaccharide, probably is due to the α -glucosidase activity produced by *Penicillium chrysogenum* sp.23 invertase. The presence of invertase activity in the α -galactosidase preparations could contribute to the complete hydrolysis of the raffinose oligosaccharides, because they are substrates for both enzymes (fig.5).

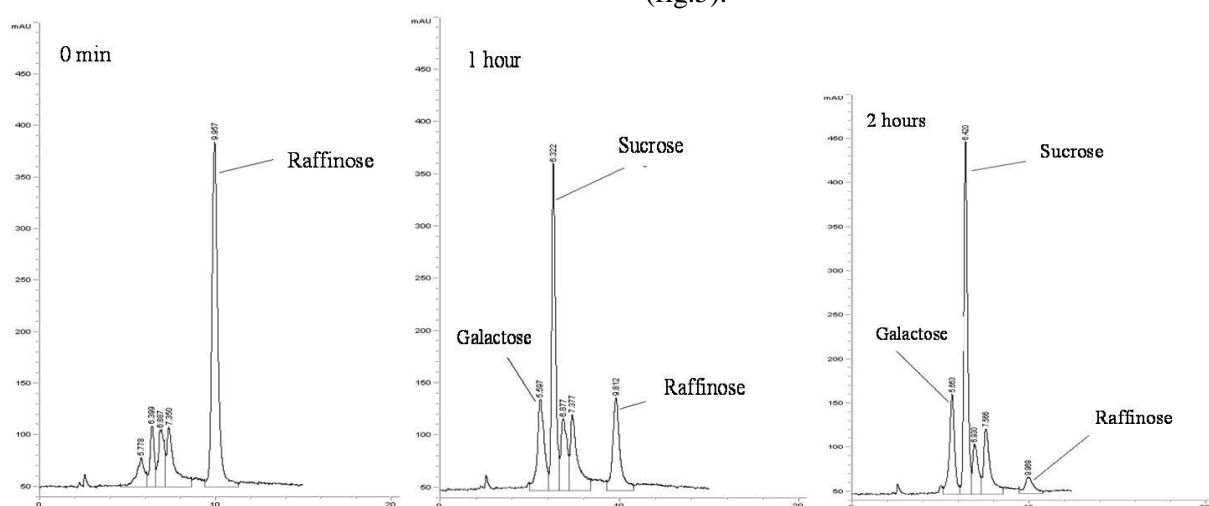


Fig 4. HPLC chromatograms of the hydrolysis of raffinose catalyzed by the enzyme sample from *Humicola lutea*. 120-5 with α - galactosidase activity - 2U.

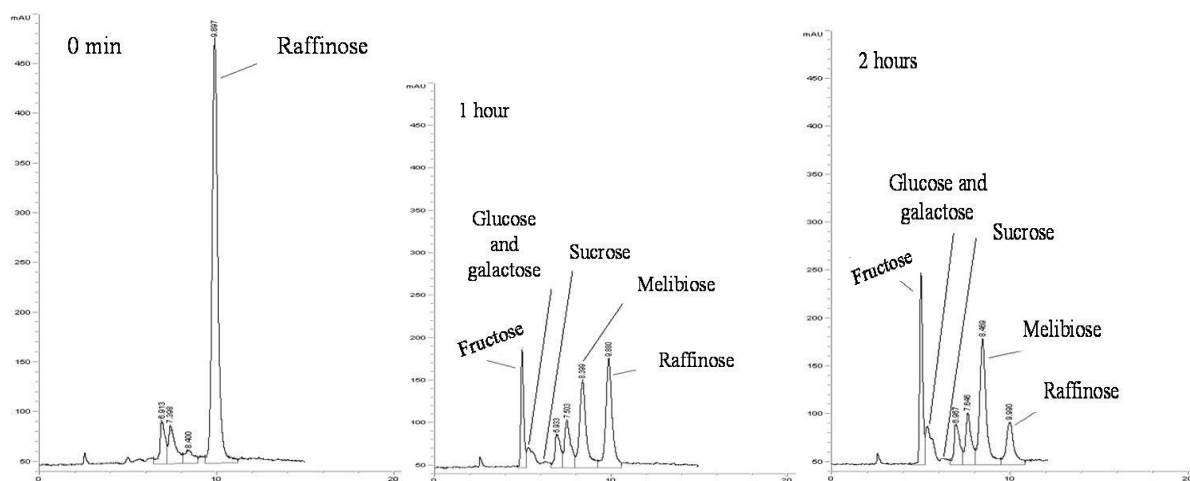


Fig. 5. HPLC chromatograms of the hydrolysis of raffinose catalyzed by an enzyme preparation of *Penicillium chrysogenum* sp.23 with α - galactosidase activity - 2U.

The obtained results show that the partially purified enzyme sample from *Penicillium chrysogenum* sp.23 should be particularly beneficial in the processing of soy crops for food purposes because of action of the two enzymes. This makes α -galactosidase of *Penicillium chrysogenum* sp.23 very promising for application in the food industry, since this enzyme has a much higher activity compared to the α -galactosidases produced by other strains.

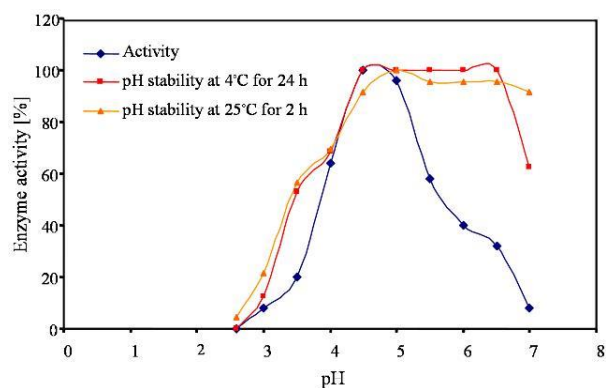


Fig. 6. Effect of pH on α -galactosidase activity and stability.

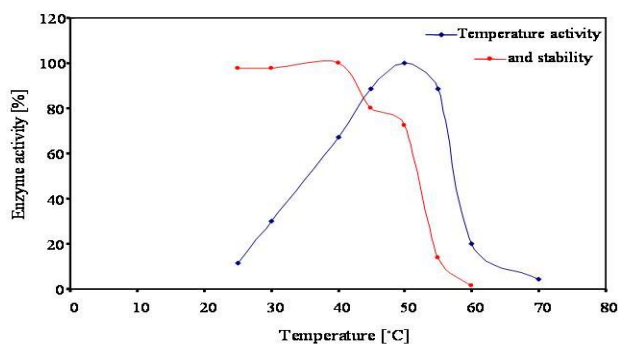


Fig. 7. Effect of the temperature on α -galactosidase activity and stability

It was established that the enzyme has a pH optimum 4.5-5.0, and pH stability extends over a wide range of 4.5-6 (fig.6).

The temperature optimum of α -galactosidase was 50°C, and the enzyme is stable from 25 to 40°C, at 45°C the activity falls to 80%, at 50°C falls to 72% and at 60°C the activity is completely lost (fig.7).

Most α -galactosidases are stable over a broad range of activity. For example the α -galactosidase from *Penicillium* sp. F63 CGMCC1669 has an optimum pH of 5.0 and an optimum temperature of 45 degrees C. The enzyme is stable between pH 5.0 and 6.0 below 40°C [14].

CONCLUSION

In this paper was proven that the fungus strain *Penicillium chrysogenum* sp.23 produces both enzymes α -galactosidase and invertase. By gel-filtration chromatography was partially purified a crude extract of the enzyme sample obtained from *Penicillium chrysogenum* sp.23. The purification was achieved of α -galactosidase from accompanying substances by ion exchange chromatography, but does not achieve separation of the invertase and α -galactosidase from each other. This requires the research of more efficient methods for the separation of the two enzymes. The ability of fungus strain of *Penicillium chrysogenum* sp.23 to produce both α -galactosidase and invertase makes it especially attractive for industrial applications. Due to the synergism of action of the two enzymes it is expected fast hydrolysis of oligosaccharides in soy foods and legumes releasing digestible monosaccharides and removing discomfort of flatulence.

REFERENCES

1. H. Jooyandeh., *Middle-East Journal of Scientific Research* **7**(1), 71 (2011).
2. D. Tsangalis, J. Ashton, A. McGill, N. Shah, *J.Food Sci*, **67**, 3104 (2012).
3. K.S Dhananjay., V.H. Mulimani, *Biotechnol. Lett.*, **30**, 1565 (2008).
4. P. M.. Dey and J.B. Pridham ‘ *Adv. Enzimol.*, **36**, 911, (1972).
5. G. P. Aravind Goud and V. H. Mulimani *Biotechnol. Bioprocess Eng.* **13**, 354 (2008)
6. S. J. Prashanth, V. H. Mulimani., *Process Biochem.* **40**, 1199 (2005).
7. M. M. Fuller, Lovejoy, D. A. Brooks, M. L. Harkin, J. J. Hopwood and P. J. Mickle.. *Clin. Chem.*, **50**, 1979 (2004).
8. M. L.Olsson, C. A. Hill, H. Dela Vega, Q. P. Liu, M. R. Stroud, and J. Valdinocci.. *Transfus. Clin. Biol.* **11**, 33 (2004).
9. C. Goosen, Xiao-Lian Yuan, M. Jolanda van Munster, F. Arthur, J.Ram. *EUKARYOTIC CELL*, 674 (2007).
10. H. Winter, SC. Huber .*Crit Rev Plant Sci.*, **19**, 31 (2000).
11. A. Tazuin and T. Giardina *Frontiers in Plant Science*, **5**, 293 (2014).
12. M. Giraldo, T. da Silva, F. Salvato, H. Terenzi, J. Jorge, L. Guimaraesh *World J.of Microb. and Biotechnol.*, **28**, 463 (2012).
13. G. Arumugam, A. Sadiq , M. Nagalingam., and A. Panneerselvam, *European Journal of Experimental Biology*, **4**, 29 (2014).
14. P.M. Dey, S. Patel, M.D.Brownleader *Biotechnol. Appl. Biochem.*, **17**, 361 (1993)
15. S. T. de Rezende., C.R. Felix *Biotechnol. Lett.*, **19**, 217 (1997).
16. G. L. Miller, *Anal. Chem.*, **31**, 426 (1959).
17. O. Lowry, N. Resenbrough, A. Farr, K. Rawdall *J. Biol. Chem.*, **193**, 265 (1951).

АЛФА-ГАЛАКТОЗИДАЗА ОТ *PENICILLIUM CHRYSOGENUM* SP.23: ПРЕЧИСТВАНЕ, ХАРАКТЕРИСТИКИ И ХИДРОЛИЗА НА РАФИНОЗА В ПРИСЪСТВИЕТО НА ИНВЕРТАЗА

Б. К. Якимова, Б. П. Чорбанов, И. Б. Стойнева

Лаб.Химия и биофизика на белтъци и ензими, Институт по Органична Химия с Център по Фитохимия, Българска Академия на Науките, ул. Акад.Г. Бончев, бл.9, 1113, София, България

Постъпила на 30 септември, 2016 г.; Коригирана на 3 февруари, 2017 г.

(Резюме)

В това изследване установихме, че шамът *Penicillium Chrysogenum* sp.23 може да продуцира едновременно α -галактозидаза и инвертаза с максимална ензимна активност (4000 U.l^{-1}) когато се използва екстракт от соево брашно, съдържащ 5% сухо вещество като среда. Определени са оптималните параметри рН 4,5-5,0 и температура 50°C на α -галактозидазата фракция чрез използване на р-нитрофенил- α -D-галактопиранозид като субстрат. Хидролизата на рафиноза катализирана от α -галактозидаза, съпътствана от инвертаза е регистрирана с високоефективна течна хроматография.

Установено е, че в присъствие на инвертаза се наблюдава преобразуване на рафинозата главно до мелибиоза и фруктоза. Ензимната хидролиза на рафинозните олигозахариди, която се осъществява от α -галактозидаза и/или инвертаза в соевите семена използвани в храната на човека и животните води до подобряване на нейните хранителни свойства и значително намалява или отстранява стомашния дискомфорт. Получените резултати показват, че частично пречистен ензимен препарат от *Penicillium chrysogenum* sp.23 би бил много полезен при преработката на соеви култури за хранителни цели, тъй като се реализира синергизъм в действието на двата ензима.

Kinetic of inhibition of lipoxygenase in presence of natural amino acid serine

R.N. Raykova¹, E. Carvalho², L.S. Manovski¹, D.L. Danalev*¹, D.A. Marinkova¹, T.I. Pajpanova³, S.A. Yaneva⁴, L.K. Yotova¹

¹University of Chemical Technology and Metallurgy, Biotechnology Department, Sofia 1756, Bulgaria

²University of Cergy-Pontoise, France

³Institute of Molecular Biology “Roumen Tsanev”, Bulgarian Academy of Sciences, Sofia 1113, Bulgaria

⁴University of Chemical Technology and Metallurgy, Department of Fundamentals of Chemical Technology Sofia 1756, Bulgaria

Received October 01, 2016; Revised January 15, 2017

Lipoxygenase (LOX) is an enzyme, found in many plants and animals, which catalyses the oxygenation of polyunsaturated fatty acids (PUFA) to form fatty acid hydroperoxides. The latter are present in a wide range of biological organs and tissues, particularly abundant in grain legume seeds (beans and peas) and potato tubers. Lipoxygenase from different sources, catalyses oxygenation at different points along the carbon chain, which is referred as regio - specificity. Such specificity has significant implications for the metabolism of the formed hydroperoxides into a number of important secondary metabolites. According to the literature, it is known that primary alcohols and amines inhibit lipoxygenase activity. Herein, we report our studies on inhibitory effect of natural amino acid serine on lipoxygenase, isolated from avocado. The affinity of LOX is higher with L-Ser, compared to D-Ser. It means that natural amino acid is more compatible for the enzyme, but at the same time K_i values reveal that D-Ser has stronger inhibitory effect against LOX from avocado.

L-Serine shows competitive type of inhibition against LOX and for D-Serine the inhibition type of enzyme catalyzed reaction is mixed.

Key words: Lipoxygenase, inhibitors, serine, amino acid

INTRODUCTION

Lipoxygenases catalyze the oxidation of unsaturated fatty acids and have a wide range of biomedical applications. In mammals, LOX aid in the production of leukotrienes and lipoxins, which regulates responses in inflammation and immunity [1, 2]. Thus, LOX inhibitors have been used as drug agents for treatment of inflammatory diseases such as asthma, atherosclerosis, and psoriasis [3]. In addition, LOX inhibitors are promising cancer chemotherapeutics [4-7]. Numerous kinetic studies of LOXs have been carried out using soybean LOX-1 [8] and human LOX [9] with linoleic acid (LA) as a substrate [10]. They all reveal the same mechanism of action (Figure 1), where the pro-S hydrogen atom from carbon atom C11 of LA is transferred to the Fe(III)-OH cofactor, forming a radical intermediate substrate and Fe(II)-OH₂ [8, 11]. Authors also described that a subsequent reaction with molecular oxygen could be further realized and it eventually leads to hydroperoxyoctadecadienoic acid and Fe (III)-OH [8].

LOX pathway has become important therapeutic target for prevention of different inflammatory diseases and cancer treatments. The Food and Drug Administration (FDA) approved drugs for diseases, caused by LOX, but some of them have been reported to exhibit various side effects [12]. Hence, it is essential to implement specific inhibitor which will not interfere with the other normal physiological functions (Fig. 2).

In this global context finding new inhibitors of LOX could be a promising alternative as chemotherapeutics for prevention and treatment of different diseases, where LOX plays a key role.

LOX can be inhibited by several natural products, including flavonoids [14, 15], thiourea and the derivatives [16-18], etc. Rioux N. et al. conclude in their work that alcohols and primary amines are good LOX inhibitor [7]. Taking into account this information, we decided to study the effect of amino acid serine for its ability to inhibit LOX.

EXPERIMENTAL

Chemicals

Linolenic acid was purchased from Sigma Aldrich. L- and D-Serine were obtained from Riedel-de haen. Isolation and purification of avocado LOX and its characteristics (activity, pH

* To whom all correspondence should be sent:
E-mail: dancho.danalev@gmail.com

and temperature optimum) were previously described in [19]. 0.1M acetate buffer with pH 6.5

was used for all kinetic studies.

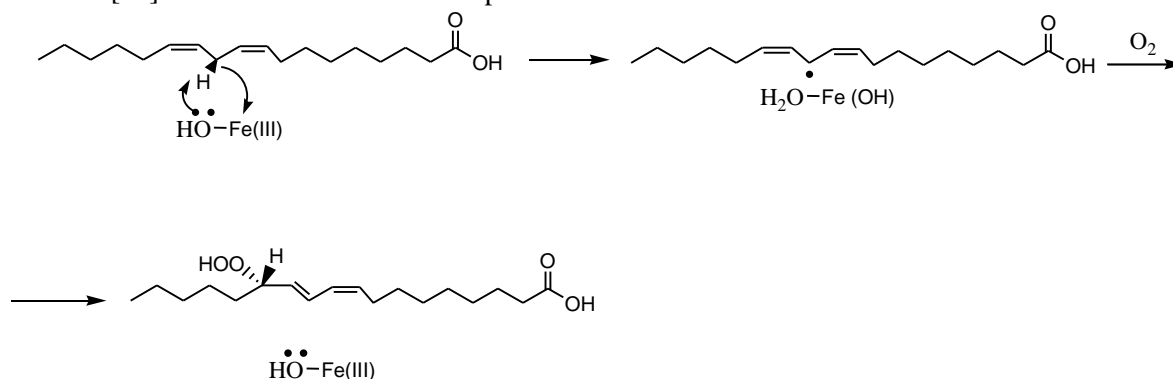


Fig. 1. Proposed mechanism of soybean lipoxygenase [8]. The net hydrogen atom transfer from the linoleic acid substrate to the Fe (III) – OH cofactor is on focus.

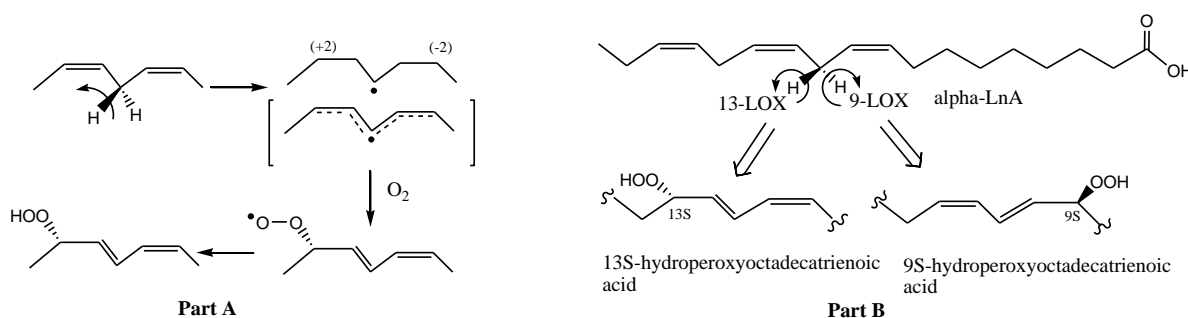


Fig.2. LOX reaction showing the principal steps of LOX reaction (Part A), and the actual reactions of plant LOXs and α -linolenic acid (Part B) [13].

KINETIC STUDIES

Substrate preparation

0.1 ml linolenic acid (LnA) was dissolved in 60 ml 95% EtOH. The obtained solution was diluted to 100 ml with distilled water and stirred for 1 hour. Before activity measurement, the needed quantity was diluted 5 times with 0.2 M acetate buffer, pH 6.5 [20].

Enzyme solution preparation

Enzyme solution with concentration 1 mg/ml in 0.1 M acetate buffer, pH 6.5, was prepared. Before measurement the protein content was diluted 5 times up to final concentration 20 μ g/ml [20-22].

Determination of avocado LOX kinetics

Kinetics of enzyme catalyzed reactions in presence of avocado LOX and LnA were measured spectrophotometrically on Perkin Elmer Lambda 2 spectrophotometer at 234 nm.

Michaelis constant, K_m and V_{max} were calculated using Lineweaver-Burk plot (L-B plot) [23, 24]. Different concentrations of LnA for the enzyme catalyzed reactions were investigated and applied.

Kinetics of inhibition of avocado LOX

Control sample of 2.4 ml solution of inhibitor and 0.1 ml substrate solution was prepared. Concerning the sample, 2.1 ml solution of inhibitor and 0.1 ml substrate solution were incubated. At zero time 0.3 ml enzyme with concentration 20 μ g/ml was added and the measurement of $\Delta A/min$ was obtained by UV-spectrophotometer at 234 nm for 10 min, taking into account the linear range of reactions [25].

RESULTS AND DISCUSSION

Serine is a natural amino acid including both primary amino and primary hydroxyl functions (Figure 3).

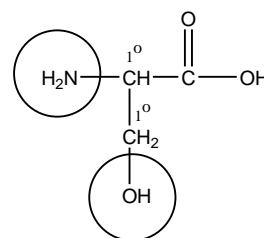


Fig. 3. Serine structure

Structurally serine includes all necessary moieties, according to Rioux N. et al., to be a

potent LOX inhibitor [7]. Taking into account this information, we investigated kinetics of inhibition of avocado LOX in presence of L- and D-Serine.

For our purpose substrate solutions with several concentrations (Table 1) were prepared, starting from a stock solution described in experimental section.

The obtained curve for reaction kinetics, in absence of inhibitor for avocado LOX and presence of LnA as a substrate, is presented on Figure 4.

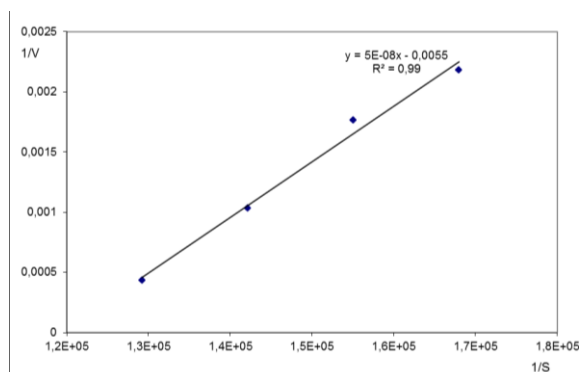


Fig. 4. L-B plot for avocado LOX kinetics with linolenic acid

Calculated kinetic parameters, according to the presented L-B plot are: K_m $9,09 \cdot 10^{-6}$ M and V_{max} $181,82$ M.sec⁻¹.

Further, our work continued with determination of kinetic parameters in presence of L- and D-Serine as inhibitors. For this purpose, inhibitor

solutions with several concentrations were prepared (Table 2).

In order to determine type of inhibition in presence of L-Ser the following concentrations of substrate and inhibitor were applied: initial substrate concentrations: $2,69 \cdot 10^{-3}$ M; $2,94 \cdot 10^{-3}$ M; $3,23 \cdot 10^{-3}$ M; $3,59 \cdot 10^{-3}$ M; initial L-Ser concentrations: $0,6 \cdot 10^{-3}$ M; $1,0 \cdot 10^{-3}$ M; $3,0 \cdot 10^{-3}$ M.

The obtained data for kinetic reactions with both inhibitors are presented on Figure 5 and 6, respectively.

The obtained results show a competitive type of inhibition, which can be also noticed from the calculated K_i and K_m parameters – in cases of competitive inhibition K_i shows lower values than K_m , overcoming the effect of increased substrate concentration.

In order to calculate K_i , K_m and V_{max} the following concentrations were used: initial substrate concentrations: $2,69 \cdot 10^{-3}$ M; $2,94 \cdot 10^{-3}$ M; $3,59 \cdot 10^{-3}$ M; initial L-Ser concentrations: $0,3 \cdot 10^{-3}$ M; $0,6 \cdot 10^{-3}$ M; $1,0 \cdot 10^{-3}$ M; $3,0 \cdot 10^{-3}$ M.

By applying Dixon plot, we determined the following values for kinetic parameters in presence of L-Serine: K_i $1,1394 \cdot 10^{-5}$ M, K_m $2,26 \cdot 10^{-5}$ M and V_{max} $0,2005$ M.sec⁻¹.

The probable role of L-Ser as a drug agent, taking into account the expressed competitive inhibition, might be to increase the intracellular concentration of LnA and in that way to accumulate the substrate and inhibit its utilization if needed.

Table 1. Substrate concentrations used for enzyme kinetic measurements.

Substrate	Stock solution concentration, 10^{-3} M	Solution concentration in cuvette (kinetics in absence of inhibitor), 10^{-6} M	Solution concentration in cuvette (kinetics in presence of inhibitor), 10^{-5} M
LnA	3,59	8,60	0,052
	3,23	7,74	0,046
	2,94	7,04	0,042
	2,69	6,45	0,039

Table 2. Concentrations of LOX inhibitors, used for determination of type of inhibition and calculation of kinetic parameters of the enzyme catalyzed reactions.

Inhibitor	Stock solution concentration, 10^{-3} M	Solution concentration in cuvette, 10^{-5} M
L-Ser	0,3	12,0
	0,6	24,0
	1,0	40,0
	3,0	120,0
D-Ser	0,1	8,0
	0,3	25,2
	0,6	50,4
	1,45	121,8

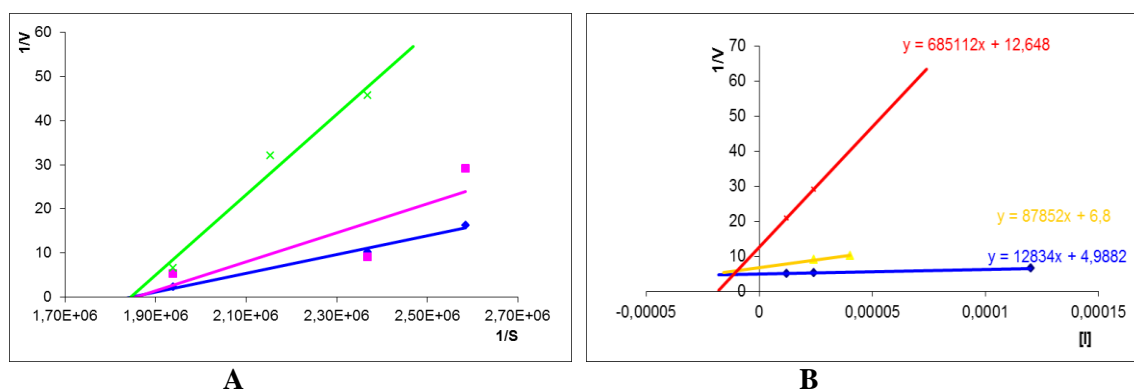


Fig. 5. Kinetics of inhibition of LOX in presence of L-Ser: **A.** L-B double reciprocal plot for determination of type of inhibition; **B.** Dixon plot for determination of kinetic parameters.

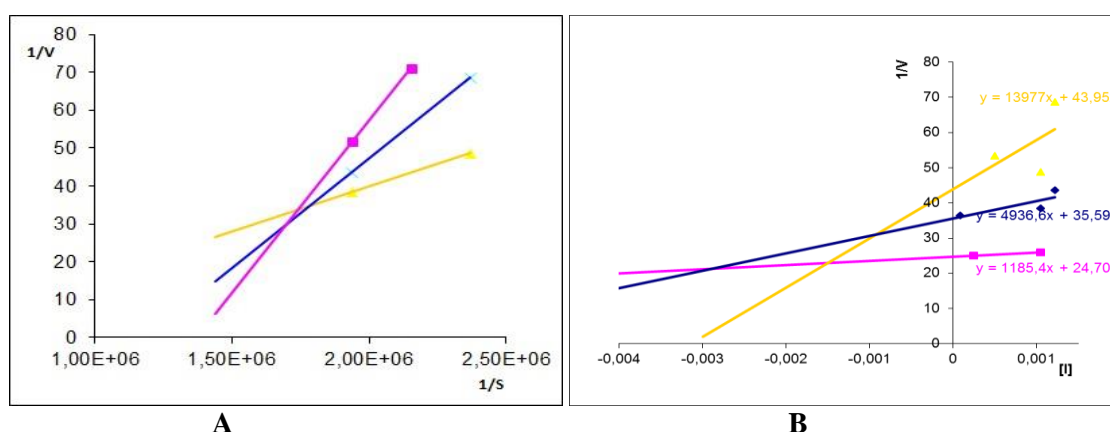


Fig. 6. Kinetics of inhibition of LOX in presence of D-Ser: **A.** L-B double reciprocal plot for determination of type of inhibition; **B.** Dixon plot for determination of kinetic parameters.

Table 3. Values of kinetic parameters in presence of inhibitors in case of avocado LOX reaction

Inhibitor	Ki [M]	Km [M]	Vmax [M.sec ⁻¹]
L-Serine	1,14.10 ⁻⁵	2,26.10 ⁻⁵	0,2005
D-Serine	1,91.10 ⁻⁶	6,23.10 ⁻⁵	0,1239
Absence of inhibitor	-	9,09.10 ⁻⁶	181,82

In order to determine the type of inhibition of D-Ser against avocado LOX the precise concentrations were used: initial substrate concentrations 2,69.10⁻³M; 2,94.10⁻³M; 3,23.10⁻³M; 3,59.10⁻³M; initial D-Ser concentrations 0,3.10⁻³M; 0,6.10⁻³M; 1,45.10⁻³M. The obtained results reveal a mixed type of inhibition, where typical is increasing of K_m value (substrate binding) and decreasing of V_{max} value (hamper catalysis).

Further, applying Dixon plot representation, we prepared: initial substrate concentrations 2,94.10⁻³M; 3,23.10⁻³M; 3,59.10⁻³M; initial D-Ser concentrations 0,1.10⁻³M; 0,3.10⁻³M; 0,6.10⁻³M; 1,45.10⁻³M and determined the following values of kinetic parameters, representing the qualitative effect of the inhibitor against LOX: K_i 1,91.10⁻⁶ M, K_m 6,23.10⁻⁵ M and V_{max} 0,1239 M.sec⁻¹.

All data for calculated parameters is summarized in Table 3.

Most of the pharmaceutical inhibitors are competitive and a few are mixed ones, lowering V_{max} and increasing K_m . For this reason, D-Ser is hopeful alternate inhibitor for LOX reactions and their place in cell processes.

CONCLUSIONS

K_m values in case of L- and D-Ser inhibition process show that the affinity of LOX from avocado is higher in presence of L-Ser, compared to D-Ser. It means that natural amino acid is highly recognized and interfered to the active site of the enzyme, but K_i values reveal that D-Ser shows significantly stronger inhibitory effect against LOX.

The type of inhibition in cases of L- and D-Ser differs. The effect of L-Serine occurs in competitive inhibition, whilst D-Ser inhibiting mechanism is mixed.

Acknowledgments: The present work was supported by "National Fund Scientific Research", project DUNK 01/03, 2009.

REFERENCES

1. R. Casey, Lipoxygenases. In: R. Casey, P.R. Shrewy (eds.) Seed proteins. London, Chapman and Hall, 1998.
2. .B. Samuelsson, S.-E. Dahlen, J. A. Lindgren, C. A. Rouzer, C.N. Serhan, *Science*, **237**, 1171 (1987).
3. V.E. Steele, C.A. Holmes, E.T. Hawk, L. Kopelovich, R.A. Lubet, J.A. Crowell, C.C. Sigman, G.J. Kelloff, *Cancer Epidemiology, Biomarkers & Prevention*, **8**, 467 (1999).
4. J. Ghosh, C.E. Myers, *Proc. Natl. Acad. Sci. USA*, **95**, 13182 (1998).
5. E.R. Lewis, E. Johansen, T.R. Holman, *JACS*, **121**, 1395 (1999).
6. D. Nie, G.G. Hillman, T. Geddes, K. Tang, C. Pierson, D.J. Grignon, K.V. Honn, *Cancer Res*, **58**, 4047 (1998).
7. N. Rioux, A. Castonguay, *Carcinogenesis*, **19**, 1393 (1998).
8. E.N. Segraves, T.R. Holman, *Biochemistry*, **42**, 5236 (2003).
9. K.W. Rickert, J.P. Klinman, *Biochemistry*, **38**, 12218 (1999).
10. M.J. Knapp, K.W. Rickert, J.P. Klinman, *JACS*, **124**, 3865 (2002).
11. G.A. Veldink, M.P. Hilbers, W.F. Nieuwenhuizen, J.F.G. Vliegthart, In: A.F. Rowley, K. Kühn, T. Schewe (eds.) Plant lipoxygenase: structure and mechanism in eicosanoids and related compounds in plants and animals, Portland Press, 1998.
12. M.C. Liu, L.M. Dube, J. Lancaster, *J. Allergy Clin. Immunol.*, **98**, 859 (1996).
13. V.S. Chedea, M. Jisaka, *Publisher: InTech*, **6**, 3 (2011).
14. M.G. Grütter, G. Fendrich, R. Huber, W. Bode, *EMBO J*, **7**, 345 (1988).
15. Y. Hamamoto, H. Nakashima, T. Matsui, A. Matsuda, T. Ueda, N. Yamamoto, *Antimicrobial Agents and Chemotherapy*, 907 (1987).
16. D. A. Walz, D. Hewett-Emmett, W. H. Seegers, *Proc. Natl. Acad. Sci. USA*, **74**, 1969 (1977).
17. J.M. Mates, C. Perez-Gomez, I.N. De Castro, *Clin. Biochem.*, **32**, 595 (1999).
18. Y.J. Wang, M.H. Pan, A.L. Cheng, L.I. Lin, Y.S. Ho, C.Y. Hsieh, J.K. Lin, *J. Pharm. Biomed. Anal.*, **15**, 1867 (1997).
19. L. Manovski, V. Smedzieva, L. Yotova, *JCTM*, **50**, 249 (2015).
20. G. E. Anthon, D. M. Barrett, *J. Agric. Food Chem.*, **49**, 32 (2001).
21. WBC, Worthington Enzyme Manuel, Freehold, New Jersey, 1972.
22. L. Yotova, D. Marinkova, *BioPS'08*, III.37–III.46 (2008).
23. H. Lineweaver, D. Burk, *JACS*, **56**, 658 (1934).
24. И. В. Березин, А. А. Клесов, Практический курс химической и ферментативной кинетики. Изд. Моск. У-та, 65 (1976).
25. F.J. Torriani, M. Rodriguez-Torres, J.K. Rockstroh, E. Lissen, J. Gonzalez-Garcia, A. Lazzarin, G. Carosi, J. Sasadeusz, C. Katlama, J. Montaner, H. Sette Jr, S. Passe, J. De Pamphilis, F. Duff, U.M. Schrenk, D.T. Dieterich, *J. Med.*; **351**; 438 (2004).

КИНЕТИКА НА ИНХИБИРАНЕ НА ЛИПОКСИГЕНАЗА В ПРИСЪСТВИЕ НА ПРИРОДНАТА АМИНОКИСЕЛИНА СЕРИН

Р.Н.Райкова¹, Е.Карвальо², Л.С.Мановски¹, Д.Л.Даналев¹, Д.А.Маринкова¹, Т.И.Пайпанова³, С.А.Янева⁴, Л.К. Йотова¹

¹Химикотехнологичен и металургичен университет, катедра "Биотехнология", София 1756, България

²Университет на Cergy-Pontoise, Франция

³Институт по молекулярна биология „Румен Цанев“, Българска академия на науките, София 1113, България

⁴Химикотехнологичен и металургичен университет, катедра "Основи на химичните технологии", София 1756, България

Постъпила на 01 октомври, 2016 г.; Коригирана на 15януари, 2017 г.

(Резюме)

Липоксигеназата (ЛГ) е ензим, който се среща в много растения и животни и катализира процеса на окисление на полиненаситените мастни киселини (PUFA) до образуване на техни хидропероксиди. Тя присъства в големи количества в биологични органи и тъкани и по-специално е в изобилие в зърната на бобовите растения (боб и грах) и картофите. ЛГ от различни източници катализира процеса на окисление в различни части от въглеродната верига, т.е. притежава региоселективност. Това има огромно значение за метаболизирането на образуваните хидропероксиди в някои важни вторични метаболити. Според литературни данни първични алкохоли и амини инхибират липоксигеназната активност. В настоящата работа ние докладваме изследвания за инхибиторният ефект на природната аминокиселина серин (Ser) върху ЛГ, изолирана от авокадо. Нашите изследвания показваха, че афинитета на ЛГ е по-висок към L-Ser в сравнение с D-Ser. Това означава че природната форма на аминокиселината е по-съвместима с ензима, но в същото време K_i стойностите показват, че D-Ser притежава по-мощен инхибиторен ефект. L-Ser показва конкурентен тип на инхибиране, докато при D-Ser той е от смесен тип.

Chemical stability of new neurotensin (8-13) analogues

S. Michailova¹, T. Dzimbova², K. Kalikova³, E. Tesařová³, T. Pajpanova^{2*}

¹Medical University of Varna "Prof. Dr. Paraskev Stoyanov", Faculty of Pharmacy, 55 Marin Drinov str., Varna 9002, Bulgaria

²Institute of Molecular Biology "Roumen Tsanev", Bulgarian Academy of Sciences, Acad. G. Bonchev str., block 21, Sofia 1113, Bulgaria

³Charles University in Prague, Faculty of Natural Science, Department of Physical and Macromolecular Chemistry, Albertov 2030, 128 43 Prague, Czech Republic

Received December 21, 2016; Revised February 20, 2017

Hydrolytic stability of the peptides is one of the most important properties regarding their application in a practice. Early information on the stability is essential for the pharmacokinetic behavior in the body, for the storage conditions, the occurrence of toxic effects associated with its degradation products, etc. The purpose of this study was to evaluate the hydrolytic stability of synthesized NT(8-13) analogues under physiological conditions such as body temperature at 37°C and physiological pH values of 1.2 (stomach), 7.4 (blood plasma) and 8.5 - 9.0 (thin intestine).

Key words: neurotensin, canavanin, hydrolytic stability

INTRODUCTION

Neurotensin (NT) is a peptide consisting of 13 amino acids (pGlu-Leu-Tyr-Glu-Asn-Lys-Pro-Arg-Arg-Pro-Tyr-Ile-Leu) that has been originally isolated from calf hypothalamus [1]. Like other neuropeptides, neurotensin has different functions. It is a neurotransmitter and neuromodulator in the central nervous system and a local paracrine hormone in the periphery, particularly in the gastrointestinal tract [2-5].

Three different receptors for neurotensin (NTS1, NTS2, and NTS3) have been cloned and studied thus far [6-8]. Among the known NT receptors, it has been shown that NTS1 is over-expressed in various relevant tumors, including ductal breast cancer and pancreatic tumors [9-12]. Structure-activity studies have demonstrated that the minimal sequence required for full biological activity is the C-terminal part NT(8-13) (Arg-Arg-Pro-Tyr-Ile-Leu) [13] and has therefore been selected as a lead structure for medicinal chemists [6, 14-18].

Application of the neurotensin, or any other endogenous peptide as clinical available drugs has been impeded by their relatively poor receptor selectivity, rapid degradation *in vivo*, and inefficient to penetrate the blood-brain barrier.

In addition, the pH value of the medium is one of the most important factors influencing the stability of the compounds and drugs, including those of the peptides also. The metabolism of the drugs often was associated with hydrolysis of an ester or amide bond, and its rate depends on the temperature and pH of the solution. The

knowledge of "pH profile" of the compound helps us to define the values for which it is most susceptible to degradation. This also enables us to determine that pH value, which will provide optimum stability of the molecule and retains its structure and concentration over time.

We recently reported the synthesis of five new NT(8-13) mimetics, the pilot studies on their toxicity and central nervous activity [19]. The purpose of this study was to evaluate the hydrolytic stability of these neurotensin analogues in different values of pH, available physiologically.

EXPERIMENTAL

Peptide synthesis

Reagents, resins and Fmoc-amino acids used in peptide synthesis were purchased from Merck (Darmstadt, Germany) and Iris Biotech GMBH (Germany). Solvents of dimethylformamide (DMF) and dichloromethane (DCM) were purchased from Merck (Darmstadt, Germany). Electrophoretic experiments were performed using a BeckmanP/ACE (Beckman Coulter Inc., Pasadena, CA, USA).

Synthesis of all peptides was performed by the conventional and manual stepwise Fmoc solid-phase synthesis on 2-chlorotriyl chloride resin with substitution, 1.4 mmol/g. The coupling of each amino acid was performed in the presence of 3 mol excess of Fmoc-amino acid, 3 mol excess of N-hydroxybenzotriazole (HOBt), 3 mol excess of diisopropylcarbodiimide (DIC), and 5 mol excess of diisopropylamine (DIPEA) in dimethylformamide (DMF). Completion of

* To whom all correspondence should be sent:
E-mail: tamara@bio21.bas.bg

coupling reactions were monitored by the Kaiser test and the Fmoc groups were removed by adding 20% piperidine in DMF. The peptides were cleaved from the resin and the final deprotection was done in a cocktail containing trifluoroacetic acid (TFA), triisopropylsilane (TIPS), thioanisole, and water (92.5: 2.5: 2.5: 2.5). The crude peptides were precipitated into cold petroleum ether/diisopropyl ether (50:50). Then, the precipitate was dissolved in 10% CH₃COOH and desalted by gel filtration on a Sephadex G25. The chemical purity of peptides was characterized by RP-HPLC and capillary electrophoresis.

Analysis

Purity: HPLC analysis were performed with LKB Bromma (Sweden) and Waters Alliance® (Waters Corporation, USA) instruments, variable detector using column: XTerra® MS C18, 3,5µm, 3.0 x 150 mm; eluent: ACN/0.05%TFA 5/95 (v/v), flow 0.4ml/min, 25°C, 220 nm, inj. volume 20 µL.

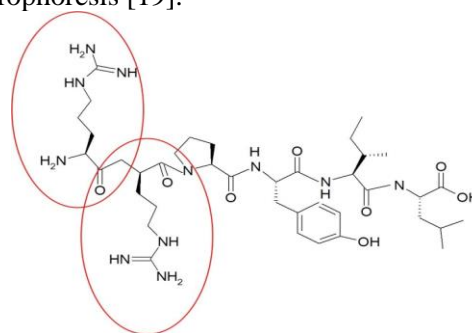
Stability: The hydrolytic stability of the peptides was determined by UV spectroscopy. For stability testing, a concentration 0.5.10⁻⁴ mol/l respectively of each of the peptides (NT - NT5) were dissolved in 10 ml of buffers: pH=1,2 (0.063 mol/l HClO₄); pH=7,4 (0.1 mol/l Na₂HPO₄ + 0.1 mol/l NaH₂PO₄); pH=9,0 (0.1 mol/l Na₂B₄O₇). The obtained solution of the peptides was tempered in the incubator ES-20 LKB (Sweden) at 37°C. The testing samples were placed in a Beckman DU 650 spectrophotometer (Beckman Instruments, USA) equipped with a temperature-controlled cell changer; 1 ml quartz cuvettes were used. The decrease in the absorbance at 220 nm (UV maximum of the peptide) was monitored.

RESULTS AND DISCUSSION

The chemical stability of peptides is very dependent on amino acid composition and sequence. The two main cleavage bonds in the metabolic deactivation of NT(8–13) are Arg⁸–Arg⁹, Pro¹⁰–Tyr¹¹ and Tyr¹¹–Ile¹². To avoid such degradation, the terminal Arg units was replaced by canavanine (Cav), which was recently described as a non-proteinogenic Arg analogue. Because lysine was shown to be an attractive alternative basic residue [14], lysine replacement of the first/or second arginine moiety was also performed (Fig. 1.).

In this context our first objective was to synthesize the neurotensin mimetics in high yields and purities. Following purification by gel filtration on a Sephadex G25, peptides were isolated in high yields (86–91%), and excellent purities (>95%)

confirmed by RP-HPLC (Fig. 2.) and capillary electrophoresis [19].



Code	Peptides
T0	Arg-Arg-Pro-Tyr-Ile-Leu
T1	Lys-Cav-Pro-Tyr-Ile-Leu
T2	Cav-Lys-Pro-Tyr-Ile-Leu
T3	Cav-Cav-Pro-Tyr-Ile-Leu
T4	Arg-Cav-Pro-Tyr-Ile-Leu
T5	Cav-Arg-Pro-Tyr-Ile-Leu

Fig. 1. Neurotensin (8-13) analogues.

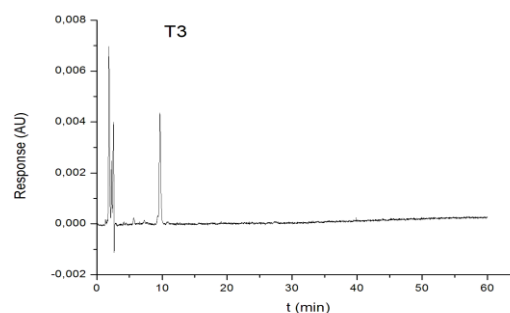


Fig. 2. RP-HPLC chromatogram at 220 nm of Cav⁸-Cav⁹-neurotensin (8-13) analogue

Therefore, in order to determine the hydrolytic stability of the synthesized neurotensin mimetics, we investigated their behaviour in three different physiological pH values of 1.2 (stomach), 7.4 (blood plasma) and 8.5 - 9.0 (thin intestine) using UV-spectroscopy and RP-HPLS as well. At defined intervals of the time we measured the absorbance at 220 nm. For each of the studied peptide has plotted graphics depending on time/concentration.

The hydrolytic stability of the native peptide Arg-Arg-Pro-Tyr-Ile-Leu (T0) is presented in Fig. 3. In acidic range the concentration of peptide remains constant during the first hour of the study and then gradually decreased. On the fourth hour it was under 40% and of the sixth hour zero. The stability of T0 in neutral and alkaline media was even smaller. On the sixtieth minute, the

concentration of T0 was under 50%, and of the third hour of experiment lower than 10%.

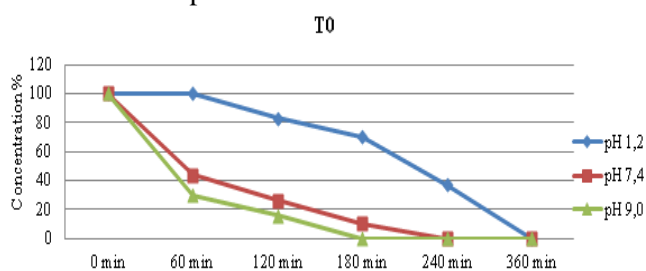


Fig. 3. Hydrolytic stability of T0 on different pH measured at 220 nm by UV – spectroscopy. As shown in Figure 4 at neutral pH, the peptide **Lys-Cav-Pro-Tyr-Ile-Leu** (T1) was stable for 60 minutes and the concentration was about 90%. Such a high stability at pH = 7,4 was observed only for the T3 analogue. Better stability in neutral zone, can significantly affect the biological potential of this NT analogue. The hydrolysis of peptide in acidic media goes slowly, as the concentration (80%) was maintained until the third hour. At the end of the experiment concentration of T1 was 40%. It is also evident from the graph, that the hydrolysis goes at a high speed at an alkaline pH (pH = 9.0).

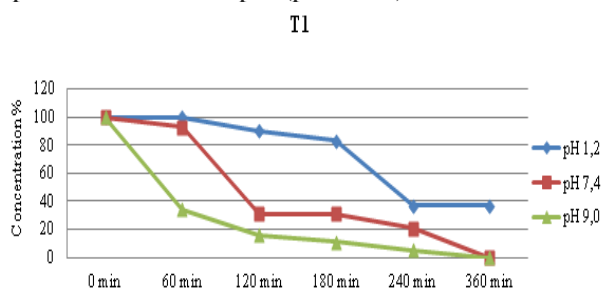


Fig. 4. Hydrolytic stability of T1 on different pH measured at 220 nm by UV – spectroscopy.

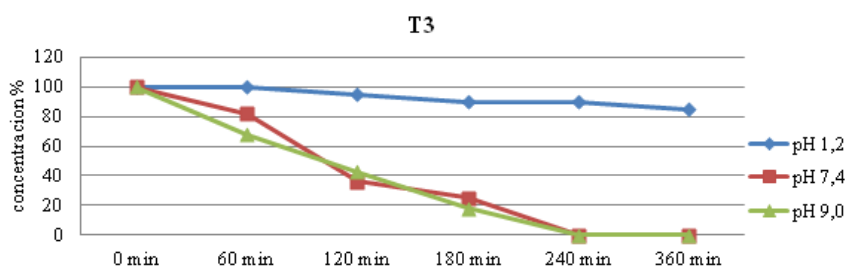


Fig. 6. Hydrolytic stability of T3 on different pH measured at 220 nm by UV – spectroscopy.

The stability of **Cav-Cav-Pro-Tyr-Ile-Leu** (T3) in the acidic pH (Fig. 6.) was the highest from the all tested NT analogues. The measured absorbance at 220 nm and pH 1.2 is slowly declining and the concentration remained relatively constant during the study, and on the sixth hour it was over 80%. A greater stability was observed for this peptide at pH = 7,4, in comparison to the other synthesized analogues. At neutral pH, it retained 90% of its concentration until the 60th minute, then hydrolytic stability gradually decreases. This stability in the

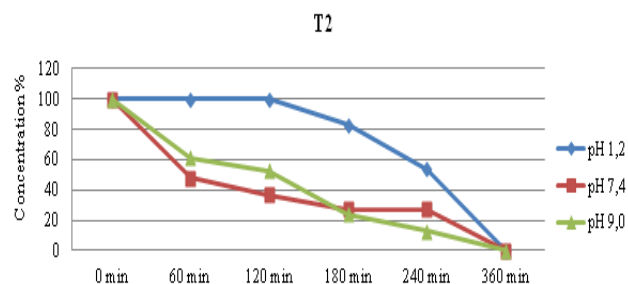


Fig. 5. Hydrolytic stability of T2 on different pH measured at 220 nm by UV – spectroscopy.

As shown in Figure 4 at neutral pH, the peptide **Lys-Cav-Pro-Tyr-Ile-Leu** (T1) was stable for 60 minutes and the concentration was about 90%. Such a high stability at pH = 7,4 was observed only for the T3 analogue. Better stability in neutral zone, can significantly affect the biological potential of this NT analogue. The hydrolysis of peptide in acidic media goes slowly, as the concentration (80%) was maintained until the third hour. At the end of the experiment concentration of T1 was 40%. It is also evident from the graph, that the hydrolysis goes at a high speed at an alkaline pH (pH = 9.0).

On the Figure 5 is visible that at pH = 1,2 the hydrolysis proceeds slowly up to 180 minute and the concentration of **Cav-Lys-Pro-Tyr-Ile-Leu** (T2) remained high (80%). After the third hour the concentration of the peptide decreased rapidly and the end of the way of expression drops to 0. At pH = 7.4 and pH = 9,0, absorption quickly decreases, indicating more rapid hydrolysis rate and a lower stability of the peptide. The dynamics of the two curves is similar.

neutral media may be very important at a later stage, when defining the route of administration of peptides and for testing its biological effects. The dynamics of the curve at pH = 9,0 also show better hydrolytic stability of T3 compared to the other analogues.

The compound **Arg-Cav-Pro-Tyr-Ile-Leu** (T4) was also unstable in alkaline and neutral condition. The process of hydrolysis goes at high speed for the first hour. On the 60th minute the concentration of the substance was 40% and 60% respectively. It

can be seen from the graph in Fig. 7. that in the solution with pH = 1,2 hydrolysis was more slowly than at pH = 7,4 and pH = 9,0, but the peptide T4 was less stable than T5 under the same conditions.

It can be seen on Fig. 8. that at the beginning of the study, the hydrolysis goes with a very high speed at the neutral (pH = 7,4) and alkaline (pH = 9,0) range. On the 60 minutes, the concentration of Cav-Arg -Pro-Tyr-Ile-Leu (T5) dropped almost in half in the alkaline solution and is only about 10% in the neutral. In the acidic range (pH = 1,2), the concentration of T5 remains relatively constant until the third hour of the study (90%), and then decreases gradually to 40% at the end of the measurement.

The chemical stability during storage represent possibility for any substance to left unchanged due to the influences of the type of an internal reaction or external factors such as air, heat, light and etc. All studied for hydrolytic stability peptides were stored at a temperature -10°C for 1 year. Using UV-spectroscopy and analytical RP-HPLC we checked hydrolytic stability of the peptides at neutral and alkaline pH. It was found that they remained unaltered, as well as, their physical and chemical, and thus it can be considered to be chemically stable under these conditions.

For example we presented hydrolytic stability of the compound T3 at neutral and alkaline pH. In the previous experiment (Fig. 6.) the peptide T3 showed the highest stability in comparison with the other analogues. The rate of the hydrolysis and reducing concentration of determined peptide by HPLC are consistent with the data that we received by UV-spectroscopy. The better stability of T3

during the first hour in the neutral and alkaline pH was confirmed once again.

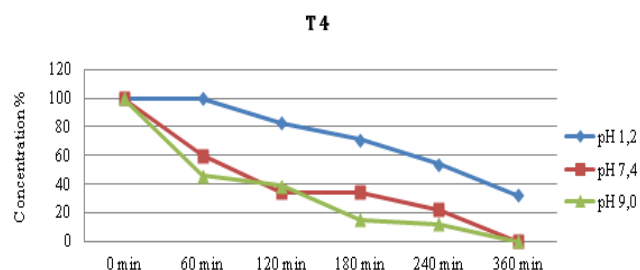


Fig. 7. Hydrolytic stability of T4 on different pH measured at 220 nm by UV –spectroscopy.

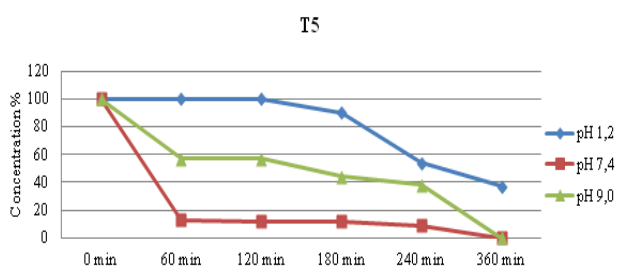


Fig. 8. Hydrolytic stability of T5 on different - pH measured at 220 nm by UV –spectroscopy.

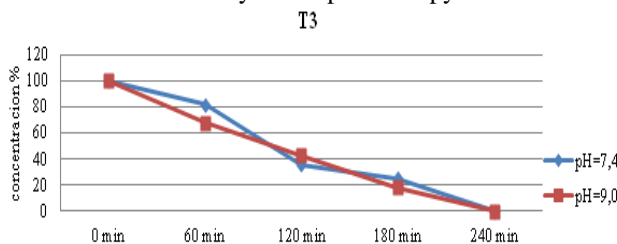


Fig. 9. Hydrolytic stability of T3 after 1 year storage measured at 220 nm by UV –spectroscopy.

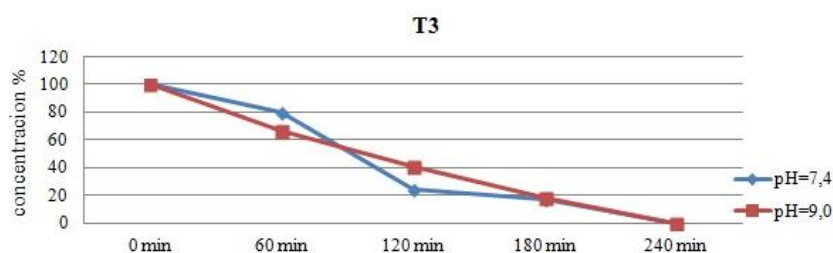


Fig. 10. Hydrolytic stability of T3 after 1 year storage measured at 220 nm by RR-HPLC.

The dynamics of curves presented in Fig. 9. is the same with that presented in Fig. 6. That gives us reason to conclude that T3 was stable even after 1 year of storage.

In addition the rate of the hydrolysis and reducing concentration of determined peptide by RP-HPLC are consistent with the data that we received by UV-spectroscopy. The better stability of T3 during the first hour in the neutral and alkaline pH was confirmed once again.

CONCLUSION

As a result of the experiments it can be concluded that:

- The dependence time / concentrations of T0 shows the low hydrolytic stability of native NT fragment and confirmed a need to develop a new, more stable analogues;

- The stability of the newly synthesized NT-analogues in acidic range is higher than that of the native (8-13) fragment of the NT;
- The hydrolysis of T3 in the acid buffer (pH = 1,2) takes place with very low speed, thereby retaining about 90% of its initial concentration. This gives us reason to believe that the analogue was stable at this pH;
- From all tested NT-analogues, compounds T1 and T3 showed the highest stability at neutral pH. On 60 minute their concentration is about 90%;
- The replacement of arginine residues with canavanine increased hydrolytic stability of the peptide analogues, and this is most likely due to the lower basicity of the oxy-guanidine group of canavanine compared to those of the guanidino group of arginine;
- The hydrolytic stability of the synthesized analogues was retained after one year of storage.

Acknowledgements: The work was supported by Medical University of Varna and CEEPUS, CIII-RO-0010.

REFERENCES

1. R. Carraway, S.E. Leeman, *J. Biol. Chem.*, **248**, 6854 (1973).
2. M. Boules, Z. Li, K. Smith, *Front. Endocrinol.*, **4**, 36 (2013).
3. M.M. Boules, P. Fredrickson, A.M Muehlmann, *Behav. Sci.*, **4**, 125 (2014).
4. P.R. Dobner, *Peptides*, **27**, 2405 (2006).
5. F. Saint-Gelais, C. Jomphe, L.E. Trudeau, *J. Psychiatry. Neurosci.*, **31**, 229 (2006).
6. B.M. Tyler-McMahon, M. Boules, E. Richelson, *Regul. Pept.*, **93**, 125 (2000).
7. J.P. Vincent, J. Mazella, P. Kitabgi, *Trends Pharmacol. Sci.*, **20**, 302 (1999).
8. E. Hermans, J.M. Malateaux, *Pharmacol. Ther.*, **79**, 89 (1998).
9. S. L. Swift, J. E. Burns, N. J. Maitland, *Cancer Res.*, **70**, 347 (2010).
10. R. E. Carraway, A. M. Plona, *Peptides*, **27**, 2445 (2006).
11. P. Gromova, B. P. Rubin, A. Thys, C. Erneux, J. M. Vanderwinden, *PLoS One*, **6**, e14710 (2011).
12. J. G.; Wang, N. N. Li, H. N. Li, L. Cui, P. Wang, *Neuropeptides*, **45**, 151 (2011).
13. C. Granier, J. van Rietschoten, P. Kitabki, C. Poustis, P. Freycht, *E. J. Biochem.*, **124**, 117 (1982).
14. K.P. Kokko, M.K. Hadden, K.L. Price, K.S. Orwig, R.E. See, T.A. Dix, *Neuropharmacol.*, **48**, 417 (2005).
15. M. Boules, P. Frederickson, E. Richelson, *Peptides*, **27**, 2523 (2006).
16. A. Mascarini, I.E. Valverde, T.L. Mindt, *Med. Chem. Commun.*, **7**, 1640 (2016).
17. E. Garcia-Garayoa, V. Maes, P. Blauenstein, A. Blanc, A. Hohn, D. Tourwe, P. A. Schubiger, *Nucl. Med. Biol.*, **33**, 495 (2006).
18. R. M. Myers, J. W. Shearman, M. O. Kitching, A. Ramos-Montoya, D. E. Neal, S. V. Ley, *ACS Chem. Biol.*, **4**, 503 (2009).
19. T. Dzimbova, S. Stoeva, L. Tancheva, A. Georgieva, R. Kalfin R, T. Pajpanova, In: *Peptides 2014, Proceedings of 33rd EPS*, (E. Naydenova, D. Danalev, E. Pajpanova, Eds.), Bulgarian Peptide Society, Sofia, Bulgaria, 260 (2015).

ХИМИЧНА СТАБИЛНОСТ НА НОВИ АНАЛОЗИ НА НЕВРОТЕНЗИН(8-13)

С. Михайлова¹, Т. Дзимбова², К. Каликова³, Е. Тежарова³, Т. Пайпанова²

¹Медицински университет „Проф. д-р Парашкев Стоянов“, Варна, Фармацевтичен факултет, ул. „Марин Дринов“ № 55, Варна 9002, България

²Институт по молекулярна биология „Акад. Румен Цанев“, Българска академия на науките, ул. „Акад. Г. Бончев“ бл. 21, София 1113,

³Карлов университет на Прага, Факултет природни науки, Катедра физико- и макромолекулна химия, „Албертов“ 2030, Прага 128 43, Чехия

Постъпила на 21 декември, 2016 г.; Коригирана на 20 февруари, 2017 г.

(Резюме)

Хидролитичната стабилност на пептидите е едно от най-важните свойства по отношение на тяхното приложение в практиката. Ранната информация за стабилността е основна за фармакокинетичното поведение в тялото при условия на съхранение, появата на токсични ефекти, свързани с неговите разпадни продукти и т.н. Целта на това изследване е да се проучи хидролитичната стабилност на новосинтезирани пептиди при физиологични условия, като телесна температура при 37°C и рН стойности при 1.2 (стомах), 7.4 (кръвна плазма) и 8.5-9.0 (тънки черва).

Involvement of hippocampal angiotensin II type 1 receptors in locomotor activity in rats with a model of depression

R.E. Tashev^{1,2*}, M.S. Ivanova³, S.P. Belcheva^{2,4}, I.P. Belcheva²

¹Department of Pathophysiology, Medical University of Sofia, 2 Zdrave Str., 1431 Sofia (Bulgaria)

²Department of Behaviour Neurobiology, Institute of Neurobiology, Bulgarian Academy of Sciences, 1113 Sofia Bulgaria

³Department of Physiology and Pathophysiology, Medical University Varna, M. Drinov str.55, Varna, 9000, (Bulgaria)

⁴Faculty of Pre-School and Primary School Education, SU "St. Kl. Ohridsky", 1574 Sofia, (Bulgaria)

Received October 08, 2016; Revised February 13, 2017

The octapeptide angiotensin II (Ang II) is the major effector of the renin-angiotensin system. Ang II exerts its effects by binding to Ang II type 1 (AT1) and Ang II type 2 (AT2) receptors. The olfactory bulbectomy (OBX) model is an animal model of depression that produces behavioural, physiological, and neurochemical alterations resembling clinical depression. To examine the involvement of Ang II and AT1 receptors in locomotion we studied the effects of Ang II, losartan (AT1 receptor antagonist) infused uni- and bilaterally into hippocampal CA1 area of OBX-rats. The changes in locomotor activity were registered in an Opto Varimex apparatus. The increased locomotor activity is a typical behavioural phenomenon in OBX rats. Microinjected bilaterally and left-side into the hippocampal CA1 area Ang II (0.5 µg) increased the number of horizontal and vertical movements in bulbectomized rats, while losartan (100 µg) infused bilaterally and the left-side, but not into the right-side, decreased the number of both horizontal and vertical movements in OBX rats, as compared to saline-treated OBX controls. It was found that the effects of Ang II and losartan were opposite and asymmetric in left and right CA1 area. These data reveal a pronounced lateralized Ang II effect on the locomotor activity of OBX rats and suggest a possible involvement of AT1 receptors in the mechanisms of the olfactory bulbectomy syndrome in rats.

Key words: Angiotensin II, Losartan, Locomotor activity, Asymmetry, Hippocampus, Depression

INTRODUCTION

The octapeptide angiotensin II (Ang II) is the major effector of the renin-angiotensin system (RAS). The brain RAS is independent of the circulating RAS. The brain RAS includes the biologically active angiotensin peptides: Ang II, Ang III, Ang IV and Ang-(1-7) [1]. There are four types of angiotensin receptors: Ang II type 1 and type 2 receptors (AT1, AT2), Ang IV-specific receptor (AT4), and Ang-(1-7)-selective receptor [2, 3, 4]. AT1 and AT2 are structurally similar, G-protein coupled receptors, AT4 is a protein, which is not G-protein-linked, while Ang-(1-7) exerts its actions via the G protein-coupled Mas receptor.

It is known that the concentration of Ang II and the expression of its different receptor types are particularly high in the hippocampus [4, 5]. In the CA1 region of the hippocampus, Ang II directly excites pyramidal neurons [6]. Ang II is a full agonist at the AT1 and AT2 receptors in accordance with the nomenclature (Guide to Receptors and Channels).

It has been reported that ATII injected intracerebroventricularly (i.c.v.) or into hippocampal CA1 area affects exploratory behaviour, locomotor activity, learning and memory in rats [7, 8]. Previous studies showed behavioural asymmetries in locomotor-exploratory activity, anxiety, learning and memory following unilateral infusions of Ang II into CA1 area [9]. We have found that losartan, a specific antagonist of AT1 receptors, microinjected bilaterally or into the left hippocampal CA1 area suppressed the exploratory activity, while the right-side losartan administration showed no effect as compared to the controls.

Recently, it has been reported that orally administered losartan can suppress the enhancing effect of voluntary running on cell proliferation in the rat hippocampus [10].

The bilateral olfactory bulbectomy (OBX) in rats is widely accepted as an animal model of depression. The OBX in rats leads to numerous behavioural, physiological, neurochemical and neuroendocrine changes that are used to model of major depression, but may also be a valuable tool in the study of neurodegenerative disorders such as Alzheimer's disease. Behavioural abnormalities of

*To whom all correspondence should be sent:
E-mail: romantashev@gmail.com

OBX rats include exploratory hyperactivity in response to a novel environmental stress, memory deficits, anxiety symptom-resembling behaviour, etc. [11, 12]. The bulbectomy-induced behavioural deficits are attributable to a retrograde degeneration of neurons from the olfactory bulbs which project to cortical, amygdala, and hippocampal regions [11, 13]. Saavedra and co-workers [14] have showed that blockade of brain AT1 receptors ameliorates stress, anxiety, brain inflammation and ischemia. In addition, losartan has been shown to ameliorate depression in mice, as determined by the forced swim test [15].

Baring in mind the suggested role for hippocampal dysfunction in depression, as well as our previous findings on the behavioral effects of Ang II and losartan administration into the hippocampal CA1 area, the aim of the present study was to investigate the effects of Ang II and losartan after uni- and bilateral infusion into CA1 hippocampal area on locomotor activity of rats with a model of depression.

EXPERIMENTAL

Animals

Male Wistar rats (200 - 220g at the time of surgery) were housed individually in polypropylene boxes with free access to food and water. The animals were maintained in a constant temperature environment ($22 \pm 2^\circ\text{C}$) on a 12 h light/dark cycle (lights on at 6:00am). The behaviour experiments were carried out between 10:00am and 1:00pm.

The experiments were carried out according to the "Principles of laboratory animal care" (NIH publication No. 85-23, revised 1985), and the rules of the Ethics Committee of the Institute of Neurobiology, Bulgarian Academy of Sciences.

Experimental model of depression

Bilateral olfactory bulbectomy (OBX) was carried out according to the method depicted by Kelly et al. [13].

Stereotaxic implantation and drug injection into hippocampal CA1 area of OBX rats

Seven days after bilateral olfactory bulbectomy guide cannulae (right and left) were implanted into CA1 hippocampal area according coordinates to the stereotaxic atlas of Pellegrino and Cushman [16] (P = 3.8 mm; L = \pm 3.0 mm; h = - 3.0 mm) as described previously [17].

Rats were microinjected into both hippocampal CA1 areas with Angiotensin II (0.5 μg), Losartan (100 μg) or saline (doses active in earlier experiments) [17]. Angiotensin II (Sigma) or

Losartan (Sigma) were dissolved ex tempore in saline and microinjected into CA1 hippocampal area. The substances were injected through an injection cannula connected by polyethylene tubing with a constant rate microsyringe (Hamilton, Reno, NV, USA). 0.5 μl of the Ang II (pH 7.4) solution or 0.5 μl of the losartan (pH 7.4) solution or 0.5 μl saline were infused over a period of 1 min and the injection cannula was left in place for another 30s.

Just before scarification, the animals were injected with 0.5 μl 2% Fast green dye through the injection cannula. Brains were removed, and successful bulbectomy was verified macroscopically by comparison with the bulbs of an intact rat brain. Animals in which < 80% of the bulbs had been removed were omitted from the analysis. Injection sites were then verified histologically post-mortem in 25 μm coronal brain sections cut through the hippocampus. Animals excluded by the cannula placement and the diffusion of dye were beyond the CA1 area of the hippocampus as depicted in the stereotaxic atlas [16] or were not symmetrical. Animals with cannulae placement outside the CA1 area or not symmetrical within both CA1 areas were excluded from the statistical analysis.

Locomotor activity

Locomotor activity was recorded in an Opto Varimex apparatus (Columbus Instruments, USA). The experimental chamber was 50 cm X 50 cm X 25 cm. This apparatus records the number of photobeam interruptions during the movements of the animal. It provides selective counting of the number of horizontal and vertical movements in arbitrary units (AU). The information obtained was recorded automatically every 5 minutes in the observation period (5-30 min). The experiments were carried out at one and the same time (between 10:00 a.m. and 1:00 p.m.). The rats were placed in the central quadrant of the activity monitor 15 min after the microinjection of Ang II or losartan.

Statistical analysis

One way ANOVA was used to analyze the data obtained for effect of bilateral Ang II and losartan microinjections. Two-factor ANOVA analysis with factors: drug - 3 levels (Ang II, losartan, saline,) and side of injection - 2 levels (right, left) was used for evaluation of data about unilateral injections. ANOVA data were further analyzed by post hoc t-test, where appropriate.

RESULTS AND DISCUSSION

Effects of bilateral microinjection of Ang II and losartan into CA1 area of OBX rats

Separate one way ANOVA analysis of the total number of horizontal or vertical movements for a 30-minute period of observation showed a significant effect for factor “drug” ($F_{3,27} = 99.775$; $P \leq 0.001$) for the number of horizontal movements, and for the number of vertical movements ($F_{3,27} = 37.149$; $P \leq 0.001$).

Post hoc t-test showed that infused bilaterally into CA1 area of OBX rats, Ang II increased, while losartan decreased, the total number of both horizontal ($P \leq 0.003$; $P \leq 0.001$, respectively) and vertical movements ($P \leq 0.005$; $P \leq 0.01$, respectively), as compared to the respective saline-treated OBX rats (Fig. 1, Fig. 2).

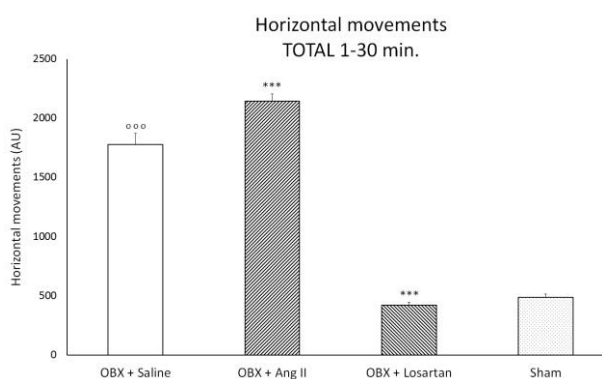


Fig. 1. Effect of Ang II and losartan microinjected bilaterally into the hippocampal CA1 area on the total number of horizontal movements for the whole period of observation (30 min). $n=7$. Means (\pm S.E.M.) are presented. Asterisks depict - drug treated OBX rats vs. respective OBX saline-treated. *** $P \leq 0.001$. Circles depict - sham vs. OBX saline-treated. ○○○ $P \leq 0.001$.

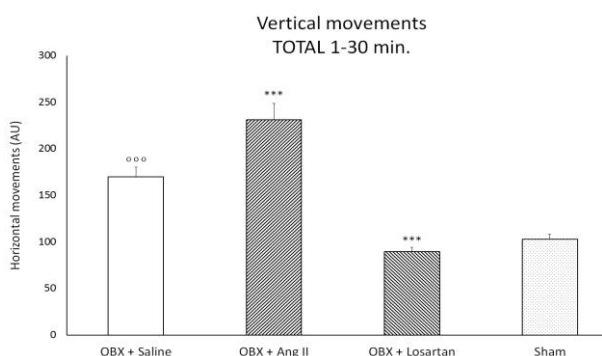


Fig. 2. Effect of Ang II and losartan microinjected bilaterally into the hippocampal CA1 area on the total number of vertical movements for the whole period of observation (30 min). $n=7$. Means (\pm S.E.M.) are presented. Asterisks depict - drug treated OBX rats vs. respective OBX saline-treated. *** $P \leq 0.001$. Circles

depict - sham vs. OBX saline-treated ○○○ $P \leq 0.001$.

Effects of unilateral microinjection of Ang II and losartan into CA1 area of OBX rats

Two-way ANOVA analysis on the effect of unilateral Ang II (0.5 μ g) and losartan (100 μ g) microinjection on the total number of horizontal movements in OBX rats for a 30-min period of observation showed a significant effects for the factor “drug” ($F_{2,47} = 92.508$; $P \leq 0.001$), the factor “side” ($F_{1,47} = 71.183$; $P \leq 0.001$) and a significant interaction between the factors “drug” X “side” ($F_{2,47} = 36.967$; $P \leq 0.001$).

Ang II administered into the left CA1 area of OBX rats increased the total number of horizontal movements ($P \leq 0.05$), while the microinjection of Ang II into the right CA1 area had no significant effect on the total number of horizontal movements ($P = \text{NS}$) as compared to the saline-treated OBX controls (Fig.3). Losartan (100 μ g) microinjected into the left CA1 area significantly decreased the total number of horizontal movements as compared to the left saline-treated OBX controls ($P \leq 0.001$) and compared to the right-side infused losartan ($P \leq 0.001$) (Fig.3).

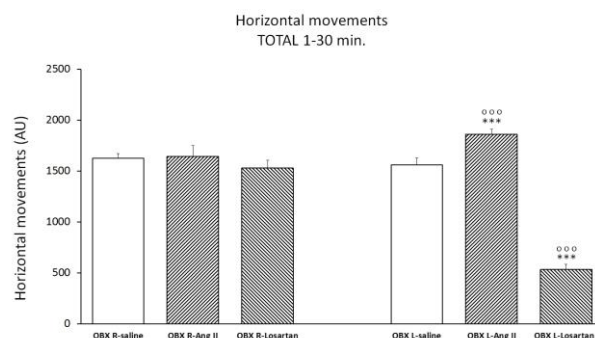


Fig. 3. Effect of Ang II and losartan microinjected unilaterally (right or left) into the hippocampal CA1 area on the total number of horizontal movements for the whole period of observation (30 min). $n=8$. Means (\pm S.E.M.) are presented. Asterisks depict - drug treated OBX rats vs. respective OBX saline-treated. *** $P \leq 0.001$. Circles depict - left-side vs. right-side ○○○ $P \leq 0.001$.

Two-way ANOVA on the effect of Ang II and losartan on the total number of vertical movements of OBX rats demonstrated a significant effects of factors “drug” ($F_{2,47} = 18.250$; $P \leq 0.001$), “side” ($F_{1,47} = 172.601$; $P \leq 0.001$) and an interaction between “side” X “drug” ($F_{2,47} = 40.032$; $P \leq 0.001$).

The number of vertical movements was significantly increased upon microinjection of Ang II into the left CA1 area ($P \leq 0.001$). The injection of losartan into left-side significantly decreased the number of vertical movements compared to the left

saline-treated OBX rats ($P \leq 0.001$) and compared to the right-side injected losartan ($P \leq 0.001$) (Fig.4).

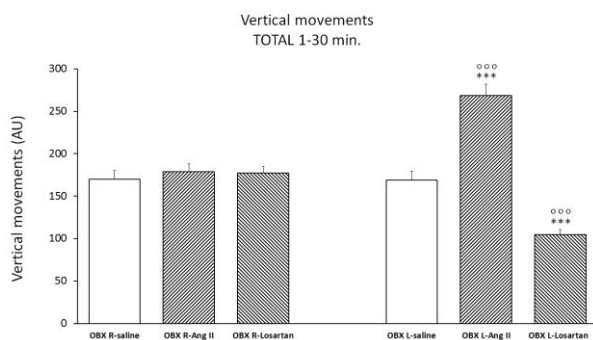


Fig. 4. Effect of Ang II and losartan microinjected unilaterally (right or left) into the hippocampal CA1 area on the total number of vertical movements for the whole period of observation (30 min). $n=8$. Means (\pm S.E.M.) are presented. Asterisks depict - drug treated OBX rats vs. respective OBX saline-treated. *** $P \leq 0.001$. Circles depict - left-side vs. right-side ○○○ $P \leq 0.001$.

In our previous studies we have found that bilateral administration of losartan at a dose of 100 μg into CA1 areas decreased exploratory activity of rats [18]. It has been also demonstrated that bilateral bulbectomy leads to hyperactivity of rats in an Opto Varimex apparatus (increased total number of both horizontal and vertical movements) [18]. This locomotor hyperactivity is a typical behavioural phenomenon in OBX rat and it is accepted as an index of depressive-like behaviour [13]. Considering these findings, we were interested to investigate the role of Ang II and Ang II receptors in the locomotor hyperactivity induced by OBX.

The bilateral microinjection of Ang II into hippocampal CA1 stimulated locomotor activity of OBX rats, expressed by an increase of both horizontal and vertical movements. The bilateral infusion of losartan significantly decreased the total number of both horizontal and vertical movements, i.e. suppressed the locomotion of OBX rats as compared to the saline-treated OBX controls. Thus, Ang II administration augmented the hyperactivity of OBX rats and aggravated the depression-like state, while the inhibition of AT1 receptors by losartan demonstrated antidepressant effect.

Bilateral olfactory bulbectomy is accompanied by changes in many neurotransmitter systems [13]. After bulbectomy, degeneration of neurons in cortex, hippocampus [19, 20], impaired neurogenesis in hippocampal dentate gyrus [21] and changes in the expression of neuropeptides in some brain areas [11] have been reported. It is possible that the increased expression of Ang II or Ang II receptors in the hippocampal neurons might

contribute to the increased hyperactivity observed in our study.

The brain RAS has been implicated in the pathophysiological mechanisms of dementia and neurodegenerative diseases [22, 23]. It has also been related to the mechanisms of depression as shown in studies demonstrating antidepressant effect of captopril in hypertensive patients that also suffered from depression [24, 25, 26]. From the viewpoint of asymmetry we investigated the effects of equal doses of Ang II or losartan microinjected unilaterally (left or right) into CA1 hippocampal area on the locomotor activity. The unilateral topical administration of the drugs showed different effects on locomotion. Thus, when injected into the left CA1 area, Ang II increased locomotor activity, while losartan decreased it. The microinjection of the drugs into the right CA1 area induced no changes in locomotion.

The present findings are in agreement with studies showing asymmetric effects on exploratory behaviour after administration of Ang II into CA1 area. Belcheva and co-workers [9] have shown that only left-side injections affected exploratory behaviour, while Ang II administered into the right CA1 area had no effect.

Several studies support the hypothesis that the RAS is a part of the neurochemical dysregulation underlying negative affective states, anxiety disorders, and ethanol dependence [27]. Something more, it has been suggested that the increased RAS activity may increase the relative risk of depression [22, 28], while the blockade of AT1 receptors could be potentially useful for the treatment of stress-induced disorders [29].

The different behavioural effects of Ang II microinjected into the left or right CA1 hippocampal area suggest a different distribution of Ang II receptors, high concentrations of which are found in the hippocampus [4]. The presence of AT1 and AT2 receptors, involved in the modulation of exploratory behaviour, learning and memory processes, etc., has been demonstrated in rat hippocampus [22, 23].

CONCLUSION

This study the first time provides information on the locomotion-stimulatory effect of Ang II and locomotion-inhibitory effect of losartan when injected into the left but not into the right CA1 hippocampal area of OBX rats. This implies that the injection of the drugs in the left side only can modulate the depressive-like behavior. The asymmetry of the Ang II- related behavioral

responses upon administration in the left or right hippocampus could be related to a different distribution of AT1 receptors in the two hemispheres.

REFERENSES

- 1 O. von Bohlen und Halbach, D. Albrecht. *Cell Tissue Res.*, **326**, 599 (2006).
- 2 M. de Gasparo, K.J. Catt, T. Inagami, J.W. Wright, T. Unger. International Union of Pharmacology XXIII. *Pharmacol. Rev.*, **52**, 415 (2000)
- 3 R.A. Santos, A.C. Simoes e Silva, C. Maric, D.M. Silva, R.P. Machado, I. de Buhr, S. Heringer-Walther, S.V. Pinheiro, M.T. Lopes, M. Bader, E.P. Mendes, V.S. Lemos, M.J Campagnole-Santos, H.P. Schultheiss, R. Speth, T. Walther. *Proc. Natl. Acad. Sci. U S A.* **100**, 8258 (2003).
- 4 J.W. Wright, J. W. Harding. *Reg. Peptides*, **59**, 269 (1995).
- 5 O. von Bohlen und Halbach, D. Albrecht. *Reg. Peptides*, **78**, 56 (1998).
- 6 H.L. Haas, D. Felix, M.R. Celio, T. Inagami. *Experientia*, **36**, 1395 (1980).
- 7 J. J. Braszko, K. *Peptides*, **9**, 475 (1988).
- 8 I. Belcheva, V. Georgiev, M. Chobanova, C. Hadjiivanova. *Neuropeptides*, **31**, 60 (1997).
- 9 I. Belcheva I, M. Chobanova, V. Georgiev. *Reg. Peptides*, **74**, 67 (1998).
- 10 T. Mukuda, H. Sugiyama. *Neurosci. Res.*, **58**, 140 (2007).
- 11 C. Song, B.E. Leonard. *Neurosci. Biobehav. Rev.*, **29**, 627 (2005).
- 12 D. Wang, Y. Noda, H. Tsunekawa, Y. Zhou, M. Miyazaki, K. Senzaki, T. Nabeshima. *Behav. Brain Res.*, **178**, 262 (2007).
- 13 J.P. Kelly, A. Wrynn, B.E. Leonard. *Pharmacol. Ther.*, **74**, 299 (1997).
- 14 J.M. Saavedra., E. Sánchez-Lemus, J. Benicky. *Psychoneuroendocrinology*, **36**, 1 (2011).
- 15 P.R. Gard, A. Mandy, M.A. Sutcliffe. *Biol. Psychiatry*, **45**, 1030 (1999).
- 16 L. Pellegrino, A. Cushman. A stereotaxic atlas of the rat brain. New York, Appleton-Century-Crofts, 1967.
- 17 R. Tashev, M. Stefanova. *Acta Neurobiol. Exp.*, **75**, 48 (2015).
- 18 R.Tashev, M. Ivanova. *Compt. Rend. Acad. Bulg. Sci.*, **67**, 871(2014).
- 19 J. Carlsen, J. De Olmos, L. Heimer. *J. Comp. Neurol.*, **208**, 196 (1982).
- 20 I. Nesterova, N. Bobkova, N. Medvinskaia, A. Samokhin, I. Aleksandrova. *Morfologiya*, **131**, 32 (2007).
- 21 N. Shioda, Y. Yamamoto, F. Han, S. Moriguchi, Y. Yamaguchi, M. Hino, K. Fukunaga. *J. Pharmacol. Exp. Therap.*, **333**, 43 (2010).
- 22 D. Albrecht. *Br. J. Pharmacol.*, **159**, 1392 (2010).
- 23 J.W. Wright, J.W. Harding. *Progress in Neurobiol.*, **95**, 49 (2011).
- 24 R.F. Deicken. *Biol. Psychiatry*, **12**, 1425 (1986).
- 25 L. Germain, G. Chouinard. *Biol. Psychiatry*, **23**, 637 (1988).
- 26 L. Germain, G. Chouinard. *Biol. Psychiatry*, **25**, 489 (1989).
- 27 W.H. Sommer, J.M. Saavedra. *J. Mol. Med.*, **86**, 723 (2008).
- 28 J.A .Stewart, O. Kampman, M. Huuhka, S. Anttila, K. Huuhka, T. Lehtimaki, E. Leinonen. *Neurosci. Lett.*, **458**, 122 (2009).
- 29 J.M. Saavedra, J. Benicky. *Stress*, **10**, 185 (2007).

УЧАСТИЕ НА ХИПОКАМПАЛНИТЕ АНГИОТЕНЗИН II ТИП 1 РЕЦЕПТОРИ В ДВИГАТЕЛНАТА АКТИВНОСТ НА ПЛЪХОВЕ С МОДЕЛ НА ДЕПРЕСИЯ

Р. Е. Ташев^{1,2*}, М. С. Иванова³, С. П. Белчева^{2,4}, И. П. Белчева²

¹Катедра по патофизиология, Медицински факултет, МУ-София, ул. Здраве 2, 1431 София, България

²Направление поведенческа невробиология, Институт по невробиология, БАН, бул. Акад. Г. Бончев, бл. 23, 1113 София, България

³Катедра по физиология и патофизиология, Медицински университет, МУ-Варна, ул. М. Дринов, 55, 9000 Варна, България

⁴Катедра по специална педагогика и логопедия, Факултет по начална и предучилищна педагогика, СУ "Св.Климент Охридски", бул. Шипченски проход 69А, 1574 София, България

Постъпила на 08 октомври, 2016 г.; Коригирана на 13 февруари, 2017 г.

(Резюме)

Октапептидът ангиотензин II (Ang II) е основният ефектор на ренин-ангиотензиновата система. Ang II упражнява ефектите си чрез свързване с Ang II тип 1 (AT1) и Ang II тип 2 (AT2) рецепторите. Олфакторната булбектомия (ОВХ) е животински модел на депресия, която води до поведенчески, физиологични и невротимични промени, наподобяващи клиничната депресия. За да проучим участието на Ang II и AT1 рецепторите в двигателната активност ние сме изследвали ефектите на Ang II и лозартан (антагонист на AT1 рецепторите), въведени едностранно и двустранно в хипокампащото СА1 поле на ОВХ плъхове. Промените в локомоторната активност са регистрирани в апарат Opto Varimex. Повишената двигателна активност е типичен поведенчески феномен при ОВХ плъхове. Ang II (0.5 µg), микроинжектиран двустранно и само в лявото СА1 поле на хипокампа, повишава броя на хоризонталните и вертикалните движения на булбектомизирани плъхове, докато лозартан (100 µg) въведен двустранно и в лявото СА1 поле, но не и в дясно, намалява броя на хоризонтални и вертикални движения на ОВХ плъхове, в сравнение с третираните с физиологичен разтвор ОВХ контроли. Установено е, че ефектите на Ang II и лозартан са противоположни и асиметрични в лявото и дясното СА1 хипокампадно поле. Тези данни показват ясно изразен латерализиран ефект на Ang II върху двигателната активност на ОВХ плъховете и предполагат възможното участие на AT1 рецепторите в механизмите на синдрома на олфакторната булбектомия при плъхове.

Some physicochemical characteristics of anti-platelet fraction isolated from *Galega officinalis* L.

A.T. Atanasov^{1*}, S. Radev², I.B.Stoinea³

¹Department of Physics and Biophysics, Medical Faculty, Trakia University, Bulgaria,

²Department of Pharmacology, Medical Faculty, Trakia University, Bulgaria

³Institute of Organic Chemistry with Centre of Phytochemistry,
Bulgarian Academy of Sciences, 1113 Sofia, Bulgaria

Received September 30, 2016; Revised January 31, 2017

Some physicochemical characteristics of a 100-140 kDa fraction isolated from *Galega officinalis* L. were studied. The water soluble fraction inhibits platelet aggregation initiated by ADP, thrombin and collagen. The enzyme-treated fraction changes negligible inhibiting effect on platelet aggregation. The isolated fraction appears to have a polysaccharide nature, including 23 % protein. No loss in the activity of the fraction after storage for several months at 4 °C in N₃H-H₂O solution with neutral pH, and after freezing of liophilized fraction at -10 °C. The fraction shows maximum activity in the temperature diapason of 10°C-42°C and pH diapason of pH 5.5-9.8. The micro-calorimetric analyses show two protein subunits in the fraction. Anti-platelet fraction may find application in medicine, similarly to dextrans.

Key words: *Galega officinalis* L., isolation, anti-platelet fraction, characteristics

INTRODUCTION

Galega officinalis L. is a medicinal plant wide spread in West Europe, Italy and Bulgaria. The plant has been used in a traditional medicine system in treatment of *diabetes mellitus* [1, 2]. Over 15 biologically-active substances are isolated from *Galega officinalis*: galegine, hydroxygalegine, peganine, vasicinone, lutein (alkaloids), pentahydroxyflavone 5-glucoside, luteolin, galuteoline, luteolin 5-glucoside (glucosides); flavonoids, glucosidessaponins and γ - γ dimethylallylamidin [3, 4]. The previous experimental investigations of Atanasov et.al indicate that the 100-140 kDa fraction isolated from *G. officinalis* has wide spectrum of effects on platelet and blood-plasma functions [5, 6] as :

- Inhibition of platelet release reaction [3]
- Inhibition of spontaneous platelet aggregation [3]
- Inhibition of platelet aggregation initiated by ADP, thrombin and collagen [5, 6]
- Inhibition of platelet aggregation initiated by free-radical compounds [3]
- Inhibition of spontaneous blood-plasma coagulation [3]

In vivo inhibition of platelet aggregation after intravenous injection in animals [7]

In manuscript are presented some physicochemical characteristics of fractions from *Galega officinalis*, which are important for biomedical approach on living organisms.

EXPERIMENTAL

Platelet aggregation measurement and fraction's activity

Blood was taken from volunteers (3 males and 3 females aged 20-23 years) wich was not treated with medicine for 15 days prior to blood collection. Blood was collected in disposable syringes and diluted at a ratio of 1 part 3,8 % trisodium citrate and 9 parts venous blood. Platelet-rich plasma (PRP) was prepared by centrifugation (180 x g for 10 min) and diluted to 300 x 10⁶ platelets per ml with autologous platelet-poor plasma (1800 x g for 15 min). The platelet aggregation was studied by a photometric method according Born and Zucker [8]. The extinction change that takes place during the aggregation of 400 μ l platelet-rich plasma compared with platelet-poor plasma (whose extinction was taken as zero) after adding aggregating agent at final concentration 25 μ M ADP, 100 μ g/ml collagen or 0.8 U/ml thrombin at 37°C was the basis of measurement of the aggregating effect. Aggregation (A) is calculated by the formula:

$$A, \% = (E_o - E_{\text{sample}})/(E_o - E_{\text{plasma}}).100\%,$$

* To whom all correspondence should be sent:
E-mail: atanastod@abv.bg

where E_0 is the initial extinction of the platelet-rich plasma, E_{plasma} is the extinction of the poor plasma and E_{sample} is the extinction after platelet aggregation. The fraction activity was evaluated by degree of platelet aggregation (A, %).

Purification procedures

The purification of the fraction was made by 4 steps: 1) gel-filtration of crude extract on Sephadex G-25; 2) gel-filtration on Sepharose 4B ; 3) ion-exchange chromatography on DEAE-cellulose and 4) gel-filtration on Sephadex G-100, accordingly to procedures given in [3, 9].

Amino acid analyses

Amino acid analysis of the fractions was performed by method given in BNS (Bulgarian National Standard) 11374-86. The amino acid content was determined by hydrolysis of the active component with 6N HCl. For determination of S-content amino acids methionine and cysteine were used [3, 9]. The amino acid quantity was determined over the ionit " OSTION LG ANB" on "AMINO ACID ANALYSER T 339 M" column (Microtechna-Praha), D(0.37 x 36 cm) using sodium citrate buffers with pH 3.5, 4.25 and 9.45. Ninhydrin was used as reagent for visualization. The absorbance was measured by photometry at 525 nm using interferent filter. "Computing integrator-CI 100" (Laboratorni Pristoje-Praha) was used for computing of the signal from the aminoanalyser.

Solubility of the fraction

The solubility of the final biologically active fraction (BAF) was studied after dissolution in various hydrophilic and hydrophobic solvents. 1mg IVBAF was dissolved in H₂O:EtOH solutions at 18°C for 24h. The activity of the IVBAF was determined by ability of 50µg BAF to inhibits aggregation of 1ml PRP, initiated by 25µM ADP. The activity of the fraction was presents like level of platelet aggregation (A, %).

Ultraviolet, visible and infrared spectrum of BAF

Spectrophotometric study of a fraction in ultraviolet (UV) and visible (VIS) area was mesasured by spectrophotometer "LKB - ULTROSPEC" – Sweden. The infrared (IR) spectrum of BAF was mesasured on spectrophotometer Bruker IFS 113v into tablets of potassium bromid (KBr).

pH dependence of a fraction activity

4% water solution of the fraction was treated with different amount of HCl and NaOH in pH range of 3.0-11.0. The activity of fraction was measured and present by mean ± SD.

Temperature dependence of a fraction activity

Water solution of 3mg final sample in 6 ml H₂O-NH₃ (pH 7.4) was heated for 20min in temperature range of 20-100°C. The activity of the fraction was measured and present by mean ± SD. A non-treated fraction was taken as control.

Microcalorimetric study of a fraction

The differential scanning microcalorimetric measurement was made on DASM-4 microcalorimeter. The sample with final concentration 200 µM (pH 7.3) was heated with in range of 1.5 °C/min. All heating curves were corrected using an instrument baseline obtained by heating the buffer.

Fraction activity after treatment with chemical substances and enzymes

Denaturing effect of chemical agents (containing divalent metal ions Ca²⁺, Zn²⁺, Mg²⁺, Mn²⁺, Co²⁺) and effect of proteolytic enzymes (Chymotrypsin, Chymopapain, Trypsin, α-amilase, β-amilase and alkaline protease were purchued from Sigma Co., USA) on fraction activity was studies. 1mg BAF was incubated for 24h at 30°C in 0.01 M Tris-HCl buffer, pH 7.0 with chemical agents and enzymes. On 1ml platelet-rich plasma was added 15-20µg BAF (control or treated). Aggregation was initiated by 25µM ADP. The level of platelet aggregation (A, %) was present as mean ± S.D.

RESULTS AND DISCUSSION

Purification steps and fraction's activity

The purification steps from the crude extract to the final fractions are given on Table 1.

For crude extract: IC₅₀ was 1.1mg; after Sephadex G-25: IC₅₀ was 0.030mg; after Sepharose 4B: IC₅₀ was 0.012mg; after DEAE-cellulose: IC₅₀ was 0.011mg; after Sephadex G-100: IC₅₀ was 0.0093mg.

The activity of the fractions was detrmind by photometric method according Born and Zucker and the protein content was determined method of Loury accordingly to procedures given in 'Aminoacid analyses'.

Table 1. The purification steps from crude extract to fractions

Purification step	Total (mg)	Specific activity (U/mg)*	Total activity (U)	Protein content (%)
Crude extract	1000×10 ³	0.9	900×10 ³	0.17 %
Sephadex G-25	24×10 ³	32	770×10 ³	6.3 %
Sepharose 4B	6×10 ³	83	500×10 ³	15.1 %
DEAE-Cellulose	2.5×10 ³	90	225×10 ³	16.9 %
Sephadex G-100	2.0×10 ³	108	216×10 ³	23 %

*One unit for specific activity for extract or fraction was taken to be IC₅₀ - this quantity extract or fraction that inhibits 50% platelet aggregation of 1ml platelet-rich plasma initiated by 25µM ADP.

The homogeneity of the IV BAF was tested by SDS electrophoresis with and without mercaptoethanol. In both cases it was found one band only on, colored as polysaccharide. No loss in the activity of the fraction after storage for several months at 4 °C in N₃H-H₂O solution at neutral pH, and after freesing of liophilized fraction at -10 °C.

The results of gel-filtration procedures can be used as a base for semi-industrial production of the BAF by two steps. By filtration through a capillary dialyzer to remove low molecular weight fraction (less than 10-15 kDa) at the first step. By second step realizing ultrafiltration trough separation membranes to remove fractions with molecular weight less than 100 kDa fig.2.

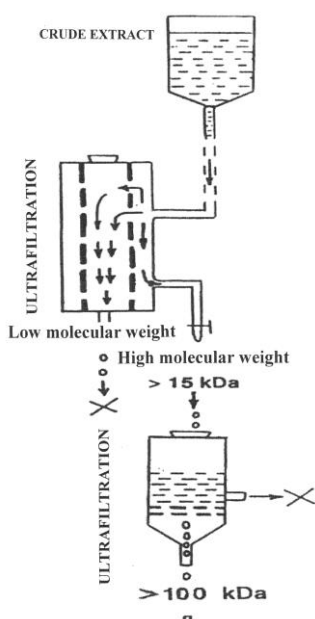


Fig. 1. Scheme of a semi-industrial yeald of IV BAF from *Galega officinalis* L.

Protein content in crude extract and fractions

The protein content of crude extract is about 0.1% [3]. Seven amino-acids (aspartic acid, arginine, alanine, glycine, lysine, serine and valine) consist 46.23% from the total amino-acid content of the final IV fraction [9]. In the final fraction the hydrophilic amino-acids consist 70% while the hydrophobic amino-acids consist 30%. These data are in good agreement with high solubility of the fraction in water solution and low slubility in hydrophobic solvents. The specific activity of the fraction increases with each step of purification (Table 1). This shows a strong relationship between fraction’s specific activity and protein content - Fig.2.

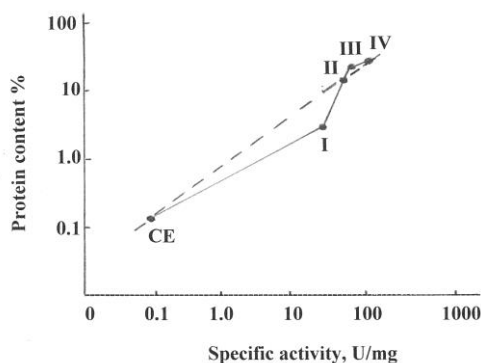


Fig.2. Relationship between protein content and specific fraction activity in log-log plot.

Solubility of the final IV fraction

The solubility of the IV fraction was studied in hydrophilic and hydrophobic solvents-Table 3. The fraction was 100% soluble and active in water solutions. In binary H₂O: EtOH solutions the fraction was well soluble and active up to ratio 4/1 between H₂O and EtOH. For H₂O: EtOH solutions in ratio 3/1 the fraction was maximum 50% active.

For H₂O: EtOH solutions in ratio 1/1 the fraction was about 8% active. In hydrophobic solvents the fraction was not soluble and has no activity.

Table 2. Solubility and residual activity of IV fraction (mean ± SD, n=3)

Solvents	Solubility	Activity of BAF (A%)
H ₂ O (pH 6-9.5)	soluble	100% active
H ₂ O : EtOH	90 : 10	96% ± 3.4 %
	80 : 20	84% ± 3.8 %
	70 : 30	52% ± 4.1 %
	60 : 40	24% ± 4.0 %
	50 : 50	8% ± 4.3 %
Chlorophorm, eter, aceton	non-solubility	non-active
Dimethylformamide dimethylsulfoxide	poorsoluble	non-active

Ultraviolet (UV), visble (VIS) and infrared (IR) spectra of BAF

The UV and VIS spectrum of IV BAF in water (pH 7.0) is given on Fig.3. The UV and VIS spectrum of the BAF was similar to heparin spectrum in diapason of 200-420 nm. In the two spectra was observed maximum of absorbance (extinction) at 280 nm. This result could be explained with the fact that BAF and heparin appear high-molecular polysaccharides.

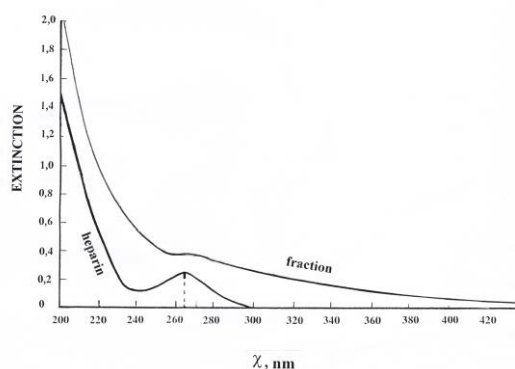


Fig.3. UV and VIS spectrum of IV BAF and heparin (0.1mg BAF and heparin in 5ml dH₂O, pH 7)

The IR spectrum of BAF into tablets of potassium bromid (KBr) gives information for amount of polysaccharides in the fraction-Fig.4. The first part of IR spectrum of BAF from 400 to 2200 cm⁻¹ (signed as I) was similar to infrared spectrum of poor alginic acid (Fig.5), which is

polysaccharide with high molecular weght. Infrared spectrum of IV fraction consist some bands with absorbance at 1400, 1650, 1050, 3400 and 2925 cm⁻¹. The well expressed band with maximum at 3400 cm⁻¹ corresponds to hydrohillic O - H groups, while the weekly expressed band at 2925 cm⁻¹ corresponds to aromatic hydrohillic O - H groups. A well expressed band at 1650 cm⁻¹ is specific for C = O group, and at 1050 cm⁻¹ is specific for C - O group. At 1400 cm⁻¹ is observed a week band specific for C - H group [10]. Alginic acid contained same bands of absorbance as IV BAF : at 3400 cm⁻¹, 2925 cm⁻¹, 1050 cm⁻¹ and 1400 cm⁻¹. The only exception is the absorbance at 1610 cm⁻¹ in alginic acid, unlike absorption at 1650 cm⁻¹ of BAF. Accordingly to previous NIR spectrometry analyses of BAF about 74% of total fraction content was polysaccharides [9]. Giving in the mind 23% protein in a fraction, about 97% of the fraction's content was determined.

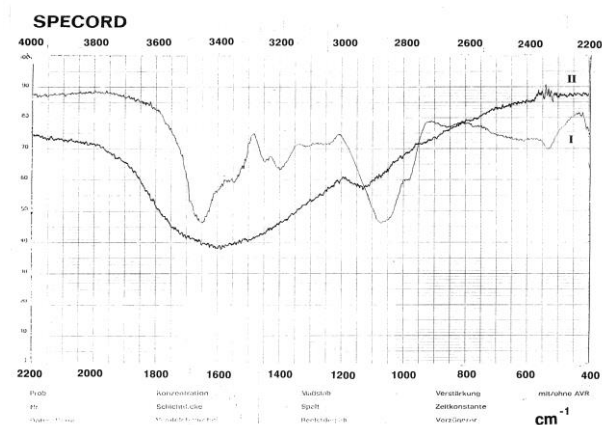


Fig.4. Infrared spectrum of IV BAF into tablets of KBr

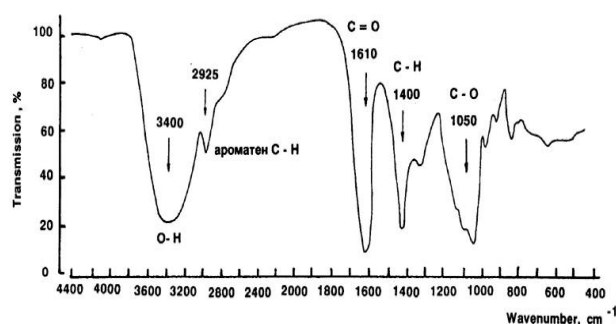


Fig.5. Infrared spectrum of alginic acid into tablets of KBr

pH dependence of the fraction activity

The pH dependence of a fraction activity was studied in pH range from 3.0 to 11.5 - Fig.6. The optimum of the fraction's activity was between pH 5.5 and 9.8. The fraction show losses activity below pH 3.5 and over 11.0. In the range of pH 4.0 – 5.5

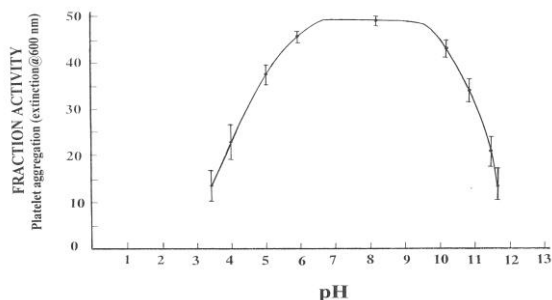


Fig. 6. Effect of pH on fraction's activity

and pH 10.0 -10.5 the fraction inhibits platelet aggregation between 10% and 60%. We did not observed decrease in inhibitory activity of the fraction stored for three monts at pH 7.3 and temperature 4°C-18°C.

Temperature dependence of the fraction activity

The temperature dependence of a fraction activity was study in temperature interval 10-100°C, cf. Fig.7.

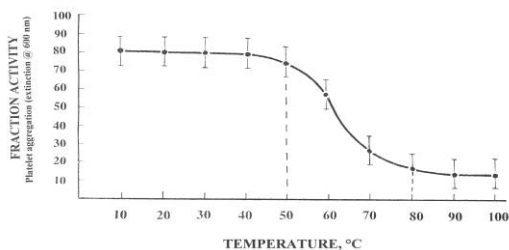


Fig.7.Effect of temperature on fraction's activity

The fraction keeps high inhibitory activity in range of 10- 42°C. In temperature range of 42 - 80°C the activity slow decreases and over 80°C the activity losses. The activation energy of the fraction inhibitory deactivation was evaluated to be 70 ± 4.5 kJ/mol. This activation energy is typical for polysaccharides. This result shows that it is possible the polysaccharides participate in inhibiting mechanism of the fraction.

Microcalorimetric study of the BAF

Upon uniformly heating of BAF in differential scanning microcalorimeter it was registered endothermic process within range of 65°-92°C with two maximums-Fig.7: Ist - corresponding to denaturation process at 73° C and IInd - corresponding to denaturation process at about 85°C. This is indication that the fraction contains two proteins and/or protein subunits. The beginning of denaturation at 65°C coincides with the most significant loss of fraction's activity. This fact confirms the participation of fraction's protein in inhibitory mechanisms of the fraction.

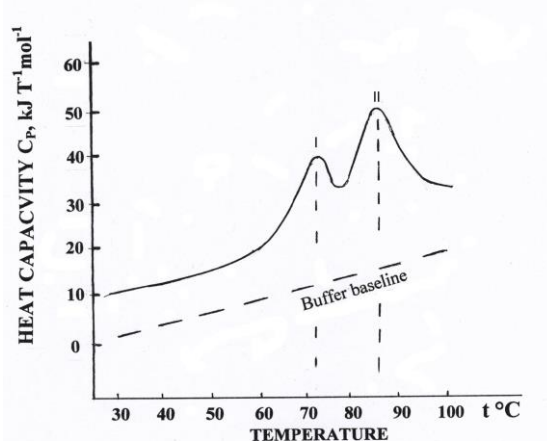


Fig. 8. Microcalorimetric thermogramm of BAF. Concentration of sample and a heating rate are 2, 4%, and 1.5°C/min, respectively

Fraction activity after treatment with chemical substances and enzymes

The residual fraction activity after treatment with chemical agents and enzymes presents interest before *in vivo* study on laboratory animals. The influence of chemical substances and enzymes on the fraction's activity is given on Table 4 and Table 5.

Table 3. Inhibition effect of BAF after treatment with chemical agents (mean± SD, n=5)

Chemical agent	mg agent/mg BAF	Activity of BAF (A, %)
Control		95.0 ± 4.9 %
Control + BAF		10.0 ± 3.2 %
EDTA, Urea	1/4	9.5 ± 2.3 %
Guanidin hydrochloride	3/4	12.3 ± 2.7 %
Bacitracin	1U/4mg	11.9 ± 1.8 %
CuSO ₄ .5H ₂ O, MgCl ₂ .6H ₂ O	0.5/4	10.2 ± 1.5 %
Zn(CH ₃ COO) ₂ Pb, (CH ₃ COO) ₂ Pb	0.5/4	6.6 ± 0.94 %

The ion salts (Cu⁺, Mg⁺, Zn⁺ and Pb⁺) had no influence on fraction activity. Exceptions are the Fe⁺ ions, which inactivate BAF. EDTA as agen forming chelate complexes with metal ions does not alter the inhibitory effect of BAF. The agents that denatured protein structures (urea, guanidine hydrochloride and bacitracin) do not affect the inhibitory effect of BAF on platelet aggregation.

The treatment of the fraction with α -amylase, β -amylase, papain, trypsin and hymotripsin did not influence the activity of the fraction-Fig.5. The treatment with alkaline protease only leads to decreases of the fraction activity. The results show the protein part of the fraction to play major role in platelet-inhibiting effect

Table 4. Effects of enzymes on fraction activity (mean \pm SD, n = 5)

Enzyme	Enzyme/BAF ratio	Activity of BAF (A %)
Control extract		100 %
Control + BAF		50 \pm 4.0 %
Chymotrypsin	1/10	46 \pm 5.6 %
Chymopapain	1/10	10 \pm 1.8 %
Trypsin	1/10	45 \pm 3.0 %
α -amylase	1/5	38 \pm 3.3 %
β -amylase	1/10	51 \pm 3.6 %
Albumin	1/10	49 \pm 4.0 %
Protease (alkaline)	1/10	70 \pm 6.0 %
Blood plasma	0.4 mg BAF/0.1ml plasma	50 \pm 3.3 %

The incubation of BAF in albumin and blood plasma did not change their activity. An additional,

we found that the fraction do not lysate and do not agglutinate erythrocytes or platelets and do not precipitate the serum and plasma proteins.

CONCLUSSION

Sustainability of BAF to action of denaturing chemical agents and proteases (α -amylase, β -amylase, trypsin, hymotripsin and hymopapain) and lack of destructive influence of fraction on blood cells gives us reason to think that BAF can find practical app like dextran, as a component of blood plasma.

REFERENCES

1. H.R. Rasekh, P. Nazari, M. Kamli-Nejad, L. Hosseinzadeh, *Journal of Ethnopharmacology*, **116**, 21 (2008).
2. D. Egamberdieva, G. Berg, K. Lingström, L.A. Räsäen. *Plant Soil*, **369**, 453 (2013).
3. A. T. Atanasov, Monograph, COTA(ed)., Stara Zagora, 2006.
4. P.G. Peiretti, F. Gai, *Animal Feed Science and Technology*, **130**, 257 (2006).
5. A.T Atanassov, B. Tchobanov, *Biotechnology and Biotechnology Equipment*, **23**, 1109 (2009).
6. A.T. Atanasov, *Anniversary Conference of the Roumen Tsanev Institute of Molecular Biology*, 5-6 October, 2015.
7. A.T. Atanasov, *Journal of Herbs, Spices & Medicinal Plants*, **3**, 71 (1995).
8. M.B. Zucker, *Methods in Enzymology*, **169**, 118 (1989).
9. A.T. Atanasov, B. Tchobanov, *Comptes rendus de l'Academie Bulgare des Sciences*, **56**, 31 (2003).W. Kemp, *Organic Spectroscopy*, 3rd edition, MacMillan Educational, Basingstoke, UK, 1991.

НЯКОИ ФИЗИКОХИМИЧНИ ХАРАКТЕРИСТИКИ НА АНТИТРОМБОЦИТНА ФРАКЦИЯ ИЗОЛИРАНА ОТ *Galega officinalis* L.

А. Т. Атанасов^{1*}, С. Радев², И. Б. Стойнева³

¹Катедра физика и биофизика, Медицински факултет, Тракийски Университет, Стара Загора, България,

²Катедра по фармакология, медицински факултет, Тракийски Университет, Стара Загора, България

³Институт по органична химия с Център по фитохимия, БАН, ул. Акад. Г. Бончев, бл. 9, 1113 София, България

Постъпила на 30 септември, 2016 г.; Коригирана на 31 януари, 2017 г.

(Резюме)

Проучени са някои физикохимични характеристики на 100-140 kDa фракция, изолирана от лечебното растение *Galega officinalis* L. Получената фракция е водноразтворима и потиска тромбоцитната агрегация инициирана с аденозиндифосфат, тромбин и колаген. Третирането на фракцията с протеолитични ензими не влияе върху способността и да инхибира тромбоцитната агрегация. Изолираната фракция представлява високомолекулен полизахарид, съдържащ 23% протеин. Активността на фракцията се запазва след съхраняване и за няколко месеца при -4°C в N₃H-H₂O разтвори при неутрално рН, както и след лиофилизация. Фракцията проявява максимална активност в температурния диапазон 10°C-42°C и в разтвори с рН 5.5- 9.8. Микрокалориметричният анализ на фракцията показва, че тя съдържа две белтъчни субединици. Получената антиромбоцитната фракция може да намери приложение подобно на високомолекулените декстриани.

A.T. Atanasov et al.: Some physicochemical characteristics of anti-platelet fraction isolated from Galega officinalis L.

антиромбоцитната фракция може да намери приложение подобно на високомолекулните декстриани.

Modulating effect of new neuropeptide on central nervous system and on dopamine neurotransmission in mice

S. Stoeva¹, L. Tancheva^{1*}, L. Alova¹, M. Stefanova¹, T. Pajpanova², R. Kalfin¹

¹Institute of Neurobiology, Bulgarian Academy of Sciences, "Acad. G. Bonchev" str., Block 23, Sofia 1113, Bulgaria

²Institute of Molecular Biology "Roumen Tsanev", Bulgarian Academy of Sciences, "Acad. G. Bonchev" str., Block 21, Sofia 1113, Bulgaria

Received October 27, 2016; Revised February 28, 2017

The neuropeptide with code P2 (Nociceptin analogue, modified in position 13 with unnatural amino acid canavanine, Cav) is object of present work. We investigated its central nervous system (CNS) activity and modulating effect on dopamine levels in mice brain. The substitution of Lys¹³ by Cav in the nociceptin molecule affects the selectivity of the peptide action. P2 has dose-dependent antinociceptive effect in mice and also changed some brain neuromediators via decrease of dopamine uptake. The synthesized nociceptin analogue has promising pharmacological effects on CNS.

Key words: neuropeptide, hexobarbital narcosis, nociception, dopamine uptake

INTRODUCTION

Neuropeptides as signaling molecules in the brain are engaged in many physiological functions. They influence activities in the brain and body, such as analgesia, food intake, learning and memory.

The Nociceptin/Orphanin FQ (N/OFFQ) is involved in a wide range of physiological responses with effects noted in the nervous system (central and peripheral) but the mechanisms are complex and not well understood yet [1-2].

The modern drug design develops new ligands on the basis of well-known active peptides with improved pharmacokinetic properties [1-6]. Several groups have active structure-activity relationship programmes that are based on native Nociceptin [3-6].

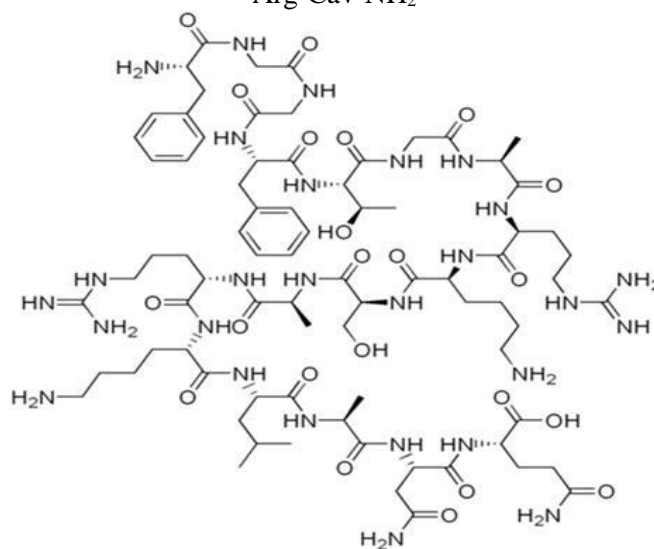
Object of this study is one short-chain neuropeptide analogue of Nociceptin (with code P2), containing unnatural amino acid canavanine on position 13 [7,8]

Having in mind its molecular design we decided to study its effects on central nervous system (CNS) and dopamine (DA) uptake.

Previous studies established significant biological activity and low oral and intraperitoneal toxicity of the compound (unpublished data).

P2 – FQ (1–13) NH₂ Nociceptin analogue

H-Phe-Gly-Gly-Phe-Thr-Gly-Ala-Arg-Lys-Ser-Ala-Arg-Cav-NH₂



Nociceptin

Purpose: To study the central nervous system activity of P2 and its modulating effects on dopamine levels in mice brain.

EXPERIMENTAL

Materials and methods. Chemicals

The peptide **P2** was synthesized by Pajpanova et al. [8] in the Institute of Molecular Biology at the Bulgarian Academy of Sciences. Acetic acid and Hexobarbital sodium salt were provided by SIGMA-ALDRICH.

The new neuropeptide was applied daily on adult male ICR mice in effective dose.

*To whom all correspondence should be sent:
E-mail: lyubkatancheva@gmail.com

Animals

Albino male ICR mice (body weight 18–20 g) were supplied by Experimental Breeding Base-Slivnitsa at the Institute of Neurobiology (Bulgarian Academy of Sciences). Animals were housed in plexiglass cages (6 per cage), under standard laboratory conditions (ambient temperature $20^{\circ}\text{C} \pm 2^{\circ}\text{C}$ and humidity $72\% \pm 4\%$), water and standard pelleted food ad libitum. All performed procedures were approved by the Institutional Animal Care Committee and the principles stated in the European Convention for the Protection of Vertebrate Animals used for Experimental and other Scientific Purposes (ETS123) were strictly followed throughout the experiment.

Methods

Studies for effect of P2 on nociception

New compound applied in an effective dose of 4 mg/kg was studied for its activity on nociception using Acetic acid test [9]. The number of abdominal cramps for 20 minutes after acetic acid application was measured. Dose-effect analgesic activity of compound P2 was studied in doses 4, 8 and 16 mg/kg b.wt. i.p. according to the same method.

Modulation of brain neurotransmission

In another experiment dopamine (DA) uptake in mouse brain was determined. After decapitation of animals the brain was cold removed. The brain samples were homogenized in 10 volume of 0.32 M sucrose and centrifuged at $1000 \times g$ for 19 min. The supernatant was carefully removed and centrifuged at $20\,000 \times g$ for 30 min. The resulting pellet was suspended in 10 volume of 10 mM Tris-HCl buffer, pH 7.7 and assayed for DA uptake and protein content. Synaptosomal DA uptake was measured according to Lai et al. [10]. Protein was measured by the method of Lowry et al. [11] with bovine serum albumin as a standard.

Effects of the new compound on CNS

The activity of the new compound on the CNS was studied evaluating its influence on the hexobarbital narcosis (HB – 100 mg/kg b.wt. i.p.). HB was used as central nervous active agent, but also as known model substrate of hepatic cytochrome P-450 monooxygenases. An effective dose 4 mg/kg i.p. of new compound was applied 20 minutes before HB administration. The changes in duration of HB narcosis (in minutes) were estimated in the groups according to the reflex of reversal [12].

Statistical analysis

Experimental results were performed using t-test of Student Fisher.

RESULTS AND DISCUSSION

Antinociceptive activity of P2

In our experiments we established that P2 had significant anti-nociceptive effect. In effective dose 4 mg/kg i.p. it decreases abdominal cramps with over 25%. This effect is dose-dependent and significant (Fig. 1 and Fig. 2).

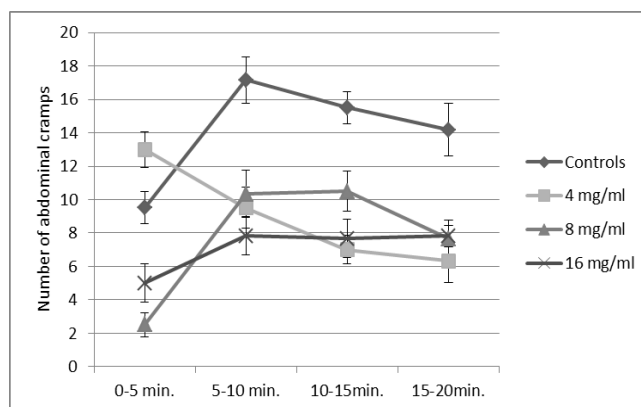


Fig. 1. Dose dependent analgesic effect of P2 according Acetic acid test

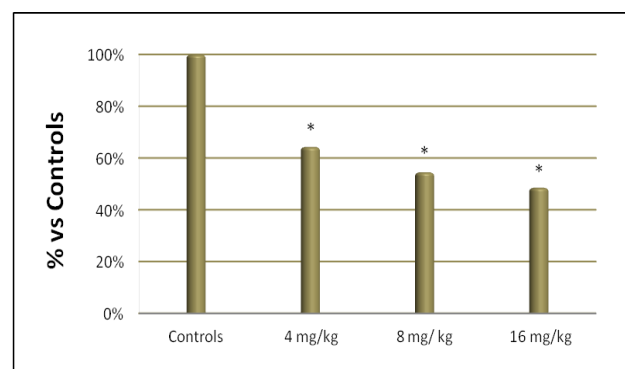


Fig. 2. Dose-dependent analgesic effect of P2 (% vs Controls) (*P<0.05)

The chemical similarity of P2 structure as nociceptive analogue probably makes it to act as ligand of N/OFQ receptors. Probably the pain modulation by P2 is result of possible interactions with N/OFQ receptor/s and deserves further experimental studies.

Influence of compounds on brain mediators

Established antinociceptive effect of P2 is accompanied by significant decrease of brain DA

uptake (by 77% in compare to control group) (Fig.3).

It is well known that DA (as antipsychotic drug) acts as blockers of DA receptors (in particular D2-like receptors) [13]. We assume existing connection between increased content of DA (as result of decrease DA uptake) and established antinociceptive effect of P2.

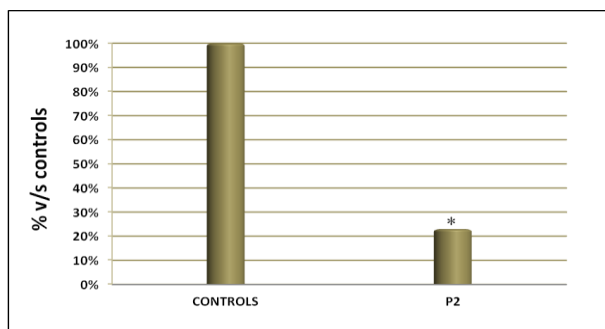


Fig. 3. Decrease of brain Dopamine uptake (* $P < 0.05$)

There is a proof in literature that N/OFQ can modulate rat dopamine neurons. Microdialysis studies have identified a suppressive effect of NOP on dopamine release from mesolimbic neurons [14]. Our data are in agreement with some reports about potent inhibition of the uptake of rat DA transporter by N/OFQ. Established inhibitory effect of P2 on DA uptake probably is mediated via NOP receptors. Maybe a new Nociceptin analogue P2 also is a ligand for this opioid receptor/s.

Established results suggest that P2 is a modulator of dopamine transport and that it affects on CNS at least partly by inhibiting dopamine transporter and directly affecting dopamine transmission [15]. Obviously studied analogue of N/OFQ is active and modulates pain together with dopamine content in brain.

Influence of compounds on the HB-narcosis

We established also in our experiments that P2 decreased significantly duration of HB narcosis (by over 40%), but the mechanism is still unknown (Fig. 4).

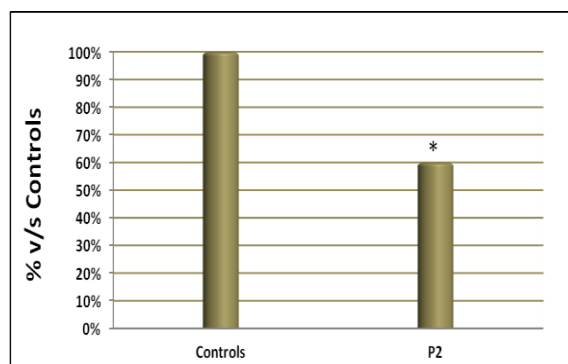


Fig. 4. Effect of P2 on Hexobarbital narcosis (* $P < 0.05$)

It is possible the substance P2 accelerates the elimination of HB via stimulating hepatic metabolism. But this interaction with HB can be due also to functional antagonism between HB and new neuropeptide on the level of CNS and/or to receptor interactions. It is known that N/OFQ receptor is a target with broad therapeutic potential. It is involved in a wide range of responses and thus has wide potential for drug development [16]. N/OFQ peptide and its receptor have been implicated also in a host of brain functions and diseases.

Further experiments could clarify whether the mechanism of this interaction is on the metabolic level or on CNS level.

CONCLUSIONS

Compound P2 as N/OFQ analogue possess significant dose-dependent antinociceptive activity due probably to its interaction with N/OFQ receptors in brain. P2 can modulate effectively brain DA uptake and also antagonized HB narcosis by unknown for now mechanism.

REFERENCES:

1. R. K. Reischeid, A. Ardati, F. J. Monsma Jr, O. Civelli, *J. Biol. Chem.*, **271**, 14163 (1996).
2. J. L. Butour, C. Moisan, H. Mazarguil, C. Mollereau, J. C. Meunier, *Eur. J. Pharmacol.*, **321**, 97 (1997).
3. G. Calo, R. Guerrini, R. Bigoni, A. Rizzi, C. Bianchi, D. Regoli, S. Sal-vadori, *J. Med. Chem.*, **41**(18) 3360 (1998).
4. R. Guerrini, A. Rizzi, K. Varani, G. Toth, S. Gessi, E. Hashiba, Y. Hashimoto, D. G. Lambert, *J. Med. Chem.*, **43**, 2805 (2000).
5. R. Guerrini, G. Calo, A. Rizzi, R. Bigoni, D. Regoli, S. Salvadori, *Peptides*, **21**, 923 (2000).
6. E. Naydenova E., V. Zhivkova, R. Zamfirova, L. Vezenkov, Y. Dobrinova, P. Mateeva, *Bioorg. Med. Chem. Lett.*, **16**, 4071 (2006).
7. T. Pajpanova, S. Stoev, E. Golovinsky, G-J. Krauss, J. Miersh, *Amino Acids*, **12**, 191 (1997).

8. P. Mateeva, R. Zamfirova, T. Pajpanova, E. Naydenova, L. Vezekov, *C. rend. acad. bulg. Sci.*, **64**, 1645 (2011).
9. MS Kaneria, SR Naik, RK Kohli, *Indian J. Experimental Biol.*, **45**, 279 (2007)
10. J. C. Lai, T. K. Leung, J. F. Guest, L. Lim, A. N. Davison, *Biochemical pharmacology*, **29** (20), 2763 (1980).
11. O.H. Lowry, N. J. Rosebrough, A. L. Farr, R. J. Randall *J. Biol. Chem.*, **193**, 265 (1951)
12. C. L. Riemke, Van Strik, E. H. De Jong, Delvera *Arch Int Pharmacodyn Ther.*, **1**, 10 (1963)
13. Ces, D. Reiss, O. Walter, J. Wichmann, E. P. Prinssen, B. L. Kieffer, A. Ouagazzal, *Neuropsychopharmacology*, **37**(2), 378 (2012)
14. N.P. Murphy, A.M. Tan, H.A. Lam, *Neuroscience*, **127**, 929-40 (2004)
15. Z. Liu, Y. Wang, Zhang, *Neuroreport.*, **26**, 699 (2001)
16. David G. Lambert *Nature Reviews Drug Discovery* **7**, 694 (2008)

МОДУЛИРАЩИ ЕФЕКТИ НА НОВОСИНТЕЗИРАН НЕВРОПЕПТИД ВЪРХУ ЦЕНТРАЛНА НЕРВНА СИСТЕМА И ДОПАМИНОВАТА НЕВРОТРАНСМИСИЯ ПРИ МИШКИ

С. Стоева¹, Л. Танчева^{1*}, Л. Алова¹, М. Стефанова¹, Т. Пайпанова², Р. Калфин¹

¹ *Институт по невробиология, БАН, ул. „Акад. Г. Бончев” бл.23, София 1113, България*

² *Институт по молекулярна биология „Румен Цанев”, БАН, ул. „Акад. Г. Бончев”, бл.21, София 1113, България*

Постъпила на 28 октомври, 2016 г.; Коригирана на 28 февруари, 2017 .

(Резюме)

Обект на представената работа е неuropeпид P2 (ноцицептинов аналог, модифициран в 13-та позиция с аминокиселината Канаваинин /Cav/). Изследвана е активността му върху централната нервна система (ЦНС), както и модулиращият му ефект върху допаминовото ниво в мозък на мишки. Замяната на Lys¹³ с Cav в ноцицептиновата молекула повлиява селективността на пептидното действие. P2 демонстрира доза-зависим антиноцицептивен ефект при мишки и променя нивата на някои мозъчни невротрансмитери чрез намаляване на допаминовото поемане. Новосинтезираният ноцицептинов аналог има обещаващи фармакологични ефекти върху ЦНС.

Effect of high- fructose diet on plasma leptin levels, morphological and biochemical parameters in ovariectomized rats

S.M. Mihajlova¹, A.A. Dimitrova³, T.I. Vlaykova¹, T.T. Tacheva¹, V. Tsoneva²,
K. Nancheva-Koleva², R. V. Sandeva^{1*}

¹Medical Faculty, Trakia University, Stara Zagora, Bulgaria

²University Hospital – Stara Zagora, Bulgaria

³Medical University, Pleven, Bulgaria

Received October 17, 2016; February 23, 2017

Leptin, the obese gene product, is an adipocyte-derived hormone that regulates body weight and metabolism by influencing food intake and energy expenditure. Postmenopausal status and high consumption of fructose are associated with increased incidence of visceral obesity and risk of metabolic syndrome, type 2 diabetes and cardiovascular diseases. The main objective of this study was to determine alterations in body weight, abdominal fat mass, plasma leptin levels, serum glucose and lipid profile (total cholesterol, triacylglycerol, high-density lipoprotein cholesterol and low-density lipoprotein cholesterol) in ovariectomized rats subjected to a fructose rich diet. Twenty-four adult female Wistar rats were divided into four groups: control sham-operated (SHAM, n = 6), ovariectomized (OVX, n = 6), sham-operated plus fructose (SHAM-F, n = 6) and ovariectomized plus fructose (OVX-F, n = 6). Fructose was given to the rats as 10% solution in drinking water for 8 weeks. The results indicated that plasma leptin levels were increased significantly in OVX and OVX-F groups compared with SHAM and SHAM-F groups (4466.66 ± 179.23 pg/ml and 2758.33 ± 682.47 pg/ml vs. 1965.33 ± 179.23 pg/ml and 1706.50 ± 232.15 pg/ml, respectively). Although leptin levels were not significantly different in the sham-operated and sham-operated plus fructose groups, there is a tendency for lower leptin levels in the sham-operated plus fructose group. The body weight was significantly increased in the OVX, OVX-F and SHAM-F groups compared with the SHAM group. Abdominal adipose tissue and biochemical parameters were significantly higher in OVX and OVX-F compared to those of control animals. In conclusion, excessive consumption of fructose may contribute to metabolic disorders and expressed predisposition to chronic non-infectious diseases observed in the postmenopausal condition. Furthermore, the results showed that a high-fructose diet and ovariectomy affect leptin levels in different directions, which may be due to interference on the various signal-transduction mechanisms in leptin synthesis and secretion.

Key words: leptin, ovariectomy, obesity, metabolic syndrome, high-fructose diet

INTRODUCTION

The lack of ovarian function in the postmenopausal period is associated with a high incidence of visceral type obesity and several metabolic disorders [1]. Estrogen deficiency has been proposed as an important obesity-triggering factor [2]. Experimental studies in rodents and humans support the involvement of estrogen in the control of energy balance [3], food intake [4], and body fat distribution [5]. In ovariectomized rodents – an animal model used to study human menopause – higher body weight and visceral adipose tissue have been observed than in sham-operated rodents. These ovariectomy disorders have been reversed by estradiol administration [6]. Postmenopausal women who have low levels of estrogen showed a significant increase in waist-to-hip ratio compared

with postmenopausal women receiving hormone replacement therapy [7].

Together with changes in fat distribution and metabolic disorders, the lack of estrogen is accompanied by abnormalities in the synthesis and signaling pathways of a number of peripheral peptides which participate in the regulation of energy homeostasis, such as leptin. Leptin is a 16-kDa peptide hormone that is secreted mainly by adipose cells [8]. It reduces feeding and increases energy expenditure by acting at sites primarily within the central nervous system [9], where it binds to leptin receptors (OB-Rs). There are multiple OB-Rs isoforms, all of which are products of a single OB-Rs gene, and it is thought that a long form of leptin receptor (OB-RL) is mainly responsible for regulating energy balance [10]. An intimate relationship between leptin and estrogen was described in many in vitro and in vivo studies, demonstrating a direct effect of estrogen on leptin expression [11] and leptin signaling in the brain [12].

* To whom all correspondence should be sent:
E-mail: rossisandeva@yahoo.com

In recent decades, there is a tendency to increase energy intake due to the widespread use of high-fructose corn syrup in beverages. High fructose consumption has been linked to the development of insulin resistance, dyslipidemia and visceral obesity [13]. An animal study has observed that dietary fructose leads to a decrease in serum leptin levels, increased food intake and weight gain [14]. Accordingly, the objective of this study was to investigate the effect of a high-fructose diet on weight gain, abdominal fat mass, lipid profile, serum glucose level and plasma leptin concentration in ovariectomized and sham-operated rats.

MATERIALS AND METHODS

Experimental Animals.

Female Wistar rats weighing 190 – 220 g were studied. The rats were kept in the accredited vivarium of the Medical Faculty, Trakia University at 25±1 °C with a light/dark photoperiod of 12/12 hours and free access to chow diet and water for a week before the study.

Experimental design.

The twenty-four experimental animals were randomly divided into two groups: ovariectomized group (n=12) and sham-operated-group (n=12). The ovariectomy procedure was performed by a dorsal midline skin incision through which the ovaries were bilaterally clamped and removed. The uterine horns were tied and the uterus was left intact. In the sham-operated group, the ovaries were exteriorized to create similar stress, but were not clamped and removed. After surgery, the animals were allowed to recover for 4 weeks. After recovery, the ovariectomized and sham-operated groups were each subdivided into two new groups, based on the type of diet: control sham-operated (SHAM, n=6), sham-operated plus fructose (SHAM-F, n=6), ovariectomized (OVX, n=6) and ovariectomized plus fructose (OVX-F, n=6). During the 8-week period, all the rats were fed with a standard diet; in addition, the fructose groups received a 10% solution of fructose in drinking water. Body weight was measured at the end of the recovery period and at the end of every two weeks during the experiment. At the end of the experiment, the rats fasted overnight were anesthetized with a mixture of ketamine - xylazine (90 and 10 mg/kg, respectively, i.p.). Blood samples were collected for serum and plasma separation by abdominal aorta puncture. The mesenteric (MAT), retroperitoneal (RAT) and subcutaneous (SAT) adipose tissue were

dissected and externalized. The fat was weighed immediately after dissection in order to avoid weight loss by evaporation.

The experiment was conducted in compliance with the requirements of national legislation and the European Directive 2010/63/EU of 22.09.2010 on the protection of animals used for scientific purposes.

Determination of glucose and lipid profile.

Glucose and lipid parameters (triglycerides, total cholesterol, HDL- and LDL-cholesterol) in serum were examined using an automatic analyzer Mindray BS300.

Determination of leptin levels.

All samples were centrifuged and the plasma was stored at -20 °C until analysis. Levels of plasma leptin were assessed using ELISA kit (BioVendor Mouse and Rat Leptin ELISA kit) according to the manufacturer's instructions.

Statistical analysis

The data were analyzed using the Student's t-test on Statsoft Statistica v.8. Results were expressed as mean ± standard deviation (SD) and values of $p > 0.05$ were considered statistically insignificant, while those of $p < 0.05$ were considered significant.

RESULTS AND DISCUSSION

Body weight and adipose tissue. Figure 1 shows the changes in body weight of the different groups for the duration of the study. As expected, after recovery for 4 weeks the OVX rats exhibited the highest body weight. This is consistent with other clinical [15] and experimental studies [6] which demonstrate that lower levels of estrogen after ovarian function failure are associated with weight gain (Fig. 1).

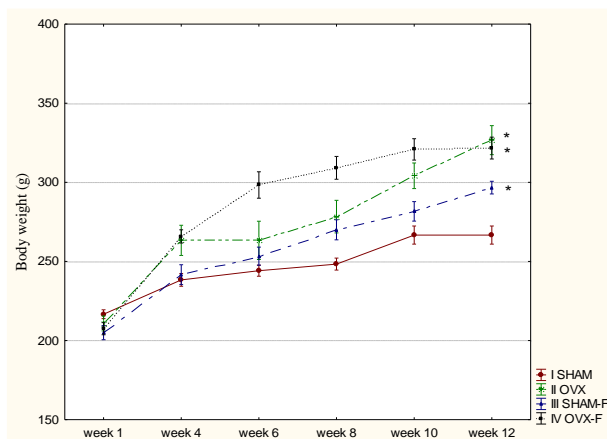


Fig. 1. Changes in body weight of different studied groups for the duration of the study, * $p < 0.05$.

After the 8-week feeding period with 10% fructose solution, a statistically significant difference ($p < 0.05$) was found between the mean body weight of the OVX, OVX-F and SHAM-F groups compared with the SHAM group. Mesenteric and retroperitoneal fat were significantly increased in the OVX and OVX-F groups compared with the SHAM group. Moreover, the OVX-F group showed a significant increase in MAT when compared with the SHAM-F group; while retroperitoneal fat depot weight was significantly higher in the OVX group than in the SHAM-F group (Table 1).

Bocarsly et al. [16] observed such changes in body weight and fat depot weight after 7 months of a high-fructose diet in female rats with intact ovarian function. Another study has demonstrated that the application of a 10% fructose solution in drinking water for 24 weeks in female rats increases visceral fat accumulation but does not alter body weight [17].

Our results demonstrate that ovariectomy leads to a significant increase in visceral fat depot. These results align with others previously reported [7]. It has been proposed that estrogen can modulate body fat distribution, adipocytes size and number [18] as well as adipocyte lipolysis [19]. This is supported by the presence of estrogen receptors in the abdominal and subcutaneous fat [20]. Moreover, estrogen receptors have been found to be expressed

in hypothalamic nuclei which are linked to the regulation of energy homeostasis [21].

Plasma Leptin Concentrations. In the OVX group and OVX-F group, leptin levels were significantly elevated compared with the SHAM and SHAM-F groups (4466.66 ± 179.23 pg/ml and 2758.33 ± 682.47 pg/ml vs. 1965.33 ± 179.23 pg/ml and 1706.50 ± 232.15 pg/ml, respectively). No statistical difference was found in plasma leptin levels between SHAM and SHAM-F groups. However, there was a tendency for lower leptin levels in the SHAM-F group. Moreover, the OVX group showed significantly higher plasma leptin levels compared with the OVX-F group (Fig. 2).

Our results support other authors who have demonstrated that estrogen deficiency is accompanied with higher plasma leptin levels [22, 23] and this may be explained by the effect of estrogen on leptin synthesis in adipose tissue [24] and on leptin sensitivity in the hypothalamus [25, 26]. However, other researchers have found a positive correlation between serum estrogen and leptin concentration [27]. Interestingly, Chu et al. have demonstrated that ovariectomy in rats leads to an initial decrease in serum leptin levels, followed by an increased production of leptin [28].

Table 1. Changes in anthropometrical and biochemical parameters in SHAM, OVX, SHAM-F and OVX-F rats at the end of the experimental period. Values are presented as mean \pm SD; *a* - $p < 0.05$ significantly different from the SHAM group, *b* - $p < 0.05$ significantly different from the OVX group, and *c* - $p < 0.05$ significantly different from the SHAM-F group.

Parameters	SHAM	OVX	SHAM-F	OVX-F
Serum total cholesterol (mmol/l)	3,5 \pm 0,6	4,9 \pm 0,2 ^{a,c}	4,0 \pm 0,3	5,5 \pm 0,5 ^{a,c}
Serum HDL-cholesterol (mmol/l)	1,19 \pm 0,1	1,3 \pm 0,1	1,2 \pm 0,2	1,2 \pm 0,1
Serum LDL-cholesterol (mmol/l)	1,7 \pm 0,6	3,2 \pm 0,3 ^{a,c}	2,2 \pm 0,4	3,7 \pm 0,6 ^{a,c}
Serum TAG (mmol/l)	1,9 \pm 0,1	2,0 \pm 0,4	2,2 \pm 0,1	2,6 \pm 0,2
Serum glucose (mmol/l)	4,9 \pm 0,8	8,8 \pm 1,8 ^{a,c}	6,5 \pm 1,2	9,8 \pm 1,7 ^{a,c}
Retroperitoneal fat depot weight (g)	3,6 \pm 0,4	6,1 \pm 1,2 ^{a,c}	4,4 \pm 0,8	5,5 \pm 1,4 ^a
Mesenteric fat depot weight (g)	4,4 \pm 0,7	6,4 \pm 1,6 ^a	5,5 \pm 1,0	7,1 \pm 1,2 ^{a,c}
Subcutaneous fat depot weight (g)	2,9 \pm 0,5	3,3 \pm 0,7	3,2 \pm 0,4	3,1 \pm 0,2

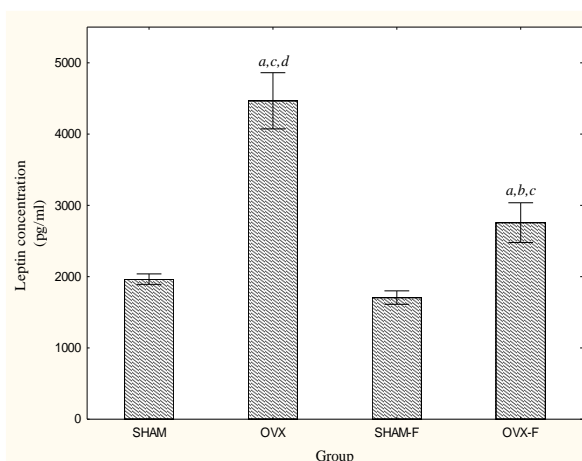


Fig. 2. Leptin concentration in plasma (pg/mL) of different studied groups at the end of the study. a: significantly different from the SHAM group, b: significantly different from the OVX group, and c: significantly different from the SHAM-F group, d: significantly different from the OVX-F group, $p < 0.05$.

In this study we have found that dietary fructose decreases plasma leptin levels in the OVX-F and SHAM-F groups compared with the OVX group. This supports the results obtained by Teff et al. [14]. Another study has found that fructose, unlike glucose, does not stimulate insulin secretion [29]. Low levels of insulin in a high-fructose diet could explain the increased food intake through the following mechanisms. First, in the central nervous system, insulin has a direct inhibitory effect on food intake [30] and second, insulin may modulate food intake by its effects on leptin secretion [31]. Another study has suggested that fructose consumption may induce central leptin resistance, while serum leptin levels, body weight and fat mass remain unchanged [32]; this may be due to the impairment of leptin transport across the blood-brain barrier, which includes leptin receptors and can be easily saturated [33]. An important role in the saturation of this transport mechanism is attributed to hypertriglyceridemia associated with a high-fructose diet [34].

Serum glucose and lipid profile. We have observed that in the OVX-F and OVX groups the levels of serum glucose, total cholesterol and LDL cholesterol were significantly increased when compared to the SHAM and SHAM-F groups (Table 1).

The present study shows that ovariectomy causes serious disturbances in the lipid profile, expressed in increased total cholesterol and LDL-cholesterol accompanied by impaired glucose homeostasis. We have found no significant difference in serum triglyceride levels in all of the studied groups. Regarding serum glucose, our

results show that administration of a 10% fructose solution for 8 weeks in sham-operated as well as in ovariectomized animals is accompanied by high levels of fasting blood glucose. Insulin resistance has been proposed as a major cause of impaired glucose tolerance in a high-fructose diet [35]. Moreover, we have found that ovariectomy leads to impaired glucose tolerance, which may also be due to impaired insulin-mediated glucose utilization as a result of estrogen deficiency [36]. However, the exact mechanism of insulin resistance in the absence of ovarian function remains unclear.

CONCLUSION

This study demonstrates that 8 weeks of administration of a high-fructose diet as a 10% solution in drinking water on ovariectomized Wistar rats leads to manifest metabolic and morphologic disturbances and an alteration in leptin metabolism. Low plasma levels of leptin as a result of a high-fructose diet suggest that fructose affects mostly leptin production and secretion. This indicates that fructose could contribute to decreased satiety and increased food intake. In contrast, estrogen deficiency is associated with higher plasma concentrations of leptin, which could be due to its influence on leptin signal transduction. In conclusion, disturbances in leptin metabolism determine a positive energy balance and weight gain. Further studies are needed to elucidate the role of a high-fructose diet on leptin action in the regulation of food intake and to provide detailed understanding of the mechanisms of postmenopausal obesity.

REFERENCES

1. M.J. Toth, A. Tchernoﬀ, C.K. Sites, E.T. Poehlman, *Int J Obes Relat Metab Disord*, **24**, 226 (2000).
2. J. Haarbo, U. Marslew, A. Gotfredsen, C. Christiansen, *Metabolism*, **40**, 1323 (1991).
3. M. L. Laudenslager, C. W. Wilkinson, H. J. Carlisle, H. T. Hammel, *Am J Physiol*, **238**, 400 (1980).
4. D.M. Roesch, *Physiol Behav*, **87**, 39 (2006).
5. T.M. Price, S.N. O'Brien, B.H. Welter, R. George, J. Anandjiwala, M. Kilgore, *Am J Obstet Gynecol*, **178**, 101 (1998).
6. S. Sanchez-Mateos, C. Alonso-Gonzalez, A. Gonzalez, C.M. Martinez-Campa, M.D. Mediavilla, S. Cos, E.J. Sanchez-Barcelo, *Maturitas*, **58**, 91 (2007).
7. A. Arabi, P. Garnero, R. Porcher, C. Pelissier, C.L. Benhamou, C. Roux, *Hum Reprod*, **18**, 1747 (2003).
8. V. V. Harmelen, S. Reynisdottir, P. Eriksson, A. Thörne, J. Hoffstedt, F. Lönnqvist, P. Arner, *Diabetes*, **47**, 913 (1998).

9. S. Dryden, P. King, L. Pickavance, P. Doyle, G. Williams, *Clin Sci (Lond)*, **96**, 307 (1999).
10. C. Bjørnbæk, S. Uotani, B. da Silva, J.S. Flier, *J Biol Chem*, **272**, 32686 (1997).
11. L. Pinilla, L.M. Seoane, L. Gonzalez, E. Carro, E. Aguilar, F.F. Casanueva, C. Dieguez, *Eur J Endocrinol*, **140**, 468 (1999).
12. R. Matysková, B. Zelezná, J. Maixnerová, D. Koutová, M., L. Maletínská, *Horm Metab Res*, **42**, 182 (2001).
13. K.L. Stanhope , J.M. Schwarz, N.L. Keim, S.C. Griffen, A.A. Bremer, J.L. Graham, B. Hatcher, C.L. Cox, A. Dyachenko, W. Zhang, J.P. McGahan, A. Seibert, R.M. Krauss, S. Chiu, E.J. Schaefer, M. Ai, S. Otokoza, K. Nakajima, T. Nakano, C. Beysen, M.K. Hellerstein, L. Berglund, P.J. Havel, *J Clin Invest*, **119**, 1322 (2009).
14. K.L. Teff, S.S. Elliott, M. Tschöp, T.J. Kieffer, D. Rader, M. Heiman, R.R. Townsend, N.L. Keim, D. D'Alessio, P.J. Havel, *J Clin Endocrinol Metab*, **89**, 2963 (2004).
15. M. Gambacciani , M. Ciaponi , B. Cappagli, L. Piaggese, L. De Simone, R. Orlandi, A.R. Genazzani, *J Clin Endocrinol Metab*, **82**, 414 (1997).
16. M.E. Bocarsly, E.S. Powell, N.M. Avena, B.G. Hoebel, *Pharmacol Biochem Behav*, **97**, 101 (2010)
17. M.B. Pektaş, G. Sadi, F. Akar, *Cell Physiol Biochem*, **37**, 1407 (2015).
18. L.A. Anderson , P.G. McTernan, A.H. Barnett, S. Kumar, *J Clin Endocrinol Metab*, **86**, 5045 (2001)
19. R.E. Van Pelt, W.S. Gozansky, R.C. Hickner, R.S. Schwartz, W.M. Kohrt, *Obesity*, **14**, 2163 (2006).
20. M.N. Dieudonné, M.C. Leneuve, Y. Giudicelli, R. Pecquery, *Am J Physiol Cell Physiol*, **286**, 655 (2004).
21. S Musatov, W. Chen, D.W. Pfaff, C.V. Mobbs, X.J. Yang, D.J. Clegg, M.G. Kaplitt, S. Ogawa, *Proc Natl Acad Sci U S A*, **104**, 2501 (2007).
22. L. Pinilla, L.M. Seoane, L. Gonzalez, E. Carro, E. Aguilar, F.F. Casanueva, C. Dieguez, *Eur J Endocrinol*, **140**, 468 (1999).
23. R. Meli, M. Pacilio, G.M. Raso, E. Esposito, A. Coppola, A. Nasti, C. Di Carlo, C. Nappi, R. Di Carlo, *Endocrinology*, **145**, 3115 (2004).
24. F. Machinal, M.N. Dieudonne , M.C. Leneuve , R. Pecquery , Y. Giudicelli . *Endocrinology*, **140**, 1567 (1999).
25. M. Kimura, M. Irahara, T. Yasui, S. Saito, M. Tezuka, S. Yamano, M. Kamada, T. Aono, *Biochem Biophys Res Commun*, **290**, 1349 (2002)
26. R. Matysková, B. Zelezná, J. Maixnerová, D. Koutová, M., L. Maletínská, *Horm Metab Res*, **42**, 182 (2001).
27. L. Beytur, M. Şimşek, E. Sapmaz, A. Yaşar, G. Baydaş, *Fırat Üniversitesi Sağlık Bilimleri Tıp Dergisi*, **23**, 145 (2009).
28. S.C. Chu, Y.C. Chou, J.Y. Liu, C.H. Chen, J.C. Shyu, F.P. Chou, *Life Sci*, **64**, 2299 (1999).
29. D.L. Curry, *Pancreas*, **4**, 2 (1989).
30. I. Sato, H. Arima, N. Ozaki, M. Watanabe, M. Goto, M. Hayashi, R. Banno, H. Nagasaki, Y. Oiso, *J Neurosci*, **21**, 8657 (2005).
31. M. Tsai, A. Asakawa, H. Amitani, A. Inui, *Indian J Endocrinol Metab*, **16**, 543 (2012)
32. A. Shapiro, W. Mu, C. Roncal, K.Y. Cheng, R.J. Johnson, P.J. Scarpace, *Am J Physiol Regul Integr Comp Physiol*, **295**, 1370 (2008)
33. B Burguera, M.E. Couce, G.L. Curran, M.D. Jensen, R.V. Lloyd, M.P. Cleary, J.F. Poduslo, *Diabetes*, **49**, 1219 (2000)
34. W.A. Banks, A.B. Coon, S.M. Robinson, A. Moinuddin, J.M. Shultz, R. Nakaoke, J.E. Morley, *Diabetes*, **53**, 1253 (2004)
35. K.L. Stanhope , P.J. Havel , *Curr Opin Lipidol*, **19**, 16 (2008)
36. Z. Suba, *Pathol Oncol Res*, **18**, 123 (2012).

ЕФЕКТ НА ВИСОКОФРУКТОЗНАТА ДИЕТА ВЪРХУ ПЛАЗМЕНИТЕ ЛЕПТИНОВИ НИВА, МОРФОЛОГИЧНИ И БИОХИМИЧНИ ПОКАЗАТЕЛИ ПРИ ОВАРИЕКТОМИРАНИ ПЛЪХОВЕ

С. М. Михайлова¹, А. А. Димитрова³, Т. И. Влайкова¹, Т. Т. Тачева¹, В. Цонева², К. Нанчева-Колева², Р. В. Сандева¹

¹Медицински факултет, Тракийски университет, ул., Армейска"11, 6000 Стара Загора (България)

²Университетска болница – тара Загора (България)

³ Медицински Университет, ул., Климент Охридски" 1, 5800 Плевен (България)

Постъпила на 16 октомври, 2016 г.; Коригирана на 23 февруари, 2017 г.

(Резюме)

Лептинът е продукт на об-гена и адипокин, който регулира телесното тегло и метаболизма чрез повлияване приема на храна и разхода на енергия. Постменопаузата и високата консумация на фруктоза са свързани с повишена честота на висцерално затлъстяване и риск от метаболитен синдром, диабет тип 2 и сърдечно-съдови заболявания. Основната цел на това проучване е да се определят промените в телесното тегло, мастната тъкан, плазмените нива на лептина, серумната глюкоза и липидния профил (общ холестерол, триацилглицерол, HDL- и LDL-холестерол) в овариектомирани плъхове, подложени на богатата на фруктоза диета. Двадесет и четири възрастни женски Wistar плъхове бяха разделени в четири групи: контролна фалшиво оперирани (Sham, 6 броя), овариектомирани (OVX, 6 броя), фалшиво оперирани плюс фруктоза (Sham-F, 6 броя) и овариектомирани плюс фруктоза (OVX-F, 6 броя). Фруктозата беше давана на плъховете като 10% разтвор в питейната вода за 8 седмици. Резултатите показват, че плазмените нива на лептина се увеличават значително в OVX и OVX-F групи в сравнение с Sham и Sham-F групи ($4466,66 \pm 179,23$ pg/ml и $2758,33 \pm 682,47$ pg/ml срещу $1965,33 \pm 179,23$ pg/ml и $1706,50 \pm 232,15$ pg/ml, съответно). Въпреки че лептиновите нива не се различават сигнификантно във фалшиво оперираната и фалшиво оперираната плюс фруктоза групи, се наблюдава тенденция за намаляване на нивата на лептина във фалшиво оперираната плюс фруктоза група. Телесното тегло е значително повишено в OVX, OVX-F и Sham-F групи в сравнение с Sham-групата. Теглата на абдоминалната мастна тъкан и стойностите на биохимичните параметри са сигнификантно по-високи в OVX и OVX-F в сравнение с тези на контролните животни. В заключение, прекомерната консумация на фруктоза може да допринесе за метаболитни нарушения и предразположение към хронични неинфекциозни заболявания, наблюдавани в периода на постменопаузата. Освен това резултатите показват, че високофруктозната диета и овариектомията повлияват лептиновите нива в различни посоки, което може да се дължи на смущения на различни сигнално-трансдукционни механизми в лептиновия синтез и секреция.

Unacylated ghrelin in plasma of Wistar rats after consumption of fructose, sucrose and aspartame

R.V. Sandeva^{1*}, A.A. Dimitrova², T.T. Tacheva¹, S.M. Mihajlova¹, G.N. Sandeva¹, T.I. Vlaykova¹

¹Medical Faculty, Trakia University, Stara Zagora, Bulgaria

²Medical University, Pleven, Bulgaria

Received September 17, 2016; Revised February 20, 2017

Unacylated ghrelin (UAG) amounts to 80-90% of the circulating orexigenic hormone ghrelin. Studies suggest that both acyl ghrelin (AG) and UAG may mediate peripheral biological actions and UAG can act as a potent functional inhibitor of ghrelin. The aim of this study was to track changes in unacylated ghrelin in plasma in a control and three experimental (fructose, sucrose and aspartame) groups of rats and to compare them with some morphological and metabolic parameters. An 8-week burdening of 28 male Wistar rats with 15% fructose (Group F, n = 7), 10% sucrose (Group S, n = 7) and 0.3% aspartame solutions (Group A, n = 7) was carried out. An increase in average body weight was found in the following order: sucrose group > fructose group > aspartame group > controls. Significant difference was found in the mesenteric fat depot weight of Group F vs. Group C. An increase in unacylated ghrelin levels and in general metabolic parameters (glucose, triglycerides, total and LDL-cholesterol, AST, ALT) of the fructose and sucrose groups compared to controls was registered. Moreover, changes in some metabolic markers in the aspartame group were also seen. In conclusion, the results of the current study suggest that elevated unacylated ghrelin might trigger changes in the regulation of food intake and further development of obesity, metabolic disorders and chronic noninfectious diseases.

Keywords: unacylated ghrelin, metabolic syndrome, fructose, sucrose, aspartame, Wistar rats

INTRODUCTION

Excessive consumption of sucrose and fructose (in the form of high fructose corn syrup) is one of the most serious causes of obesity and comorbidities, such as hypertension, diabetes, nonalcoholic fatty liver disease and coronary heart diseases, which are associated with a significant increase in morbidity and mortality rates [1,2,3,4]. In order to reduce sucrose and fructose consumption they are replaced with artificial sweeteners like aspartame. Sweeteners are widely used in many products, such as desserts and diet beverages, as a mean to prevent body mass gain, metabolic syndrome, diabetes, and several risk factors for heart disease. In 2012, the American Heart Association and American Diabetes Association concluded that there are still insufficient data to determine the role played by artificial sweeteners in the regulation of energy balance, body weight, and influence on cardiometabolic risk factors [5]. There is evidence that non-caloric sweeteners increase appetite, promote overeating, and lead to body mass gain [6, 7, 8]. The mechanisms by which this occurs remain unknown. It is probable that a significant role in this mechanism is played by the sweet taste

receptors T1R2 and T1R3 (G-coupled receptor proteins), which have also been found in the duodenum, small intestine and pancreas. Stimulation of this taste receptors by sugars or artificial sweeteners activates intracellular signaling elements, which stimulate peripheral gustatory nerves and, in turn, brain gustatory pathways [9, 10]. The artificial sweeteners weaken a natural predictive relationship between sweet taste and the calorie intake during eating.

One of the main factors for the regulation of the energy homeostasis is ghrelin. It can be found as two isoforms in the circulation: acylated ghrelin (AG) and unacylated ghrelin (UAG). Acylation is catalyzed by the enzyme ghrelin O-acyl transferase. The appetite-stimulating function of AG was identified secondary to its effect on the growth hormone release from somatotroph cells of the anterior pituitary [11]; however, AG is the first known peripheral hormone to display orexigenic effects through its action on the hypothalamic appetite-regulating pathways [12]. AG activates NPY/AgRP neurons [13] of the hypothalamic arcuate nucleus through its receptor, GHS-R1a, promoting production and secretion of their orexigenic neuropeptides to suppress pro-opiomelanocortin neuronal activity while stimulating food intake. There is evidence to show that ghrelin is important in the short-term regulation of appetite and energy balance. The pre-prandial

* To whom all correspondence should be sent:
E-mail: rossisandeva@yahoo.com

rise and post-prandial fall in plasma ghrelin levels support the hypothesis that ghrelin acts as an initiator signal for meal consumption in humans [14]. Ghrelin also appears to be involved in the regulation of long-term energy homeostasis [14]. This peptide hormone has been described as the peripheral counterpart of insulin and leptin, and adenosine monophosphate-activated protein kinase also appears to be involved in its peripheral metabolic effects [15]. Ghrelin reduces the use of fat as a metabolic fuel and promotes an increase in adipose tissue and body weight [16]. Circulating ghrelin induces abdominal obesity, independently of its central orexigenic activity, via GHS-R-dependent lipid accumulation in fat depots [17].

UAG is considered to be an inert degradation product of AG, UAG (or des-acyl ghrelin) nowadays emerges as an important hormone, apart from the other proghrelin-derived peptides, AG and obestatin. UAG amounts to 80-90% of the circulating orexigenic hormone ghrelin. UAG appears to have its own receptor, and it can share this receptor with AG, under experimental conditions at least. An increasing number of studies suggest that UAG can act as a potent functional inhibitor of ghrelin. It can even strongly suppress ghrelin production in obese human diabetic subjects [18]. Moreover, UAG can improve postprandial glycemia, especially in those subjects in whom preprandial acylated ghrelin levels are high, which makes UAG, or UAG-analogs strong potential candidates for the development of drugs for the treatment of metabolic disorders or other conditions in which elevated AG/UAG ratios occur, such as diabetes, obesity and Prader-Willi syndrome [19].

Therefore, the aim of this study was to track changes in UAG in plasma of experimental rats and to compare them with some morphological and metabolic parameters.

EXPERIMENTAL

Animal models

Male albino Wistar rats weighing circa 250 g were kept in the accredited Vivarium at the Medical Faculty, Trakia University at $25\pm 1^\circ\text{C}$ with a photoperiod light/dark of 12/12 hours and free access to water and food. The standard diet was composed of starch - 50%, protein - 20%, fat - 3%, cellulose - 5%, standard vitamin and mineral mix. After adaptation (one week) an 8-week treatment of the 28 male rats with drinking water (control Group C, $n = 7$), 15% fructose solution (Group F, $n = 7$), 10% sucrose solution (Group S, $n = 7$), and 0.3% aspartame solution (Group A, $n = 7$) was carried

out. Food intake was recorded daily and animal weight was monitored at the end of the 2nd, 4th, 6th and 8th week. The containers with water and sweet solutions were supplemented every two days, once a week the amount consumed by all groups was calculated and the average intake of solutions in g/100 g body weight per day for the experimental groups was determined.

At the end of the experiment the rats were fasted overnight and anesthetized with a mixture of ketamine-xylazine (90 and 10 mg/kg respectively, i.p.). Blood samples were collected for serum and plasma separation by abdominal aorta puncture. Depots of retroperitoneal, mesenteric (visceral) and subcutaneous adipose tissue of the back were removed and weighed immediately after dissection in order to avoid weight loss by evaporation. Fat depots were measured in mg/100 g body weight.

The experiment was conducted in compliance with the requirements of both the national legislation and the European Directive 2010/63/EU of 22.09.2010 on the protection of animals used for scientific purposes.

Blood collection and biochemical analyses

In sera from venous blood collected from the tail vein at the beginning and from the abdominal aorta (under ketamine-xylazine anesthesia) at the end of the experimental period glucose, lipid parameters (triglycerides, total cholesterol, HDL- and LDL-cholesterol), and the levels of uric acid, ALT and AST were examined using an automatic analyzer Mindray BS300.

Blood collection and measurement of unacylated ghrelin in plasma

Blood samples from the abdominal aorta were collected in tubes containing EDTA. Samples were centrifuged at 3,500 rpm for 10 minutes at $+4^\circ\text{C}$ and then supernatants were transferred into separate tubes. Samples were stored at -20°C until analysis. Levels of plasma unacylated ghrelin were assessed using the BioVendor Rat Unacylated Ghrelin ELISA kit, based on a double-antibody sandwich technique (BioVendor - Laboratorni medicina, Czech Republik) according to the manufacturer's instructions. The assay sensitivity was 8 pg/ml.

Statistical analysis

The results were analyzed by Student's t-test on Statistica v.12 (StatSoft, Inc.). Correlation analysis with determination of correlation coefficient r was also performed. Differences were considered significant if $p < 0.05$.

RESULTS AND DISCUSSION

Following the changes in body weight of the control and experimental groups of rats, it was observed that all experimental groups had higher mean body weight at the end of the 8-week period than the controls (Fig. 1). However, only the animals overloaded with sucrose had significantly higher mean body weight than controls ($p < 0.05$).

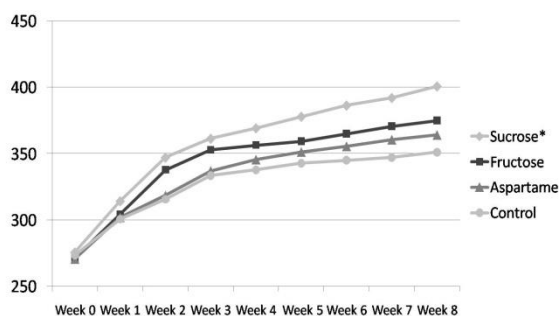


Fig. 1. Dynamics in group mean weight (g) for eight week period, * $p < 0.05$.

Moreover, rats from Group S elicited greater body mass gain than rats from the other experimental groups. This could be due to the

presence of both glucose and fructose derived from hydrolysis of sucrose. Glucose is metabolized widely in the body for energy, glycogen storage or synthesis of fatty acids, while fructose is metabolized mainly in the liver in *de novo* lipogenesis of fatty acids and TAG synthesis. It is noteworthy that, based on the differences in the metabolic pathways for fructose and glucose, fructose consumption gives less satiety, leads to increased food intake and body mass gain compared to glucose. Fructose, unlike glucose does not stimulate insulin secretion. Low levels of insulin in a high-fructose diet could explain the increased food intake [20, 21]. Similar changes in body weight after fructose, sucrose and aspartame consumption found several authors [6, 22, 23].

Increase of the mean retroperitoneal and mesenteric fat deposits was also observed in the following order: Group F > Group S > Group A > Group C, although the differences were not significant in most cases besides the mesenteric fat depot weight of Group F vs. Group C (Table 1). An increase in visceral fat depots in fructose fed animals found Stanhope and Havel [4].

Table 1. The main biochemical and morphological parameters for the four experimental groups of rats. Data are presented as mean value \pm SD

Parameter	Control (C)	Fructose (F)	Sucrose (S)	Aspartame (A)
Serum glucose (mM)	5.43 \pm 0.75	9.76 \pm 2.48*	7.04 \pm 0.77*	4.97 \pm 1.08
Serum total cholesterol (mM)	1.75 \pm 0.12	2.1 \pm 0.42	1.95 \pm 0.17*	1.79 \pm 0.09
Serum HDL-cholesterol (mM)	0.5 \pm 0.08	0.39 \pm 0.05*	0.66 \pm 0.04*	0.69 \pm 0.03*
Serum LDL-cholesterol (mM)	0.73 \pm 0.07	0.85 \pm 0.04*	0.88 \pm 0.05*	0.77 \pm 0.04
Serum TAG (mM)	0.72 \pm 0.24	1.91 \pm 0.87*	1.14 \pm 0.22*	0.9 \pm 0.28
Serum UA (μ mol/L)	17.43 \pm 5.25	76.85 \pm 26.49*	31.86 \pm 12.96*	21.57 \pm 12.2
AST (U/L)	117.57 \pm 19.18	162.86 \pm 34.28*	171.71 \pm 32.98*	119.00 \pm 10.26
ALT (U/L)	41.14 \pm 12.21	60.57 \pm 15.25*	51.43 \pm 7.69	45.86 \pm 13.37
Retroperitoneal fat depot weight (mg/100g bw)	815.9 \pm 240.15	1137.8 \pm 332.24	1082.78 \pm 389.75	1035.37 \pm 351.75
Mesenteric fat depot weight (mg/100g bw)	1075.64 \pm 254.42	1763.45 \pm 709.98*	1572.67 \pm 602.58	1112.05 \pm 492.48
Subcutaneous posterior fat depot weight (mg/100gbw)	124.63 \pm 53.13	154.0 \pm 61.47	208.72 \pm 126.16	163.69 \pm 39.83

* $p < 0.05$ compared with the control group

Bursać et al. [24] analyzed the effects of 9-week consumption of 60% fructose solution on dyslipidemia, insulin and leptin sensitivity, and adipose tissue histology in male Wistar rats. The total body mass of fructose-fed rats was not changed, but the mass of visceral omental adipose tissue, as well as the relative ratio of visceral omental fat mass to total body mass was increased by fructose diet, pointing to visceral adiposity. Their results also showed elevated triglycerides and hypothalamic leptin resistance accompanied by stimulated glucocorticoid signaling and NPY mRNA elevation. Fructose consumption shifted the balance between glucocorticoid receptor and adipogenic transcriptional factors (PPAR γ , SREBP-1 and lipin-1) in favor of adipogenesis judged by distinctly separated populations of small adipocytes observed in this tissue. They concluded that high-fructose-diet-induced alterations of glucocorticoid signaling in both hypothalamus and adipose tissue result in enhanced adipogenesis, possibly serving as an adaptation to energy excess in order to limit deposition of fat in nonadipose tissues, which are the key events leading to the development of insulin resistance and type 2 diabetes.

Increased hepatic *de novo* lipogenesis induced by fructose is another possible mechanism which promotes obesity [25]. In healthy volunteers there are data of reduced insulin sensitivity of the liver due to high consumption of fructose [26]. A dose-dependent increase in the fat content of the liver has been observed only after several weeks on a diet rich in fructose [27]. In our study body weight gain reflected the amount of food consumed and was the highest in rats given sucrose, followed by the fructose and aspartame group of rats, which indicate that the non-caloric sweetener aspartame may also increase food intake and cause an increase in body weight. Martinez et al. [6] showed that rats who drank water with aspartame and sucralose were fatter than both control and sucrose groups, in spite of the fact that total caloric intake in the sucrose group was higher than in both groups with artificial sweeteners.

The results of human studies show that consumption of artificial sweeteners in beverages at least daily was associated with significantly greater risk of select metabolic syndrome components (36% greater) and type 2 diabetes (67% greater) [28]. Body mass gain and overeating after consumption of products containing artificial sweeteners can be explained by the hypothesis that artificial sweeteners disrupt the body's natural ability to predict the caloric contents of food on the basis of sweet taste, which leads to greater body mass gain through increased food intake during the next meal to compensate the energy deficit [29].

Sweet tastes are known to evoke numerous physiological responses that help to maintain energy homeostasis by signaling the imminent arrival of nutrients in the gut and by facilitating the absorption and utilization of energy contained in food. This failure to anticipate calories and sugar appropriately when they do arrive could ultimately lead to the negative health consequences associated with artificial sweeteners, by impairing the ability of sweetness to predict the arrival of energy in the gut accurately, thereby reducing the efficient utilization of that energy and perhaps weakening the cascade of events that initiate satiety.

Table 1 shows that consumption of sweeteners causes serious disturbances in the lipid profile expressed in significant increased total (Group S) and LDL-cholesterol (Group F and S), TAG (Group F and S), accompanied by impaired glucose homeostasis (Group F and S). In accordance with our results other authors indicate insulin resistance as a major cause of impaired glucose tolerance [4,30,31].

Also in Table 1 are presented the significant elevations of uric acid and AST in Group F and S, and ALT in Group F, compared with the control group. Increased uric acid is considered a minor criterion in the definition of metabolic syndrome and explains the higher incidence of gout, renal calculosis and type 2 diabetes in those patients due to the creation of pre-receptor insulin resistance. Uric acid inhibits the synthesis of the vasodilator nitric oxide and is considered one of the causes of fructose-induced hypertension. According to Douard and Ferraris [32] for this hypertension contribute expression of the glucose transporter protein (GLUT 5), increased intestinal salt reabsorption and reduced renal salt excretion.

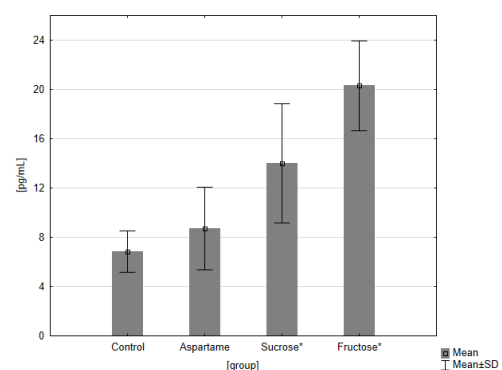


Fig. 2. Levels of plasma UAG at the end of the study period (Mean \pm SD); * $p < 0.05$ compared with the control group.

ALT is an important enzyme found predominately in the liver. Elevated ALT levels correlate strongly with non-alcoholic fatty liver disease and other liver diseases, because significantly elevated activity of ALT in serum

reflects hepatocyte damage. ALT is a more specific indicator of liver inflammation than AST, as AST may also be elevated in diseases affecting other organs.

In our experiment the animals overloaded with sweeteners had higher mean UAG levels than controls in the following order: Group F > Group S > Group A > Group C. Fig. 2 shows significant increase in UAG levels in Group F and Group S. After consumption of fructose (that gives less satiety) or sucrose activation of ghrelin production and AMP-activated protein kinase (AMPK) participation in its peripheral metabolic effects has been described [15]. Kola and Korbonits summarize data about intracellular mechanisms of the appetite-inducing effect of ghrelin in the hypothalamus: AMPK is a key metabolic enzyme involved in appetite regulation. Calmodulin kinase 2 has been identified as an upstream kinase of AMPK and a key mediator in the effect of ghrelin on AMPK activity. The fatty acid pathway, hypothalamic mitochondrial respiration, and uncoupling protein 2 have been outlined as downstream targets of AMPK and mediators of ghrelin's appetite stimulating effect. The increase of UAG levels in Group A, although not significant, may be due to a weaker natural relationship between sweet taste and caloric intake after aspartame consumption [29].

Positive correlations were found between plasma UAG levels and several biochemical parameters: serum glucose ($r = 0.65$; $p = 0.0002$), total cholesterol ($r = 0.46$; $p = 0.01$), LDL-cholesterol ($r = 0.55$; $p = 0.002$), serum triglycerides ($r = 0.47$; $p = 0.01$), uric acid ($r = 0.67$; $p = 0.0001$), AST ($r = 0.5$; $p = 0.006$), ALT ($r = 0.22$; $p = 0.01$), as well as between UAG levels and mesenteric fat depot weights ($r = 0.48$; $p = 0.01$). Negative correlation was observed between UAG and HDL-cholesterol levels ($r = -0.43$; $p = 0.02$). The observed correlations suggest some important links between levels of UAG and the general metabolic parameters. Unfortunately, lack of relevant data from similar experiments in literature limits available resources for discussion.

CONCLUSIONS

The relative elevation of unacylated ghrelin after fructose ingestion in the present study suggests that a failure of fructose to suppress ghrelin could contribute to decreased satiety and increased food intake during long-term fructose consumption.

The development of morphological and metabolic disturbances and an increase of UAG in experimental rats after 8-week consumption of fructose, sucrose and aspartame demonstrates the need to limit the intake of these sweeteners in

humans as an opportunity to reduce the current global epidemic of obesity.

Further studies need to elucidate the physiological role of ghrelin in the regulation of food intake. It is possible that detailed understanding of the mechanisms, involved in this process, can lead to the development of therapeutic strategies for some serious nutritional disorders.

REFERENCES

1. L. Tappy, K.A. Le, *Physiol. Rev.*, **90**(1), 23 (2010).
2. K.L. Stanhope, S.C. Griffen, B.R. Bair, M.M. Swarbrick, N.L. Keim, P.J. Havel, *Am. J. Clin. Nutr.*, **87**(5), 1194 (2008).
3. J.S. Lim, M. Mietus-Snyder, A. Valente, J.M. Schwarz, R.H. Lustig, *Nat. Rev. Gastroenterol. Hepatol.*, **7**(5), 251 (2010).
4. K.L. Stanhope, P.J. Havel, *Curr. Opin. Lipidol.*, **19**(1), 16 (2008).
5. C. Gardnem, J. Wylie-Rosett, S. Gidding, L.M. Steffen, R.K. Johnson, D. Reader, A. Lichtenstein, *Diabetes Care*, **35**(8), 1798 (2012).
6. C. Martinez, E. Gonzalez, R.S. Garcia, G. Salas, F. Constantino-Cassas, L. Marcias, *Open Obes. J.*, **2**, 116 (2010).
7. W.D. Pierce, C.D. Heth, J.C. Owczarczyk, J.C. Russell, S.D. Proctor, *Obesity*, **8**, 1969 (2007).
8. S.E. Swithers, T.L. Davidson, *Behav. Neurosci.*, **122**(1), 161 (2008).
9. H.J. Jang, Z. Kokrashvili, M.J. Theodorakis, *Proc. Natl. Acad. Sci. USA*, **104**(38), 15069 (2007).
10. A. Scrafani, *Proc. Natl. Acad. Sci. USA*, **104**(38), 14887 (2007).
11. M. Korbonits, A.B. Grossman, *Eur. J. Endocrinol.*, **1**, 67 (2004).
12. M. Nakazato, N. Murakami, Y. Date, M. Kojima, H. Matsuo, K. Kangawa, S. Matsukura, *Nature*, **409**, 194 (2001).
13. L.M. Seoane, M. Lopez, S. Tovar, F.F. Casanueva, R. Senaris, C. Dieguez, *Endocrinology*, **144**, 544 (2003).
14. D.E. Cummings, J.Q. Purnell, R.S. Frayo, K. Schmidova, B.E. Wisse, D.S. Weigle, *Diabetes*, **50**, 1714 (2001).
15. B. Kola, M. Korbonits, *J. Endocrinol.*, **202**, 191 (2009).
16. M. Tschop, D.L. Smiley, M.L. Heiman, *Nature*, **407**, 908 (2000).
17. J.S. Davies, P. Kotokorpi, S.R. Eccles, S.K. Barnes, P.F. Tokarczuk, S.K. Allen, H.S. Whitworth, I.A. Guschina, B.A. Evans, A. Mode, J.M. Zigman, T. Wells, *Mol. Endocrinol.*, **23**, 914 (2009).
18. B. Ozcan, J.C. Sebastian, M.M. Negggers, A.R. Miller, H. Yang, V. Lucaites, T. Atribat, S. Allas, M. Huisman, J.A. Visser, A.P. Themmen, E.J. Sijbrands, P.J. Delhanty, A.J. van der Lely, *Eur. J. Endocr.*, **170**(6), 799 (2013).
19. P.J. Delhanty, S.J. Negggers, A.J. van der Lely, *Endocr. Dev.*, **25**, 112 (2013).

20. K.L. Teff, S.S. Elliott, M. Tschop, T.J. Kieffer, D. Rader, M. Heiman, *J. Clin. Endocrinol. Metab.*, **89**(6), 2963 (2004).
21. M.D. Lane, S.H. Cha, *Biochem. Biophys. Res. Commun.*, **382**(1), 1 (2009).
22. A. Lindqvist, A. Baelemans, C. Erlanson-Albertsson, *Regul. Pept.*, **150**(1-3), 26 (2008).
23. M.E. Bocarsly, E.S. Powell, N.M. Avena, B.G. Hoebel, *Pharmacol. Biochem. Behav.*, **97**(1), 101 (2010).
24. B.N. Bursać, A.D. Vasiljević, N.M. Nestorović, N.A. Veličković, D.D. Vojnović Milutinović, G.M. Matić, A.D. Djordjevic, *J. Nutr. Biochem.*, **25**, 446 (2014).
25. A.C. Rutledge, K. Adeli, *Nutr. Rev.*, **65**, 13 (2007).
26. D. Faeh, K. Minehira, J.M. Schwarz, R. Periasamy, S. Park, L. Tappy, *Diabetes*, **54**(7), 1907 (2005).
27. V. Lecoultre, L. Egli, G. Carrel, F. Theytaz, R. Kreis, P. Schneiter, A. Boss, K.A. Le, K. Zwyzgart, M. Bortolotti, C. Boesch, L. Tappy, *Obesity*, **21**(4), 782 (2013).
28. J.A. Nettleton, J.F. Polak, R. Tracy, G.L. Burke, D.R. Jacobs, *Am. J. Clin. Nutr.*, **90**(3), 647 (2009).
29. S.E. Swithers, T.L. Davidson, *Behav. Neurosci.*, **122**(1), 161 (2008).
30. G. D'Angelo, A.A. Elmarakby, D.M. Pollock, D.W. Stepp, *Hypertension*, **46**(4), 806 (2005).
31. C. Catena, G. Giacchetti, M. Novello, G. Colussi, A. Cavarape, L.A. Sechi, *Am. J. Hypertens.*, **16**, 973 (2003).
32. V. Douard, R.P. Ferraris, *J. Physiol.*, **591**(2), 401 (2013).

НЕАЦИЛИРАН ГРЕЛИН В ПЛАЗМАТА НА ПЛЪХОВЕ ВИСТАР СЛЕД КОНСУМАЦИЯ НА ФРУКТОЗА, ЗАХАРОЗА И АСПАРТАМ

Р. В. Сандева¹, А. А. Димитрова², Т. Т. Тачева¹, С. М. Михайлова¹, Г. Н. Сандева¹, Т. И. Влайкова¹

¹Медицински факултет, Тракийски университет, ул., „Армейска“ 11, 6000 Стара Загора (България)

²Медицински Университет, ул., „Климент Охридски“ 1, 5800 Плевен (България)

Постъпила на 21 януари 2013 г.; Коригирана на 21 май, 2013 г.

(Резюме)

Неацилираният грелин (НАГ) съставлява 80-90% от циркулиращия орексигенен хормон грелин. Проучванията показват, че и двете форми - ацил грелин (АГ) и НАГ могат да медирират периферни биологични функции и НАГ може да действа като мощен функционален инхибитор на грелина. Целта на настоящото изследване бе да се проследят промените в НАГ в плазмата на контролна (К) и три експериментални (фруктозна, захарозна и аспартамна) групи плъхове и да се сравнят с някои морфологични и метаболитни показатели. Проведе се 8 седмично проследяване на 28 мъжки плъхове Вистар (по 7 в група), получаващи питейна вода (група К), 15% фруктозен (група Ф), 10% захарозен (групата З) и 0.3% аспартамен разтвор (група А). Установи се увеличение на средната телесна маса в следния ред: захарозна група > фруктозна група > аспартамна група > контролна група. Намери се сигнификантна разлика в теглото на мезентериалната мастна тъкан при група Ф в сравнение с група К. Регистрира се увеличение на НАГ и на основните метаболитни параметри (глюкоза, триглицериди, общ и LDL-холестерол, AST, ALT) при фруктозната и захарозна групи в сравнение с контролите. Промени в някои метаболитни маркери се установиха и в аспартамната група. В заключение, резултатите от настоящото изследване показват, че увеличената консумация на подсладители като захароза, фруктоза и аспартам води до повишаване на неацилирания грелин, което от своя страна може да предизвика промени в регулацията на приема на храна с последващо развитие на затлъстяване, метаболитни нарушения и хронични неинфекциозни заболявания.

Effects of new neurotensin analogue on brain activity in rat Parkinson's disease model

A. Popatanasov¹, S. Stoeva¹, M. Lazarova¹, L. Traikov², T. Pajpanova³, R. Kalfin¹, L. Tancheva^{1,4*}

¹Institute of Neurobiology, Bulgarian Academy of Sciences, Acad. G. Bonchev Str., bl. 23, Sofia, Bulgaria

²Faculty of Medicine, Medical University, Zdrave Str. 2, Sofia, Bulgaria

³Institute of Molecular Biology, Bulgarian Academy of Sciences, Acad. G. Bonchev Str., bl. 21, Sofia, Bulgaria

⁴Weston Visiting Professor of Weizmann Institute of Sciences, Herzl Str. 234, Rehovot, Israel

Received November 4, 2016; Revised March 6, 2017

Parkinson's disease (PD) results in progressive loss of dopamine (DA) neurons and leads to motor disturbances. The close connection between DA-ergic neurotransmitter system and Neurotensin (NT) mediation was established which suggests that NT is associated with PD. It was reported that NT can modulate the activity of DA neurons. Our previous data demonstrated significant CNS-activity in rodents of some new NT-analogues. The aim of the present study was to evaluate the potential modulating effect of new NT-analogue on the behavior and brain activity in rats with model of PD which was induced in male Wistar rats via unilateral injections of 6-hydroxydopamine (6-OHDA) and verified by apomorphine test. Animals were treated 5 days with new NT analogue in effective doses after the induction of PD. Standard test was used for evaluation of neuro-muscular coordination (Rot-a-Rod). Electroencephalography (EEG) was used also to measure the brain activity in inactive condition. Experimental data were processed by Student-Fisher, or Mann-Whitney or Kruskal–Wallis test. Rot-a-rod test showed gradual improvement in the motor performance of NT-treated animals compared to control PD- rats with saline. In the same time EEG showed differences in spectral composition and patterns above the lesioned areas and their hemispheric counterparts in the PD-animals treated with NT-analogue compared to saline treated PD-rats and similarities with the healthy ones. In conclusion the new NT-analogue is promising anti-PD agent and deserves further investigations.

Keywords: Neurotensin, Parkinson's disease, 6-hydroxydopamine, Neuropeptides, EEG

INTRODUCTION

Parkinson's disease (PD) results in progressive loss of dopaminergic (DA) neurons and leads to motor disturbances. The close connection between DA-ergic neurotransmitter system and Neurotensin (NT) mediation was established which suggests that NT is associated with PD. Moreover, it was reported that NT modulates the activity of DA neurons [1]. NT is a 13-amino-acid peptide and it is demonstrated that in mammals there are NT-containing neurons in some specific central nervous structures as striatum and substantia nigra pars reticulata [2]. The biologic effect of NT results from the specific interaction of the peptide with three different cell-surface receptors referred to as NTS1, NTS2 and NTS3/sortilin [3]. Like many other neuropeptides, NT acts as a neuromodulator in the nervous system and it has been shown to modulate DA release in some brain regions including striatum [4].

However, peptides are rapidly metabolized in plasma by endogenous peptidases, terminating their

biologic effect under physiologic conditions. Therefore, the object of the present study is a promising long-lasting NT analogue - NT2 (Fig. 1) synthesized by Pajpanova et al [5].

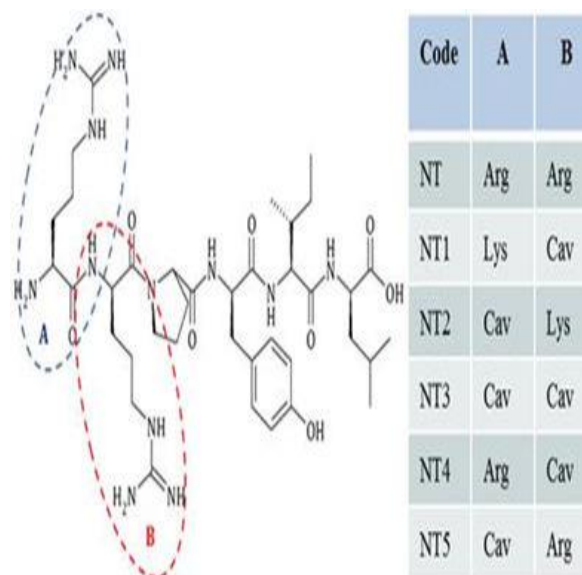


Fig. 1. The amino acid sites replaced with non-proteinogenic amino acids in synthesized NT-analogue [5].

The basic sequence was fragment 8–13 of NT, to which some modifications were introduced in

* To whom all correspondence should be sent:
E-mail: lyubkatancheva@gmail.com; and_atanasov@abv.bg

order to improve its metabolic stability. The terminal Arg unit (position A on Fig. 1) was replaced by canavanine (Cav), which was described as a non-proteinogenic Arg analogue [6]. Our previous unpublished data demonstrated significant CNS-activity in rodents of some NT-analogues.

We aimed to evaluate the potential modulating effect of one new NT-analogue on the brain activity on experimental model of PD in rats.

EXPERIMENTAL

All experiments have been performed according to the "Principles of laboratory animal care" (NIH publication No. 85-23), and the rules of the Ethics Committee of the Institute of Neurobiology, Bulgarian Academy of Sciences (registration FWA 00003059 by the US Department of Health and Human Services).

Synthesis of NT analogue:

NT-analogue (with code NT2) was synthesized through standard solid-phase method. The peptide chain was assembled on a Wang resin (0.1 mmol scale) with a Fmoc/Boc strategy. The coupling of each amino acid was performed in the presence of 3 mol excess of Fmoc-amino acid, 3 mol excess of HOBt, 3 mol excess of DIC and 5 mol excess of DIPEA. The cleavage step from the resin and the final deprotection of all remained protecting groups was done in a standard cocktail containing TFA, TIPS, thioanisole, and water [5].

Surgical procedures

A total of 24 male Wistar rats weighting 220 – 250 g at the beginning of the experiment were used. They were housed four per cage in a temperature-controlled room with a 12 h light-dark cycle, and had free access to food and water. The rats were anaesthetized with chloralhydrate (400 mg/kg, i.p), their heads were shaved and skin cleaned with 70 % alcohol. Then the rats were positioned in the stereotaxic apparatus. PD model was induced via unilateral and stereotaxic injection of 2 µl/20 µg 6-hydroxydopamine (6-OHDA, (Sigma-Aldrich, USA)); calculated as free base, dissolved in ice-cold saline with 0.02 % ascorbic acid) in right striatum [7]. The target coordinates for striatum were AP=0; LR=3.5; H=+5 from the bregma, according to the stereotaxic atlas [8]. Sham operated (SO) group received only 2 µl saline. The wound was closed and animals returned to their cages for recovering.

All animals were treated intraperitoneally (i.p.) for 5 days before the induction of PD and were divided into the following groups: SO and 6-OHDA controls were treated daily with 5 ml/kg saline, 6-OHDA + NT and 6-OHDA + NT2 were treated with 5 mg/kg i.p, NT and NT2, respectively.

In postmortem histological analysis it was found that the lesions were located in the striatum.

Electrode implantation

The electrodes were implanted above the lesioned areas with stereotaxic coordinates AP=0; LR=3.5; H=+0.5 from the bregma and symmetrically to the skull midline above their hemispheric counterparts [8]. After the implantation the electrodes were fixed permanently with acrylic to the skull bone. The common ground wire was above the right hemisphere. The position of the electrodes was controlled on custom stereotaxic apparatus with Narishige micromanipulators (Narishige, Japan).

Postmortem histological analysis was performed to validate electrode placement and neurotoxin effects. The placements of the electrodes was in most cases in deep cortical layers AP=0; LR=3.5; H=+0.5-1.5 [8].

Behavioral tests

Rot-a-Rod standard test was used for evaluation of changes in neuro-muscular coordination [9]. On the second week after surgery each animal was placed on a gyrotory (7 rot/min) and the number of falls for 3min was determined.

Electrophysiological methods

Cortical electroencephalography (cortical EEG) was used to measure the brain activity in inactive condition in calm lab environment. The cortical EEG recordings were sampled at 200 Hz with bio-amplifier ETH-255 iWorx (iWorx, USA). To reduce the stress of the new environment the animals were placed in the restrainer for 20 minutes few times in the 2-3 days before the recording sessions on the second week after the surgery.

Immediately after all tests the animals were euthanized via CO₂ inhalation for biochemical and histological studies.

Statistical and data analysis

Results were expressed as means ± SEM. Experimental data were analyzed by Student's *t*-test or Mann-Whitney test, or Kruskal-Wallis test. Differences were considered significant at *P* < 0.05.

Cortical EEG spectral analysis algorithms were used for processing of the data according to Shi *et*

al., 2015 [10]. Schematically the EEG analysis of power spectra was performed in the following order. For a given behavioral recording period, all available EEG recordings were divided in segments of 2 seconds. A second order notch filter at frequency 50 Hz (AC) component was applied to remove power line noise. For every segment estimation of the power spectral density was performed by using the fast Fourier transform. Afterward we normalized the data, using relative power spectra by dividing the power spectral density in the different frequency ranges for each segment to the total power in the segment.

RESULTS AND DISCUSSION

Rot-a-rod test was performed at the second week post lesion (Fig. 2).

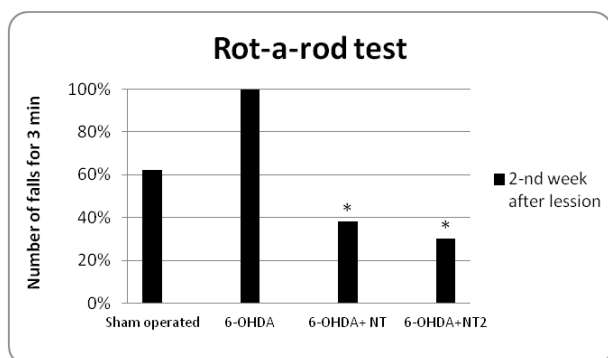


Fig. 2. Effects of new NT analogue and NT as referent on the Rot-a-rod test in rat model of Parkinson's disease; $n = 6$, * $P < 0.05$ vs 6-OHDA group

While the untreated 6-OHDA group showed an average of 1.33 falls/3min, all animals in 6-OHDA group, treated with NT and new NT analogue (NT2) demonstrated a gradual improvement in motor performance. They showed a significant decrease in number of falls for 3 minutes on the second week after lesion (NT by 62, 41% and NT2 by 69, 92%) in compare to saline treated 6-OHDA group.

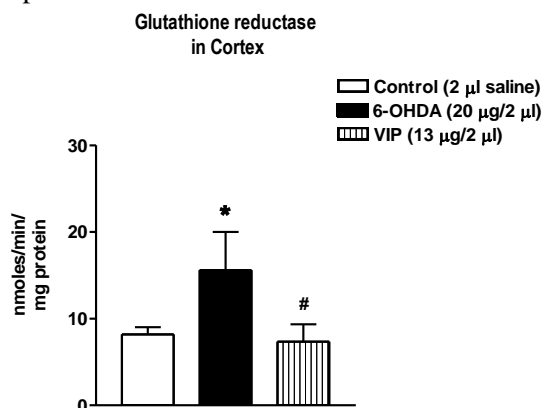


Fig. 3. Levels of glutathione reductase in the cortex of control and Parkinsonian rats. $n = 5$; * $P < 0.05$ vs Control; # $P < 0.05$ vs 6-OHDA-lesioned rats.

EEG analysis: Cortical EEGs showed differences in spectral composition and patterns above the lesioned areas and their hemispheric counterparts in the animals treated with NT-analogue compared to saline treated PD-rats and similarities with the SO ones (Fig. 4 and Fig. 5).

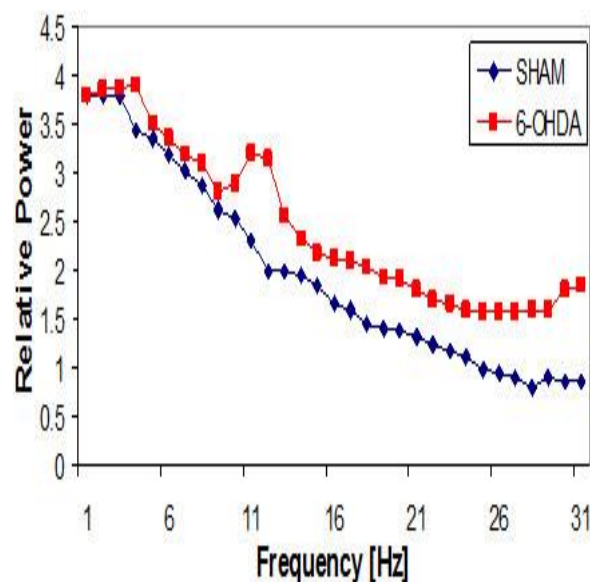


Fig. 4. Power spectra of the sham operated rats vs 6-OHDA (Parkinsonian) group

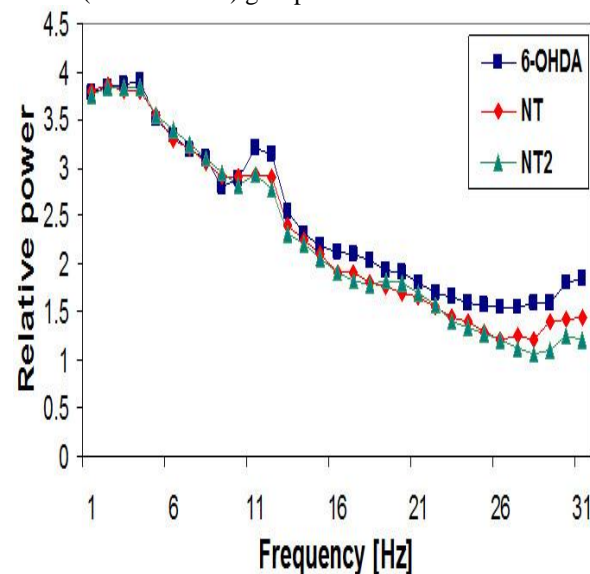


Fig. 5. Power spectra of the NT or NT-analogue treated rats vs 6-OHDA (Parkinsonian) group

The comparison between non-treated 6-OHDA and SO groups showed large increase in the power density through all beta band oscillations range (10-31 Hz) in the former group. Here the beta band oscillations range (10-31 Hz) refers to a new PD specific EEG bands classification proposed by

Gatev et al. in 2006 [12]. These differences were especially well pronounced in the ranges (8-13 Hz) and (26-31 Hz). The averaged values from the sessions for the peak frequency 13 Hz were 3.14 ± 0.16 , 2.1 ± 0.12 and for peak frequency 30 Hz were 1.86 ± 0.17 and 0.85 ± 0.13 for the 6-OHDA and SO group accordingly.

Comparing the NT and NT-analogue treated groups to the non-treated one there was a general decrease in the beta oscillations bandwidth with more pronounced peaks at frequency range of lower (9-13Hz) and upper beta (28-31Hz). The averaged values from the sessions for the peak frequency 13 Hz were 3.14 ± 0.16 , 2.90 ± 0.14 and 2.78 ± 0.15 ; for peak frequency 30 Hz were 1.86 ± 0.17 , 1.44 ± 0.15 and 1.22 ± 0.13 for the 6-OHDA, NT and NT2 group, respectively. According to the Kruskal–Wallis non-parametric test, $P < 0.05$ the differences at these peaks between the OHDA, NT and NT2 groups were significant with $\chi^2=14,02$ and 14.72 , the differences between NT, NT2 and SO groups also followed this trend with $\chi^2=14,92$ and 14.71 .

The curve pattern of the NT and NT2 treated groups (Fig. 5, 6) was relatively similar in the beta band range except at the above mentioned peaks.

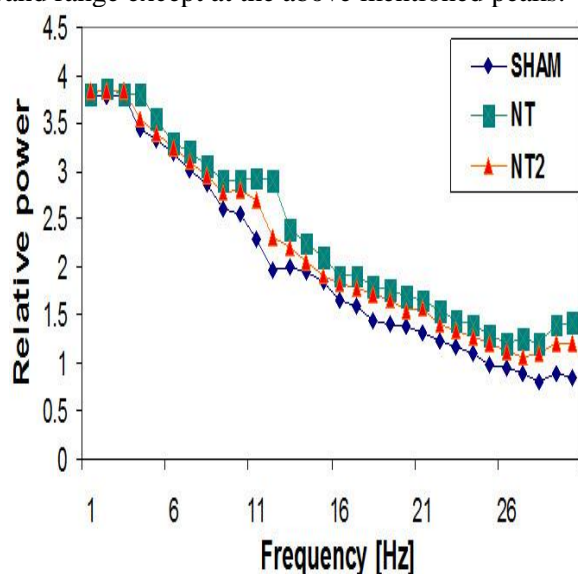


Fig. 6. Power spectra of the NT-analogue treated rats vs sham operated group

The averaged value differences in the frequency range 14-27 Hz were within 0.1 ± 0.05 . Additionally the peaks at 13 Hz and 30 Hz were compared with the Mann-Whitney test and the results showed that the differences were significant at $P < 0.05$ for the former peak.

DISCUSSION

The results of our experiments showed that there was a valuable improvement the motor functions in

both groups of the NT-analogue treated animals over the non-treated 6-OHDA animals which were among the most affected in the PD. The improving effect of NT2 on motor coordination was better than the effect of the referent NT.

Classically EEG oscillations have been grouped into frequency bands as follows: delta (0.5–3.5 Hz), theta (3.5–7.5 Hz), alpha (7.5–12.5 Hz), beta (12.5–30 Hz) and gamma (>30 Hz) [11]. However with the data accumulation from experiments with animal models and patients with PD in 2006 Gatev et al. [12] proposed a new division in the frequency range 3-35 Hz: i). frequencies at the Parkinsonian rest tremor (3-7 Hz) and ii). higher frequencies (10-35 Hz) termed beta band oscillations. Beta band oscillations generally are associated with motor and cognitive functions in normal human and mammal subjects. Our research reconfirms the importance of such specific PD division for EEG since the most pronounced differences in the power spectra were observed in the range of beta band oscillations. In the results of the EEG analysis, the increase in the power density at frequencies 9-13 Hz corresponds to the lower beta bandwidth [12]. Also there's increase in the power density at the frequencies range 26-30 Hz which corresponds to the higher beta-bandwidth. This effect was more pronounced in the NT-treated animals than the NT2-treated ones.

Beta activity is synchronized within and between functionally interconnected circuitries in the basal ganglia, thalamus and cortex. The elevated beta-band activity in the resting brain state showed that the neuromodulatory significance of beta oscillations for information processing in the motor output is impaired in PD rats. Therefore, the dopaminergic medication (or the treatment with NT analogues) reduced the beta-band activity within and between structures of this functional loop in PD rats.

This global increase of absolute power in PD rats is a pathophysiological reaction of dopamine denervation on basal ganglia-thalamo-cortical circuitries. NT analogue-induced modulation of inhibitory basal ganglia output to the thalamus may reduce abnormal thalamo-cortical rhythmicity and normalize high frequency oscillatory power in cortical networks.

The analysis of brain activity recordings in the animal groups treated with NT and NT-analogue showed power spectral pattern closer to the one of the SO or healthy rats and the effects of the NT analogue were better in comparison to the referent NT.

Based on these results we can suggest that the newly synthesized NT-analogue facilitates the survival and compensatory functioning of more DA-neurons in the 6-OHDA affected brain regions and the preservation of the networks in which they are engaged.

CONCLUSION

The new NT-analogue is promising anti-PD agent and deserves further exploration and development.

REFERENCES

1. F. St-Gelais, C. Jomphe, L. É. Trudeau. *J. Psychiatr. Neurosci.*, **31**, 229 (2006).
2. M. N. Castel, P. Morino, P. Frey, L. Terenius, T. Hökfelt. *Neuroscience*, **55**, 833 (1993).
3. J. P. Vincent, J. Mazella, P. Kitabgi. *Trends Pharmacol. Sci.*, **20**, 302, (1999).
4. E. Hetier, A. Boireau, P. Dubedat, J. C. Blanchard. *Naunyn Schmiedebergs Arch. Pharmacol.*, **337**, 13 (1988).
5. T. Dzimbova, S. Stoeva, L. Tancheva, A. Georgieva, R. Kalfin, T. Pajpanova, in: Peptides 2014, (Proc. 33rd European Peptide Symp., Sofia, 2014). E. Naydenova, T. Pajpanova, D. Danalev (Eds). European Peptide Society, Sofia, p. 260, (2014).
6. T. Dzimbova, T. Pajpanova, in: L-Arginine in Clinical Nutrition. V. B. Patel, V. R. Preedy, R. Rajendram. (eds), Springer-Verlag, Berlin,, p. 55 (2016).
7. S. Przedborski, M. Levivier, H. Jiang, M. Ferreira, V. Jackson-Lewis, D. Donaldson, D. M. Togasaki. *Neuroscience*, **67**, 631 (1995).
8. G. Paxinos, C. Watson, The Rat Brain in Stereotaxic Coordinates, Elsevier Acad. Press, San Diego, (2005).
9. J. H. Rosland, S. Hunskaar, K. Hole. *Pharm. Toxicology*, **66**, 382 (1990).
10. Y. F. Shi, Y. Han, Y. T. Su, J. H. Yang, Y. Q. Yu. *PLoS ONE*, **10**, e0130130 (2015).
11. W. Freeman, R. Q. Quiroga. *Springer Science & Business Media* (2012).
12. E. Stein, I. Bar-Gad, *Exp. Neurol.*, **245**, 52 (2013).
13. A. K. Engel, P. Fries. *Curr. Opin. Neurobiol.*, **20**, 156 (2010).

ЕФЕКТИ НА НОВ НЕВРОТЕНЗИНОВ АНАЛОГ ВЪРХУ МОЗЪЧНАТА АКТИВНОСТ ПРИ МОДЕЛ НА БОЛЕСТТА НА ПАРКИНСОН ПРИ ПЛЪХОВЕ

А. Попатанасов¹, С. Стоева¹, М. Лазарова¹, Л. Трайков², Т. Пайпанова³, Р. Калфин¹, Л. Танчева^{1,4*}

¹Институт по невробиология, БАН, ул. Акад. Г. Бончев, бл. 23, София 1113, България

²Факултет по медицина, Медицински университет, ул. Здраве 2, София, България

³Институт по молекулярна биология, БАН, ул. Акад. Г. Бончев, бл. 21, София 1113, България

^{4*}Уестон гост-професор във Вайцман научни институти, ул. Херцел 234, Реховот, Израел

Постъпила на 4 ноември, 2016 г.; Коригирана на 6 март 2017 г.

(Резюме)

Болезтта на Паркинсон (БП) причинява прогресивна загуба на допаминергични (DA) неврони и води до двигателни нарушения. Установена е тясна връзка между допаминергичната невротрансмитерна система и невротензиновата (НТ) медиация, което предполага, че НТ е свързан с болестта на Паркинсон. Данните в научната литература показват, че НТ може да модулира активността на DA-неврони. В наши предишни изследвания беше установено, че някои от новосинтезираните от нас НТ-аналози могат да оказват силно влияние върху активността на ЦНС при гризачи.

Целта на настоящото изследване бе да се изследва потенциалния модулаторен ефект на нов НТ-аналог върху поведението и мозъчната активност при плъхове с модел на БП, който бе индуциран при мъжки плъхове от породата Wistar чрез едностранно инжектиране на 6-хидроксидопамин (6-OHDA) и бе верифициран чрез апоморфинов тест. Животните бяха третирани в продължение на 5 дни с НТ или с новия НТ-аналог с ефективни дози след индукция на БП. Стандартен Рот-а-род тест бе използван за оценка на нервно-мускулната координация. Електроенцефалография (ЕЕГ) бе използвана за измерване на мозъчната активност в неподвижно състояние. Експерименталните данни бяха обработени с теста на Стюдънт-Фишер, на Ман-Уитни или на Крускал-Уоллис. Резултатите от Рот-а-род теста показаха постепенно подобрене на двигателната дейност при третираните с НТ-животни в сравнение с контролните животни с БП, третирани с физиологичен разтвор. В същото време ЕЕГ показва наличие на разлики в спектъра и патерните над областите с индуцирани лезии при болните животни третирани с НТ или НТ-аналог в сравнение с плъховете с БП, третирани с физиологичен разтвор, и сходства със здравите опитни животни. В заключение може да се каже, че новия НТ-аналог е обещаващ антипаркинсонов агент и заслужава по-нататъшно изследване.

Effects of nociceptin neurotransmitter system on nociception in 6-hydroxydopamine model of hemiparkinsonism in rat

H. Nocheva^{1*}, E. Naydenova², N. Pavlov², A. Bocheva¹

¹ Medical University of Sofia, Department of Pathophysiology

² University of Chemical Technology and Metallurgy, Department of Organic Chemistry

Received September 20, 2016; Revised February 20, 2017

The aim of the present study was to investigate the analgesic effects of N/OFQ(1-13)NH₂, JTC-801 (a NOP receptor antagonist) and a newly synthesized analog on analgesia in a 6-hydroxydopamine model of hemiparkinsonism in rats.

The experiments were carried out on male Wistar rats (180-200g at the time of the surgery). Right-sided hemiparkinsonism has been induced by stereotaxic microinjection of 6-hydroxydopamine into the ventrolateral striatum. Experiments started 15 days after surgery. All the evaluated substances were injected intraperitoneally. Changes in nociception were measured by paw-pressure test and adopted as a sensitivity indicator.

The results showed that N/OFQ(1-13)NH₂ and the newly synthesized analog decreased the pain threshold compared to the control animals. JTC-801 led to a more expressed decrease in pain threshold compared to N/OFQ(1-13)NH₂ and the analog.

We tried to elucidate the participation of the nociceptinergic mediator system in the sensory disorders in Parkinson's disease. The results obtained suggest that the effect is more a modulating one, since the NOP-receptor agonist and the antagonist led to unidirectional changes that differ in magnitude. We assume that the nociceptinergic system is involved in sensory modulation in the adopted model of hemiparkinsonism.

Keywords: nociceptin, N/OFQ(1-13)NH₂, JTC-801, NOP ligands, analgesia, Parkinson disease model

INTRODUCTION

Parkinson disease (PD) is the second most common age-related progressive neurodegenerative disease after Alzheimer's disease. Described first by James Parkinson in 1817 in his monograph "Essay on the Shaking Palsy", more than a century had to pass before its central pathological feature was discovered. In 1958 Arvid Carlsson made the discovery of dopamine (DA) in the mammalian brain. Then the pathologic hallmark of PD was established to be a degeneration of dopaminergic neurons in the substantia nigra pars compacta (SNpc). Loss of SNpc neurons leads to striatal DA deficiency. This neurotransmitter regulates excitatory and inhibitory outflow of the basal ganglia [1, 2] and is responsible for the major symptoms of PD resulting from the depletion of striatal dopamine [2-4].

From a clinical point of view PD is characterized principally by the syndrome of bradykinesia, tremor, rigidity, and postural instability.

Along with the motor dysfunction there is an increasing recognition of non-motor symptoms in PD patients, some of which may precede the onset of motor symptoms by many decades. Non-motor

symptoms such as pain, dementia, anxiety, and depression are common in PD [5].

As a common problem in PD pain can either be directly caused by PD or secondary - due to other reasons [6]. The exact mechanisms of the phenomenon have still to be elucidated.

Different studies report a prevalence of pain in PD between 40 and 85% [7-13]. The variation in prevalence rates may be related to inclusion criteria, to definition of pain or to differences in patient population across centers. Specific features of pain including its localization were evaluated in some studies [14, 15].

Pain is reported by nearly half of patients with PD and its prevalence is higher than in general population [8- 12]. Furthermore PD patients' cases are reported with pain symptoms antedating the onset of motor symptoms [10, 16]. Other non-motor dysfunctions, like olfactory dysfunction, are even considered as a useful diagnostic marker of preclinical PD, because pathological changes are recognized before the motor symptoms' development [17].

The heptadecapeptide Nociceptin/Orphanin FQ (N/OFQ) is an endogenous ligand of the opioid-like receptor named ORL₁ or N/OFQ peptide (NOP) receptor, a novel member of the opioid receptor family [18-20]. Through its receptor N/OFQ modulates a number of biological functions in the

* To whom all correspondence should be sent:

E-mail: dr_inna@yahoo.com

central and the peripheral nervous system [20, 21], and is relevant for the modulation of pain perception, locomotion, etc. Its receptor is expressed both spinally and supraspinally in the central nervous system [18, 19].

N/OFQ(1-13)NH₂ is the shortest sequence of the N/OFQ molecule preserving its biological effects [22].

The understanding of the role of the N/OFQ/NOP system depends upon the development of selective and highly potent ligands. Among them are N/OFQ related peptides and small peptides, identified by screening of peptide combinatorial libraries [23].

Based on the templates Ac-Arg-Phe-Met-Trp-Met-Lys-NH₂ (opioid receptor antagonist) [25] and Ac-Arg-Tyr-Tyr-Arg-Trp-Lys-NH₂ (highly potent and selective NOP-receptor agonist) [24] new series of hexapeptides were recently synthesized and evaluated by our group [26, 27].

Our recent results showed that the presence of a N-methyl β^2 -tryptophan residue in position 5 in Ac-Arg-Tyr-Tyr-Arg-Trp-Lys-NH₂ modified the selectivity of the referent peptide. The same group in position 4 did not change the properties of Ac-Arg-Phe-Met-Trp-Met-Lys-NH₂, while the 5-methoxy β^2 -tryptophan residue led to significant changes in peptides' selectivity and affinity [27]. Replacement of Trp with β^2 -tryptophan analogues in position 4 of Ac-Arg-Phe-Met-Trp-Met-Lys-NH₂ led to increased and longer lasting analgesic effect [26].

The interrelations between N/OFQ, its receptor NOP, and PD are subjected to intense research [7, 9]. N/OFQ exerts an inhibitory control on locomotion through inhibition of DA neurons in the SN [28]. Literature data show that dopamine depletion in PD increases N/OFQ expression in SN [1, 29-31].

Most of the scientists investigating PD are still interested in motor dysfunctions and the possibility to influence them. Our interest was focused on sensory dysfunctions and how the nociceptin system influenced pain perception in a rat model of PD.

The effect of N/OFQ(1-13)NH₂, JTC-801 (NOP-receptor antagonist), and novel hexapeptides containing β^2 -tryptophan analogues on nociception were evaluated in a rat model of hemiparkinsonism. The effects of the latter on nociception were compared to N/OFQ(1-13)NH₂.

EXPERIMENTAL

Animals

The experiments were carried out on male Wistar rats (200-240 g at the time of experiments). The rats were housed individually in polypropylene boxes with free access to food and water and maintained in a constant temperature environment (22 \pm 2°C) on a 12 h light/dark cycle (lights on at 6.00 a.m.). The behaviour experiments were carried out between 10:00 a.m. and 1:00 p.m.

The experiments were carried out according to the "Principles of laboratory animal care" (NIH publication No. 85_23, revised 1985), and the rules of the Ethics Committee of the Institute of Neurobiology, Bulgarian Academy of Sciences.

Stereotaxic drug injection into the ventrolateral striatum

After intraperitoneal anaesthesia with a mixture of ketamine (75 mg/kg), acepromazine (0.75 mg/kg) and rompun (4 mg/kg), the animals were placed in a stereotaxic apparatus (Stoelting, USA). Burr hole was drilled at the following coordinates for ventrolateral striatum according to the stereotaxic atlas of Pellegrino and Cushman (1967) relative to bregma: posterior 1.1 mm; lateral 3.1 mm. 8 μ g (free base weight) 6-OHDA (RBI) was dissolved *ex tempore* in 2 μ l of 0.2% ascorbic acid with 0.9% normal saline. 2 μ l of the solution was microinjected through Hamilton micro-syringe (Hamilton, Reno, NV) at a depth of 6 mm below the dura over a period of 2 min (rate 0.5 μ l /m) and the injection cannula was left in place for additional 30 seconds. The control group was microinjected with 2 μ l saline into the same area. Immediately prior to sacrificing the animals were injected with 1 ml 2% Fastgreen dye through the injection cannula.

Injection sites were then anatomically verified post-mortem in 25 mm coronal brain sections cut through the hippocampus by an investigator, blind to the behavioural results. Results from animals with cannulas' placements outside the ventrolateral striatum area were excluded from the statistical analysis.

After the model of right hemiparkinsonism was performed a 15-days period was observed before the beginning of the experiments.

All the evaluated substances were dissolved in sterile saline (0.9% NaCl) solution and were injected intraperitoneally (i.p.). N/OFQ(1-13)NH₂ and the new hexapeptides were administered at a dose of 10 μ g/kg, while JTC-801 was administered at a dose of 0.5 mg/kg. N/OFQ(1-13)NH₂ and JTC-801 were obtained by Sigma. The substituted NOP-

receptor ligands were synthesized in the Department of Organic Chemistry of the University of Chemical Technology and Metallurgy - Sofia [26].

Nociceptive test

Paw-pressure test (Randall-Selitto test). The changes in the mechanical nociceptive threshold of the rats were measured by the use of an analgesiometer (Ugo Basile). Increasing pressure (g) was applied to the hind-paw and the value required to elicit a nociceptive responses (a squeak or struggle) was taken as the mechanical nociceptive threshold. A cut-off value of 500 g was observed in order to prevent damage of the paw.

The results were statistically assessed by one-way analysis of variance ANOVA followed by t-test comparison. Values are mean \pm S.E.M. Values of $p \leq 0.05$ were considered to indicate statistical significance.

The experimental procedures were carried out in accordance with the requirements of the Ethical Committee of the Medical University of Sofia.

RESULTS

Nociception in animals with right-side hemiparkinsonism (RSHP) was investigated. The left paw without 6-OHDA lesion was regarded as auto-control (AC).

In the first series of experiments N/OFQ(1-13)NH₂ or the NOP-receptor antagonist JTC-801 was applied to the animals. Measuring the pain threshold started 10 min after injection of the substances.

The left paw (AC) had the higher pain threshold as compared to the control group ($p < 0.01$). Right paws showed higher pain threshold in comparison both to the control ($p < 0.001$) and AC-paws during the whole time investigated (Fig. 1).

On the 10th min after N/OFQ(1-13)NH₂ administration at a dose of 10 μ g/kg the pain threshold was decreased for AC- and RSHP-paws compared to AC- ($p < 0.01$) and RSHP-paws ($p < 0.01$) of animals without the substance respectively. The pain threshold for AC of animals with N/OFQ(1-13)NH₂ on the 10th min was comparable to the controls.

An additional decrease in pain thresholds was observed on the 20th min after N/OFQ(1-13)NH₂ administration for both AC- and RSHP-paws of animals with N/OFQ(1-13)NH₂ compared to the AC- ($p < 0.001$) and RSHP-paws ($p < 0.001$) of animals without the substance respectively.

Compared to the control animals on the 20th min the AC-paws in animals with N/OFQ(1-13)NH₂ showed a tendency toward hyperalgesia ($p < 0.01$), while the pain threshold for RSHP-paws of the same animals was comparable to the controls (Fig. 1).

Hence, N/OFQ(1-13)NH₂ affected pain perception both in auto-control paws and the RSHP ones. The nociceptive effects were more pronounced and pain thresholds of both the estimated paws were lower than the controls on the 20th min of the evaluation (Fig. 1).

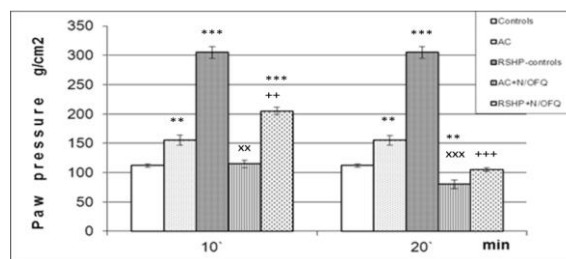


Fig. 1. Effects of N/OFQ(1-13)NH₂ (10 μ g/kg, i.p.) on the pain threshold in animals with experimental 6-OHDA-RSHP. The results are represented as mean values \pm S.E.M. AC and RSHP-animals were compared to controls (^{***} $p < 0.001$; ^{**} $p < 0.01$); AC with N/OFQ(1-13)NH₂ were compared to controls (^{**} $p < 0.01$) and to AC without the substance (^{xxx} $p < 0.001$; ^{xx} $p < 0.01$); RSHP-animals with N/OFQ(1-13)NH₂ were compared to controls (^{***} $p < 0.001$) and to RSHP-controls (RSHP-animals without N/OFQ(1-13)NH₂) (⁺⁺⁺ $p < 0.001$; ⁺⁺ $p < 0.01$).

Administration of the NOP-receptor antagonist JTC-801 at a dose of 0.5 mg/kg led to a statistically significant decrease in pain threshold both for AC- and the RSHP-paws (Fig. 2). In AC-paws of animals with JTC-801 the nociception increased compared to AC of animals without the substance. On the 10th min the pain threshold of RSHP-paws in animals with JTC-801 was significantly lower than RSHP-paws of animals without the antagonist administration, but higher than the control animals (Fig. 2).

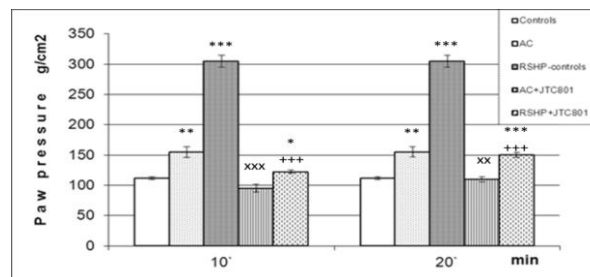


Fig. 2. Effects of JTC801 (0.5 mg/kg, i.p.) on pain threshold in animals with experimental 6-OHDA-RSHP. The results are represented as mean values \pm S.E.M. AC and RSHP-animals were compared to controls

(*** $p < 0.001$; ** $p < 0.01$); AC with JTC801 were compared to controls (** $p < 0.001$; ** $p < 0.01$) and to AC without the substance (xxx $p < 0.001$; xx $p < 0.01$); RSHP-animals with JTC801 were compared to controls (** $p < 0.001$; * $p < 0.05$) and to RSHP-controls (RSHP-animals without JTC801) (++++ $p < 0.001$).

On the 20th min the nociception for AC+JTC-801 was still comparable to the controls and higher than the AC without the antagonist. RSHP-paws of animals with JTC-801 showed lower pain thresholds than the RSHP-paws of animals without the antagonist; values were comparable to the AC (Fig. 2).

Hence, NOP-receptor antagonist JTC 801 affected pain perception of both AC- and RSHP-paws in animals with hemiparkinsonism. The nociceptive effect was most pronounced on the 10th in of the experiment.

Since both the NOP-receptor agonist and the antagonist JTC 801 led to a decrease in the pain thresholds for both AC- and RSHP-paws compared to animals without substances administration, an additional comparison was made for AC- and RSHP-paws with N/OFQ(1-13)NH₂ and JTC 801(Fig. 3).

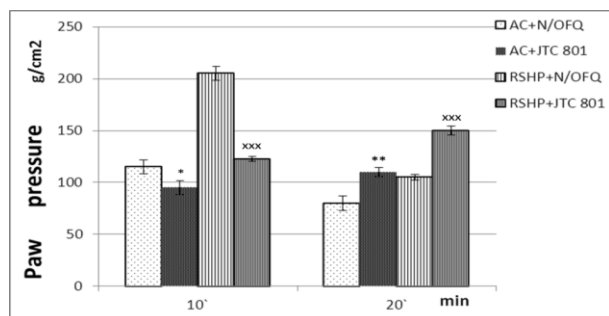


Fig. 3. Comparison between the nociceptive effects of N/OFQ(1-13)NH₂ and JTC801 administrated in AC and RSHP-animals. The results are represented as mean values \pm S.E.M. AC with JTC801 were compared to AC with N/OFQ(1-13)NH₂ (** $p < 0.01$; * $p < 0.05$); RSHP-animals with JTC801 were compared to RSHP-animals with N/OFQ(1-13)NH₂ (xxx $p < 0.001$).

The comparison between the nociceptive effects of N/OFQ(1-13)NH₂ and JTC 801 administered in animals with hemiparkinsonism showed that on the 10th min of the experiment both AC- ($p < 0.05$) and RSHP-paws ($p < 0.001$) of animals with the NOP-receptor antagonist had lower pain thresholds, while on the 20th min AC- ($p < 0.01$) and RSHP-paws ($p < 0.001$) of animals with the NOP-receptor agonist had the lower pain thresholds (Fig. 3).

An additional series of experiments was conducted with first JTC801 administration (0.5 mg/kg, i.p.) and 10 min later N/OFQ(1-13)NH₂ (10 μ g/kg, i.p.) administration in animals with

experimental RSHP. The results were represented in two figures – one for the AC-paws (Fig. 4) and one for the RSHP-paws (Fig.5).

On the 10th min of the experiment the Paw pressure test showed that the pain threshold for AC+ N/OFQ(1-13)NH₂ + JTC801 was comparable to the controls, the AC + N/OFQ(1-13)NH₂, and the AC + JTC801.

On the 20th min of the experiment the nociception for AC + N/OFQ(1-13)NH₂ + JTC801 was increased in respect to controls ($p < 0.001$, AC without any substances ($p < 0.001$), and AC with the antagonist ($p < 0.01$), but was comparable to the AC with N/OFQ(1-13)NH₂ (Fig. 4).

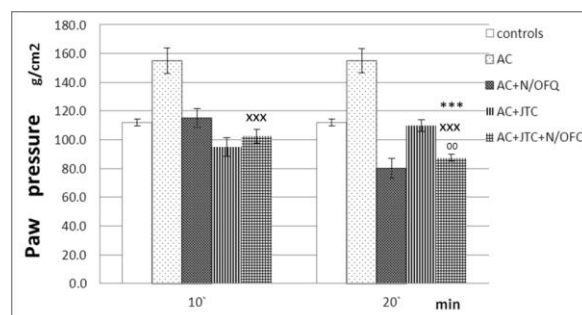


Fig. 4. Effects of N/OFQ(1-13)NH₂ (10 μ g/kg, i.p.) applied after JTC801 (0.5 mg/kg, i.p.) on the pain threshold in auto-control (AC) animals with experimental 6-OHDA-RSHP. The results are represented as mean values \pm S.E.M. AC-animals with both JTC801 and N/OFQ(1-13)NH₂ were compared to controls (** $p < 0.001$), to AC without any substances (xxx $p < 0.001$), to AC with N/OFQ(1-13)NH₂ (without statistically relevant difference), and to AC with JTC801 (00 $p < 0.01$).

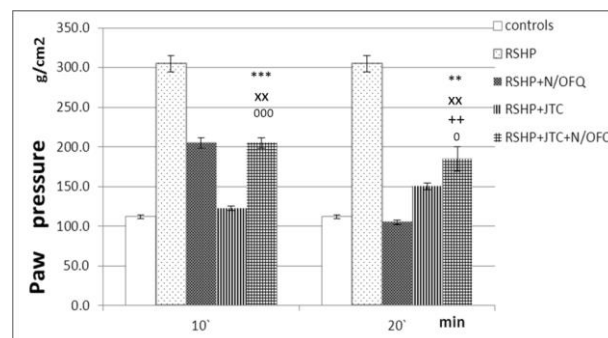


Fig.5. Effects of N/OFQ(1-13)NH₂ (10 μ g/kg, i.p.) applied after JTC801 (0.5 mg/kg, i.p.) on the pain threshold in animals with experimental 6-OHDA-RSHP. The results are represented as mean values \pm S.E.M. RSHP-animals with both JTC801 and N/OFQ(1-13)NH₂ were compared to controls (** $p < 0.001$; ** $p < 0.01$); to RSHP without any substances (xx $p < 0.01$); to RSHP with N/OFQ(1-13)NH₂ (++++ $p < 0.01$), and to RSHP with JTC801 (000 $p < 0.001$; 0 $p < 0.05$).

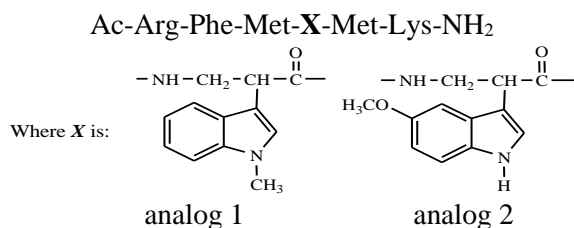
As to RSHPpaws+N/OFQ(1-13)NH₂+JTC801, the pain threshold on the 10th min was comparable

to RSHP-paws of animals with N/OFQ(1-13)NH₂. The nociception for RSHP-paws in animals with both N/OFQ(1-13)NH₂ and JTC801 was decreased compared to the controls (p<0.001) and the RSHP-paws of animals with JTC801(p<0.001), but increased in comparison to RSHP-paws of animals without any substances (p<0.01).

On the 20th min the pain threshold of RSHP-paws + N/OFQ(1-13)NH₂ +JTC801 was still lower than RSHP-paws of animals without any substances (p<0.01), but was higher than controls (p<0.01) and animals with the NOP receptor agonist (p<0.01) and antagonist (p<0.05) separately administered (Fig. 5).

In another series of experiments we investigated the effects on nociception of two newly synthesized hexapeptides modified in 4th position with β²-tryptophan analogs containing methyl group (analog 1) and methoxy group (analog 2) in the indole functional group.

The novel hexapeptides containing β²-tryptophan analogues have the following sequences:



Analog 1's administration in animals with hemiparkinsonism did not change AC-paws' pain threshold during the whole period of observation compared to AC-paws in animals without the substance. Analog 2's administration led to a decrease in AC-paws' pain threshold compared to AC-paws of animals without the substance (p<0.01) only on the 20th min of the evaluated period (Fig. 6).

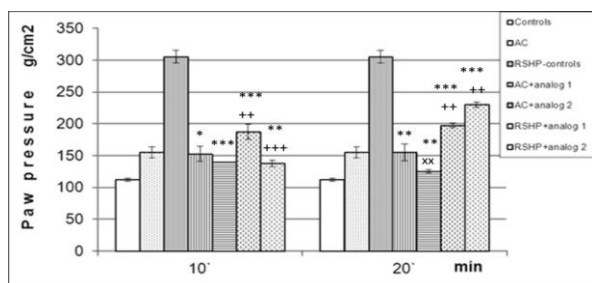


Fig. 6. Effects of hexapeptides 1 and 2 (10 µg/kg, i.p.) on pain threshold in animals with experimental 6-OHDA-RSHP. The results are represented as mean values ± S.E.M. AC with analogs 1 and 2 were compared to controls (**p<0.001; *p<0.01; p<0.05) and to AC without the substances (xx p<0.01); RSHP-animals with analogs 1 and 2 were compared to controls

(***p>0.001) and to RSHP without the substances (+++ p<0.001; ++p<0.01).

Analog's injection led to a statistically significant decrease in pain threshold of RSHP-paws compared to RSHP-paws of the animals without substances' administration. After analog 1 an increase of nociception was observed for the whole estimated period in RSHP-paws compared to the same paws in animals without the substance (p<0.01). On the 10th min analog 2 led to a more pronounced decrease in RSHP-paws' pain threshold compared to analog 1. On the 20th min a decrease in nociception was detected for RSHP-paws of animals with analog 2 compared to the same paws of animals with analog 1 and RSHP-paws of animals with analog 2 on the 10th min (Fig 6).

DISCUSSION

Pain is a frequently reported symptom in PD-patients [7-12]. It can be attributed to changes in sensory centers of the brain (primary pain) or can be caused by rigidity, dystonia or dyskinesia (secondary pain) [32].

Over the last decade researchers have extended their interest to objective alteration of sensory information processing. Patients with PD have altered central somatosensory processing [33]. Animal studies suggested that basal ganglia act as a sensory analyzer that integrates and focuses adequate sensory impulses, therefore modulating motor performance [34]. Although the degeneration of dopaminergic neurons in the SNpc is retained to be the pathologic hallmark of PD, and the regulating role of the dopaminergic system in excitatory and inhibitory outflow of the basal ganglia is well established [1, 2], some clinical trials report no correlation between motor symptoms, dopaminergic medication and pain [9, 10]. Some results also suggest that neurodegeneration of other non-dopaminergic basal ganglia neurotransmitter systems may be responsible for the sensory abnormalities in PD [33].

N/OFQ and its receptor represent a neuropeptide system that bears structural and functional analogies with classical opioid systems but possesses a pharmacological profile of its own [20]. NOP receptor expression and binding are widespread throughout the rodent and primate brain, supporting that the N/OFQ-NOP receptor system plays a substantial role in the modulation of central functions such as sensory nociceptive processing, learning and memory, reward, mood, feeding, stress, and movement [21, 35]. Preclinical

and clinical studies revealed a link between N/OFQ and Parkinson's disease [29, 36, 37].

Literature data suggest changes in N/OFQ-NOP receptor system in patients with PD, concerning NOP receptor gene expression [30], N/OFQ expression and release in the SN [31, 37], and N/OFQ levels in the cerebrospinal fluid of parkinsonian patients [37].

It's known that N/OFQ is released from SN GABA neurons [38]. Exogenously administrated N/OFQ inhibits nigrostriatal DA transmission *in vivo* [39] and elevates glutamate (GLU) release in the SN reticulata *in vivo* [40]. Some data suggest an endogenous N/OFQ tone in the regulation of motor functions, and different selective antagonists [20, 41] improve nigrostriatal DA transmission and motor behavior, and inhibit glutamate release from substantia nigra [39, 40, 42].

Since most of the efforts were to establish the effect of N/OFQ on motor functions, our interest was to estimate potential changes in pain perception. Our results showed that experimental hemiparkinsonism in rats led to an increase in pain thresholds both for the paws unilateral (AC) and contralateral to the lesion (experimental-hemiparkinsonism-affected paws) as compared to control animals. Administration of the NOP-receptor agonist decreased the pain thresholds in auto-control paws as well as in experimental-hemiparkinsonism-affected paws of the animals. The pro-nociceptive effect of N/OFQ(1-13)NH₂ has been documented by other research groups [43], while others report the pro-analgesic effect of the substance [44, 45].

Acute pain activates C- and A δ -nociceptive pain fibers, but the presence of the NOP receptor on them hasn't been documented till now. Experimental data rather suggest that the receptor is transported to either the sensory projections endings in laminae II and III, or to the nerve terminals in peripheral tissues [46, 47]. Concentration of N/OFQ-immunoreactivity was detected in fibers that innervate the superficial layers of the dorsal horn and such immunoreactivity was not altered by unilateral dorsal rhizotomy, suggesting that N/OFQ is not predominantly produced in primary afferent neurons whose cell bodies are located in dorsal root ganglia, but rather is produced within the spinal cord [48]. Such observations support the idea that N/OFQ can modulate pain transmission by activating NOP-receptors located in the central nervous system.

An endogenous tone of the N/OFQ has been proposed since NOP-antagonists produced antinociception when given alone [49, 50].

Surprisingly, in our experiments JTC-801 administration alone also led to a decrease in pain threshold for paws both homo- and contralateral to the lesion. Such results can hardly be explained since literature data point out that NOP-receptor antagonists antagonized agonist's effects independently whether pro-analgesic or pro-nociceptive [51]. A possible reason might be that disease-related changes in pain-perception account for the results observed.

A comparison between agonist's and antagonist's effect showed that the latter's pro-nociceptive action occurred earlier, on the 10th min, while N/OFQ(1-13)NH₂ had the more pronounced effect on the 20th min of the experiment both with AC- and RSHP-paws. When N/OFQ(1-13)NH₂ was injected 10 min after JTC-801 the results obtained for the AC on the 20th min were comparable to those for agonist's alone administration, while for RSHP-paws such a relationship was obtained on the 10th min. Additional experiments are needed to discover the complex interrelations underlying pain perception in parkinsonism.

As to the two newly synthesized hexapeptides, the parent molecule Ac-Arg-Phe-Met-Trp-Met-Lys-NH₂ was originally proved to act as an opioid antagonist. The substitution in position 4 with a 5-methoxy β^2 -tryptophan residue conferred to the newly synthesized substance the characteristics of a weak NOP-receptor agonist, while the substitution in the same position with N-methyl β^2 -tryptophan residue did not change the affinity of the parent molecule [27]. Despite nociceptin doesn't interact with opioid receptors [21, 52] some authors showed that nociceptin antagonized some analgesic opioid effects [53] which suggests a potential interrelation between systems involved in nociception and additionally complicates the interpretation of the experimental data obtained. Our experiment showed that the effects of analog 1 (opioid receptor antagonist) on nociception both in AC- and RSHP-paws had no paragon with the dynamic curve of animals with N/OFQ(1-13)NH₂, but changes in pain perception were still observed compared to animals with N/OFQ(1-13)NH₂. Analog 2 (the one with affinity reverted to weak NOP-receptor agonist) showed for AC-paws a dynamic curve similar to the one for AC+N/OFQ(1-13)NH₂. In RSHP-paws such a similarity was not observed, probably due to disease's influence over the pain perception pathways.

CONCLUSION

Our experiments tried to elucidate the participation of the nociceptinergic mediatory

system in the sensory disorders in Parkinson's disease. The effect seemed to be more a modulating one, since NOP-receptor agonist and antagonist led to unidirectional changes that differ in magnitude.

Our data showed that administered alone JTC-801 led to a decrease in pain threshold for paws both homo- and contralateral to the lesion. These results are difficult to explain and aren't supported by any other literature data since now. They point out that NOP-receptor antagonists antagonized agonist's effects independently whether pro-analgesic or pro-nociceptive.

After analogs' injection in animals with experimental Parkinsonism a decrease in pain threshold was observed. Analog 1 increased nociception for the whole estimated period in RSHP-paws of the animals compared to RSHP-paws of the animals without the substance, while analog 2 led to a more pronounced decrease in pain threshold in RSHP-paws compared to analog 1 on the 10th min. On the 20th min a decrease in nociception was detected for RSHP-paws of animals with analog 2 compared to RSHP-paws of animals with analog 1 and RSHP-paws of animals with analog 2 on the 10th min. The results showed that the effects of the two analogs were time-dependent.

The newly synthesized hexapeptides also suggest that there is a possible interrelation between opioid and NOP-receptor pathways in mediation of pain perception in Parkinson's disease.

The authors declare no potential conflict of interest.

Acknowledgments: The study was supported by Grant DTK 02/61 of the National Research Fund, Sofia, Bulgaria.

REFERENCES

1. J.M. Brown, S. Gouty, V. Iyer, J. Rosenberger, B.M. Cox, *J. Neurochem.*, **98**, 495 (2006).
2. T. Simuni, Medscape Neurolog [on line]; www.medscape.com. (2007).
3. K.S. McNaught, C.W. Olanow, *Neurobiol. Aging*, **27**, 530 (2006).
4. P. Jenner, C.W. Olanow, *Neurology*, **66**, S24 (2006).
5. K. R. Chaudhuri, D. G. Healy, A. H. V. Schapira, *Lancet Neurol.*, **5**, 235 (2006).
6. J.I. Sage, *Curr Treat Options Neurol*, **6**, 191 (2004).
7. C.G. Goetz, C. M. Tanner, M. Levy, R. S. Wilson, D. C. Garron, *Mov Disord*, **1**, 45 (1986).
8. A. Lee, R.W. Walker, T.J. Hildreth, W.M. Prentice, *J. Clin. Neurosci.*, **32**, 462 (2006).
9. M. Tinazzi, C. Del Vesco, E. Fincati, S. Ottaviani, N. Smania, G. Moretto, A. Fiaschi, D. Martino, *J. Neurol. Neurosurg. Psychiatry*, **77**, 822 (2006).
10. G. Defazio, A. Berardelli, G. Fabbrini, D. Martino, E. Fincati, A. Fiaschi, G. Moretto, G. Abbruzzese, R. Marchese, U. Bonuccelli, P. Del Dotto, P. Barone, E. De Vivo, A. Albanese, A. Antonini, M. Canesi, L. Lopiano, M. Zibetti, G. Nappi, E. Martignoni, P. Lamberti, M. Tinazzi, *Arch. Neurol.*, **65**, 1191 (2008).
11. L. Nègre -Pagès, W. Rezagui, D. Bouhassira, H. Grandjean, O. Rascol, *Mov Disord*, **23**, 1361 (2008).
12. A.G. Beiske, J.H. Loge, A. Rønningen, E. Svensson, *Pain*, **141**, 173 (2009).
13. H.A. Hanagasi, S. Akat, H. Gurvit, J. Yazici, M. Emre, *Clinical Neurol. Neurosurg.*, **113**, 11 (2011).
14. F. Etchepare, S. Rozenberg, T. Mirault, A.M. Bonnet, C. Lecorre, Y. Agid, P. Bourgeois, B. Fautrel, *Joint Bone Spine*, **73**, 298 (2006).
15. D. Broetz, M. Eichner, T. Gasser, M. Weller, J.P. Steinbach, *Mov Disord*, **22**, 853 (2007).
16. S.S. O'Sullivan, D.R. Williams, D.A. Gallagher, L.A. Massey, L. Silveira-Moriyama, A.J. Lees, *Mov Disord*, **23**, 101 (2008).
17. H. Braak, K. Del Tredici, U. Rub, R. A. de Vos, E. N. Jansen Steur, E. Braak, *Neurobiol Aging*, **24**, 197 (2003).
18. J.C. Meunier, C. Mollereau, L. Toll, C. Suaudeau, C. Moisand, P. Alvinerie, J. Butour, J.C. Guillemont, P. Ferrara, B. Monsarrat, H. Mazaguil, G. Vassart, M. Parmentier, J. Constantini, *Nature*, **377**, 532 (1995).
19. R.K. Reinscheid, H.P. Nothacker, A. Bourson, A. Ardati, R.A. Henningsen, J.R. Bunzow, D.K. Grandy, H. Langen, F.J. Jr Monsma, O. Civelli, *Science*, **270**, 792 (1995).
20. G. Calo', R. Guerrini, A. Rizzi, S. Salvadori, D. Regoli, *Brit. J. Pharmacol.*, **129**, 1261 (2000).
21. J.S. Mogil, G.W. Pasternak, *Pharmacol. Rev.*, **53**, 381 (2001).
22. S. Molinari, V. Camarda, A. Rizzi, G. Marzola, S. Salvadori, E. Marzola, P. Molinari, J. McDonald, M.C. Ko, D.G. Lambert, G. Calo', R. Guerrini, *Brit. J. Pharmacol.*, **168**, 151 (2013).
23. R. Guerrini, G. Calo', R. Bigoni, A. Rizzi, K. Varani, G. Toth, S. Gessi, E. Hashiba, Y. Hashimoto, D.G. Lambert, P.A. Borea, R. Tomatis, S. Salvadori, D. Regoli, *J. Med. Chem.*, **43**, 2805 (2000).
24. C.T. Dooley, C.G. Spaeth, I.P. Berzetei-Gurske, K. Craymer, I.D. Adapa, S.R. Brandt, R.A. Houghten, L. Toll, *J Pharmacol Exp Ther*, **283**, 735 (1997).
25. C.T. Dooley, N.N. Chung, P.W. Shiller, R.A. Houghten, *Proceedings of the National Academy of Sciences of the U.S.A.*, **90**, 10811 (1993).
26. A. Bocheva, H. Nocheva, N. Pavlov, P. Todorov, M. Calmès, J. Martinez, E. Naydenova, *Amino Acids*, **45**, 983 (2013).
27. R. Zamfirova, N. Pavlov, P. Todorov, P. Mateeva, J. Martinez, M. Calmès, E. Naydenova, *Bioorg. Med. Chem. Lett.*, **23**(14), 4052 (2013).
28. R. Viaro, PhD dissertation, University of Ferrara (2007-2009).
29. M. Marti, F. Mela, M. Fantin, S. Zucchini, J.M. Brown, J. Witta, M. Di Benedetto, B. Buzas, R.K.

- Reinscheid, S. Salvadori, R. Guerrini, P. Romualdi, S. Candeletti, M. Simonato, B.M. Cox, M. Morari, *J Neurosci.*, **95**, 9591 (2005).
30. M. Di Benedetto, C. Cavina, C. D'Addario, G. Leoni, S. Candeletti, B.M. Cox, P. Romualdi, *Neuropharmacol.* **56**, 761 (2009).
31. S. Gouty, J.M. Brown, J. Rosenberger, B.M. Cox, *Neuroscience*, **169**, 269 (2010).
32. L. Velaa, K.E. Lyonsb, C. Singerc, A.N. Liebermand, *Parkinsonism&Related Disorders*, **13**, 189 (2007).
33. A. Berardelli, A. Conte, G. Fabbrini, M. Bologna, A. Latorre, L. Rocchi, A. Suppa, *Parkinsonism&Related Disorders*, **18S1**, S226 (2012).
34. H. Boecker, A. Ceballos-Baumann, P. Bartenstein, A. Weindl, H.R. Siebner, T. Fassbender, *Brain*, **122**, 1651 (1999).
35. D.G. Lambert, *Nat Rev Drug Discov*, **7**, 694 (2008).
36. M. Marti, C. Trapella, R. Viaro, M. Morari, *J. Neurosci.*, **27**, 1297 (2007).
37. M. Marti, S. Sarubbo, F. Latini, M. Cavallo, R. Eleopra, S. Biguzzi, C. Lettieri, C. Conti, M. Simonato, S. Zucchini, R. Quatrале, M. Sensi, S. Candeletti, P. Romualdi, M. Morari, *Mov Disord*, **25**, 1723 (2010).
38. C.S. Norton, C.R. Neal, S. Kumar, H. Akil, S.J. Watson, *J. Comp. Neurol.*, **444**, 358 (2002).
39. M. Marti, F. Mela, C. Veronesi, R. Guerrini, S. Salvadori, M. Federici, N.B. Mercuri, A. Rizzi, G. Franchi, L. Beani, C. Bianchi, M. Morari, *J. Neurosci.*, **24**, 6659 (2004).
40. M. Marti, R. Guerrini, L. Beani, C. Bianchi, M. Morari, *Neuroscience*, **112**, 153 (2002).
41. H. Kawamoto, S. Ozaki, Y. Itoh, M. Miyaji, S. Arai, H. Nakashima, T. Kato, H. Ohta, Y. Iwasawa, *J. Med. Chem.*, **42**, 5061 (1999).
42. M. Marti, F. Mela, R. Guerrini, G. Calo, C. Bianchi, M. Morari, *J. Neurosci.*, **91**, 1501 (2004).
43. D. Reiss, J. Wichmann, H. Tekeshima, B.L. Kieffer, A.M. Ouagazzal, *Eur. J. Pharmacol.*, **579**, 141 (2008).
44. S. Katsuyama, H. Mizoguchi, T. Komatsu, C. Sakurada, M. Tsuzuki, S. Sakurada, T. Sakurada, *Peptides*, **32**, 1530 (2011).
45. J. Mika, I. Obara, B. Przewlocka, *Neuropeptides*, **45**, 247 (2011).
46. C. Mollereau, L. Mouldous, *Peptides*, **21**, 907 (2000).
47. G. Monteillet-Agius, J. Fein, B. Anton, C.J. Evans, *J. Comp. Neurol.*, **399**, 373 (1998).
48. M. Riedl, S. Shuster, L. Vulchanova, J. Wang, H.H. Loh, R. Elde, *Neuroreport*, **7**, 1369 (1996).
49. G. Calo, A. Rizzi, D. Rizzi, R. Bigoni, R. Guerrini, G. Marzola, M. Marti, J. McDonald, M. Morari, D. G. Lambert, S. Salvadori, D. Regoli, *Brit. J. Pharmacol.*, **129**, 1183 (2000).
50. G. Calo, A. Rizzi, D. Rizzi, R. Bigoni, R. Guerrini, G. Marzola, M. Marti, J. Mc-Donald, M. Morari, D.G. Lambert, S. Salvadori, D. Regoli, *Brit. J. Pharmacol.*, **136**, 303 (2002).
51. B. Fioravanti, T.W. Vanderah, *Curr. Topics Med. Chem.*, **8**, 1442 (2008).
52. S.Z. Meis, *Neuroscientist*, **9**, 158 (2003).
53. H. Wang, C.B. Zhu, X.D. Cao, G.C. Wu, *Sheng Li Xue Bao*, **50**, 263 (1998).

ЕФЕКТИ НА НОЦИЦЕПТИНОВАТА НЕВРОТРАНСМИТЕРНА СИСТЕМА ВЪРХУ НОЦИЦЕПЦИЯТА ПРИ 6-ХИДРОКСИДОПАМИНОВ МОДЕЛ НА ХЕМИПАРКИНСОНИЗЪМ ПРИ ПЛЪХ

Х. Ночева^{1*}, Е. Найденова², Н. Павлов², А. Бочева¹

¹Катедра по патофизиология, Медицински университет – София

²Катедра по органична химия, Химикотехнологичен и металургичен университет - София

Постъпила на 20 септември, 2016 г.; Коригирана на 20 февруари, 2017 г.

(Резюме)

Целта на настоящето проучване бе изследване ефекта на N/OFQ(1-13)NH₂, JTC-801 (NOP-рецепторен антагонист), както и на новосинтезирани ноцицептинови аналози върху аналгезията при 6-хидроксидопаминов модел на хемипаркинсонизъм при плъхове.

Експериментите бяха проведени върху мъжки плъхове от породата Wistar (180-200 гр по времето на интервенцията). Десностранен хемипаркинсонизъм бе индуциран чрез стереотаксично микроинжектиране на 6-хидроксидопамин във вентролатералния стриатум. Експериментите започваха 15 дена след интервенцията. Изследваните субстанции се въвеждаха интраперитонеално. Промените в ноцицепцията се определяха посредством raw-pressure test.

Резултатите показаха, че N/OFQ(1-13)NH₂ и неговият новосинтезиран аналог понижават болковия праг в сравнение с контролните животни.

Чрез описаните експерименти бе направен опит за изясняване участието на ноцицептин-ергичната система в сетивните нарушения при Паркинсонова болест. Получените резултати показаха, че ефектът ѝ е по-скоро модулаторен, тъй като както агонистът, така и антагонистът на NOP-рецептора показаха еднопосочно повлияване, но в различна степен. Приемаме, че ноцицептин-ергичната система модулира сетивността при изпозвания модел на хемипаркинсонизъм.

Parkinson`s disease: influence of cannabinoid and peptidergic systems on pain

D.S. Kochev*, H.H. Nocheva¹, L. Traikov

Medical University of Sofia, Department of Neurology

¹ *Medical University of Sofia, Department of Pathophysiology*

Received September 20, 2016; Revised February 13, 2017

Parkinson`s disease (PD) results primarily from the death of dopaminergic neurons in the substantia nigra, but it is now clear that its pathogenesis is underlined by interaction of different mediatory systems. The endocannabinoid system (ECS) is vastly distributed in the central nervous system and represents a potential therapeutic approach for a number of neurologic diseases, PD among them. MIF-1 and Tyr-MIF-1`s modulating action on ECS is also of interest as well as ECS and peptides combined effect on pain perception in PD.

Cannabinoids` and neuropeptides` interactions were estimated in a rat model of 6-hydroxydopamine hemiparkinsonism by Paw pressure test.

Anandamide and AM251 influenced pain perception in control animals as well as in animals with experimental PD. MIF-1 and Tyr-MIF-1 modulated ECS in PD while naloxone changed nociception in PD animals compared to controls.

MIF-1 and Tyr-MIF-1 neuropeptides interact with ECS and modulate pain perception.

Keywords: Parkinson`s disease, pain perception, cannabinoid system, MIF-1, Tyr-MIF-1

INTRODUCTION

Parkinson`s disease (PD) first described by James Parkinson in 1817 represents a chronic incurable progressive neurodegenerative condition characterized by predominantly motor disturbances – tremor, rigidity, bradykinesia, and postural disorders [1]. It affects between 1 and 3% of the population over 50 years of age. Its pathological hallmark is specific degeneration of dopaminergic neurons in the substantia nigra pars compacta [2, 3]. The complex integrative system of the basal ganglia in the central nervous system (CNS) comprises substantia nigra, putamen, nucleus caudatus, nucleus accumbens, and globus pallidus. The effectiveness of the system described depends on the synaptic transmission that represents itself the outcome of interaction (and integration) of different neurotransmitters and neuromodulators [4, 5]. Animal studies suggested that basal ganglia play also a role as a sensory analyzer integrating and focusing adequate sensory impulses, and finally modulating motor performance [6]. Such a sensorimotor integration links sensory input to the motor output producing adequate voluntary movements [7], and probably accounts for the pathogenesis of bradykinesia in PD.

Over the last decade researchers have focused their interest on purely sensory functions in PD. Along with motor dysfunctions 75% of PD patients manifest also sensory disorders with pain among them [8]. Living organisms possess a complex

mechanism to control pain sensations. The antinociceptive pathways integrate two interrelated components – an opioid and a non-opioid one [9].

The first component is connected with the opioid system, which comprises the opioid receptors (μ -, δ -, κ -, λ -, σ -) and their endogenous ligands (β -endorphins, enkephalins, and dynorphin) [10]. The non-opioid component of analgesia integrates different neuromodulator/neurotransmitter systems - the adrenergic, the serotonergic, the nitric-oxide, the endocannabinoid systems.

Experimental data support the importance of the endocannabinoid system (ECS) in CNS and the peripheral nervous system. The ECS consists of two types of cannabinoid receptors (CB1 and CB2), their endogenous ligands and the enzyme systems involved in their synthesis and degradation [11].

CB1 predominates in the brain and especially in the basal ganglia. In the last years several experiments proved that the endocannabinoids exerted an important role in the striatum: they influence its normal functions, interact with dopamine and mediate the changes after dopamine depletion [5, 12]. It has been proved that endocannabinoid levels in the striatum increase after dopamine depletion [5, 13]. The role of endocannabinoid and peptidergic neurotransmissions in the pathogenesis of motor dysfunctions in PD has also been confirmed [14, 15].

The peptides of the Tyr-MIF-1 family exert opioid as well as anti-opioid effects [16-18]. MIF-1 and Tyr-MIF-1 have also modulating effect on the dopaminergic neurotransmission [19-23].

* To whom all correspondence should be sent:

E-mail: doctor.kochev@gmail.com

Changes in dopaminergic neurotransmission are undoubtedly crucial to the pathogenesis of motor dysfunctions in PD, and it is also important in modulating pain perception and natural analgesia within supraspinal striatal and extra-striatal regions. Yet there are some evidences questioning the dopaminergic transmission role in pain processing [24]. It is then possible that other non-dopaminergic basal ganglia neurotransmitter systems may account for the sensory abnormalities in PD and thus influence the sensorimotor integration.

In the present study, we evaluated the changes in pain thresholds after injection of: 1) CB-1 agonists and antagonists; 2) MIF-1 and Tyr-MIF-1 neuropeptides; 3) MIF-1 or Tyr-MIF-1 after CB1 agonist. The experiments were performed in a rat model of 6-hydroxydopamine (6-OHDA)-induced Parkinsonism which is one of the most common animal models of PD. 6-OHDA is a hydroxylated analogue of natural dopamine that selectively destroys catecholamine neurons. It also leads to production of reactive oxygen species (ROS) which damage proteins, lipids and DNA, causes mitochondrial inhibition and impairment, and ATP deficiency [25-27].

EXPERIMENTAL

Animals

The experiments were carried out on male Wistar rats (200-240 g at the beginning of study), housed individually in polypropylene cages (40 × 60 × 20 cm) at a temperature-controlled colony room maintained at 21 ± 3 °C under 12:12 h light/dark cycle with lights on at 6:00 a.m. The animals were given free access to tap water and standard rat chow. All procedures were carried out according to the "Principles of laboratory animal care" (NIH publication No. 85_23, revised 1985), and the rules of the Ethics Committee of the Institute of Neurobiology, Bulgarian Academy of Sciences.

Stereotaxic drug injection into the ventrolateral striatum

Rats were anesthetized with intraperitoneal injection of a mixture of ketamine (75 mg/kg), acepromazine (0.75 mg/kg) and rompun (4 mg/kg). The animals were placed in a stereotaxic apparatus (Stoelting, USA). 8 µg (free base weight) 6-OHDA (RBI) was dissolved *ex tempore* in 2 µl of 0.2% ascorbic acid with 0.9% normal saline and 2 µl of the solution was microinjected through Hamilton micro-syringe (Hamilton, Reno, NV) at the following coordinates: AP "4.4 mm, ML

1.2 mm relative to bregma, and DV "7.5 mm from the dura over a period of 2 min (rate 0.5 µl /min) and the injection cannula was left in place for additional 30 seconds.

The control group was microinjected with 2 µl saline into the same area.

Immediately prior to sacrificing, the animals were injected with 1 ml 2% Fastgreen dye through the injection cannula.

Injection sites were then anatomically verified post-mortem in 25 mm coronal brain sections cut through the hippocampus by an investigator, blind to the behavioural results. Results from animals with cannulas' placements outside the ventrolateral striatum area were excluded from the statistical analysis.

Drugs and treatment

All drugs were obtained from Sigma. Anandamide (arachidonoyl ethanolamide, AEA) at a dose 1mg/kg, and AM251 at a dose 1,25mg/kg dissolved in DMSO were injected intraperitoneally (i.p.). MIF-1 and Tyr-MIF-1 were dissolved in sterile saline solution (0.9% NaCl) and injected i.p. at a dose 1mg/kg. When evaluating the neuropeptides' effect on cannabinoids MIF-1 and Tyr-MIF-1 were administered 10 min after anandamide or AM251.

Nociceptive test

Paw-pressure test (Randall-Selitto test). The changes in the mechanical nociceptive threshold of the rats were measured by analgesiometer (Ugo Basile). Increasing pressure (g) was applied to the hind-paw and the value required to elicit a nociceptive response (a squeak or struggle) was taken as the mechanical nociceptive threshold. A cut-off value of 500 g was observed in order to prevent damage of the paw.

Statistical analysis

The results were statistically assessed by one-way analysis of variance ANOVA followed by t-test comparison. Values are mean ± S.E.M. Values of $p \leq 0.05$ were considered to indicate statistical significance.

RESULTS AND DISCUSSION

Left-sided injection of 6-OHDA led to right-sided hemiparkinsonism (RSHP). The right paws of the animals were regarded as RSHP-paws, while the homolateral to the lesion ones were regarded as auto-controls (AC). Animals with saline microinjection were taken in consideration as controls.

The evaluations started 10 min after drugs administration

Estimation of pain thresholds of the control animals, the AC, and the RSHP without any substances administrated showed that AC and RSHP had higher values than controls with RSHP being the highest (Fig. 1).

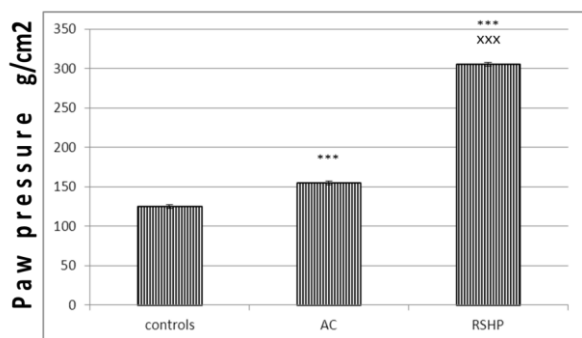


Fig. 1. Pain thresholds of control animals, left auto-control-paws (AC) and right 6-OHDA-hemiparkinsonian paws (RSHP) before evaluated substances administration. The results are represented as mean values \pm S.E.M. AC and RSHP were compared to controls (** $p < 0.001$); RSHP were compared to AC (XXX $p < 0.001$).

After AEA injection the pain thresholds of AC and RSHP increased in respect to the control values. AC+AEA values were higher than AC on the 10th min (Fig. 2), and similarly RSHP+AEA were higher than RSHP (Fig. 3).

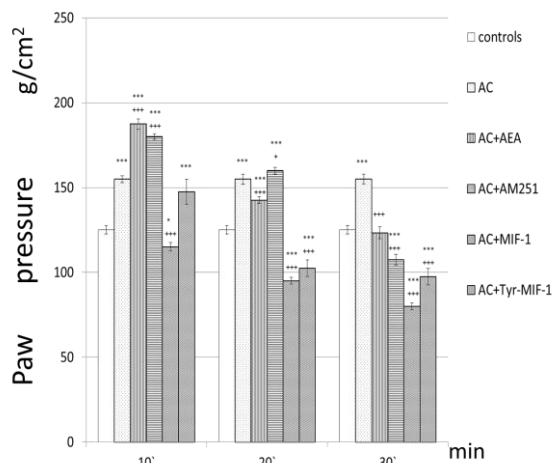


Fig. 2. Effects of AEA (1.0 mg/kg, i.p.), AM251 (1.25 mg/kg, i.p.), MIF-1 (1.0 mg/kg, i.p.), and Tyr-MIF-1 (1.0 mg/kg, i.p.) on the pain threshold of the auto-control (AC) paws in animals with experimental 6-OHDA-RSHP. The results are represented as mean values \pm S.E.M. AC, AC+AEA, AC+AM251, AC+MIF-1, and AC+Tyr-MIF-1 were compared to controls (** $p < 0.001$; ** $p < 0.01$; * $p < 0.05$); AC+AEA, AC+AM251, AC+MIF-1 and AC+Tyr-MIF-1 were compared to AC (XXX $p < 0.001$; + $p < 0.05$).

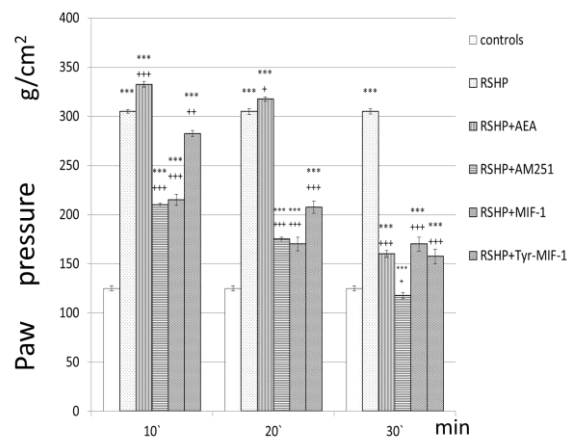


Fig. 3. Effects of AEA (1.0 mg/kg, i.p.), AM251 (1.25 mg/kg, i.p.), MIF-1 (1.0 mg/kg, i.p.), and Tyr-MIF-1 (1.0 mg/kg, i.p.) on the pain thresholds of the lesioned paws in animals with experimental 6-OHDA-RSHP. The results are represented as mean values \pm S.E.M. RSHP, RSHP+AEA, RSHP+AM251, RSHP+MIF-1, and RSHP+Tyr-MIF-1 were compared to controls (** $p < 0.001$); RSHP+AEA, RSHP+AM251, RSHP+MIF-1, and RSHP+Tyr-MIF-1 were compared to RSHP (XXX $p < 0.001$; ++ $p < 0.01$; + $p < 0.05$).

In a second series of experiments the effects of MIF-1 and Tyr-MIF-1 neuropeptides on nociception in rats with 6-OHDA-RSHP were estimated.

Administration of neuropeptides decreased pain thresholds of both AC- and RSHP- paws compared to values of animals without the substances (Fig. 2 and 3).

In AC-paws the effect was statistically relevant on the 20th and the 30th min of the experiment. Both peptides increased nociception in comparison to AC as well as to controls (Fig. 2).

In RSHP-paws the pronociceptive effect after MIF-1 and Tyr-MIF-1 administration was obvious as soon as the 10th min and remained visible for the whole experimental time. Pain thresholds were lower compared to RSHP without substances, but higher than control values (Fig. 3).

In the next series of experiments the modulating effect of the two neuropeptides on the cannabinoid system in animals with experimental hemiparkinsonism was evaluated.

MIF-1 and Tyr-MIF-1 administration after AEA in animals with experimental RSHP led to a statistically relevant decrease in pain thresholds of both AC- and lesioned paws compared to AC- and lesioned paws in animals with AEA without the peptides (Fig. 4 and 5).

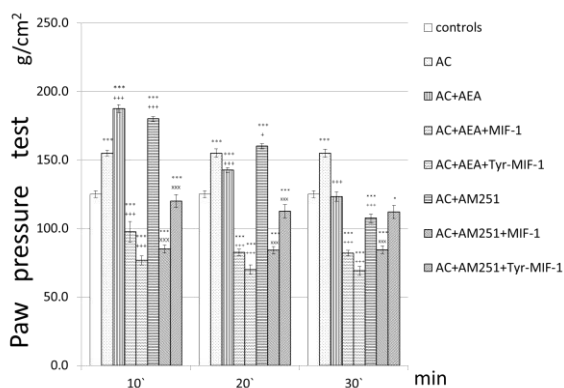


Fig. 4. Effects of MIF-1 and Tyr-MIF-1 (both at 1.0 mg/kg, i.p.) on auto-control (AC) paws pain thresholds of animals with experimental 6-OHDA-RSHP injected with AEA (1mg/kg, i.p.) or AM251 (1.25 mg/kg, i.p.). Results are represented as mean values \pm S.E.M. All thresholds of experimental animals were first compared to controls (** $p < 0.001$; * $p < 0.05$); AC+AEA, AC+AEA+MIF-1 and AC+AEA+Tyr-MIF-1 were compared to AC (++ $p < 0.001$, + $p < 0.05$); AC+AM251+MIF-1 and AC+AM251+Tyr-MIF-1 were compared to AC+AM251(^{xxx} $p < 0.001$).

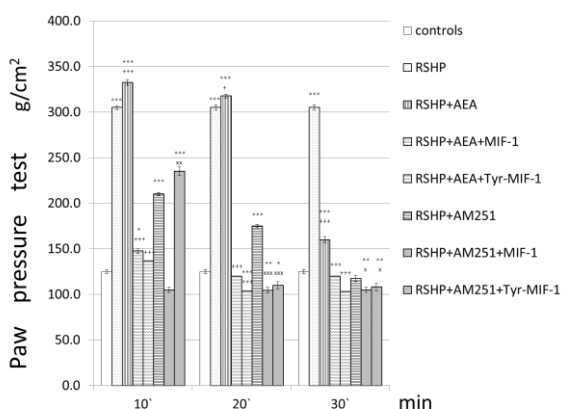


Fig. 5. Effects of MIF-1 and Tyr-MIF-1 (both at 1.0 mg/kg, i.p.) on lesioned paws pain thresholds in animals with experimental 6-OHDA-RSHP injected with AEA (1mg/kg, i.p.) or AM251 (1.25 mg/kg, i.p.). Results are represented as mean values \pm S.E.M. All thresholds of experimental animals were first compared to controls (** $p < 0.001$; ** $p < 0.01$; * $p < 0.05$); AC+AEA, AC+AEA+MIF-1 and AC+AEA+Tyr-MIF-1 were compared to AC (++ $p < 0.001$, + $p < 0.05$); AC+AM251+MIF-1 and AC+AM251+Tyr-MIF-1 were compared to AC+AM251(^{xxx} $p < 0.001$; ^{xx} $p < 0.01$; ^x $p < 0.05$).

AC+peptides-thresholds decreased for the whole estimated period and were lower than controls, AC, and AC+AEA. A tendency toward hyperalgesia was observed (Fig. 4).

RSHP-paws thresholds showed a statistically relevant decrease in respect to RSHP and RSHP+AEA for the whole experimental time.

Compared to controls a slight tendency

toward hyperalgesia was detected only for Tyr-MIF-1 on the 20th and 30th min (Fig. 5).

Administration of the CB1 receptor antagonist AM251 increased the pain thresholds of AC-paws compared to animals without the substance on the 10th and 20th min. Compared to the agonist the CB1 antagonist led to comparable thresholds on the 10th min, and even higher thresholds on the 20th min (Fig. 2).

Vice versa CB1 receptor antagonist decreased the pain thresholds of RSHP+AM251 compared to RSHP and RSHP+AEA for the whole estimated time (Fig. 3).

Administration of MIF-1 or Tyr-MIF-1 after CB1 antagonist AM251 decreased the pain thresholds of the AC-paws (AC+AM251+peptides) on the 10th and the 20th min compared to animals with AM251 but without the peptides (AC+AM251). The effect was more pronounced for MIF-1, and a tendency toward hyperalgesia was observed (fig. 4).

The pain thresholds of RSHP-paws after both AM251 and MIF-1 were lower than controls, RSHP, and RSHP+AM251 without peptides. Tyr-MIF-1 led to increase in the pain thresholds on the 10th min, while for the remaining time the values were comparable to MIF-1's (fig. 5).

The aim of the present study was not to delimitate changes in pain perception from pure motor dysfunctions. Such discrimination would be difficult given the complex interconnection and interrelation between sensory input and motor output underlying motor activity. The purpose was more to establish whether the simultaneous activation of different systems would exert an effect different from the individual effects of each of the systems.

Separately administrated AEA, MIF-1 and Tyr-MIF-1 increased pain thresholds of RSHP-paws of 6-OHDA-hemiparkinsonian animals compared to the controls. Injection of the neuropeptides 10 min after AEA didn't lead to a cumulative effect, but instead decreased the thresholds toward values equal to the controls'. Paradoxically injection of the neuropeptides 10 min after the antagonist AM251 led to comparable effects. This is substantial with findings of other trials searching relief of bradykinesia using CB1 receptor antagonists – the effects were similar to those described also after CB1 receptor agonists and the inhibitors of the endocannabinoid inactivation, the so-called indirect agonists [28-32]. The presence of CB1 receptors in multiple sites, both in excitatory and inhibitory synapses within the basal ganglia circuitry, might explain such controversial findings.

The AC-paws` thresholds showed statistically relevant differences compared to control values even though, being ipsilateral to the 6-OHDA lesion, they should not be affected by changes. We assume that sensorimotor integration accounts for such findings, since sensorimotor actions demand the synchronized activity of medullar, subcortical and cortical levels, making circuits in series and parallel [33].

Comparison between AC- and RSHP-paws showed that the increase in pain thresholds of individually administered AEA and the peptides was more expressed in RSHP-paws than in AC-ones. The decrease in the thresholds after the combined administration of AEA and the peptides was more pronounced for the AC-paws than for RSHP-ones. A possible explanation may be that the cannabinoid signaling through the CB1 receptor type is altered during the course of nigral degeneration in PD [34], changing the impact of the receptor activation. Statistically relevant differences in pain thresholds of AC- and RSHP-paws have also been observed after antagonizing CB1 receptors by AM251. Additional complication for the results` explanation arises from the implication of MIF-1 and Tyr-MIF-1`s receptors. MIF-1 does not interact with opioid receptors and has its own non-opioid receptor [35] and it has been demonstrated that it can modulate the dopaminergic neurotransmission in the nigrostriatal pathways [36]. Tyr-MIF-1 interacts with μ -opioid receptors [35], and AM251 has been demonstrated to act as a μ -opioid receptor antagonist as well as CB1`s one [34]. Such complex interactions account for the final effect.

In conclusion, Parkinson`s disease is characterized by a complex pathogenesis with derangement in many of the mediating and modulating systems. Beside the dopaminergic, the cannabinoid, and the opioidergic, other systems (utilizing adenosine, glutamate, GABA, serotonin) also take part in the basal ganglia circuits [37, 38]. Such a constellation complicates the interpretation of experimental data but gives the opportunity for differential approaches to Parkinson`s disease by targeting the different mediatory systems alone and in combinations.

Acknowledgments: The study was supported by the Bulgarian Scientific Fund, Grant 27/2013.

REFERENCE

1. J. Parkinson, London: Shenwood, Nesly & Jones, 1817.
2. J.L. Lanciego, N. Luquin, J.A. Obeso, *Cold Spring Harb Perspect Med.*, (2012).
3. P. McNamara, K. Stavitsky, E. Harris, O. Szent-Imrey, R. Durso, *Int J Geriatr Psychiatry.*, **25**, 519 (2010).
4. A. Graybiel, *Trends Neurosci.*, **13**, 244 (1990).
5. D.M. Lovinger, *Neuropharmacology*, **58**(7), 951 (2010).
6. H. Boecker, A. Ceballos-Baumann, P. Bartenstein, A. Weindl, H.R. Siebner, T. Fassbender, F. Munz, M. Schwaiger, B. Conrad, *Brain*, **122**, 1651 (1999).
7. G. Abbruzzese, A. Berardelli, *Mov Disord.*, **18**, 231 (2003).
8. K.R. Chaudhuri, D.G. Healy, A.H.V. Schapira, *Lancet Neurol.*, **5**, 235 (2006).
9. J.S. Mogil, W.F. Sternberg, H.J. Balian, C. Liebeskind ohn, B. Sadowski, *Physiol Behav.*, **59**(1), 123 (1996).
10. B.L. Kieffer, *Cell Mol Neurobiol.*, **15**, 615 (1995).
11. A.C. Howlett, F. Barth, T.I. Bonner, G. Cabral, P. Casellas, W.A. Devane, C.C. Felder, M., Herkenham, K. Mackie, B.R. Martin, R. Mechoulam, R.G. Pertwee, *Pharmacol Rev.*, **54**(2), 161 (2002).
12. J. Fernandez-Ruiz, *Br J Pharmacol.*, **156**(7), 1029 (2009).
13. P. Gubellini, B. Picconi, M. Bari, N. Battista, P. Calabresi, D. Centonze, G. Bernardi, A. Finazzi-Agro, M. Maccarrone, *J Neurosci.*, **22**, 6900 (2002).
14. M. García-Arencibia, C. García, J. Fernández-Ruiz, *CNS & Neurological Disorders - Drug Targets.*, **8**, 432 (2009).
15. O. Sagredo, M. García-Arencibia, E. de Lago, S. Finetti, A. Decio, J. Fernández-Ruiz, *Mol. Neurobiol.*, **36**, 82 (2007).
16. C. Hara, A.J. Kastin, *Pharmacol Biochem Behav.*, **24**, 1785 (1986).
17. C. Hara, A.J. Kastin, *Pharmacol Biochem Behav.*, **25**, 757 (1986).
18. R.K. Mishra, S. Chiu, P. Chiu, C.P. Mishra, *Methods Find Exp Clin Pharmacol.*, **5**, 203 (1983)
19. G.E. Drucker, R.F. Ritzmann, L.J. Wichlinski, K. Engh, J.H. Gordon, J.Z. Fields, *Pharmacol Biochem Behav.*, **47**, 141 (1994).
20. R.K. Mishra, E.R. Marcotte, A. Chugh, C. Barlas, D. Whan, R.L. Johnson, *Peptides*, **18**, 1209 (1997).
21. R.K. Mishra, L.K. Srivastava, R.L. Johnson, *Prog Neuropsychopharmacol Biol Psychiatry*, **14**, 821 (1990).
22. M. Rodriguez, P. Barroso-Chinea, P. Abdala, J. Obeso, T. González-Hernández, *Exp Neurol.*, **169**, 163 (2002).
23. L.K. Srivastava, S.B. Bajwa, R.L. Johnson, R.K. Mishra, *J. Neurochem.*, **50**, 960 (1988).
24. G. Defazio, A. Berardelli, G. Fabbrini, D. Martino, E. Fincati, A. Fiaschi, G. Moretto, G. Abbruzzese, R. Marchese, U. Bonuccelli, P. Del Dotto, P. Barone, E.

- De Vivo, A. Albanese, A. Antonini, M. Canesi, L. Lopiano, M. Zibetti, G. Nappi, E. Martignoni, P. Lamberti, M. Tinazzi, *Arch Neurol.*, **65**(9), 1191 (2008).
25. D. Blum, S. Torch, N. Lambeng, M. Nissou, A.L. Benabid, R. Sadoul, J.M. Verna, *Prog Neurobiol.*, **65**(2), 135 (2001).
26. W. Dauer, S. Przedborski, *Neuron.*, **39**(6), 889 (2003).
27. R. Kumar, M.L. Agarwal, P.K. Seth, *J Neurochem.*, **64**, 1701 (1995).
28. J.M. Brotchie, *Mov. Disord.*, **13**, 871 (1998).
29. J.M. Brotchie, *Curr. Opin. Pharmacol.*, **3**, 54 (2003).
30. B. Ferrer, N. Asbrock, S. Kathuria, D. Piomelli, A. Giuffrida, *Eur. J. Neurosci.*, **18**, 1607 (2003).
31. S.H. Fox, B. Henry, M. Hill, A. Crossman, J.M. Brotchie, *Mov. Disord.*, **17**, 1180 (2002).
32. R. Soto-Otero, E. Mendez-Alvarez, A. Hermida-Ameijeiras, A.M. Munoz-Patino, J.L. Labendeira-Garcia, *J Neurochem.*, **77**, 1605 (2000).
33. S. Machado, M. Cunha, B. Velasques, D. Minc, S. Teixeira, C.A. Domingues, J.G. Silva, V.H. Bastos, H. Budde, M. Cagy, L. Basile, R. Piedade, P. Ribeiro, *Rev Neurol.*, **51** (7), 427 (2010).
34. W. Pan, A.J. Kastin, *Peptides*, **28**, 2411 (2007).
35. K.A. Seely, L.K. Brents, L.N. Franks, M. Rajasekaran, S.M. Zimmerman, W.E. Fantegrossi, P.L. Prather, *Neuropharmacology*, **1** (2012).
36. M.C. Ott, R.K. Mishra, R.L. Johnson, *Brain Research*, **737**, 287 (1996).
37. A. Dray, *Journal de Physiologie*, **77**(2-3), 393 (1981).
38. G.L. Gerdeman, J. Fernández-Ruiz, *Cannabinoids and the Brain*, A. Kőfalvi (ed.), 2008, 21.

ПАРКИНСОНОВА БОЛЕСТ: ПОВЛИЯВАНЕ НА БОЛКАТА ОТ КАНАБИНОИДНАТА И ПЕПТИДЕРГИЧНАТА СИСТЕМИ

Д. Кочев^{1*}, Х. Ночева², Л. Трайков¹

¹ Катедра по Неврология, Медицински Университет – София

² Катедра по Патопфизиология, Медицински Университет – София

Постъпила на 20 септември 2016 г.; Коригирана на 13 февруари, 2017 г.

(Резюме)

Паркинсоновата болест (ПБ) е резултат от дегенерация на допаминергичните неврони в substantia nigra, като е изяснено, че в патогенезата на заболяването участват множество взаимодействащи си системи. Ендогенната канабиноидна система (ЕКС) е широко разпространена в централната нервна система и повлияването ѝ представлява потенциален терапевтичен подход при различни патологични неврологични състояния, в т.ч. и ПБ. Модулаторният ефект на пептидите MIF-1 и Tyr-MIF-1 върху ЕКС също представлява интерес, като е ясно и съвместното им влияние върху болковата чувствителност при ПБ.

Съвместното повлияване на болката от страна на канабиноидите и неuropeптидите MIF-1 и Tyr-MIF-1 бе изследвано върху 6-хидроксидопаминов модел на паркинсонизъм у плъх посредством метода Paw pressure test.

Резултатите показаха, че анандамидът и AM251 повлияват болковата перцепция, а MIF-1 и Tyr-MIF-1 модулират ефекта на канабиноидите при ПБ. След антагонизирането на действието на пептидите чрез налоксон болковата перцепция на експерименталните животни се изравни с тази на контролните.

Vasoactive intestinal peptide and Parkinson's disease

R.E. Kalfin^{1*}, M.I. Lazarova¹, P.I. Mateeva¹, L.M. Yankova¹, S.P. Belcheva^{1,2}, R.E. Tashev^{1,3}

¹*Department of Synaptic Signaling and Communications, Institute of Neurobiology, Bulgarian Academy of Sciences, Acad. Georgi Bonchev Str., Bl. 23, 1113 Sofia, Bulgaria*

²*Faculty of Pre-School and Primary School Education, SU "Sv. Kl. Ohridsky", Shipchenski Prohod Str. 69A, 1574 Sofia, Bulgaria*

³*Department of Pathophysiology, Medical University of Sofia, 2 Zdrave Str., 1431 Sofia, Bulgaria*

Received October 11, 2016; Revised January 21, 2017

Using an experimental model which represents the end-stage of Parkinson's disease (PD), we aimed to measure the levels of glutathione reductase activity, lipid peroxidation in different brain regions (cortex, hippocampus) in the presence or absence of vasoactive intestinal peptide (VIP), which is a 28-amino acid "brain-gut" neuropeptide. A total of 20 male Wistar rats, weighing 150-200 g at the time of surgery, were randomly divided in groups and housed in cages with free access to rat chow and water. The rats were anesthetized with chloral hydrate (400 mg/kg, i.p.), had their heads shaved, and placed in a stereotaxic apparatus. The target coordinates were: AP = +0.2; LR = -3.0; H = -5.6 according to the stereotaxic atlas. The experimental group received an injection of 20 µg/2 µl of 6-hydroxydopamine (6-OHDA), while the control group received an injection of 2 µl saline. All injections were made into the right striatum area by a Hamilton microsyringe at a rate of 1 µl/min. The wound was closed with stainless steel clips and the rat was allowed to recover before being returned to its cage. VIP (13µg/2 µl) was injected into the right striatum 15 min before 6-OHDA lesion and at the 21st day after surgery. Our experiments showed that the neuropeptide decreased the activity of enzyme glutathione reductase and inhibited lipid peroxidation in the experimental model of Parkinson's disease counteracting in such way against membrane damage and ameliorating the cell viability.

Keywords: Vasoactive intestinal peptide; Parkinson's disease; Lipid peroxidation; Glutathione reductase

INTRODUCTION

Parkinson's disease (PD) is currently regarded as the most common neurodegenerative disorder of the aging brain after the Alzheimer's dementia. Clinically, PD is characterized by the tremor at rest, slowness of voluntary movements, rigidity, and postural instability [1]. The cardinal biochemical abnormality in PD is the profound deficit in brain dopamine level, primarily, but not exclusively, attributed to the loss of neurons of the nigrostriatal dopaminergic pathway [2]. Parkinson's disease is among the causes of death in people over 65 years of age. For example the boxing legend Muhammad Ali, who recently died, suffered from PD. Although the pathogenesis of PD are still unknown there is increasing evidence that impairment of mitochondrial function, oxidative damage and inflammation are certainly involved [3]. Some new knowledge about this neurodegenerative disorder has been achieved by in vitro and in vivo experimental models of PD [2]. Most popular of them is 6-hydroxydopamine-induced Parkinson's disease rat model. Injected stereotaxically, unilateral in striatum this dopamine analog

produces a more protracted retrograde degeneration of nigrostriatal system which can last from 1-3 weeks after lesion [4, 5]. The toxic effects of 6-OHDA are due to enhanced oxidative stress, inflammatory processes and apoptosis [6].

We aimed to measure the levels of glutathione reductase activity and lipid peroxidation in different brain regions (cortex, hippocampus) in the presence or absence of vasoactive intestinal peptide (VIP) by means of 6-hydroxydopamine-induced PD rat model, which represents the end-stage of this disease.

EXPERIMENTAL

All experiments have been performed according to the "Principles of laboratory animal care" (NIH publication No. 85-23), and the rules of the Ethics Committee of the Institute of Neurobiology, Bulgarian Academy of Sciences (registration FWA 00003059 by the US Department of Health and Human Services).

Surgical procedures

A total of 20 male Wistar rats, weighing 150-200 g at the time of surgery, were randomly divided in groups and housed in cages with free access to rat chow and water. The rats were anesthetized with

* To whom all correspondence should be sent:
E-mail: reni_kalfin@abv.bg

chloral hydrate (400 mg/kg, i.p.), had their heads shaved, and placed in a stereotaxic apparatus. The scalp was cleaned with a jodine solution, incised on the midline and a burr hole was drilled through the skull at the appropriate location. The target coordinates were: AP = +0.2; LR = -3.0; H = -5.6 according to the stereotaxic atlas [7]. The experimental group received an injection of 20 µg/2 µl of 6-OHDA (Sigma-Aldrich, St. Louis, MO, USA; calculated as free base, dissolved in ice-cold saline with 0.02 % ascorbic acid) while the control group received an injection of 2 µl saline. All injections were made into the right striatum area by a Hamilton microsyringe at a rate of 1 µl/min. The needle was left in place an additional 2 min before being slowly withdrawn. The wound was closed with stainless steel clips and the rat was allowed to recover before being returned to its cage. VIP (13µg/2µl) was injected in the striatum twice: 15 min before 6-OHDA lesion and at the 21st day after surgery.

Biochemical procedures

Protein content was measured by the method of Lowry et al. [8]. Lipid peroxidation in the absence and in the presence of an inducer (5.10–5 M Fe²⁺) was determined by the amount of the thiobarbituric acid-reactive substances, formed in fresh preparations for 60 min at 37°C [9]. The absorbance was read at 532 nm against appropriate blanks; the absorbance at 600 nm was considered to be a non-specific baseline and was, therefore, subtracted from A532. Glutathione reductase activity was measured by the method of Pinto & Bartley [10].

Statistical analysis

Results were expressed as mean ± S.E.M. Statistical analysis of the data was performed by Student's *t*-test for unpaired data or by one-way analysis of variance (ANOVA) followed by Newman-Keuls post-test. *P*-values < 0.05 were considered significant.

RESULTS AND DISCUSSION

It is considered that the reduction of apomorphine-induced rotational behavior in 6-OHDA-lesioned rats is the most utilized method for assessing functional efficacy in this model of PD [11]. The rotations were measured according to a method as described previously [12]. Briefly, the animals were allowed to habituated for 10 min and then 1 min after the injection (apomorphine 2mg/kg, s.c), the rotations were counted. Number of rotations was monitored in a cylindrical container

(a diameter of 33 cm and a height of 35 cm) for 1 hour in a dimly-lighted room. The ipsilateral rotation was not significant (Fig. 1). All animals that made more than 30 turns/30 min opposite to the lesion were selected for the experiments (Fig.2).

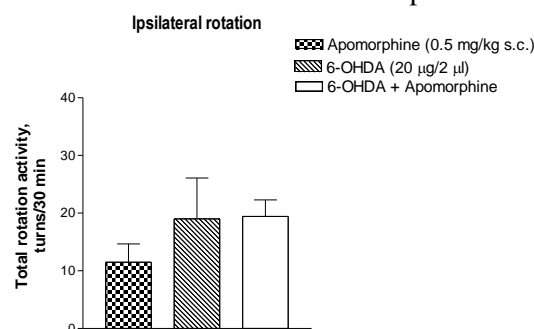


Fig. 1. Rotational behavior of rats to the same side of the lesion.

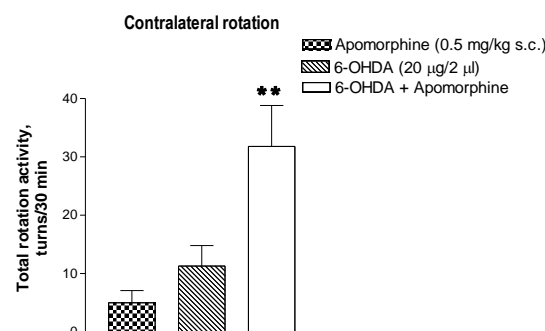


Fig. 2. Rotational behavior of rats opposite to the side of the lesion; ***P* ≤ 0.01.

Vasoactive intestinal peptide (13µg/2 µl), injected into the right striatum 15 min before 6-OHDA lesion and at the 21st day after surgery decreased the levels of enzyme glutathione reductase significantly in the cortex (Fig. 3) and lowered it in the hippocampus of Parkinsonian rats (Fig. 4).

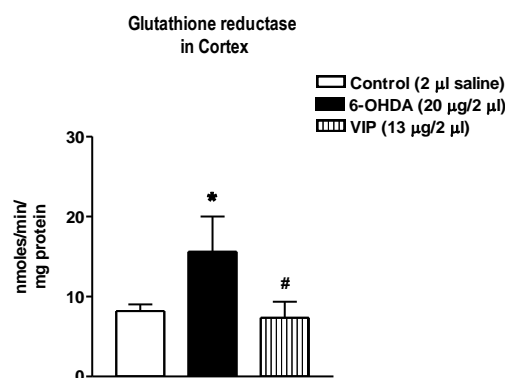


Fig. 3. Levels of glutathione reductase in the cortex of control and Parkinsonian rats. *n* = 5; **P* ≤ 0.05 vs Control; #*P* ≤ 0.05 vs 6-OHDA-lesioned rats.

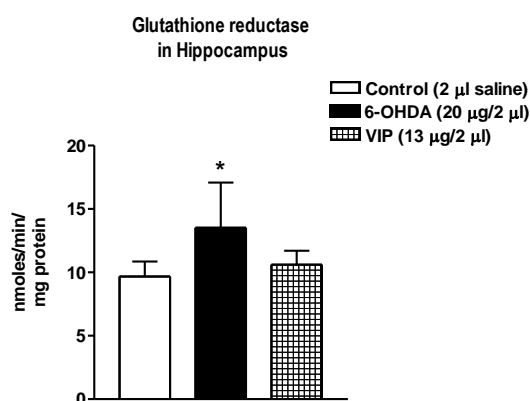


Fig. 4. Levels of glutathione reductase in the hippocampus of control and Parkinsonian rats. $n = 5$; * $P \leq 0.05$ vs Control.

Vasoactive intestinal peptide is now recognized as a major neuropeptide in the brain, with function ranging from neurotransmission to neuromodulation with neurotrophic properties. This neuropeptide is found in high concentration in the cerebral cortex, amygdala, striatum, hippocampus, midbrain [13]. VIP is a peptide with potent anti-inflammatory, anti-oxidant and anti-apoptotic effect [14, 15, 16]. Neuroprotective effect of vasoactive intestinal peptide in a mouse model of Parkinson's disease by blocking microglial activation was shown [17]. Moreover, the team of professor IllanaGozes reported neuroprotection by stearyl-Nle17-VIP, vasoactive intestinal peptide, and NAP (8aa) against the buthioninesulfoximine, a selective inhibitor of glutathione synthesis, suggesting that the mechanism may involve the glutathione antioxidant system [18]. Our results are in accordance with the above-mentioned hypothesis, showing that vasoactive intestinal peptide decreased the activity of the enzyme glutathione reductase in a Parkinson's disease model.

We also demonstrated that VIP (13 µg/2 µl) decreased lipid peroxidation both in cortex (Fig. 5) and hippocampus (Fig. 6) in the 6-hydroxydopamine-induced rat model of Parkinson's disease. Lipid peroxidation is a crucial step in the pathogenesis of several disease states in adult and infant patients. The reactive oxygen species (hydroxyl radical, hydrogen peroxide etc.) readily attack the polyunsaturated fatty acids of the fatty acid membrane, initiating a self-propagating chain reaction. The destruction of membrane lipids and the end-products of such lipid peroxidation reactions are especially dangerous for the viability of cells, even tissues. Since lipid peroxidation is a self-propagating chain-reaction, the initial oxidation of only a few lipid molecules can result in significant tissue damage. Lipid peroxidation has

been implicated in Parkinson's disease. It was also reported that both VIP and PACAP have neuroprotective effects in PD models by inhibiting the production of inflammatory mediators [19]. Vasoactive intestinal peptide family was proved to be a therapeutic target for Parkinson's disease [20].

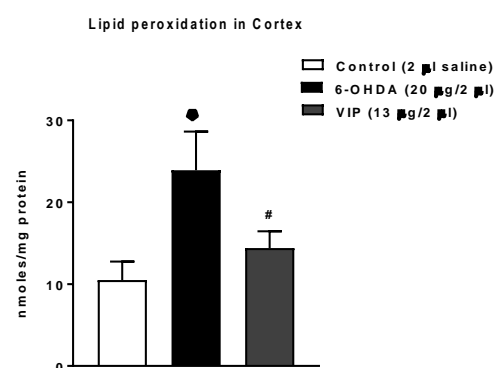


Fig. 5. Levels of Fe-ascorbat induced lipid peroxidation in the cortex of control and Parkinsonian rats. $n = 4$; * $P \leq 0.05$ vs Control; # $P \leq 0.05$ vs 6-OHDA-lesioned rats.

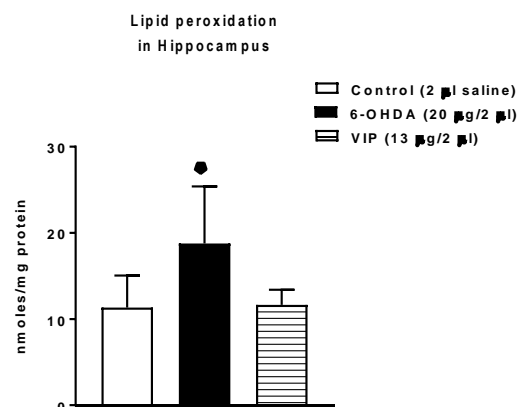


Fig. 6. Levels of Fe-ascorbat induced lipid peroxidation in the hippocampus of control and Parkinsonian rats. $n = 4$; * $P \leq 0.05$ vs Control.

CONCLUSION

In the present study we demonstrated that vasoactive intestinal peptide decreased the activity of enzyme glutathione reductase and inhibited lipid peroxidation in the experimental model of Parkinson's disease counteracting in such way against membrane damage and ameliorating the cell viability.

REFERENCES

1. S. Fahn, S. Przedborski, Merritt's Neurology (L. P. Rowland, ed) New York, Lippincott Williams & Wilkins, 2000, 679.
2. W. Dauer, S. Przedborski, *Neuron*, **39**, 889 (2003).

3. C. Henchcliffe, M.F. Beal, *Nat. Clin. Pract. Neurol.* **4**, 600 (2008).
4. S. Przedborski, M. Levivier, H. Jiang, M. Ferreira, V. Jackson-Lewis, D. Donaldson, D.M. Togasaki, *Neuroscience*, **67**, 631 (1995).
5. H. Sauer, W.H. Oertel, *Neuroscience*, **59**, 401 (1994).
6. X. Mu, G. He, Y. Cheng, X. Li, B. Xu, G. Du, *Pharmacol. Biochem. Behav.*, **92**, 642 (2009).
7. T. Pellegrino, G. Cushman, *The Rat Brain in Stereotaxic Coordinates*, New York, Academic Press (1967).
8. O.H. Lowry, N.J. Rosenbrough, A.L. Farr, R.J. Randal, *J. Biol. Chem.*, **193**, 265 (1951).
9. F. Hunter, J. Gebinski, P. Hoffstein, J. Weinstein, A. Scott, *J. Biol. Chem.*, **238**, 828 (1963).
10. R.E. Pinto, W. Bartly, *Biochem. J.*, **112**, 109 (1969).
11. R.J. Mandel, *Exp. Neurology*, **161**, 212 (2000).
12. M. Roghani, A. Niknam, M. R. Jalali-Nadoushan, Z. Kiasalari, M. Khalili, T. Baluchnejadmojarad, *Brain Res. Bull.*, **82**, 279 (2010).
13. S.I. Said, *J. Endocrinol. Invest.*, **9**, 191 (1986).
14. M. Delgado, C. Abad, C. Martinez, M. G. Juarranz, A. Arranz, R. P. Gomariz, *J. Mol. Med.* **80**, 16 (2002).
15. R. P. Gomariz, C. Martinez, C. Abad, J. Leceta, M. Delgado, *Curr. Pharm. Des.*, **7**, 89 (2001).
16. S.I. Said, K.G. Dickman, *Regul. Pept.*, **93**, 21 (2000).
17. M. Delgado, D. Ganea, *FASEB J.*, **17**, 944 (2003).
18. D. Offen, Y. Sherki, E. Melamed, M. Fridkin, D.E. Brenneman, I. Gozes, *Brain Res.*, **854**, 257 (2000).
19. D.R. Staines, *Medical Hypotheses*, **69**, 1208 (2007).
20. E. Gonzalez-Rey, A. Chorny, A. Fernandez-Martin, N. Varela, M. Delgado. *Expert Opin. Ther. Targets*, **5**, 923 (2005).

ВАЗОАКТИВЕН ИНТЕСТИНАЛЕН ПЕПТИД И БОЛЕСТ НА ПАРКИНСОН

Р. Е. Калфин^{1*}, М. И. Лазарова¹, П. И. Матеева¹, Л. М. Янкова¹, С. П. Белчева^{1,2}, Р. Е. Ташев^{1,3}

¹Направление синаптична сигнализация и комуникации, Институт по невробиология, БАН, бул. Акад. Г. Бончев, бл. 23, 1113 София, България

²Катедра по специална педагогика и логопедия, Факултет по начална и предучилищна педагогика, СУ "Св.Климент Охридски", бул. Шипченски проход 69А, 1574 София, България

³Катедра по патофизиология, Медицински факултет, МУ-София, ул. Здраве 2, 1431 София, България

Постъпила на 11 октомври, 2016 г.; Коригирана на 21 януари, 2017 г.

(Резюме)

Цел на нашите експерименти беше, използвайки експериментален модел на болестта на Паркинсон, да се проследят промените в активността на ензима глутатион редуктаза и нивата на липидна пероксидация в две различни мозъчни структури (мозъчна кора и хипокам) в присъствие или отсъствие на vasoактивен интестинален пептид (ВИП), който е 28 аминокиселинен пептид, принадлежащ към групата на „мозъчно-чревните“ пептиди. Използвани бяха 20 мъжки, половозрели плъха от породата Wistar с тегло 150-200 г. Животните бяха разделени на групи на случаен принцип със свободен достъп до храна и вода. Плъховете бяха анестезирани с хлоралхидрат (400 mg/kg, интраперитонеално), главата им се обръсваше и се поставяха на стереотаксичен апарат. Таргетните координати за стриатум бяха: AP = +0.2; LR = -3.0; H = -5.6 в съответствие със стереотаксичен атлас. На експерименталната група животни се инжектираше 20 µg/2 µl of 6-хидроксидопамин (6-OHDA), а на контролната 2 µl физиологичен разтвор. При всички групи животни инжектираната се осъществяваша в десен стриатум посредством микроспринцовка Хамилтон при скорост на вливането 1 µl/min. Раната се затваряше чрез неръждаеми клипсове след което плъховете се оставяха да се възстановят. ВИП (13 µg/2 µl) се инжектираше в десен стриатум 15 минути преди лезията с 6-OHDA и на 21^{ия} ден след операцията. Получените от нас резултати показват, че при използвания експериментален модел на болестта на Паркинсон е налице понижение в активността на ензима глутатион редуктазата и потискане на липидната пероксидация, което означава, че увреждането на клетъчните мембрани е намалено, а жизнеспособността на клетките е повишена.

Intrahippocampal administration of losartan improves learning and memory in rats with model of depression

M.S. Ivanova¹, R.E. Tashev^{2,3*}

¹ Department of Physiology and Pathophysiology, Medical University of Varna, M. Drinov Str., 55, Varna, Bulgaria,

² Department of Pathophysiology, Medical University of Sofia, Zdrave Str., 2., Sofia, Bulgaria;

³ Department of Behavior Neurobiology, Institute of Neurobiology, Bulgarian Academy of Sciences, Acad. G. Bonchev Str., 23, Sofia Bulgaria,

Received October 8, 2016; Revised February 14, 2017

The brain renin-angiotensin system is involved in learning and memory, but the role of angiotensin II and its receptors in these processes is not well established. The effects of losartan (angiotensin type 1 receptor antagonist) and angiotensin II, microinjected bilaterally into CA1 hippocampal area on learning and memory in rats with a model of depression (bilateral olfactory bulbectomy), using two avoidance paradigms: active avoidance (shuttle box) and passive avoidance (step through) were investigated. After stereotaxic implantation of guide cannulas into the CA1 area of dorsal hippocampus angiotensin II (0.5 µg) and losartan (100 µg) were microinjected separately, 5 minutes before each training session. It was found that intra-CA1 losartan reverses memory deficits induced by bulbectomy unlike angiotensin II which did not show any effect. The data suggest an involvement of angiotensin type 1 receptors in modulating memory processes in rats with model of depression.

Key words: Losartan, Angiotensin II, Hippocampus, Depression, Learning, Memory

INTRODUCTION

The brain renin-angiotensin system (RAS) includes a number of bioactive angiotensin (Ang) peptides (Ang II, Ang III, Ang IV and Ang-(1-7) which show variable neurological activities [1]. Four receptor types have been proposed within the RAS: the Ang II type 1 and 2 receptors (AT1, AT2), Ang IV-specific receptor (AT4), and a putative Ang-(1-7)-selective receptor. Angiotensin II (Ang II) is the most important angiotensin peptide, which binds selectively AT1 and AT2 receptors.

Recent studies have revealed that Ang II regulates synaptic transmission in several brain regions including the hippocampus [2]. The hippocampus is known to be involved in a variety of learning tasks and there the concentration of Ang II and the expression of the various angiotensin receptor subtypes are particularly high [3, 4].

There are few reports about the involvement of hippocampal angiotensin receptors in cognitive processes using the avoidance paradigms. It was demonstrated that when administered to the hippocampus, Ang II impaired retention of the single

trial step through shock avoidance response by activation of AT1 receptors [5]. Other studies provided evidence that Ang II applied to the CA1 area blocked memory formation through a mechanism involving the activation of AT2 receptors [6]. Recently, a possible role of hippocampal Ang II receptors in voluntary exercise-induced enhancement of learning and memory in rats was suggested [7]. It has been reported that orally administered losartan (an antagonist of the AT1 receptors) suppresses the enhancing effect of voluntary running on cell proliferation in the rat hippocampus [8].

The first suggestion that brain RAS may be important in depression was observed in hypertensive patients undergoing captopril treatment [9-11]. Captopril treatment has also been shown to protect animals against the forced swim induction method of learned helplessness. Evidence accumulates that the brain RAS is involved in the mediation of stress responses and depression [12, 13].

The olfactory bulbectomized rat (OBX) is a well-validated animal model of depression. OBX is associated with a variety of behavioral abnormalities such as hyperactivity in the “open-field” test, appetite-motivated behaviors, decreased fear-related behavior, extensive cognitive impairments, and

* To whom all correspondence should be sent: © 2017 Bulgarian Academy of Sciences, Union of Chemists in Bulgaria
E-mail: romantashev@gmail.com

others [14-16]. Hippocampal degeneration has been suggested to be the basis for the cognitive deficits in Alzheimer's disease (AD) [17]. As far as bulbectomy is associated with increased levels of beta-amyloid protein in neocortex and hippocampus [18] and induces some behavioral and biochemical phenotypes of Alzheimer's disease, such as an increase of locomotor activity and cognitive defects [19, 20] it has been used also as an AD model.

Taking into account the high density of AT1 receptors in the hippocampus and the role of this limbic structure in the cognitive processes, the aim of the present study was to examine the effects of Ang II and losartan (a selective AT1 receptor antagonist) after bilateral infusion into CA1 hippocampal area on learning and memory processes in rats with an OBX model.

MATERIAL AND METHODS

Animals

Male Wistar rats (200 - 220g at the time of surgery) were housed individually in polypropylene boxes with free access to food and water. The animals were maintained in a constant temperature environment ($22 \pm 2^\circ\text{C}$) on a 12 h light/dark cycle (lights on at 6:00am). The behavioral experiments were carried out between 10:00am and 1:00pm.

The experiments were carried out according to the "Principles of laboratory animal care" (NIH publication No. 85-23, revised 1985), and the rules of the Ethics Committee of the Institute of Neurobiology, Bulgarian Academy of Sciences (registration FWA 00003059 by the US Department of Health and Human Services).

Surgical procedures

Bilateral olfactory bulbectomy (OBX), stereotaxic implantation and drug microinjections into the hippocampal CA1 area were published previously [14, 21, 22]. OBX was performed according to the method described by Kelly et al. [14]. Seven days after OBX, guide cannulas were implanted bilaterally (right and left) into CA1 hippocampal area of OBX rats ($P = 3.8 \text{ mm}$; $L = \pm 3.0 \text{ mm}$; $h = - 3.0 \text{ mm}$). After surgery, the animals were allowed 7 days to recover before the beginning of the behavioral tests, e.g. 15 days after OBX. During the recovery period, the rats were handled daily.

Rats were microinjected into both CA1 areas with

0.5 μl of Ang II (pH 7.4) or 0.5 μl of losartan (pH 7.4) or 0.5 μl saline. Following the termination of the experiments and immediately prior to the sacrifice, the rats were injected through the injection cannula with 0.5 μl 2 % Fast Green dye for verification of cannula placement into hippocampal CA1 area. Animals with cannula placement outside the CA1 area or not symmetrical within both CA1 areas were excluded from the statistical analysis.

Behavioral methods

The behavioral tests were carried out 15 days after the bilateral olfactory bulbectomy. The animals were tested in two learning and memory tests: two-way active avoidance test (shuttle box) and passive avoidance test (step-through) as described previously [21]. The experimental rats were divided into 2 main groups for each of avoidance test (shuttle box and step through): A) - rats without cannulas and without treatments - OBX operated rats and sham-operated rats B) - OBX rats with bilaterally implanted cannulas into CA1 areas microinjected with Ang II; losartan and saline. The drugs were injected 5 minutes prior to each training session.

Statistical analysis

One-way ANOVA was used to analyze the data obtained for bilateral olfactory bulbectomy. Separate one-way ANOVA was used to analyze the data obtained for number of avoidances for learning (1st and 2nd training day) and memory test (24 hours after the 2nd training day). ANOVA data were analyzed further by post-hoc Student-Newman-Keuls (SNK). T-test was used for post-hoc comparisons between left- and right-side injections. Analysis of the passive avoidance data was performed using χ^2 tests.

RESULTS AND DISCUSSION

Shuttle box test

One-way ANOVA on the number of avoidances of OBX rats (without implanted cannulas) demonstrated a significant effect on the 1st training day ($F_{1,11} = 34,090$; $P \leq 0.001$), 2nd training day ($F_{1,11} = 60,500$; $P \leq 0.001$) and on the retention test ($F_{1,11} = 74,387$; $P \leq 0.001$) at the active avoidance paradigm. Post-hoc SNK showed that the avoidances of OBX rats were significantly lower as compared to the sham-OBX controls on 1st day ($P \leq 0.001$), 2nd day ($P \leq 0.001$) and on the retention test, 24 h after the 2nd day ($P \leq 0.001$) (Fig. 1).

One way ANOVA after bilateral infusions of Ang II and losartan on the number of avoidances of OBX rats showed a significant effect for “drug” on the 1st day ($F_{2,17} = 4,078$; $P \leq 0.03$), on the 2nd day ($F_{2,17} = 6,0465$; $P \leq 0.01$), and at the retention test ($F_{2,17} = 5,248$; $P \leq 0.01$). Post-hoc test revealed that losartan significantly increased the number of avoidances during the 1st day ($P \leq 0.005$), the 2nd day ($P \leq 0.005$), and at the retention test ($P \leq 0.0001$), as compared to the saline-treated OBX-controls, while Ang II did not produce any significant effect (Fig. 2).

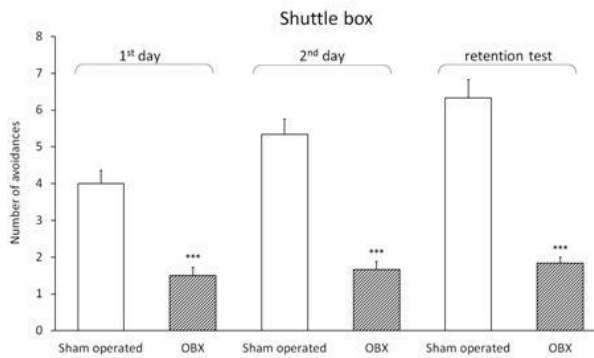


Fig. 1. Effect of olfactory bulbectomy (OBX) on the number of avoidances (shuttle box). *** $P < 0.001$. Asterisks depict comparisons of the number of avoidances in OBX rats vs. sham operated controls. $n=6$. Means (\pm S.E.M.) are presented.

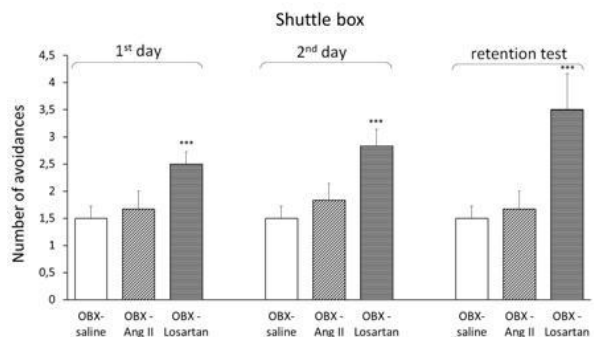


Fig. 2. Effects of Ang II and losartan microinjected bilaterally into the CA1 hippocampal area of OBX rats on the number of avoidances (shuttle box). *** $P < 0.001$. Asterisks depict comparisons of the number of avoidances, following infusions of the drugs vs. respective OBX saline treated controls. $n=6$. Means (\pm S.E.M.) are presented.

Step-through test

ANOVA on the latent time of OBX rats (passive avoidance task) demonstrated a significant effect on the retention tests: 3rd h after training ($F_{1,11} = 182,931$; $P \leq 0.001$) and 24th after training ($F_{1,11} = 250,372$; $P \leq 0.001$). The OBX rats showed a

significant decrease of the latent time on 3rd h ($P \leq 0.001$) and 24th h ($t = 3.98$, $P \leq 0.001$) as compared to the sham-OBX controls. The number of OBX rats to fulfill the learning criteria diminished to 0 % at both retention tests ($P \leq 0.001$) as compared to the controls (Fig.3).

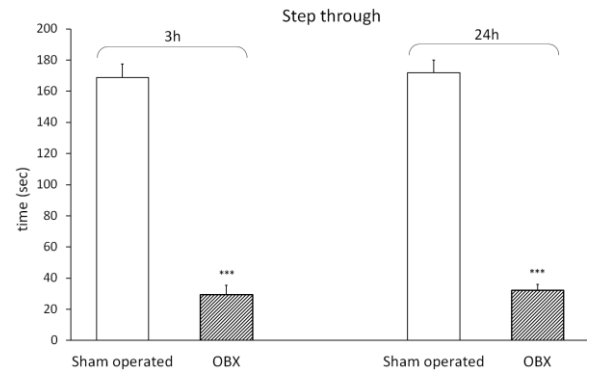


Fig. 3. Effect of olfactory bulbectomy (OBX) on the latent time (step through). *** $P < 0.001$. Asterisks depict comparisons of the latent time in OBX rats vs. respective sham operated controls. $n=6$. Means (\pm SEM) are presented.

ANOVA after infusions of Ang II and losartan on the latent time of OBX rats showed a significant effect for “drug” on the 3rd h ($F_{2,23} = 19,917$; $P \leq 0.001$) and 24th h ($F_{2,23} = 71,941$; $P \leq 0.001$). Losartan significantly enhanced the cognitive performance of OBX rats. It prolonged the latent time on 3rd h ($P \leq 0.04$) and 24th h ($P \leq 0.001$) and increased the percentage of the rats reaching the learning criteria on 3rd h (38% - $\chi^2 = 5.333$; $P \leq 0.02$) and 24th h (63% - $\chi^2 = 7.237$; $P \leq 0.01$) as compared to the saline-treated OBX rats. Ang II administered into the CA1 areas did not produce significant effects on memory-related behavior of OBX rats (Fig.4).

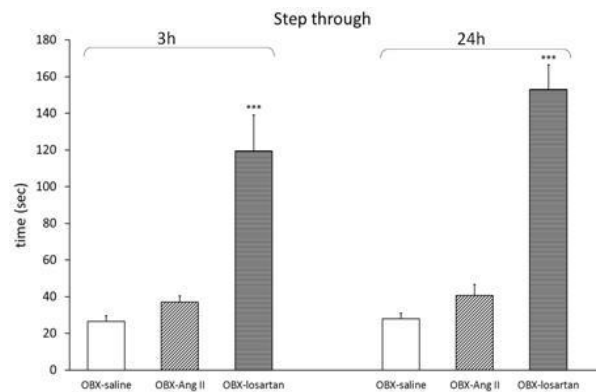


Fig. 4. Effects of Ang II and losartan microinjected bilaterally into the CA1 hippocampal area of OBX rats on the latent time (step through). *** $P < 0.005$. Asterisks depict

comparisons of the latent time, following infusions of the drugs vs. respective OBX saline treated controls. n=8. Means (\pm S.E.M.) are presented.

The present study extended our understanding about the learning and memory effects of Ang II and losartan infused separately into the hippocampal CA1 area of OBX rats. The bilateral bullectomy impaired the performance of rats in both avoidance paradigms as it has been demonstrated previously [23, 24]. The microinjections of Ang II failed to produce any effect on the performance of OBX rats as compared to the saline-treated OBX controls, while losartan significantly ameliorated the learning and memory-related behavior impairment. Based on our results we can make only some speculative assumptions to explain the memory ameliorating effect of losartan on OBX-induced learning deficits in the avoidance tests.

The brain RAS has been implicated in the pathophysiological mechanisms of dementia and neurodegenerative diseases. However, its role on the impairment of learning and memory-related behavior induced by OBX has not been examined yet. The bilateral removal of bulbi olfactorii is associated with a variety of behavioral abnormalities in rodents including cognitive impairments, with deficits in learning and memory [14, 16, 23, 24]. After bullectomy degeneration of neurons in cortex, hippocampus [25, 26] and impaired neurogenesis in hippocampal dentate gyrus have been reported [27]. The present findings provided new insights concerning the modulatory role of RAS on cognitive processes in rats with olfactory bullectomy.

Data are lacking about the expression of angiotensin receptors in the brain of OBX rats, but the neurodegenerative changes might be accompanied with abnormalities in RAS in different brain regions, similarly to the observed alterations on AT receptor subtypes in patients with neurodegenerative disorders [28, 29]. It could be suggested that the above-mentioned neurodegenerative changes in the hippocampus after bullectomy and the following compensatory neuronal reorganization could explain the effects of the drugs on the performance of OBX rats. The memory enhancing effects of losartan in OBX rats may indicate that it is able to ameliorate the impaired cognitive functions only in the conditions of neurodegeneration and impaired activity of many neurotransmitter systems, increased oxidative stress and inflammation, which have been reported following bullectomy.

AT1 receptor blockers have shown powerful neuroprotective effect in vivo and their use may be beneficial for the treatment of many brain disorders [30, 31]. Recent studies showed that telmisartan protects mouse dopaminergic neurons, inhibits the microglial response in a mouse MPTP of Parkinson's disease [32] and attenuates hypertension-induced learning and memory deficits [33, 34].

Brain inflammation has been implicated in the pathophysiology of brain diseases such as major depression, Parkinson's disease, Alzheimer's disease, and traumatic brain injury. Evidence accumulates suggesting that ARBs may protect the brain from different types of injury resulting in parenchyma inflammation and neuronal damage. Inflammation has been linked to the etiology of OBX-induced depression. Ablation of olfactory bulbs is associated with production of oxygen reactive species, saturation of antioxidant enzymes, increased lipid peroxidation, etc.[35]. In addition to oxidative stress, OBX syndrome involves generation of pro-inflammatory cytokines in brain [36, 37] and promotes pathological damage by accompanying inflammatory reactions [38]. Oxidative stress contributes to the cognitive impairments in experimental animals [39]. Reports indicate that oxidative stress is increased in the brain of Alzheimer's disease and other neurodegenerative disorders [40]. The neuroprotective effects of ARBs may be partially related to their ability to decrease oxidative stress. Recently, complex interactions between Ang II, behavioral processes and neuronal oxidative stress have been reported. Bild et al. [2] found significant correlations between some memory-related behavioral parameters and the oxidative stress markers from the hippocampus. The central administration of Ang II induced memory deficits in two different cognitive tasks and increased oxidative stress status in the hippocampus, while the administration of losartan significantly improved the performance of rats [2]. Following this line of reasoning, it is likely the anti-inflammatory and antioxidant effects of losartan to contribute for its ability to ameliorate the OBX-induced deficits in the avoidance paradigms.

The ability of Ang II receptor antagonists to interfere with the activity of some neurotransmitter systems, all being involved in the cognitive processes might also contribute to the memory enhancing effect of losartan in the OBX model. As far as in rodents AT1 receptors are expressed in brain regions

involved with fear memory such as hippocampus and amygdala, the implication AT1 receptor inhibition in the mechanisms of fear memory and extinction [3, 41, 42] could also be taken into account.

CONCLUSION

This study demonstrated that the bilateral administration of the AT1 receptor antagonist losartan into the CA1 hippocampal area of OBX rats significantly ameliorated the memory deficits in both active and passive avoidance tasks. These findings could contribute to understanding the potential of the central RAS manipulation for the treatment of cognitive disorders.

REFERENCES

1. O. von Bohlen und Halbach, D. Albrecht, *Cell Tissue Res.*, **326**, 599 (2006).
2. W. Bild, L. Hritcu, C. Stefanescu, A. Ciobica, *Prog. Neuropsychopharmacol. Biol. Psychiatry*, **43**, 79 (2013).
3. O. von Bohlen und Halbach, D. Albrecht, *Regul. Pept.*, **78**, 51 (1998).
4. J. Wright, J. Harding, *J. Renin Angiotensin Aldosterone Syst.*, **9**(4), 226 (2008).
5. E.H. Lee, Y.L. Ma, M.J. Wayner, D.L. Armstrong, *Peptides*, **166**, 1069 (1995).
6. D. Kerr, L. Bevilacqua, J. Bonini, J. Rossato, C. Köhler, J. Medina, I. Izquierdo, M. Cammarota *Psychopharmacology (Berl)* **179**, 529 (2005).
7. M. Akhavan, M. Emami-Abarghoie, B. Sadighi-Moghaddam, M. Safari, Y. Yousefi, A. Rashidy-Pour, *Brain Res.* **1232**, 132, (2008).
8. T. Mukuda, H. Sugiyama, *Neurosci. Res.* **58**, 140, (2007).
9. R. Deicken, Captopril treatment of depression. *Biol Psychiatry* **21**, 1425, (1986).
10. L. Germain, G. Chouinard, *Biol. Psychiatry* **23**, 637, (1988).
11. L. Germain, G. Chouinard, *Biol. Psychiatry* **25**, 489 (1989).
12. M. Ruiz-Ortega, O. Lorenzo, M. Ruperez, V. Esteban, Y. Suzuki, S. Mezzano, J. Plaza, J. Egido, *Hypertension* **38**, 1382 (2001).
13. P. Gard, J. Rusted, *Expert. Rev. Neurother.* **4**, 87, (2004).
14. J.P. Kelly, A. Wrynn, B.E. Leonard, *Pharmacol. Ther.* **74**, 299 (1997).
15. C. Mucignat-Caretta, M. Bondí, A. Caretta, *Physiol. Behav.* **89**, 637, (2006).
16. R.Tashev, M. Ivanova, T. Toromanov, M. Marinov, S. Belcheva, I. Belcheva, *Compt. Rend. Acad. Bulg. Sci.* **63**, 617, (2010).
17. P. Thompson, K. Hayashi, G. De Zubicaray, A. Janke, S. Rose, J. Semple, M. Hong, D. Herman, D. Gravano, D. Doddrell, A. Toga, *Behav. Brain Res.*, **138**, 9, (2003).
18. M. Ivanova, S. Belcheva, I. Belcheva, N. Negrev, R. Tashev, *Psychopharmacology*, **221**, 561 (2012).
19. R. Tashev, M. Stefanova, *Acta Neurobiol. Exp.*, **75**, 48, (2015).
20. C. Mucignat-Caretta, M. Bondí, A. Caretta, *Physiol. Behav.* **89**, 637, (2006).
21. C. Song, B.E. Leonard, *Neurosci. Biobehav. Rev.* **29**, 627, (2005).
22. J. Carlsen, J. De Olmos, L. Heimer, *J. Comp. Neurol.* **208**, 196, (1982).
23. I. Nesterova, N. Bobkova, N. Medvinskaja, A. Samokhin, I. Aleksandrova, *Morfologija*, **131**, 32, (2007).
24. N. Shioda, Y. Yamamoto, F. Han, S. Moriguchi, Y. Yamaguchi, M. Hino, K. Fukunaga, *J. Pharmacol. Exp. Ther.*, **333**, 43, (2010).
25. J. Ge, N.M. Barnes, *Eur. J. Pharmacol.*, **297**, 299, (1996).
26. E. Savaskan, C. Hock, G. Olivieri, S. Bruttel, C. Rosenberg, C. Hulette, F. Müller-Spahn, *Neurobiol. Aging*, **229**, 541, (2001).
27. J. Saavedra, *Clin. Sci. (Lond)*, **123**, 567, (2012).
28. J. Wang, T. Pang, R. Hafko, J. Benicky, E. Sanchez-Lemus, J.M. Saavedra, *Neuropharmacology* **79**, 249, (2014).
29. P. Garrido-Gil, B. Joglar, A.I. Rodriguez-Perez, M.J. Guerra, J.L. Labandeira-Garcia, *J. Neuroinflammation* **9**:38. doi: 10.1186/1742-2094-9-38, (2012).
30. B. Sharma, N. Singh, *Pharmacol. Biochem. Behav.*, **102**, 101, (2012).
31. T. Kishi, Y. Hirooka, K. Sunagawa, *J. Cardiol.*, **60**, 489, (2012).
32. I. Tasset, F.J. Medina, J. Peña, I. Jimena, M. Del Carmen Muñoz, M. Salcedo, C. Ruiz, M. Feijóo, P. Montilla, I. Túnez, *Physiol. Res.* **59**, 105, (2010).
33. A. Myint, H. Steinbusch, L. Goeghegan, D. Luchtman, Y. Kim, B. Leonard, *Neuroimmunomodulation* **14**, 65, (2007).
34. P. Rinwa, A. Kumar, *Neuroscience* **255**, 86, (2013).
35. C. Song, X. Zhang, M. Manku, *J. Neurosci.* **29**(1), 14, (2009).
36. R. Liu, I.Y. Liu, X. Bi, R.F. Thompson, S.R. Doctrow, B. Malfroy, M. *Proc. Natl. Acad. Sci. USA*, **100**(14), 8526, (2003).
37. X. Zhu, A.K. Raina, H.G. Lee, G. Casadesus, M.A. Smith, G. Perry, *Brain Res.*, **1000**, 32, (2004).
38. P.J. Marvar, J. Goodman, S. Fuchs, D.C. Choi, S. Banerjee, K.J. Ressler, *Biol. Psychiatry* **75**, 864, (2014).
39. T.L. Lazaroni, C.P. Bastos, M.F. Moraes, R.S. Santos, G.S. Pereira, *Neurobiol. Learn. Mem.*, **127**, 27, (2015).

ЛОСАРТАН ВЪВЕДЕН В ХИПОКАМП НА ПЛЪХОВЕ С МОДЕЛ НА ДЕПРЕСИЯ ПОДОБРЯВА ОБУЧЕНИЕТО И ПАМЕТТА

М. С. Иванова¹, Р. Е. Ташев^{2,3*}

¹Катедра по патофизиология, Медицински факултет, МУ-София, ул. Здраве 2, 1431 София, България

²Направление поведенческа невробиология, Институт по невробиология, БАН, бул. Акад. Г. Бончев, бл. 23, 1113
София, България

³Катедра по физиология и патофизиология, Медицински университет, МУ-Варна, ул. М. Дринов, 55, 9000 Варна,
България

Постъпила на 08 октомври, 2016 г.; Коригирана на 14 февруари, 2017 г.

(Резюме)

Мозъчната ренин-ангиотензиновата система е въввлечена в обучителните и паметовите процеси, но ролята на ангиотензин II и неговите рецептори в тези процеси все още не е добре установена. Изследвани са ефектите на лосартан (антагонист на ангиотензин тип 1 рецепторите) и ангиотензин II, микроинжектирани двустранно в СА1 полето на хипокампа върху обучението и паметта на плъхове с модел на депресия (двустранна олфакторна булбектомия), при два метода за памет и обучение: активно избягване (shuttle box) и пасивно избягване (step through). След стереотаксично имплантиране на водещи канюли в СА1 полето на задния хипокамп, ангиотензин II (0.5 µg) и лосартан (100 µg) се микроинжектират поотделно, 5 минути преди всяка тренировъчна сесия. Установено е, че лосартан въведен в СА1 полето премахва паметовия дефицит, предизвикан от булбектомията, за разлика от ангиотензин II, който не показва ефект. Получените данни говорят, че ангиотензин тип 1 рецепторите са въввлечени в процесите на обучение и памет на плъховете с модел на депресия.

Angiotensin II-induced motility of reservoir smooth muscle organs from ghrelin and melatonin-treated diabetic rats

P.V. Hadzhibozheva^{1*}, Ts. K. Georgiev¹, R. E. Kalfin², G. S. Ilieva¹, A. N. Tolekova¹

¹*Department of Physiology, Pathophysiology and Pharmacology, Medical Faculty, Trakia University, 11 Armeiska Str., Stara Zagora 6000, Bulgaria*

²*Institute of Neurobiology, Bulgarian Academy of Sciences, 23 Akad. Georgi Bonchev Str., Sofia 1113, Bulgaria*

Received September 29, 2016; Revised February 13, 2017

The purpose of the study was to assess the effect of short-term ghrelin (GHR) or melatonin (MLT) treatment on Angiotensin II (AngII)-provoked motility of stomach, rectum and urinary bladder of rats with streptozotocin (STZ)-induced diabetes. Mature Wistar rats were divided into 4 groups: control; STZ-treated: by a single STZ injection; MLT-treated: single STZ injection, followed by MLT treatment for 7 consecutive days; GHR-treated: single STZ injection, followed by GHR treatment for 7 consecutive days. The experiment lasted 42 days and in the end, preparations from the reservoir organs were prepared and influenced by AngII. The analysis of power and kinetic parameters of the obtained contractions was made by KORELIA Software.

STZ-induced diabetes affected differently AngII-provoked contractile activity of reservoir organs. In the MLT-treated group, powerful responses to Ang II of the stomach (1.91 ± 0.07 g) and weak Ang II-induced contractions of urinary bladder preparations (1.12 ± 0.11 g) in comparison to controls (1.14 ± 0.13 g and 1.74 ± 0.22 g, respectively) were observed. Administration of GHR almost completely recovered the normal force characteristics of urinary bladder contractions and accelerated the duration of stomach contractions. The responses to Ang II of rectal preparations from animals treated with GHR or MLT were not improved.

Although partial, there were registered favorable effects of short-term application of MLT or GHR in animals with STZ-induced diabetes. The beneficial effect on Ang II-induced stomach and urinary bladder motility was probably due to antioxidant and pro-kinetic properties of MLT or GHR on the smooth muscle.

Key words: Angiotensin II, Ghrelin, Melatonin, diabetes, smooth muscle

INTRODUCTION

The stomach, rectum and urinary bladder serve mainly as reservoir organs and perform evacuating functions. This is why the maintenance of their adequate tone is essential for a normal quality of life. The precisely coordinated and complex smooth muscle activity of reservoir organs is regulated by the interplay between neural and endocrine control mechanisms. The octapeptide Angiotensin II (Ang II) is an important factor for blood pressure regulation and maintenance of electrolyte homeostasis. Furthermore, as the main effector of the Renin-Angiotensin System (RAS), Ang II has various actions, many of them affecting the activity of visceral smooth muscles from gastrointestinal (GI) and urogenital tract [1,2]. Leung et al. [3] have found that Ang II has a potent contractile action on the musculature of the GI tract, rather than on the aorta. In the GI tract, Ang II plays multiple roles, influencing water-salt balance, blood flow, motility and inflammation. There is evidence for the involvement of Ang II in the development of gastro-esophageal reflux [2], internal anal sphincter

incontinence [4] and Crohn's disease [2,5]. It has also been shown that Ang II causes dose-dependent contractions of smooth muscle strips from the urinary bladder. This directs many researchers to the hypothesis that Ang II is likely to influence the process of micturition and probably acts as a modulator of neurotransmission in the bladder [6]. A large number of studies reveal the presence of receptors for Ang II in different parts of the GI and urogenital tracts [2,5]. Most of the effects of Ang II on the digestive system, especially those concerning the contractile activity, are attributed mainly to the effects mediated by the AT1 receptors [2,4,6].

Nowadays, the growing incidence of disorders in many smooth muscle organs is frequently observed in diabetic patients. The gastroparesis, fecal incontinence/constipation and cystopathy are among the first significant complications connected with the progression of diabetes mellitus [7,8]. The reason for these diabetic complications is the impaired smooth muscle function due to oxidative stress and the accumulation of glycated products [9]. Considering the leading role of oxidative stress in the pathogenesis of diabetes, the scientific efforts are directed to the search for effective antioxidants [10]. Such possible antioxidants with a therapeutic

* To whom all correspondence should be sent:

E-mail: petia_hadjibojeva@abv.bg

potential for treatment of diabetic smooth muscle dysfunction could be the hormones melatonin (MLT) and ghrelin (GHR).

Melatonin (MLT)

MLT positively affects a wide range of diabetic complications by reducing the oxidative stress. It has been found that MLT is a more powerful antioxidant than Vitamin E, displaying nearly 10-fold times more potent free radicals trapping ability, especially in the brain [11]. An intraperitoneal injection of MLT, made a few days before STZ-induced diabetes in rats, prevents severe lesions of β -cells in the pancreas [12]. Klepac et al. [13] found that even a single dose of MLT (20 mg / kg) has an antioxidant activity in the plasma of STZ-treated rats, increases the action of antioxidant enzymes and reduces the production of superoxide radicals.

Ghrelin (GHR)

Irako et al. [14] are the first who found that a subcutaneous injection of GHR could prevent the hyperglycemia, caused by the STZ application in newborn rats. The authors have registered a significant increase in insulin production and secretion in the experimental animals [14]. In similar experiments, Granata et al. [15] described that the administration of GHR results in an improvement of glucose metabolism and a conservation of mass of pancreatic island cells. This is a prerequisite for a good therapeutic potential of GHR in conditions associated with an impaired β -cell function [15]. GHR favorably affects the gastropathy, stimulates the motility and emptying of the stomach and accelerates the delayed by the diabetes intestinal passage [16-18].

The established role of RAS in the pathogenesis of hypertension in diabetes mellitus [19] focused our interest to study the effects of Ang II on diabetic visceral smooth muscles. Despite the observed development of diabetic smooth muscle dysfunction in a number of organs, the information about the changes in the smooth muscle response of reservoir organs to Ang II, in this disease, is insufficient. The hormones MLT and GHR are with proven protective and antioxidant effects and possess a promising action in the prevention of the emergence and development of diabetic complications. Currently, there is no information in the literature how the application of these hormones could influence Ang II - stimulated responses of diabetic visceral smooth musculature.

The aim of this study was to assess whether short-term application of MLT or GHR on rats with streptozotocin (STZ)-induced diabetes will

affect the Ang II - induced motility of the stomach, rectum and urinary bladder.

EXPERIMENTAL

Experimental animals

Mature Wistar rats, weighting 250-300 g, were divided into 4 groups: control group – healthy rats, injected 8 consecutive days from the beginning of the experiment with saline; STZ-treated group (diabetic group) - rats injected once on the first day of the experiment with a single dose of STZ; MLT-treated group (diabetic animals treated with MLT) - rats injected once on the first day of the experiment with a single dose of STZ, followed by 7 consecutive days administration of MLT; GHR-treated group (diabetic animals treated with GHR) - rats injected once on the first day of the experiment with a single dose of STZ, followed by 7 consecutive days administration of GHR.

Experimental model of diabetes mellitus and treatment with MLT and GHR

The induction of diabetes was made by a single intraperitoneal injection of streptozotocin (STZ) at a dose of 60 mg/kg. STZ was dissolved in cold 0.1 M citrate buffer, pH 4.5. The injected volume did not exceed 0.1 ml in each experimental animal. 72 hours after STZ application (the third day of the experiment), blood glucose levels were measured and only animals with blood glucose above 16 mmol/l were considered diabetic and were left in the experiment.

MLT was administered in the diabetic animals at a dose of 10 mg / kg i.p. This dosage and the route of administration of MLT were made as it was described by some authors [20,21]. GHR was administered in the diabetic animals at a dose of 100 μ g/kg s.c. This dosage and the route of administration of GHR were made as it was described by Irako et al. [14] and Granata et al. [15].

The experiment lasted 42 days and in the end, preparations from the reservoir organs were made and influenced by Ang II.

Sample Preparation

The study was performed on stomach, rectal and urinary bladder smooth muscles, isolated from the experimental animals. The animals were anesthetized with Nembutal 50mg/kg i.p. and exsanguinated. The experiments were carried out in accordance with the National regulations and the Directive 2010/63/EU of the European parliament and of the Council (22 September, 2010)

concerning the protection of animals used for scientific purposes.

Abdominal and pelvic cavity were opened and the stomach, rectum and urinary bladder were dissected out and immediately placed in cold Krebs solution (3 °C), containing the following composition (in mmol): NaCl 118.0, KCl 4.74, NaHCO₃ 25.0, MgSO₄ 1.2, CaCl₂ 2.0, KH₂PO₄ 1.2, and glucose 11.0. The surrounding tissue was dissected and longitudinal sections from the organs (approximately 8-10 mm long) were prepared. The two ends of each preparation were tied with ligatures. The distal end was connected to the organ holder; the proximal end was stretched and attached to a mechano-electrical transducer FSG-01 (Experimetria Ltd., Hungary) via a hook. The preparations were placed in organ baths TSZ-04/01 (Experimetria Ltd., Hungary), containing Krebs solution, pH 7.4, continuously bubbled with Carbogen (95% O₂, 5% CO₂). The organ baths were mounted in parallel above an enclosed water bath, maintaining the solution temperature at 37 °C. Preparations were placed under an initial tension (preload) of 1 g and allowed to equilibrate for at least 75 min (three periods: 15 min, 45 min and 15 min and two washes with Krebs solution between them). After the equilibration period, preparations were influenced by Ang II in a dose of 1 μmol (10⁻⁶ M).

Recording of mechanical activity and technical equipment

Mechanical activity was digitized and recorded by using ISOSYS-Advanced 1.0 Software (Experimetria Ltd., Hungary). Data processing and storage for subsequent analysis were performed with specialized software KORELIA [22]. With the module KORELIA-Processing [23] a transformation of data from ISOSYS-Advanced 1.0 was performed and their primary processing (filtering, smoothing, scaling, etc) was made.

Chemicals and drugs

Ang II (Sigma-Aldrich, Germany) was solubilized in bidistilled water. STZ and all reagents for the preparation of Krebs solution were purchased from Sigma-Aldrich Chemie GmbH, Germany. MLT (Sigma-Aldrich, Germany) and was dissolved in 1:90 ethanol/saline immediately prior to injection of the experimental animals. GHR (PolyPeptide Group, Sweden) was dissolved in saline immediately prior to injection of the experimental animals.

Data processing

The duration of the interval for analysis of Ang II - induced smooth muscle contractions was defined as follows: from the beginning of the contraction, until the moment at which the amplitude dropped to 50% of its maximum. This definition was made in order to calculate uniformly the various in duration contractions (Fig.1).

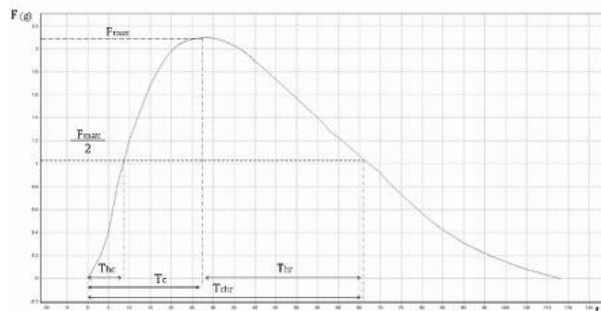


Fig. 1. Time-parameters of Ang II-induced contraction: F_{max} – maximal force of the smooth muscle contraction (SMC), $F_{max}/2$ – half of maximal force of the SMC, T_{hc} – half-contraction time: the time interval between the start of the SMC and $F_{max}/2$, T_c – contraction time: time interval between the start of the SMC and F_{max} , T_{hr} – half-relaxation time: the interval between F_{max} and $F_{max}/2$, T_{chr} – contraction plus half-relaxation time: the interval between the beginning of the SMC until the amplitude fell to $F_{max}/2$

The recorded force-vs.-time curves allowed the determination of the amplitude and the integral force of the contraction (the latter represented by the area under the curve - AUC). The different phases of the Ang II - induced tonic contractions, were clarified and analyzed by the application of a time -parameter analysis, similar to that made in the study of the skeletal muscle contraction [24]. The following time-parameters [25] were defined (Fig.1): half-contraction time (T_{hc}), contraction time (T_c), half-relaxation time (T_{hr}), contraction plus half-relaxation time (T_{chr}). Their calculation was made by KORELIA-Dynamics Program [26]. The averaged time-parameters were processed by spline interpolation and graphical visualization of the different patterns of contractile activity was obtained.

Statistical analysis

Obtained data were processed by the statistical program Statistica Version 6.1 (StaSoft, Inc., Tulsa, OK, USA) and presented as a mean ± standard error. A P-value less than or equal to 0.05 was considered to be statistically significant.

RESULTS

Stomach

The comparison in force parameters of Ang II-induced contractions (Fig.2) showed that the stomach preparations of the MLT-treated group developed the strongest answer to Ang II (amplitude and AUC respectively 1.99 ± 0.07 g and 315.65 ± 25.50 gs). The AUC of the contractions of the other three groups did not differ statistically ($P > 0.05$). Ang II-induced contractions of the stomach preparations from the STZ-treated group were with similar force parameters as those of the control group (Fig.2).

Time-parameters analysis revealed that the developed response to Ang II of the preparations from the diabetic group was faster and all the parameters were significantly shortened compared to those of control, with the exception of T_c (Table 1).

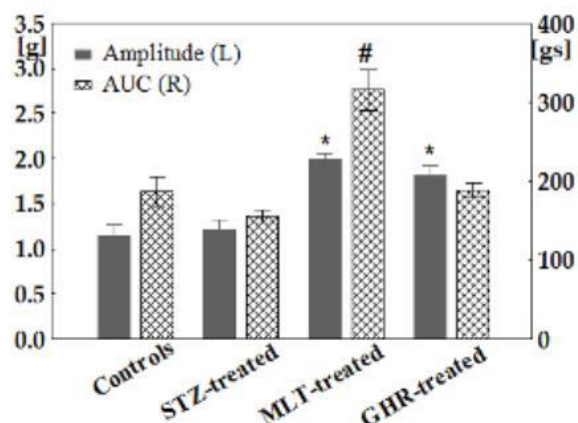


Fig. 2. Amplitude and AUC of Ang II - induced contractions of gastric preparations from the different groups. * $P < 0.05$ vs amplitudes of contraction of gastric preparations of controls and STZ-treated group # $P < 0.05$ vs AUC of contraction of gastric preparations of controls, STZ- and MLT-treated animals.

The contractions of the preparations from the GHR-treated group were the fastest, with most

shortened time-parameters (Table 1). This pattern of contractile activity was clearly visualized when interpolation was performed (Fig.5-A). Graphical visualization of Ang II - induced activity of stomach preparations of the different groups revealed the similarity between the contractions of preparations from MLT-treated and control groups (Fig.5-A).

Rectum

The responses to Ang II of rectal preparations of STZ-, MLT- and GHR-treated animals were with similar, significantly lower amplitude, when compared to controls (Fig.3). The latter developed the most powerful contraction: AUC 332.71 ± 35.78 gs, while the AUC of preparations from the GHR-treated group was significantly reduced: 143.17 ± 18.69 gs (Fig.3).

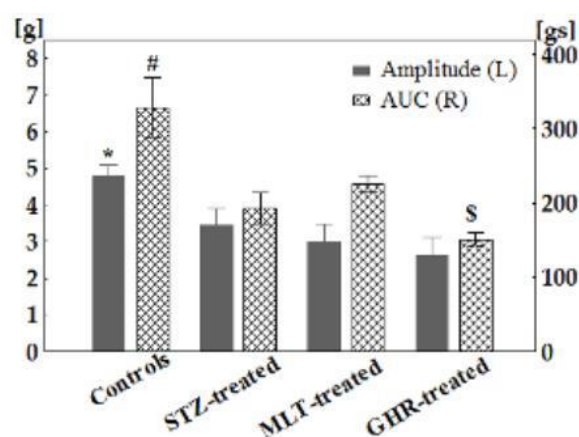


Fig.3. Amplitude and AUC of Ang II - induced contractions of rectal preparations from the different groups. * $P < 0.05$ vs amplitudes of contraction of rectal preparations from STZ-, MLT- and GHR-treated animals. # $P < 0.05$ vs AUC of contraction of rectal preparations of STZ-, MLT- and GHR-treated animals. \$ $P < 0.05$ vs AUC of contraction of rectal preparations of controls, STZ- and MLT-treated animals.

Table 1. Calculated time - parameters of Ang II - induced stomach contractions from the different groups.

Group	T_{hc} (s)	T_c (s)	T_{hr} (s)	T_{chr} (s)
Controls	28.69 ± 2.53	78.18 ± 3.35	146.73 ± 9.84	224.91 ± 11.64
STZ-treated	18.00 ± 0.96	77.75 ± 1.69	105.50 ± 5.18	183.25 ± 4.98
MLT-treated	17.20 ± 1.02	66.00 ± 0.71	157.01 ± 1.41	222.81 ± 2.11
GHR-treated	27.33 ± 4.84	63.66 ± 6.97	94.00 ± 7.10	157.67 ± 4.59

Table 2. Calculated time - parameters of Ang II - induced rectal contractions from the different groups.

Group	T_{hc} (s)	T_c (s)	T_{hr} (s)	T_{chr} (s)
Controls	9.58 ± 1.52	39.74 ± 3.23	48.43 ± 5.74	87.86 ± 7.83
STZ-treated	13.50 ± 0.92	44.33 ± 4.83	50.50 ± 4.14	94.83 ± 5.73
MLT-treated	12.17 ± 1.40	42.32 ± 3.95	72.67 ± 2.01	115.02 ± 5.77
GHR-treated	8.33 ± 0.76	29.00 ± 2.98	53.17 ± 5.66	82.17 ± 6.44

The time-parameters analysis (Table 2) did not reveal significant differences between the contractions of the preparations from the control and the STZ-treated group.

This similarity in the response to Ang II of these two groups was further observed when graphic images of contractions were performed (Fig.5-B): the two patterns of Ang II-induced activity differed only in force parameters.

Interestingly, the Ang II – provoked contractions of the rectal preparations from the GHR-treated group, also displayed similar duration in time, while the contractions of MLT-treated rats were significantly prolonged, with increased T_{hr} and T_{chr} (Table 2, Fig.5-B).

Urinary bladder

The application of Ang II on urinary bladder preparations from control and GHR-treated group caused contractions with similar force parameters: amplitude 1.74 ± 0.22 g and 1.63 ± 0.19 g, respectively and AUC 121.13 ± 13.73 gs and 121.11 ± 6.96 gs, respectively.

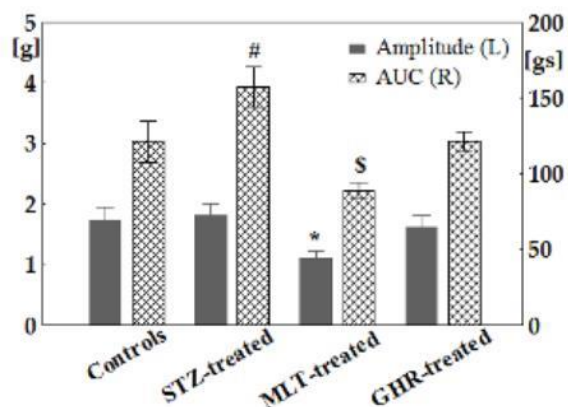


Fig. 4. Amplitude and AUC of Ang II - induced contractions of urinary bladder preparations from the different groups. * $P < 0.05$ vs amplitudes of contraction of bladder preparations from controls, STZ- and GHR-treated animals. # $P < 0.05$ vs AUC of contraction of bladder preparations of controls, MLT- and GHR-treated animals. \$ $P < 0.05$ vs AUC of contraction of bladder preparations of controls, STZ- and GHR-treated animals.

The amplitude of Ang II-induced response of preparations from STZ-treated rats (1.81 ± 0.18 g) did not differ statistically from the above, but the integral force was significantly increased (157.43 ± 13.13 gs). Preparations from MLT-treated group displayed the weakest reaction to Ang II (amplitude 1.12 ± 0.11 g and AUC 88.93 ± 5.40 gs) (Fig.4).

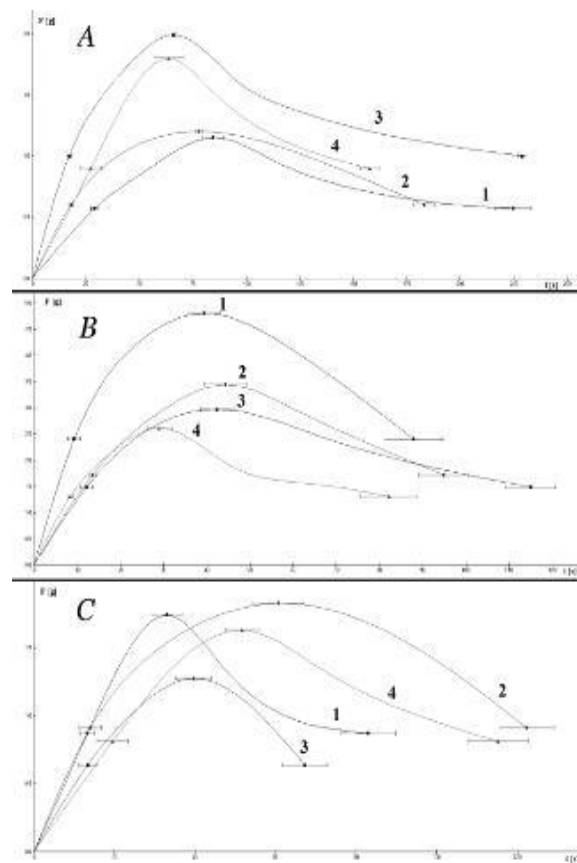


Fig. 5. Graphic images of Ang II - induced activity of smooth muscle preparations from: healthy animals: control group (1); diabetic animals: STZ-treated group (2); diabetic animals, treated additionally with MLT: MLT-treated group (3); diabetic animals, treated additionally with GHR: GHR-treated group (4). **A.** Preparations of stomach, **B.** Preparations of rectum, **C.** Preparations of urinary bladder

The comparison of the contractions by time-parameters (Table 3) showed that Ang II-induced responses of the four groups had similarity in reaching T_{hc} . T_c and T_{chr} however, were significantly prolonged in the contractions of preparations from STZ-treated and GHR-treated groups, while T_{hr} of preparations from MLT-treated animals was shortened (Table 3).

The graphical visualization of the contractile process (Fig.5-C) showed different models of Ang II-provoked urinary bladder activity in the different groups.

There were observed similarities between the contractile patterns of STZ-treated and GHR-treated groups from one side, and control and MLT-treated group from another.

Table 3. Calculated time – parameters of Ang II – induced urinary bladder contractions from the different groups.

Group	T _{hc} (s)	T _c (s)	T _{hr} (s)	T _{chr} (s)
Controls	13.28 ± 1.69	33.00 ± 3.14	50.28 ± 5.14	83.00 ± 6.95
STZ-treated	14.00 ± 2.78	60.71 ± 8.46	61.71 ± 6.58	122.43 ± 7.89
MLT-treated	13.33 ± 1.45	39.67 ± 4.59	30.60 ± 2.66	67.33 ± 3.88
GHR-treated	19.50 ± 4.88	51.67 ± 7.14	63.67 ± 4.94	115.33 ± 7.98

DISCUSSION

STZ-induced diabetes and smooth muscle dysfunction of reservoir organs

The similarity in force characteristics of the responses to Ang II of stomach and urinary bladder preparations from control and STZ-treated group, respectively, show that probably 6-week period after administration of STZ was not sufficient to reveal the characteristic changes in the function of these organs. Some authors also do not establish any differences between cholinergic responses of such preparations from healthy rats and rats with STZ-induced diabetes, lasted 6-8 weeks [27,28]. It is likely that this lack of apparent differences in the contractile response of preparations from healthy and diabetic animals to be due to not yet occurred or compensated changes in the smooth musculature.

However, we observed an accelerated time for contraction (T_{hc}) and relaxation (T_{hr}) of Ang II – induced gastric reaction in STZ-treated animals. This is an evidence for a more rapid duration of Ang II – stimulated contractile process in the stomach during diabetes. Such increased motor function of the stomach in diabetic patients has already been described [29,30]. It is believed that this dysfunction is caused by the hyperglycemia and the subsequent neuropathy, damage of gastric pacemaker cells and myopathy [29]. Probably this accelerated gastric emptying is a preliminary stage of the later observed delayed stomach evacuation [30]. According to He et al. [31], Ang II also takes part in the pathogenesis of the diabetic gastropathy. The authors reported that in patients with diabetes, the activity of RAS and Ang II, in particular, are increased. In a study of Tobu et al. [32] on rats with STZ-induced diabetes, an increased expression of AT1 receptors in smooth muscle cells of the urinary bladder was described. The authors believe that the persistent hyperglycemia probably activates the local RAS in the bladder.

The contractions of bladder preparations from STZ-treated animals were with delayed contraction time (T_c), which led to a prolonged development of smooth muscle process and an increased AUC. Such an increased activity of the bladder in STZ-treated animals might be associated with increased

release of neurotransmitters, improved activity of Ca²⁺ -channels or increased calcium sensitivity [28].

The analysis of rectal contractions of STZ-treated animals found exactly the opposite response to Ang II: a significant reduction of force parameters. This is consistent with Touw et al. [33], who reported for a less motor activity of large intestine in diabetic mice. In diabetes, there is a reduced entry of Ca²⁺ in smooth muscle cells of the rectum, resulting in decreased and disturbed contractile activity. Furthermore, Jancsó et al. [34] have found that the large intestine is more sensitive to the oxidative stress, caused by diabetes, when compared to the small intestine. The primary defect that leads to a less rise in intracellular Ca²⁺ concentration is a violation of L-type Ca²⁺ -channels, probably due to accumulation of glycated products [33].

Effect of MLT treatment

The fact, that contractions of the preparations from MLT-treated group differed when compared to controls and STZ-treated ones, revealed that: 1) short-term administration of MLT at the beginning of the experiment was not enough to influence entirely the smooth muscle dysfunction, caused by diabetes; 2) yet, there was some effect of the application of MLT in the diabetic animals.

The registered decreased response to Ang II of the urinary bladder from MLT-treated group is probably due to influence on the mechanism of contraction. There is evidence that MLT inhibits Ca²⁺-calmodulin complex and directly affects the ion channels on the urinary bladder smooth muscle cells, thus preventing the contractile process [35]. A similar type of MLT action could be suggested for the rectal preparations, where Ang II-provoked contractions were also with reduced force characteristics.

Regarding the stomach, the observed differences between the responses to Ang II of preparations from STZ- and MLT-treated groups indicate a beneficial effect of short-term MLT application. Even though the force parameters were increased, the time-parameters of gastric contractions from MLT-treated group were nearly identical to the controls. It is known that, due to its antioxidant properties, MLT stimulates the immune system,

improves the microcirculation and epithelial regeneration, and thus protects the digestive tract [36]. According to Peschke [37], MLT can significantly reduce the levels of protein glycation. Considering the role of ROS and glycation end products for the impaired smooth muscle activity in diabetes, it can be assumed that the favorable effect on the duration of stomach contraction is due to all the mentioned above properties of MLT. It should be also taken into account, that the disorders of the intestinal and gastric function during the diabetes do not show correlation between each other. For example, disturbances in the upper GI tract may occur in later stages of the disease, compared to the large intestine [38].

Effect of GHR treatment

In our experiments, we found differences between Ang II - stimulated contractions of the preparations from GHR-treated group, and the other groups. This indicates that short-term application of GHR had effect on the STZ-induced diabetes. The diverse contractile pattern of the stomach, rectum and bladder revealed a different influence of GHR on the diabetic smooth muscle activity.

The registered rapid response to Ang II of gastric preparations from GHR-treated group was in agreement with Qui et al. [17,18]. In a series of experiments with diabetic animals, these researchers have found that the treatment with GHR accelerates gastric and small intestinal contractile activity and leads to an increase in the amplitude of the carbachol-induced contractions. It is suggested that the stimulatory effect on the activity of the stomach is due to the activation of peripheral cholinergic pathways in the enteric nervous system [17,18]. GHR and its agonists also contribute to the restoration of the gastric mucosa damaged by oxidative stress in diabetes. These gastro-protective properties are likely to be due to the established antioxidant activity of the peptide [16]. In experiments with STZ-induced diabetes in rats, Ariga et al. [39] found high levels of GHR in the blood plasma of the animals and increased gastric evacuation activity. The authors suggest that during the early stages of diabetes, the elevated levels of the endogenous GHR improve the coordination between the fundus and pylorus of the stomach and accelerate the evacuation of the food. Moreover, a study of patients with a chronic heart failure reveals that serum levels of GHR correlated with Ang II levels and GHR can inhibit Ang II-induced cardiomyocyte apoptosis by down-regulating AT1 receptors [40]. Considering that during diabetes the levels of endogenous GHR are higher [39], the

activity of Ang II rises [31] and the expression of AT1 is increased [32], such correlation between GHR and Ang II levels and suppression of AT1 receptors could be supposed.

The Ang II-stimulated contractions of bladder preparations from GHR- treated group showed similar force parameters, when compared to the control group. These results indicated that GHR application had a beneficial effect on the urinary bladder activity. We could assume that this effect is due to the antioxidant or the described above interaction between GHR and AT1 receptors.

Interestingly, the rectal preparations of GHR-treated animals responded to Ang II with weaker reaction. According to Zhao et al. [41], GHR can play a role as pro-inflammatory peptide in the large intestine, thus promoting the formation of inflammatory cytokines in this region of the GI tract. Taking into account that the large intestine is more sensitive to the oxidative stress, caused by the diabetes [34], probably the seven-day administration of GHR on diabetic animals have caused an additional damage in the rectum, hence affecting the Ang II-stimulated contractile activity. In support of this hypothesis is the research conducted by Liu et al. [42], who found that the activation of the GHR receptors in the large intestine contributes to the development of colitis, probably by enhancing the pro-inflammatory cytokines and activation of macrophages.

In conclusion, the seven-day administration of MLT or GHR on rats with experimentally induced diabetes mellitus had a positive effect on some parameters of the Ang II –induced response of the preparations from stomach and urinary bladder. This beneficial effect was probably due to antioxidant and pro-kinetic properties of MLT or GHR on the smooth musculature of these organs. On the other hand, the responses to Ang II of rectal preparations from animals treated with GHR or MLT were not improved. Obviously, Ang II-mediated contractile activity of the rectum is seriously impaired by the diabetes and could not be enhanced by a short-term application of these hormones.

Acknowledgements: This study was supported by **Grant DDVU-02-24/2010** from National fund, Sofia, Bulgaria and **Grant 22/2014** from Trakia University, Stara Zagora, Bulgaria.

REFERENCES

1. S.I. Shimuta, A.C. Borges, R.N. Prioste, T.B. Paiva, *Eur. J. Pharmacol.*, **367**, 59 (1999).
2. L. Fändriks. *J. Renin Angiotensin Aldosterone Syst.*, **11**, 43 (2010).
3. E. Leung, J.M. Rapp, L.K. Walsh, K.D. Zeitung, R.M. Eglén, *J. Pharmacol. Exp. Ther.*, **267**, 1521 (1993).
4. S. Rattan, R.N. Puri, Y.P. Fan, *Exp. Biol. Med.*, **228**, 972 (2003).
5. G.D.Wang, X.Y.Wang, H.Z. Hu, X.C. Fang, S. Liu, N. Gao, Y. Xia, J.D. Wood, *Am. J. Physiol. Gastrointest. Liver Physiol.*, **289**, 614 (2005).
6. K. Andersson, A. Arner, *Physiol. Rev.*, **84**, 935 (2004).
7. P. Kashyap, G. Farrugia, *Neurogastroenterol. Motil.*, **23** (2), 111 (2011).
8. Frimodt-Møller, *Ann. Int. Med.*, **92**, 318 (1980).
9. M.J. Chang, J.H. Xiao, Y. Wang, Y.L. Yan, J. Yang, J.L. Wang, *PLoS One*, **7**(12), e50291 (2012).
10. A.Chatzigeorgiou, A. Halapas, K. Kalafatakis, E. Kamper, *In Vivo*, **23**, 245 (2009).
11. G. Baydas, H. Canatan, A. Turkoglu, *J Pineal Res.*, **32**, 225 (2002).
12. O. Yavuz, M. Cam, N. Bukan, A. Guven, F. Silan, *Acta Histochem.*, **105**, 261 (2003).
13. N. Klepac, Z. Rudes, R. Klepac, *Biomed. Pharmacother.*, **60**, 32 (2006).
14. T. Irako, T. Akamizu, H. Hosoda, H. Iwakura, H. Ariyasu, K. Tojo, N. Tajima, K. Kangawa, *Diabetologia.*, **49**, 1264 (2006).
15. R. Granata, M. Volante, F. Settanni, C. Gauna, C. Ghé, M. Annunziata, B. Deidda, I. Gesmundo, T. Abribat, A.J. van der Lely, G. Muccioli, E. Ghigo, M. Papotti, *J. Mol. Endocrinol.*, **45**, 9 (2010).
16. H. Suzuki, J. Maztsizaki, T. Hibi, *J Clin. Biochem. Nutr.*, **48**, 1 (2010).
17. W.C. Qiu, Z.G. Wang, R. Lv, W.G. Wang, X.D. Han, J. Yan, Y. Wang, Q. Zheng, K.X. Ai, *World J. Gastroenterol.*, **14**, 2572 (2008)
18. W.C. Qiu, Z.G. Wang, W.G. Wang, J. Yan, Q. Zheng, *World J Gastroenterol.*, **14**, 1419 (2008).
19. A. Ribeiro-Oliveira, A.I. Nogueira, R.M. Pereira, W.W. Boas, R.A. Dos Santos, A.C. Simões e Silva, *Vasc. Health Risk. Manag.*, **4**, 787 (2008).
20. H. Vural, T. Sabuncu, S.O. Arslan, N. Aksoy, *J. Pineal. Res.*, **31**, 193 (2001).
21. A. Armagan, E. Uz, H.R. Yilmaz, S. Soyupek, T. Oksay, N. Ozcelik, *Asian J. Androl.*, **8**, 595 (2006).
22. K. Yankov, D. Ilieva., *Tr. J. Sci.*, **13**, 420 (2015).
23. K. Yankov *Tr. J. Sci.*, **8**, 41 (2010).
24. R. Raikova, H. Aladjov, *J. Electromyogr. Kinesiol.*, **14**, 227 (2004).
25. K. Yankov, in: Proceedings of the International Conference on Information Technologies (InfoTech-2011), R. Romanski (eds.), 2011, p. 225.
26. K. Yankov, in: Proceedings of the International Conference on Information Technologies (InfoTech-2012), R. Romanski (eds.), 2012, p. 114.
27. N. Bektaş, Y. Öztürk, *Turk. J. Med. Sci.*, **42**, 211 (2012).
28. G. Liu, F. Daneshgari, *Chin. Med. J. (Engl.)*, **127**, 1357 (2014).
29. L.A. Szarka, M. Camilleri, *J. Diabetes Sci. Technol.*, **4**, 180 (2010).
30. V.J. Horváth, F. Izbéki, C. Lengyel, P. Kempler, T. Várkonyi, *Curr. Diab. Rep.*, **14**, 527 (2014).
31. L. He, Y. Sun, Y. Zhu, R. Ren, Y. Zhang, F. Wang, *Genet. Mol. Res.*, **13**, 7163 (2014).
32. S. Tobu, M. Noguchi, T. Hatada, K. Mori, M. Matsuo, H. Sakai, *Curr. Urol.*, **6**, 62 (2012).
33. K. Touw, S. Chakraborty, W. Zhang, A.G. Obukhov, J.D. Tune, S.J. Gunst, B.P. Herring, *Am. J. Physiol. Gastrointest. Liver. Physiol.*, **302**, 66 (2012).
34. Z. Jancsó, N. Bódi, B. Borsos, É. Fekete, E. Hermes, *Int. J. Biochem. Cell Biol.*, **62**, 125 (2015).
35. J.H. Han, I.H. Chang, S.C. Myung, M.Y. Lee, W.Y. Kim, S.Y. Lee, S.Y. Lee, S.W. Lee, K.D. Kim. *Korean J Physiol Pharmacol.*, **16**, 37 (2012).
36. I.M. Kvetnoy, I.E. Ingel, T.V. Kvetnaia, N.K. Malinovskaya, S.I. Rapoport, N.T. Raikhlín, A.V. Trofimov, V.V. Yuzhakov, *Neuro Endocrinol Lett.*, **23**, 121 (2002).
37. E. Peschke, *J. Pineal Res.*, **44**, 26 (2008).
38. E.C. Ebert, *Dis. Mon.*, **51**, 620 (2005).
39. H. Ariga, K. Imai, C. Chen, C. Mantyh, T.N. Pappas, T. Takahashi, *Am. J. Physiol. Regul. Integr. Comp. Physiol.*, **294**, 1807 (2008).
40. C. Yang, Z. Liu, K. Liu, P. Yang, *PLoS One.*, **9**, e85785 (2014)
41. D. Zhao, Y. Zhan, H. Zeng, M.P. Moyer, C.S. Mantzoros, C. Pothoulakis, *J. Cell. Biochem.*, **97**, 1317 (2006).
42. Z.Z. Liu, W.G. Wang, Q. Li, M. Tang, J. Li, W.T. Wu, Y.H. Wan, Z.G. Wang, S.S. Bao, J. Fei, *Cell Biosci.*, **5**, 12 (2015).

АНГИОТЕНЗИН II – ПРЕДИЗВИКАНА АКТИВНОСТ НА РЕЗЕРВОАРНИ ГЛАДКО-МУСКУЛНИ ОРГАНИ ОТ ТРЕТИРАНИ С ГРЕЛИН И МЕЛАТОНИН ДИАБЕТНИ ПЛЪХОВЕ

П. В. Хаджибожева^{1*}, Ц. К. Георгиев¹, Р. Е. Калфин², Г. С. Илиева¹, А. Н. Толева¹

¹*Катедра Физиология, патофизиология и фармакология, Медицински Факултет, Тракийски Университет, ул. „Армейска“ 11, Стара Загора 6000 (България)*

²*Институт по Невробиология, Българска Академия на Науките, ул. „Акад. Георги Бончев“ 23, София 1113 (България)*

Постъпила на 29 септември, 2016 г.; Коригирана на 13 февруари, 2017 г.

(Резюме)

Целта на изследването беше да се установи ефекта от краткосрочното приложение на грелин (ГРЛ) или мелатонин (МЛТ) върху ангиотензин II (Анг II)-провокирана активност на стомах, ректум и пикочен мехур от плъхове със стрептозотозин (СТЗ)-предизвикан диабет. Половозрели плъхове, линия Wistar, бяха разделени в 4 групи: контрола; СТЗ-третиран: с единична доза СТЗ; МЛТ-третиран: единична доза СТЗ, последвано от приложение на МЛТ за 7 последователни дни; ГРЛ-третиран: единична доза СТЗ, последвано от приложение на ГРЛ за 7 последователни дни. Експериментът продължи 42 дни и в края му препарати от резервоарните органи бяха изработени и повлияни с Анг II. Анализът на силовите и кинетични параметри на получените гладко-мускулни съкращения бе осъществен със софтуер KORELIA.

СТЗ-предизвиканият диабет засегна в различна степен Анг II-провокираната активност на резервоарните органи. При групата, третирана с МЛТ, се установи силен отговор на стомаха към Анг II (1.91 ± 0.07 g) и слаба реакцията на препаратите от пикочен мехур (1.12 ± 0.11 g), в сравнение с контролната група (съответно 1.14 ± 0.13 g и 1.74 ± 0.22 g). Приложението на ГРЛ почти напълно възстанови нормалните силови характеристики на съкращението на пикочния мехур и доведе до ускорено протичане на стомашните контракции. Отговорът към Анг II на ректалните препарати от третираните с ГРЛ или МЛТ животни, не беше подобрен.

Въпреки че бяха частични, се регистрираха благоприятни ефекти от краткосрочното приложение на МЛТ или ГРЛ при животните със СТЗ-индуциран диабет. Благоприятният ефект върху Анг II-предизвиканата активност на стомах и пикочен мехур вероятно се дължи на антиоксидантните и про-кинетици въздействия на МЛТ и ГРЛ върху гладката мускулатура.

Endocrine cells in pig's gallbladder, ductus cysticus and ductus choledochus with special reference to ghrelin

M.V. Gulubova^{1*}, I.V. Valkova², K.V. Ivanova¹, I.G. Ganeva¹, D.K. Prangova¹,
M.M.K. Ignatova¹, S.R. Vasilev³, I.S. Stefanov²

¹ Department of General and Clinical Pathology, Medical Faculty, Trakia University, Stara Zagora, Bulgaria

² Department of Anatomy, Medical Faculty, Trakia University, Stara Zagora, Bulgaria

³ Department of Physiology, Pathophysiology and Pharmacology, Medical Faculty, Trakia University, Stara Zagora, Bulgaria

Received September 14, 2016; Revised March 5, 2017

In human biliary pathways and gallbladder there have been several reports describing endocrine cells (ECs) mainly in chronic inflammation. In pigs' biliary structures we couldn't find data about ECs. Ghrelin is peptide hormone participating in the growth-hormone-release and in modulation of food intake. It has also pro-inflammatory functions. Ghrelin-positive ECs are the main source of Ghrelin. The present study reveals the presence of ghrelin+ ECs in pigs' gallbladder cystic and choledochal duct – by immunohistochemistry. In pigs gallbladder ECs are very rare. Single Chromogranin A⁺, Somatostatin⁺ and Serotonin⁺ ECs were observed. In choledochal duct there are Chromogranin A⁺, Somatostatin⁺, Gastrin⁺ and Ghrelin+ECs more in number as compared to gallbladder. Most ECs were located in d.cysticus. They were also Chromogranin A⁺, Somatostatin⁺, Gastrin⁺ and Ghrelin+ ECs. In conclusion we support that various ECs including Ghrelin exert action on physiology and pathology conditions in biliary tree in pigs.

Key words: endocrine cells, ghrelin, pigs' biliary system

INTRODUCTION

Endocrine cells had been found to be widely distributed in the epithelial structures in gastrointestinal tract [1, 2]. In human embryo, the first anlage of the bile ducts and the liver was the hepatic diverticulum or liver bud, that occurred on eighteen day in the anterior intestinal portal [3] and it's endodermal origin was already demonstrated [2]. Endocrine cells in human gallbladder and biliary pathways were investigated mainly in disease [4]. In human biliary pathways endocrine cells presence was associated with dysplasia and metaplasia around malignant tumors [5, 6], developmental mistakes and in chronic conditions [7, 8].

Endocrine cells and nerve structures had been investigated in the gastrointestinal tract of different animal species [9-14]. There existed some reports on the existence of endocrine cells in the biliary and pancreatic ducts of rabbit, rat, cat and sheep [15, 16, 17]. At least eight immunohistochemically distinct endocrine cell types were described in the bile ducts of some vertebrate species as followed: motilin and substance P (SP) in rabbits [16]; insulin, glucagon, somatostatin, pancreatic polypeptide (PP) and cholecystokinin (CCK) in rat

common pancreatic bile duct [18]; insulin, glucagon, CCK, PP and somatostatin in rat bile duct in diabetes [19]; serotonin and somatostatin in pigs' bile duct and gallbladder [12]; somatostatin in pigs' gallbladder and biliary pathways [12]; insulin, glucagon, PP, somatostatin in extrahepatic bile ducts of hilar region in mice [20]. Our previous investigation on endocrine cells in human common bile duct in obstructive jaundice showed chromogranin A (CHA), synaptophysin, somatostatin (SOM), serotonin (SER), gastrin (GAS) and secret in immunoreactivity (IR) in choledochal endocrine cells and an increase of these cells in chronic inflammation [7].

Ghrelin-immunoreactivity (IR) cells were identified mainly in vertebrate stomach [21, 22, 23]. Ghrelin consists of 28 aminoacids, including O-n-octanoylated Ser³ residue essential for growth hormone release [21]. Ghrelin's physiological and pathophysiological significance had been extensively studied since its discovery in 1999 [24, 25]. In rodents ghrelin-producing cells were observed all over the gastrointestinal tract: gastric body, antrum, duodenum, ileum, cecum, colon [26]. Ghrelin IR was described in distinct cells of pancreas, pituitary, lung and thyroid [27-32]. Ghrelin positivity was observed also in some immune cells in human (T cells, B cells and neutrophils), [33]. Ghrelin mRNA was amplified

* To whom all correspondence should be sent:
E-mail: mgulubova@hotmail.com

from multiple tissues, but for many of these any cellular confirmation is still lacking [34].

To our knowledge there was no data about endocrine cells and about ghrelin-positive endocrine cells in pigs' gallbladder, cystic duct and choledochal duct. The aim of the present study was to describe chromogranin-, somatostatin-, serotonin-, gastrin- and ghrelin-positive endocrine cells in pig's gallbladder, cystic and choledochal ducts.

MATERIALS AND METHODS

Animals and tissues sampling

The material was obtained from the gallbladder's neck, middle parts of ductus cysticus and ductus choledochus of 6 male pigs (Landras X Danube White). The animals aged 6 months, weighing 92-98 kg, slaughtered for meat consumption in a slaughterhouse in accordance with the Bulgarian laws. In the current study cross serial sections of the mentioned organs were used. A total of 6 pigs were used in this study.

Immediately after slaughtering, small specimens from gallbladder's neck, middle part of ductus choledochus and ductus cysticus were taken for each animal. The samples (total number=18) were promptly fixed in 4% para-formaldehyde in 0.01 M phosphate-buffered saline (PBS), pH 7.4, for 24 h at 4°C. After that the specimens were dehydrated in graded series of ethanol, cleared with xylene and embedded in paraffin. Microtome sections (4 µm-thick) were cut and collected onto slides treated with poly-L-lysine. One section of each sample was stained with hematoxylin and eosin (HE) and examined under a light microscope (LEICA DM 1000, Germany) to assess the morphology and exclude pathological changes. The other sections were treated by immunohistochemistry.

Immunohistochemistry

Immunohistochemical staining for chromogranin (CHA), gastrin (GAS), somatostatin (SOM), serotonin (SER), ghrelin (GHR), (Table 1), was performed using avidin-biotin-peroxidase complex technique on formalin-fixed and paraffin-embedded tissue sections as described earlier [7]. Paraffin sections 4µm thick were dewaxed in two xylenes at 56°C for 1 h, and were rehydrated in ethanol. Later, they were washed in 0.1 M PBS, pH 7.4, boiled for 20 min at 100°C, cooled at room temperature, incubated in 1.2 % hydrogen peroxide in methanol for 30 min, and rinsed in 0.1 M phosphate buffer, pH 7.4, for 15 min. The sections were then blocked for 30 min with normal

mouse/rabbit serum (DAKO). After incubating with the primary mouse/rabbit antibodies overnight, they were washed in PBS, pH 7.4, and incubated with a secondary antimouse/antirabbit biotinylated antibody (DAKO ready-to-use LSAB®2 System, HRP K0675) for 4h, and subsequently with the streptavidin-HRP complex (DAKO ready-to-use LSAB®2 System, HRP K0675) for 4 h. All incubations were performed in a moist chamber. The reaction was made visible by using a mixture of 3 mg 3,3'-diaminobenzidine (DAB) (Sigma, St. Louis MO, USA) in 15 ml 0.05 Tris-HCL buffer, pH 7.5, and 36 µl 1% hydrogen peroxide for 10-20 min, rinsed in distilled water. The sections were dried overnight at room temperature, and then mounted with entellan for light microscopy. They were counterstained with Mayer's hematoxylin.

Sections incubated with non-immune sera instead of the primary antibodies were used as negative controls.

RESULTS

The structure of different swine gallbladders and bile ducts was judged to be fully normal in the different studied samples.

Gallbladder

In pig's gallbladder endocrine cells were very rare. From six different specimens endocrine cells could be observed in only two. Endocrine cells were found mainly in the intramural glands. They were CHA- (Fig. 1), SER-, and SOM- positive.

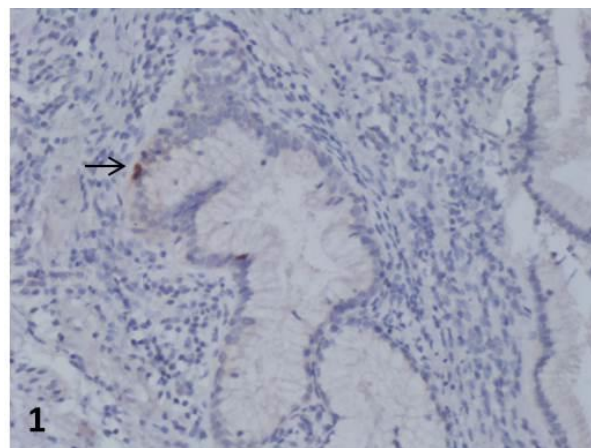


Fig. 1. Chromogranin A positive endocrine cell (arrow) in gallbladder (x 200).

Endocrine cells were located mainly on the basement membrane of the glands and were of closed type.

Ductus choledochus

From all six samples endocrine cells were observed in five of them, in mural glands. The

density of endocrine cells was increased as compared to that in gallbladder. CHA-positive cells

were most numerous (Fig.2a).

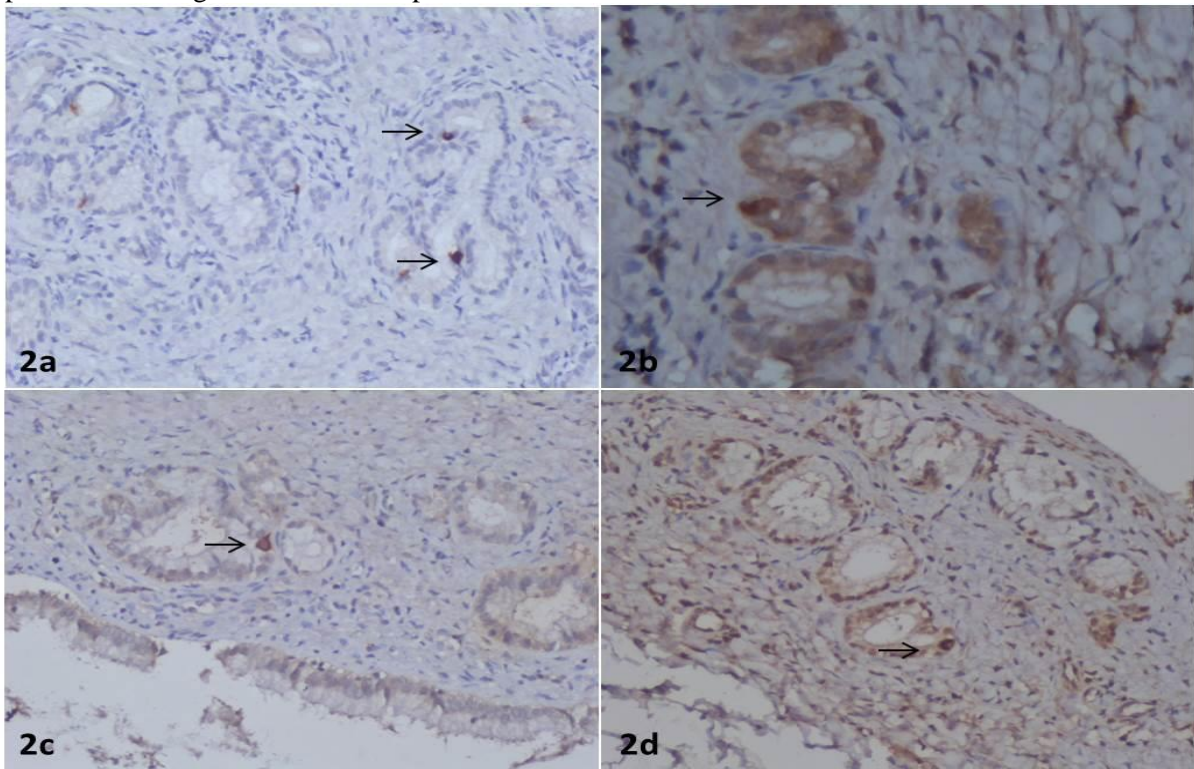


Fig. 2. a) Chromogranin A positive endocrine cells (arrows) in ductus choledochus (x 100); b) Somatostatin positive endocrine cell (arrow) in ductus choledochus (x 200); c) Gastrin positive endocrine cell (arrow) in ductus choledochus (x 200); d) Ghrelin positive endocrine cell (arrow) in ductus choledochus (x 100).

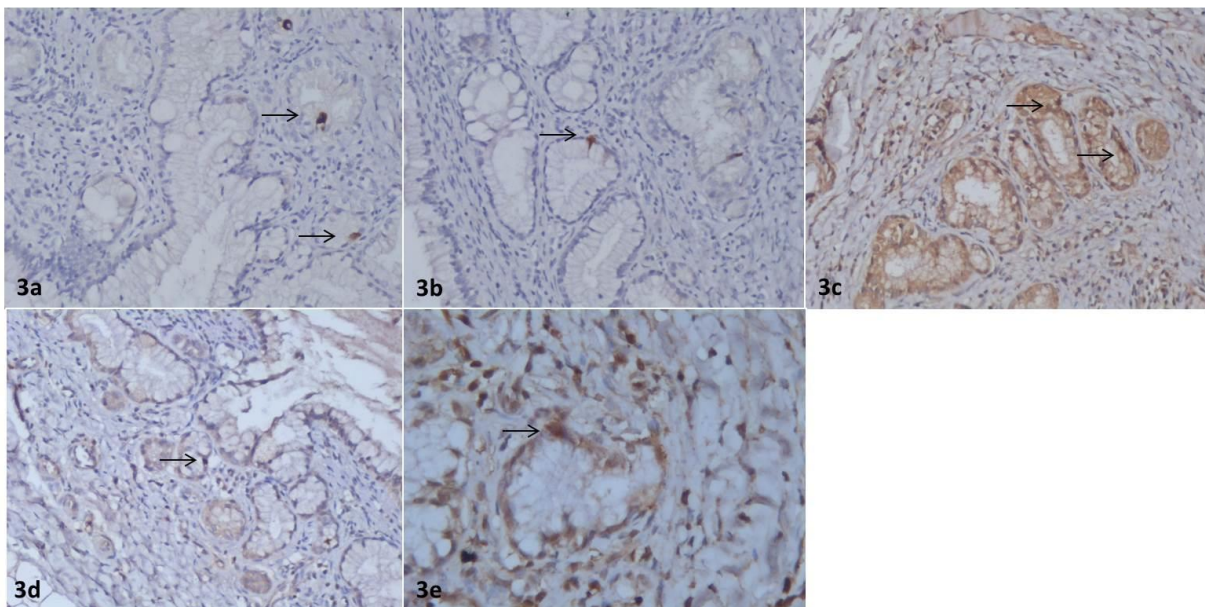


Fig. 3. a,b) Chromogranin A positive endocrine cells (arrows) in ductus cysticus (x 100); c) Somatostatin positive endocrine cells (arrows) in ductus cysticus (x 100); d) Gastrin positive endocrine cell (arrow) in ductus cysticus (x 100); e) Ghrelin positive endocrine cell (arrow) in ductus cysticus (x 200).

SOM immunoreactive (IR) endocrine cells were seen at the base of glands (Fig.2b). In the connective tissue around glands there could be observed SOM-positive peptidergic nerve fibers.

SER-positive endocrine cells were also scattered in some glands. Single GAS-positive endocrine cells were located in glands structures beneath the surface epithelium (Fig. 2c).

GHR-positivity was observed in endocrine cells in the intramural glands (Fig. 2d), in some nerve fibers and connective tissue cells (mast cells).

Ductus cysticus

Endocrine cells were observed in all six samples and were more as compared to the other two locations. Of them CHA-positive cells were most numerous. Most of these endocrine cells were in close proximity to goblet cells in the same glands and were from the closed type (Fig. 3a).

Some endocrine cells showed opened type (Fig. 3b). SOM-positive endocrine cells were observed in the glands and surface epithelium (Fig. 3c). GAS IR endocrine cells and peptidenergetic nerve fibers were seen in the glands and muscle tissue (Fig. 3d). SER-positive endocrine cells were also detected.

GHR-positive endocrine cells and inflammatory cells were found in glands and around them in all specimens (Fig. 3e). We could find also ghrelin immunoreactivity in the intramural nerve ganglionic cells.

DISCUSSION

The gallbladder- biliary pathways system played an important role in modulating bile flow, secreting mucous substances and maintaining biliary motility [35]. Previous studies reported vasointestinal polypeptide (VIP), SP, somatostatin and met-enkephalin IR nerves in the gall bladder and biliary pathway of the guinea pig [12]. Their secreted hormones exerted neuronal control on biliary motility [36].

In the present study it was showed for the first time that ghrelin-positive endocrine cells existed in swine gallbladder, ductus cysticus and choledochus. The presence of SOM-, SER-, GAS- and CHA-positive endocrine cells was also described there.

Endocrine cells were most numerous in cystic duct followed by common bile duct and were less in the neck region of the gallbladder. Our unpublished observations showed single endocrine cells in human gallbladder, and plenty of endocrine cells in the lower third of human common bile duct in mechanic jaundice [7].

We have found SOM-positive endocrine cells in all studied sites located in the mural glands and in the surface epithelium.

SOM IR endocrine cells were found in human extrahepatic bile ducts [5, 7]. SOM-positive D cells were detected in common bile duct of guinea pig [12] and bile duct of pigs [36]. Unlike Sand et al., 1993 we detected SOM-positive nerve fibers in bile

ducts. It could be suggested that SOM is a biliary neurotransmitter.

SOM played mainly an inhibitory role in endocrine secretion, biliary motility etc. [12]. In the guinea pig there had been demonstrated lack of effect of SOM on the motility of the gallbladder [37].

SOM that was a neuropeptide and hormone had been reported to inhibit spontaneous and CCK-induced gallbladder motility [38]. The authors showed that when the gallbladder smooth muscle was contracted by electrical stimulation, SOM decreased the contraction by suppressing acetylcholine release.

SOM was known to inhibit the effect of some peptide hormones such as CCK that induced relaxation of the sphincter of Oddi [39]. In diabetes, SOM IR ECs increased in biliary pathways and the increased hormone release induced contraction on sphincter of Oddi muscles and concomitant bile stasis and stone formation [19]. SOM stimulated sphincter of Oddi activity that favoured the reduced flow of bile into the duodenum and facilitated gallbladder filling [40].

Single SER-positive endocrine cells were observed in the intramural glands in gallbladder neck and in the ductus cysticus and choledochus. SER IR endocrine cells were found to be exclusively low in number in the rat pancreatic and bile duct system [19] in pig bile duct and gallbladder [36] or missing in rat bile duct [18]. In a previous study we described that SER-positive endocrine cells increased in number in chronic cholangitis [7]. Serotonin is an important neurohumoral signaling molecule [13]. SER-positive endocrine cells are sensory transducers that responded to mechanical or chemical stimulation of the mucosa by releasing serotonin [41] that regulated visceral sensation and gut motility [13].

Gastrin-positive endocrine cells were found in cystic duct and choledochal duct in our study. Something more, GAS-positive nerves were detected in these structures. In a previous study [7] it was observed G cells in human common bile duct, whose ultrastructure was similar to that of gastric G cells. Our present finding confirmed our previous suggestion that GAS-positive (G cells) were part of the gastrointestinal triangle. The latter consisted in GAS-positive cells in the junction of the cystic duct with common bile duct, the junction between the second and the third portions of the duodenum and by the junction between the neck and body of the pancreas [42]. In humans and pigs G cells were most numerous in antrum and stimulated gastric acid secretion [43, 44]. Presence

of G cells and GAS-positive nerve fibers in biliary structures could be explained with initiating contraction of their smooth muscle cells and with modulation of their motility [45].

Ghrelin was mainly described in endocrine cells of human digestive, respiratory and urinary system and in particular cells of some endocrine glands [27]. In human stomach (oxyntic region) the relative percentages of main four endocrine cell types were 30% for ECL cells (histamine-positive), 20% for P/D₁-like cells (GHR), 22% for D cells (SOM), and 7% for EC cells (SER) [46]. GHR-positive cells accounted for 23% of CHA-positive cells there [46]. It was established that GHR-positive cells co-localized with CHA and VMAT2 [27, 46]. In pig's stomach GHR-positive cells encountered about 84.79 cells/mm² in corpus (the greatest number) and showed decreased frequency in cardia, pylorus and small intestine [47].

Endocrine cells in biliary system were rarely described in animals [18, 19, 36] and in humans [7]. There were no data about GHR-positive cells in human biliary pathways [20] and in pig's biliary structures. Our study demonstrated GHR-positive endocrine cells in glands and GHR positivity in some nerve fibers and ganglionic cells in gallbladder, cystic duct and choledochal duct in pigs. In human's gallbladder there was detected ghrelin and ghrelin receptor mRNA expression [34] but ghrelin tissue localization wasn't described yet. Based on our finding of GHR presence in nerve structures of biliary pathways, ghrelin neurotransmitter function could be supposed. There existed data about ghrelin localization in central nervous system [48] and in Auerbach nerve plexus [26, 49]. GHR had structural similarities with motilin [50] and co-existed in one and the same cell. It was reported that motilin initiated and realized gallbladder emptying [50] and stimulated contraction of smooth muscle cells in human gallbladder [51]. Ghrelin on its side was a growth hormone-secretagogue and the last increased gallbladder motility [52]. It was shown that in humans low ghrelin serum levels were seen in metabolic syndrome and in gallstone disease [53]. Ghrelin receptors might exist on mucosal cells and signals for GHR production might come from the lumen. Another explanation for GHR presence in biliary mucosal endocrine cells might be for its role in stimulating the growth hormone secretion that is necessary for cell proliferation.

We had demonstrated ghrelin positivity in some immune cells in biliary pathways.

It was already shown that GHS-RmRNA expression was found in human lymphoid

organs [54] or in purified human T cells [55]. The majority of T cells from human donors express and secrete low levels of ghrelin constitutively and high levels upon cellular activation [55]. Therefore our finding of Ghr positivity in some immune cells in pig's biliary pathways confirmed the presence of basal ghrelin expression in some inflammatory cells. The endogenous GR inhibited proinflammatory cytokine expression (IL-1a, IL-1b, IL-6) [55] and it would be supposed that Ghr may function as an important signal modulator among the endocrine, nervous and immune systems. The presence of GHR in endocrine and immune cells in biliary pathways confirmed the integrity between this hormone and immune reactions in organism.

REFERENCES

1. F. Sandler, R. Hakanson, *Elsevier*, **6**, 219 (1988).
2. A. Andrew, B. Kramer, B.B. Rawdon, *J Pathol*, **186**, 117 (1998).
3. T. Roskams, V. Desmet, *The Anatomical record*; **291**, 628 (2008).
4. H. Kurumaya, G.F. Ohta, K. Nakanuma, *Arch Pathol Lab Med*, **113**, 143 (1989).
5. H. Dancigier, U. Klein, U. Leuschner, K. Hubner, M. Classen, *Gastroenterology*, **86**, 892 (1984).
6. M.P. Hoang, L.A. Muracata, A.L. Pedilla-Rodriguez, J. Albores-Saavedra, *Mod Pathol*, **14**, 1119 (2001).
7. M.V. Gulubova, P. Hadjipetkov, D. Sivrev, G. Ilieva. *Hepato-Gastroenterology*, **59** (2012).
8. J. Ducla-Soares, M. Ferreira, C. Campos, *Am J Gastroenterol*, **87**, 668 (1992).
9. J.C. Doss, C.C. Grone, T.J. Rosol. *Vet Pathol*, **35**, 312 (1998).
10. F.J. Esteban, J.B. Jimenez, J.A. Barroso, M.L. Pedrosa, J. Del Moral, J. Rodrigo, M.A. Peinado. *J Anat*, **193**, 241 (1998).
11. P. Chen, B. Hu, Q. Tan, L. Liu, D. Li, C. Jiang, H. Wu, J. Li, C. Tang. *Neurogastroenterol Motil*, **22**, 935 (2010).
12. W-Q. Cai, G. Gabella. *J Anat*, **136**, 97 (1983).
13. H. Zhao, I. Sovadinova, V.M. Swope, G.M. Swain, M.M. Kadrofske, X. Bian. *Neurogastroenterol Motil*, **23**, 161 (2011).
14. A.K. Patnaik, P.H. Liberman, R.A. Erlandson, C. Antoanescu. *Vet Pathol*, **42**, 331 (2005).
15. M.Y. Lee. *J Cathol. Med. Coll*, **41**, 787 (1988).
16. P. Heitz, J.M. Polak, C.M. Kasper, A.G.E. Pearse, *Histochemistry*, **50**, 319 (1977).
17. R.T. Gemmell, T. Heath, *J Anat*, **115**, 221 (1973).
18. I-S. Park, M. Bendayan, *The Anatomical Record*, **232**, 247 (1992).
19. I-S. Park, M. Bendayan, *Pancreas*, **9**, 566 (1994).
20. J.R. Dutton, N.L. Chillingworth, D. Eberhard, C.R. Brannon, M.A. Hornsley, D. Tosh, J.M.W. Slack, *J Cell Sci*, **120**, 239 (2006).

21. M. Grönberg, A.V. Tsolakis, L. Magnusson, E.T. Janson, J. Saras, *J HistochemCytochem*, **56**, 793 (2008).
22. T. Hayashida, K. Nakahara, M.S. Mondal, Y. Date, M. Nakazato, M. Kojima, K. Kangawa, N. Murakami, *Journal of Endocrinology*, **173**, 239(2002).
23. C-M. Zhao, M.A. Furnes, B. Stenstrom, B. Kulseng, D. Chen, *Cell Tissue Res*, **331**, 575 (2008).
24. M. Kojima, H. Hosoda, Y. Date, M. Nakazato, H. Matusio, K. Kangawa, *Nature*, **402**, 656 (1999).
25. M. Kojima, A. Kanagawa, *Nat ClinPractEndocrinolMetab*, **2**, 80 (2006).
26. Sakata I, Sakai T. Ghrelin, *Int J Pept*, **7** (2010).
27. G. Rindi, V. Necchi, A. Savio, A. Torsello, M. Zoli, V. Locatelli, F. Raimondo, D. Cocchi, E. Solcia, *Histochem Cell Biol*, **117**, 511 (2002).
28. C. Tomasetto, S.M. Karam, S. Ribieras, R. Masson, O. Lefebvre, A. Staub, G. Alexander, M-P. Chenard, M-C.Rio, *Gastroenterology*, **119**, 395 (2000).
29. Y. Date, M. Nakazato, S. Hashiguchi, K. Dezaki, M.S. Mondal, H. Hosoda, M. Kojima, K. Kangawa, T. Arima, H. Matsuo, T. Yada, S. Matsukura, *Diabetes*, **51**, 124 (2002).
30. M. Volante, E. Allia, E. Fulcheri, P. Cassoni, E. Ghigo, G. Muccioli, M. Papotti, *Am J Pathol*, **162**, 645 (2003).
31. G. Muccioli, M. Papotti, V. Locatelli, E. Ghigo, R. Deghenghi, *J Endocrinol Invest*, **24**, RC7 (2001).
32. G. Rindi, A. Torsello, V. Locatelli, E. Solcia. *ExpBiol Med*, **229**, 1007 (2004).
33. N. Hattori, T. Saito, T. Yagyu, B.H. Jiang, K. Kitagawa, C. Inagaki, *J ClinEndocrinolMetab*, **86**, 4284 (2001).
34. S. Gnanapavan, B. Kola, S.A. Bustin, D.G. Morris, P. McGee, P. Fairclough, S. Bhattacharya, R. Carpenter, A.B. Grossman, M. Korbonits, *J ClinEndocrinolMetab*, **87**, 2988 (2002).
35. J.P. Ryan. Motility of the gallbladder and biliary tree. In: Physiology of the Gastrointestinal Tract. Jonson, LR, ed. Raven Press, New York, 1987, 665.
36. J. Sand, H. Tainio, I. Nordback, *Dig Dis Sci*, **38**, 694 (1993).
37. P. Poitras, T. Yamada, J.H. Walsh, *Journal of Physiology and Pharmacology*, **58**, 179 (1979).
38. K. Milenov, R. Rakovska, R. Kalfin, P. Mantovani. *Nuropeptides*, **17**, 75 (1990).
39. G.P. Adami, R. Leandri, J.C. Sarles, *GastroenterolClinBiol*, **10**, 108 (1986).
40. J. Huang, R.T.A. Padbury, A.C. Schloithe, M.R. Cox, M.E. Simula, J.R. Harvey, R.A. Baker, J. Toouli, G.T.P. Saccone, *Gastroenterology*, **115**, 672 (1998).
41. K. Racke, A. Reiman, H. Schoworer, H. Kilbinger. *Behav Brain Res*, **73**, 83 (1996)
42. B.E. Stabile, D.J. Morrow, E. Passaro, *Am J Surg*, **147**, 25 (1984).
43. E. El-Omar, I. Penman, C.A. Dorrian, J.E.S. Ardill, K.E.L. McColl, *Gut*, **34**, 1060 (1993).
44. J.C.P. Silva, J.L. Santos, A.J.A. Barbosa, *J Comp Path*, **126**, 235 (2002).
45. M.R. Cox, R.T.A. Padbury, T.L. Snelling, A.C. Schloithe, J.R. Harvey, J. Toouli, G.T.P. Saccone. *Dig Dis Sci*, **43**, 1275 (1998).
46. Y. Date, M. Kojima, H. Hosoda, A. Sawaguchi, M.S. Mondal, T. Sukanuma, S. Matsukura, K. Kangawa, M. Nakazato, *Endocrinology*, **141**, 4255 (2000).
47. F. Vitari, A. Di Giancamillo, D. Deponti, V. Carollo, C. Domeneghini. *Vet Res Commun*, **36**, 71 (2012).
48. S. Lu, J.L. Guan, Q.P. Wang, K. Uehara, S. Yamada, N. Goto, Y. Date, M. Nakazato, M. Kojima, K. Kangawa, S. Shioda. *Neurosci Lett*, **321**, 157 (2002).
49. L. Xu, I. Depoortere, C. Tomasetto, M. Zandecki, M. Tang, J.P. Timmermans, *RegulPept*, **124**, 119 (2005).
50. B. De Smet, A. Mitselos, I. Depoortere, *PharmacolTher*, **123**, 207 (2009).
51. T. Yamasaki, K. Chijiwa, Y. Chijiwa. *J Surg Res*, **56**, 89 (1994).
52. A. Moschetta, T.B. Twickler, J.F. Rehfeld, N. A. van Ooteghem, M.C. Cabezas, P. Portincasa, G. P. van Berge-Henegouwen, K.J. van Erpecum, *Dig Dis Sci*, **49**, 529 (2004).
53. N. Mendez-Sanchez, G. Ponciano-Rodriguez, L. Bermejo-Martinez, A.R. Villa, N.C. Chavez-Tapia, D. Zamora-Valdes, R. Pichardo-Bahena, B. Barredo-Prieto, M.H. Uribe-Ramos, M.H. Ramos, H.A. Baptista-Gonzalez, M. Uribe. *World J Gastroenterol*, **12**, 3096 (2006).
54. S. Gnanapavan, B. Kola, S.A. Bustin, D.G. Morris, P. McGee, P. Fairclough, S. Bhattacharya, R. Carpenter, A.B. Grossman, M. Korbonits. *J ClinEndocrinolMetab*, **87**, 2988 (2002).
55. V.D. Dixit, E.M. Schaffer, R.S. Pyle, G.D. Collins, S.K. Sakthivel, R. Palaniappan, J.W. Jr Lillard, D.D. Taub, *J Clin Invest*, **114**, 57 (2004).

ЕНДОКРИННИ КЛЕТКИ В ЖЛЪЧНИЯ МЕХУР, DUCTUS CYSTICUS И DUCTUS CHOLEDOCHUS ПРИ ПРАСЕТА СЪС СПЕЦИАЛНО ОТНОШЕНИЕ КЪМ ГРЕЛИНА

М. В. Гълъбова^{1*}, И. В. Вълкова², К. В. Иванова¹, И. Г. Ганева¹, Д. К. Прангова¹,
ММ. К. Игнатова¹, С. Р. Василев³, И. С. Стефанов²

¹Катедра „Обща и клинична патология“, Медицински факултет, Тракийски университет, Стара Загора, България

²Катедра „Анатомия“, Медицински факултет, Тракийски университет, Стара Загора, България

³Катедра „Физиология, Патифизиология и Фармакология“ Медицински факултет, Тракийски университет, Стара Загора, България

Постъпила на 14 септември 2016г.; Коригирана на 5 март 2017г.

(Резюме)

Съществуват няколко съобщения, в които са описани ендокринните клетки (ECs) в жлъчният мехур и жлъчните пътища при човека, свързани с хронично възпаление. При прасето обаче ние не открихме данни за присъствието ECs в тези структури. Грелинът е пептиден хормон, участващ в освобождаването на растежния хормон и в модулирането на приема на храна. Той притежава също проинфламаторни функции. Грелин позитивните ECs са основен източник на грелин. Настоящото изследване разкрива имунохистохимично присъствието на грелин⁺ ECs в жлъчния мехур и *ductus choledochus*. Ендокринните клетки в жлъчния мехур са твърде малко. Наблюдавани са единични Chromogranin A⁺, Somatostatin⁺ и Serotonin⁺ECs. В *ductus choledochus* са установени по-голям брой Chromogranin A⁺, Somatostatin⁺ и Serotonin⁺ECs в сравнение с жлъчния мехур. Най-много ECs бяха локализирани в *d.cysticus*. Те са също Chromogranin A⁺, Somatostatin⁺, Gastrin⁺ и Ghrelin⁺ECs. В заключение, предполагаме, че ECs, включително грелин позитивните ECs упражняват действие върху физиологичните и патологичните състояния в жлъчните пътища при прасета.

Effect of N-[N'-(2-chloroethyl)-N'-nitrosocarbamoyl-glycine amide of 2,2,6,6-tetramethyl-4-aminopiperidine-1-oxyl (SLCNUgly) on Angiotensin II-mediated smooth muscle activity of organs in pelvic cavity

T.K. Georgiev^{1*}, P.V. Hadzhibozheva¹, E.D. Georgieva², Y.D. Karamalakova², G.D. Nikolova², V.G. Gadjeva², A.M. Zheleva², A.N. Tolekova¹

¹Department of Physiology, Pathophysiology and Pharmacology, Medical Faculty, Trakia University, Stara Zagora, Bulgaria

²Department of Chemistry and Biochemistry, Medical Faculty, Trakia University, Stara Zagora, Bulgaria

Received September 29, 2016; Revised February 21, 2017

Persistent hyperglycemia during diabetes mellitus impairs contractile responses of smooth muscles to pressor hormones like Angiotensin II (Ang II). The main etiological factor for this diabetic disturbance is the excessive formation of reactive oxygen radicals leading to oxidative stress and disrupted cell calcium signaling machinery. Therefore antioxidants have the potential to improve smooth muscle diabetic dysfunction.

The purpose of this study was to assess the effects of administration of SLCNUgly on the oxidative and glycemic status and on Ang II – induced motility of organs from the pelvic cavity of rats.

Mature female Wistar rats were divided into three groups: control group (intact animals); STZ-treated group (single injection of 60 mg/kg STZ); group, treated seven consecutive days after STZ injection with 10mg/kg SLCNUgly. In the end of experimental period, longitudinal strips from the urinary bladder, rectum and uterus were prepared and influenced by Ang II (1µmol). The obtained contraction curves were analyzed by calculation of force and time-parameters of the contractile process. The concentrations of ascorbate radicals, ROS production and lipid peroxidation (malondialdehyde) were evaluated in tissue homogenates from the liver, kidney and pancreas.

The seven-day administration of SLCNUgly improved significantly the glycemic status. It caused an additional reduction of Ang II-mediated response and greatly decreased the half relaxation phase of the myometrial response. Rectal preparations from SLCNUgly-treated diabetic rats responded to Ang II with reduced force parameters. The nitrosourea tends to normalize force and time-parameters of the urinary bladder. SLCNUgly has a small effect over amelioration of tissue oxidative damages.

Key words: Angiotensin II, SLCNUgly, smooth muscle contraction, oxidative stress, Streptozotocin

INTRODUCTION

Diabetes mellitus (DM) comprises a group of metabolic disorder characterized by varying or persistent hyperglycemia, due to decreased production of insulin or impaired utilization of glucose. DM is a major and increasingly significant worldwide health problem. World Health Organization predicts increase the incidence of diabetes to 5% for the period until 2030 [1]. The persistent hyperglycemia leads to long-term organ damages, thus affecting all the systems in the organism [2]. Most of the manifested symptoms of DM are related to smooth muscle dysfunction [3]. There are numbers of articles, which described the impaired urinary bladder activity [4], rectal incontinency [5] and uterine dysfunction [6]. The etiology of the impaired smooth muscle motility in DM is multifactorial [7], but the main factor for this diabetic disturbance is the excessive formation of reactive oxygen species (ROS) leading to oxidative

stress and disrupted cell calcium signaling machinery [8]. Considering the role of oxidative stress in the development of structural and functional cell damage and the progression of DM, many scientific efforts are directed towards search and application of effective antioxidants [9]. Possible agent with therapeutic antioxidant potential for treatment of DM, is the newly synthesized nitrosourea N-[N'-(2-chloroethyl)-N'-nitrosocarbamoyl-glycine amide of 2, 2, 6, 6-tetramethyl- 4- aminopiperidine- 1- oxyl (SLCNUgly), spin-labeled analog of CCNU [10]. Previously reported *in vitro* physico-chemical properties determined higher alkylating activity, shorter half-life (29 min for SLCNUgly and 54 min for CCNU), and almost twice lower carbamoylating activity comparing to CCNU. *In vivo* SLCNUgly exhibited higher anti-leukaemic activity, anti-melanomic and immunomodulatory properties [11,12], and represent as a new class for tumor scintigraphy, radioprotectors which may have application as general antioxidant for *in vivo* radiotherapy and tumor localization [13].

* To whom all correspondence should be sent:
E-mail: phript@gmail.com

The purpose of this study was to assess the effects of administration of SLCNUgly on the oxidative and glycemic status and on Ang II – induced motility of organs from the pelvic cavity of rats.

EXPERIMENTAL

Animals

18 non-pregnant female Wistar rats, weighing 200-250 g were used. The animals were divided into the following groups: Group 1: controls; Group 2: diabetic animals; Group 3: diabetic animals, treated with SLCNUgly. DM was induced by a single intraperitoneal injection of Streptozotocin (STZ) 60 mg/kg BW. STZ was dissolved in cold 0.1M citrate buffer, pH 4.5. 72 hours after STZ administration, only animals with blood glucose levels higher than 16 mmol/l were considered to be diabetic and left in the experiment. The experiment lasted 8 days. SLCNUgly was administered in a dose of 10 mg/kg i.p. The application of SLCNUgly started in the next day, after STZ injection and lasted 7 consecutive days. The control group was injected with saline i.p. for 8 consecutive days.

Sample preparations and experimental protocols

In the end of experimental period, animals were anesthetized with Nembutal 50 mg/kg i.p. and preparations of the urinary bladder (UB), uterine horns (UH) and rectum (R) were made. The experimental protocol of the study was approved by the Institutional Animal Care and was in accordance with the national regulations and European Directive of 22.09.2010 (210/63/EU) concerning the protection of animals used for scientific and experimental purposes.

The preparation of the tissue samples and the recording of mechanical activity were conducted as it was previously described [14,15]. After the equilibration period, preparations were influenced by Ang II in a dose of 1 μ mol (10^{-6} M).

Chemicals, drugs and equipment

Ang II, STZ and all reagents for preparation of Krebs solution and citrate buffer were purchased from Sigma-Aldrich Chemie GmbH, Germany. Blood glucose levels were measured by Medisign mm810 glucomer (Empecs Medical Device Co., Ltd., China).

Spin-labeled drug SLCNUgly was synthesized according to Zheleva et al. [10]. Dimethyl sulfoxide (DMSO), N-tert-butyl-alpha-phenylnitron (PBN), 2-(4-carboxyphenyl)-4,4,5,5-tetra-methylimidazoline-1-oxyl-3-oxide (Carboxy-

PTIO.K) and PBS were purchased from Sigma Chemical Co, St. Louis, USA. All the other chemicals used in this study were with analytical grade.

Data analysis and statistical processing

The mechanical activity was transformed by a mechanical-force sensor, amplified, digitized and recorded using digital acquisition software ISOSYS-ADVANCED 1.0, produced by Experimetria Ltd., Hungary. The conversion of the data and primary data processing was performed with KORELIA-Processing software [16]. The recorded force-vs.-time curves permit determination of amplitudes of contraction and integrated force of contraction (represented by the area under the curve - AUC). The following time-parameters of smooth muscle contraction (SMC) were defined and calculated: half-contraction time (T_{hc}) - time interval between the beginning of SMC and half of the maximal force ($F_{max}/2$); contraction time (T_c) - time interval between the beginning of SMC and F_{max} ; half-relaxation time (T_{hr}) - time interval between F_{max} and $F_{max}/2$; contraction plus half-relaxation time (T_{chr}) - time interval between the start of the SMC and $F_{max}/2$. The duration of the interval for analysis of tonic contraction was 5 minutes. Reported amplitudes, integrated force and time-parameters of uterine SMC were analyzed with KORELIA-Dynamics software [17].

For all Electron Paramagnetic Resonance measurements an X-band EMXmicro spectrometer (Bruker, Germany) equipped with standard Resonator was used. Spectral processing was performed using Bruker WIN-EPR and SimFonia software. The levels of the Asc., NO radicals and ROS products in the tissue/organ homogenates were calculated after double integration of the plots under the corresponding EPR spectra and expressed in arbitrary units. The level of ROS products was studied according to Shi et al. [18] with some modifications by Zheleva et al. [19]. Asc. radicals were studied by Buettner & Jurkiewicz [20], and •NO radicals according to methods of Yoshioka et al. [21] and Yokoyama et al. [22] with slight modifications.

The data obtained were processed by statistical program Statistica Version 6.1 (StaSoft, Inc., Tulsa, OK, USA) and presented as mean \pm standard error. Statistical analysis was performed using one-way ANOVA and Student t-test to determine significant differences among data groups. A *P*-value less than or equal to 0.05 was considered as statistically significant.

RESULTS AND DISCUSSION

Smooth muscle activity

Urinary Bladder

As is shown in Figure 1 and table 1, the registered force parameters of the UB preparations from group 2, were increased. Ang II-mediated response of the UB strips of group 3 was approaching to the controls. In regard to time-parameters, there was no statistical difference between the three groups.

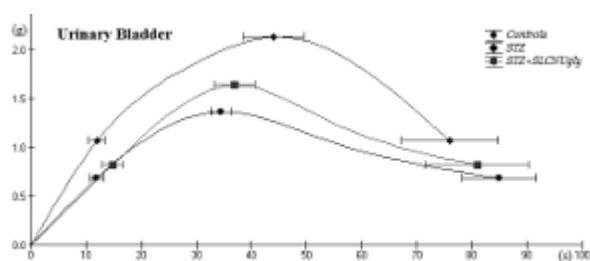


Fig. 1. Graphic visualization of SMC from rat urinary bladder after Ang II stimulation.

Table 1. Parameters of SMC from Urinary bladder of rats after Ang II stimulation.

	Ampl. (g)	AUC (gs)	T _{hc} (s)	T _c (s)	T _{hr} (s)	T _{chr} (s)
Con-trols	1.37±0.19	120±10	11.92±1.36	34.5±2	50.5±4.6	84.9±6.731
STZ	2.14±0.41*	123.83±229.62	10.79±1.52	46.67±5.5*	33.67±6.93*	76±8.87
SLCN Ugly	1.64±0.33	94.83±28.53	14.83±1.94	37±3.79	43.83±6.69	80.8±9.47

**P*<0.05 vs. Controls.

Uterus

The amplitude and the AUC of the Ang II-mediated response of the UH from group 2 were significantly reduced compared to the controls (Fig. 2 and Table 2). Ang II-stimulated response of the UH from group 3 demonstrated a tendency to increase the force parameters of the SMC, but the statistical significance compared to the controls still existed. In regard to the time-parameters was observed greatly reduced T_{hr} and T_{chr} compared to the controls and group 2.

Rectum

In regard to rectal SMC Ang II-induced response of group 2 was with decreased amplitude and AUC compared to the controls (Fig. 3 and

Table 3). Very interesting, the 7 consecutive day application of SLCNUgly caused an additional significant decrease in the amplitude and the AUC of the UH Ang II-provoked activity. With respect to the time-parameters there were no statistical significance differences between the three groups.

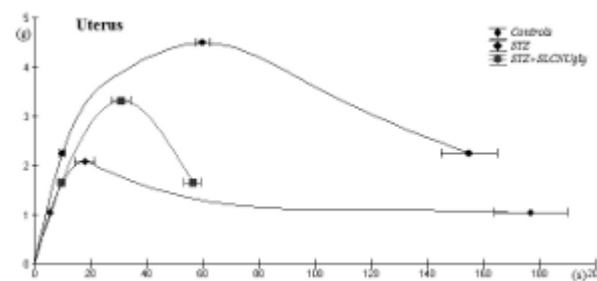


Fig. 2. Graphic visualization of SMC from rat uterus after Ang II stimulation.

Table 2. Parameters of SMC from Uterus of rats after Ang II stimulation.

	Ampl. (g)	AUC (gs)	T _{hc} (s)	T _c (s)	T _{hr} (s)	T _{chr} (s)
Con-trols	4.5±0.35*	465±31.4*	10±1	60±2.5*	95±7.5*	155±10
STZ	2.08±0.28	219.25±15.1	5.5±0.22 ^{\$}	17.8±3.6	159.4±11	177±13
SLCN Ugly	3.32±0.28 ^{&}	129.5±10.75 ^{&}	10.13±1.22	32±2.5 ^{&}	24.5±3 ^{&}	56.5±3 [#]

**P*<0.05 vs. STZ and SLCNUgly, [#]*P*<0.05 vs. Controls and STZ, [&]*P*<0.05 vs. STZ, ^{\$}*P*<0.05 vs. Controls and SLCNUgly.

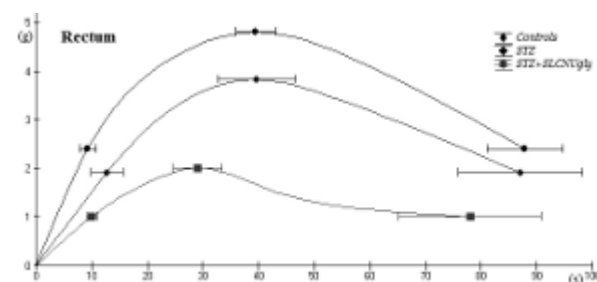


Fig. 3. Graphic visualization of SMC of rat rectum after Ang II stimulation.

Blood glucose levels

As it was expected, the animals treated only with a single STZ injection demonstrated a very high level of blood glucose. The rats injected with SLCNUgly 7 consecutive days presented significantly lower values compared to the STZ treated rats (Table 4).

Table 3. Parameters of SMC from Rectum of rats after Ang II stimulation.

	Ampl. (g)	AUC (gs)	T _{hc} (s)	T _c (s)	T _{hr} (s)	T _{chr} (s)
Con-trols	4.8±0.44*	328.5±75*	9.27±1.52	39.43±3.53	49.43±3.3	88±6.83
STZ	3.82±0.42	192±24	12.75±2.86	39.58±7.1	38.92±5.47	87±11.2
SLCNUgly	2.02±0.29&	104.8±14&	10.1±1	29.2±4.36#	49.1±4.2	78.3±12.8

*P<0.05 vs. STZ and SLCNUgly, #P<0.05 vs. Controls and STZ, &P<0.05 vs. STZ.

Table 4. Blood glucose level.

Blood Glucose	Controls	STZ	SLCNUgly
mM/L	6.8±0.3*	29±2.0	18.7±1.7&

*P<0.05 vs. STZ and SLCNUgly, &P<0.05 vs. STZ.

Ex vivo assay the levels of ROS products, Asc. and NO radicals, in tissue homogenates of rats by EPR spectroscopy.

ROS products

As can be seen in all three organs were not found statistically significant differences in levels of ROS products measured in group 1 and group 2 when compared with the control group (Fig. 4).

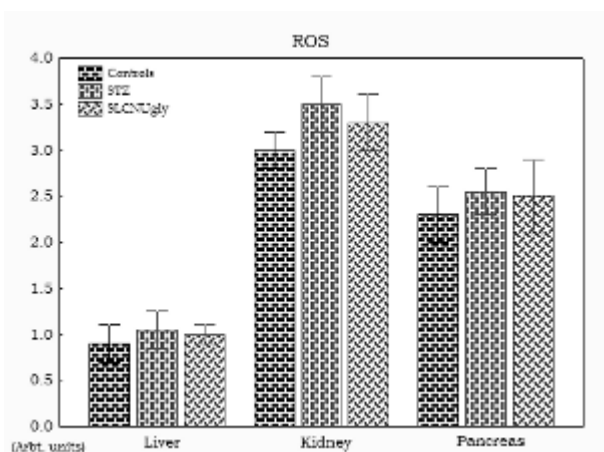


Fig. 4. Levels of ROS in tissues homogenates.

However, should be noted, that in the livers and kidneys of rats treated with STZ + SLCNUgly was found a reduction in the levels of ROS and bringing them to those of the control group. EPR settings were as follows: center field 3503 G; sweep width 10.0 G; microwave power 12.83 mW; receiver gain

1x10⁶; mod. amplitude 5.00 G; time constant 327.68 ms; sweep time 81.92 s; 5 scans per sample.

The nitric oxide levels.

In kidney homogenates were not statistically different levels of NO measured in STZ and STZ+SLCNUgly as compared to control group (Fig. 5). In the liver and pancreas homogenates of rats treated with STZ+SLCNUgly levels of NO radicals were statistically higher compared to the controls (Fig 5). The EPR settings were as follows: center field 3505 G; microwave power 6.42 mW; mod. amplitude 5 G; sweep width 75 G; gain 2.5x10²; time constant 40.96 ms; sweep time 60.42 s; 1 scan per sample.

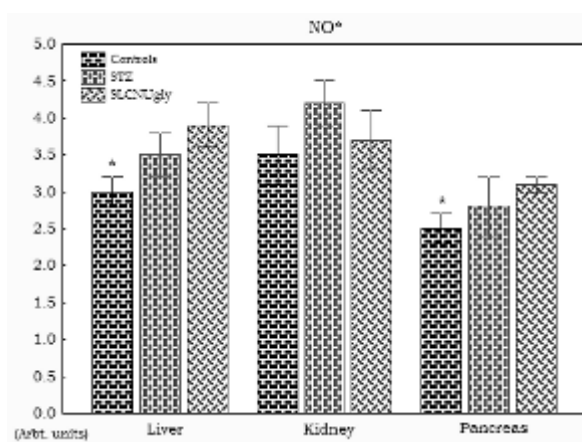


Fig. 5. Levels of NO* in tissues homogenates. *P<0.05 vs. SLCNUgly

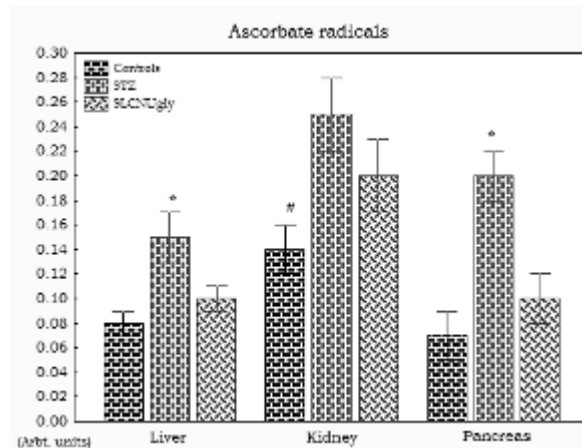


Fig. 6. Levels of Ascorbate radicals in tissues homogenates. *P<0.05 vs. Controls and SLCNUgly, #P<0.05 vs. STZ and SLCNUgly.

Ascorbate radicals

As is seen from Fig. 6 the levels of ascorbate radicals in all three organ homogenates isolated from rats treated only with STZ were statistically significant higher than those of controls. It is

interesting to note that in the livers and pancreas of rats treated with STZ + SLCNUgly levels of Asc. were almost comparable to that of controls and statistically significant reduced comparing to that measured in the same organs of rats injected with STZ, only. Such a reduction is also found in the kidney homogenates, but the decrease was not statistically significant compared to STZ treated group. EPR settings were as follows: center field 3503 G; sweep width 10.0 G; microwave power 12.83 mW; receiver gain 1x106; mod. amplitude 5.00 G; time constant 327.68 ms; sweep time 81.92 s; 5 scans per sample.

Lipid peroxidation (MDA) in the tissue homogenates of rats measured spectrophotometrically:

As is seen the lowest levels of MDA were found in control group in all homogenates, but with no statistical difference compared to the other groups with exception of the pancreas of the rats, treated with STZ only (Table 5). It should be mentioned, that MDA levels measured in the homogenates of the group treated by STZ + SLCNUgly were closer to those of the controls when compared with the MDA levels of the STZ treated group.

Table 5. Levels of MDA in tissues homogenates.

MDA / microM	Liver	Kidneys	Pancreas
Controls	1.74±0.51	4.052±0.62	2.65±0.33
STZ	1.891±0.54	4.322±0.89	3.24±0.06*
SLCNUgly	1.86±0.65	4.137±0.73	2.89±0.72

*P<0.05 vs. Controls.

Smooth muscle activity

The Ang II-mediated response of the smooth muscle in the pelvic cavity was different in each organ.

In urinary bladder, there was no difference between the control group and the group with administration of STZ+SLCNUgly. In another hand, the group treated with STZ demonstrated hyper contractility of the bladder. In previously experiment lasting 42 days, we obtained no differences regarding the amplitude of SMC between diabetic and control group [23]. This different response in the present experiment is most likely due to the described from Nakahara et al. [24] negative feedback triggering by MaxiK channels. The authors found that there is hyper activity of the bladder due to higher sensitivity of

the L-type Ca²⁺ channels, which in turn is compensated with MaxiK channels triggering feedback. Apparently, L-type Ca²⁺ channels high sensitivity is developing faster and 8 days were not enough to switch on K⁺ channels feedback. The antioxidant properties of the SLCNUgly could explain the better response to Ang II of the UB in the group with SLCNUgly application.

The main feature of the uterus is predominantly expression of AT2 type receptors [25] in myometrium and the uterine artery [26]. Under this condition, the STZ application influenced negatively the Ang II- mediated uterine contractile activity, while the combination STZ+SLCNUgly demonstrated tendency to improve the amplitude of SMC and to reduce the relaxation. The neuropathy, myopathy [27] and reduction of calmodulin levels and Ca²⁺-desensitization, caused by the hyperglycemia and ROS excess [28,29] are the main factors associated with these results. ROS concentration and pH determine developing of SMC [30,31]. This is why we could suppose that SLCNUgly as an agent with some antioxidant properties reduces the levels of oxidative stress in uterus, thus improving of the contractility. Also, it was very interesting that the application of SLCNUgly caused the significant decrease of relaxation phase. Activation of NO synthesis by endothelial cells [32] or alkylation of Ang II derivate [33] are possible reasons for development of this short relaxation. Moreover, the alkylation of AT1 receptors described by Dhanoa et al. [34] can disrupt the AT1 receptors signaling. Although for the developing of uterine SMC is necessary interaction between AT1 and AT2 receptors [35], leading role of AT2 receptors in this condition would lead to a fast relaxation.

Ang II-mediated response in rectum smooth muscle strips was the only one where the application of SLCNUgly caused a strong reduction of the amplitude of contraction. The other two groups – controls and STZ injected rats, demonstrated similar non-significant response. Nitrosoureas as alkylating agents are used in treatment of adenocarcinomas, especially in colorectal cancer [36]. SLCNUgly, as a new class nitrosourea, might have a high concentration in the rectum after 7 consecutive day application, which may cause an additional damage and reinforcement of STZ effects in the rectum.

In this study was observed a pronounced tendency in reducing the levels of blood glucose after 7 consecutive days of administration of SLCNUgly. Formerly, was demonstrated a statistically significant decrease in blood glucose

levels of healthy mice treated once with SLCNUgly [37]. The observed decrease in the level of blood glucose the same authors explained with the presence of glycine structure in SLCNUgly. In many studies was shown that per os intake of glycine causes increase in insulin concentration in the sera of healthy volunteers [38,39]. It is known that glycine participates in gluconeogenesis and any increase of its concentration in hepatocytes would cause disturbance in the control of blood glucose level.

Analysis of the results obtained for the levels of oxidative stress parameters namely, ROS products, Asc., NO and MDA reactive substances in both groups treated with STZ and combination of STZ + SLCNUgly showed that SLCNUgly behaves as an antioxidant comparing to STZ. Previously, was reported that due to presence of the stable nitroxyl radical structure (spin labeled) SLCNUgly could successfully scavenged ROS in particular superoxide radicals and to prevent formation of high toxic species like ·OH radicals [40]. It was documented that concentration of ascorbate free radical was a reliable, real-time and quantitative marker of free radical generation could be used as an indicator of oxidative stress *in vitro* and *in vivo* [20,41]. Based on both: 1) Levels of ascorbate radicals registered in the three organ homogenates of the group treated with STZ + SLCNUgly were close to those of the control group and 2) were considerably lower than those registered in the group treated only with STZ, might be concluded that obviously SLCNUgly induced to a lesser extent oxidative stress than the other nitrosoarea. We believe that this drug has double effect over blood sugar regulation. On the one hand, we can speculate that SLCNUgly has direct effect on insulin release by closing of ATP-sensitive K-channels in the beta-cell plasma membrane similar to the anti-diabetic drug sulfonylurea [42]. On the other hand, both SLCNUgly and STZ are nitrosoareas. We believe that there might be a competition between them for the GLUT 2 transporter. In this way, the additional administration of SLCNUgly leads to a prevention of the toxic effects of STZ.

CONCLUSION

STZ induced hyperglycemia and oxidative stress produced different changes in Ang II-provoked motor activity of organs in pelvic cavity: from hypo reactivity - uterus, no changes - rectum to hyper reactivity - UB. The effect of the antioxidant protection depends on different functional characteristics of pelvic organs and interplay between Ang II receptors and SLCNUgly.

The seven-day administration of SLCNUgly improved significantly glycemic status of the rats, but obviously the duration of the treatment with SLCNUgly or/and the dose was not enough for the complete amelioration of tissue oxidative damages and to restore oxidative balance. The beneficial effect of SLCNUgly allows us to a future development of our research in this direction.

Acknowledgements: This study was supported by Grant DDVU-02-24/2010 from National fund, Sofia, Bulgaria and Grant 25/2014 from Trakia University, Stara Zagora, Bulgaria.

REFERENCES

1. A. Amos, D. Mccarty, P. Zimmet, *Diab. Med.*, **14**, 1 (1997).
2. A. M. Abu El-Asrar, *Middle East Afr. J. Ophthalmol.*, **20**, 273 (2013).
3. J. Stamler, O. Vaccaro, J. D. Neaton, *Diabetes Care*, **16**, 434 (1993).
4. C. Frimodt-Moller, *Ann. Int. Med.*, **92**, 318 (1980).
5. L. R. Schiller, C. A. Santa Ana, A. C. Schmulen, R. S. Hendler, W. V. Harford, J. S. Fordtran, *N. Engl. J. Med.*, **307**, 1666 (1982).
6. G. Falkay, G. Spiegl, D. Csonka, I. Zupkó, *Neurochem. Int.*, **51**, 306 (2007).
7. M. J. Chang, J. H. Xiao, Y. Wang, Y. L. Yan, J. Yang, J. L. Wang, *PLoS One.*, **7**, 50291 (2012).
8. T. J. Lyons, *Diabet Med.*, **8**, 411 (1991).
9. A. Chatzigeorgiou, A. Halapas, K. Kalafatakis, E. Kamper, *In Vivo*, **23**, 245 (2009).
10. A. Zheleva, Z. Raikov, M. Ilarionova and D. Todorov, *Pharmazie*, **50**, 25 (1995).
11. M. V. Ilarionova, A. M. Zheleva, Z. D. Raikov, D. K. Todorov, A. P. Dudov, *J. Chemotherapy*, **5**, 786 (1993).
12. A. Zheleva, S. Stanilova, Z. Dobрева, Z. Zhelev, *Int. J. Pharmaceutics*, **222**, 237 (2001).
13. Y. Karamalakova, K. Chuttani, R. Sharma, A. Zheleva, V. Gadjeva, A. Mishra, *Biotechnol. & Biotechnol. Equip.*, **28**, 1172 (2014).
14. A. Tolekova, P. Hadzhibozheva, R. Iliev, Ts. Georgiev, K. Trifonova, R. Sandeva, R. Kalfin, G. Ilieva, *Reg. Pep.*, **162**, 79 (2010).
15. Ts. K. Georgiev, P. V. Hadzhibozheva, A. N. Tolekova, *Scripta Sci. Med.*, **44**, 93 (2012).
16. K. Yankov, *Trakia J. Sci.*, **8**, 41 (2010).
17. K. Yankov, in: Proceedings of the International Conference on Information Technologies (InfoTech-2012), R. Romanski (edr), 2012, p.114.
18. H. H. Shi, Y. X. Sui, X. R. Wang, Luo Yand, L. L. Jia, *Comp. Biochem. Physiol. C Toxicol. Pharmacol.*, **140**, 115 (2005).
19. A. Zheleva, Y. Karamalakova, G. Nikolova, R. Kumar, R. Sharma, V. Gadjeva, *Biotechnol. & Biotechnol. Equipment*, **26**, 146 (2011).
20. G. R. Buettner and B. A. Jurkiewicz, *Free Radic. Bio. Med.*, **14**, 49 (1993).

21. T. Yoshioka, N. Iwamoto, and K. Ito, *J. Am. Soc. Nephrol.*, **7**, 961 (1996).
22. K. Yokoyama, K. Hashiba, H. Wakabayashi, K. Hashimoto, K. Satoh, T. Kurihara, N. Motohashi and H. Sakagami, *Anticancer Res.*, **24**, 3917 (2004).
23. P. Hadzhibozheva, PhD Thesis, INB, BAS, Sofia 2015.
24. T. Nakahara, A. Mitani, Y. Kubota, T. Maruko, K. Sakamoto, Y. Tanaka, K. Koike, K. Shigenobu, K. Ishii, *J. Smooth Muscle Res.*, **40**, 97 (2004).
25. T. Matsumoto, N. Sagawa, M. Mukoyama, I. Tanaka, H. Itoh, M. Goto, H. Itoh, M. Horiuchi, V. J. Dzau, T. Mori, K. Nakao, *J. Clin. Endocr. Metab.*, **81**, 4366 (1996).
26. R. E. Hannan, T. A. Gaspari, E. A. Davis, R. E. Widdop, *Brit. J. Pharmacol.*, **141**, 1024 (2004).
27. L. A. Szarka, M. Camilleri, *J Diabetes Sci Technol.*, **4**, 180 (2010).
28. Y. Ozturk, S. Aydin, A. T. Ozcelikay, V. M. Altan, N. Yaldizoglu-Ari, *Eur. J Pharmacol.*, **31**, 59 (1997).
29. H. Suzuki, I. Usui, I. Kato, T. Oya, Y. Kanatani, Y. Yamazaki, S. Fujisaka, S. Senda, Y. Ishii, M. Urakaze, A. Mahmood, S. Takasawa, H. Okamoto, M. Kobayashi, K. Tobe, M. Sasahara, *Diabetologia*, **54**, 2953 (2011).
30. I. Appiah, S. Milovanovic, R. Radojicic, *Brit. J. Pharmacol.*, **158**, 1932 (2009).
31. R. C. Heaton, M. J. Taqqart, S. Wray, *Pflugers Arch.*, **422**, 24 (1992).
32. V. M. Rudichenko, W. H. Beierwaltes, *J. Vasc. Res.*, **32**, 100 (1995).
33. K. Hsieh, G. R. Marshall, *J. Med. Chem.*, **24**, 1304 (1981).
34. D. S. Dhanoa, S. W. Bagley, R. S. L. Chang, V. J. Lotti, T. B. Chen, S. D. Kivlighn, G. J. Zingaro, P. K. S. Siegl, A. A. Patchett, W. J. Greenlee, *J. Med. Chem.*, **36**, 4230 (1993).
35. Ts. K. Georgiev, A. N. Tolekova, R. E. Kalfin, P. V. Hadzhibozheva, *Physiol. Res.*, in press
36. M. E. Katz, J. H. Glick, *Cancer Clin. Trials.*, **2**, 297 (1979).
37. A. Zheleva, A. Tolekova, P. Goicheva, *Trakia J. Sci.*, **6**, 49 (2008).
38. M. Gannon, J. A. Nuttall, F. Q. Nuttall, *Am. J. Clin. Nutr.*, **76**, 1302 (2002).
39. M. Gonzalez-Ortiz, R. Medina-Santillan, E. Martinez-Abundis, C. R. von Drateln, *Horm. Metab. Res.*, **33**, 358 (2001).
40. A. M. Zheleva, V. G. Gadjeva, *Int. J. Pharmaceutics*, **212**, 257 (2001).
41. <http://slideplayer.com/slide/6626563/>.
42. F. M. Ashcroft, *Horm. Metab. Res.*, **28**, 456 (1996).

ЕФЕКТ НА N-[N'-(2-ХЛОРОЕТИЛ)-N'-НИТРОЗОКАРБАМОИЛ-ГЛИЦИН АМИД НА 2,2,6,6-ТЕТРАМЕТИЛ-4-АМИНОПИПЕРИДИН-1-ОКСИЛ (SLCNUGLY) ВЪРХУ АНГИОТЕНЗИН 2-МЕДИИРАНАТА ГЛАДКОМУСКУЛНА АКТИВНОСТ НА ОРГАНИ В ТАЗОВАТА КУХИНА

Ц. К. Георгиев¹, П. В. Хаджибожева¹, Е. Д. Георгиева², Я. Д. Карамалакова², Г. Д. Николова²,
В. Г. Гаджева², А. М. Желева², А. Н. Толева¹

¹Катедра по физиология, патофизиология и фармакология, Медицински факултет, Тракийски университет, Стара Загора, България

²Катедра по химия и биохимия, Медицински факултет, Тракийски университет, Стара Загора, България

Постъпила на 29 септември, 2016 г.; Коригирана на 21 февруари, 2017 г.

(Резюме)

Хипергликемията, съпътстваща захарния диабет нарушава отговора на гладките мускули към хормони с контрактилна активност като Ангиотензин 2 (Анг 2). Основният етиологичен фактор за това смущение е прекомерното образуване на кислородни радикали, което води до оксидативен стрес и нарушение на калциевата сигнализация в клетките. Ето защо веществата с антиоксидантна активност имат потенциал за подобряване на гладкомускулната диабетна дисфункция.

Целта на това проучване е да се оцени въздействието на SLCNUgly, върху оксидативния и гликемичния статус на диабетни плъхове, както и Анг 2 - индуцираната съкратителна активност на органи от тазовата кухина.

Женски полови зрели плъхове, линия Wistar, бяха разделени в три групи: контролна група (здрави животни); Стрептозотозин (СТЗ) третирана група (единична инжекция от 60 мг/кг); група, третирана седем последователни дни, след СТЗ инжектирането с 10 мг/кг SLCNUgly. В края на експерименталния период, бяха изготвени надлъжни гладкомускулни ивици от пикочен мехур, ректум и матка, на които бе въздействано с Анг 2 (1 микромол). Получените контрактилни криви бяха анализирани чрез изчисляване на силови и времеви характеристики на процеса. В тъканни хомогенати от черен дроб, бъбреци и панкреас, бяха изчислени концентрациите на аскорбатни радикали, продукцията на кислородни радикали и липидната пероксидация (малондиалдехид).

Седемдневното приложение на SLCNUgly подобри значително гликемичния статус на плъхчетата. Също така нитрозурейта причини допълнително намаление на Анг 2-медиацията контрактилен отговор и значително скъси фазата на полурелаксация на миоетралната контракция. Препаратите от ректум изготвени от SLCNUgly-третираните диабетни плъхове, отговориха на Анг 2 стимулацията с намаление във силовите параметри на контракцията. Приложението на нитрозурейта показва тенденция за нормализиране на силовите и времевите характеристики на контрактилния процес при препаратите от пикочен мехур. SLCNUgly имаше слаб ефект по отношение на подобряване тъканните увреди вследствие от оксидативния стрес.

Evaluation of opioid system participation in endocannabinoids` effects on SIA after three models of stress

H. Nocheva*, A. Bocheva

Medical University of Sofia, Department of Pathophysiology

Received September 20, 2016; Revised January 14, 2017

During stress several physiological functions, pain perception among them, undergo changes. Decreased nociception during stress is known as stress-induced analgesia (SIA), and its mechanisms of development include an opioid and a non-opioid component.

The opioid system comprises several receptor subtypes (μ , δ , κ) and their endogenous ligands, while in non-opioid one epinephrine, serotonin, nitric oxide, and endocannabinoids take place.

The aim of our study was evaluation of opioid system participation in endocannabinoids` effects on SIA after different stresses (immobilization, heat and cold stress). In order to achieve the goals we excluded the effects of opioid receptors through administration of the non-selective opioid receptor antagonist naloxone.

The experiments were carried out on male Wistar rats subjected to 1 hour acute immobilization, heat or cold stress. The opioid receptor antagonist naloxone was administered after the end of each stress, and additionally, the cannabinoid receptor (CB1) agonist anandamide was injected.

Pain perception was assessed by Paw pressure and Hot plate test.

All procedures were approved by the Animal Care and Use Committee of the Medical University of Sofia.

Our results showed that antagonization of opioid receptors decreased mostly heat stress-induced analgesia (heat-SIA, where the opioid component is most expressed). Immobilization- and cold-SIA were affected to a lesser extent (the opioid component in development of both stresses is less expressed than in heat-SIA).

Keywords: opioidergic system, endocannabinoid system, stress-induced analgesia, pain perception

INTRODUCTION

First adopted by Hans Selye, the term *stress* includes different types of physical or psychological impact on the organism during which its adaptation abilities are tested to maintain the dynamic equilibrium with the environment despite the increased demands [1, 2]. During stress several physiological mechanisms as well as the functions of different organs and systems change. It is possible that short-lasting but intense stress as well as relatively mild but long-lasting one onsets pathological reactions and processes that permanently impair the functions of the systems, and especially the nervous, the endocrine, the immune, the cardio-vascular, the gastrointestinal, and the reproductive systems. The impact of stress on the whole body can permanently threaten its health, impair the quality and shorten the expectancy of life, with serious social and economic consequences [3, 4, 5]. This is why elucidation of the mechanisms of stress development as well as the pathways of its interacting with and damaging the organs` and systemic functions represents a promising and important direction of scientific area.

During stress several physiological functions, pain perception among them, undergo changes. Decreased nociception during stress is known as stress-induced analgesia (SIA) [6, 7] and its mechanisms of development include an opioid and a non-opioid component [8, 9].

The opioid system comprises several receptor subtypes (μ , δ , κ) and their endogenous ligands [for a review see 10]. The two components in the mechanism of SIA have different ratios of participation in different stresses: the opioid component prevails in heat-SIA, while the non-opioid is better expressed in cold-SIA; immobilization stress equally triggers both the components [8].

The aim of our study was evaluation of opioid system participation in endocannabinoids` effects on SIA after different stresses (immobilization, heat and cold stress). In order to achieve the goals we excluded the effects of opioid receptors through administration of the non-selective opioid receptor antagonist naloxone [11, 12].

EXPERIMENTAL

Animals

The experiments were carried out on male Wistar rats (180-200 g), housed in polypropylene cages (40 × 60 × 20 cm, 6–8 rats in each) at a

* To whom all correspondence should be sent:
E-mail: dr_inna@yahoo.com

temperature-controlled colony room maintained at 21 ± 3 °C under 12:12 h light/dark cycle with lights on at 6:00 a.m. The animals were given free access to tap water and standard rat chow. The experiments were carried out between 9.00 and 12.00 a.m.

All procedures were carried out according to the ‘‘Principles of laboratory animal care’’ (NIH publication No. 85_23, revised 1985), and by the Animal Care and Use Committee of the Medical University of Sofia.

Acute models of stress

Immobilization stress: The animals were placed in plastic tubes with adjustable plaster tapes on the outside to prevent moving. Holes were left for breathing.

Cold stress: The animals were placed in refrigerating chamber at 4°C for 1 hour.

Heat stress: The animals were placed in thermal chamber at 38°C for 1 hour.

Drugs and treatment

All drugs were obtained from Sigma and administered intraperitoneally (i.p). The non-selective opioid receptor antagonist naloxone (Nal, at a dose of 1.0 mg/kg, dissolved in 0.9% NaCl) was administered immediately after the end of stress and 20 min before anandamide (AEA, at a dose 1 mg/kg, dissolved in DMSO) or AM251 (1,25 mg/kg, dissolved in DMSO).

Evaluation of pain perception started 10 min after administration of AEA or AM251.

Paw-pressure test (Randall-Selitto test): The changes in the mechanical nociceptive threshold of the rats were measured by an analgesimeter (Ugo Basile). The pressure was applied to the hind-paw and the pressure (g) required to eliciting a nociceptive response such as squeak or struggle was taken as the mechanical nociceptive threshold. A cut-off value of 500 g was used to prevent damage of the paw.

Hot plate test: The latency of response to pain was measured from the moment the animal was placed on the metal plate (heated to 55 ± 0.5 °C) till the first signs of pain (paw licking, jumping). A cut-off time of 30 s was observed in order to avoid injury of the animals.

Data analysis: The results were statistically assessed by one-way analysis of variance (ANOVA) followed by Newman-Keuls post-hoc comparison test. Values were mean \pm S.E.M. Values of $p < 0.05$ were considered to indicate statistical significance.

RESULTS AND DISCUSSION

1 Hour of cold (1h CS), immobilization (1h IS), and heat (1h HS) stress increased pain thresholds of experimental animals compared to the controls (Fig. 1, Fig. 2, and Fig. 3).

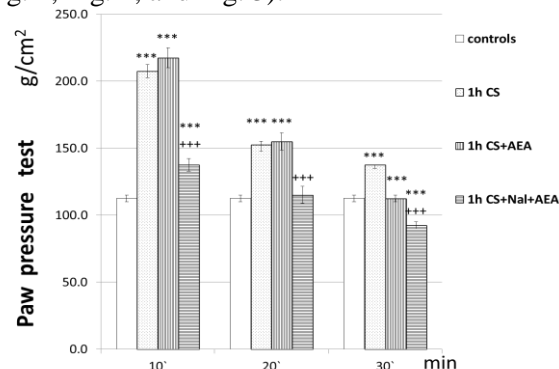


Fig. 1. Effects of naloxone (Nal, 1 mg/kg, i.p.) on anandamide (AEA, 1 mg/kg, i.p.) after 1 hour of cold stress (1h CS). The results are represented as mean values \pm S.E.M. Pain thresholds of experimental animals were compared to controls (***) $p < 0.001$); pain thresholds of animals after 1h CS+Nal+AEA were compared to 1h CS+AEA (+++ $p < 0.001$).

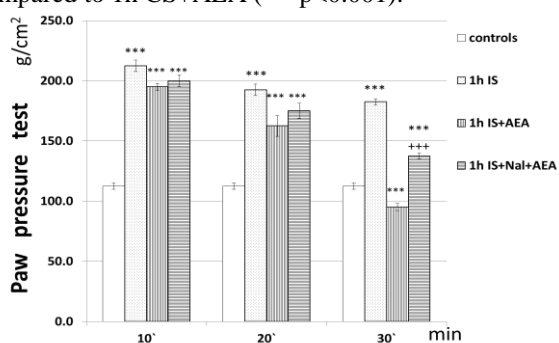


Fig. 2. Effects of naloxone (Nal, 1 mg/kg, i.p.) on anandamide (AEA, 1 mg/kg, i.p.) after 1 hour of immobilization stress (1h IS). The results are represented as mean values \pm S.E.M. Pain thresholds of experimental animals were compared to controls (***) $p < 0.001$); pain thresholds of animals after 1h IS+Nal+AEA were compared to 1h IS+AEA (+++ $p < 0.001$).

Administration of AEA immediately after ending of each stress led to a tendency toward increase of 1h CS-animals` pain thresholds, but a statistically relevant decrease in pain thresholds of animals after 1h IS and 1h HS was observed (Fig. 1, Fig. 2, and Fig. 3).

Administration of naloxone immediately after ending of stress and 20 min before AEA (1h CS+Nal+AEA; 1h IS+Nal+AEA; 1h HS+Nal+AEA) differently influenced analgesia induced by 1h CS, 1h IS, and 1h HS. Animals after 1h CS+Nal+AEA showed decreased pain thresholds compared to animals after 1h CS and animals after 1h CS+AEA; pain thresholds on the

20th and 30th min of the experiment were comparable to the control values. PP-values of animals after 1h HS+Nal+AEA were similar to 1h HS+AEA. Animals after 1h IS+Nal+AEA presented with pain thresholds relatively lower than 1h IS, but comparable to 1h IS+AEA on the 10th and 20th min; on the 30th min of the experiment the PP-values were higher than 1h IS+AEA even being lower than 1h IS. During the whole time of the experiment PP-values were higher than control ones (Fig. 1, Fig. 2, and Fig. 3).

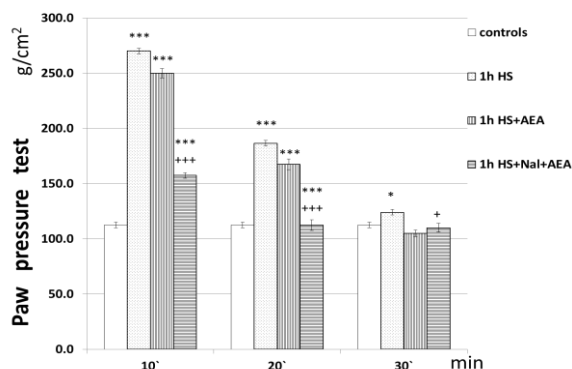


Fig. 3. Effects of naloxone (Nal, 1 mg/kg, i.p.) on anandamide (AEA, 1 mg/kg, i.p.) after 1 hour of heat stress (1h HS). The results are represented as mean values ± S.E.M. Pain thresholds of experimental animals were compared to controls (**p<0.01; ***p<0.001); pain thresholds of animals after 1h HS+Nal+AEA were compared to 1h HS+AEA (*** p<0.001; +p<0.05).

Administration of AM251 after CS and IS led to an immediate decrease in pain thresholds in animals compared to the respective stress with values comparable to the controls (Fig. 4 and Fig. 5). After HS higher values were observed on the 10th min compared to the controls, but yet lower than HS (Fig. 6).

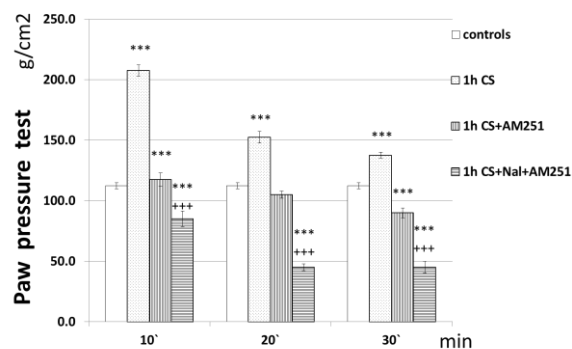


Fig. 4. Effects of naloxone (Nal, 1 mg/kg, i.p.) and AM251 (1.25 mg/kg, i.p.) on 1 hour cold stress-induced analgesia (1h CS). The results are represented as mean values ± S.E.M. Pain thresholds of experimental animals were compared to controls (**p<0.01; ***p<0.001); pain thresholds of animals after 1h CS+Nal+AM251 were compared to 1h CS+AM251 (*** p<0.001).

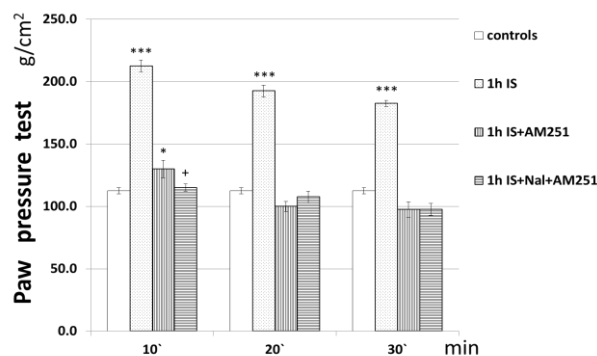


Fig. 5. Effects of naloxone (Nal, 1 mg/kg, i.p.) and AM251 (1.25 mg/kg, i.p.) on 1 hour immobilization stress-induced analgesia (1h IS). The results are represented as mean values ± S.E.M. Pain thresholds of experimental animals were compared to controls (**p<0.01; ***p<0.001); pain thresholds of animals after 1h IS+Nal+AM251 were compared to 1h IS+AM251 (+p<0.05).

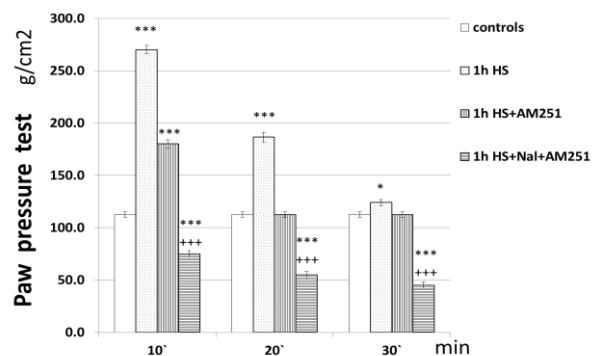


Fig. 6. Effects of naloxone (Nal, 1 mg/kg, i.p.) and AM251 (1.25 mg/kg, i.p.) on 1 hour heat stress-induced analgesia (1h HS). The results are represented as mean values ± S.E.M. Pain thresholds of experimental animals were compared to controls (**p<0.01; ***p<0.001); pain thresholds of animals after 1h HS+Nal+AM251 were compared to 1h HS+AM251 (*** p<0.001).

Administration of Nal immediately after the end of stress and before the CD1-receptors antagonist decreased all the pain threshold values: they were comparable to the controls for animals after IS+Nal+AM251, while for animals after CS+Nal+AM251 and HS+Nal+AM251 even a tendency toward hyperalgesia was observed (Fig. 4, Fig. 5, and Fig. 6).

It's known that two components – an opioid and a non-opioid one, interact in SIA development. The two components show different interrelations during different types of stress. Immobilization stress triggers both of them at equal degree, while cold and hot stresses rely predominantly upon one of them: cold stress upon the non-opioid one, and heat stress upon the opioid component of SIA [8, 9]. Given such predisposition it's likely to have a

different influence of each type of SIA (immobilization, heat, cold) after antagonizing the μ -opioid receptors.

The results observed surprised us, since we expected the most prominent decrease of pain thresholds after heat stress (where the opioid component is the most expressed); and the least decrease we expected after cold stress (where the non-opioid component prevails).

Our results showed that antagonizing the μ -opioid receptors led to an approximately equal decrease in both cold (36.78%) and heat (37%) SIA on the 10th min of the experiment; on the 30th min of the experiment cold SIA was decreased by 17.7% compared to animals without Nal, while heat SIA was increased by 4.76% compared to animals without Nal.

Are the two components so closely interrelated that they depend on each other to the extent that when one is antagonized both of them fail to develop? But if so, how can we explain results after immobilization stress where both the components are equally triggered?

We dare to propose a speculation: the activation of opioid and non-opioid receptors to a different degree leads to differences in their interactions and such differences produce different effects.

Administration of both μ - and CB1-receptors antagonists revealed that simultaneous inhibition of opioid and cannabinoid effects differently modulated pain perception. The tendency toward hyperalgesia, observed in animals injected with both antagonists after cold- and heat-stress, was never manifested after the CB1 agonist AEA or after IS where both opioid and non-opioid components are equally activated.

CONCLUSION

We may say that the opioid system influences the endocannabinoid system effects after different models of stresses.

It would be interesting to evaluate interactions between the different non-opioid components: adrenergic, serotonergic, nitric oxide-ergic systems between them and with the endocannabinoid system.

Acknowledgements: This work was supported by a Grants №№ 4/2010, 10/2011, and 61/2013 from the Council of Medical Science, MU-Sofia.

REFERENCES

1. H. Selye, *Montreal: Acta Inc.* (1952).
2. H. Selye, *New York: McGraw-Hill.* (1956).
3. K.S. Kendler, R.C. Kessler, E.E. Walters, C. MacLean, M.C. Neale, A.C. Heath, L.J. Eaves, *Am. J. Psychiatry*, **152**, 833 (1995).
4. E. Lambo, *The economy and health Health Policy*, **23(3)**, 247 (1993).
5. I.P. Burges Watson, M. Brüne, A.J. Bradley, *Neuroscience & Biobehavioral Reviews*, **68**, 134 (2016).
6. R.J. Bodnar, D.D. Kelly, M. Brutus, M. Glusman, *Neurosci Biobehav Rev.*, **4**, 87 (1980).
7. R.K. Butler, D.P. Finn, *Prog Neurobiol*, **88**, 184 (2009).
8. K. Pacák, M. Palkovits, *Endocr Rev.* **22(4)**, 502 (2001).
9. I.B. Lapo, M. Konarzewski, B. Sadowski, *Physiol. Behav.*, **78**, 345 (2003).
10. R. J. Bodnar, *Peptides*, **32**, 2522 (2011).
11. P. Sacerdote, P. Mantegazza, A.E. Panerai, *Brain Research*, **359(1-2)**, 34 (1985).
12. L. Kriianac-Bengez, M. BoraniC', N.G. Testa, *Biomed & Pharnmcother*, **49**, 27 (1995).

ОПРЕДЕЛЯНЕ УЧАСТИЕТО НА ОПИОИДЕРГИЧНАТА СИСТЕМА В ЕФЕКТИТЕ НА ЕНДОКАНАБИНОИДИТЕ ВЪРХУ СТРЕС-ИНДУЦИРАНАТА АНАЛГЕЗИЯ СЛЕД ТРИ МОДЕЛА НА СТРЕС

Х. Ночева*, А. Бочева

Катедра по Патопфизиология, Медицински Университет – София

Постъпила на 20 септември, 2016 г.; Коригирана на 14 януари, 2016 г.

(Резюме)

По време на стрес редица физиологични параметри, в т.ч. и болковата перцепция, се променят. Намалената по време на стрес ноцицепция се означава като стрес-индуцирана аналгезия (СИА) и нейните механизми на развитие включват опиоидна и неопиоидна компоненти.

Опиоидната система включва няколко рецепторни подтипа (μ , δ , κ), както и техните ендогенни лиганди, докато в не-опиоидната компонента на СИА се включват адреналин, серотонин, азотен оксид, ендоканабиноиди и др.

Целта на настоящето проучване бе определяне участието на опиоидната система в ефектите на ендоканабиноидите върху СИА след различни модели на стрес (имобилизационен, топлинен, студов). С оглед постигане на поставената цел бе изключен ефектът на опиоидните рецептори посредством приложението на неселективния антагонист на опиоидните рецептори налоксон.

Експериментите бяха проведени върху мъжки плъхове от породата Wistar, подложени на едночасов имобилизационен, топлинен или студов стрес. Налоксонът бе въведен незабавно след прекратяването на стреса, а агонистът на канабиноидните рецептори анандамид – след него.

Болковата перцепция бе определяна посредством Paw pressure и Hot plate тестове.

Резултатите показаха, че антагонизирането на опиоидните рецептори понижава в най-висока степен топлинната СИА, където опиоидната компонента е най-добре изразена. Имобилизационната и студовата СИА бяха понижени в по-слаба степен в сравнение с топлинната.

Comparative studies on two isomeric L-valine peptidomimetics for neuropharmacological effects in rodents

E.N. Encheva^{1*}, D. Tsekova², L. Tancheva³, L. Alova⁴, L. Shikova⁴, M. Kaneva⁴

¹Department of Physiology, Medical Faculty, Medical University of Sofia, G. Sofijski Str. 1, 1431 Sofia, Bulgaria

²Department of Organic Chemistry, University of Chemical Technology and Metallurgy, 8, Kl. Ohridsky Blvd., 1756 Sofia, Bulgaria

³Behavior Neurobiology, Institute of Neurobiology, Bulgarian Academy of Sciences, Acad. G. Bonchev St., Block 23, 1113 Sofia, Bulgaria

⁴Isotope Laboratory, Institute of Neurobiology, Bulgarian Academy of Sciences, Acad. G. Bonchev St., Block 23, 1113 Sofia, Bulgaria

Received October 06, 2016; Revised January 10, 2017

It is well known that biological activity is a function of chemical structure of the compounds, and that positional isomers frequently differ in biological activity. Positional isomerism is a subtype of structural isomerism. Two new compounds which are isomeric peptide mimetics, derivatives of L-Valine, and contain hydrophobic spacers of six methylene groups and moieties of either nicotinic or isonicotinic acid were studied for their neurobiological effects *in vivo*.

Aim of the present study was to evaluate the neuropharmacological activity of these peptide mimetics on rodents with experimental model of social isolation. Male Albino ICR mice and Wistar rats, treated with effective daily doses in 3 consecutive days were used. Their cognitive functions (learning and memory - Step-through test, exploratory activity - Hole-board test) were evaluated. The effects of the compounds on release and reuptake of serotonin in hippocampus and on stimulated acetylcholine release also were studied in hippocampal slices of Wistar rats.

Our results revealed a significant dose-dependent effect of the positional isomers. They both modulated cognitive functions and changed the release of Serotonin (5-HT) and the reuptake of Acetylcholin (Ach) in brain differently. The CNS effects are most probably related to the presence of L-Valine and a hydrophobic spacer which increases liposolubility of the compounds. The main reason for differences in the modulating effect on cognitive functions of rodents, and upon neuromediator levels is most probably the positional isomerism of the nicotinic and isonicotinic residues.

Key words: isomeric peptidomimetics, L-valine, nicotinic and isonicotinic acid, memory, neuromediators

INTRODUCTION

Medicinal chemistry, as well as drug development, is an interdisciplinary field with a focus on various chemical formulations possessing possible therapeutic effect in humans and animals alike. As it is well known, positional isomerism is a subtype of structural isomerism, and positional isomers frequently differ in biological activity.

Objects of our research were two newly synthesized peptidomimetics, representatives of the so called small molecular weight gelators, derivatives of the amino acid L-valine and nicotinic, respectively, isonicotinic acid, recently synthesized by some of us [1].

Right after their synthesis, the compounds M6 and P6 (Fig.1) have been studied mostly as organogelators, because of their ability to self-assemble. Unique is their ability, even though they

are low molecular weight compounds, to form supramolecular complexes based on hydrogen bonds, and even in solutions having very low concentrations, to self-assemble into ordered structures, often forming gels [2]. Interest in similar gels lately is great, as those are widely used in everyday life, for example in cosmetics (creams, shampoos, toothpastes), and it is mandatory that they be safe and non-toxic. Of medical and biological point of view, a curious fact is that the derivatives which we work with have never been used in drug synthesis.

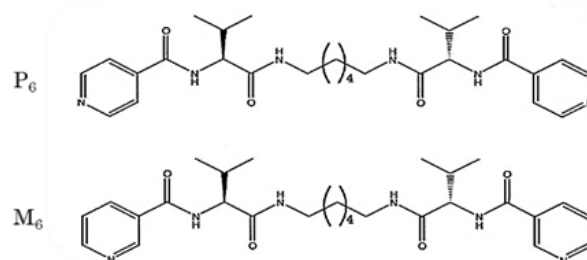


Fig. 1 Chemical formulae of the two isomeric peptidomimetic dimers

* To whom all correspondence should be sent:

E-mail: Eleonora.e@gmail.com

The classical strategy for inclusion of endogenous substances in a molecule has been employed in the synthesis of the substances object of our study, and is known as useful in creating a vast array of medications (e.g. antihypertensive, anticoagulant, anti-tumour, etc. [3-5]).

On the other hand, the presence of the essential branched chain amino acid (BCAA) L-valine in the molecule of the compound, together with 2 functional residues of nicotinamide / isonicotinamide, depending on the isomer, are expected to contribute to outstanding biological activity, especially on the central nervous system (CNS), as evidenced by numerous literature data on the activity of the lead substances (generic compounds) and derivatives [6-9].

It was our aim to study and compare the neuropharmacologic effects of the two unique isomeric dimers on an experimental model of social isolation.

Social factors are well known to influence neuronal plasticity and cognitive functions of humans and animals, which has been established by observation of autistic children, elderly people with dementia, and others. Often, poor communication and lack of social environment are associated with the development of aggressive and depressive disorders in early as well as in later life.

Many of the changes in brain morphology and neurochemical level after social deprivation in early life or in adulthood are specific and are described in the literature as social isolation syndrome [10-12]. The diffuse mechanisms of impaired neurotransmission and changes in memory function in SI syndrome are still being widely discussed. A complex interplay between social and pharmacological factors in humans and animals has yet to be clarified.

As a model for exploring neurodevelopmental changes in brain structures and neurotransmitter systems being changed under chronic stress, social isolation rearing of animals has no alternative and serves as a valuable and successful tool in experimental neuropharmacology.

So here we have an essential BCAA and vitamin B₃ and its isomer, incorporated into a combined chemical structure of two isomeric dimers.

- Bioactivity = f (Chemical structure)
- Hydrophobic spacer + L-valine = Increase in liposolubility, which suggests permeability across blood-brain barrier
- We assume the isomers will exert biological activity upon the CNS not just in grouped, but also in animals with changed brain

functions due to the presence of a vitamin of the B-group.

MATERIAL AND METHODS

Socially isolated male Albino ICR mice and Wistar rats (n=10 in each group) were treated with effective daily doses (125-150 mg/kg b.w. daily) for 3 consecutive days. Administration of the compounds was intraperitoneal. The dry substance, in view of the proven liposolubility of compounds, was dissolved in Oleum Helianthi. The two control groups: of socially isolated mice and rats, were administered for three days with the solvent only.

Behavioral methods for testing cognitive functions were used (learning and memory - Step-through test, exploratory activity - Hole-board test) to evaluate these vs controls on day 1 and on day 7 after training.

The effects of the compounds after 3 days of administering of the compounds in vivo on stimulated release and reuptake of [³H] 5-HT, in hippocampus of rats/whole brain tissue of mice and on stimulated [³H] Ach release were also studied in hippocampal slices of Wistar rats, via radiolabelling techniques.

RESULTS AND DISCUSSION

The two isomeric peptidomimetics modulated cognitive functions (memory and exploratory behavior) in socially isolated and aggressive rats and mice, which proves their neuropharmacological efficacy. This is well illustrated in Figures 2 (mice) and 3 (rats) for aversive stimulus memory and Figures 4 (mice) and 5 (rats) for exploratory behavior (spatial memory and exploration).

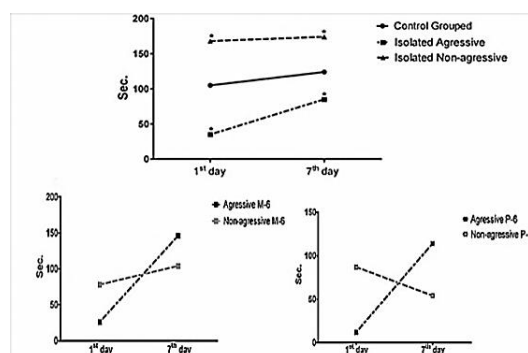


Fig.2. Opposite effects of M6 and P6 upon memory of socially isolated mice versus non-aggressive mice

The very interesting thing about the dimers is that there is clearly a diverse effect upon neuropharmacological behavior parameters depending on whether they are administered to mice or to rats. These differences in effects could be due to inter-species differences in

neurotransmitter systems / metabolism of the two types of rodents.

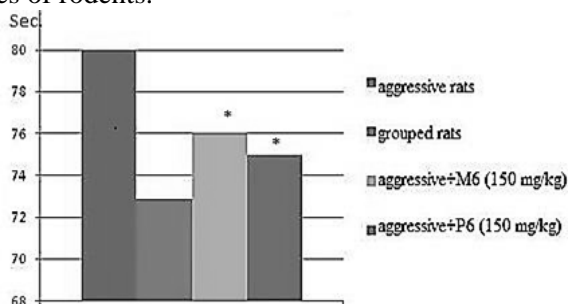


Fig.3. Effects of isomers on memory of rats tested with the Step-through test.

* $p < 0.001$ vs. aggressive controls On the Y-axis: Sec. = Latency to step through of rats into the dark compartment

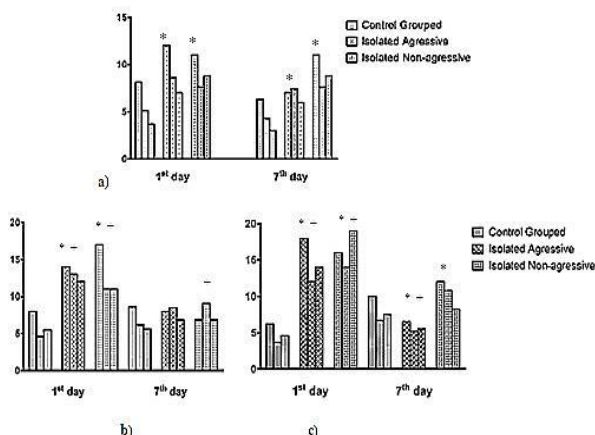


Fig.4. Effects of isomers on the number of peeks in the holes of the Hole-board for every single minute in the course of 3-minute observation, on the 1st and 7th days after 3 days of i.p. treatment with M6 (b) and P6 (c);

+ $p < 0.05$ vs controls isolated animals from Fig.4.a;
* $p < 0.05$ vs grouped control mice, treated with the respective isomer.

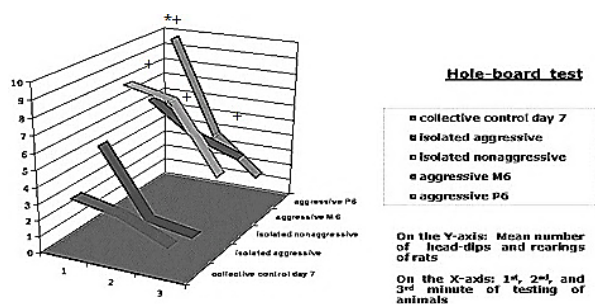


Fig.5. Effects of isomers on the number of peeks in the holes of the Hole-board for every single minute in the course of 3-minute observation, on the 7th day after 3 days of i.p. treatment with M6 and P6;

+ $p < 0.01$ vs controls isolated rats; * $p < 0.05$ significance of difference between M6-treated rats' vs P6-treated.

The effects of the compounds on release and reuptake of serotonin in hippocampus of Wistar rats and whole brain tissue of mice and also on stimulated acetylcholine release in hippocampal slices of rats were also studied. The change in neurotransmitter release and reuptake is also related to memory modulation. Both isomers exerted the same decreasing effect upon serotonin reuptake, as evident in Fig. 6a– (mice whole brain tissue) and 6b – (in rats' hippocampus) alike.

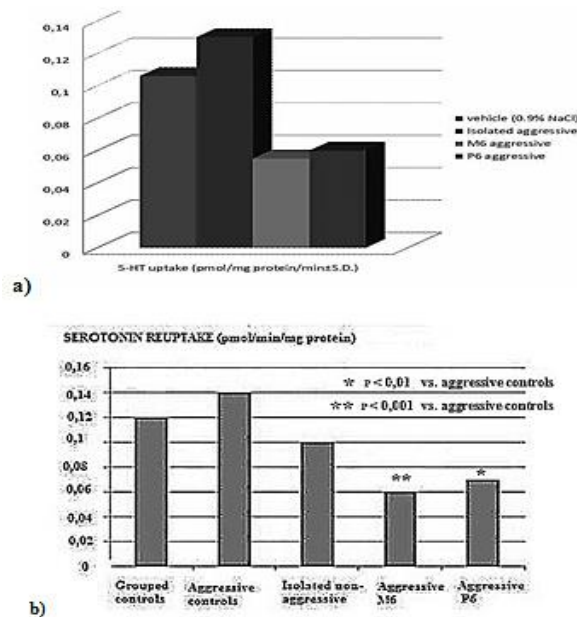


Fig. 6. Reuptake of [³H]-5-HT in synaptosomes of whole brain of mice (a), and in synaptosomes of hippocampal tissue of rats (b).

The compounds were administered for 3 days, daily dose 150 mg/kg body weight

Our results revealed also different effects of the two isomers on neurotransmission. Serotonin (5-HT) release and Ach release from hippocampal slices of aggressive rats were changed differently by the two isomers (Fig. 7b and Fig. 8).

The effects of the two isomers upon [³H] 5-HT release in slices of hippocampus of rats and of whole brain of mice with aggressive behavior were the opposite – M6 increased serotonin release, while P6 decreased it both in whole brain tissue of aggressive mice and in hippocampal tissue of aggressive rats, as seen on Fig. 7. a) /mice/ and b)/rats/.

It is very interesting that similar opposite effects of the two isomers upon [³H] ACh release in hippocampus of rats with aggressive behavior after social isolation were also found: M6 having a neutral vs P6 a definitely decreasing effect on neurotransmitter release (Fig.8).

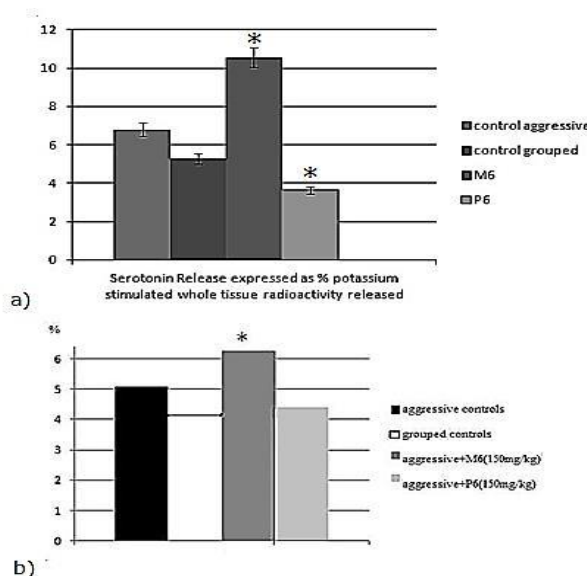


Fig.7. Stimulated release of [³H] 5-HT in brain tissue (%) a) – of whole brain of mice; b) in hippocampal slices of rats

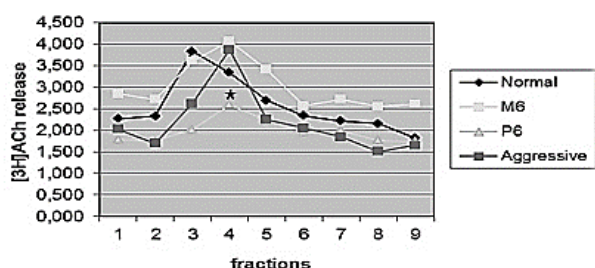


Fig.8. Electrically stimulated Acetylcholine release from hippocampal slices of rat (% radioactivity of fractions compared to initial level)

The CNS effects are most probably related to the presence of L-Valine and a hydrophobic spacer which increases liposolubility of the compounds. The main reason for differences in the modulating effect on cognitive functions of rodents, and upon neuromediator release is obviously the positional isomerism of the nicotinic/isonicotinic residues. We could consider also another reason – interspecies differences in neurotransmission systems of the brain in aggressive rodents that were reported by Kulikov, Carillo, Vergnes and other authors [13-15].

CONCLUSIONS

M6 and P6 improve memory on the 7th day of the Step through test in aggressive mice after long term social isolation.

Both L-valine peptidomimetics decrease serotonin reuptake in synaptosomes of whole brain

of mice and of hippocampal tissue of rats, compared to grouped and aggressive controls, M6 increases, while P6 decreases KCl-stimulated serotonin release in whole brain slices of socially isolated aggressive mice and of hippocampal slices of socially isolated aggressive rats.

The effects of M6 and P6 upon electrically stimulated release of ACh from hippocampal slices of socially isolated aggressive rats are opposite: M6 slightly increases, while P6 significantly decreases ACh release, correlating with the effect of this isomer upon memory in the aggressive rats.

We believe that peptidomimetic drug design and experimental neuropharmacology are indispensable tools, to be used together, in exploration of the brain and of neurotransmitter interactions at the level of chemical synapses in brain structures.

REFERENCES

1. D.S. Tsekova, B. Escuder, J.F. Miravet, *Cryst Growth Des*, **8**, 11 (2008).
2. D. S. Tsekova, J. A. Saez, B. Escuder, J. F. Miravet, *Soft Matter*, **5**, 3727 (2008).
3. G.Fear, S. Komarnytsky, I. Raskin, *Pharmacology and therapeutics*, **113**(2): 354 (2007)
4. J.J. Ferguson, M. Zaqa, *Drugs*, **58**(6), 965 (1999)
5. L.D.Walensky, A.L.Kung, I Escher, T.J. Malia, S. Barbuto, R. D. Wright, G. Wagner, G. L. Verdine, S.J. Korsmeyer, *Science*, **305**, 1466 (2004)
6. J.T. Cole, C.M. Mitala, S. Kundu, A.Verma, J.A. Elkind, I.Nissim, A. S Cohen, *Proceedings of the National Academy of Sciences*, **107**(1), 366 (2010).
7. .R. Aquilani, P. Iadarola, A. Contardi, M.Boselli, M.Verri, O.Pastoris, F. Boschi, P. Arcidiaco & S.Viglio, **86**(9), *Arch. Phys. Med. Rehabil* 1729 (2005).
8. J. Chen, M. Chopp, *The Open Drug Discovery Journal*, **2**, 181 (2010).
9. R.A. Maxwell; S.B. Eckhardt *Drug discovery*. Humana Press, 1990, 143.
10. L.Valzelli, *Psychopharmacologia*, **31**(4), 305 (1973).
11. C.A. Heidbreder, I.C. Weiss, A.M. Domeney, C. Pryce, J. Homberg, G. Hedou, J. Feldon, M.C. Moran & P. Nelson, *Neuroscience*, **100**(4), 749 (2000).
12. N. Wongwitdecha, C.A. Marsden. *Behavioural brain research*, **75**(1) 27 (1996).
13. V.Kulikov, D.V. Osipova, V.S. Naumenko, E.Terenina, P. Mormède, N.K. Popova, *Behavioural brain research*, **233**(1), 113 (2012).
14. M Carrillo, L.A. Ricci, G.A. Coppersmith, R.H. Melloni. *Psychopharmacology*, **205**, 349 (2009)
15. M Vergnes, A Depaulis, A Boehrer. *Physiology and Behavior*, **36**, 653 (1986).

СРАВНИТЕЛНИ ПРОУЧВАНИЯ НА ДВА ИЗОМЕРНИ L-ВАЛИНОВИ ПЕПТИДОМИМЕТИЦИ ЗА НЕВРОФАРМАКОЛОГИЧНИ ЕФЕКТИ У ГРИЗАЧИ

Е. Н. Енчева^{1*}, Д. Цекова², Л. Танчева³, Л. Алова⁴, М. Стефанова⁴, Л. Шикова⁴, М. Кънева⁴

¹ Катедра по физиология, Медицински факултет, МУ-София, Бул. Георги Софийски 1, 1431 София, България

² Катедра по органична химия, ХТМУ, Бул. Кл. Охридски 8, 1756 София, България

³ Поведенческа невробиология, Институт по Невробиология, БАН, Акад. Г. Бончев, бл. 23,1113 София, България

⁴ Радиоизотопна Лаборатория, Институт по Невробиология, БАН, Акад. Г. Бончев, бл. 23,1113 София, България

Постъпила на 6 октомври, 2016 г.; Коригирана на 10 януари, 2017 г.

(Резюме)

Позиционната изомерия е вариант на структурната изомерия. Известно е, че биологичната активност е функция на химичната структура на съединенията, и също, че позиционните изомери често се различават по биологична активност. Две нови съединения, които са изомерни пептидни миметици, производни на L-валин, и съдържащи хидрофобен мост с шест метиленови групи, и остатъци на никотиновата, съответно на изоникотиновата киселина, очакваме да проявяват различни ефекти *in vivo*.

Цел на настоящото проучване е да се оцени въздействието на тези пептидни миметици върху ориентировъчното поведение и паметта у гризачи. Социално изолирани мъжки гризачи: бели ICR мишки и Wistar плъхове, бяха третирани с ефективни дневни дози за 3 последователни дни. Техните когнитивни функции бяха оценени (обучение и памет – с помощта на Step through, ориентировъчно поведение с Hole board тест). Ефектите на съединенията също са изследвани върху освобождаването и обратното захващане на серотонина в хипокампа и върху стимулираното ацетилхолиново освобождаване в хипокампални срези на Wistar плъхове.

Нашите резултати показват значителен доза-зависим ефект на позиционните изомери. Серотониновото (5-HT) и ацетилхолиновото освобождаване в срези на хипокамп бяха променени по различен начин от двата изомера. Ефектите върху ЦНС са вероятно свързани с присъствието на L-валин и хидрофобен спейсер, което увеличава липоразтворимостта на съединенията. Основната причина за разликите в ефектите върху когнитивните функции на гризачи, и върху невромедиаторните нива е най-вероятно позиционната изомерия на никотиновите или изоникотиновите остатъци.

Ghrelin and gastric cancer

I.S. Stefanov ^{1*}, J.R. Ananiev ², A.N. Tolekova ³, K.I. Dinkova ², S. Hamza ¹, M. K. Ignatova ²,
M. V. Gulubova ²

¹ Department of Anatomy, Medical Faculty, Trakia University, Stara Zagora, Bulgaria

² Department of General and Clinical Pathology, Medical Faculty, Trakia University,
Stara Zagora, Bulgaria

³ Department of Physiology, Pathophysiology and Pharmacology, Medical Faculty, Trakia University, Stara Zagora,
Bulgaria

Received September 28, 2016; Revised February 13, 2017

Ghrelin is a recently discovered peptide, described predominantly in gastric endocrine cells. Gastric ghrelin – positive cells were studied in chronic atrophic gastritis, H. Pylori-related gastritis and gastric carcinoids mainly. Presence of ghrelin- positive cells in gastric cancer was less investigated. The aim of the present study was to describe ghrelin-positive cells in gastric cancer of diffuse and intestinal types and in surrounding mucosa from antral, fundic and corpus regions. Endocrine cells were revealed immunohistochemically with antibodies against chromogranin (Cha), gastrin (Gas), somatostatin (Som), serotonin (Ser) and ghrelin (Ghr). Ghrelin positive cells were found in all cancers (diffuse type gastric cancer), (1,93±1,76 cells/mm²). In antral mucosa Ghr⁺ cells were between 42,37±4,8 cells/ mm² followed by corpus mucosa between 27,6±1,27 cells/ mm² and by fundus mucosa between 25,2±6,3 cells/ mm². Co-localization studies showed that some of the Cha⁺ cells, Gas⁺ cells, and Som⁺ cells were also Ghr⁺. In conclusion we may state that in gastric cancer from the diffuse type there could be detected Ghr⁺ ECs. Ghrelin could be secreted not only by separate Ghr⁺ ECs but also by ECs positive for gastrin and somatostatin.

Keywords: ghrelin, endocrine cells, gastric cancer

INTRODUCTION

Ghrelin structure and production

Ghrelin was described by Kojima et al. [1] as a novel growth-hormone-releasing peptide, which was originally isolated from rat and human stomachs. It was also reported that human ghrelin is homologous to rat ghrelin except for two amino acids. This ligand for growth hormone secretagogue receptor (GHS-R) is a peptide consists of 28 amino acids. Its serine 3 residue is n-octanoylated. The acylated peptide was established to release growth hormone (GH) both in vivo and in vitro, and O-n-octanoylation at serine 3 is very important step in its activation. Circulating ghrelin contains more than 90% of desacyl ghrelin and less than 10% acyl ghrelin [2]. However, according to Kojima et al. [1, 3] the acyl group of ghrelin is essential for its binding to GHS-R and the simultaneous activation of the inositol triphosphates-calcium pathway).

The human ghrelin gene is located on the short segment of chromosome 3 (3p25-26) and comprises 4 introns and six exons (2 are noncoding) and encodes a 511 bp mRNA [4, 5, 6]. In relation to the chemical properties of its precursors, Korbonits et al. [7] reported that proghrelin (117 AA) contains 23 AA signal peptide and a 94AA segment

corresponding to proghrelin. Proghrelin is made of the 28AA ghrelin peptide and a 66AA carboxyterminal peptide named C-ghrelin [6, 8, 9]. C-ghrelin can be transformed to a 23AA peptide called obestatin [10]. On the other hand, some authors give information for the alternative splicing of the human ghrelin gene produces additional transcripts coding for other peptides including des-Gln14-ghrelin [6, 11]. The enzymes responsible for transforming proghrelin into ghrelin include signal peptidase cleaving at Arg23, prohormone convertase 1/3 (PC 1/3) cleaving at Arg51 (producing ghrelin 1–28) [12], and carboxypeptidase-B like enzyme cleaving at Pro50 (producing ghrelin 1–27) [13].

As mentioned above, two ghrelin peptides are described as a result of human ghrelin gene transcription and translation. The main metabolic pathway is the acylation of the hydroxyl group of the Ser3 [1]. Both ghrelin 1–28 and ghrelin 1–27 undergo to acylation, mainly by an octanoyl group (C8:0) and more rarely by a decanoyl (C10:0) or decanoyl (C10:1) group [Hosoda et al., 2003]. Enzyme involved in ghrelin acylation is ghrelin O-acyl transferase (GOAT), which is a member of the family of membrane O-acyl transferases (MBOAT) [14, 15]. Gutierrez et al. [14] found out that ghrelin and GOAT are co-expressed in X/A like cells of gastric mucosa. The addition of C8 medium-chain or C10 medium chain triglycerides in diets

* To whom all correspondence should be sent:
E-mail: ivstefanov@abv.bg

modificate the proportions of octanoyl or decanoyl ghrelin involved in the same granules in gastric X/A like cells, suggesting that GOAT uses the most available substrate to catalize ghrelin acylation [16]. It is known that ghrelin acylation is performed in the endoplasmic reticulum prior to the processing of proghrelin by proteases on either the proghrelin or the proghrelin precursors [12, 15, 17, 18]. GOAT acylates ghrelin with fatty acids ranging from C:7 to C:12 [14]. Yang et al. (2008) described acyl-CoA as donors of acyl group. After that, Ohgusu et al. (2009) proved that *in vitro* GOAT prefers *n*-hexanoyl-CoA to *n*-octanoyl-CoA as an acyl donor.

Biological activities of ghrelin depend on the presence of acyl group on Ser3 [19, 20]. C8:0 Ser3 defines maximal ghrelin activity, which is maintained by C10:0 Ser3, C12:0 Ser3, and C16:0 Ser3 but decreased by C4:0 Ser3 or C2:0 Ser3 [19]. The replacement of Ser3 by Trp3 maintains the activity of ghrelin, but its replacement by aliphatic AA (such as Val, Leu, or Ile) inhibits its activity [19]. The N-terminal positive charge and Phe4 are necessary for ghrelin activity and recognition by GHS-R1A [21]. Systematic C-terminal reduction of ghrelin identified the N-terminal pentapeptide of ghrelin, including C8:0 Ser3, to be the minimal peptide fragment with the same power like ghrelin [20, 22]. In addition, amidation of the C-terminus increased the activity of the ghrelin fragments [20, 22] while N-acetylation decreased it [21, 22].

In human, circulating ghrelin contains desacyl ghrelin (more than 90%), acyl ghrelin, and C-ghrelin [2, 8, 23]. Desacyl ghrelin mostly circulates as a free peptide, while acyl ghrelin is bound to lipoproteins [24, 25]. The acyl group is needed for ghrelin interaction with lipoproteins bound with triglycerides and low-density lipoprotein, while N- and C-terminal ends of ghrelin are needed for its coupling to high-density lipoproteins and very high-density lipoproteins. In this regard, De Vriese et al. [24] hypothesized that triglyceride-rich lipoproteins predominantly transport acyl ghrelin, while high-density and very high-density lipoproteins transport both acyl and desacyl ghrelin.

Ghrelin receptor (GHS-R)

GHS-R is a type of G-protein coupled receptors (GPCR), characterized by seven transmembrane helix domains [26]. The localization of human GHS-R was established on chromosome 3 (3q26.2) consisting of 2 exons and 1 intron. Exon 1 codes for the GHS-R region from the extracellular N-terminal end to the 5th transmembrane helix, while exon 2 codes for the rest of the receptor GHS-R is

represented by GHSR1A and GHS-R1B. GHS-R1A is a 366AA protein consisting of 7 transmembrane helix domains, while GHS-R1B is a 289AA protein consisting of 5 transmembrane helix domains [27].

Binding of GHS-R1A to G-protein involves the 3rd intracellular loop. The lack of a 3rd intracellular loop in GHS-R1B prevents its binding to G-proteins. GHS-R1A activation causes the activation of phospholipase C, inositols triphosphates, and intracellular calcium pathways [28]. At physiological concentrations, only acyl ghrelin binds to GHS-R1A, while at supraphysiological concentrations (1 μ M) desacyl ghrelin couples to the receptor as well [29, 30]. Acyl ghrelin and desacyl ghrelin are electrostatically attracted to membranes by their basic residues, but acyl ghrelin penetrates deeper by its acyl group [30]. GHS-R1A was shown to function as homodimer [31, 32] and it also forms heterodimers with members of the prostanoid receptor family such as vasodilator prostacyclin receptor (IP), the vasoconstrictor prostaglandin E2 receptor subtype EP3-I (EP3-I), and thromboxane A2 (TP α) [33].

GHS-R1B, considered in the past to be functionally inactive, is now believed to act as an important modulator in ghrelin-induced GHS-R1A signaling. Indeed, GHS-R1B is able to heterodimerize with GHS-R1A and to decrease the constitutive activity of GHS-R1A [32, 34, 35, 36]. GHS-R1B exerts a dominant negative effect via a conformational restriction of the GHS-R1A that becomes unable to subsequently activate G protein and recruit β -arrestin [37].

GHS-R1B is unable to bind acyl or desacyl ghrelin and acts as a modulator in ghrelin-induced GHS-R1A signaling. GHS-R1B is able to heterodimerize with GHS-R1A and decrease the constitutive activity of GHS-R1A [32, 34, 35, 36]. GHS-R1B exerts a negative effect through a conformational constraint of the GHS-R1A which becomes unable to activate G protein and strengthen β -arrestin [37].

The role of ghrelin in physiological processes

Ghrelin expression is mainly detected in the digestive tract, with highest levels in the gastric mucosa [1, 38]. Gastric mucosa involves five endocrine cell types, represented by enterochromaffin cells (EC), enterochromaffin-like cells (ECL), D cells, G cells, and X/A like cells which, respectively, secrete serotonin, histamine, somatostatin, gastrin, GABA, and ghrelin. Human and rat gastric mucosa are, respectively, composed of 30%/60–70% ECL cells, 20%/20% X/A-like cells,

22%/2.5%Dcells, and 7%/0–2% of EC and G cells [39, 40]. Ghrelin is mainly located in the oxyntic mucosa of the gastric fundus in neuroendocrine cell subtype of P/D₁ cells which represent 20% of all neuroendocrine cells at this place [41, 42]. In the normal mucosa of stomach corpus, ghrelin-positive cells were located between parietal cells and chief cells in the lower part of the fundic glands. In man, ghrelin cells (147 nm) were characterised by round, electron-dense secretory granules [42]. Ghrelin has been known as a multifunctional hormone. Various studies have investigated ghrelin and its systemic effects regarding growth hormone release from the pituitary gland, appetite regulation and its impact on body weight [43, 44]. However, ghrelin is also a hormone with gastro-protective local effects. It stimulates propulsion and mucus secretion and contributes to the healing process after a mucosal injury. Therefore, ghrelin is essential for maintaining the mucosal barrier of the human stomach [45, 46]. The mechanism for the action of ghrelin on feeding, growth hormone secretion, secretion of gastric acid and the gastric contractility was studied and demonstrated that the vagal nerve was involved in the action of ghrelin [47, 48]. Yakabi et al., [49] established that ghrelin stimulates gastric acid secretion via a mechanism involving activation of vagal efferent nerve and histamine release from gastric enterochromaffin-like cells. In humans, peripheral administration of ghrelin stimulate gastric emptying [50] with no modification of orocecal and colonic transit [51]. Moreover, ghrelin strengthens the human migrating motor complex [52]. Furthermore, ghrelin has been established to be useful for the treatment of gastrointestinal motility disorders [53, 54]. Future studies are needed to study the beneficial effects of novel ghrelin receptor agonists in gastrointestinal motility disorders.

The role of ghrelin and its receptors in pathological processes of the human stomach

The role of ghrelin in pathological processes has been described in different aspects. Several studies have reported that ghrelin is able to exert anti-inflammatory actions by inhibiting the production of proinflammatory cytokines [55, 56, 57, 58]. Ghrelin anti-inflammatory actions were found out in inflammatory bowel disease, pancreatitis, sepsis, arthritis [59, 60, 61, 62].

Rau et al., [63] investigated the influence of ghrelin in several pathological situations of the stomach. For example, in autoimmune gastritis, Rau et al. [63] established a new gastrin-mediated mechanism for ghrelin suppression. In autoimmune

gastritis, ghrelin-positive cells comprised up to 50% of the investigated nodules of neuroendocrine cell hyperplasia. Neoplastic ghrelinomas have also been described by several authors [64, 65, 66, 67]. Some authors claim that ghrelin plays an autocrine/paracrine role in a number of processes related to cancer progression, including cell proliferation [68, 69], cell migration [70], and apoptosis [71]. According to Duxbury et al. [72] ghrelin increases cell proliferation, migration and invasion in pancreatic cancer cell lines via PI3K/Akt pathway [72], which is associated with an increase in cell motility and invasion. The participation of ghrelin in proliferation of gastric cancer was also reported by Tian and Fan [73]. These authors found out that ghrelin and des-acyl ghrelin stimulate the proliferation of gastric cancer cells via the activation of the ERK1/2 and PI3K/Akt pathway. While a number of studies have demonstrated that ghrelin stimulates cell proliferation, some reports indicate that ghrelin may inhibit proliferation. These include thyroid [74], prostate [75] and breast cancer [76] and small cell lung carcinoma [77] cell lines. Ghrelin is expressed in a wide range of cancer tissues and plays a role in a number of key processes in cancer progression, including cell proliferation, cell migration and invasion, and apoptosis. As there have been a number of conflicting reports, it is currently unclear whether ghrelin promotes cancer or inhibits its development..

The data about ghrelin expression in gastric cancer cases is too limited, but it is different for neuroendocrine tumors. In gastric cancer, Rau et al. [63] did not detect any ghrelin-expressing cells. Papotti et al. [64] demonstrated that the majority of gastric carcinoids and a fraction of intestinal endocrine tumors show immunoreactivity for ghrelin. It was established that 75% gastric carcinoids were immunoreactive for ghrelin in a variable percentage of tumor cells. Cellular ghrelin reactivity was observed as a diffuse, finely granular cytoplasmic staining, as strong as that of peritumoral gastric endocrine cells. Intratumoral stromal or inflammatory cells were not stained. Although gastric carcinoids are rare and generally benign conditions, Papotti et al. [64] observed two aggressive cases and an additional low grade tumor with a lymph node metastasis. Ghrelin was found to be produced by two of these tumors, which means that its expression is probably independent from the biological aggressiveness of the tumor. These findings suggest that assessment of circulating ghrelin levels may be useful in diagnosis of atrophic gastritis and associated neuroendocrine

cell growths as well as of gastrointestinal tumors of neuroendocrine nature. Tsolakis et al. [66] studied a patient with a malignant gastric neuroendocrine tumor secreting ghrelin as the main hormone. This might be a new tumor entity of the stomach, and it is suggested that patients with malignant gastric neuroendocrine tumors should be investigated for ghrelin production, for example ghrelin immunoreactivity in tumor cells as well as total and active ghrelin concentrations in the blood.

It was reported that ghrelin-expressing cells are a cell type differs from the enterochromaffin-like cells, but intermingle with them as derivatives from type A-like cells. However, the idea of enterochromaffin-like cell hyperplasia is derived from the idea of a direct gastrin influence on these cells which still has to be shown for ghrelin-positive cells [78]. Gastrin is known to have growth stimulating effects on neuroendocrine cells in the gastric fundus [78, 79] but it is unknown if it interacts with ghrelin-expressing cells. Some authors presented data that shows synergistic effects of gastrin and ghrelin on gastric acid secretion and histamine production by gastric mucosa which involves the vagal nerve [80, 45].

However, Rau et al. [64] confirmed the existence of the gastrin/cholecystokinin (CCKB) receptor for the first time on human ghrelin-positive cells, which corresponds to data from animal models [45]. The finding of this receptor on

ghrelin-expressing cells suggests a possible influence by gastrin. For example, Rau et al. [63] observed dose-dependent ghrelin suppression by gastrin.

MATERIALS AND METHODS

We used specimens from two patients with intestinal type of gastric cancer who undergo of total gastrectomy in Surgical Department in University Hospital in Stara Zagora. Tissue specimens were fixed in 10% buffered formalin, embedded in paraffin and cut to 4 μm thickness. Specimens were deparaffinated and endogenous peroxidase was blocked for 5 minutes with blocking reagent according to the protocol. Then the slides were washed 3 times with PBS and incubated with primary antibody for 1 hour followed by incubation with marked polymer and washed again.

Tissue samples were incubated with DAB substrate-chromogen and after washing counterstained by Mayer's hematoxylin.

Table 1 shows immunohistochemistry panel of applied antibodies and components, their manufacturer, dilution and reaction:

Table 1. Immunohistochemistry panel of applied antibodies and components

N°	Antibody	Manufacture	Dilution	Reaction
1.	Monoclonal Mouse Anti-Human Chromogranin A	M0869, DAKO	1:100	Cytoplasmatic
2.	Polyclonal Rabbit Anti-Human Gastrin	A 0568, DAKO	1:500	Cytoplasmatic
3.	Monoclonal Mouse Anti-Human Serotonin	M0758, DAKO	1:100	Cytoplasmatic
4.	Polyclonal Rabbit Anti-Somatostatin	A0566, DAKO	1:200	Cytoplasmatic
5.	Polyclonal Rabbit Anti-Human Ghrelin	H-40 Santa Cruz Biotechnology	1:100	Cytoplasmatic
6.	EnVision™ FLEX+, Mouse, High pH, (Link)	K8002, DAKO	-	-

RESULTS AND DISCUSSION

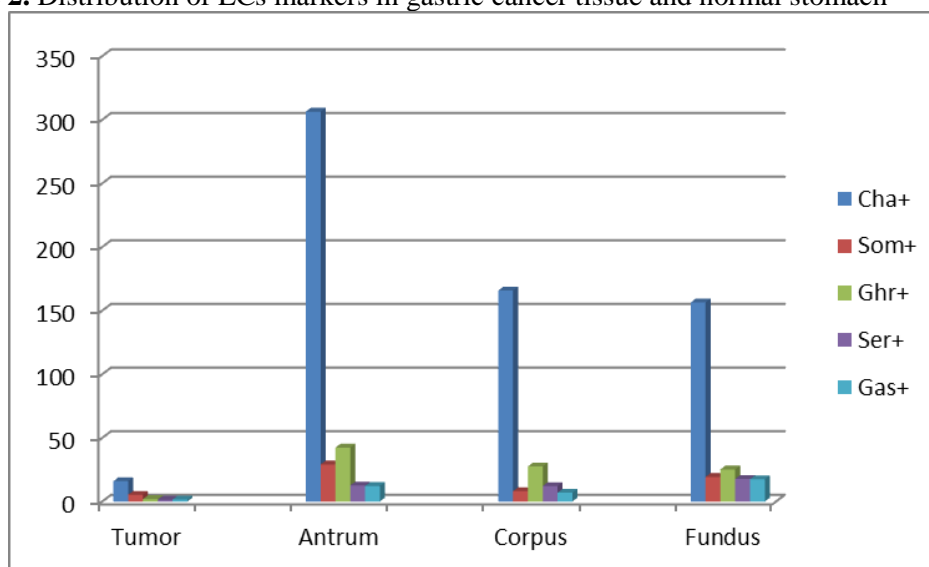
After analysis, we found endocrine positive cells (ECs) for all investigated markers in tumor parenchyma and in the overlying mucosa of gastric antrum, corpus and fundus (Table 1, Fig. 1, Fig. 2 and Fig. 3).

The most common ECs in the tumor tissue were cells positively for Chromogranin ($15,9 \pm 8,5$ cells/mm²), followed by somatostatin positive ($5,33 \pm 1,25$ cells/mm²), Ghrelin⁺ ($1,93 \pm 1,76$ cells/mm²), gastrin positive ($1,59 \pm 0,32$ cells/mm²) and serotonin positive cells ($1,47 \pm 1,44$ cells/mm²). In normal tissue from gastric antrum and gastric

fundus the distribution of ECs was similar: Cha⁺cells (306,35±6,97 and 156,5±1,6 cells/mm² respectively), Ghr⁺cells (42,37±4,8 and 25,2±6,3 cells/mm², respectively), Som⁺cells (29,14±5,93 and 19,4±7,2 cells/mm², respectively), Ser⁺cells (and 17,8±4,14 cells 12,1±6,9 cells/mm², respectively). cells/mm², respectively), and ECs positively for gastrin were least (12,2±8,4 for antrum and 17,6±2,03 cells/mm² for fundus).

Finally after investigation of gastric corpus the result shown that the most common type of ECs was again chromogranin positive (165.76±3,13cells/mm²), followed by ghrelin positive (27,6±1,27 cells/mm²), serotonin + (12,6±1,4 somatostatin positive (8,1±0,04 cells/mm²), /mm²) and gastrin positive (6,89±1,4 cells/mm²).

Table 2. Distribution of ECs markers in gastric cancer tissue and normal stomach



Ghrelin has a number of functions, including roles in the regulation of growth hormone release, metabolism, appetite, the cardiovascular system and insulin secretion [1]. Another function of ghrelin is that it increases the secretion of gastric acid via nitric oxide which stimulates mucosal blood flow [81]. Ghrelin cell density was found by to be positively correlated with the degree of diarrhea and inversely correlated with the degree of constipation [82]. Therefore, changes in ghrelin cell density play a decisive role in the development of diarrhea and constipation in irritable bowel syndrome patients.

In addition the role of ghrelin and its receptor GHS-R is not clear. It was reported that GHSR 1a expression differs from that of GHSR 1b in cancer. For instance, in a number of cancers, GHSR 1a expression is downregulated or absent [76, 83, 84, 85], while the non-functional form of the receptor, GHSR 1b is widely expressed in cancer and expression may be upregulated compared to normal tissues [86]. Some autors state that gastric cancers arised after different types of mucosal injury, but today we know that ghrelin is also a hormone with

gastro-protective local effects. It stimulates propulsion and mucus secretion and contributes to the healing process after a mucosal injury. Therefore, ghrelin is essential for maintaining the mucosal barrier of the human stomach [44, 45].

Ghrelin is expressed in a wide range of cancer tissues and plays a role in a number of key processes in cancer progression, including cell proliferation, cell migration and invasion, and apoptosis. As there have been a number of conflicting reports, it is currently unclear whether ghrelin promotes cancer or inhibit its development and it is possible that it could have both stimulatory and inhibitory effects.

Since in the literature data is scarce, our results suggest that ghrelin and some from the other endocrine markers in gastric cancer tissue and normal mucosa may play an important role in carcinogenesis, and its expression will be a valuable prognostic marker for prognosis and prediction in gastric cancer patients.

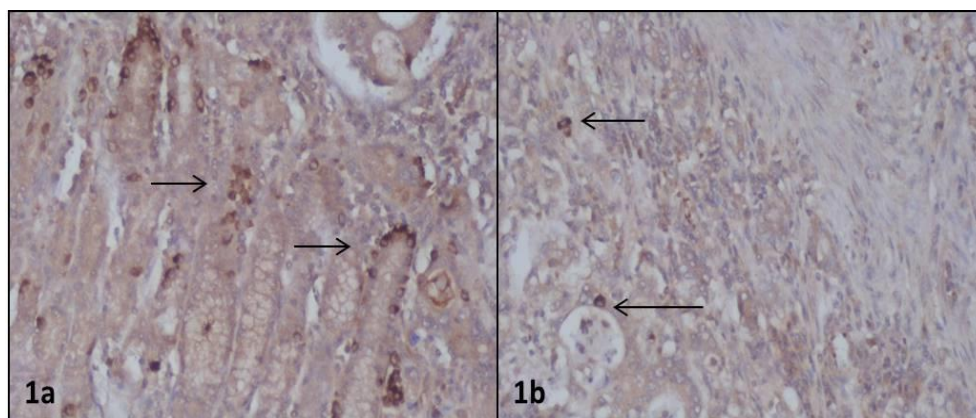


Fig. 1a) Ghrelin positive ECs (arrows) hyperplasia in transitional mucosa and in tumor (x200); **b)** Ghrelin positive ECs (arrows) in tumor (x200).

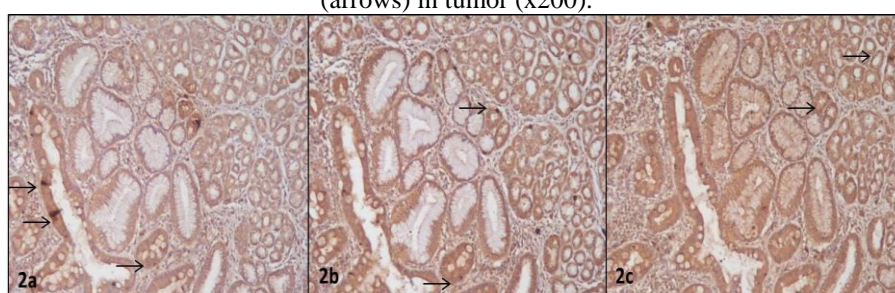


Fig. 2a) Gastrin positive ECs (arrows) in gastric fundus (x200); **b)** Ghrelin positive ECs (arrows) in gastric fundus (x200); **c)** Somatostatin positive ECs (arrows) in gastric fundus (x200)

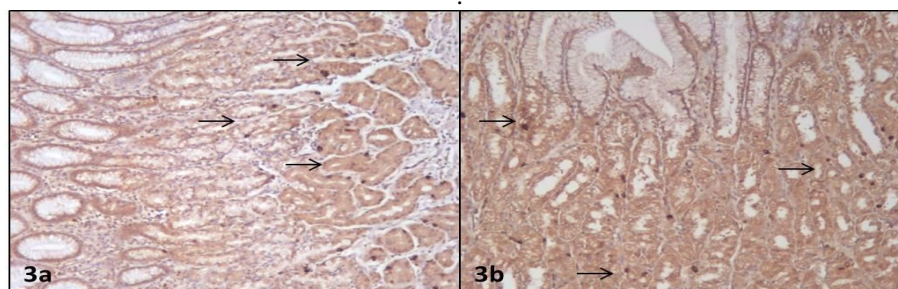


Fig. 3. a) Ghrelin positive ECs (arrows) in pylor (x100); **b)** Ghrelin positive ECs (arrows) in corpus (x100).

REFERENCES

1. M. Kojima, H. Hosoda, Y. Date, M. Nakazato, H. Matsuo, K. Kangawa. *Nature*, **402**, 656 (1999).
2. M. Patterson, K. G. Murphy, C.W. le Roux, M. A. Ghatei, S. R. Bloom, *J. Clin. Endocrinol. Metab.*, **90**(4), 2205 (2005).
3. M. Kojima, H. Hosoda, and K. Kangawa, *Horm. Res.*, **56**, suppl. 1, 93 (2001).
4. N. Kanamoto, T. Akamizu, T. Tagami, Y. Hataya, K. Moriyama, K. Takaya, H. Hosoda, M. Kojima, K. Kangawa, K. Nakao, *Endocrinology*, **145**(9), 4144 (2004).
5. N. Nakai, M. Kaneko, N. Nakao, T. Fujikawa, K. Nakashima, M. Ogata, M. Tanaka, *Life Sci.*, **75**(18), 2193 (2004).
6. I. Seim, C. Collet, A. C. Herington, L. K. Chopin, *BMC Genomics*, **8**, 298 (2007).
7. M. Korbonits, A. P. Goldstone, M. Gueorguiev, A. B. Grossman. *Front. Neuroendocrinol.*, **25**(1), 27 (2004).
8. C. Pemberton, P. Wimalasena, T. Yandle, S. Soule, M. Richards, *Biochem. Biophysic. Res. Commun.*, **310**(2), 567 (2003).
9. A. S. Bang, S. G. Soule, T. G. Yandle, A. M. Richards, C. J. Pemberton, *J. Endocrinol.*, **192**(2), 313 (2007).
10. J. V. Zhang, P.-G. Ren, O. Avsian-Kretschmer, C. W. Luo, R. Rauch, C. Klein, A. J. Hsueh. *Science*, **310**(5750), 996 (2005).
11. H. Hosoda, M. Kojima, H. Matsuo, K. Kangawa, *J. Biol. Chem.*, **275**(29), 21995 (2000).
12. X. Zhu, Y. Cao, K. Voogd, D. F. Steiner, *J. Biol. Chem.*, **281**, 38867 (2006).

11. H. Hosoda, M. Kojima, T. Mizushima, S. Shimizu, K. Kangawa. *J. Biol. Chem.*, **278**(1), 64 (2003).
12. J. A. Gutierrez, P. J. Solenberg, D. R. Perkins, J. A. Willency, MD Knierman, Z. Jin, D. R. Witcher, S. Luo, J. E. Onyia, J. E. Hale, *Proc. Natl. Acad. Sci. U S A.*, **105**(17), 6320 (2008).
13. J. Yang, M. S. Brown, G. Liang, N. V. Grishin, J. L. Goldstein, *Cell*, **132**(3), 387 (2008).
14. Y. Nishi, H. Mifune, A. Yabuki, Y. Tajiri, R. Hirata, E. Tanaka, H. Hosoda, K. Kangawa, M. Kojima, *Front. Endocrinol.*, **4**(84), 1 (2013).
15. Kojima M. and K. Kangawa, *Results Probl. Cell Differ.*, **50**, 185 (2010).
16. H. Ohgusu, K. Shirouzu, Y. Nakamura, Y. Nakashima, T. Ida, T. Sato, M. Kojima, *Biochem. Biophys. Res. Commun.*, **386**(1), 153 (2009).
17. M. Matsumoto, H. Hosoda, Y. Kitajima, N. Morozumi, Y. Minamitake, S. Tanaka, H. Matsuo, M. Kojima, Y. Hayashi, K. Kangawa. *Biochem. Biophys. Res. Commun.*, **287**(1), 142 (2001a).
18. M. A. Bednarek, S. D. Feighner, S.-S. Pong, K. McKee, D. L. Hreniuk, M. V. Silva, V. A. Warren, A. D. Howard, L. H. Van Der Ploeg, J. V. Heck, *J. Med. Chem.*, **43**(23), 4370 (2000).
19. M. van Craenenbroeck, F. Gregoire, P. de Neef, P. Robberecht, J. Perret, *Peptides*, **25**(6), 959 (2004).
20. M. Matsumoto, Y. Kitajima, T. Iwanami, Y. Hayashi, S. Tanaka, Y. Minamitake, H. Hosoda, M. Kojima, H. Matsuo, K. Kangawa, *Biochem. Biophys. Res. Commun.*, **284**(3), 655 (2001b).
21. H. Hosoda, K. Doi, N. Nagaya, H. Okumura, E. Nakagawa, M. Enomoto, F. Ono, K. Kangawa. *Clin. Chem.*, **50**(6), 1077 (2004).
22. C. De Vriese, M. Hacquebard, F. Gregoire, Y. Carpentier, C. Delporte, *Endocrinology*, **148**(5), 2355 (2007).
23. N. J. Beaumont, V. O. Skinner, T. M.-M. Tan, B. S. Ramesh, D. J. Byrne, G. S. MacColl, J. N. Keen, P. M. Bouloux, D. P. Mikhailidis, K. R. Bruckdorfer, M. P. Vanderpump, K. S. Srai. *Journal of Biological Chemistry*, **278**(11), 8877 (2003).
- A. D. Howard, S. D. Feighner, D. F. Cully, J. P. Arena, P. A. Liberator, C. I. Rosenblum, M. Hamelin, D. L. Hreniuk, O. C. Palyha, J. Anderson, P. S. Pares, C. Diaz, M. Chou, K. K. Liu, K. K. McKee, S. S. Pong, L. Y. Chaung, A. Elbrecht, M. Dashkevich, R. Heavens, M. Rigby, D. J. Sirinathsinghji, D. C. Dean, D. G. Melillo, A. A. Patchett, R. Nargund, P. R. Griffin, J. A. DeMartino, S. K. Gupta, J. M. Schaeffer, R. G. Smith, L. H. Van der Ploeg, *Science*, **273**(5277), 974 (1996).
24. K. K. McKee, O. C. Palyha, S. D. Feighner, D. L. Hreniuk, C. P. Tan, M. S. Phillips, R. G. Smith, L. H. Van der Ploeg, A. D. Howard. *Mol. Endocrinol.*, **11**(4), 415 (1997).
25. R. G. Smith, O. C. Palyha, S. D. Feighner, C. P. Tan, K. K. McKee, D. L. Hreniuk, L. Yang, G. Morriello, R. Nargund, A. A. Patchett, A. D. Howard, *Horm. Res.*, **51**, 1 (1999).
26. C. Gauna, B. van de Zande, A. vanKerkwijk, A. P. N. Themmen, A. J. van der Lely, P. J. D. Delhanty, *Mol. Cell. Endocrinol.*, **274**, 30 (2007).
27. E. Staes, P.-A. Absil, L. Lins, R. Brasseur, M. Deleu, N. Lecouturier, V. Fievez, A. Rieux, M. P. Mingeot-Leclercq, V. Raussens, V. Pr at, *Bioch. Biophys. Acta*, **11**, 2102 (1798)
28. B. Holst, E. Brandt, A. Bach, A. Heding, T. W. Schwartz. *Mol. Endocrinol.*, **19**(9), 2400 (2005).
29. P.-K. Leung, K. B. S. Chow, P.-N. Lau, K. M. Chu, C. B. Chan, C. H. Cheng, H. Wise. *Cell Signal.*, **19**(5), 1011 (2007).
30. K. B. S. Chow, P.-K. Leung, C. H. K. Cheng, W.-T. Cheung, H. Wise, *Int. J. Biochem. Cell Biol.*, **40**(11), 2627 (2008).
31. C.-B. Chan and C. H. K. Cheng, *Mol. Cell. Endocrinol.*, **214**, 81 (2004).
32. K.-M. Chu, K. B. S. Chow, P.-K. Leung, P. N. Lau, C. B. Chan, C. H. Cheng, H. Wise. *Int. J. Biochem. Cell Biol.*, **39** (4), 752 (2007).
33. K. B. S. Chow, J. Sun, K. M. Chu, W. Tai Cheung, C. H. Cheng, H. Wise. *Mol. Cell Endocrinol.*, **348**(1), 247 (2012).
34. S. J. Mary, A. Fehrentz, M. Damian, G. Gaibelet, H. Orcel, P. Verdi , B. Mouillac, J. Martinez, J. Marie, J. L. Ban res. *J. Biol. Chem.*, **288**, 24656 (2013).
35. H. Ariyasu, K. Takaya, T. Tagami, Y. Ogawa, K. Hosoda, T. Akamizu, M. Suda, T. Koh, K. Natsui, S. Toyooka, G. Shirakami, T. Usui, A. Shimatsu, K. Doi, H. Hosoda, M. Kojima, K. Kangawa, K. Nakao, *J. Clin. Endocrinol. Metab.*, **86**(10), 4753 (2001).
36. E. Solcia, G. Rindi, R. Buffa, R. Fiocca, C. Capella, *Regul. Pept*, **93**, 31 (2000).
37. M. Simonsson, S. Eriksson, R. Hakanson, T. Lind, H. L nroth, L. Lundell, D. T. O'Connor, F. Sundler, *Scand. J. Gastroenterol.*, **23**(9) 1089 (1988).
38. Y. Date M. Kojima, H. Hosoda, A. Sawaguchi, M. S. Mondal, T. Suganuma, S. Matsukura, K. Kangawa, M. Nakazato. *Endocrinology*, **141**, 4255 (2000)
39. G. Rindi, V. Necchi, A. Savio, A. Torsello, M. Zoli, V. Locatelli, F. Raimondo, D. Cocchi, E. Solcia. *Histochem. Cell Biolol.*, **117**(6), 511 (2002)
40. D. E. Cummings J. Q. Purnell, R. S. Frayo, K. Schmidova, B. E. Wisse, D. S. Weigle, *Diabetes*, **50**, 1714 (2001)
41. D. Perez-Tilve, R. Nogueiras, F. Mallo S. C. Benoit, M. Tschoep, *Endocrine*, **29**, 61 (2006)
42. P. C. Konturek, T. Brzozowski, R. Pajdo, A. Nikiforuk, S. Kwiecien, I. Harsch, A. Nikiforuk, S. Kwiecien, I. Harsch, D. Drozdowicz, E. G. Hahn, S. J. Konturek. *J Physiol Pharmacol*, **55**, 325 (2004)
43. K. Fukumoto, K. Nakahara, T. Katayama, M. Miyazatao, K. Kangawa, N. Murakami, *Biochem. Biophys. Res. Commun.*, **374**, 60 (2008)
44. Y. Masuda, T. Tanaka, N. Inomata, N. Ohnuma, S. Tanaka, Z. Itoh, H. Hosoda, M. Kojima, K. Kangawa, *Biochem. Biophys. Res. Commun.* **276**, 905 (2000).

45. Y. Date, N Murakami, K Toshinai, S Matsukura, A Nijijima, H Matsuo, K Kangawa, M Nakazato, *Gastroenterology*, **123**, 1120 (2002)
46. K. Yakabi ., S. Ro, T. Onouhi, T. Tanaka, S. Ohno, S. Miura, Y. Johno, K. Takayama, *Dig. Dis. and Sciences*, **51**(8), 1313 (2006).
47. F. Levin, T. Edholm, P. T. Schmidt, P. Grybäck, H. Jacobsson, M. Degerblad, C. Höybye, J. J. Hols , J. F. Rehfeld, P. M. Hellström, E. Näslund. *J. Clin. Endocrinol. Metab.*, **91**, 3296 (2006).
48. Y. Falkén, P. M. Hellström, G. J. Sanger, O Dewit, G Dukes, P Grybäck, J. J. Holst, E. Näslund. *Neurogastroenterol. Motil.*, **22**(6), 192 (2010).
49. K. E. Wortley, K. D. Anderson, K. Garcia, J. D. Murray, L. Malinova, R. Liu, M. Moncrieffe, K. Thabet, H. J. Cox, G. D. Yancopoulos, S. J. Wiegand, M. W. Sleeman, *Proc. Natl. Acad. Sci. USA*, **101**(21), 8227 (2004).
50. B. Avau, B. De Smet, T. Thijs, A. Geuzens, J. Tack, P. Vanden-Berghe, I. Depoortere, *Neurogastroenterol. Motil.*, **25**, 599 (2013).
51. C. de Vriese, J. Perret, C. Delporte, Current and future clinical applications of ghrelin. In *Endocrine Disease*, IConcept Press Ltd, 2014.
52. L. Chang, J.-B. Du, L.-R. Gao, Y.-Z. Pang, C.-S. Tang, *Acta Pharmacol. Sin.*, **24**, 45 (2003).
- A. Dembinski, Z. Warzecha, P. Ceranowicz, R Tomaszewska, J. Stachur, S. J. Konturek, P. C. Konturek, *J. Physiol. Pharmacol.*, **54**(4), 561 (2003).
53. V. D. Dixit, E. M. Schaffer, R. S. Pyle, G. D. Collins, S. K. Sakthivel, R Palaniappan, J. W. Lillard, D. D. Taub, *J. Clinical Invest.*, **114**(1), 57 (2004).
54. Q. Xia, W. Pang, H. Pan, Y. Zheng, J.-S. Kang, S.-G. Zhu. *Regul. Pept.*, **122** (3), 173 (2004).
55. Z. Warzecha, P. Ceranowicz, A. Dembinski, J. Cieszkowski, B. Kusnierz-Cabala, R. Tomaszewska, A. Kuwahara, I. Kato. Therapeutic effect of ghrelin in the course of cerulein induced acute pancreatitis in rats. *J. Physiol. Pharmacol.*, **61**(4), 419 (2010).
56. M. Granado, T. Priego, A. I. Martín, MA Villanúa, A. López-Calderón, *Am. J. Physiol. Endocrinol. Metab.*, **288**, 486
57. Chorny, P. Anderson, E. Gonzalez-Rey, M. Delgado, *J. Immunol.*, **180**(12), 8369 (2008).
58. M. D. Deboer, *International Journal of Peptides*, **2011**, 10 (2011) doi:10.1155/2011/189242
59. T. T. Rau A. Sonst, A. Rogler, G. Burnat, H. Neumann, K. Oeckl, W. Neuhuber, A. Dimmler, G. Faller, T. Brzozowski, A. Hartmann, P.C. Konturek, *J. Physiol. Pharmacol.*, **64**, (6) 719 (2013)
60. M. Papotti, P. Cassoni, M. Volante, R. Deghenghi, G. Muccioli, E. Ghigo. Ghrelin producing endocrine tumors of the stomach and intestine. *J. Clin. Endocrinol. Metab.*, **86**, 5052 (2001).
61. A. Srivastava, A. Kamath, S. A. Barry, Y. Dayal, *Endocrine Pathology* **15**, 47 (2004).
62. V. Tsolakis, G. M. Portela-Gomes, M. Stridsberg, L. Grimelius, A. Sundin, B. K. Eriksson, K. E. Oberg, E. T. Janson. Malignant gastric ghrelinoma with hyperghrelinemia. *J. Clin. Endocrinol. Metab.*, **89**, 3739 (2004).
63. S. Checchi, Montanaro A, L. Pasqui, C Ciuoli, G Cevenini, F Sestini, C Fioravanti, F Pacini. *J. Clin. Endocrinol. Metab.*, **92**, 4346 (2007)
64. P.L. Jeffery, A.C. Herington, L.K. Chopin, *J. Endocrinol.*, **172**, 7 (2002)
65. P. L. Jeffery, A. Herington, L. Chopin, *Cytokine Growth Factor Rev.*, **14**, 113 (2003)
66. V. D. Dixit, A. T. Weeraratna., H. Yang., D Bertak., A. Cooper-Jenkins., G. J. Riggins, C. G. Eberhart, D. D. Taub, *J. Biol. Chem.*, **281**, 16681 (2006).
67. J. Fung, S. Ieim, D. Wang, A. Obermair, L.K. Chopin, C. Chen. *Horm. Cancer*, **1**, 245 (2010).
68. Duxbury, M., T. Waseem, H. Ito ,M. K. Robinson, M. J. Zinner, S. W. Ashley, E. E. Whang, *Biochem. Biophys. Res. Commun.*, **309**(2), 464 (2003).
69. P. Y. Tian and X. M. Fan, *J. Dig. Dis.*, **13**(9), 453 (2012).
70. M. Volante, E. Allia, P. Gugliotta, A. Funaro, F. Broglio, R. Deghenghi, G. Muccioli, E. Ghigo, M. J. *Clin. Endocrinol. Metab.*, **87**, 1300 (2002).
71. N. Diaz-Lezama, M. Hernandez-Elvira, A. Sandoval, A. Monroy, R. Felix, E. Monjaraz. *Biochem. Biophys. Res. Commun.*, **403**, 24 (2010)
72. P. Cassoni, M. Papotti, C. Ghe, F. Catapano, A. Sapino, A. Graziani, R. Deghenghi, T. Reissmann, E. Ghigo, G. Muccioli, *J. Clin. Endocrinol. Metab.*, **86**, 1738 (2001).
73. P. Cassoni, E. Allia, T. Marrocco, C. Ghe, E. Ghigo, G. Muccioli, M. Papotti, *J. Endocrinol. Invest.* **29**, 781 (2006).
74. V. G. Weis and J. R. Goldenring. *Gastric Cancer*; **12**, 189 (2009)
75. J. Kawashima S. Ohno, T. Sakurada, H. Takabayashi, M. Kudo, S. Ro, S. Kato, K. Yakabi. *J. Gastroenterol.*, **44**, 1046 (2009).
76. S. Ro, T. Tanaka, M. Ochiai, K. Yakabi, *Gastroenterology*; **26**, A147 (2004).
77. H. M. Bilgin, C. Tumer, H. Diken, M. Kelle, A. Sermet, *Physiol. Res.*, **57**, 563 (2008).
78. M. El-Salhy, E. Lillebø, A. Reinemo , L. Salmelid, *Int. J. Mol. Med.*, **23**(6), 703 (2009).
79. L. Barzon, M. Pacenti, G. Masi, A.L. Stefani, K. Fincati, G. Palu, *Oncology*, **68**, 414 (2005).
80. Ghe, P. Cassoni, F. Catapano, T. Marrocco, R. Deghenghi, E. Ghigo, G. Muccioli, M. Papotti, *Endocrinology* **143**, 484 (2002).
81. K. Takahashi, C. Furukawa, A. Takano, N. Ishikawa, T. Kato, S. Hayama, C. Suzuki, W. Yasui, K. Inai, S. Sone, T. Ito, H. Nishimura, E. Tsuchiya, Y. Nakamura, Y. Daigo, *Cancer Research*, **66**, 9408 (2006).
82. T. Waseem, Ur. R. Javaid, F. Ahmad, M. Azam, M. A. Qureshi, *Peptides*, **29**, 1369 (2008).

ГРЕЛИН И РАК НА СТОМАХА

И. С. Стефанов^{1*}, Ю. А. Ананиев², А. Н. Толева³, К. И. Динкова,² С. Хамза¹, М. К. Игнатова²,
М. В. Гълъбова²

¹ Катедра "Анатомия", Медицински факултет, Тракийски университет, Стара Загора, България

² Катедра „Обща и клинична патология“, Медицински факултет, Тракийски университет, Стара Загора,
България

³ Катедра „Физиология, патофизиология и фармакология“ Медицински факултет, Тракийски университет,
Стара Загора, България

Постъпила на 28 септември, 2016 г.; Коригирана на 13 февруари, 2017 г.

(Резюме)

Грелинът е наскоро установен пептид, описан предимно в ендокринните клетки на стомаха. В стомаха, грелин позитивни клетки са описани основно при хроничен атрофичен гастрит, Н. Рудолф- свързан гастрит и стомашни карциноиди. Присъствието на грелин позитивни клетки при рак на стомаха е слабо проучено. Целта на настоящото изследване е да опишем грелин позитивните клетки при дифузен и интестинален тип рак на стомаха и в околната лигавица на антрума, фундуса и тялото на стомаха. Ендокринните клетки са установени имунохистохимично с антитела срещу хромогранин (Cha), гастрин (Gas), соматостатин (Som), серотонин (Ser) и грелин (Ghr). Грелин позитивни клетки са наблюдавани във всички видове стомашен карцином (дифузен тип) ($1,93 \pm 1,76$ cells/mm²). Най-много Ghr⁺ клетки $42,37 \pm 4,8$ cells/mm² са открити в антралната лигавица на стомаха, последвани от тези ($27,6 \pm 1,27$ cells/mm²) в лигавицата на тялото и най-малко - $25,2 \pm 6,3$ cells/mm² в лигавицата на фундуса на стомаха. Извършената колокализация с използваните антитела показва, че някои от Cha⁺ клетки, Gas⁺ клетки и Som⁺ клетки са едновременно и Ghr⁺. В заключение, Ghr⁺ECs могат да бъдат идентифицирани в стомашния карцином от дифузен тип. Грелинът може да бъде секретиран не само от определени Ghr⁺ ECs, но също от позитивни за гастрин и соматостатин ендокринни клетки.

Anti-inflammatory and analgesic activity of newly synthesized peptides including pyrrole moiety

M. Tzvetkova¹, H. Nocheva^{1*}, D. L. Danalev², St. P. Vladimirova³, S. A. Yaneva⁴, A. I. Bocheva¹

¹Medical University of Sofia, Department of Pathophysiology

²Sofia, University of Chemical Technology and Metallurgy, Biotechnology Department

³Sofia, University of Chemical Technology and Metallurgy, Department of Organic synthesis and fuels

⁴Sofia, University of Chemical Technology and Metallurgy, Department of Fundamentals of Chemical Technology

Received September 20, 2016; Revised February 20, 2017

Peptides have important functions in human's body. Tyr-MIF-1 represents a tetrapeptide with opioid activity and good selectivity in binding to μ -receptors. In the same time lots of pyrrole-containing drugs with different activities take part in medical practice. A series of hybrid molecules representing Tyr-MIF-1 mimetics incorporated in a pyrrole heterocycle, with potential analgesic activity, was synthesized. The synthesis of the peptide moiety was realized by peptide synthesis in solution. Pyrrole cycle and aimed hybrid structures were obtained by Paal-Knorr reaction.

The aim of the present study was to investigate the analgesic and anti-inflammatory effects of Tyr-MIF-1 mimetics during acute pain in rats.

The experiments were carried out on male Wistar rats. The analgesic effects were evaluated using Paw-pressure and Hot-plate tests and the anti-inflammatory effect was evaluated by Digital Water Plethysmometer.

All drugs were administered intraperitoneally at a dose of 1mg/kg, dissolved in sterile saline (0.9% NaCl) solution. The results showed that some of the newly synthesized peptides possessed analgesic activity and the opioid system took part in such effects.

The anti-inflammatory activity of the newly synthesized compounds with manifested analgesic activity was evaluated, but showed to be lower than the referent substance indomethacin.

Keywords: Tyr-MIF-1's mimetics, nociception, inflammation.

INTRODUCTION

Pain and inflammation are ordinary participants in every-day's life. Innumerable factors can be responsible for painful and inflammatory conditions, causing distress and sometime severe disorders in people's social and economic life. Given the unpleasant and adverse consequences of pain and inflammation, different fields' specialists are involved in the search of means to fight such undesirable conditions.

Each day doctors prescribe large number of painkiller drugs belonging to different groups - corticosteroids, non-steroidal anti-inflammatory drugs (NSAIDs), etc. [1]. Since the last century there was a strong exploration of the properties of various heterocyclic compounds including pyrrole as anti-inflammatory and anti-pain agents [2]. A number of molecules containing pyrrole heterocycle in their structure were approved as drugs with different application in medical practice [3-8].

Since pain and inflammation represent stressful conditions for the human body, the organism possesses also natural mechanisms to slow down

and oppose their adverse consequences. Different systems take part in anti-stress activity, with the opioid, endocannabinoid, adrenergic ones being among the most important ones [9- 12].

The opioid system includes opioid receptors (e.g. μ -, δ -, κ - receptors) and their endogenous ligands (e.g. endorphins, enkephalins, dynorphin) [13]. Some natural occurring molecules including peptides perform a variety of functions in the human body. They can be neurotransmitters, neuromodulators, hormones, etc. Tyr-MIF is a tetrapeptide well known from the literature for its opioid activity and good selectivity binding to μ -receptors [9-11]. A series of hybrid molecules representing Tyr-MIF-1 mimetics with a pyrrole heterocycle incorporated possessing potential analgesic and anti-inflammatory activity was synthesized. Such modifications in the structure of the natural opioid peptide combined into hybrid structure with various heterocyclic compounds are investigated as promising alternatives to existing commercial non-steroidal anti-inflammatory and opioid agents.

The aim of the present study was to investigate the analgesic and anti-inflammatory effects of Tyr-MIF-1 mimetics during acute pain in rats.

* To whom all correspondence should be sent:

E-mail: dr_inna@yahoo.com

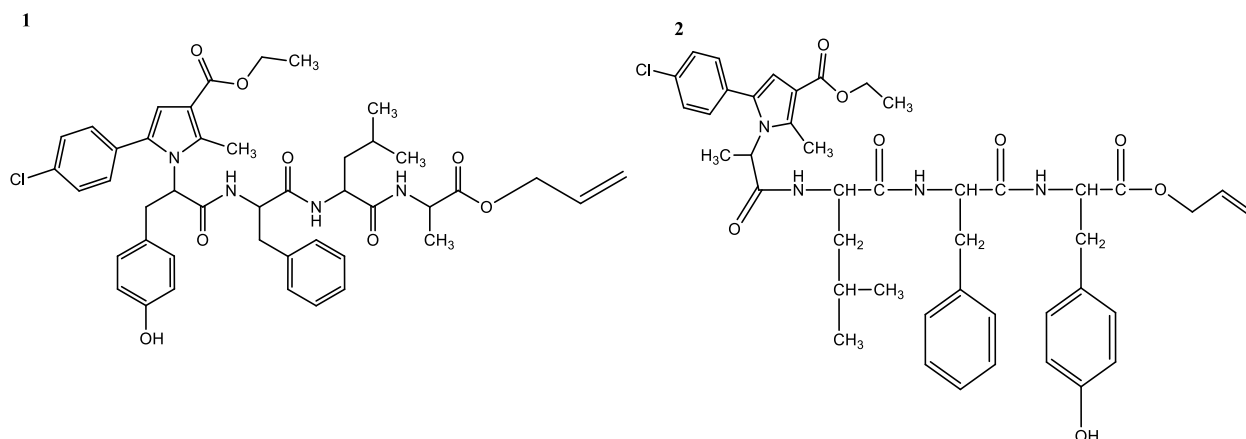


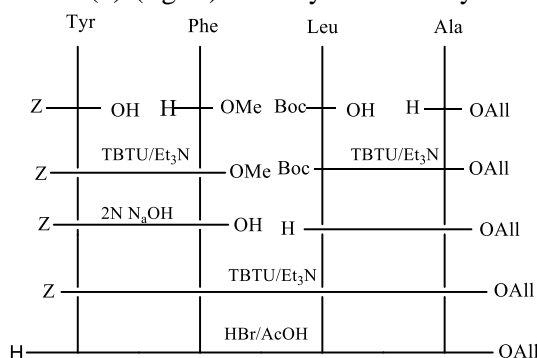
Fig.1. Structure of Pyrrole modified Tyr-MIF analogues (1) and (3)

EXPERIMENTAL

Chemical synthesis

All used solvents are purchased by Valerus (Bulgaria) and used without any additional treatments. All amino acids are purchased by IRIS Biotech (Germany).

Both compounds analogues of Tyr-MIF, Pyr-Tyr-Phe-Leu-Ala-OAll (1) and Pyr-Ala-Leu-Phe-Tyr-OAll (3) (fig. 1) were synthesized by reaction



of Paal-Knorr between modified pyrrole and tetrapeptides H-Tyr-Phe-Leu-Ala-OAll and H-Ala-Leu-Phe-Tyr-OAll in acetic acid as a solvent.

Both necessary tetrapeptides were synthesized by standard peptide synthesis in solution by means of 2+2 Scheme (fig. 2).

Compound Pyr-Tyr-Phe-Leu-Ala-OH (2) with free COOH-function at C-terminus is obtained starting by substance 1 by treatment with Pd(PPh₃)₄ for around 5 h (TLC control) in Ar atmosphere.

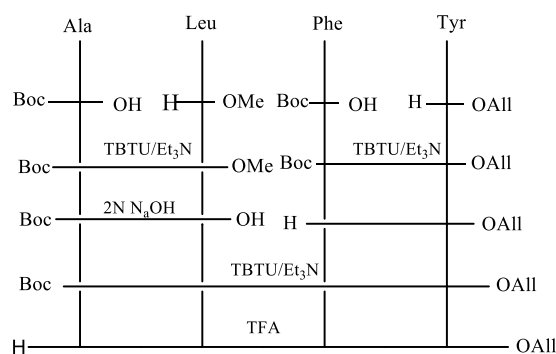


Fig. 2. Schemes of synthesis of tetrapeptides analogues of Tyr-MIF.

Animals

The experiments were carried out on male Wistar rats (180-220 g). The rats were housed individually in polypropylene boxes with free access to food and water and kept in a constant temperature environment (22 ± 2°C) on a 12:12 h light/dark cycle.

The newly synthesized substances (Peptides 1, 2, and 3) were administered intraperitoneally (i.p.) at a dose of 1mg/kg, dissolved in sterile saline (0.9% NaCl) solution.

Along with estimation of analgesic activity of newly synthesized peptides the involvement of the opioid system in such effects was evaluated by

blocking opioid receptors with the non-selective opioid-receptors antagonist naloxone (Nal, at a dose 1 mg/kg, i.p., dissolved in saline).

All procedures were approved by the Animal Care and Use Committee of the Medical University of Sofia.

Nociceptive tests

Pain perception was estimated between 10:00 a.m. and 1:00 p.m. by mechanical (Paw pressure test) and thermal (Hot plate test) stimuli.

Paw pressure test (Randall-Selitto test)

The changes in the mechanical nociceptive threshold of the rats were measured by the use of an analgesiometer (Ugo Basile). Increasing pressure (g) was applied to the hind-paw and the value required to elicit a nociceptive responses (a squeak or struggle) was taken as the mechanical nociceptive threshold. A cut-off value of 500 g was observed in order to prevent damage of the paw.

Hot plate test

The latency of response to pain was measured from the moment an animal was placed on a metal plate (heated to $55 \pm 0.5^\circ \text{C}$) to the first signs of pain (paw licking, jumping). A cut-off time of 30 sec was observed.

Anti-inflammatory activity of the newly synthesized substances was estimated by a *Digital Water Plethysmometer* designated to provide highly precise measurement of small volume changes due to inflammation. The test typically follows the evolution of the inflammatory response experimentally induced in rodents and screens potential anti-inflammatory or anti-edema properties of pharmacological substances. The volume transducer consists in two tubes interconnected and filled with conductive solution and an electrode for each chamber. The animal paw immersed in the measuring tube displaces some water and the displacement produced is then reflected into the second tube, inducing a change in the conductance between the two electrodes. The Plethysmometer Control Unit detects the conductance changes and generates an output signal to the digital display indicating the volume displacement measured (0.01 ml resolution).

The anti-inflammatory effect of the newly synthesized peptides with analgesic activity was then compared to the referent substance indomethacin (2 mg/kg, i.p.).

All results were statistically assessed by one-way analysis of variance ANOVA followed by t-test comparison. Values are mean \pm S.E.M. Values of $p \leq 0.05$ were considered to indicate statistical significance.

The experimental procedures were carried out in accordance with the requirements of the Ethical Committee of the Medical University of Sofia.

RESULTS AND DISCUSSION

The biological activity of newly synthesized substances was first compared to Tyr-MIF-1. The results showed that on the 10th min Peptide 2 expressed a statistically relevant higher analgesic

activity compared to the referent substance ($p < 0,01$) and even higher on the 20th min ($p < 0,001$).

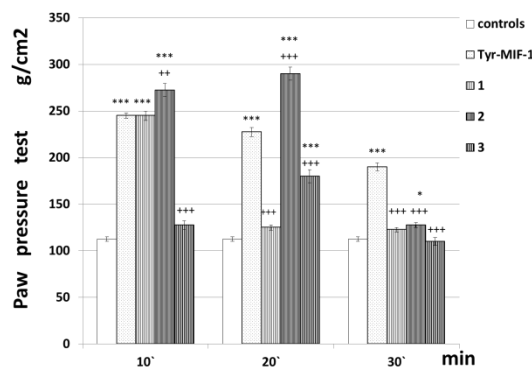


Fig. 3. Effects of newly synthesized Peptides 1, 2, and 3 measured by Paw pressure test. The results are represented as mean values \pm S.E.M. *** $p < 0,001$ relative to control; * $p < 0,05$ relative to control; +++ $p < 0,001$ relative to Tyr-MIF-1; ++ $p < 0,01$ relative to Tyr-MIF-1.

The analgesic activity of Peptide 1 was equal to Tyr-MIF-1's on the 10th min and comparable to the control values for the remaining time of the experiment. Peptide 3 showed no analgesic activity compared to Tyr-MIF-1 for the whole time of the experiment (Fig. 3).

On hot plate evaluation Peptide 2 showed an analgesic activity comparable to the control values for the entire time of the experiment and without statistically relevant differences compared to Tyr-MIF-1 on the 10th and 20th min, while on the 30th min its analgesic activity was higher than the referent substance's one ($p < 0,001$). Peptides 1 and 3 showed no analgesic activity and even a tendency toward hyperalgesia both compared to the referent substance and controls (Fig. 4).

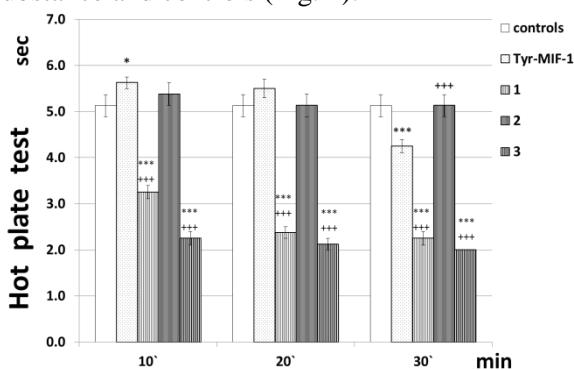


Fig. 4. Effects of newly synthesized Peptides 1, 2, and 3 measured by Hot plate test. The results are represented as mean values \pm S.E.M. *** $p < 0,001$ relative to control; * $p < 0,05$ relative to control; +++ $p < 0,001$ relative to Tyr-MIF-1.

Involvement of the opioid system in analgesic effects of the newly synthesized Peptides was

assessed due antagonizing opioid receptors with Nal. A brisk decline in analgesic activity of Peptides 1 ($p < 0,001$) and 3 ($p < 0,001$) after administration of opioid receptors antagonist was assessed for the entire time of the experiment compared to animals without naloxone and controls, while Peptide 2 maintained its analgesic activity on the 10th min compared to controls ($p < 0,001$) even pain thresholds being lower than those of animals without naloxone (Fig. 5).

On hot plate evaluation all latencies were shorter the controls and the respective group of animals without Nal (Fig. 6).

The estimated anti-inflammatory activity of Peptides 1 and 2 (showing the most expressed analgesic activity) was estimated. It resulted lower than the referent substance's one (Table 1).

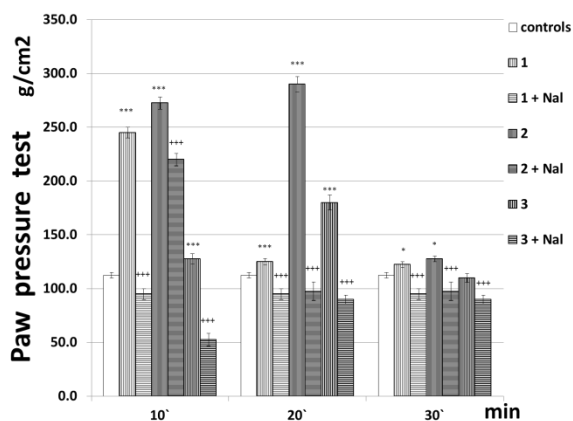


Fig. 5. Effects of newly synthesized peptides (1, 2, and 3) evaluated by PP test in animals without and with naloxone (Nal, 1 mg/kg, i.p.). The results are represented as mean values \pm S.E.M. *** $p < 0,001$ relative to control; * $p < 0,05$ relative to control; +++ $p < 0,001$ relative to Tyr-MIF-1.

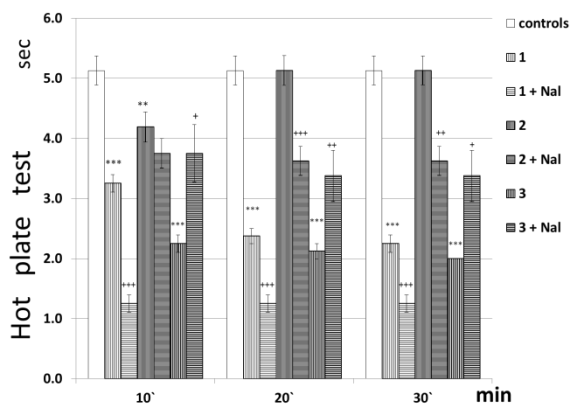


Fig. 6. Effects of newly synthesized peptides (1, 2, and 3) evaluated by HP test in animals without and with naloxone (Nal, 1 mg/kg, i.p.). The results are represented as mean values \pm S.E.M. *** $p < 0,001$ relative to control; ** $p < 0,01$ relative to control; +++ $p < 0,001$ relative to Tyr-

MIF-1; ++ $p < 0,01$ relative to Tyr-MIF-1; + $p < 0,05$ relative to Tyr-MIF-1.

Table 1. Anti-inflammatory effects of newly synthesized peptides (1 and 2) estimated by decrease (%) of edema caused by carrageenan (100 μ g/paw) compared to indomethacin (2 mg/kg, i.p.).

Substance	Edema on the 4 h and 10 min after the substance administration	Decrease (%) of edema due to carrageenan (100 μ g/paw)
Indomethacin 2 mg/kg, i.p.	2.20 \pm 0.2	54,6
1, 1 mg/kg, i.p.	2.69 \pm 0.1	44.5
2, 1 mg/kg, i.p.	2.84 \pm 0.1	41.4

Searches of new substances with analgesic and anti-inflammatory activity is justified, on one hand, because both acute and chronic pain, as well as inflammation accompany many diseases and clinical conditions decreasing quality of life, and, on the other hand, most of the already known drugs possess undesired collateral effects (ulcerogenic effect, drug-dependence, etc.). In order to avoid/decrease undesired collateral effects more than one drugs, possessing each one a lower effect, are often prescribed together relying on their agonistic final effect. Such therapeutic approach allows decreasing the dose of each drug thus avoiding/decreasing the individual collateral effect of each one of them. Two of the new substances showed an analgesic effect, and an anti-inflammatory effect even lower than the referent substance's one was also present. Such findings could represent a starting position for additional searches.

In the same time it's important to understand the mechanisms of the newly synthesized substances action in order to establish the best way of administration and to predict possible interactions with other drug components.

Our study tried to elucidate the participation of the opioid system in the mechanisms of action of the newly synthesized substances. The experiments demonstrated the participation of the opioid system in the analgesic effects of the three new peptides.

Acknowledgements: The work was supported by Grant 61/2014 from the Bulgarian National Scientific Research Foundation.

REFERENCES

1. R.H. Dworkin, M. Backonja, M.C. Rowbotham, R.R. Allen, C.R. Argoff, G.J. Bennett, M.C. Bushnell, J.T. Farrar, B.S. Galer, J.A. Haythornthwaite, D.J. Hewitt, J.D. Loeser, M.B. Max, M. Saltarelli, K.E. Schmader, C. Stein, D. Thompson, D.C. Turk, M.S. Wallace, L.R. Watkins, S.M. Weinstein, *Arch. Neurol.*, **60(11)**, 1524 (2003).
2. J.A.H. Lainton, J.W. Huffman, B.R. Martin, D.R. Compton, *Tetrahedron Lett.*, **36(9)**, 1401 (1995).
3. W. Malinka, M. Sieklucka-Dziuba, G. Rajtar, R. Rejdak, K. Rejdak, Z. Kleinrok, *Pharmazie*, **55(1)**, 9 (2000).
4. N. Amishiro, A. Okamoto, C. Murakata, T. Tamaoki, M. Okabe, H. Saito, *J. Med. Chem.*, **42(15)**, 2946 (1999).
5. P.R. Bovy, J.T. Collins, R.E. Manning, US Patent 6,008,368 (1999)
6. Y. Fumoto, T. Eguchi, H. Uno, N. Ono, *J. Org. Chem.*, **64(17)**; 6518 (1999).
7. J.R. Carson, R.J. Carmosin, P.M. Pitis, J.L. Vaught, H.R. Almond, J.P. Stables, H.H. Wolf, E.A. Swinyard, H.S. White, *J. Med. Chem.*, **40(11)**, 1578 (1997).
8. M. Artico, R. Silvestri, E. Pagnozzi, B. Bruno, E. Novellino, S.M. Greco, A. Ettorre, A.G. Loi, G.F. Scintu, P. La Colla, *J. Med. Chem.*, **43(9)**, 1886 (2000).
9. M.N. Hill, J.G. Tasker, *Neuroscience*, **204**, 5 (2012).
10. I. Barna, D. Zelena, A.C. Arszovszki, C. Ledent, *Life Sci.*, **75**, 2959 (2004).
11. R. Przewlocki, *Elsevier*, 289 (2009).
12. D. Jefferys, J.W. Funder, *Endocrinology*, **121**, 1006 (1987).
13. W. Pan, A.J. Kastin, *Peptides*, **28**, 2411 (2007).

ПРОТИВОВЪЗПАЛИТЕЛНА И АНАЛГЕТИЧНА АКТИВНОСТ НА НОВОСИНТЕЗИРАНИ ПЕПТИДИ, ВКЛЮЧВАЩИ ПИРОЛ

М. Цветкова¹, Х. Ночева^{1*}, Р. Хаджиолова¹, Д. Даналев², С. Владимирова³, С. Янева⁴, А. Бочева¹

¹ Катедра по Патифизиология, Медицински Университет – София

² Катедра Биотехнология, Химикотехнологичен и металургичен Университет - София

³ Катедра Органичен синтез и горива, Химикотехнологичен и металургичен Университет - София

⁴ Катедра Основи на химичните технологии, Химикотехнологичен и металургичен Университет - София

Постъпила на 20 септември, 2016 г.; Коригирана на 20 февруари, 2017 г.

(Резюме)

Пептидите притежават важни функции в човешкия организъм. Туг-MIF-1 представлява тетрапептид с опиоидна активност и добра селективност по отношение свързването му с μ -рецепторите. В същото време множество пирол-съдържащи медикаменти с различно приложение намират място в терапевтичната практика. Във връзка с това бе синтезирана серия хибридни молекули, представляващи Туг-MIF-1-миметици, съдържащи пиролов хетероцикъл, с потенциален аналгетичен ефект. Синтезът на пептидите бе реализиран посредством стандартна SPPS (Fmoc/Ot-Bu стратегия). Пироловият цикъл и хибридните структури бяха получени чрез Paal-Knorr - реакция.

Целта на проучването бе определяне аналгетичния и противовъзпалителен ефект на Туг-MIF-1-миметиците при остро възпаление при плъхове.

Експериментите бяха проведени върху мъжки плъхове от породата Wistar. Аналгетичният ефект бе определен посредством методите raw-pressure и hot-plate, докато противовъзпалителната активност бе изследвана посредством дигитален воден плетизмометър.

Изследваните вещества бяха въведени интраперитонеално.

Резултатите показаха, че някои от новосинтезираните пептиди притежават аналгетична активност, като опиоидната система участва в тези ефекти.

Противовъзпалителната активност на новосинтезираните вещества бе по-слаба от тази на референтния препарат индометацин.

CONTENTS

<i>Preface</i>	5
<i>A.A. Balacheva, M.K. Lambev, I. Pashov, R.L. Detcheva, P. Sázelova, G.Ts. Momekov, V. Kašička, T.I. Pajpanova, E.V. Golovinsky</i> , Synthesis, analysis and biological evaluation of new RGD mimetics	7
<i>B. K. Yakimova, D. Petkova, N. K. Karapetrova and I. B. Stoineva</i> , Molecular design and chemical synthesis of peptide inhibitors of Angiotensin I converting enzyme (ACE) for prevention and therapy of hypertension.....	11
<i>B. Stoykova, M. Chochkova, L. Georgiev, G. Ivanova, L. Mukova, N. Nikolova, L. Nikolaeva-Glomb, Ts. Milkova, M. Šticha</i> , Amino acids amides of anti-influenza drugs: synthesis and biological activities.....	16
<i>F.I. Sapundzhi, T.A. Dzimbova, N.S. Pencheva, P.B. Milanov</i> , QSAR modelling and molecular docking studies of three models of delta opioid receptor.....	23
<i>P. Todorov, P. N. Peneva, Z. N. Genova, E. D. Naydenova</i> , Synthesis and characterization of new endomorphin analogs with N-terminal phosphonate.....	31
<i>P.I. Mateeva, R. Y. Prodanova, M. N. Marinov, E. D. Naydenova, P.T. Todorova, R. N. Zamfirova</i> , Rapid screening of anti-inflammatory properties of newly synthesized derivatives of indomethacin.....	35
<i>M. N. Marinov, E. D. Naydenova, R. Y. Prodanova, S. H. Tsoneva, N. M. Stoyanov</i> , Synthesis of new indometacin derivatives with 3-aminospirohydantoins and 3-amino-5-methyl-5-phenylimidazolidine-2,4-dione.....	40
<i>I.I. Kostadinova, N.D. Danchev, I.N. Nikolova, L.T. Vezenkov, Tch. B. Ivanov, M.G. Georgieva</i> , Pharmacological and toxicological investigations of newly synthesized benzazepine derivatives comprising peptide fragment.....	46
<i>M.A. Rangelov, N. H. Todorova, I. G. Tsacheva</i> , In silico investigation of single-chain variable fragment (scFv) antibody, structurally similar to native C1q globular heads.....	50
<i>T.A. Dzimbova, R.K. Georgiev, A.G. Chapkanov</i> , Synthesis and FT-IR spectral elucidation of dipeptide with aromatic amino acid.....	54
<i>K. Chuchkov, D. Mitreva, V. Markova, I. Stankova</i> , Chemical stability of thiazole analogues of rimantadine and amantadine.....	58
<i>R.Chayrov, L. Mukova, A. Galabov, Y. Mitrev, I. Stankova</i> , Amantadine analogues - synthesis and biological activity.....	61
<i>S. A. Yaneva, D. A. Marinkova, L. Ilieva, L. T. Vezenkov, L. K. Yotova, D. L. Danalev</i> , Kinetic investigation and tyrosinase inhibition activity of peptide analogues of galanthamine.....	64
<i>M. Chochkova, B. Stoykova, P. Petrova, N. Gyoshkova, G. Ivanova, M. Šticha, T. Milkova</i> , Synthesis and radical scavenging activity of cinnamic acid esters.....	68
<i>M.G. Georgieva, R.L. Detcheva, T.I. Pajpanova</i> , Synthesis and study of cytotoxic effect of novel AVPI-RGD hybrid peptides.....	74
<i>M.B. Aliosman, I.Z. Eneva, M. Durmus, I.B. Stoineva, V.N. Mantareva</i> , Aminophenoxy-substituted zinc(II) phthalocyanines as basic photosensitizers for conjugation with biologically active peptides: Synthesis and photophysical properties.....	79
<i>S. P. Vladimirova, D. L. Danalev, D. A. Marinkova, R. N. Raykova, D. S. Manova, S. R. Marinova, D. I. Marinova</i> , Synthesis and antibacterial activity of amino acids modified with specifically substituted pyrrole heterocycle.....	86
<i>S. A. Yaneva, I. I. Stoykova, L. I. Ilieva, L. T. Vezenkov, D. A. Marinkova, L. K. Yotova, R. N. Raykova, Dancho L. Danalev</i> , Acetylcholinesterase inhibition activity of peptide analogues of galanthamine with potential application for treatment of Alzheimer`s disease.....	90
<i>P. Petrova, I. Karadjova, M. Chochkova, I. Dakova, M. Karadjov</i> , New amino acid modified silica gel sorbents for solid phase extraction of Au (III).....	95
<i>B.K. Yakimova, B.P. Tchorbanov, I.B. Stoineva</i> , Alpha-galactosidase and invertase from <i>Penicillium chrysogenum</i> sp.23: purification, characteristics and hydrolysis of raffinose.....	101
<i>R.N. Raykova, E. Carvalho, L.S. Manovski, D.L. Danalev, D.A. Marinkova, T.I. Pajpanova, S.A. Yaneva, L.K. Yotova</i> , Kinetic of inhibition of lipoxygenase in presence of natural amino acid serine.....	107

<i>S. Michailova, T. Dzimbova, K. Kalikova, E. Tesařová, T. Pajpanova</i> , Chemical stability of new neurotensin (8-13) analogues.....	113
<i>R.E. Tashev, M.S. Ivanova, S.P. Belcheva, I.P. Belcheva</i> , Involvement of hippocampal angiotensin II type 1 receptors in locomotor activity in rats with a model of depression.....	118
<i>T. Atanasov, S. Radev, I.B. Stoineva</i> , Some physicochemical characteristics of anti-platelet fraction isolated from <i>Galega officinalis</i> L.....	124
<i>S. Stoeva, L. Tancheva, L. Alova, M. Stefanova, T. Pajpanova, R. Kalfin</i> , Modulating effect of new neuropeptide on central nervous system and on dopamine neurotransmission in mice.....	130
<i>S.M. Mihajlova, A.A. Dimitrova, T.I. Vlaykova, T.T. Tacheva, V. Tsoneva, K. Nancheva-Koleva, R.V. Sandeva</i> , Effect of high- fructose diet on plasma leptin levels, morphological and biochemical parameters in ovariectomized rats.....	134
<i>R. V. Sandeva, A. A. Dimitrova, T. T. Tacheva, S. M. Mihajlova, G. N. Sandeva, T. I. Vlaykova</i> , Unacylated ghrelin in plasma of wistar rats after consumption of fructose, sucrose and aspartame.....	140
<i>A.Popatanasov, S. Stoeva, M. Lazarova, L. Traikov, T. Pajpanova, R. Kalfin, L. Tancheva</i> , Effects of new neurotensin analogue on brain activity in rat Parkinson's disease model.....	146
<i>H. Nocheva, E. Naydenova, N. Pavlov, A. Bocheva</i> , Effects of nociceptin neurotransmitter system on nociception in 6-hydroxydopamine model of hemiparkinsonism in rat.....	151
<i>D.S. Kochev, H.H. Nocheva, L. Traikov</i> , Parkinson`s disease: influence of cannabinoid and peptidergic systems on pain.....	159
<i>R. E. Kalfin, M. I. Lazarova, P. I. Mateeva, L. M. Yankova, S. P. Belcheva, R. E. Tashev</i> , Vasoactive intestinal peptide and Parkinson`s disease.....	165
<i>M.S. Ivanova, R.E.Tashev</i> , Intrahippocampal administration of losartan improves learning and memory in rats with model of depression.....	169
<i>P.V. Hadzhibozheva, Ts. K. Georgiev, R. E. Kalfin, G. S. Ilieva, A. N. Tolekova</i> , Angiotensin ii-induced motility of reservoir smooth muscle organs from ghrelin and melatonin-treated diabetic rats.....	175
<i>M. V. Gulubova, I. V. Valkova, K. V. Ivanova, I. G. Ganeva, D. K. Prangova, MM. K. Ignatova, S. R. Vasilev, I. S. Stefanov</i> , Endocrine cells in pig`s gallbladder, ductus cysticus and ductus choledochus with special reference to ghrelin.....	184
<i>T. K. Georgiev, P. V. Hadzhibozheva, E. D. Georgieva, Y. D. Karamalakova, G. D. Nikolova2, V. G. Gadjeva, A. M. Zheleva, A. N. Tolekova</i> , Effect of N-[N'-(2-chloroethyl)-N'-nitrosocarbamoyl-glycine amide of 2,2,6,6-tetramethyl-4-aminopiperidine-1-oxyl (SLCNUgly) on Angiotensin II-mediated smooth muscle activity of organs in pelvic cavity.....	191
<i>H. Nocheva, A. Bocheva</i> , Evaluation of opioid system participation in endocannabinoids` effects on SIA after three models of stress.....	199
<i>E. N. Encheva, D. Tsekova, L. Tancheva, L.Alova, L. Shikova, M. Kaneva</i> , Comparative studies on two isomeric L-valine peptidomimetics for neuropharmacological effects in rodents.....	204
<i>S. Stefanov, J.R. Ananiev, A.N. Tolekova, K.I. Dinkova, S. Hamza, MM. K. Ignatova, M. V. Gulubova</i> , Ghrelin and gastric cancer.....	209
<i>M. Tzvetkova, H. Nocheva, R. Hadjiolova, D. Danalev, S.Vladimirova, B.Borisov, A. Bocheva</i> , Anti-inflammatory and analgesic activity of newly synthesized peptides including pyrrole moiety.....	218

СЪДЪРЖАНИЕ

<i>A.A. Балачева, М.К. Ламбев, И. Пашов, Р. Л. Дечева, П. Сазелова, Г.Ц. Момаков, В. Кашичка, Т.И. Пайпанова, Е.В. Головински, Синтез, анализ и биологична оценка на нови RGD миметици.....</i>	10
<i>Б. Якимова, Д. Петкова, И. Стойнева, Молекулен дизайн и синтез на пептидни инхибитори на ангиотензин I превръщащия ензим за лечение и превенция на хипертония.....</i>	15
<i>Б. Стойкова, М. Чочкова, Л. Георгиев, Г. Иванова, Л. Мукова, Н. Николова, Л. Николаева-Гломб, Ц. Милкова, М. Щиха, Аминокиселинни амиди на противогрипни лекарствени средства: синтез и биологично действие.....</i>	22
<i>Ф. И. Сапунджи, Т. А. Дзимбова, Н. С. Пенчева, П. Б. Миланов, QSAR моделиране и докинг експерименти с три модела на δ-опиоиден рецептор.....</i>	30
<i>П. Т. Тодоров, П. Н. Пенева, З. Н. Генова, Е. Д. Найденова, Синтез и охарактеризиране на нови N-модифицирани аналози на ендоморфините с фосфонатен остатък.....</i>	34
<i>П. И. Матеева, Р. Й. Проданова, М. Н. Маринов, Е. Д. Найденова, П. Т. Тодорова, Р. Н. Замфирова, Бърз скрининг на противовъзпалителните свойства на новосинтезирани производни на индометацин.....</i>	39
<i>М. Н. Маринов, Е. Д. Найденова, Р. Й. Проданова, С. Х. Цонева, Н. М. Стоянов, Синтез на нови индометацинови производни с 3-аминоспирохидантоини и 3-амино-5-метил-5-фенилимидазолидин-2,4-дион.....</i>	45
<i>И. И. Костадинова, Н. Д. Данчев, И. Н. Николова, Л. Т. Везенков, Ч. Иванов, М. Г. Георгиева, Фармакологични и токсикологични изследвания на новосинтезирани бензазепинови производни с пептиден фрагмент.....</i>	49
<i>М. А. Рангелов, Н. Х. Тодорова, И. Г. Цачева, In silico изследване на едноверижни антители (scfv), структурно подобни на нативните глобуларни фрагменти на <i>Clq</i>.....</i>	53
<i>Т. Е. Дзимбова, Р. К. Георгиев, А. Г. Чапкънов, Синтез и ИЧ-ФТ спектрално изясняване на дипептиди с ароматна аминокиселина.....</i>	57
<i>К. Чучков, Д. Митрева, В. Маркова, И. Станкова, Химична стабилност на тиазолови производни на римантадин и амантадин.....</i>	60
<i>Р. Чайров, Л. Мукова, А. Гълъбов, Я. Митрев, И. Станкова, Амантадинови аналози – синтез и биологична активност.....</i>	63
<i>С. А. Янева, Д. А. Маринкова, Л. И. Илиева, Л. Т. Везенков, Л. К. Йотова, Д. Л. Даналев, Изследване инхибиторната активност върху тирозиназа на пептидни аналози на галантамин.....</i>	67
<i>М. Чочкова, Б. Стойкова, П. Петрова, Н. Гьошкова, Г. Иванова, М. Щиха, Ц. Милкова, Синтез и изследване на радикалулавяща активност на естери на канелените киселини.....</i>	73
<i>М.Г. Георгиева, Р.Л. Дечева, Т.И. Пайпанова, Синтез и анализ на цитотоксичния потенциал на нови AVPI-RGD хибридни пептиди.....</i>	78
<i>М. Б. Алиосман, И. З. Енева, М. Дурмуш, И. Б. Стойнева, В. Н. Мантарева, Аминофенокси заместени цинкови (II) фталоцианини като основни фотосенсибилизатори за конюгиране с биологични активни пептиди: синтез и фотофизични характеристики.....</i>	85
<i>С. П. Владимирова, Д. Л. Даналев, Д. А. Маринкова, Р. Н. Райкова, Д. С. Манова, С. Р. Маринова, Д. И. Маринова, С.А. Янева, Синтез и антибактериална активност на аминокиселини модифицирани със специфично заместен пиролов хетероцикл.....</i>	89
<i>С. А. Янева, И. И. Стойкова, Л. И. Илиева, Л. Т. Везенков, Д. А. Маринкова, Л. К. Йотова, Р. Н. Райкова, Д. Л. Даналев, Изследване инхибиторната активност върху ацетилхолинестераза на пептидни аналози на галантамин, с потенциално приложение при пациенти с болестта на Алцхаймер.....</i>	94
<i>П. Петрова, И. Караджова, М. Чочкова, И. Дакова, М. Караджов, Силикагел модифициран с аминокиселини като сорбент за твърдофазна екстракция на Au (III).....</i>	100
<i>Б. К. Якимова, Б.П. Чорбанов, И.Б. Стойнева, α-Галактозидаза от <i>Penicillium Chrysogenum</i> SP.23: пречистване, характеристики и хидролиза на рафиноза в присъствието на инвертаза.....</i>	106

Р. Н. Райкова, Е. Карвалхо, Л. С. Мановски, Д. Л. Даналев, Д. А. Маринкова, Т. И. Пайпанова, С. А. Янева, Л. К. Йотова, Кинетика на инхибиране на Липоксигеназа в присъствие на природната аминокиселина серин.....	112
С. Михайлова, Т. Дзимбова, К. Каликова, Е. Тежарова, Т. Пайпанова, Химична стабилност на нови аналози на невротензин(8-13).....	117
Р. Е. Ташев, М. С. Иванова, С. П. Белчева, И. П. Белчева, Участие на хипокампалните ангиотензин ii тип 1 рецептори в двигателната активност на плъхове с модел на депресия	123
А. Т. Атанасов, С. Радев, И. Б. Стойнева, Някои физикохимични характеристики на антитромбоцитна фракция изолирана от <i>Galega Officinalis</i> L.....	129
С. Стоева, Л. Танчева, Л. Алова, М. Стефанова, Т. Пайпанова, Р. Калфин, Модулиращи ефекти на новосинтезиран невропептид върху централна нервна система и допаминовата невротрансмисия при мишки.....	133
С. М. Михайлова, А. А. Димитрова, Т. И. Влайкова, Т. Т. Тачева, В. Цонева, К. Нанчева-Колева, Р. В. Сандева, Ефект на високофруктозната диета върху плазмените лептинови нива, морфологични и биохимични показатели при овариектомирани плъхове.....	139
Р. В. Сандева, А. А. Димитрова, Т. Т. Тачева, С. М. Михайлова, Г. Н. Сандева, Т. И. Влайкова, Неацилиран грелин в плазмата на плъхове вистар след консумация на фруктоза, захароза и аспартам.....	145
А. Попатанасов, С. Стоева, М. Лазарова, Л. Трайков, Т. Пайпанова, Р. Калфин, Л. Танчева, Ефекти на нов невротензинов аналог върху мозъчната активност при модел на болестта на Паркинсон при плъхове.....	150
Х. Ночева, Е. Найденова, Н. Павлов, А. Бочева, Ефекти на ноцицептиновата невротрансмитерна система върху ноцицепцията при б-хидроксидопаминов модел на хемипаркинсонизъм при плъх.....	158
Д. Кочев, Х. Ночева, Л. Трайков, Паркинсонова болест: повлияване на болката от канабиноидната и пептидергичната системи.....	164
Р. Е. Калфин, М. И. Лазарова, П. И. Матеева, Л. М. Янкова, С. П. Белчева, Р. Е. Ташев, Вазоактивен интестинален пептид и болест на Паркинсон.....	168
М. С. Иванова, Р. Е. Ташев, Лосартан въведен в хипокамп на плъхове с модел на депресия подобрява обучението и паметта.....	174
П. В. Хаджибожева, Ц. К. Георгиев, Р. Е. Калфин, Г. С. Илиева, А. Н. Толекова, Ангиотензин ii – предизвикана активност на резервоарни гладко-мускулни органи от третиран с грелин и мелатонин диабетни плъхове	183
М. В. Гълъбова, И. В. Вълкова, К. В. Иванова, И. Г. Ганева, Д. К. Прангова, ММ. К. Игнатова, С. Р. Василев, И. С. Стефанов, Ендокринни клетки в жлъчния мехур, <i>Distus Cysticus</i> и <i>Distus Choledochus</i> при прасета със специално отношение към грелина	190
Ц. К. Георгиев, П. В. Хаджибожева, Е. Д. Георгиева, Я. Д. Карамалакова, Г. Д. Николова, В. Г. Гаджева, А. М. Желева, А. Н. Толекова, Ефект на N-[N'-(2-хлороетил)-N'-нитрозокарбамоил-глицин амид на 2,2,6,6-тетраметил-4-аминопиперидин-1-оксил (slcnugly) върху ангиотензин 2-медираната гладкомускулна активност на органи в тазовата кухина	198
Х. Ночева, А. Бочева, Определяне участието на опиоидергичната система в ефектите на ендоканабиноидите върху стрес-индуцираната аналгезия след три модела на стрес	203
Е. Н. Енчева, Д. Цекова, Л. Танчева, Л. Алова, М. Стефанова, Л. Шикова, М. Кънева, Сравнителни проучвания на два изомерни L-валинови пептидомиметици за неврофармакологични ефекти у гризачи	208
И. С. Стефанов, Ю. А. Ананиев, А. Н. Толекова, К. И. Динкова, С. Хамза, М. К. Игнатова, М. В. Гълъбова, Грелин и рак на стомаха	217
М. Цветкова, Х. Ночева, Р. Хаджиолова, Д. Даналев, С. Владимирова, С. Янева, А. Бочева, Противовъзпалителна и аналгетична активност на новосинтезирани пептиди, включващи включващи пирол.....	222